ICEFIELD RANGES RESEARCH PROJECT

SCIENTIFIC RESULTS

VOLUME 1

PUBLISHED JOINTLY BY THE
AMERICAN GEOGRAPHICAL SOCIETY
AND THE
ARCTIC INSTITUTE OF NORTH AMERICA

ICEFIELD RANGES RESEARCH PROJECT
ADVISORY COMMITTEE
(1961 – 1965)

Dr. Walter A. Wood, *Chairman*
2561 North Vermont Street
Arlington, Virginia 22207

Dr. Henri Bader
Institute of Marine Science
University of Miami
Miami, Florida 33146

Dr. William O. Field
American Geographical Society
Broadway at 156th Street
New York, New York 10032

Dr. G. D. Garland
Department of Physics
University of Toronto
Toronto 5, Ontario, Canada

Dr. Richard P. Goldthwait
Chairman, Department of Geology
The Ohio State University
125 South Oval Drive
Columbus, Ohio 43210

Mr. Trevor A. Harwood
Defense Research Telecommunications Establishment
Shirley Bay
Ottawa 4, Ontario, Canada

Dr. Geoffrey F. Hattersley-Smith
11 Madawaska Drive
Ottawa 1, Ontario, Canada

Dr. Calvin J. Heusser
Department of Biology
New York University
Sterling Forest
P.O. Box 608
Tuxedo, New York 10987

† Dr. Charles B. Hitchcock
American Geographical Society
Broadway at 156th Street
New York, New York 10032

Dr. Mark Meier
General Hydrology Branch
U.S. Geological Survey
1305 Tacoma Avenue, South
Tacoma, Washington 98402

Dr. Svenn Orvig
Department of Meteorology
McGill University
Montreal 2, P.Q., Canada

Dr. John C. Reed
Arctic Institute of North America
1619 New Hampshire Avenue, N.W.
Washington, D.C. 20009

Dr. George P. Rigsby
Department of Geology
U.S. International University
Elliot Campus
San Diego, California 92128

Mr. Graham W. Rowley
245 Sylvan Road
Ottawa 2, Ontario, Canada

Prof. Robert P. Sharp
Department of Geological Sciences
California Institute of Technology
Pasadena, California 91109

† Deceased

ICEFIELD RANGES RESEARCH PROJECT
SCIENTIFIC RESULTS

Volume 1

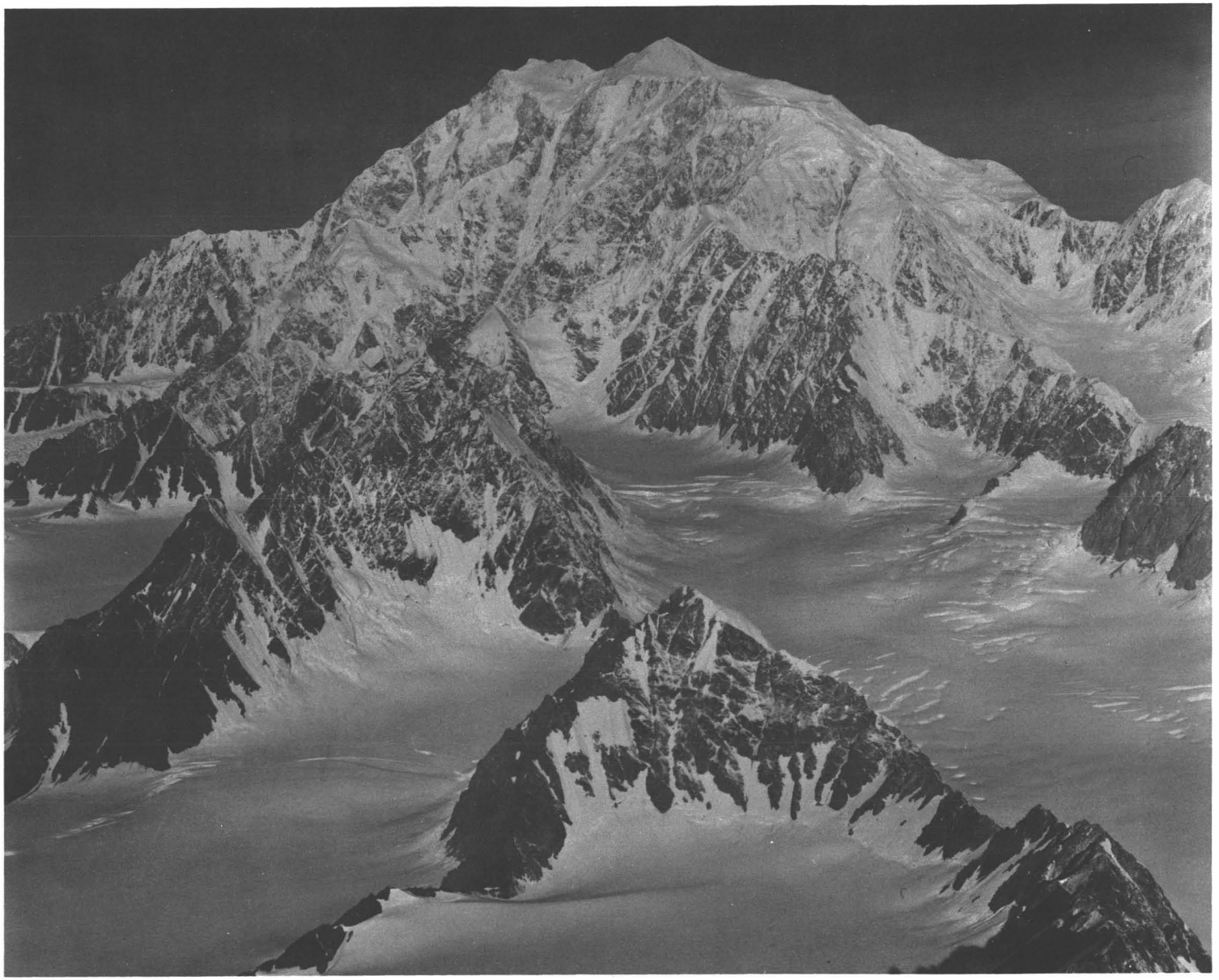

Mt. Logan, Canada's highest peak (19,850 ft.), seen from the southeast. The true summit is the culmination of the "Hummingbird Ridge" seen in profile (left). "Catenary Ridge" descends in profile (right) from East Peak. The massif rises 13,500 ft. above the snows of Seward Glacier (lower left) and Hubbard Glacier (right). (September 3, 1948; 10:30; 11,500 ft.)

ICEFIELD RANGES RESEARCH PROJECT SCIENTIFIC RESULTS

Volume 1

Edited by

VIVIAN C. BUSHNELL

American Geographical Society

and

RICHARD H. RAGLE

Arctic Institute of North America

Foreword and Introduction *by*

WALTER A. WOOD

Published jointly by

AMERICAN GEOGRAPHICAL SOCIETY, NEW YORK

and

ARCTIC INSTITUTE OF NORTH AMERICA, MONTREAL

1969

Library of Congress Catalog Number: 70-90351

This series of volumes is dedicated to

the people of Yukon Territory.

Contents

Foreword

Human reactions to the high mountains of the earth are as varied as the environments in which the ranges rise. Throughout all but a microdecimal of the time man has inhabited this planet, he has regarded mountains in either positive or negative terms: either as protective to his way of life or as antagonistic to his dreams of conquest; as beneficial to his crops and harvests or as detrimental to his communications. Until only yesterday in man's timetable, the high places have reared their summits as symbols of mystery and foreboding, as areas of refuge for ill doers, as havens of safety for the oppressed. For only two hundred years have men crossed the threshold of the tree line in search of recreation, and only in this century has the promise of economic benefits lured men to exploit the water resources that are banked in the snow and ice of alpine regions.

Although in the past man may have had little urge to obtain knowledge of the high mountains by any methods other than those of trial and error, the twentieth century's surge of scientific inquiry into all aspects of our natural environment has carried with it an increasing awareness of the high ranges of the earth and of the role they play in our individual, national, and global lives.

One endeavor in man's quest for knowledge of mountain regions is the Icefield Ranges Research Project. Under the institutional sponsorship of the Arctic Institute of North America and the American Geographical Society, this project seeks understanding of the multiple facets that comprise the natural environment of the St. Elias Mountains of Alaska and Yukon Territory. Its approach to the task is truly geographical, within the widely accepted current meaning of geography as an integrator among the scientific disciplines. Not only is the project multidisciplinary in its areas of research, but it is also interdisciplinary in its approach to its objectives. Then, too, the benefits of the project, some of which are included in this volume and many more of which are scheduled to follow in ensuing numbers of this publication series, are not to be found solely in the printed pages. No fewer than thirteen authors of this initial volume came into the field as graduate students under a project philosophy that sought the double dividend of fundamental knowledge in harmony with educational advancement. These young researchers represented nine universities in the United States and Canada, and they profited not only by field association with their own academic colleagues, but also by professional contact with senior men, who were themselves drawn to IRRP by the research opportunities offered within its structure and facilities.

The Icefield Ranges Research Project has now completed eight field seasons, and the contents of this volume are representative of field work performed during the first four, from 1961 to 1965. Succeeding volumes will present the products of later research.

I first saw and lived among the St. Elias Mountains in 1935, and by 1961 I had revisited them during eight summer field seasons. It was during these visits that I became impressed not only with the vastness and beauty of the high mountain architecture and the variety of geographical contrasts presented within the physical landscape, but also

with the evident role that these elevations play in shaping the character of immediate, adjacent, and even distant climates. It was obvious, too, that no single person or expedition could hope to do more than guess at the scientific opportunity in store for those who would accept the challenge of studying this region. It was in response to these impressions that the concept of studying a high mountain region in terms of its total environment was born in 1960. The area of endeavor was to be the St. Elias Mountains.

Having been on hand at the birth of the Icefield Ranges Research Project, I could easily compile a historical record of its inception, the unfolding of its research and inquiry, and the fruition of the project, which is now at hand. But a chronological sequence of events is of little moment as compared with accomplishment within the period during which the events occurred. Similarly, it is of little consequence to enumerate the number of performances given by a theatrical company. Far more significant are the players themselves and how they play their parts; and it is the participants in IRRP and their roles in throwing intellectual light on the many unsolved problems of mountain environments that are the essence of this volume.

The comparison between theatrical productions and scientific projects can be carried a bit further in that both require "angels." Confidence of theatrical sponsors is inspired by hopes of material gain, whereas in scientific research rewards are measured in the dividends of expanded knowledge and of maturity gained by experience. Faith in a concept finds expression in many ways. None is more welcome nor more effective than institutional sponsorship. The Icefield Ranges Research Project is fortunate in having two organizational parents, the Arctic Institute of North America and the American Geographical Society. Attainment of the project's objectives is encouraged in different ways by both institutions, by the Arctic Institute through its binational structure and its basic aim to advance the knowledge of polar and subpolar environments, and by the American Geographical Society through its long established position in the field of geographical research and publication. No more considerate parents could be imagined, and special gratitude must be expressed to the Arctic Institute for its dynamic response to the multitude of administrative and technical demands that inevitably punctuate the calendar of any major field undertaking.

Faith in the Icefield Ranges Research Project has come from many sources and, happily, with favorable balance between the federal and private sectors and also between Canada and the United States. For this confidence in project objectives, and especially in the men and women who have been its essence, grateful acknowledgement is made to the following institutions: the National Science Foundation (U.S.); the U.S. Army Research Office – Durham; the U.S. Army Terrestrial Sciences Center (formerly Cold Regions Research and Engineering Laboratory); the U.S. Army Natick Laboratories; the Department of Energy, Mines and Resources (Canada); and the National Research Council of Canada. From the independent community has come a variety of support as diverse in origin as the programs it has made possible. Not only have these financial sponsors had the vision of furthering a scientific quest for knowledge, but they also have placed their confidence in young men and women who have been able to work within the framework of IRRP chiefly because of this interest and assistance. Deep appreciation is hereby expressed to the National Geographic Society for a succession of grants in support of broad programs, and to the Research Corporation, the Alfred P. Sloan Foundation, the Louwana Fund,

Inc., The American Alpine Club, and The Explorers Club for the funding of individual undertakings. To Dr. Oshin Agathon, Allan Bemis, Dr. Richard B. Dominick, Dr. William O. Field, Henry S. Hall, Dr. Lowell Thomas, Sr., George R. Wallace, III and C. Thomas Clagett, Jr., goes our gratitude for spontaneous response to the general needs of the project.

We are indebted, also, to many persons and organizations in Yukon Territory for the numerous ways in which they have shown cordial cooperation. Our appreciation goes to all of them and especially to the Canadian Army and later the Department of Public Works, whose highway maintenance facilities assured the upkeep of our landing strip. And we are grateful, too, for the interest, the friendly cooperation, and the watchful eye of the Royal Canadian Mounted Police detachment at Haines Junction. Not least, we acknowledge the generosity of the Department of Indian Àffairs and Northern Development in granting the exclusive use of the land adjacent to the Kluane airstrip for the duration of the project's existence.

Finally, it is one of the rewards of the Project Director – a capacity in which I was pleased to serve from 1961 to 1968 – to single out those cornerstones of the IRRP structure whose qualities of leadership and inspiration have directed the field programs through their infancy and adolescence to full maturity, and who have inspired the more than three hundred people of IRRP by their wisdom and their dedication. On behalf of all of those who have come to know the St. Elias Mountains through the window of the Icefield Ranges Research Project, I extend gratitude and affection beyond expression to Richard H. Ragle, Robert C. Faylor, Philip Upton, and Melvin Marcus, who have made the dream a reality.

WALTER A. WOOD, *Chairman*
Icefield Ranges Research Project
Advisory Committee

Editors' Preface

During an informal Sunday morning session at Kluane Lake in the summer of 1967, senior investigators of the Icefield Ranges Research Project discussed how best to present, in an authoritative and scholarly manner, the results of the scientific efforts thus far completed. Within this setting, in the locale where much field work was being supported, many ideas were bandied about. As a result of this discussion and others since then, a series of volumes is to be published. They will include reports on all the research in the physical, biological, and social sciences emerging from IRRP's investigations of a total environment – an environment dominated by one of the largest snow- and ice-covered mountain ranges in the world, an area influenced by both marine and continental exposure. Thus, these volumes will reflect the multiformity of research and the variety of its treatment by both graduate students and postdoctoral investigators. The diversity of material is, I believe, understandable in an environmental study of so large and complex a region as the Icefield Ranges of the St. Elias Mountains.

Volume I is composed of long and short papers concerned with the physical sciences. Written by both graduate students and senior investigators, they reflect, individually and collectively, a synthesis of divergent interests, an interlacement of purposes important, indeed necessary, to every investigator no matter where he stands on the ladder of education and research. Much has been learned, but more remains to be studied; new questions have arisen as fast as old ones have been answered.

The reader, then, must consider this volume as the first product of an amalgam of efforts by student and scholar. Some of these papers are original contributions to this volume, some are graduate dissertations, some have been published in professional journals, and some have appeared in a university or institution report series. Each of the reports brought together between these covers makes a significant contribution in its own area and also contributes to the broad spectrum of technique and presentation that distinguishes IRRP research.

In using this volume, the observant reader who has seen some of the articles in their previously published forms will notice that the present versions differ in some respects from the original. The changes that have been made fall into three general categories: (1) matters of style, (2) omissions of, or changes in, illustrative material, and (3) condensation of lengthy reports.

Style changes include such things as revision of the format of reference lists, the manner in which the literature is cited in the body of the text, and the use and form of abbreviations. In most instances, names of the field camps and meteorological stations utilized throughout the research program have been changed when they differed from those of the map on the back cover of the present volume. The names "Yukon Territory" and "Canada" have been deleted from titles because the repetition of these names throughout a volume devoted to the same general region seemed unnecessary.

Location maps used with the original articles have been omitted when the map in the back of the present volume was thought to be an adequate substitute. In a few instances, photographs have been replaced either because the original is not available or because a somewhat better photo has become available. Several drawings that were originally presented as oversize plates have been modified to allow greater reduction, and in one instance, a small map has been redrafted for greater clarity.

Articles which originally appeared as Institute of Polar Studies Reports have been condensed chiefly by deleting parts of the text selected by the authors.

The maps in the back of this volume were drawn at the American Geographical Society according to specifications arrived at in consultation with Walter Wood.

VIVIAN C. BUSHNELL
RICHARD H. RAGLE

INTRODUCTION

The Icefield Ranges Research Project

*Walter A. Wood**

Birth of a Dream

The Icefield Ranges Research Project came into being as the outgrowth of the concept of studying a high, mountainous region in terms of its total environment. To the purist such an objective must appear impossible to accomplish if his interpretation foresees the mining of all basic knowledge that can be extracted from a selected region. Such, however, was not the intent. Rather, the total environment of a high mountain region was thought of as offering a broad spectrum of research opportunities in the earth and life sciences throughout a vertical range not afforded by less pronounced land forms of the earth's surface. Moreover, it is no longer necessary to be a practiced mountaineer to tackle this environment; man's ability to function in high mountain regions has been so enhanced by a variety of recently developed logistic tools that relatively inexperienced investigators can now work efficiently with a minimum of concern for their own well-being. Thus the multidisciplinary and interdisciplinary approach to environmental studies is encouraged.

The science of geography has been many things to many people, and geographers who live by definitions have found themselves to be widely at variance with their colleagues in their attempt to apply rigid boundaries of meaning to the word. This is neither the time nor the place to resolve or continue the debate. Rather, it is more useful to briefly state that the Icefield Ranges Research Project was conceived as a field exercise in scientific inquiry with geography playing the role of an integrator between the several scientific elements inherent in the environment under study.

From these basic considerations one fact was obvious: no broad approach to an understanding of the many facets of a high mountain region could be undertaken in a single season. The basic planning, then, had to assume the invalidity of the classic expeditionary approach and, in its place, substitute an organizational structure flexible as to duration, and adaptable to a variety of logistic requirements and investigative techniques. On these ideas depended the choice of the geographical area for study.

Early in the planning of the project, it was recognized that there was in the basic concept another potential, as rewarding as the realization of scientific dividends. If, indeed, such dividends were to be achieved, a major role would have to be played by assistants in support of principal investigators. Here, then, was an opportunity to expose new persons to high mountain environments, to train them to deal with the problems of living and working in those regions, and thus to contribute to a reserve of experience which will certainly be needed in the future development of boreal regions. Therefore, if junior participants were to be needed, why not offer these openings to graduate students seeking advanced degrees in disciplines represented in the natural laboratory? Thus would the interests of science be served and a double dividend of education be earned.

With education a companion of scientific inquiry, the maximum effort in the field would have to be scheduled to accommodate the academic calendar. Moreover, a wakeful eye would have to be focused on operating costs in order to make possible full participation by scientific aspirants. The watchword would have to be minimum cost to the project with maximum benefit to the investigator. Since time is said to be money, this factor loomed large in the selection of the study area and came to be fully equated with other qualifying conditions.

Goals of the Project

There is no such thing as the unique high mountain environment. High relief is the denominator common to all mountains; but beyond that characteristic, the mountain ranges of the earth differ among themselves as widely as do the peoples who inhabit our planet. Of what topographic expression, in what natural setting, were we thinking as the concept of IRRP emerged?

We in North America are, by and large, a people of dramatic perspective and enormous technical competence. At the same time, however, we are inclined not to heed our childhood training and clear our plates before we hurry on to dessert. For example, we scan and probe the secrets of the moon before we have more than a half knowledge of our own planet and, of current import, we propound the existence of ice in the surface layers of the moon and weigh its significance to space exploration before we have begun to truly assess the fresh water resource of terrestrial ice, or to explain the dynamics and mechanics of a surging glacier.

Prior to 1941, activity in North American glaciology was focused largely on an orderly approach to an understanding of the physical properties and behavior of

*American Geographical Society

temperate glaciers. Then came World War II and an intensified interest in far northern areas and in land and sea ice. The International Geophysical Year and its several outgrowths fully opened the door to glaciological opportunity, especially in Antarctica; and at this point the magnetism for the vast and the dramatic in our nature asserted itself, and we launched ourselves into scientific appraisal of enormous polar areas – most successfully and commendably. The only problem was that this concentration of scientific concern led to an unbalanced approach to glacier studies, for it diverted attention from temperate glaciers and the orderly progress attained before the International Geophysical Year. It seemed, then, that the target area for studies in a high mountain environment might well be one giving opportunity to restore the balance of interest within the field of glaciology, and with it to open the way to extended studies of the physical and biological processes associated with a glacierized and glaciated landscape.

The Chosen Locale

Once the basic character of the topography of a study area was defined, there remained the selection of a geographical site which would meet this definition and also qualify under the following criteria:

(1) Accessibility by the major air transportation networks of the continent and, if possible, by the highway complex
(2) Availability of a supply point with major air facilities and produce outlets
(3) A base of air-ground operations for project aircraft within short flying distances of the various study areas
(4) Topographic conditions favorable to the takeoff and landing of the aircraft at points within the study areas

Although a number of areas in North America satisfy these criteria to some degree, none, in 1961, appeared to offer advantages comparable with those of the Icefield Ranges of the St. Elias Mountains.

The St. Elias Mountains form a major element of the Pacific mountain systems of the North American cordillera between latitudes 59°N and 62°N and longitudes 137°W and 142°W. Rising as a high barrier between the Pacific Ocean and the continental interior, they comprise a number of roughly parallel ranges that form a shallow arc through nearly 300 mi. In width they span a distance of more than 100 mi. between the Gulf of Alaska and the Yukon plateau. The topography is that of a high alpine region and its major valleys are largely submerged beneath the most extensive mantle of snow and ice in continental North America. Bostock (1948, pp. 98-100), in his classic description of the St. Elias Mountains of Canada, subdivides them into a number of physiographic regions, and to the highest central core, little known at the time of his writing, he ascribed the name "Icefield Ranges." It was from this designation that the project took its name.

Mt. St. Elias is probably the most prominent physical feature ever to have played a central role in geographic discovery. Rising 18,000 ft. above the Gulf of Alaska, and barely 20 mi. from tidewater, it was the landfall of Vitus Bering's voyage of 1741 (Golder, 1922, p. 93). Its sighting by Lt. Waxel of Bering's ship *St. Peter* marked the first discovery of land at any point along the vast stretch of the Alaskan coastline between two widely separated limits of previous exploration: Cape Addington at latitude 55°N, and Cape Prince of Wales on the Bering Strait. Prominent as is Mt. St. Elias, it is but one of a galaxy of high summits that tower above Pacific waters and so dominate their lesser neighbors that they are visible from great distances on the Yukon plateau to the east. No fewer than 13 peaks of the St. Elias Mountains exceed 15,000 ft. in elevation, scores surpass 12,000 ft., and hundreds rear their crests above the 10,000-ft. contour. King of them all is Mt. Logan, 19,850 ft. high, second only, in North America, to Mt. McKinley and probably unchallenged among the mountains of the world for its massive stature. If Mt. Logan were to be truncated at the 15,000-ft. level, the resulting plateau would comfortably accommodate Manhattan Island. Vastness is a word that characterizes this great mountain landscape, and it applies no less to the glaciers than to the peaks themselves. Straddling the topographic divide between Yukon and Pacific drainages is a high (7,000 ft. – 9,000 ft.) level area of snow accumulation from which drain, in an almost starlike pattern, five of the longest glaciers on earth outside the polar regions. These are the Hubbard (75 mi.), flowing southward to the Pacific Ocean; the Walsh (60 mi.), flowing westward to the Chitina River of Alaska; the Donjek and Kluane (35 and 30 mi. respectively), flowing northeastward to the drainage of the Yukon River; and the Kaskawulsh (45 mi.), flowing eastward to both the Pacific and Yukon drainages. Across this "land of desolation," as it was described by members of the International Boundary Commission Survey (1918, p. 92) passes the frontier between the United States and Canada.

From the foregoing description it might be assumed that the St. Elias Mountains form a continuous physical barrier throughout their length. This is not true, for they are breached by the valley of the Alsek River, and the waters of Lake Dezadeash, deep in Yukon Territory, reach the Pacific Ocean through this trench. Wahrhaftig (1965, p. 41), in his delineation of the physiographic elements of Alaska, divides the St. Elias Mountains into two parts, the Icefield Ranges and associated physiographic elements to the north and west of the Alsek River, and the Fairweather Range to its south and east. To date, the programs of the Icefield Ranges Research Project have dealt exclusively with the former region.

There remains one major influence on the environment of the St. Elias Mountains to which reference must be made, for it was well recognized prior to the birth of the Icefield Ranges Research Project, and it played a major role in planning the operational phases of the project. This mountain belt is characterized by a wet-cold climate on the slopes that fringe the Gulf of Alaska, and by a dry-cold, even semi-arid climate in the continental interior. Records at Yakutat, Alaska, on the Pacific coast show that an annual precipitation of 125 in.

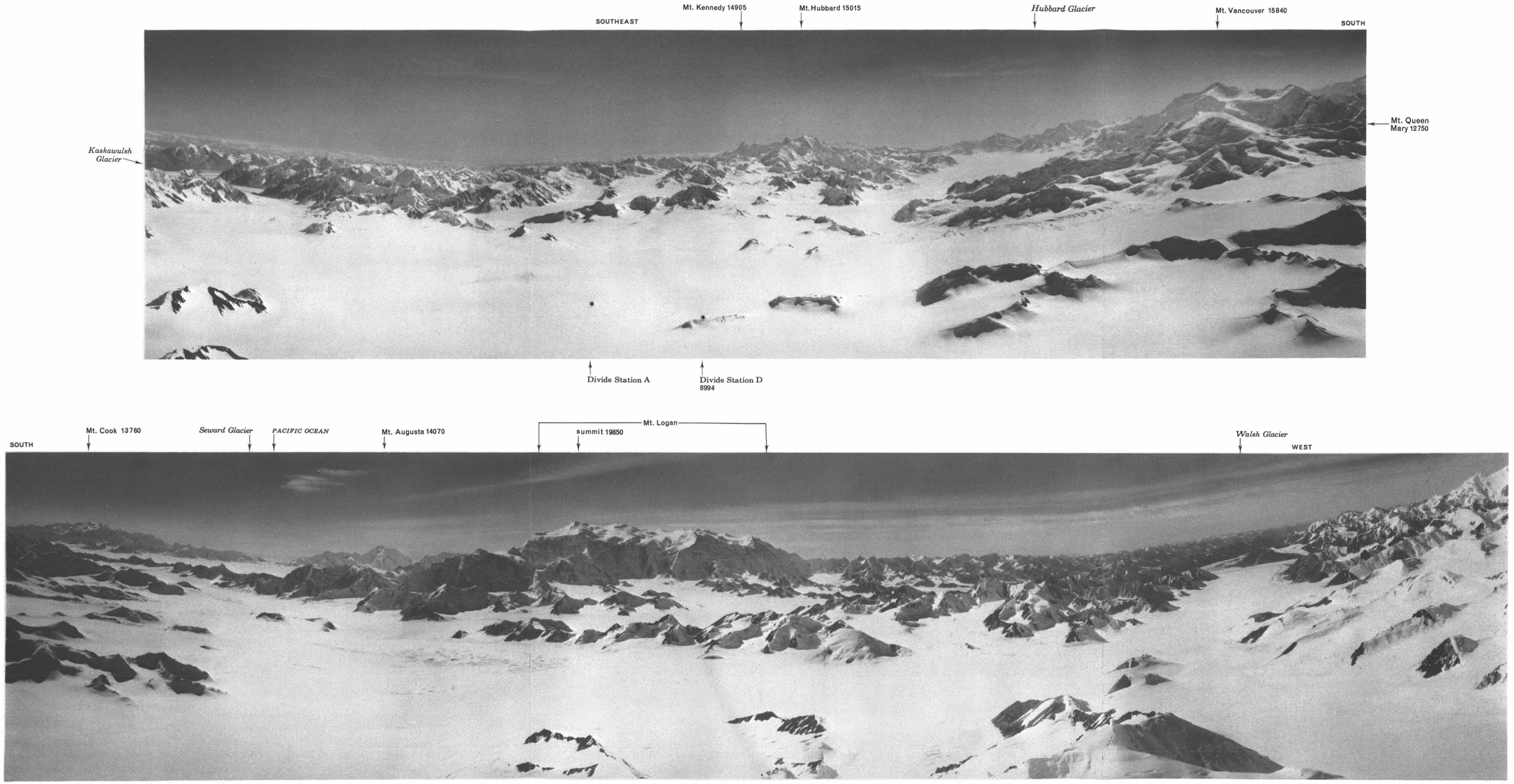

Fig. 1. Aerial panorama, central Icefield Ranges, St. Elias Mountains. *Upper panel:* accumulation area of north arm, Kaskawulsh Glacier (left); Kaskawulsh — Hubbard divide (center foreground). *Lower panel:* head snows of Hubbard Glacier (left foreground); Hubbard — Walsh divide (center). The top panel is made up of three overlapping photographs and the bottom one of four. In a panorama of this type, the horizon will not be a continuous straight line because the

Fig. 2. Mt. St. Elias from the south. The mountain, 18,008 ft. above sea level, rises 16,000 ft. above the Libbey Glacier in the foreground. Haydon Peak (11,945 ft.) is left of center. (August 2, 1949; 10:45; 5000 ft.)

Fig. 3. Barnard Glacier, St. Elias Mountains (61°10'N, 141°30'W). A classic example of a compound glacier trunk. View looking northeast with Mt. Natazhat (left) and Mt. Bear (right). (August 21, 1949; 11:15; 12,500 ft.)

is common there whereas, at Kluane, 110 mi. away at the foot of the eastern scarp of the mountains, precipitation probably does not average more than 15 in. a year. Such a contrast, when added to other opportunities presented by the high mountain environment, was challenging indeed, provided that a means of extracting the ore of knowledge could be devised and applied with efficiency and safety.

Logistical Planning

An ingredient essential to the recipe for successful field studies in remote areas is logistics, which includes the primary movement of all supplies, equipment, and personnel to the base of operations, and the support of all elements of the program within the study area. If this ingredient is lacking or is of inferior quality, the pudding will not gel, now matter how tasteful or potentially nutritious may be the other ingredients of the recipe. In undeveloped high mountain regions, overland access to scientific targets may be difficult and time consuming, particularly where auxiliary support in the form of human or animal transport is lacking or inapplicable. Since field seasons are short when geared to academic schedules, time is of the essence, and the means must be found to take full advantage of it. Moreover, steps must be taken to relieve the field investigators of logistic burdens and of as much of the housekeeping as possible. In the St. Elias Mountains, overland transport of important necessities is out of the question if the project is to be scientifically productive within the time span of the field season. Further, history has shown that no major objective has been reached in these ranges in the last thirty years without the use of air support (Wood, 1967). Therefore, in considering the St. Elias Mountains as a target for scientific field studies we immediately recognized that the solution to all logistic problems within the mountain complex must be found in airborne techniques. To make this possible a variety of other assets was necessary, and they were found in ample supply in the emerging development of southwestern Yukon Territory. Here the Alaska Highway fringes the northeastern flank of the St. Elias Mountains, providing a basic link with the transportation network of the North American heartland. In Whitehorse, the capital of Yukon Territory, we were assured of a major supply point, provisioned as it is by sea and rail via Skagway, Alaska, from continental outlets via the Alaska Highway, and by air through two major airlines. Moreover, Whitehorse is the hub of light aircraft operations in northwestern Canada and thus provides facilities for routine servicing and maintenance.

Some 140 mi. west of Whitehorse lies Kluane Lake, girdled on its south and west by the Alaska Highway. At its southern end was an abandoned airstrip, a relic of the Northwest Staging Route of World War II. Its gravel surface was in good condition and its 2500-ft. length was adequate for the needs of all types of light aircraft. Its proximity to the Alaska Highway assured regular mail and telephone service as well as the delivery of all housekeeping and equipment requirements. Finally, and most importantly, the semi-arid climate of Kluane Lake and, indeed, of the mountains adjacent to it, offered advantages to local air operations that found no counterpart in the marine environment of the North Pacific coast. This combination of assets made possible the transportation of project personnel, equipment, and subsistence to an operating base within the perimeter of the high mountains, afforded a major supply point amply capable of providing all but the most specialized project necessities, and offered the means of adding or replacing technical requirements from manufacturing sources with a minimum of delay. The airstrip at Mile 1054 of the Alaska Highway became, then, the focal point on which all planning was based, and since 1961 it has served as the operating headquarters for successive annual phases of the Icefield Ranges Research Project.

Selection and Testing of Equipment

When we had defined broad geographical objectives and theorized on field organization and logistics, it became time to put theory into practice, and the first consideration was the aircraft that would make our dreams a reality. Fortunately, by 1960 the air age had so advanced the design and performance characteristics of airplanes that it was no longer a question of adapting terrain to suit the best of a limited number of aircraft but rather one of selecting from a considerable range of aircraft types that plane whose characteristics would most effectively adapt to the topographic conditions and the logistic requirements.

The ideal aircraft for the predicted needs of the Icefield Ranges Research Project was one of rugged construction, high maneuverability at low flying speeds, slow landing and takeoff capability, optimum performance to 12,000 ft., and ease of maintenance in the field. A payload of 1000 lbs. was foreseen as adequate and the accommodation of ski-wheel landing gear was mandatory. Finally, low operating cost was an obvious necessity. From a number of light aircraft types, final selection fell on the Helio Courier, H391B, a single engine, highwing, Short Takeoff and Landing (STOL) airplane. The wisdom of this choice has been amply demonstrated in eight field seasons of IRRP during which more than 2500 hours of flying time have been logged.

Topographic texture is, of course, a major factor governing human mobility, but long association with the St. Elias Mountains had convinced me that, in the central highlands at least, the sweeping expanses of snow above the firn line offered an almost unlimited choice of aircraft landing sites and, from them, straightforward access to wide areas of scientific study. Thus, the effective formula for efficiently conducted scientific investigations would be one of establishing,

Fig. 4. Alaska Highway, airstrip and base of IRRP operations (lower center); Kluane Lake and Slims River valley (right). The St. Elias Mountains fringe the lake with the Icefield Ranges in the distance. (August 10, 1961; 15:30; 13,000 ft.)

by air, well selected and supplied hubs of research at and from which field programs could be carried out. With the airplane replacing the pack train as the primary means of establishing and supplying such operating bases, there remained a secondary logistic consideration, that of mobility within a localized area.

The dog team is the traditional mode of long distance travel over snow surfaces, and it has been used effectively in the St. Elias Mountains (Washburn, 1936); however, as a means of logistic support for scientific teams operating from key sites in the Icefield Ranges, dog power leaves much to be desired. Not the least of its disadvantages is the inexperience of modern day investigators who have little more than a romantically induced notion of dog driving or dog handling; the mental picture of untrained dog drivers attempting to cope with a confusion of traces, harnesses, sled, cargo, and snarling dogs was enough to turn us to other means of locomotion. We settled on motorized oversnow vehicles and, specifically, the Polaris Snow Traveler, Model B 57. Powered with a 5.75 horsepower gasoline engine that drives a longitudinal track, the Traveler was ideal for the job at hand. It was light in weight – 230 lbs. – and when uncoupled, a single vehicle could be accommodated in the Helio Courier aircraft. At a conservative operating speed of 5 mi./hr. on snow, it was found capable of towing a sled with a useful load of 250 lbs. and a man on skis. Thus it was possible for a team of two men or more to travel freely within a given study area and return to camp at the end of each day with a minimum of effort on the parts of the driver and passengers. The use of these vehicles obviated the need for outlying camps; the saving in equipment, both in weight and cost, fully justified our dependence on them. During the first IRRP field season in 1961, two Snow Travelers logged a total of 250 mi., completely trouble free.

There will be come who will feel that I have taken

too cavalier an attitude in dismissing the dog team from our plans. For them, let me provide a little fuel for their argument – and for their pride in a vanishing hallmark of exploration. We were fully aware that travel over glacier surfaces, however gentle the slope, is not free of danger, and we speculated on the ability of a man on skis to apply a successful rope belay on a driver, should the vehicle break through the bridge of a crevasse. In 1961 our pilot, fully acquainted with the behavior of skis through his experience with our aircraft, insisted that he could apply a rope belay to the driver of a Snow Traveler. It was a little too much to risk a vehicle, or a driver, in a real crevasse, so it was arranged that, at an unknown moment, the pilot, on skis, would apply a sudden rope belay on the surveyor of the project, who would be driving the Snow Traveler. The test took place at a camp on the Pacific – Yukon watershed, before an audience divided in its opinions on the outcome. When all was ready, our pilot, on skis and loosely belaying our surveyor in the driver's seat, was towed at cruising speed past the witnesses. Abruptly, the skier swung into a sharp turn, plunged his ice axe into the snow and secured the surveyor who, as the rope came taut, sailed upward and backward into space. The only hitch came when the surveyor in midair accidentally kicked the throttle of the vehicle into the wide open position. Free of all encumbrances, the Snow Traveler leaped forward and headed for the horizon some five miles away. By ironic coincidence the only obstacle in its path was the tent of the principal investigators of the experiment. Through its walls rammed the run-away, tearing a large rent as it did so. Once inside it chewed its way across two sleeping bags, collapsed the center pole, and came to a vibrating halt in a tangle of shredded clothing, feathers and canvas. No dog team would or could have created such havoc with so little provocation!

The final link in the organization of such a project as IRRP is radio communications. Not only is such contact a morale factor in the daily lives of isolated groups, but it is a necessity to certain elements of the project programs. Mention has been made of the effect of a high mountain barrier on the climate of a region. Better to understand this effect we incorporated meteorological and climatological studies in the basic framework of IRRP. Synoptic weather data from the St. Elias Mountains was totally lacking in 1961, and such information was of interest to the forecasting officers of the Meteorological Service of Canada in Whitehorse. To be meaningful to forecasters this information must be timely, and to achieve it, radio transmission of weather data on a regular and reliable basis was mandatory. But the most important role of communication was that of the safety of all members of the field parties, and leading the list of priorities was the well-being of our aircraft in flight. It was imperative, therefore, that rigid flight procedures be established, and these depended on reliable communications between surface units of the project and the aircraft. Without going into the technicalities involved, it is sufficient to state that the communications network of IRRP functioned, with some minor problems at the outset. But as we gained experience in matters of favorable operating frequencies, power needs, and the vagaries of radio blackouts, our communications lacunae have approached the vanishing point, especially in the air–ground phase of the network.

High mountain flying is a specialized chapter of bush aviation. Mountain pilots are not born, they are made; and their survival and maturity result not only from skill in handling and maintaining aircraft, but from observation, interpretation and experience of the behavior of the atmosphere in its contact with the terrain. Pilots are human and so are the manufacturers of aircraft. This being so, the possibility of error or mechanical malfunction is ever present and, on a project such as IRRP, the consequences of emergencies are more serious than in general aviation for not only is the well being of pilot and passengers at stake but also that of all personnel in the field, who depend on aircraft for their daily needs. IRRP well recognizes these risks, and its response to them is to reduce to an absolute minimum the consequences of an emergency. Accordingly, a rigid set of procedures has been established and is in force whenever the Helio Courier is in the air. Not the least of these procedures are the filing of flight plans with the IRRP flight controller and the reporting by radio of the plane's three dimensional coordinates at 10-minute intervals. These are recorded and plotted on a gridded map. Should an emergency arise, and with it a break in communications, search and rescue operations would be set in motion immediately. We have never had to exercise the latter, but on two occasions in eight field seasons, engine failure has occasioned forced landings. In both instances the pilot's report was monitored by at least two radio stations of the project network, and in each case the crippled plane was reached and the occupants evacuated in less than two hours.

The Dream's Fulfillment

It was with the broad scientific and educational objectives and within the framework of the geographical and organizational planning described above, that IRRP went into the field in 1961. The first season was largely devoted to geographical reconnaissance and to testing of the operational concepts developed during the planning stage. It is pleasant to recall that the various logistical considerations were integrated with a rewarding degree of success.

Any head of a family knows full well that a new domestic environment is frought with surprises. The oven is inclined to overdo or undercook until its idiosyncrasies are understood; the heating may not produce the desired climate until the thermostats have

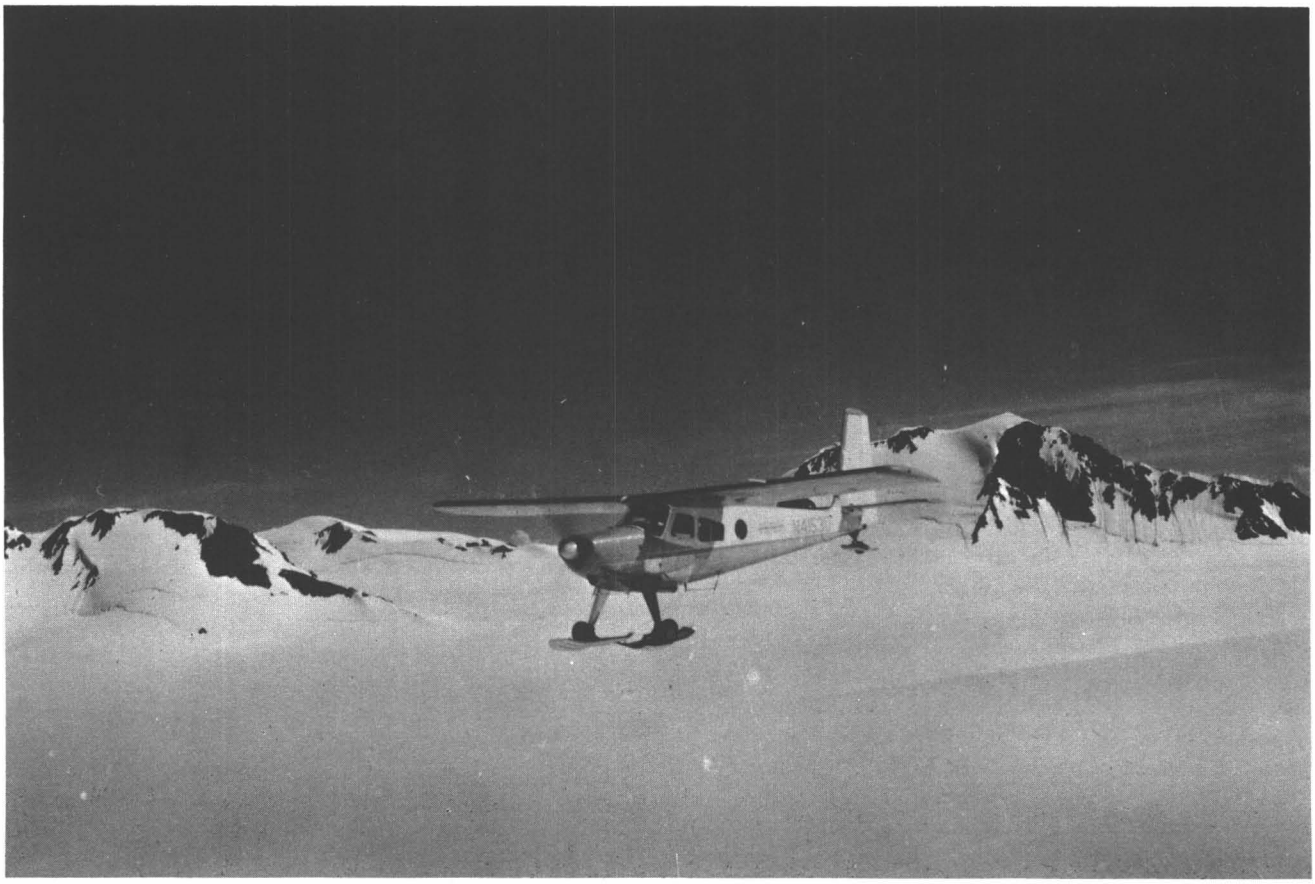

Fig. 5. Helio Courier aircraft in flight over the Hubbard – Kaskawulsh divide. Plane is flying at 10,000 ft.; elevation of snowfield in foreground, 8500 ft. (August 4, 1962; 08:30; 10,000 ft.). Reprinted from the *Geographical Review,* Vol. 53, 1963, copyrighted by the American Geographical Society.

been adjusted; the house will creak and groan until it settles into structural comfort. But, basically, the judgment that led to domesticity was sound. And so it was with IRRP. Our base establishment beside the abandoned airstrip in Kluane Lake proved quite adequate for our initial needs and comforts. The Helio Courier aircraft, equipped with unaccustomed ski-wheels, began probing the high mountain skies to bring topographical familiarity to its pilots. Despite an obvious distaste for deep snow, which required modification and realignment of its skis, the plane rapidly demonstrated the benefits we had sought. N4153D, and later her younger companion, 4166D, showed that they had the capability to operate with safety through a broader spectrum of conditions than we had hoped for, and in 1961, our two pilots, Richard Ragle and Philip Upton, initiated a sequence of air operations that have opened wide the doors to scientific opportunity, and is unsurpassed anywhere in the mountain world. Through 1968 this record included more than 2500 flying hours, and for each hour flown, a landing and takeoff have been made on and from unprepared surfaces away from the project's operating base. These surfaces have ranged in texture from the powder of broad unobstructed snowfields to the unsorted gravels of outwash plains in narrow valleys. In elevation, field parties have been supported from the 2500-ft. level of Kluane Lake to 17,500 ft. on the roof of Mt. Logan. In compiling this record, the judgment and skill of the pilots and the reliability of the aircraft have been such that, weather permitting, no member of the project has had to be more than a few minutes late for a meal because of air-transportation problems.

It has sometimes been implied that too much emphasis is placed upon logistics, and the facilities and aids that make field investigations possible. Or perhaps the point of view has been expressed that these aspects of field research should be taken for granted or at least subordinated to the task at hand, the gleaning of basic knowledge. With the first point of view I most emphatically disagree, while with the latter, there can be no argument provided the backup that makes field work possible has been fully thought out beforehand. In the environmental sciences we are dealing with nature as she expresses herself and, of course, this is true also of some of the facets of science that can be studied in institutional laboratories. Few would argue

that there is over-emphasis on the structures and research tools that make possible scientific progress within the research laboratories of our academic community. The St. Elias Mountains can be thought of as a laboratory, as a natural theater of investigation, and we of the Arctic Institute of North America and the American Geographical Society have cast ourselves in the role of creators of scientific opportunity. We have furnished access to high mountain fastnesses, arranged for environmental protection, and provided, by our project philosophy, a stimulus to learn in an intrascientific community. That there is a interest in the use of this natural laboratory has been amply demonstrated by the more than 300 men and women who are the IRRP faculty and alumni. The reports of this first volume and of volumes to come represent, in a concrete and useful way, the realization of our hopes for IRRP.

References

Bostock, H.S. (1948) Physiography of the Canadian cordillera, with special reference to the area north of the 55th parallel, CANADA GEOL. SURV. MEM. NO. 247.

Golder, F.A. (1922) BERING'S VOYAGES, Vol. 1, AM. GEOGR. SOC., RES. SER., No. 1, 371 pp.

International Boundary Commission (1918) Establishment of the boundary between the United States and Canada, Arctic Ocean to Mount St. Elias, U.S. Dept. State, Washington, 305 pp.

Wahrhaftig, C. (1965) Physiographic divisions of Alaska, U.S. GEOL. SURV. PROF. PAPER 482, 52 pp.

Washburn, B. (1936) Exploring Yukon's glacial stronghold, NAT. GEOGR. MAG., 169, 715 – 748.

Wood, W.A. (1967) A HISTORY OF MOUNTAINEERING IN THE ST. ELIAS MOUNTAINS, Yukon Alpine Centennial Expedition, Scarborough, Ontario, Canada, 45 pp.

PAPERS IN THE PHYSICAL SCIENCES

Exploration Meteorology in the St. Elias Mountains*

James M. Havens† *and David E. Saarela*‡

During the summer of 1963 the IRRP meteorology program was supported by the Earth Sciences Division, U.S. Army Natick Laboratories, Natick, Massachusetts, U.S.A., whose mission includes the geophysical exploration of remote areas for military and basic scientific needs. This preliminary report outlines the program and summarizes some of the general results.

The purpose of the weather program was two-fold: to gather general data in a relatively unknown and remote area for climatological purposes, and to undertake observations that would permit estimates of the heat balance at the snow surface in an accumulation area, both by direct measurement (radiation) and by indirect calculation (eddy heat flux).

The Stations and Their Instrumentation

The locations of the stations established in the region are shown on the map inside the back cover of this volume. They are: Divide Station B[1], the main meteorological station at 8660 ft (2640 m) above msl in the area of the ice-divide between the Hubbard and Kaskawulsh Glaciers; a secondary station at the project's base camp near the south shore of Kluane Lake, 2580 ft (787 m); and two support hygrothermograph stations, Divide Station A, the project's research station at 8488 ft (2587 m) in the area's main snowfield, two miles from Divide Station B, and Terminus Station, about 2660 ft (914 m) near the terminus of Kaskawulsh Glacier. In the area of Divide Station B (Figure 1) the snow and ice thickness was found to be of the order of 1700 ft (520 m), while maximum thicknesses of the upper Kaskawulsh Glacier exceeded 2700 ft (826 m) (G.K.C. Clarke, personal communication).

The graphic representation of the individual weather elements at Divide Station B (Figure 2), and the statistical summaries (Tables 1 and 2) indicate the general weather elements observed during the 65-day observation period. In addition, air temperatures at various levels were measured by thermocouples, and measurements of incoming and reflected short-wave radiation (Eppley pyrheliometers) and net radiation flux (Beckman and Whitley radiometer) were made during most of the period. At Base Station synoptic observations were taken twice daily, at 0900 and 2100 Yukon Standard Time (1800 and 0600 GMT). Figure 2 and Tables 1 and 2 have been designed for direct comparison with similar data collected on the main ice cap of Axel Heiberg Island, N.W.T., Canada, and reported in the June 1962 issue of *Weather*. The tabulated statistics can also be compared with other Arctic and Subarctic expedition results in this journal (for example, Orvig, 1955; Lotz and Sagar, 1960).

The Weather During the 1963 Season

The nearest permanent weather station to the area of investigation is at the Haines Junction Experimental Farm, 30 miles southeast of Kluane Lake, where climatological observations have been maintained by the Canadian Department of Agriculture since 1945. At this station the summer of 1963 was 1.2°F warmer than normal with temperatures during August running about 4°F above the long-term average. At Whitehorse, about 150 miles to the east, record high August temperatures were recorded on the 13th, 14th, 24th, and 25th. The season's maximum temperature was experienced on the 24th, a day after the record had terminated at Divide Station B. This late season warmth prolonged the melt-season in the accumulation area of the Icefield Ranges long beyond most previous years. The daily rate of snow-surface lowering toward the end of the season at Divide Station B averaged 2 to 3 cm.

Precipitation was near normal at Haines Junction during June and July but above normal at Yakutat, on the Alaska Coast. During August, areas both east and west of the St. Elias Mountains received less than normal rainfall, with Haines Junction recording only about one-tenth the usual amount. The accumulation area of the Icefield Ranges showed a net snow loss during the 1963 melt-season, although the annual snow accumulation in the area is of the order of 12 ft (4 m). The mean height of the snow surface, detailed in Figure 3, is particularly instructive in showing the increasing separation of individual stake readings during the course of the summer and

*This article originally appeared in *Weather, 1964,* Vol. 19, pp 342-352 and is reproduced here with permission; for a complete report, see Havens (1968).

†U.S. Army Natick Laboratories, Natick, Massachusetts at the time of writing, now at the University of Western Ontario, London, Canada.

‡U.S. Marine Corps, at the time of writing.

[1] Station names have been changed for this volume to conform to Plate 1 inside the back cover of this volume (see also explanation in table accompanying Plate 1).

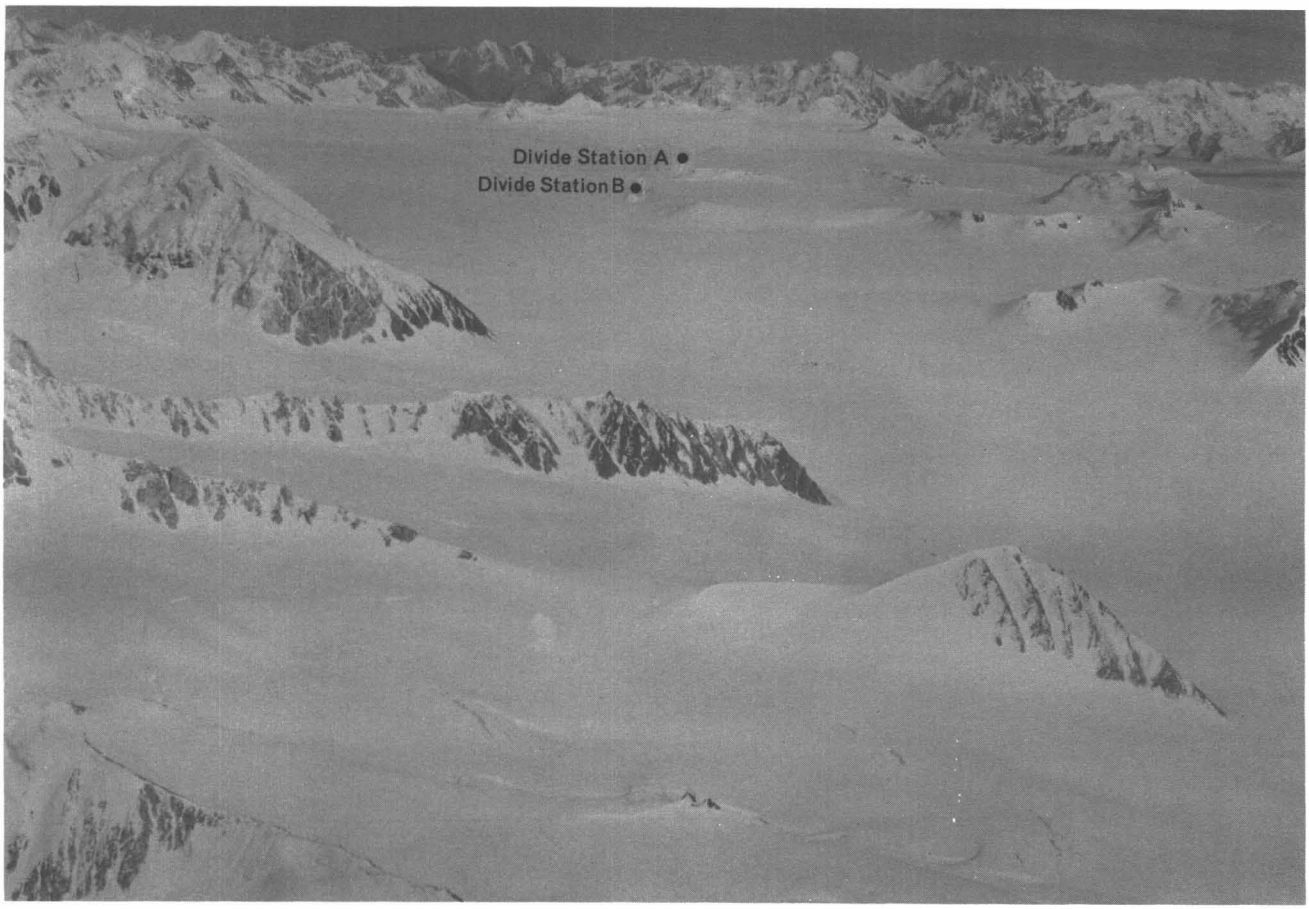

Photograph by W. A. Wood

Fig. 1. Area of ice-divide between Kaskawulsh Glacier (upper left) and Hubbard Glacier (lower right), Icefield Ranges, St. Elias Mountains.

thereby emphasizing the unrepresentativeness of readings made on a single stake. An attempt was made to measure individual snowfalls but this was impossible during falls accompanied by wind. The amounts graphed in Figure 3 should be regarded as estimates only. Raingauge collections usually included both rain and melted snow and the indicated daily rain and snow totals are, therefore, not necessarily mutually exclusive.

Depressions, crossing the area from the Gulf of Alaska, were mainly responsible for the precipitation that occurred in the area of the ice divide; isolated snow showers were rare, although convective instability, as indicated by cumulus congestus and cumulonimbus activity, was often observed to the east, over the bare ground of the Shakwak Trench.

An unusual aspect of the weather at Divide Station B was the low wind speed normally experienced there, when compared with the gradient speed indicated on the 700 mb chart. The highly irregular surface in the vicinity of the station (Figure 1) was especially effective in 'breaking' the air flow over the station.

A Note on Temperature Error

A few words are necessary to account for the high maximum temperatures at Divide Station B, listed in Table 1. These occurred during periods of strong insolation and light wind which resulted in warming of the air in the instrument screen. The screen was not mechanically ventilated. In order to obtain some idea of the magnitude and importance of this error, mean daily temperatures for July were calculated from the mean of the daily maximum temperatures indicated by (1) the maximum thermometer, (2) the daily maximum from the thermograph trace, and (3) the maximum of the 12 bi-hourly temperatures per day. The mean daily minimum temperature used with each of these three mean maxima was the minimum thermometer value.

It can be seen in Table 3 that the highest July mean is that temperature calculated using the maximum thermometer readings, next highest that registered by the thermograph, with its greater time lag, and lowest that obtained from the bi-hourly readings which were sometimes made between periods of strong heating. Until the available ther-

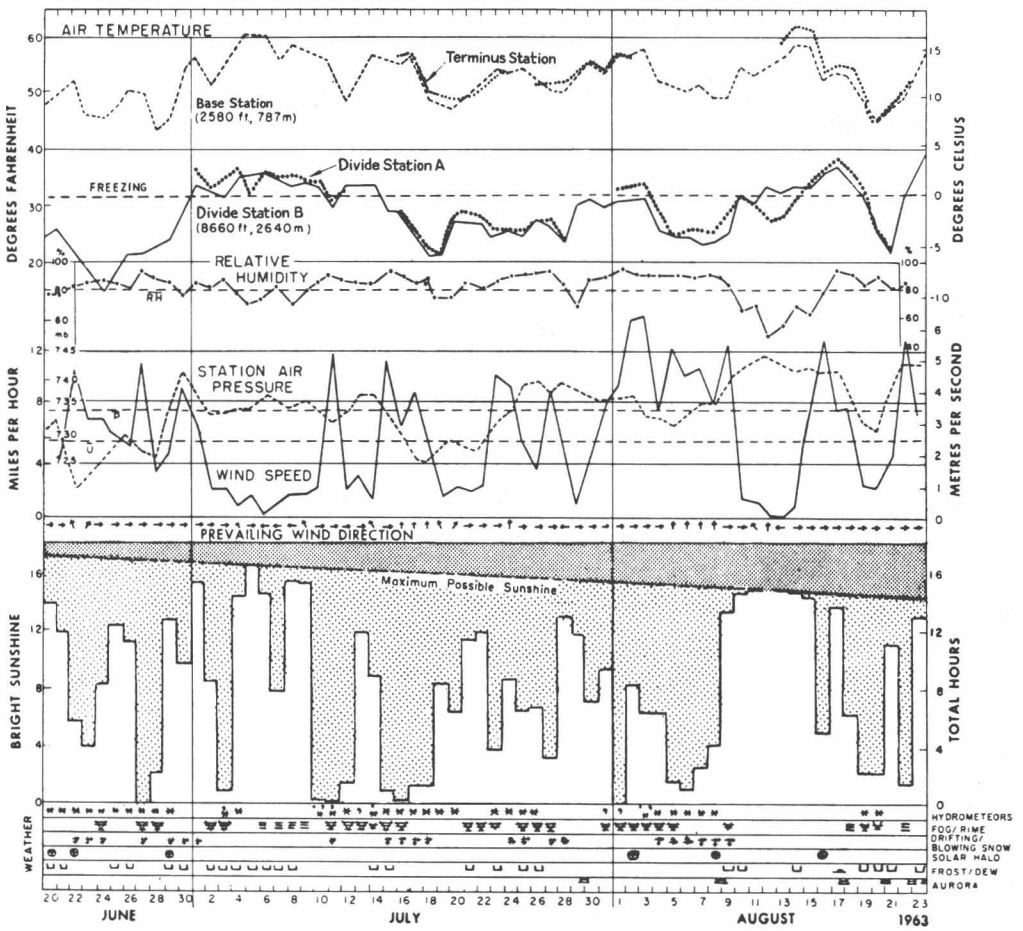

Fig. 2. Course of the weather elements at Divide Station B during the summer of 1963.

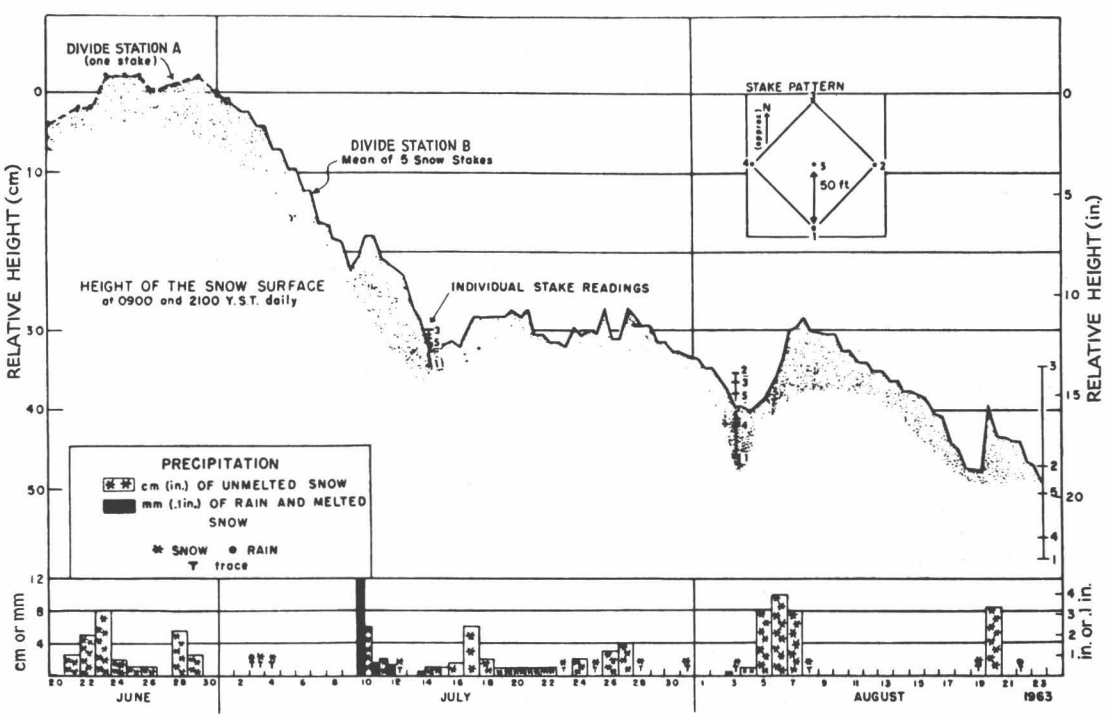

Fig. 3. Relative height of the snow surface and daily precipitation at Divide Station B, 1963.

mocouple data have been reduced by machine methods and are available for comparison, it can provisionally be concluded that the mean daily temperature for the month of July, as given in Table 1, is at least 2°F higher than the true air temperature. Since the bi-hourly readings were also affected by the heating to some extent, this estimate should be regarded as a minimum. The only comforting thought in this connection is that temperatures reported by most expeditions have not been made in mechanically ventilated screens. The temperatures reported here are, therefore, comparable, under similar wind and insolation conditions.

Some Regional Temperature and Precipitation Comparisons

Hourly data at Base Station have been compared with bi-hourly data at Divide Station B and a mean environmental lapse rate of 3.96°F/1000 ft (0.72° C/100m) is indicated for the eastern slope of the St. Elias Mountains during the summer. This lapse rate exhibits a marked diurnal variation, from 3.27°F/1000 ft at 0500 YST to 4.82°F/1000 ft at 1700 YST. Between Divide Station and Yakutat, on the Alaska coast, the over-all environment lapse rate for a comparable period is only 2.98°F/1000 ft (0.54°C/100 m), a value of rather uncertain significance because of the horizontal distance between the two stations, over 75 miles. This lower rate undoubtedly reflects both the more moist air mass on the western slope and the cooling effect of the waters of the Gulf of Alaska on Yakutat's summer temperatures.

If a zone of maximum precipitation exists in the vertical on the windward side of the St. Elias Mountains during the summer it would lie between Yakutat and Divide Station, for the former received 21.48 in. (546 mm) of rain during the period 20 June to 23 August while the project's station recorded only about 4 in. (100 mm) water equivalent. This rough estimate is slightly higher than rainfall totals reported at several other Yukon stations (e.g., Base Station, 2.43 in.; Whitehorse, 3.11 in.). The average annual precipitation in the divide area of the Icefield Ranges has been estimated from snow pits to be at least 71 in. (1800 mm).

The Solar Eclipse of July 20, 1963

Although the project was not equipped for special observations, the effect of the solar eclipse of 20 July, which was total across a large part of North America, was registered by the autographic temperature and radiation records. At Divide Station B, where the maximum coverage of the sun's diameter was about 96 percent at 1113 YST, the eclipse was viewed through a thin layer of stratocumulus. The symmetrical depression of the

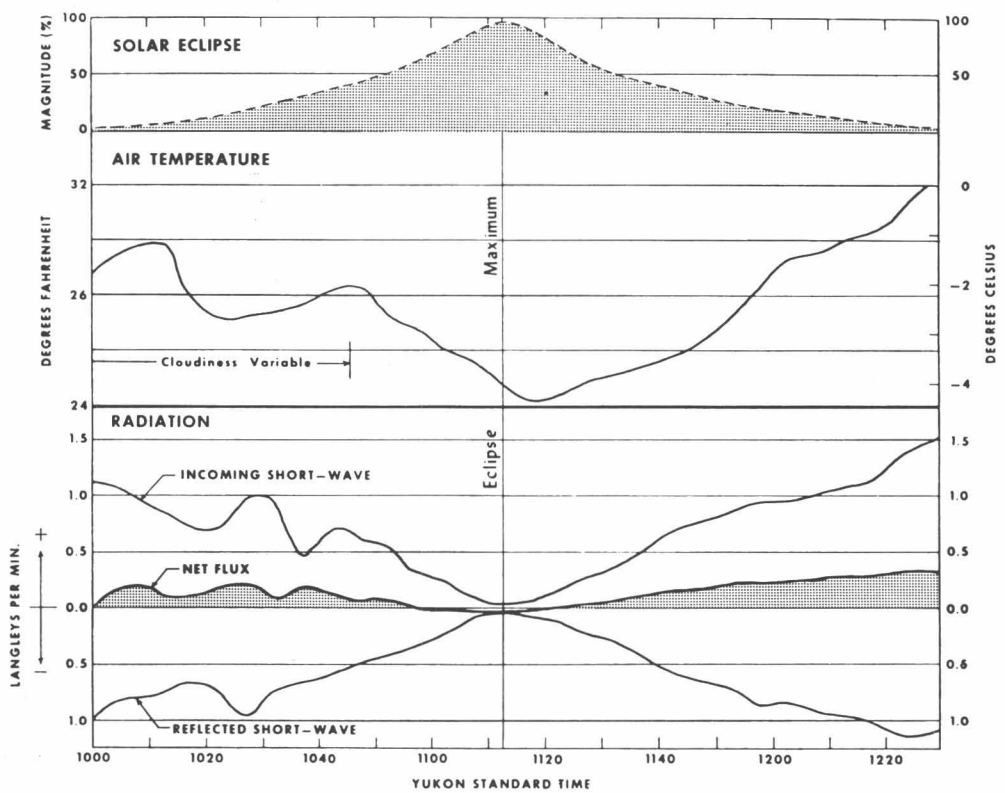

Fig. 4. Fluctuations of air temperature and radiation at Divide Station B during solar eclipse of 20 July 1963.

TABLE 1. Extracts from the Climatological Record at Divide Station B (60° 46'N, 139° 39'W, 2640 m Above msl), 1963

	July		August (1-23)		Entire Observation Period of 65 days (20 Jun – 23 Aug 1963)	
SHELTER AIR TEMPERATURE (F, 150 cm)						
Highest maximum	*51.7*	*(5)**	*51.8*	*(12)*	*51.8*	*(12 Aug)*
Mean daily maximum	*39.4*		*37.3*		*37.3*	
Mean daily	*30.6*		*29.8*		*28.8*	
Mean daily minimum	*21.7*		*22.2*		*20.3*	
Lowest minimum	*2.6*	*(19)*	*3.8*	*(21)*	*2.6*	*(19 Jul)*
SHELTER RELATIVE HUMIDITY (percent, with respect to water)						
Highest hourly	*100*	*(several)*	*100*	*(several)*	*100*	*(several)*
Mean daily	*83.6*		*81.4*		*82.8*	
Lowest hourly	*37*	*(29)*	*29*	*(12)*	*29*	*(12 Aug)*
WIND (mph, 200 cm)						
Highest bi-hourly	*20*	*(24)*	*25*	*(5)*	*25*	*(5 Aug)*
Mean daily	*4.4*		*7.2*		*5.7*	
Prevailing direction	*W*		*W*		*W*	
BRIGHT SUNSHINE						
Total no. hours	*247.7*		*190.2*		*532.2*	
Mean daily hours	*8.0*		*8.3*		*8.2*	
Percent of possible	*48.5%*		*54.4%*		*50.7%*	
SKY COVER (tenths)	*6.8*		*6.1*		*6.6*	
NET LOWERING OF SNOW SURFACE (cm of snow)	*33.2*		*16.1*		*49.3 (1 July-23 Aug)*	

*(Date)

TABLE 2. Percentage of Bi-Hourly Observations, and Number of Days on Which Precipitation, Fog, Rime, and Drifting and Blowing Snow Occurred at Divide Station B, 1963

	July	August (1-23)	Entire Observation Period of 65 days (20 Jun – 23 Aug 1963)
Frozen hydrometers	24%, 18 days	19%, 8 days	24%, 36 days
Liquid hydrometers	3%, 7 days	3%, 2 days	3%, 9 days
Precipitation (all forms)	26%, 21 days	22%, 8 days	26%, 39 days
Fog	13%, 19 days	14%, 10 days	13%, 32 days
Rime	11%, 17 days	8%, 9 days	10%, 29 days
Drifting snow ($h < 2$ m)	11%, 11 days	14%, 6 days	14%, 23 days
Blowing snow ($h > 2$ m)	1%, 2 days	2%, 2 days	1%, 4 days
Drifting and blowing snow	12%, 11 days	16%, 6 days	15%, 23 days

TABLE 3. Calculated Mean Temperatures (°F) Registered in the Instrument Screen, Which Was Not Mechanically Ventilated, at Divide Station B, July 1963

Instrument	Mean daily maximum	Mean daily minimum (min. thermometer)	Mean daily
Maximum thermometer	39.4	21.7	30.6
Thermograph	38.1	21.7	29.9
Bi-hourly readings on min. thermometer	36.0	21.7	28.8

air temperature and radiation curves during the period of the eclipse, approximately 0957 to 1229 YST, is illustrated in Figure 4.

Other Scientific Work

A total of 21 expedition members were in the field for varying lengths of time during the 1963 season. Of these, 17 conducted or assisted the individual scientific program. In the accumulation area the field investigations were centered around the subject of glaciology. They included mass movement measurements by triangulation, snow stratigraphy and diagenesis, and a geophysical study of snow/ice thickness by seismic and gravity methods. Near the terminus of the Kaskawulsh Glacier and in the Kluane area of the Shakwak Trench glacial-geological field work was mainly directed toward determination of the Pleistocene glacial sequence in the area.

Transport between the base camp and the various field parties was carried out by a Helio Courier (H391B) aircraft equipped with retractable skis. On the high-altitude snow fields two types of motor toboggans helped greatly to expedite the field work.

Acknowledgments

Sunshine recorders were generously lent to IRRP by the Department of Transport, Canada. The other instruments used were prepared for field use by Dr. Paul C. Dalrymple, Earth Sciences Division, U.S. Army Natick Laboratories, who also outlined the program that was followed, in consultation with Dr. Svenn Orvig, McGill University, a member of the project's advisory committee. The observations would have been more limited without the help of Mr. W. Philip Wagner (Divide Station), Mr. Richard Bonnett (Terminus Station), and especially Mrs. Philip Upton, who maintained the observations at Base Station.

References

Havens, J. M. (1968) METEOROLOGY 1963, ICEFIELD RANGES RESEARCH PROJECT, ST. ELIAS MOUNTAINS, YUKON TERRITORY, CANADA, 133 pp. (privately printed).

Lotz, J.R. and Sagar, R. B. (1960) Meteorological work in northern Ellesmere Island, 1957 – 60, WEATHER, 15, 397 – 406.

Orvig, S. (1955) Meteorological work in Baffin Island WEATHER, 10, 72 – 77.

Wood, W. A. (1963) The Icefield Ranges Research Project, GEOGR. REV., 53, 163 – 184.

Summer Temperature Relationships Along a Transect in the St. Elias Mountains*

Melvin G. Marcus†

ABSTRACT. During the summer of 1964, temperature readings were taken at a series of weather stations operated across the St. Elias Mountains as part of a program to establish a climatic profile from the Pacific littoral across a major topographic barrier to the continental interior. Comparisons of local temperatures were made in two areas: (1) on the Seward Glacier where one station was operated on a nunatak (6100 ft.) and another on the glacier surface (5800 ft.), and (2) at the divide of the Hubbard and Kaskawulsh Glaciers where one station was maintained on the glacier surface (8650 ft.) and two stations were located on rock ridges (8774 and 8994 ft.). Surface weather observations for 1963 and 1964 in the St. Elias Mountains were compared to radiosonde date for equivalent elevations over Whitehorse, Yukon and Yakutat, Alaska.

In both localities, the full diurnal temperature regime is lower for the glacier surface stations under clear weather conditions; this is most significant at night. At the divide, the inversion appears primarily as a result of surface cooling, while in the Seward Glacier basin, a combination of surface cooling and cold air flow appears to be responsible. Under heavy cloud cover, divide area temperatures equalize, but on the Seward, the inversion is maintained by cold air ponding.

Summer temperatures across the St. Elias Mountains reveal the great diversity that is expected in an area of high relief and varied surface characteristics. This diversity is principally a response in the boundary layer and tends to disappear at higher altitudes. Because investigators are interested in two kinds of problems — those in glacio-climatology and those in regional climatology — designation of observational sites and selection of data in the context of research objectives become critical considerations. This is clearly indicated for the St. Elias region by the comparisons of temperatures measured (1) on a trans-mountain profile, (2) at stations in the same locality, but on different surfaces, and (3) from radiosonde soundings.

Introduction

In the past three decades, few research projects involving glaciological and related research have operated without maintaining associated meteorological stations. The quality of such operations has varied from jury-rigged measurements of temperature and precipitation through the equivalent of Cooperative Weather Bureau Stations, to carefully regulated First Order Stations. Although there are many purposes to which the collected data may be put, its intended use has generally fallen into the following four categories: (1) the collection of weather data for use in regional and synoptic climatologies, (2) the analysis of mesometeorological information related to glacier regimen and behavior, (3) the evaluation of localized interactions of weather elements at the snow or ice interface, or (4) some combination of the above approaches. For each of these objectives, expeditions have achieved varying degrees of success — a reflection, in large measure, of the limitations and distortions imposed by local glacier environments.

In no case is this more apparent than in the measurement of temperature. Temperature data recorded in glacier environments must be utilized and interpreted with caution, particularly when the observations are made at sites directly over snow or ice surfaces. Depending on local wind patterns, topography, and surface characteristics, such temperature readings may be seriously misleading if taken for purposes of climatic or mesometeorological analysis; the same data may, however, be a useful indicator of thermal conditions at or near the glacier–atmosphere interface. Conversely, readings taken on nunataks or ridges adjacent to glaciers may be meaningful for synoptic purposes but significantly misleading in terms of the glacier interface. Thus, consideration of temperature observations in their environmental context is critical to interpretations in climatology and glacio-climatology.

Although field investigators may wish to bypass the problem by maintaining associated weather stations over both glacier and rock surfaces, these difficulties cannot always be avoided. For example, if an expedition's principal research is oriented to a camp near the longitudinal axis of a wide valley or piedmont glacier, the weather station usually will be located at the same site. No observations will be made on the distant rock surfaces above the glacier unless a most favorable conjunction of time, equipment, financial support, and incentive occurs. On an ice cap, there is not even the opportunity for comparative readings. The situation is, of course, often reversed. Investigators oriented to camps along glacier margins seldom have the equipment or time necessary to maintain extra weather stations well out on the ice or snow.

In the summer of 1964, as part of the climatology program of the Icefield Ranges Research Project, an effort was made to reduce such discrepancies in the meteorological record, particularly for temperature data.

*This report has previously appeared in *Man and the Earth, University of Colorado Studies, Series in Earth Sciences, 1965, No. 3,* Univ. Colorado Press, Boulder, pp. 15 — 30.

†Chairman, Department of Geography, University of Michigan, Ann Arbor.

Temperature observations were made at a series of weather stations operated across the St. Elias Mountains (Plate 1; Plate 2)[1] as part of a larger program to establish a climatic profile from the Pacific littoral across a major topographic barrier to the continental interior. This program was a continuation and amplification of previous efforts to establish a summer meteorological network in the region. During the summer field seasons of 1961 and 1962, before a climatology team was part of the project, field personnel carried out reconnaissance weather observations. In 1963, a regular meteorology program was initiated with two manned stations, one at Lake Kluane and another near the topographic divide of the Kaskawulsh and Hubbard Glaciers. An automatic station was operated on the terminal moraine of the Kaskawulsh Glacier (Havens and Saarela, 1964, and pp. 17 – 22 of this volume).

1964 Meteorology and Climatology Program

Summer meteorological observations for 1964 were made at four manned and four automatic stations. Their locations are shown in Plate 1; the grid locations, periods of record, and surface characteristics of the stations are given in Tables 1A and 1B. Three government stations, Whitehorse and Haines Junction Agricultural Station in the Yukon, and Yakutat in Alaska, were also considered part of the network since records for these stations are utilized in the climatic analysis of the St. Elias region. Information for these stations is provided in Table 1C.

The general scheme of station locations corresponds to a profile traverse of the St. Elias Mountains. Yakutat provides a reference base along the Pacific Coast while Seward Stations A and B[2] have marine exposures at higher elevations. Divide Stations B, C, and D form a triangular network near the hydrological divide of the Hubbard and Kaskawulsh Glaciers. The continental slope is represented by the Kaskawulsh and Terminus Stations, with Base Station providing an interior anchor point near the Alaska Highway. Haines Junction and Whitehorse are the continental reference stations. Originally, it was planned that an automatic marine slope station be established on the Hubbard Glacier between the Seward and Divide Stations, but this operation was abandoned because of logistical difficulties.

It should be noted that the profile roughly approximates the lowest elevations that might be encountered on a traverse of the range; stations are located in the valleys and on lower adjacent rocks. The profile is not, however, a smooth one. Total relief in the region is as great as anywhere in the world. The south wall of Mt. Logan, for example, rises from its Seward Glacier base at 1800 m to an elevation of 6050 m within 8 km. Similarly, the 5488-m summit of Mt. St. Elias is attained within less than 30 km of the Pacific shore. Many peaks have elevations in excess of 3500 m. Obviously the effect of these topographic barriers on local and regional climate is appreciable and cannot be ignored in the interpretation of weather data recorded in the glacier valleys. Thus, although a theoretically better set of station locations might have been selected, factors such as safety, ease of travel, accessibility to the project aircraft, and other logistical problems partially dictated the choice of sites. It is believed that the necessary compromise between logistics and the respective needs of the glaciology and climatology programs was optimal.

Observations at the four manned stations were taken at three-hour intervals commencing at 0300 daily (Yukon Standard Time). These included observations of temperature, amount and type of precipitation, relative humidity, wind direction and velocity, sky condition, sunshine, clouds, and other related meteorological variables. Hygrothermographic data were collected at the other four stations. Divide and Base Station observations for 0900 and 2100 Y.S.T. were coded and relayed to the Whitehorse weather station where they were used in local and airways forecasting. A complete summary of the 1964 data has been published elsewhere (Marcus, 1965).

In making measurements of temperature, thermographic data were recorded at all stations, the instruments having been calibrated against base thermometers throughout the season. In addition, at the manned stations, the three hourly observations included direct readings of temperatures from the minimum thermometer. Thermographs and thermometers were kept in standard meteorological shelters. Screens were not mechanically ventilated. Observers made their observations as close to the three-hour interval as possible, but exceptions were made for the 0300 Y.S.T. and 1500 Y.S.T. readings. Since these times correspond to the 1200 G.M.T. and 0000 G.M.T. radiosonde ascents at Whitehorse and Yakutat, icefield observations were scheduled for comparison with actual balloon ascents. Radiosonde balloons are usually released at these stations 40 minutes before the listed observation hour (for example, 1120 G.M.T. release for 1200 G.M.T. record). Assuming an average ascent rate of one minute per thousand feet, comparable icefield station readings were taken at times when the balloons should have been at the approximate elevations of the stations. The 0300 Y.S.T. and 1500 Y.S.T. observations were, therefore, taken at 0220-0230 Y.S.T. and 1420-1430 Y.S.T. respectively. Thermographic data for 0300 and 1400 Y.S.T. were extracted according to a similar scheme.

Recordings at automatic stations were generally uninterrupted, but exceptional circumstances affected the record at two locations. Seward B (on ice) should have been established only a few days after the initiation, on June 18, of Seward Station A observations (on a nunatak). An extraordinarily prolonged period of fog, low-

[1] Plates 1 and 2 are maps at the end of this volume.
[2] Names of IRRP stations have been changed from those used in the previously published report to those given on Plate 1 inside the back cover of this volume.

TABLE 1A. Manned Weather Stations, St. Elias Mountains, 1964

Station	Latitude (N)	Longitude (W)	Elevation (m)	Period of record	Type of surface
Base Station	61°03′	138°22′	786	June 1 – August 26	Gravel; 50 m NW of center of abandoned Kluane air strip
Divide Station B	60°47′	139°40′	c. 2,637	June 10 – August 17	Snow
Kaskawulsh Station A	60°44′	139°08′	c. 1,770	July 4 – August 22	Thin moraine overlaying ice
Seward Station A	60°20′	139°55′	c. 1,860	June 18 – August 14	Rock ridge approximately 20 m from nearest snow.

TABLE 1B. Automatic Weather Stations, St. Elias Mountains, 1964

Station	Latitude (N)	Longitude (W)	Elevation (m)	Period of record	Type of surface
Divide Station C	60°46′	139°42′	2,674	June 13 – August 16	Small rock nunatak. 5 m. to nearest snow. Occasional thin snow cover depending on weather
Divide Station D	60°46′	139°38′	2,741	July 13 – August 15	Snow. On ridge just east of nunatak summit.
Seward Station B	60°20′	139°56′	c. 1,780	July 6 – August 13	Snow. Approximately 1.5 km west of nunatak.
Terminus Station	60°49′	138°38′	c. 825	June 11 – August 18	Gravel. On moraine approximately 50 m from Slims River floodplain; 1 m higher than floodplain surface.

TABLE 1C. Reference Stations, Icefield Ranges Research Project, 1964

Station	Latitude (N)	Longitude (W)	Elevation (m)	Period of record	Operating agency
Experimental Farm Mile 1019, Alaska Highway, Y.T.	60°45′	137°35′	599	June 1 – August 26	Canada Department of Agriculture
Whitehorse Airport Y.T.	60°43′	135°04′	702	June 1 – August 21	Meteorological Branch, Department of Transport
Yakutat, Alaska	59°31′	139°40′	12	June 1 – August 31	U.S. Weather Bureau

lying clouds, and poor visibility delayed the operation until July 6. Travel over the untested, crevassed surface was inadvisable under those conditions. Late in July, a two-day break in the record occurred when station personnel were unable, again because of bad weather, to reach and reset the instrument. At Terminus Station, an entire week of temperature observations was lost (June 23–29) when a grizzly bear attacked and demolished the meteorological shelter and instruments therein shortly after the thermograph had been reset.

Temperature Relationships

A summary of statistics for 1964 is given in Table 2; comparative data also are given for the stations operated in 1963.[3] Data from stations maintained in both 1963 and 1964 (Divide, Base Station, Whitehorse, and Yakutat) indicate that despite a great diversity of sites, temperature trends were not masked by local effects of topography, elevation, and continental or marine exposure. Thus, general cooling or warming trends are reflected along the whole climatic profile. Only in the intensity of temperature change is site influence particularly obvious.

Comparison of the 1963 and 1964 records indicates that no significant site-induced departures occur. All categories of temperature given in Table 2 show that June 1964 was appreciably warmer than June of the preceding year. In contrast, the temperature data indicate that the months of July and August 1964 were generally colder than the same months of the preceding year. Occasional exceptions occur for the extreme maximums or minimums, but these are not considered significant since extreme values are particularly apt to reflect conditions at the immediate observational site.

[3] Although centigrade degrees and metric units are normally used in this paper, the summary statistics in Table 2 are given in Fahrenheit degrees. This is in keeping with the method established in other publications for reporting general weather data collected by the project.

Daily temperature trends are also similar on both sides of the mountain barrier. This is true for the entire summer record and is partially revealed by the dates for extreme maximums and minimums given in Table 2. Many of these dates coincide or fall closely together; other values, only slightly less extreme than these, reveal even more conclusively that all stations experienced exceptionally warm or cold weather at the same time.

TABLE 2. Summary Temperature Statistics (°F), St. Elias Mountains and Environs, 1964

	June	July	August
EXTREME MAXIMUM			
Yakutat	68.0 – 64.0 (1)	70.0 – 69.0 (14, 15)	74.0 – 76.0 (11)
Seward B	– –	53.8 (18)	47.0 (5)
Seward A	46.0 (27)	54.0 (17)	52.0 (7)
Divide B	42.0 (12)	51.3 – 51.7 (18)	43.0 – 51.8 (1,8)
Divide C	37.8 (14)	46.2 (18)	39.9 (1)
Divide D	– –	49.2 (16)	41.8 (3)
Kaskawulsh A	– –	58.1 (21)	50.3 (7)
Terminus	66.0 (16)	72.2 (16)	66.4 (11)
Base Station	74.6 – 67.0 (8)	73.5 – 73.0 (17)	66.8 – 73.0 (11)
Haines Junction	79.0 (8)	77.0 (17)	70.0 (11)
Whitehorse	79.5 – 76.9 (8)	75.8 – 81.8 (17)	74.8 – 82.3 (11)
MEAN DAILY MAXIMUM			
Yakutat	58.0 – 54.2	58.0 – 59.3	58.6 – 62.7
Seward B	–	45.9	42.9
Seward A	37.5	43.5	43.6
Divide B	33.3	34.7 – 39.4	35.1 – 37.3
Divide C	31.0	33.1	33.8
Divide D	–	37.8	32.4
Kaskawulsh A	–	46.9	45.6
Terminus	57.2	61.2	59.4
Base Station	60.5 – 56.3	61.4 – 63.4	59.5 – 64.1
Haines Junction	66.4	65.4	63.7
Whitehorse	66.7 – 59.0	65.3 – 67.9	62.6 – 71.3
DAILY MEAN			
Yakutat	52.4 – 48.3	52.9 – 54.6	53.2 – 54.8
Seward B	–	35.3	32.4
Seward A	31.4	36.3	35.9
Divide B	26.6	27.4 – 30.6	26.3 – 29.8
Divide C	26.7	26.9	27.2
Divide D	–	31.0	24.8
Kaskawulsh A	–	40.2	39.5
Terminus	44.8	49.3	47.4
Base Station	51.9 – 46.5	52.4 – 53.9	50.8 – 52.9
Haines Junction	53.1	53.3	49.9
Whitehorse	55.9 – 49.6	55.2 – 57.5	52.8 – 58.3
MEAN DAILY MINIMUM			
Yakutat	46.8 – 42.4	47.8 – 49.9	47.7 – 46.9
Seward B	–	28.8	25.9
Seward A	27.4	30.3	29.7
Divide B	19.7	20.2 – 21.7	18.9 – 22.2
Divide C	22.9	22.3	22.3
Divide D	–	26.2	20.2
Kaskawulsh A	–	33.6	33.5
Terminus	34.4	38.5	37.8
Base Station	42.4 – 36.7	43.8 – 44.5	41.0 – 40.6
Haines Junction	40.1	41.1	36.0
Whitehorse	45.1 – 40.2	45.1 – 47.0	43.0 – 45.3

TABLE 2. (Continued)

	June	July	August
EXTREME MINIMUM			
Yakutat	39.0 – 35.0 (4)	40.0 – 41.0 (21)	41.0 – 37.0 (30, 31)
Seward B	– –	24.0 (19)	19.8 (9)
Seward A	25.1 (21)	25.5 (5)	26.6 (13)
Divide B	13.5 (15)	9.8 – 2.6 (5)	12.0 – 3.8 (4)
Divide C	17.3 (15)	14.9 (6)	17.8 (14)
Divide D	– –	21.2 (23)	13.7 (14)
Kaskawulsh A	– –	29.8 (17)	30.2 (9)
Terminus	30.4 (21)	33.8 (6)	32.3 (14)
Base Station	36.7 – 30.0 (4)	38.1 – 37.0 (24)	34.6 – 31.0 (13)
Haines Junction	29.0 (4)	27.0 (6)	22.0 (22)
Whitehorse	36.2 – 32.4 (4)	36.8 – 34.0 (6)	30.6 – 32.2 (22)

NOTES

1. Whenever a second figure is given, it represents the 1963 temperature for the same location. The dates on which extreme maximums and minimums occurred in 1964 are shown in parentheses. Data for 1963 are taken from project files prepared by James M. Havens.
2. Yakutat data were taken from U.S. Department of Commerce, Weather Bureau, *Climatological Data, Alaska.* Canadian data were taken directly from the files of the Agricultural Experiment Station, Mile 1019, Alaska Highway, Yukon, and from Canada Department of Transport, Meteorological Branch, ***Annual Meteorological Summary for Whitehorse Airport, Yukon.***
3. Values for the stations can be directly compared only in selected cases; periods of record given in Table 1 should be consulted.

The presumed blockage[4] of air masses, frontal systems, or both, by the St. Elias massif is not therefore especially evident in the temperature record.

Local temperature relationships. Variations in local temperature were noted in the two areas where more than one station was operated, the Divide Stations triangle and the Seward Station area. As a result primarily of the formation of a katabatic cold layer at night, diurnal variations were generally greater over the mid-glacier surfaces than over the nunataks. Also, the greatest variations between station temperatures occurred under clear sky conditions; the least differences were associated with a combination of low, heavy clouds and fog. These relationships are not surprising, but confusion and misleading information may result if particular attention is not paid to the characteristics of the observational site. It is the writer's opinion that such unintentional misuse of glacial-meteorological data occurs frequently.

Representative examples of each of these conditions are illustrated by the superimposed thermograph traces for the Divide Stations (Figure 1 and 2). In Figure 1, temperature trends are plotted for a period when clouds generally covered less than two-tenths of the sky and sunshine hours measured between 90 percent and 100 percent of their possible duration. Although Divide Station D was located 104 m higher than Divide Station B, its temperature trace has higher values for most hours of the record. This is especially apparent at night and in the early morning hours. Since a nighttime differential of 4° to 6°C occurs between the stations, the importance of nocturnal radiation losses and cold air flooding on glacier interfaces cannot be ignored.[5] Divide Station D, on the other hand, has temperatures that more properly approximate those of the regional ambient air.

The effect of nocturnal cooling on ablation processes is especially apparent for this case. Since Divide Station D and atmospheric temperatures are at or above. freezing (radiosonde data indicate that the so-called free air is probably well above freezing), it would be a mistake to evaluate ablation or ablation potential in terms of the regional air masses; local conditions depress temperatures over the glacier far below the freezing point and inhibit ablation. Conversely, the glacier station temperatures simply are not representative of regional air mass characteristics.

The slight snow slope leading from Divide Station B to Divide Station C and the small elevational difference between them (30 m) tend to subdue the variations between these two stations. They are, however, similar to the preceding set and partially evident in Figure 1.

Figure 2 represents the alternative case: a prolonged period of stormy weather with some snowfall, high rel-

[4] The expression "presumed blockage" is used here because expected variations in air mass and frontal characteristics were seldom identified along the trans-mountain profile.

[5] Because of its position in a topographic saddle, the relative importance of cold air flooding should be minimized at Divide Station B. Indeed, this fact is indicated by the generally low wind velocities observed. However, the station is located in a concavity relative to peaks north and south of it and probably has some "cold island" characteristics.

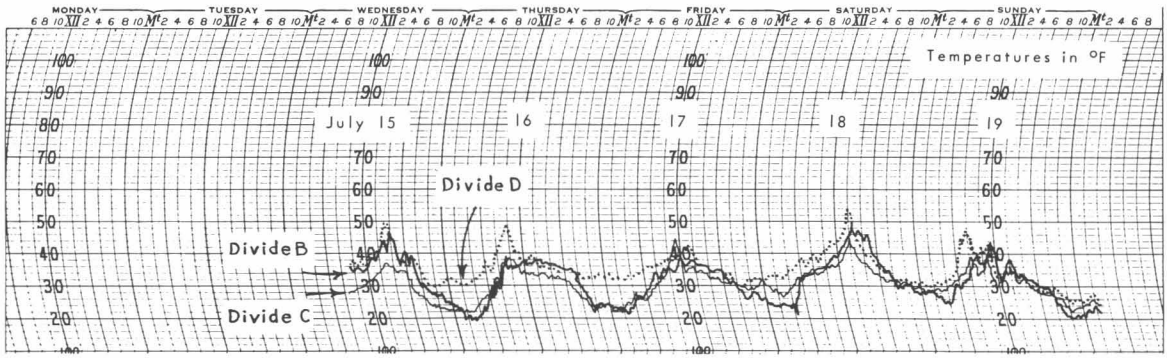

Fig. 1. Divide area temperatures during clear weather.

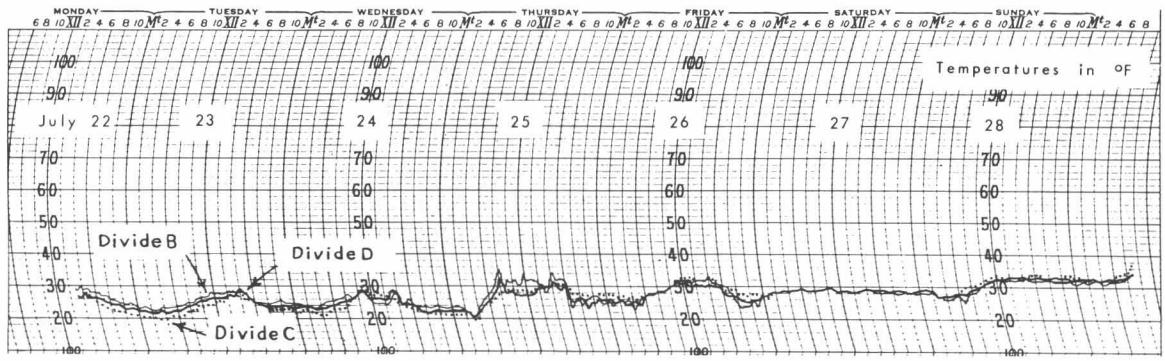

Fig. 2. Divide area temperatures during cloudy and foggy weather.

ative humidity, practically no direct sunshine, and 10-tenths cloud cover most of the time. In addition, cloud ceilings ranged from 0 to 300 m above Divide Station B. Under these circumstances, all three traces show close agreement; in fact, for July 27 they merge perfectly. Radiation loss at night from the snow surface is greatly reduced and the greenhouse effect of the cloud cover at times eliminates the minimum temperature differences that might be expected of stations slightly separated in altitude. Also, shelter temperatures over both snow and rock show closer agreement with equivalent-altitude radiosonde temperatures than in any other situation.

Between Seward Stations A and B, accentuated but similar kinds of temperature relationships exist. The extensive Seward Glacier basin is completely ringed by high peaks and its egress to the Malaspina Glacier and the Pacific Ocean is quite narrow. It thus forms an almost perfect natural catchment basin which receives and holds (even in daytime to a significant degree) downflowing cold air. Although the Seward Station B shelter is 80 m lower than Seward Station A, its temperatures frequently run 3° to 4°C colder during both day and night. Stormy weather is also less effective than in the Divide area in bringing the temperature traces together. The "cold pond" effect tends to override the greenhouse influences.

Environmental and atmospheric lapse rates. Using Whitehorse and Yakutat radiosonde data, atmospheric temperatures were calculated for altitudes equivalent to those of the project stations. Temperatures were interpolated for 0300 Y.S.T. and 1500 Y.S.T. each day and means were taken for selected periods. Calculations were done on the University of Michigan IBM 7090 digital computer. The method of interpolation is described elsewhere (Marcus, 1964). For purposes of comparison, environmental lapse rates between lowland stations and Divide Stations B and D are given in Table 3. Mean lapse rates for July 1963 are also included, and they compare favorably with 1964 data. Temperature gradients are plotted on Figure 3. It should be noted that the July periods of clear and stormy weather previously given are again cited as representative examples. Analysis of June and August data has indicated that generally temperature relationships are similar to those for July.

Summer temperature–altitude relationships shown in the tables and graphs are, for the most part, to be expected. The influence of marine and continental locations, over Yakutat and Whitehorse, respectively, is apparent in (1) differences in diurnal temperature variations – especially at and near the surface, (2) the lapse rates and their reflection of relative stability and instability in the boundary layer, (3) the effect of inversions on lapse

TABLE 3. Environmental and Atmospheric Lapse Rates (°C/100 m)

Period of record, and time (Y.S.T.)	Marine slope		Continental slope	
	Raobs: Yakutat to 2637 m	Environmental: Yakutat to 2637 m (Divide B)	Raobs: Whitehorse to 2637 m	Environmental: Base Station to 2637 m (Divide B)
1964				
Mean July				
0300	0.46	0.56	0.44	0.66
1500	0.62	0.52	0.88	0.83
July 15 – 20				
0300	0.32	0.54 (0.36)	0.38	0.65 (0.49)
1500	0.58	0.45 (0.43)	0.93	0.74 (0.70)
July 22 – 29				
0300	0.50	0.54 (0.50)	0.47	0.61 (0.55)
1500	0.58	0.53 (0.49)	0.97	0.84 (0.70)
1963				
Mean July				
0300	0.44	0.55	0.45	0.64
1500	0.57	0.51	0.88	0.81

*Environmental lapse rates for Divide Station (2741 m) are given in parentheses. Atmospheric lapse rates for Divide D are the same as those for Divide Station B.

rates and gradients, and (4) the absolute values of temperature recorded. The influence of glacier-covered mountain slopes on environmental temperatures is most pronounced for both marine and continental exposures at 0300 Y.S.T. when nocturnal radiation loss and the downslope movement of cold air are at a cumulative maximum. Finally, it should be noted that land and water effects tend to disappear above 3000 m where radiosonde temperature gradients begin to merge. Diurnal influences disappear at even lower levels. Yakutat radiosonde temperatures begin to merge within 600 m of the surface; Whitehorse values merge within 2000 m.

There are, however, important exceptions to the above. For example, the environmental lapse rate between Yakutat and Divide is greater at 0300 Y.S.T. than at 1500 Y.S.T. for all cases cited. This anomaly can be explained by the nocturnally induced bias of the environment at Divide Station B. Temperatures are lowered, and consequently the lapse rate is increased. The reversal of these values at Divide Station D, which is influenced less by the glacier, seems to verify this conclusion. The environmental temperature curves on both sides of the mountain give ample evidence that mid-glacier recordings are significantly lower, and the choice of Divide Station D or Divide Station B records for interpretation must be made in the context of particular research objectives.

The most surprising anomaly occurs in the relationship of 1500 Y.S.T. icefield surface temperatures to Yakutat radiosonde temperatures for the same altitudes. In Figure 3, it is shown that during clear weather (July 15 – 20) temperatures at Divide Stations B and C and Seward Station A exceed radiosonde values by as much as 3° to 4°C. This is meteorologically illogical and the explanation relates to instrumentation. Havens noted in 1963 that maximum thermometers at Divide Station B were reading *at least* 2°F higher than true air temperature (Havens and Saarela, 1964, and pp. 17 – 22 of this volume). These readings occurred, as did the high 1964 observations, under conditions of intense insolation and light wind. Comparisons of 1964 thermocouple data with shelter temperatures indicate that heating of the instrument screens, which are not mechanically ventilated, is undoubtedly the principal cause of error.

Others have recognized this problem which occurs even in extreme polar environments. David Miller, for example, notes that in summer over the Greenland Ice Cap "solar radiation is intense, but makes little impression on the local environment. Snow and air remain cool, although foreign objects may reach a high temperature" (Miller, 1956). One must concur with Havens that "the only comforting thought in this connection is that temperatures reported by most expeditions have not been made in ventilated screens . . . and temperatures are therefore, comparable under similar wind and insolation conditions" (Havens and Saarela, 1964, and pp. 17 – 22 of this volume). The fact remains, however, that many calculations of environmental lapse rates must be erroneous for clear weather, daytime observations – and seriously so.

Determination of freezing levels is important to an understanding of ablation–accumulation processes, and an incorrect reading of several degrees will seriously

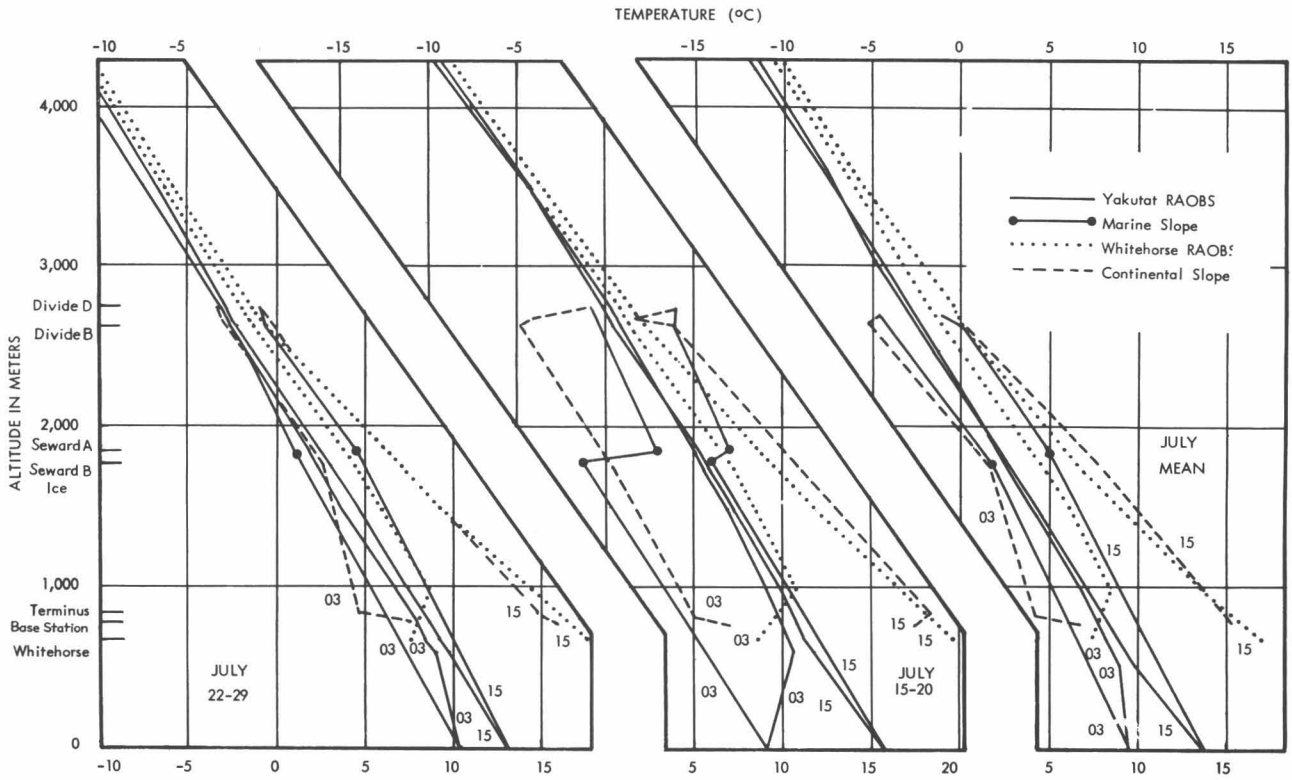

Fig. 3. Temperature gradients in the St. Elias region, July 1964.

hamper analysis of glacier – climate interactions. The range of possible freezing levels shown in Figure 3, for example, is quite impressive, and as it happens, the altitudinal zone between 2000 and 3000 m is particularly critical in the St. Elias Mountains. For the researcher who hopes, as many have done, to bypass these pitfalls by resorting to standard lapse rates, it can only be pointed out that this will probably compound the error. This is amply demonstrated by the diverse rates given in Table 3, and the same effect has been previously noted in the Juneau Ice Field region (Marcus, 1964). Thus, it is seen that a combination of instrument error, site characteristics, and research objectives leaves the investigator with a dilemma from which he can extricate himself only by the most careful manipulation of his data and considerable qualification.

Conclusions

Summer temperatures across the St. Elias Mountains reveal the great diversity that is expected in an area of high relief and varied surface characteristics. This diversity is principally a response in the boundary layer and tends to disappear at higher altitudes. Because investigators are interested in two kinds of problems – those in glacio-climatology and those in regional climatology – designation of observational sites and selection of data in the context of research objectives become critical considerations. This is clearly indicated for the St. Elias region by the comparisons of temperatures measured (1) on a trans-mountain profile, (2) at stations in the same locality, but on different surfaces, and (3) from radiosonde soundings.

There is no simple way to circumvent these problems. Expensive equipment, complicated logistics, and the concentrated efforts of several field workers in meteorological programs are necessary to their solution. In polar regions, where large-scale, government - supported expeditions have operated, this has been possible. In such instances, the climatology programs have been particularly effective because of the use of radiosonde, pilot balloons, mechanically ventilated shelters, automatic recording instruments, and other sophisticated instrumentation. Thus, it has been possible to observe and analyze the weather in the entire air column above the station surface.

Investigators interested in mountain and temperate glacier climatology have been neither as successful nor as sophisticated, except at micrometeorological scales. And with all their advantages, micrometeorological observations are not easily extrapolated beyond the instrument site. The operational scale of most studies in alpine glacial climatology has simply been too small to

obtain optimum results. The present status of knowledge in this field requires that more elaborate and sophisticated, albeit more expensive, research be undertaken. In the meantime, investigators will continue to live within the same old operational limitations; their only response can be careful, qualified use of the data they collect.

Acknowledgments

During the 1964 field season, the project's climatology program was supported by the Earth Sciences Division, U.S. Army Natick Laboratories, Natick, Massachusetts. Equipment was provided by the U.S. Army Terrestrial Sciences Center; the U.S. Army Natick Laboratories; and the Meteorological Branch, Department of Transport, Canada.

Six investigators constituted the basic climatology team: the author, who was in charge of the program; Tony Brazel and Raymond Lougeay, Rutgers University; Edward Grew, Dartmouth College; David Witter, Clark University; and Linda Upton, Arctic Institute of North America. Other members of the project were generous with their time and assistance.

The author wishes to thank the University of Michigan for use of the 7090 computer.

References

*Havens, J. M., and Saarela, D. E. (1964) Exploration meteorology in the St. Elias Mountains, Yukon, Canada, WEATHER, 19, 342 – 352.

Marcus, M. G. (1964) Climate-glacier studies in the Juneau Ice Field region, Alaska, Univ. Chicago, Dept. Geogr., RES. PAPER NO. 88, pp. 52 – 54.

Marcus, M. G. (1965) ICEFIELD RANGES CLIMATOLOGY PROGRAM, ST. ELIAS MOUNTAINS, 1964, PT. I, DATA PRESENTATION, Arctic Inst. North Am., 109 pp.

Miller, D. H. (1956) The influence of snow cover on the local climate in Greenland, J. METEOROL., 13, p. 119.

*This article is reprinted in the present volume.

The Summer Climate of the St. Elias Mountains Region

Bea Taylor-Barge *

ABSTRACT. The analysis of the climatological data collected during the summers of 1963 to 1965 in the St. Elias Mountains, the climatic records of the permanent weather stations in the mountain margins, several particular synoptic situations in the summer of 1965, and the geostrophic flow over the study area in the summers of 1964 and 1965 were examined. From these a summer transmountain climatic profile of the St. Elias Mountains region was developed.

The study indicated that (a) a climatic divide could be located between the Divide and Kaskawulsh stations on the continental slope, (b) two types of stations existed with respect to temperature records, (c) anomalously low wind speeds were experienced at the Seward and Divide stations and strong glacier winds persisted at the Kaskawulsh station, and (d) the factors determining the climate of the area could be separated into three scales of influence.

Introduction

Climatological and meteorological discussions of the southwest corner of the Yukon Territory and the adjacent portion of the Alaska panhandle invariably attribute the pronounced contrast in the climatic regimes of these two regions to the intervening mountain ranges (Hare, 1954; Mitchell, 1958; Kendrew and Kerr, 1955; Reed, 1958). The lofty peaks of the main range, the St. Elias Mountains, also form the political and topographical boundary between Alaska and the Yukon.

Until recently, only meteorological records from stations lying well to the east or west of the actual mountain barrier have been available for climatic studies of the region. In 1961, with the initiation of the Icefield Ranges Research Project, it became possible to delve into the climate of the vast areas of ice, snow, and towering mountains separating the Alaska coast and the southwestern Yukon plateau.

A study of this unknown and somewhat unusual corner of the world would in itself be of interest and of help in resolving some of the complex problems related to the climate of high mountain glacierized areas. In addition, a climatic profile across the mountain barrier would undoubtedly be useful as an aid to understanding the weather conditions to the east and west of it. Consequently, a study of the Icefield Ranges climate has been undertaken using data from the IRRP stations for the summers of 1963, 1964, and 1965, supplemented by long- and short-term climatic records from the permanent stations bordering the mountains.

The history, location, and geographical environment of the IRRP stations and the permanent meteorological stations whose records were used in this study are discussed in full elsewhere (Taylor, 1967; Marcus, 1966). Details of the meteorological program can be found in Taylor-Barge (1969) and Marcus (1966). Periods of operation of the meteorological stations and types of data are summarized in Tables 1, 2, and 3. Table 4 gives the nature of the surface on which the IRRP stations were located. The region of the study area is shown on Plates 1 and 2 in the back of this volume; the locations of the meteorological stations are given in Figure 1.

*Department of Meteorology, McGill University, Montreal, Canada

General Circulation

The study area straddles latitude 60°N. It lies in the subpolar low pressure belt on the northern edge of the mid-latitude zonal westerlies. Mitchell (1958) says of the cyclonic activity in the area: "The mountains form a cradle for the Gulf of Alaska in which the great Pacific cyclones, spawned near the Aleutians, violently spin themselves to death, and where the greatest cyclone frequencies in the entire Northern Hemisphere are to be found."

In winter the mean sea-level pressure field in the area is dominated by the Aleutian low in the Gulf of Alaska, and the extremely cold Mackenzie high east of the St. Elias Mountains. There is a moderate increase of zonal flow with height. The upper charts are characterized by a quasi-permanent, warm ridge extending across Alaska towards the pole. Hare and Orvig (1958, p. 24) point out that: "Since the high pressure cells . . . coincide with low temperatures, and low pressure cells with warmth, the pressure pattern adjusts itself rapidly with height. . . . The Icelandic and Aleutian lows are replaced by a two- or three-centred vortex directly across the polar basin. The Mackenzie high merges into the semi-permanent, warm ridge over Alaska. In short, the patterns of the mean sea-level winter map are extremely shallow, being barely discernible above about 5000 feet." This is particularly significant to the present study as all the glacier camps are above the 5000-ft. level.

TABLE 1. Meteorological Program – IRRP Manned Weather Stations (1963 – 1965)

Station	Period of record	Observation times* (YST)	Parameters recorded †, ‡
Base Station	1963 (June 5 – Aug. 24)	0900, 2100	
	1964 (June 1 – Aug. 26)	0900, 1500, 2100	Insol, Sun
	1965 (May 14 – Aug. 9)	3 hourly	Insol
Kaskawulsh Station A	1964 (July 4 – Aug. 22)	Irregular (3 hourly)	No Press record
	1965 (June 4 – Aug. 8)	3 hourly	Insol, Ablation, Upper Wind
Divide Station B	1963 (June 19 – Aug. 23)	2 hourly	Sun, Snow, Met Phenom; no Vis record
	1964 (June 10 – Aug. 17)	3 hourly	Insol, Sun, Ablation, Micromet; no Vis record
	1965 (June 4 – Aug. 8)	3 hourly	Insol, Ablation, Upper Wind; no Vis record
Seward Station A	1964 (June 18 – Aug. 14)	3 hourly	Upper Wind, Micromet
	1965 (July 9 – July 25)	3 hourly	No Press record

*3 hourly is 03, 06, 09, 12, 15, 18, 21, 24 Yukon Standard Time
2 hourly is 02, 04, 06, 08, 10, 12, 14, 16, 18, 20, 22, 24 Yukon Standard Time

†Temp, RH, Cloud, Wind, Vis, Precip, Press were recorded at all stations during all periods except where noted to the contrary

‡EXPLANATION OF TERMS

Temp – Air shelter temperature
RH – Relative humidity
Cloud – Cloud type and cloud cover
Wind – Wind direction
Vis – Visibility
Precip – Precipitation
Press – Air pressure

Insol – Incoming radiation, short wave
Sun – Duration of sunshine
Ablation – Ablation and accumulation
Upper Wind – Upper wind direction and speed
Micromet – Temperature and wind at 4 levels, net radiation balance
Snow – Snow surface classifications
Met Phenom – Meteorological phenomena

By summer, the Aleutian low on the mean surface maps has been replaced by a ridge extending north from the Pacific Ocean along the Yukon–Alaska border. The circulation is considerably weaker than that seen in the winter, due largely to the disturbed synoptic regime. The 700-mb and 500-mb charts also show a far weaker gradient in July though they resemble the winter map in shape. The Alaska ridge has, in both cases, shifted eastward. The summer pressure features are also very shallow though both the surface and upper mean flow are weak and onshore at Yakutat. In all seasons except summer, the maximum frequency of cyclonic passage lies just south of the Aleutians. Summer exhibits a weak maximum north of the Aleutian chain and another opposite northern Alaska. The mean frontal positions (Kendrew and Kerr, 1955) relate well to these cyclonic track maxima.

All accounts of mean circulation are careful to point out that, in mountainous regions, mean values are of limited use. This stems largely from the methods used to convert surface pressures to mean sea-level. At very low temperatures, the corrections give entirely fictitious results. In addition, mountain barriers create unrealistically large gradients on sea-level pressure charts, and flow in mountainous areas is decidedly non-geostrophic.

Captain Nolan Williams (in Reed, 1958) has proposed a method of analysis of surface geostrophic winds in mountainous regions, which combines surface and upper level charts. The method has been applied to the mountains of western Canada and Alaska. Reed (1959), in summarizing this method, says, "Finally it should be noted that the difficulties considered cannot be eliminated or mitigated by improved reduction formulas. In fact some of the worst fictitious 'gradients' in the present study were located in regions where all stations were at or near sea-level. The large pressure differences were sustained by intervening mountain ranges, so what was represented as a pressure gradient was, in reality, a pressure discontinuity. There is some question as to whether this point has been properly appreciated in the synoptic literature, though it is well understood in general circulation studies."

As would be expected from the foregoing discussions, commonly used mid-latitude dynamical forecast models have failed in the mountains of the Yukon and Mackenzie regions. Estoque (1957), using a two-level baroclinic model and graphical integration techniques, reports complete failure in this region. Reed (1959), on the other hand, in his two-level graphical prediction model, includes non-adiabatic and orographic effects

TABLE 2. IRRP Automatic Stations (1963 – 1965)

Station	Period of record	Parameters recorded *
Divide Station C	1965 (June 13–Aug. 16)	Temp
Divide Station D	1964 (July 13 –Aug. 15)	Temp, RH
	1965 (June 7–Aug. 11)	Temp
Kaskawulsh Station B	1965 (July 7–July 26)	Temp, RH
Kaskawulsh Station C	1965 (June 25–July 26)	Temp
Seward Station B	1964 (July 6–Aug. 15)	Temp, RH
Terminus Station	1963 (July 15–Aug. 23)	Temp, RH
	1964 (June 11–Aug. 18)	Temp

*See explanation of terms, Table 1

TABLE 3. Permanent Weather Stations in Vicinity of Study Area

Station	Latitude (N)	Longitude (W)	Elevation above MSL (ft.)	Operating agency	Type of record	Period of record of climatological normals
Aishihik	61° 37′	137° 31′	3170	Meteorological Branch, Canadian Dept. of Transport	Surface synoptic	1943 – 1960 (18 years)
Haines Junction Experimental Farm	60° 45′	137° 35′	1965	Canadian Dept. of Agriculture	Irregular surface synoptic	1944 – 1960 (17 years)
Snag	62° 22′	140° 24′	1925	Met. Branch, Canadian D.O.T.	Surface synoptic	1944 – 1960 (17 years)
Whitehorse Airport	60° 43′	135° 05′	2289	Met. Branch, Canadian D.O.T.	Surface and upper air data (First Class station)	1942 – 1960 (19 years)
Cape Yakataga				U. S. Weather Bureau	Daytime surface synoptic	
Anne H	55° 02′	131° 34′	110	U. S. Weather Bureau	Surface synoptic	1931 – 1960 (30 years)
Sitka				U. S. Weather Bureau	Surface synoptic	
Juneau Airport	58° 22′	134° 35′	12	U. S. Weather Bureau	Surface synoptic	1931 – 1960 (30 years)
Yakutat Airport	59° 31′	139° 40′	39	U. S. Weather Bureau	Surface and upper air data	1931 – 1960 (30 years)

and applies these to a major storm in the Gulf of Alaska. The results are considerably better than Estoque's. Reed further reports that when he attempted to use a dynamical prediction model in the winter, the orographic effects were considerable. On the western slopes, heights were higher than those predicted. The error pattern fits the potential vorticity theorem well (that is, air forced up decreases in vorticity). Reed also found a good quantitative relationship between the elevation and error patterns. In short, for a region of this sort, special techniques must be applied to produce reliable numerical forecasts. These problems are, however, beyond the scope of the present study.

Climatic Profile

Figure 1 is a rough topographical profile drawn from Yakutat to Whitehorse through the IRRP stations shown on Plate 1 and listed in Table 1. In Figure 1, the dashed line joining the various stations will be taken as the ideal mountain profile representing the study area. Table 4 gives the type of surface on which each IRRP station is located. Photographs typical of the regions of the Kaskawulsh, Divide, and Seward stations are shown in Figures 2, 3, and 4.

TABLE 4. Type of Surface at IRRP Stations

Station	Station No.*	Type of surface
Base Station	1	Rock
Kaskawulsh stations		
A	3	Rock (on moraine)
B	4	Ice
C	5	Rock (knoll)
Divide Stations		
B	8	Ice
C	9	Rock
D	10	Snow-covered ridge
Seward Stations		
A	11	Rock (nunatak)
B	12	Ice
Terminus Station	2	Rock

*See inset map, Figure 1

The meteorological data from the individual stations along this profile have been tabulated in Marcus, Rens, and Taylor (1966), Marcus (1965a) and Havens (1968), and plotted, analyzed, and discussed in Taylor-Barge (1969). A summary of the year round climates of the continental and maritime margins and the local summer climates of the IRRP stations follows.

The continental margins. Winters are cold [January mean: −0.6°F (−21°C)] and clear while summers are warm [July mean: 57.5°F (14°C)] and short. Annual diurnal temperature ranges are large. The area is, on the whole, isolated from the Pacific air by the St. Elias and Coast Mountains. However, the lower Pelly and Cassiar Mountains to the east allow the penetration of the Mackenzie high in winter. Precipitation is scant, and occasionally drought and forest fires result. Snow depths are small but drifting is prevalent. Fog does occur and, in winter, ice fogs are not infrequent. Wind direction and, to some extent, cloud and precipitation are controlled by topography, and the records from the meteorological stations are actually only indicative of the valley climates. In short, the climate of the mountainous southwest corner of the Yukon Territory is virtually unaffected by the moderating influence of the Pacific Ocean (as little as 80 mi. away) and open to the accentuating influence of continental Canada.

Base Station. The summer temperature regime at Base Station is definitely continental, averaging around

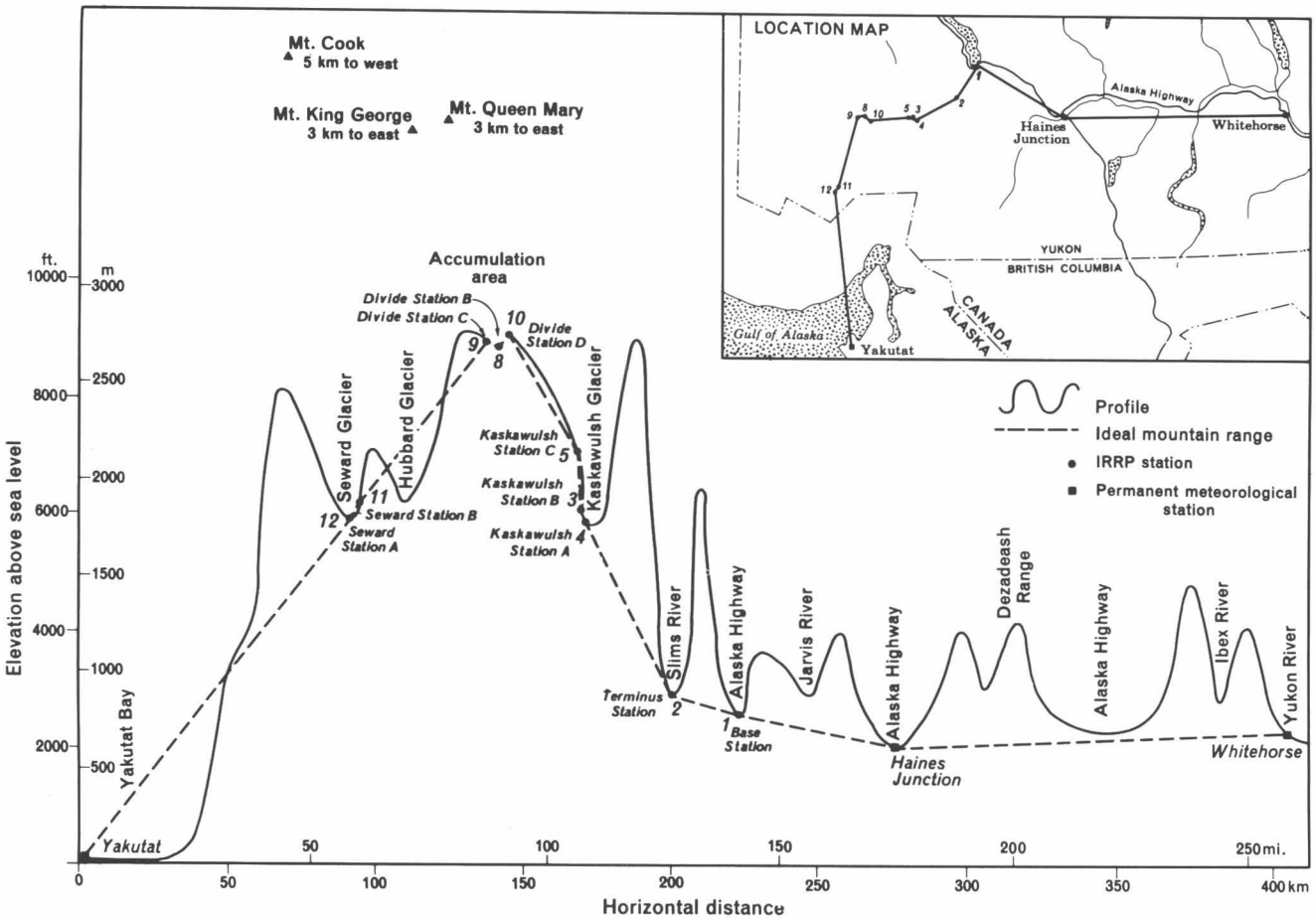

Fig. 1. Rough topographical profile, Yakutat to Whitehorse.

50°F (10°C) with a daily range of approximately 20°F. Relative humidity averages in the low 60's. There is little evidence of cooling caused by the proximity of the icefields. Winds are comparatively light (4.0 kn), tend to be south and east at night and southwest by day, and suggest an ill-defined mixing of local and synoptic scale influences. The continentality of the station is reflected by the relatively low cloud amounts, a predominance of middle and high cloud, and the presence of convective cloud after midday. Base Station, with a daily average precipitation of 0.90 mm and a probability of rain, on any one day, of 34%, appears to receive less precipitation than does Whitehorse. The precipitation falls mostly as rain though snow has been recorded in May and June. South and west winds off the mountains tend to be warm and are accompanied by cloudy skies. Winds from the lake are cold, at times moist, and bring precipitation. Winds from the valleys, on the other hand, tend to import relatively less cloud and rain. Base Station, then, has a well-defined continental climate, ill-defined wind patterns, and is in a precipitation shadow.

Kaskawulsh stations. Kaskawulsh Station A (on moraine), at an elevation of 5800 ft., has an average summer temperature around 40°F (approx. 4.0°C). The diurnal range is comparatively low (11.5°F). Relative humidity averages in the low 80's. Kaskawulsh Stations B (on ice) and C (on a knoll) prove, from the temperature and relative humidity records, to be less continental and more continental, respectively, than Kaskawulsh Station A.

Synoptic wind patterns are very poorly represented at Kaskawulsh Station A when compared with the other IRRP stations. Strong, thermally induced, down-glacier winds exist a large percent of the time, the average speed being close to 10 kn. In addition, the diurnal speed curve is quasi-sinusoidal, and there is little evidence of diurnal direction variation. In 1965, calms were infrequent.

Cloud cover at the Kaskawulsh stations appears to be somewhat decreased by thermally induced subsidence though the average cover (6 tenths) is still relatively high for this latitude. Stratocumulus clouds are the most common though cirrus and stratus also figure significantly.

Since precipitation records at the glacier stations were inadequate, the winter accumulation profile obtained by the hydrological traverse[1] was examined. The accumulation values were assumed to represent the

[1]The traverse extended from the lower Seward Glacier across the glacier divide of the Hubbard and Kaskawulsh Glaciers to the lower Kaskawulsh Glacier. Fifteen pits were excavated. The preliminary results are presented by Marcus (1965c).

CONFLUENCE OF NORTH AND CENTRAL ARMS, KASKAWULSH GLACIER.

CAMP AT KASKAWULSH STATION A, LOOKING SOUTH.

Fig. 2. Kaskawulsh camp and surroundings.

total accumulation-season precipitation, and the per day amounts have been taken as comparable to the average precipitation per day obtained for the summer season.[2] The Kaskawulsh stations lie below the firn limit. There seems to be a 50% chance of precipitation on any one day. Snow and rain have been recorded in all of the summer months.

The relationship of wind direction to the other climatic parameters is as follows. The infrequent up-glacier winds tend to be warm, moist, and light, and they bring less cloud and more precipitation than do the predominant down-glacier winds.

Strong down-glacier winds and a surprisingly low temperature range appear to be the most outstanding features of the climate at the Kaskawulsh stations.

Divide stations. Divide Station B, at 8700 ft., is well above the climatological freezing level. Temperatures here average in the high 20's (°F) and vary about 15° diurnally. Relative humidities are in the mid 80's.

Winds here are surprisingly low, averaging only 4.9 kn. Divide Station B appears to be more influenced by the synoptic situation than the other IRRP stations though the large scale mountain–glacier configuration plays a role in determining the wind direction. There is a backing tendency in the daytime. West winds have predominated during the three summers. Average cloudiness is 6.7 tenths, or the same as the average at that latitude over the ocean. Skies tend to be either almost clear or completely overcast. Orographic uplift is doubtless responsible for much of the overcast. Stratus is by far the most dominant cloud type, followed by cirrus.

Once again, as at the Kaskawulsh stations, the hydrological traverse data were used to obtain a picture of the precipitation amounts. Pit 12 near Divide Station B yielded a result of 4.5 mm per day. To date, in all the summer months, snow is the only form of precipitation that has been recorded. The probability of snow on any one day is about 65%.

Southwest winds are generally the strongest except when cyclonic passages bring strong easterlies. Strong winds tend to be cold while light winds are accompanied by warm temperatures and clear skies. Southerlies tend to be warm and moist. Clouds come mainly up the marine slope but also from the mountains. Precipitation, on the other hand, accompanies easterly cyclonically induced winds while westerlies drop least snow. At Divide Station B there seems to be a close relationship between low pressure, cloud cover and wind maxima, and precipitation. Similarly, high pressure is followed by low winds and small cloud amounts. This is not necessarily so at the other IRRP stations, and suggests that the Divide Station B best represents the synoptic situation.

[2]This many not be entirely justified. However, comparing the accumulation-season precipitation per day at Whitehorse and Yakutat with that for the ablation season, the following was found. At Whitehorse the ablation-season precipitation was 62% that of the accumulation-season, while at Yakutat the opposite was true.

Seward stations. Seward Station A (on a nunatak), which is on a marine slope at 6100 ft., has a summer temperature of 35.2°F (approx. 2°C) with a mean daily range of 12.8°F. The relative humidity averages close to 90%. Perhaps the most outstanding feature of the climate at Seward Station A is the extremely low average wind speed of 2.6 kn. During the day very light winds blow up the Seward Glacier, while at night the relatively stronger winds are down-slope, originating from the northeast on the slopes of Mt. Vancouver. Calms are frequent. These observations point to a very locally controlled wind regime.

Cloudiness averages close to 8 tenths, and fog and completely overcast skies are frequent. Stratus is, of course, the dominant cloud type followed by altostratus. As at Kaskawulsh Station A, both rain and snow have been recorded in all of the summer months. The probability of rain is the same as at Divide Station B (65%), but judging from the findings of the hydrological traverse, Seward Station A lies near the zone of maximum precipitation and should average about 5 mm a day. It appears that down-slope winds from the mountains to the north and northeast are warm, moist, and strong but tend to destroy cloud cover, while winds up the branches of the Seward Glacier to the west and southwest are cool and light, and bring much cloud and precipitation. Thus, Seward Station A exhibits a maritime climate and has even lower wind speeds than at Divide Station B.

Maritime margins. The southeast coast of Alaska is characterized, in general, by mild winters with a January mean temperature of 27.3°F (−3°C), cool summers with a July temperature mean of 54.1°F (12°C), and small annual temperature variations. The area is occasionally subject to periods of extreme cold when air from the Mackenzie high overflows the mountain barrier and sweeps down the glaciers, bringing clear skies, gusty winds, and sub-zero temperatures. Precipitation is appreciable, often over 100 in. (2540 mm) and is mainly orographic in nature. This, of course, implies that amounts are much less in the lee of high ground. Snow amounts increase with altitude, to a certain point, and the snow has a high water equivalent. Skies are usually cloudy and fog is frequent on the coast. Winds are not particularly strong and are influenced by topography; sometimes they are off-shore. Cyclonic disturbances are frequent in the Yakutat area, especially in autumn and winter. In short, the climate is that of a northerly maritime area, located in the Subarctic low pressure belt, protected from continental weather by a mountain barrier, and warmed by the Alaska current.

Climatological Divide

The extremely pronounced differences between the climates of Yakutat and Whitehorse, discussed by Taylor-Barge (1969), suggest that a climatological divide may exist. Therefore, the synoptic data have been analyzed to determine the nature and location of such a divide.

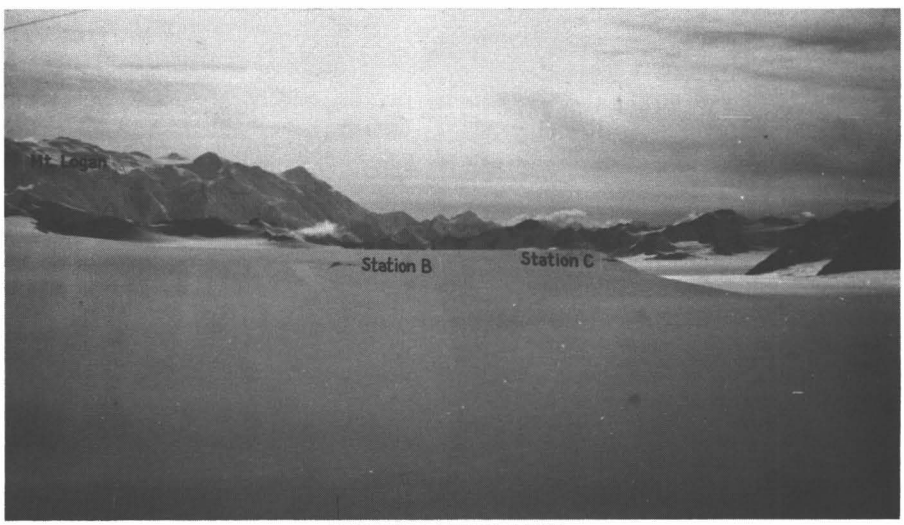

ACCUMULATION AREA.

CAMP AT DIVIDE STATION B, LOOKING SOUTH.

MOUNTAINS NORTH OF THE DIVIDE STATIONS.

Fig. 3. Divide camp and surroundings.

Temperature. From a study of the summer temperature data, it is evident that Yakutat and Seward stations were under a maritime influence, while Whitehorse, Base Station, and the Kaskawulsh stations showed the effect of continentality. Terminus Station did not exhibit as great a warming as did the other "continental" stations because of cool glacier winds. The various Divide stations do not fall easily into either a maritime or continental temperature regime. When the pronounced local moderating effects known to exist at the Kaskawulsh and Terminus stations are taken into account, temperature range considerations place the climatic divide between the Kaskawulsh and the Divide stations. A plot of atmospheric lapse rates (Marcus, 1965b) showed that the temperature divide did not extend much above 3000 m (approx. 10,000 ft.), where the temperature soundings above Yakutat and Whitehorse tended to merge. Despite the fact that a definite division could be made on the basis of average mean-temperature and temperature-range records, daily trends were the same at all stations. As noted by Marcus (1965b), this rules out a strict "blockage of air mass, frontal systems, or both, by the St. Elias massif."

Cloud cover. In the study area, cloud cover amounts increased gradually westward. However, cloud frequencies showed a decided difference between the Kaskawulsh and Divide stations, the former being much like Base Station and the latter closely resembling the Seward stations. Similarly, the Seward and Divide stations exhibited a predominance of stratus cloud while at Kaskawulsh, Base, and Whitehorse stations cumuliform clouds predominated. The flow-cloud amount relationships[3] showed a definite similarity between the cloud regimes at Seward and Divide stations. In addition, fog was far more frequent at Divide and Seward stations than at the continental slope stations.

Precipitation. From the result of the hydrological traverse, it was seen that a radical difference in precipitation amounts existed between the approximate elevation of the Seward stations on the marine slope and that of the Kaskawulsh stations on the continental slope. In accordance with the laws of physics (Walker, 1961), the precipitation maximum should occur on the windward slope at some altitude below the peak. It would not, however, have been correct to interpret this maximum as being synonymous with the division between the two precipitation regimes. On the other hand, the probability of precipitation on any one day was the same at the Divide stations as at the Seward stations, suggesting that precipitation in these two areas is subject to the same controls. Relationship between flow and precipitation were similar at Divide and Seward and were in contrast to those at the Kaskawulsh and Base stations. In addition, a plot of the diurnal precipitation march indicated that afternoon convectivity was of significant importance in producing precipitation at the Kaskawulsh, Base and Whitehorse stations, but not at the Divide and Seward stations. This was further illustrated by the fact that the Kaskawulsh and Base stations receive most precipitation in July and August when thermally induced precipitation is at a maximum.

Conclusions. It appears that temperature, cloud, and precipitation considerations definitely point to the existence of some form of climatological divide. The divide does not take the form of a blockage of air mass and frontal systems but is instead a complex modification of these systems or their surface effects. The divide is not a simple line but rather a zone much like a synoptic front, though probably much broader. The effectiveness of this divide appears to die out above 10,000 ft. in the free atmosphere. This is only a little more than 1000 ft. above the elevation of the Divide stations. This point will be examined further when the synoptic divide is discussed. All factors appear to locate this divide between the Divide and the Kaskawulsh stations on the eastern slope of the idealized mountain barrier shown in Figure 1. This is only the mean position, and depending on the synoptic situation, it oscillates back and forth much like a synoptic front.

Temperature Regimes

The temperature analysis showed that the stations were strongly affected by their position with respect to the glacier surface, as was also found by Marcus (1965b). The average summer temperatures of stations situated on nunataks, despite their greater elevations, were higher than those of the nearby stations on the glacier surface. Mean and extreme temperature ranges of the ice stations (except Kaskawulsh Station B) were greater than those of their nunatak counterparts. The environmental lapse rate between Yakutat and Divide Station B pointed to decided nocturnal cooling at Divide Station B when compared to the lapse rate between Yakutat and Divide Station D. Station to station differences were greatest under clear sky conditions. Relative humidities at the nunatak stations tended to be lower due to higher temperatures. The physical processes responsible for the phenomena described here vary from station to station, at least in magnitude, making it difficult to draw a sharp line between the two types of stations.

An attempt was made to isolate small scale influences from those of the broader maritime and continental regimes. This was done with the help of Figure 5 in which the mean summer temperatures for the stations are plotted along with the theoretical temperature that the standard atmosphere (lapse rate 0.6°C/100 m) would have at heights corresponding to those of the stations. In drawing the temperature – height curve, it

[3]The actual direction of geostrophic flow over the study area was extracted from the Central Analysis Office surface and 500-mb charts (00Zand 12Z) for the summer of 1965 and from the U.S. Weather Bureau *Daily Weather Maps* for 00Z at 500-mb and 18Z at the surface for the summer of 1964. The flow was classified according to the type of surface over which it travelled immediately before it reached the IRRP study area. The relationship of each of the synoptic parameters to the flow type was then analyzed.

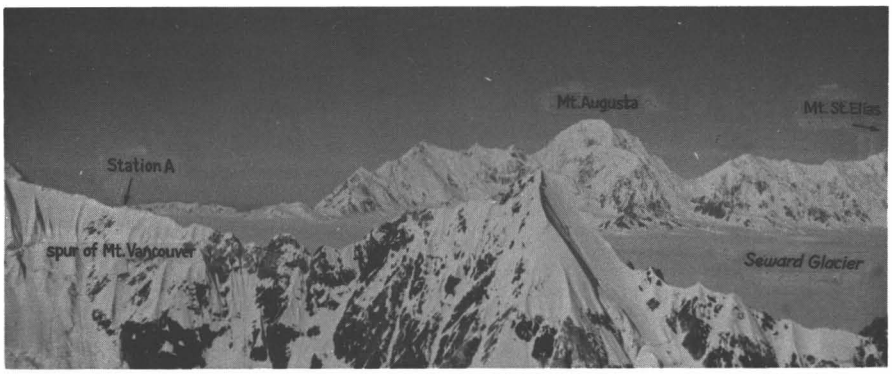

ACCUMULATION BASIN (PHOTO TAKEN FROM HUBBARD GLACIER).

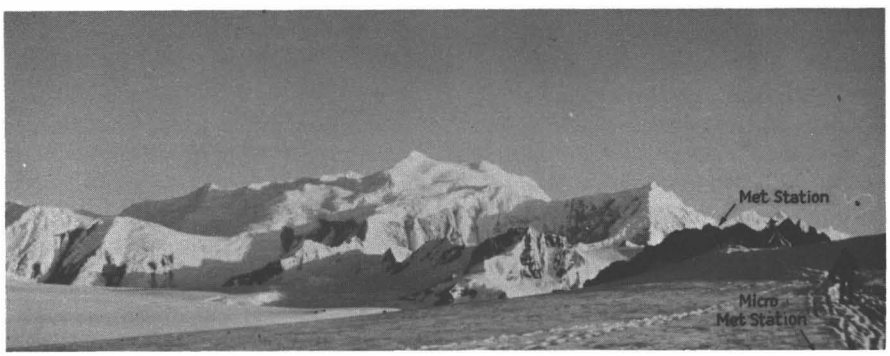

SEWARD STATION A WITH MT. COOK IN BACKGROUND.

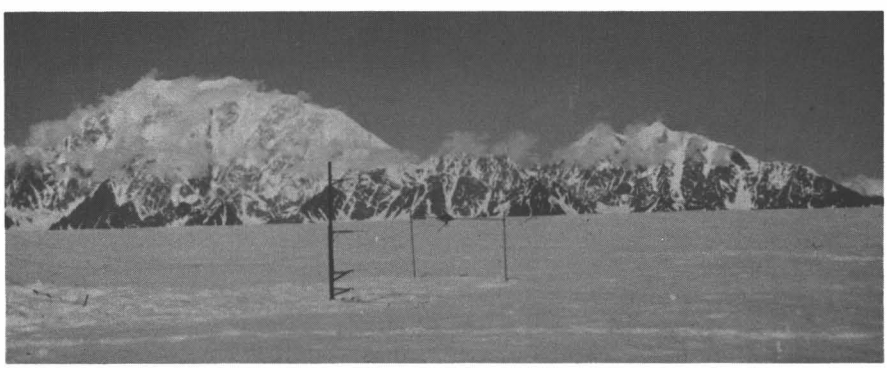

MICRO-METEOROLOGICAL STATION NEAR STATION A, WITH MT. LOGAN IN BACKGROUND.

Fig. 4. Seward camp and surroundings.

was assumed that the climatic divide lay between Divide Station D and Kaskawulsh Station A and that at the climatic divide the actual air temperature agreed with the theoretical temperature of the free atmosphere or ambient air.

The following observations can be made concerning the local temperature regimes of the various IRRP stations.

Seward stations. Radiative heating of the rock nunatak, nocturnal radiative cooling of the ice surface, and pooling of the cooled air in the impressive basin created by the ring of lofty peaks combined to produce the most distinct rock station to ice station differences of any of the IRRP stations.

Divide stations. Divide Station D, on a snow-covered ridge, appeared to be a rather good indicator of the ambient air temperature since the station was located above the cold layer but was not subject to undue radiational heating. Divide Station C, on the other hand, appeared to be somewhat heated by its rock surface but seemed not to escape the katabatic cold layer. Divide Station B, on ice, was undoubtedly subject to cooling from the cold pool. However, since the theoretical ambient air, or free atmosphere, temperature here was below freezing, it was questionable as to how effective the snow surface was in cooling the air by convective and conductive processes.

Kaskawulsh stations. Kaskawulsh Station C was more strongly heated than Base Station or Whitehorse. The explanation for this lies in the fact that the knoll on which Station C is located is a comparatively large expanse of bare rock, sheltered from the persistent down-glacier winds and raised above the cooled ice surface.

The temperature range, both mean and extreme, of the Kaskawulsh stations, was surprisingly low, and, in contrast to the case in the Divide and Seward areas, the range at the Kaskawulsh ice station (Station B) was less than that at either Station C, on a knoll, or Station A, on moraine. Both these anomalies are attributable to the following factors:

(1) During much of the summer season, the Kaskawulsh station area is below the firn line. Streams are extremely numerous and melting is so rapid that pools cover much of the surface. It appears that water surfaces exert a greater moderating effect on the air temperature than do ice surfaces.

(2) Constant, strong, down-glacier winds do not allow temperature extremes (for example, nocturnal cold layer or radiative daytime heating) to develop.

(3) Air passing over the Kaskawulsh stations has probably experienced a longer trajectory over snow or ice than that at any other stations, which suggests a cumulative moderating effect on diurnal range.

Other Stations. Figure 5 shows that Terminus Station is definitely cooled by the adjacent glacier or by winds blowing off it. Base Station and Whitehorse are heated to about the same degree as would be expected from the relative similarity of the surrounding terrain. Too little is known by the author about the Haines Junction station to explain the relatively cool temperatures there.

Factors determining the temperature. It is now possible to list some of the factors of importance in determining the temperature regime of the stations in the study area, though no definite statements can be made concerning their relative importance until a detailed quantitative study has been undertaken. The factors working locally are:

(1) The altitude of the station
(2) The radiative properties of the surface
(3) The position of the station with respect to a topographically created basin
(4) The direction and magnitude of the gradient between the surface and screen level temperatures
(5) The wind conditions – that is, the mixing and transport of cool or warm air

Factors working on a broader scale are:

(1) The latitude of the station
(2) The general circulation patterns of the area
(3) The behavior of synoptic systems or, essentially, the complex interaction of all meteorological parameters

Wind Regimes

The average wind speeds at the Divide and Seward stations (5.9 kn and 2.7 kn respectively) are appreciably lower than either the recorded upper winds above Yakutat and Whitehorse at the altitude of the Divide stations (averaging 12.1 kn at Whitehorse), or the geostrophic winds at the 700-mb level – the altitude of the Seward stations. This is not merely a surface condition at the Divide and Seward stations, but extends to significant altitudes above these stations. The most obvious explanations for this situation relate to the extremely high relief of the areas.

Divide Station B. This station is situated near the center of 200 mi.^{2} of open accumulation area. This relatively flat, undulating plain is surrounded by towering peaks, especially to the south and southwest. From the accumulation area, several glaciers flow down to lower elevations. The general circulation patterns and an analysis of the 500-mb flow in 1964 and 1965 (Taylor-Barge, 1969) indicate a predominance of southwesterly flow over the area. The high frequency of south and west winds at Divide Station B suggests that the upper flow, if not completely blocked, is diverted north or south of Mt. Logan. In addition, the broad, cold expanse of the accumulation area might support a small anticyclone. Light winds would thus be expected at Divide Station B due to their position near the center of this anticyclone and to the tendency of down-glacier winds to counteract winds invading the area up the glacier outlets (that is, the Kaskawulsh and Hubbard Glaciers).

Seward Station A. This station lies in an even more impressive basin surrounded on all sides by 12,000-ft. to 19,000-ft. peaks. The main outlet to the ocean, the south Seward Glacier channel to the Malaspina Glacier, is relatively narrow and ineffective, and furthermore, only occasionally do west winds reach the basin along

the main branch of the Seward Glacier. Thus, as at Divide Station B, the prevailing flow passes either high above the secluded basin or reaches it by such indirect channels that it no longer has any appreciable speed, and the thermodynamically induced down-glacier flow counteracts winds encroaching up these glacier channels. This leaves up- and down-slope effects to explain air movement here. All data from Seward Station A point to a dominance of such diurnal wind systems.

Kaskawulsh Station A. Strong down-glacier winds are an almost constant feature at Kaskawulsh Station A. The following factors contribute to these winds:

(1) Katabatic (gravity) winds result from nocturnal radiative surface cooling and a subsequent downward motion of the cooled air near the surface, and conversely, daytime surface heating and a subsequent progression up-slope of the warmed air. The latter can be disregarded here as the glacier surface is not heated appreciably. Down-slope and down-valley winds (the latter being likely more significant) probably do contribute to the nocturnal winds at Kaskawulsh Station A.

(2) Glacier winds are much like down-valley winds but the cooling is achieved by conduction of heat away from the overlying air to the cold ice surface. These are most significant during the day when the ice-to-air temperature difference is greatest. At the Kaskawulsh stations, where temperatures average more than 6°F above freezing, diurnal maxima average 12°F above freezing, and the mean minimum is 32.7°F. Glacier winds are presumably rather important.

(3) The rather perfect channels formed by the steep mountains bordering the north and central arms of the Kaskawulsh Glacier and their confluence, in the region of the Kaskawulsh stations, suggest the presence of a Venturi or funnelling effect.

Cyclonic systems. Analysis of the maximum-wind records leaves little doubt that cyclonic systems can, to a considerable extent, override the local effects. Naturally, the degree to which this occurs varies from station to station, being greatest at the Divide stations. Until a complete analysis of the upper winds over the IRRP stations and over Yakutat and Whitehorse has been carried out along with a study of thermodynamically induced winds in these regions, it is unlikely that the wind anomalies can be completely explained.

Precipitation and Cloud Regimes

Precipitation. Precipitation, an extremely important factor in climatic studies of a glacierized region, is unfortunately one of the most difficult parameters to measure. Rain gauges prove very ineffective in catching snow, especially when it is accompanied by wind; at times it is almost impossible to tell whether snow is falling or merely being blown around. Furthermore, precipitation amounts measured at a fixed stake are affected by ablation and drifting. Observers thus tend to call all unmeasurable snowfalls "a trace" and as the sum of many "traces" is still a "trace", both the daily and monthly totals are gross underestimates. Kaskawulsh and Divide stations are most subject to these inaccuracies. For these reasons the winter accumulation values obtained from the fifteen pits excavated along the hydrological traverse were converted to amounts of precipitation per day and used to investigate the trans-mountain precipitation profile. The shape of this profile, shown in

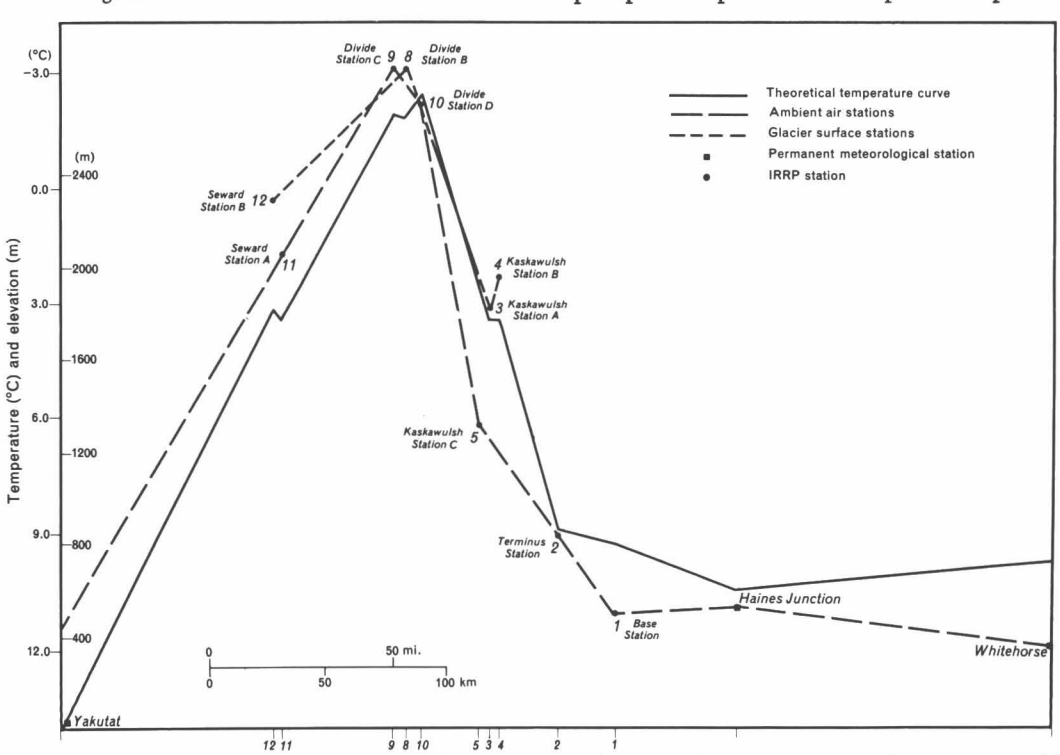

Fig. 5. Mean summer temperatures at stations on ice and stations on rock compared with the theoretical temperature of the standard atmosphere, corrected for varying elevation.

Figure 6, can be attributed to the influence of air circulation at three scales.

Considering the broadest scale of influence, it is assumed that air flows up the Seward and Hubbard Glaciers to the region of the Divide stations and then down the Kaskawulsh Glacier (that is, over a mountain range with the Divide stations at the highest point). According to Walker's (1961) theoretical calculations, this would result in a profile with the shape of the curve (long dashes) in Figure 6. The traverse data places the zone of maximum accumulation around 1800 m; this agrees well with Walker's results. Over a smaller area, as has already been mentioned, the mountains, especially Mt. Logan, are a major influence on the wind up to a considerable altitude. The precipitation shadow of Mt. Logan is also represented in Figure 6. Even more locally, topography in the form of ridges, hollows, and nunataks exerts an influence on the individual pit sites. To the windward (south) of Pits 5 and 7, for instance, nunataks present a precipitation barrier.

Base Station and Whitehorse fit well into an extension of the continental slope profile. Though Yakutat receives a rather high amount of precipitation, the precipitation value of 3.8 mm per day for summer months at Juneau fits well into the maritime slope.

The precipitation data collected at the IRRP meteorological stations proved to be more valuable in the form of precipitation probabilities than in actual precipitation amounts. The observations of precipitation type were also of use.

Clouds. An analysis of cloud observations shows cloud-amount frequencies are of more use in isolating the climate of a station than are cloud-amount averages. This suggests that cloud photography might yield useful results.

Synoptic Behavior

The climate of an area is largely a reflection of its synoptic regime. Seven synoptic situations from the summer of 1965 were analyzed in detail using (1) radiosonde ascents, (2) Central Analysis Office 500-mb, 700-mb, and 850-mb and surface weather charts, and (3) IRRP data (Taylor-Barge, 1969). A summary of the seven situations is given in Table 5 and a discussion of the significance of some of the observations follows.

Effects of the mountain barrier on the weather. There is no doubt that the St. Elias range, which lies almost perpendicular to the normal atmospheric flow, has a considerable effect on the area's climate. The synoptic analysis of the seven periods selected for study suggests the following:

(1) The degree to which the area's weather is orographically induced was perhaps best illustrated during the period when easterly flow, an uncommon phenomenon, produced, to the east of the barrier, considerable cloud, precipitation, and general cooling—all the effects

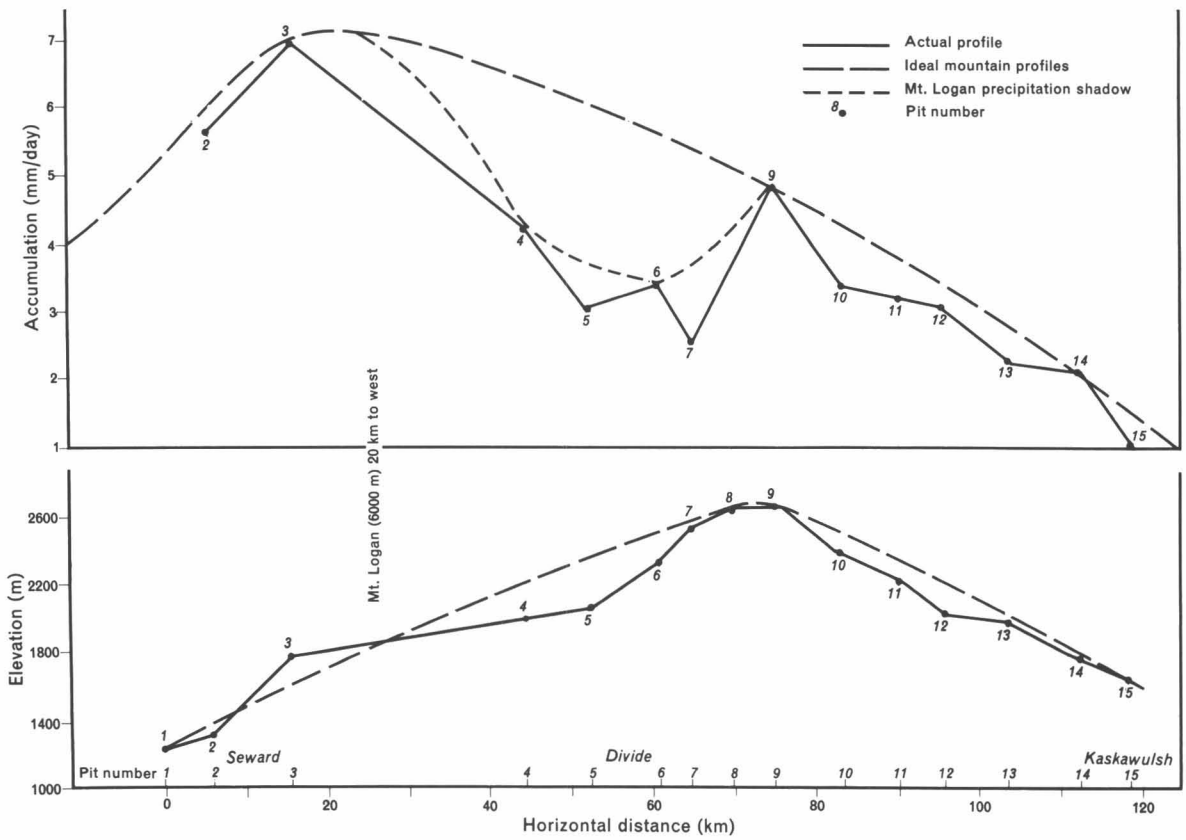

Fig. 6. Accumulation profile, St. Elias Mountains.

normally associated with the marine slope during a cyclonic passage. There was evidence of a föhn or chinook effect on the marine slopes, and Divide Station B appeared to behave as a windward slope station, grouping it with Base Station and Kaskawulsh Station A.

(2) During several of the upper cold front passages, there was definite evidence of stalling in the lower levels of the front, due to its contact with the mountain ridge.

(3) The barrier seemed to have several different effects on the horizontal alignment and motion of the fronts and trowals. A front approaching the coast and travelling perpendicular to it, unless well imbedded in a low system, tended to be deflected north or south (depending on the upper flow) along the mountains before crossing the barrier, and to be more or less aligned with the barrier during passage. On the other hand, fronts initially travelling parallel to the barrier were less affected, as were fronts accompanying very strong systems.

(4) The repeated lack of clearing on the marine slope after a cold front passage suggested a sort of piling up effect because the barrier held back the system. Once it crossed the barrier, however, the frontal system moved on relatively quickly, allowing continental slope clearing. Meanwhile, the next system had moved in and was affecting the marine slope stations.

(5) Time and again, Base Station escaped the temperature and precipitation effects of a trowal passage to an even greater degree than did Whitehorse. In addition, though the high and middle cloud associated with these systems was recorded at Base Station, low cloud was seldom present. In some cases, the weather crossing the barrier passed Base Station at upper levels only, but descended slowly, or reformed, so that it was felt at the surface at Whitehorse. On several occasions when Base Station escaped, there was evidence that the frontal effects spilt down over the saddle in which the Divide stations are located, at least as far as the Kaskawulsh stations, suggesting that by the time Base Station was reached, the cloud cover and precipitation had been destroyed by subsidence. A real föhn effect may also have been present, but further investigation would be needed to verify this. On a much more local scale, it is likely that the large, cold Kluane Lake produced some clearing in its vicinity.

In summary, the weather from the Gulf of Alaska, as it crossed the barrier, was orographically lifted, possibly deflected and aligned, and/or stalled in the lower levels. Then it spilt over the top and either descended steeply to Base Station, being partially destroyed by subsidence in the process, or descended slowly, or reformed, being felt at the surface at Whitehorse farther to the east.

Behavior of fronts. As noted above, fronts were in some cases aligned with the barrier or stalled by it in their lower levels. Cold fronts appeared to be most subject to these effects. It was evident that upper features (that is, upper warm troughs) became surface features during their passage over the mountains.

As previously stated, a satisfactory way of representing the synoptic situation over a mountainous area has not really been found. It is possible to depict, by a combination of vertical and horizontal diagrams, what is known of the behavior and modification of a frontal system crossing the barrier. However, to represent these happenings mathematically for numerical prediction is an extremely complex matter. Until it is achieved, numerical forecasts will continue to misrepresent the conditions over a mountain barrier, such as the St. Elias Mountains, and for some distance downwind of it.

It should be noted that only in two cases did the frontal systems appear to maintain their identity completely, during passage. In the first case, surface fronts passing the area were aligned perpendiculr to the barrier, while in the second the surface low was very strong, fast-moving, and well supported.

Winds. Both the actual and the geostrophic 700-mb and 500-mb winds at Whitehorse and Yakutat were frequently considerably greater than those recorded at the glacier stations; further, the highest winds at the IRRP stations did not correspond to the highest upper air or geostrophic winds. Once again, the very local character of the stations' wind regimes was evident. However, there did seem to be, on some occasions, a fairly good relationship between the 500-mb flow and the surface wind direction at Divide Station B. Generally, during the passage of a frontal system, the wind direction at Divide agreed fairly well with the surface flow. It appeared that the strongest winds resulted when the surface pressure configurations were not shallow but extended at least to the 500-mb level.

Importance of the 850-mb and 700-mb levels. As the study progressed it became obvious that the 700-mb and the 850-mb levels played a significant role in the surface weather of the study area. Not only did upper frontal systems produce surface effects when they hit the ground, which was especially evident at Divide Station B, but they also initiated considerable weather on either side of the mountains, at Yakutat and Whitehorse. From a synoptic point of view, it appeared that, for the IRRP stations, particularly those on ice surfaces, the 850-mb or even the 700-mb weather charts were a better representation of the situation than the rather fictitiously constructed sea-level charts.

The synoptic divide. General circulation features at sea-level were seen to be very shallow, and the climatic divide appeared, from Yakutat and Whitehorse radiosonde temperatures, to die out around 10,000 ft. above mean sea level, which is 1400 ft. above the surface in the region of the Divide stations. There has been some indication that surface pressure systems can be lifted almost intact over the mountains. Thus, the circulation features and the climatic divide may, in fact, be deeper than indicated by data from the mountain margins. In other words, the surfaces of these may follow the topography to some extent.

Reed's (1959) suggestion that the large trans–mountain pressure gradients are, in fact, discontinuities is interesting in view of the pronounced shadow in which Base Station is found. The results of the present study definitely do not rule out the possibility of trans-mountain discontinuities in the cloud, precipitation, wind, and pressure fields. Temperatures, however, were seen to undergo a modification rather than a strict blocking effect.

The position of the divide under various synoptic

TABLE 5. Summary of Synoptic Situation During Periods Analyzed (Summer, 1965)

		FRONTS		
Period	Pressure configuration	Number and type	Relation to pressure system	Deflection, alignment, and stalling
1	Surface: low died in Gulf of Alaska 500 mb: low died on south coast of Alaska	Trowal at 850 – 700 mb Upper both warm and cold fronts	Preceded low Passed area in trough of surface ridge	Forced north Became aligned with mountains Cold portion stalled in lower levels
2	Surface: well developed low with trough on southeast side – low moved across mountains 500 mb: deep low in good position to support surface low	Trowal at approx. 700 mb	In trough to southeast of low	Passed unaltered Initially parallel to coast Finally parallel to longitudes
3	Surface: ridge 500 mb: ridge and col	None		
4	Surface: low died in Gulf of Alaska or reformed over Yukon 500 mb; low gave fair support	Odd M front at 850 mb (Trowal) Diffuse cold A front approx. 850 mb	Preceded low Passed area in trough of surface ridge	Warm M front: forced north Initially aligned perpendicular to barrier Cold M front: aligned somewhat perpendicular to barrier during passage Retarded in lower levels
5	Surface: low south of the IRRP stations Flow – north and east 500 mb: low off Yakutat Flow – east	None		
6	Surface: dipole low	At surface: Warm M front Cold M front Cold A front	Fronts to south of low moving faster than it	M front, warm and cold: moved southeast Initially perpendicular to barrier Finally parallel to longitudes A front, cold: initially parallel to longitudes. Finally perpendicular to barrier (pivoted by surface flow)
7	Surface: not well defined 500 mb: low south of Yakutat	Odd front at 850 mb (Trowal)	Proceeding to south and moving faster than surface features	First cold front: bulges

*IRRP Station numbers used are those given in Table 4.

TABLE 5. (cont'd.)

STATIONS AFFECTED BY:*				
Temperature	Precipitation	Clearing	Period in general (compared to average)	Period
Warming: IRRP 3, 8 and at 850 mb at Whitehorse	Yakutat to IRRP 3	IRRP 1, 3, 8	Continental slope warm Marine slope cool Windy	1
Cooling: Yakutat, Whitehorse, and IRRP 1, 3, 8	All but IRRP 1		Cloudy	
Cooling: IRRP 3, 8	All but IRRP 1	Whitehorse, and IRRP 1, 3	Cold Windy (seasonal maxima) Cloudy	2
			Warm (except Yakutat) Clear	3
M front warming: IRRP 3, 8; upper at Yakutat and Whitehorse	Yakutat, Whitehorse, and IRRP 8	None	Continental slope warm Marine slope cool	4
M front cooling: all (but only a trend at IRRP 1 and Whitehorse)	Yakutat, IRRP 3	IRRP 8 to Whitehorse	Windy	
A front cooling: diffuse	All but Whitehorse			
Cooling: Whitehorse and IRRP 1, 3, 8	All (Yakutat rather small amount)	All but IRRP 8, 11	Contiental slope cool Windy except IRRP 3 Cloudy Precip amounts high on continental slope	5
M front cooling: all	All but IRRP 1, 3		Cool Cloudy	6
A front cooling: all but Whitehorse (not yet reached)	Yakutat and IRRP 11		Windy	
First cold front: IRRP 3, 8 (Yakutat, Whitehorse slowly)	All but IRRP 1	Whitehorse and IRRP 1, 3	Cool and windy (except Yakutat) Cloudy (except IRRP 3)	7
Second cold front: all but Whitehorse	Yakutat, Sitka and IRRP 11	IRRP 3, 8		

situations varied, at times being east of the Kaskawulsh stations and at times west of the Divide stations. Thus, its climatological position probably varies from year to year according to the current characteristics of the circulation, as well as other factors.

Conclusions

In this study the various climatological parameters have been discussed from a number of viewpoints. From these and from the analysis of general circulation and specific synoptic stations, a picture of the summer climate of the St. Elias Mountains region has been built up. The three years used in the study appear to be fairly representative of normal conditions.

Three scales of influence. There is evidence that the area's climate is subject to three scales of influence. Consequently, the most important manifestations of the influences, as indicated by the climatological and synoptic analysis in this study, will be discussed for each of the three scales. They are (1) broad, or synoptic influences, (2) influences of major local topography, (3) influences of minor local topography.

Broad, or synoptic, influences. The study area extends from sea-level at Yakutat on the Pacific coast across the extremely high and extensively glacierized St. Elias Mountains, and the lower Coast Mountains, to Whitehorse. Superimposed on the expected variation of temperature with height is a gradual eastward warming from the cool coastal region to the heated interior. There is a possibility of a föhn effect west of the St. Elias Mountains. Temperatures are more closely related to surface flow than to upper-air geostrophic flow. Divide Station B appears to best reflect the synoptic-scale winds. Wind directions here are more easily related to surface flow than to upper-air flow. Wind speeds, on the other hand, appear more related to 500-mb flow. The data for one of the periods analyzed suggest surface flow as the dominant factor in determining wind direction during a cyclonic passage, but the 500-mb situation apparently controlled wind direction before and after the cyclone. Cloud frequencies and types show two definite regimes, one on either side of the barrier, and cloud amounts appear to relate better to upper-air flow than to surface geostrophic flow. The trans-mountain precipitation profile and the position of the precipitation maximum agree reasonably well with Walker's (1961) theoretical model for an ideal mountain range. Precipitation probabilities exhibit the existence of two distinct regimes, as do cloud frequencies and types. The St. Elias barrier is seen to have a considerable effect on synoptic systems invading the area. Base Station experiences a greater shadow than Whitehorse.

A climatological, and to some extent a synoptic, divide can be found between the Divide stations and the Kaskawulsh stations. This position is physically reasonable if the Yakutat to Whitehorse cross section (Figure 1) is considered to be a simple, solid mountain range with the Divide station accumulation area as the effective ridge. That is, the weather is carried up the windward slope, spills some distance over the top, but generally leaves the continental slope in a decided shadow.

Conditions over the high glacierized region appeared, during a trowal passage, to be a direct result of the situation at 850 mb or 700 mb. However, during passage of deep lows, the sea-level geostrophic flow seemed to be more significant. Presumably, then, the depth of the surface features at any particular time largely determines the relative importance to the glacier stations' weather, of sea-level flow and upper air flow.

Influences of major local topography. The major topography, that is, the mountain–glacier or mountain–valley distribution, in the vicinity of each IRRP station is responsible for many of the station-to-station differences and for two interesting wind anomalies discussed in this study. Temperatures are probably least subject to this influence. However, Lake Kluane and the valley – mountain configuration in the area appear to have had some influence on Base Station temperatures. At the Kaskawulsh stations, mainly because of the nature of the wind regime, temperatures could be related to major local topography.

There is no doubt that the wind regime is most strongly influenced by major topography. Kaskawulsh Station A presents an extreme example of a topographically controlled wind regime where both speed and direction result from the channeling effect of the mountains bordering the north and central arms of the Kaskawulsh Glacier, and the air-to-glacier temperature differences. Similarly, the surprisingly low wind speeds at Seward Station A and Divide Station B result from their position in a topographic bowl and from a thermally produced miniature anticyclone effect. At Divide Station B, in 1965, wind directions related well to the distribution of mountains and glaciers around the accumulation area. Wind directions at Seward Station A are definitely locally induced.

Cloud cover is only slightly influenced by the major local topography. The distribution of snow and ice and bare rock surfaces, however, had some influence as seen by the formation of convective clouds over bare mountains and the dissipation of cloud over cold glacier surfaces.

The trans-mountain precipitation profile illustrates the shadow produced by the presence of a mountain the size of Mt. Logan in the path of the prevailing flow. It would be interesting to chart the horizontal extent of the precipitation and wind shadow caused by massifs such as Mt. Logan, Mt. St. Elias, and Mt. Cook.

Influences of minor local topography. It was seen that the presence of a relatively small amount of bare rock in the vicinity of a temperature recording station, or the elevation of that station above the glacier surface, can have a considerable effect on the temperature recorded. Seward Station B and Kaskawulsh Station C proved to be rather extreme examples of ice and nunatak stations, respectively.

Pits downwind of relatively small obstructions, such as snow ridges, showed significantly less accumulation. Thus, it is seen that wind and precipitation regimes can also be influenced by minor local topography.

Most important processes. Though the climatic influences can be separated into the three scales discussed above, it should be remembered that the same physical processes are effective at all scales.

For the area under consideration, the two major processes are radiative heating and cooling, and orographic effects. Radiative heating and cooling are responsible for (1) continental summer heating which in turn results in convective clouds and precipitation, (2) mountain-to-glacier temperature differences which in turn influence the wind and temperature regimes, and (3) nunatak-to-ice station temperature differences. Orographic effects produce wind and precipitation shadows at synoptic and local scales, that is, cyclonic systems produce precipitation, but where it occurs and how much falls is orographically determined.

Sensible and latent heat transfer effects were also observed but they are important chiefly in micrometeorological studies of ablation.

Other factors emerging from the study. The study clearly points out the necessity of exercising great care in the choice and analysis of data in an area such as this to insure that the records used are representative of the regime being investigated. For example, ablation studies must use temperatures from the ice-atmosphere boundary layer; air-mass identification, on the other hand, should use nunatak or higher-altitude temperatures. Local influences must be subtracted from wind data if they are to be used in synoptic analysis, and vice versa; all scales of topography must be taken into account in evaluating accumulation amounts.

The network of stations maintained by IRRP appears to be reasonably diversified and is quite suitable for a detailed synoptic climatological study. That they can be treated as a profile of a mountain range with the Divide stations situated near the top is also useful to such a study.

Since orographic and non-adiabatic processes were found to be of prime importance in the study area, it is not surprising that normal forecast methods, when applied to this region, fail rather badly. This will remain the case until some satisfactory way is found to include these effects in the forecasts. A systematic analysis of the relative importance, to the surface weather, of the standard pressure level configurations (that is, sea-level, 850 mb, 700 mb and 500 mb) under various synoptic conditions would doubtless shed some light on this problem.

References

Estoque, M.A. (1957) Graphic integration of a two-level model, J. METEOROL., 14, 65 – 70.

Hare, F. K. (1954) Weather and climate, in GEOGRAPHY OF THE NORTHLANDS, edited by G. H. T. Kimble and D. Good, Am. Geogr. Soc. and John Wiley and Sons, Inc., New York, pp. 58 – 83.

Hare, F. K., and Orvig, S. (1958) The Arctic circulation: a preliminary review, PUBL. IN METEOROL., NO. 12, Arctic Meteorology Research Group, McGill Univ., Montreal, 211 pp.

Havens, J. M. (1968) Meteorology 1963, Icefield Ranges Research Project, St. Elias Mountains, Yukon Territory, Canada, 133 pp. (privately printed).

Kendrew, W. G., and Kerr, D. (1955) THE CLIMATE OF BRITISH COLUMBIA AND THE YUKON TERRITORY, Queens Printer, Ottawa, 222 pp.

Marcus, M. G. (1965a) ICEFIELD RANGES CLIMATOLOGY PROGRAM, ST. ELIAS MOUNTAINS, 1964, PT. 1, DATA PRESENTATION, Arctic Inst. North Am., Washington, 109 pp.

*Marcus, M. G. (1965b) Summer temperature relationships along a transect in the St. Elias Mountains, Alaska and Yukon Territory, in MAN AND THE EARTH, UNIVERSITY OF COLORADO STUDIES, SERIES IN EARTH SCIENCES, NO. 3, Univ. Colorado Press, Boulder, pp. 15 – 30

Marcus, M. G. (1965c) A hydrological traverse of glaciers in the St. Elias Mountains, Alaska – Yukon Territory, Paper presented to the International Association for Quaternary Research, Boulder, Colo., Sept. 1965, 11 pp., (mimeographed).

Marcus, M. G., Rens, F., and Taylor, B. (1966) Icefield Ranges Climatology Program: 1965 Data presentation and Programming analysis, RES. PAPER NO. 33, Arctic Inst. North Am., Washington, 111 pp.

Mitchell, J. M., Jr. (1958) The weather and climate of Alaska, WEATHERWISE, 11, 151 – 160.

Reed, R. J. (1958) A graphic prediction model incorporating a form of nonadiabatic heating, University of Washington, 1957, J. METEOROL., 15.

Reed, R. J. (1959) Arctic circulation studies, FINAL REPORT, DEPT. METEOROL. CLIMATOL., Univ. Washington, 57 pp.

Taylor-Barge, B. (1969?) The summer climate of the St. Elias Mountains region, RES. PAPER NO. 53, Arctic Inst. North Am., Washington, 160 pp., (in press).

Walker, E. R. (1961) A synoptic climatology for parts of the Western Cordillera, PUBL. IN METEOROL. NO. 35, McGill Univ., Montreal, 218 pp.

*This article is reprinted in the present volume.

Description and Evolution of Snow and Ice Features and Snow Surface Forms on the Kaskawulsh Glacier

*W. Philip Wagner**

ABSTRACT. Investigations of numerous snow pits on the Kaskawulsh Glacier suggested that the 1963 summer could be viewed in terms of a threefold, sequential development of surface and subsurface features related to snow melt. Stage 1 was characterized by thin ice layers and rounded, medium-grained snow immediately underlying a nondescript snow surface. Stage 2 began on July 1 with a pronounced warm spell. Features characteristic of Stage 2 included surface depressions, ice and slush glands, "slush columns", and "slush walls". Lateral expansion of surface depressions and related subsurface features occurred during Stage 2. By July 21, growth of surface depressions resulted in a snow surface with conspicuous mounds (distinctive for Stage 3), remnants of the inter-depression areas of Stage 2. Stages 1 and 3 began and ended when melt began in the spring and ended in the fall, respectively; the dates of these stages are unknown.

Studies by Ahlmann (1935), Glen (1941), Sharp (1951), Benson (1962) and others have shown that a variety of features, namely ice layers, lenses, and glands, to use Benson's (1962, p. 21) terminology, are produced by summer melt diagenesis of snow. The most detailed study of these features was made by Sharp (1951) on the upper Seward Glacier, Canada. Both Benson and Sharp noted snow surface forms which they related to subsurface ice and slush glands. The purpose of this study was to follow the daily changes of subsurface snow and ice features and of the associated snow surface forms through a melt season.

Between June 21 and July 29, 1963, 42 snow pits were excavated in the percolation facies of the Kaskawulsh Glacier. Most of the pits were located on a nearly horizontal surface less than 2 km^2 in area, at an elevation of approximately 2590 m. Five of the pits were excavated to the top of the 1962 summer firn layer at approximately 4-m depth; the remaining pits were on the order of 2 m in depth.

Evolutionary Changes

On the basis of changes in the character of the snowpack, the 1963 melt season is divided into three stages which together form an evolutionary sequence.

Stage 1. The nature of the snow during this stage was relatively simple. It consisted mostly of very fine-grained,[1] angular to subrounded compact snow with a few ice layers and lenses. Near the surface the snow tended to be slightly coarser grained, with bonded and firm layers of snow interstratified with many thin ice layers generally less than 3 mm thick. The only changes which occurred during this stage were increases in the thickness of the near-surface zone and in the number and size of ice bands and bonded snow layers within this zone. The snow surface showed no features which could be readily related to subsurface melt diagenesis.

Stage 2. The break between Stages 1 and 2 occurred on July 1 when a sudden warm spell resulted in a variety of snow melt features. Walls of pits excavated on July 1 revealed layers of slushy snow and ice and a few small incipient slush and ice glands. Early in Stage 2, conspicuous surface depressions formed which were from 20 cm to 300 cm wide and 2 cm to 10 cm deep. More free water was observed in snow below surface depressions than in snow under inter-depression areas, and in vertical cross-section, slushy, wet snow was evident in areas similar in shape and dimension to the surface depressions. In three dimensions the slushy snow formed what may be termed "slush columns" under roughly circular depressions and "slush walls" under elongate and interconnecting surface depressions. Slush columns were generally more common than slush walls, which were restricted to the steeper slopes. Slush columns were thicker than slush glands and, unlike slush glands, they extended downward from the surface beneath surface depressions. The tops of the majority of glands were found at ± 30 cm below the surface. The upper limit is thought to be controlled by temperature either directly through the presence of 0°C temperatures near the surface or indirectly through impedence by coarser textured material and more complex stratification of the near-surface zone. No evidence was noted to suggest either that ice glands formed preferentially before or after slush columns, or that the two were genetically related.

There was no apparent geometric spacing or arrangement of the surface depressions except on inclined surfaces where depressions were elongated parallel to the

*Department of Geology, University of Vermont, Burlington.

[1] Grain size terminology used in this paper is from the international classification of Schaefer, Klein, and de Quervain (1951).

slope. On steeper slopes the depressions were very elongated and interconnected forming a dendritic pattern. To determine the nature of the depressions, fluorescein dye was spread along a 15-m line normal to the slope of a snow-covered nunatak where these features were well developed. After three days, 17 pits were excavated to note the distribution of the dye which was no longer visible on the snow surface. No dye was observed immediately beneath the original dye line. Traces of dye closest to the original line were found in a 2-cm ice layer approximately 35 cm below the surface and 250 cm downslope. A show of dye continued beneath a long sinuous depression for 27 m to the base of the slope where dye became concentrated in an ice layer again, at a depth of about 35 cm. Although the extent of lateral water movement on gentler slopes undoubtedly would be much less than on the nunatak slope, the experiment showed that there is subsurface lateral movement of meltwater along restricted paths which have surface expression.

As suggested by Sharp (1951) and Benson (1962) surface depressions are caused by greater densification of the snow in the immediate region of the depressions than in the adjacent areas. On the Kaskawulsh Glacier the density of snow in columns under depressions was found to be as much as 0.115 g/cm^3 higher than that of adjacent snow. This density difference is due to greater free water content and more extensive diagenetic changes in the snow under depressions than in inter-depression areas. Near the surface, strata followed the pattern of surface downwarp; with increasing depth, however, their amplitude decreased, indicating that the downwarp of strata was accompanied by a cumulative effect of densification with depth.

The only changes which occurred during Stage 2 were an overall increase in the sizes of slush columns and surface depressions, and an increase in density and downwarp of strata in columns under depressions while lower rates of densification occurred in the area of glands under inter-depression zones.

Stage 3. In contrast to the rolling surface with conspicuous depressions described in Stage 2, the snow surface in Stage 3 was generally smooth except for scattered mounds 5 cm to 10 cm high and 20 cm to 100 cm wide. Although Stage 3 began about July 21, the transition between stages unfortunately was accompanied by a snow storm which effectively masked the snow depressions until after several days of melt action when mounds appeared on the surface. There was no evidence that the storm played an essential part in the sequence but instead seemed merely to bring about a temporary cessation of snow melt. The appearance and structure of the mounds characterized Stage 3, but the internal character of the snowpack was similar in both State 2 and Stage 3.

Although the transition was not observed, the following evidence is offered to demonstrate that the mounds of Stage 3 were located in the inter-depression areas of Stage 2. During Stage 3, ice glands were found consistently closer to the surface under mounds, whereas in Stage 2, ice glands were closer to the surface below inter-depression areas. In fact, after correcting for surface lowering in the intervening time period, the depth to the tops of the ice glands in Stage 3 coincided with the depth to the tops of glands in Stage 2. Furthermore, grain size was smaller and strata were domed below the mounds in Stage 3, similar to the conditions below inter-depression areas in Stage 2. Therefore, it seems likely that topographic and structural inversion had not occurred, but that the depressions and downwarped strata of Stage 2 corresponded to the topographic lows of Stage 3.

The change in the snow surface from conspicuous depressions to conspicuous mounds may have been caused by the lateral expansion of depressions accompanying growth of slush columns, by the geometric effect produced by lowering of the snow surface as illustrated in Figure 1, and by continuing lower rates of densification of snow beneath inter-depression areas.

Sharp (1951, p. 620) found mounds which were cored by the tops of ice glands. Similar features were noted by the writer only near the firn line on the Kaskawulsh Glacier. Presumably, melt action in the study area would, if continued, lower the snow surface and eventually expose ice glands. Sharp also noted elongated patterns of mounds on steep slopes which he thought were related to the depression patterns which preceded them. The depressions and mounds described by Sharp are similar to those observed by the writer. Mounds with ice cores at the surface may be produced by a late stage melt action down-slope from the area studied.

Summary and Conclusions

Where snow is subjected to sufficiently long and intense melt action, a sequence of both surface and subsurface events may be distinguished. Three events or stages were found on the Kaskawulsh Glacier in the summer of 1963. Stage 1, with layers and lenses of snow and ice, passed to Stage 2, with the appearance of ice and slush glands, slush columns, and surface depressions. The third stage was characterized by a surface of conspicuous

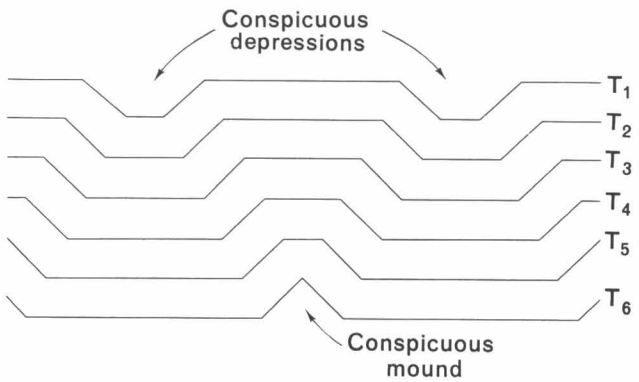

Fig. 1. Cross-sectional diagram illustrating the geometric effect of lowering the snow surface from T_1 to T_6 by equal increments in directions everywhere perpendicular to the snow surface. The result is a change from conspicuous depressions in T_1 (Stage 1) to conspicuous mounds in T_6 (Stage 3).

mounds. Although some melt occurred before and after the field study, the features described are probably representative for the melt season. Whether or not the evolutionary sequence is peculiar to the 1963 melt season and the Kaskawulsh Glacier is uncertain. By comparison with similar features described elsewhere, the sequence seems generally valid. Other areas, however, may well have a longer, shorter, or more or less complicated sequence. Similar features, though probably much more ephemeral, have been observed by the writer in mountainous areas in New England.

The sequence discussed reflects changes with time. It should be possible to find similar sequences with elevation and latitude as the independent variables. For example, if the range in elevation is sufficient, one should find the features of Stage 3 at lower elevations than the features of Stage 2, and Stage 2 features lower than those of Stage 1. Stage 1 features would be absent only where no melt diagenesis occurs or where melting occurs very rapidly. Perhaps the scheme outlined could be incorporated within the snow facies concept of Benson (1962). The recognition of surface forms might facilitate the recognition of facies where and when pit data are limited. For example, it appears likely that mounds with ice gland cores at the surface are restricted to the wetted facies.

Acknowledgments

The writer is grateful to Barry Nagle, Land Washburn, and Hugh Sellers for their assistance in the field; to the Arctic Institute of North America and American Geographical Society, and the American Alpine Club for grants supporting the 1962 and 1963 programs, respectively; and to Professor Donald F. Eschman, and Richard H. Ragle for reading the manuscript.

References

Ahlmann, H. W. (1935) The stratification of the snow and firn on Isachsen's Plateau, *Geogr. Annaler, 17,* 29 - 52.

Benson, C. S. (1962) Stratigraphic studies in the snow and firn of the Greenland Ice Sheet, *Res. Rept. 70,* U. S. Army Snow, Ice and Permafrost Res. Estab., 93 pp.

Glen, A. R. (1941) A sub-arctic glacier cap: the West Ice of North East Land, *Geogr. J., 98,* 65 - 76, 134 - 146.

Schaefer, V. J., Klein, G. J., and de Quervain, M. (1951) *Draft of an International Snow Classification,* Commission of Snow and Ice, Intern. Assoc. Sci. Hydrol., Brussels, 10 pp.

Sharp, R. P. (1951) Features of the firn on Upper Seward Glacier, St. Elias Mountains, Canada, *J. Geol., 59,* 599 - 621.

Snow Facies and Stratigraphy on the Kaskawulsh Glacier

W. Philip Wagner *

ABSTRACT. Measurements of snow temperature, density, hardness, accumulation, and stratigraphy were made during the 1963 melt season in the accumulation zone of the north and central arms of the Kaskawulsh Glacier, Yukon Territory, Canada.

The ablation facies extended from the glacier terminus at 810 m to the firn line at 1990 m. Temperature, hardness, and stratigraphic relationships located the saturation line, which separates wetted and percolation facies, between 2330 m and 2420 m. Significant melt occurred everywhere on the glacier; hence the dry snow facies was precluded.

In contrast, the variation of density with altitude, which was found to be gradational across the saturation line, as defined by temperature, hardness, and stratigraphic data, suggests that only one facies (the wetted facies) occurred everywhere in the accumulation zone. However, because density is not thought to be a useful parameter for separating wetted and percolation facies on the Kaskawulsh Glacier, the density data are rejected as a primary parameter.

It is concluded on the basis of temperature, hardness, and stratigraphy that both wetted and percolation facies were present. Thus the Kaskawulsh Glacier was subpolar in 1963.

Location and Method of Study

The area studied lies in the accumulation zone of the Kaskawulsh Glacier, one of five major valley glaciers that drain the Icefield Ranges of the St. Elias Mountains, Yukon Territory, Canada. Measurements of snow accumulation were made across the snow divide between the north arm of the Kaskawulsh Glacier and the Hubbard Glacier in 1962 and 1963 (Figure 1). At the peak of the 1963 melt season, measurements were made on the central arm along a 24-km traverse line extending from 1990 m at the firn line to 2760 m at the head. From July 29 to August 10, ram hardness was determined at 11 stations, and snow pits were excavated at five points along the central arm traverse line (Figure 1 and Table 1).

Firn temperature, density, and stratigraphy were measured in each of the pits. In three of the pits (Stations 3, 4, and 5), temperatures were determined with Fuess Thallium-Mercury liquid thermometers with a reading accuracy of ± 0.1°C. In the remaining two pits, temperatures were measured with mercury liquid thermometers with reading accuracy of ± 0.2°C. Densities were measured with 500-cc snow density tubes. Stratigraphic measurements and observations included depth and thickness of strata, grain roundness and sphericity, and grain size, using the international classification of snow grain size (Schaefer, Klein, and de Quervain, 1951). Annual accumulation on the north arm was determined by measurements of stake exposure in 1962 and 1963. A rough estimate of summer ablation was obtained by observations of stake exposure near Station 4 during 1963.

*Department of Geology, The University of Vermont, Burlington.

Stratigraphy

Because ablation exceeds accumulation during the summer, the annual stratigraphy (Figure 2) does not include a summer layer, but instead the summer season is represented by melt effects superimposed on the previous spring and winter snows. These melt effects, chiefly in the form

TABLE 1

Pit Station	Type of Observation	Elevation (m)
1	snow pit and ram hardness	1990
2	snow pit and ram hardness	2220
A	ram hardness	2260
B	ram hardness	2330
3	snow pit and ram hardness	2420
4	snow pit and ram hardness	2590
C	ram hardness	2630
D	ram hardness	2670
E	ram hardness	2700
F	ram hardness	2730
5	snow pit and ram hardness	2760

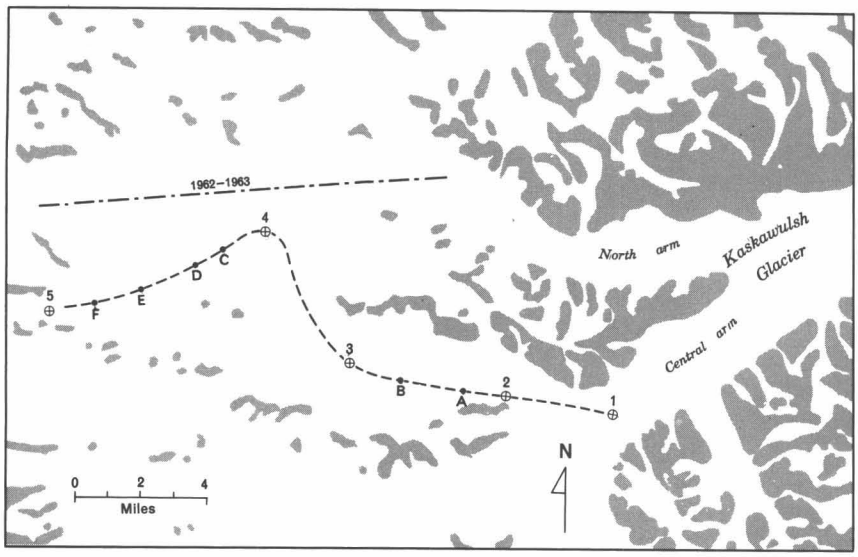

Fig. 1. Sketch map of study area showing locations of pit excavations (numbers) and ram hardness tests (letters) along 1963 traverse line. The approximate traverse line for the 1962 to 1963 measurement of stake exposure is also indicated. The shaded areas are nunataks.

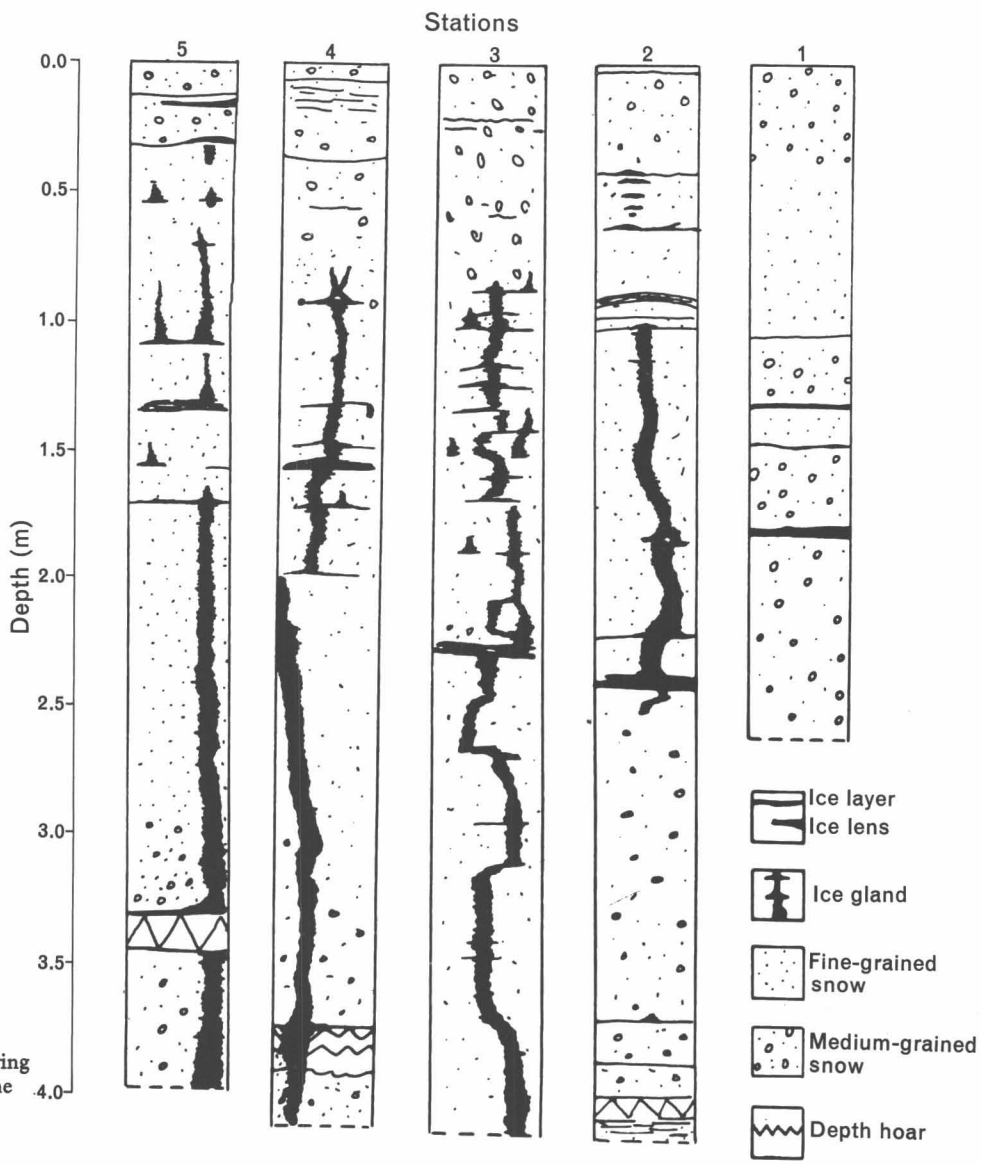

Fig. 2. Stratigraphic columns showing pit stratigraphies described in the text.

of warm, wet, medium-grained, and rounded snow associated with numerous thin ice layers and lenses, occur in the upper 40 cm at Stations 1, 2 and 5, and in the upper 80 cm at Stations 3 and 4. Not only are near surface ice layers and lenses thinner than those at greater depths, but many of those within approximately the upper 20 cm show a peculiar texture in which coarse, elongate grains are oriented parallel to each other, with the long axes predominantly vertical. Crude "thin-section" examination of a few of these layers under crossed polaroids suggests a preferred c-axis vertical crystallographic orientation. In contrast, none of the thicker ice layers at greater depths show this texture nor any preferred crystallographic orientation. More detailed study, in particular a fabric study, of such ice layers is needed for a full understanding of their significance. Thin ice layers with similar columnar textures also occur near the top of the previous budget-year snowpack; such layers may be stratigraphic markers of the tops of annual units.

Late fall, winter, and early spring snow strata are not individually distinguishable and are therefore considered as a single unit. These snows constitute the bulk of the annual accumulation. They are characterized by their stratigraphic position and fine grain-size, commonly 0.5 mm to 1 mm.

Late summer and early fall strata, which consist of medium-sized subrounded to angular grains, lie immediately below the finer grained, late fall, winter, and early spring snow.

The break between the 1962 and 1963 budget year was found as a zone marked by several features. Deformation attributable to oversnow traffic during the previous summer occurred at Station 4 as a distorted and broken, 2-cm thick ice layer at 390-cm depth. Depth-hoar layers, which probably marked the advent of cooler fall 1962 ambient air temperatures, approximately located the break at Stations 2, 4, and 5. Characteristically associated with the depth hoar layers were interbeds of thin ice layers with a texture like that of the near surface layers described above. Although depth hoar was absent at Station 1, several features may have marked the break between annual layers. The zone from 105 cm to 130 cm consisted of medium-grained, angular snow, interpreted as early fall snow. In addition, the upper 4 cm of this zone were dirty and probably marked the late summer 1962 surface. Dirty snow, which appeared at the bottom of the pit, probably represented the end of the 1961 budget year. The 1962–1963 break was below the base of the pit at Station 3.

In order to determine the 1962–1963 net winter accumulation, a pit was excavated at Station 4 early in the summer before any significant melt occurred. An estimate of net winter snow accumulation based on this pit is 430 cm (188 cm water equivalent). Because gross summer accumulation is roughly 10 cm water equivalent, gross annual accumulation is at least 198 cm water equivalent. Stake measurements at Station 4 indicate that approximately 40 cm (15 cm water equivalent) of surface lowering occurred from June 20 to July 29. This amount is taken to represent only the general magnitude of gross summer ablation and may be considerably in error. Considering the estimated amounts of gross summer accumulation and ablation, there appears to be very little net change in the summer. This is supported by comparison of pit measurements taken at Station 4 early in the melt season, which show 188 cm water equivalent, with measurements at the same place later in the melt season, which show 188.5 cm water equivalent. Estimates of net annual accumulation from the Pits 1–5 (Figure 1) of the Kaskawulsh Glacier are given in Table 2. These are minimum estimates because contributions from ice masses are not considered and because some melt water collects in the firn of the previous budget years.

During 1962, 45 stakes were placed along a nearly east-west traverse line extending along the north arm of the Kaskawulsh Glacier and across a snow divide into the arm of the Hubbard Glacier (Plate 1)[1]. Measurements at most of these stakes on June 24, 1962 and June 24, 1963 provide general information on the magnitude and variation of accumulation. Figure 3 shows accumulation at each stake along the traverse line. Curve A represents the 1962 topographic profile of the snow surface as determined by survey triangulation (unpublished data). Curve B shows the differences in 1962 – 1963 stake heights above the snow surface; the stipled area thus approximately represents the thicknesses of the annual layer. Clearly, accumulation is greater on the eastern side of the divide than on the western side. Curve C in Figure 3 depicts the variation of accumulation in water equivalents along the traverse line. Maximum accumulation occurs approximately 6.4 km east of the divide. Accumulation of drift snow in the lee of the divide probably accounts for the marked difference.

TABLE 2. Net Annual Accumulation

Station No.	Thickness of Annual Layer (cm)	Mean Density (g/cm^3)	Water Equivalent (cm)
1	120	0.153	61.6
2	400	0.515	206.0
3	420	0.500	210.0
4	380	0.496	188.5
5	340	0.475	161.5

Snow Facies

The facies concept. On the bases of snow density, temperature, hardness, and stratigraphy, a snow cover is divided into four facies which reflect the variation of melt season intensity and duration with elevation on a glacier. Figure 4 shows diagrammatically the distribution of facies. The ablation facies which occurs below the firn line is characterized by complete removal of the snow of the current budget year. The wetted facies extends from the firn line to the saturation line, located at the intersection of the 0°C isotherm with the top of the previous annual

[1] Plate 1 is a map inside the back cover of this volume.

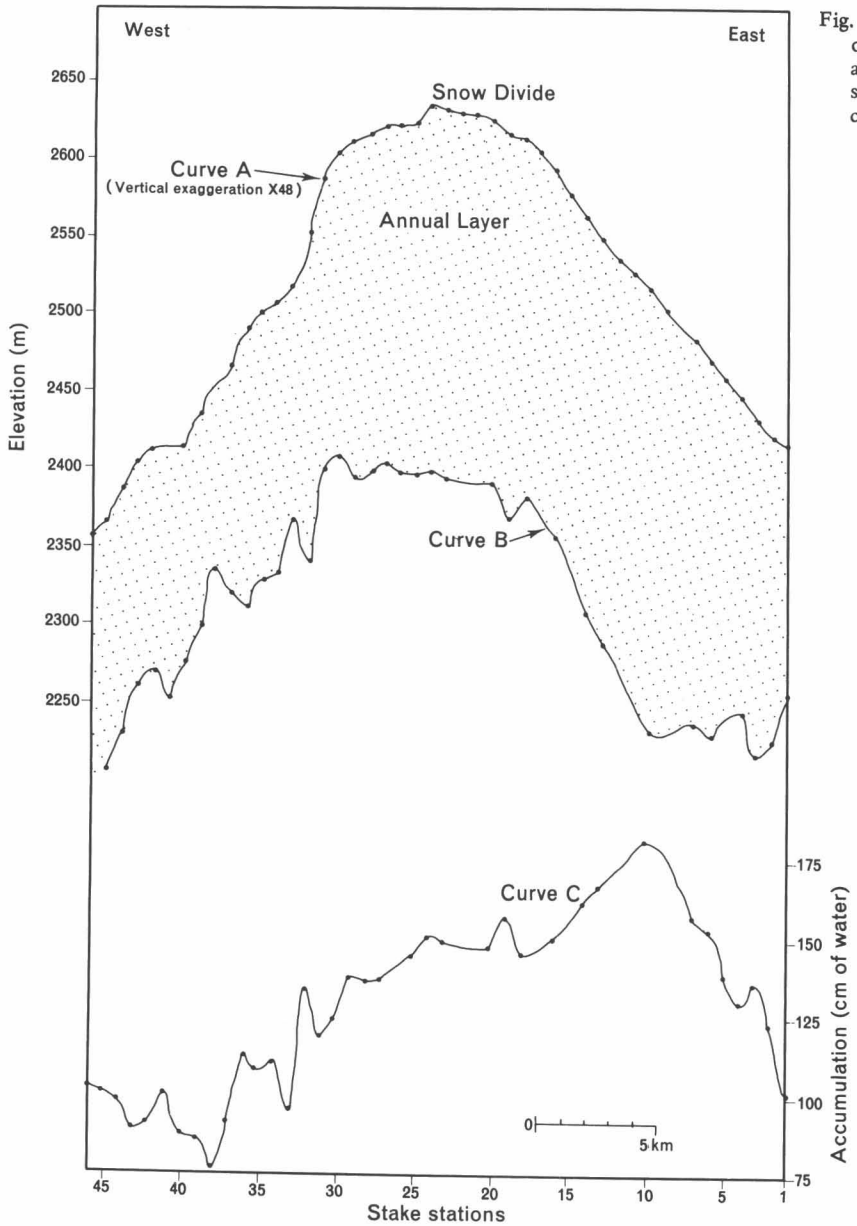

Fig. 3. Curve A is a topographic profile of the 1962 snow surface; Curve B is a topographic profile of 1963 snow surface; Curve C is accumulation in centimeters water equivalent.

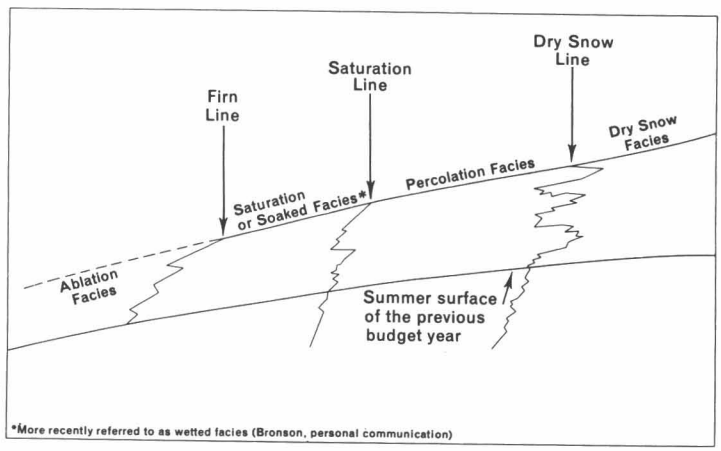

Fig. 4. Diagrammatic cross section of a glacier showing the distribution of snow facies according to the terminology of Benson (1962, Fig. 15).

layer; all of the snow in this facies is warmed to the melting point and becomes wetted. In the percolation facies, only the top part of the annual increment of snow is wetted and warmed to 0°C. The upper limit of the percolation facies is the dry snow line, located where the −5°C isotherm intersects the snow surface at the peak of the melt season.

General nature of facies on the Kaskawulsh Glacier. Before the results of the various measurements are considered, some general conclusions can be made. In 1963 the ablation facies extended from the glacier terminus at 810 m to the firn line at 1990 m. Because significant melting occurred even at the highest altitudes in the area studied, the dry snow facies was not present. Therefore, whether or not the saturation line crosses the area must be determined.

Facies in terms of temperature. Temperature variation with depth for each of the snow pits is presented in Figure 5; the location of the top of the previous budget year is indicated. At Stations 1 and 2 all of the snow in the annual layer was warmed to 0°C. However, in the pits at higher elevations, part of the annual layer retained some of the previous winter cold wave. The 0°C isotherm intersected the top of the 1962 annual layer between Stations 2 and 3. Thus the saturation line crossed the area between these two stations, or between elevations of 2220 m and 2420 m.

Facies in terms of ram hardness. Ram hardness tests were made at each of the 5 pit sites, and at 6 other sites between the pits. Hardness values were computed using the formula (Haefeli, in Bader *et al.,* 1939, p. 129):

$$R = (qQ+P) + \frac{Phn}{x},$$

Where

R = ram hardness in kg-force
q = the number of meter rods
Q = the weight of 1 rod (a constant considered equal to 1)
P = weight of hammers (1 or 3 kg)
h = height from which hammer is dropped (5—50 cm)
n = number of times the hammer is dropped per depth interval, Δx
x = penetration of the rod assemblage in centimeters

Variation of R values, with depth, at each of the ram test sites is shown in Figure 6. In general, the higher R values represent either ice or icy layers, or compact, cold snow. R values commonly increase with increasing elevation, reflecting the variation of intensity and duration of melt with increasing elevation.

In order to facilitate interpretation, Benson (1962, pp. 62-63) integrated his data. The depth intervals, Δx, are multiplied by their associated R values. The cumulative summations of products, $\Sigma R \Delta x$, in units of kg - force - cm (approximately equivalent to 10^{-3} joules), for depth intervals of 0 to 100 cm, 0 to 200 cm and 0 to 260 cm at each station are plotted in Figure 6 as dashed lines. The $\Sigma R \Delta x$ values for the 0 to 100 cm interval are consistently low. The general lack of variation with elevation indicates that the upper 100 cm of snow has everywhere approached a lower limit of resistance to penetration. The values for the 0 to 200-cm depth-interval are more variable, generally increasing with elevation. Snow at higher elevations has lower temperatures and has undergone lesser melt action in the 100 to 200-cm depth-range than snow at lower elevations. The $\Sigma R \Delta x$ values for the 0 to 260-cm interval are consistently high from Station 5 to Station 3, with a mean of 39,091 kg - force - cm, whereas below Station 3, the values are consistently low and average 16,472 kg - force - cm.The difference in $\Sigma R \Delta x$ values is caused by a marked increase in hardness at 200 to 260 - cm depth between Station 3 and the next lower ram hardness site (Figure 6). At this depth in the pits at Stations 3, 4, and 5, there is dry, fine-grained, relatively unaltered winter snow, whereas in the pits at lower elevations, the snow is medium grained and wet. Benson (1962, p. 65, Figure 42) shows that in 1953 in Greenland the $\Sigma R \Delta x$ values for the 0 to 100 - cm depth interval increase rather abruptly in passing from soaked to percolation facies. The difference appears to be on the order of 2000 kg-force-cm. By comparison the change in $\Sigma R \Delta x$ values on the Kaskawulsh Glacier appears significant. It is therefore interpreted as a facies change between the wetted and percolation facies, with the saturation line between elevations of 2420 m and 2330 m.

Facies in terms of density. Because density increases with increasing intensity and duration of summer melt, firn densities are generally higher in the wetted facies than in the percolation facies. Benson (1962) compared facies on the bases of: (1) average density in the upper 5 m; (2) load at 5-m depth; and (3) rate of load increase with depth.

From measurements in Greenland, upper Seward Glacier, Yukon Territory, and the Snow Dome, Mt. Olympus, Washington, Benson (1962, p. 71) lists the range of average density values in the upper 5 m for each of the facies. His values are given in Table 3. Densities obtained in five snow pits in the Kaskawulsh Glacier are given in Table 4. All the density values are higher than Benson's upper limit for the percolation facies. Stations 4 and 5 have averages slightly below the lowest limit for the soaked facies. Because the measurements do not include estimates for the water equivalent of ice masses, and because the depth intervals do not reach 5 m,it is felt that the values reported here are minimum estimates. The 1962 measurements at Station 4 give an average that is within the range for the soaked facies. Although all of the average densities are near the lower limit of the soaked facies, all are significantly higher than the upper limit of the percolation facies. Accordingly, these figures are interpreted as indicating that all of the area is within the soaked facies. However, Stations 4 and 5 may lie within a transition zone between percolation and soaked facies.

According to Benson (1962, p. 73) the load at 5-m depth varies between facies, as given in Table 3. Load values at 5 m for the Kaskawulsh Glacier stations, extrapolated from the curves in Figure 7, are given in Table 4. By comparison with Benson's data, the soaked facies is again indicated.

Cursory examination of depth-load variations suggests that the rates of load increase with depth are not markedly

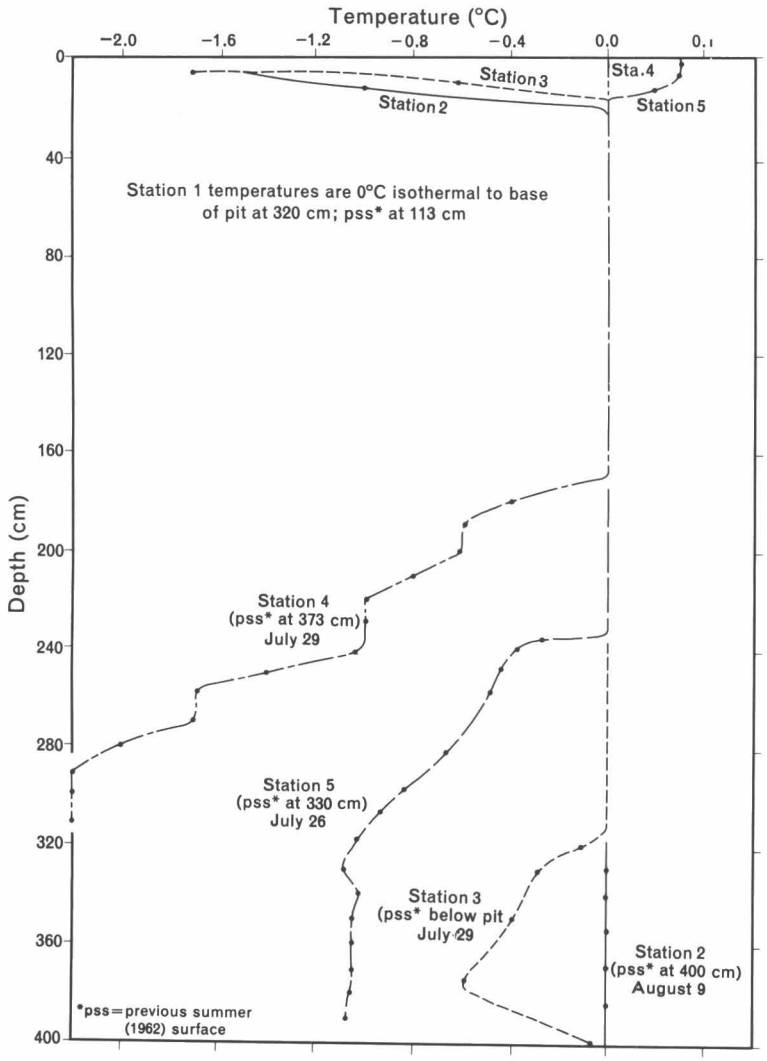

Fig. 5. Depth – temperature relations at pit stations during summer 1963.

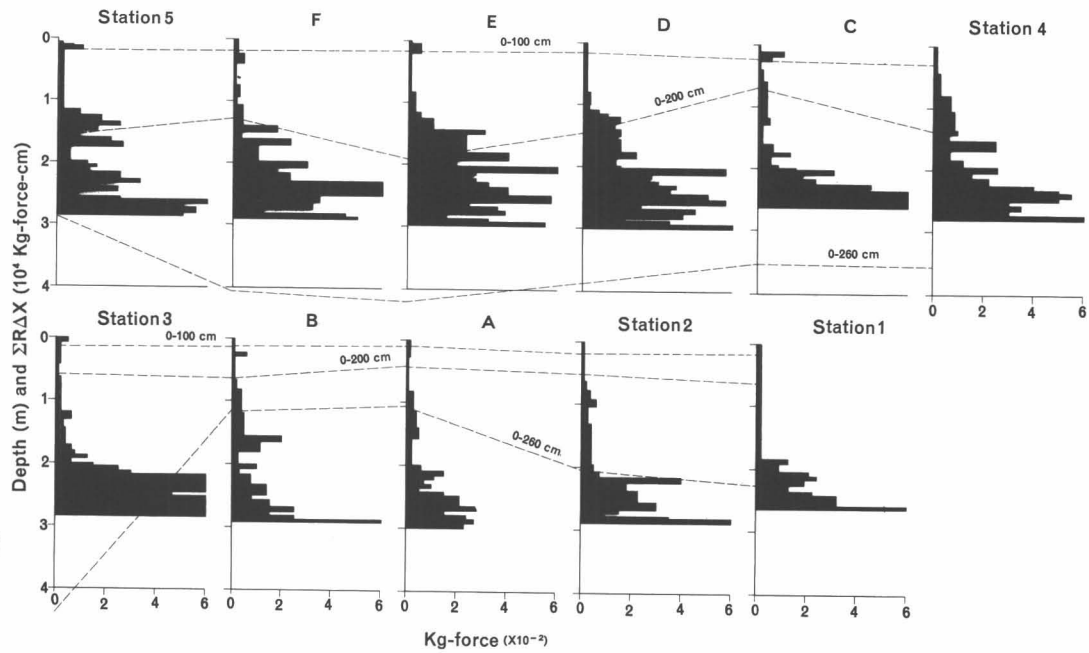

Fig. 6. Ram hardness R values (histograms) and $\Sigma R \Delta x$ values (dashed lines).

different between stations, and are similar to rates in the wetted facies. This can best be demonstrated by correlation and regression analyses. Results of these analyses, listed in Table 5, serve to substantiate the evidence for the occurrence of only the wetted facies. Using the data in Table 5, regression lines for each station are shown in Figure 7. For comparison, a curve representing Benson's (1962, Figure 45) expected lower limit of rate of load increase with depth for wetted facies is shown. Each of the Kaskawulsh stations has a rate of load increase with depth greater than Benson's curve. This suggests the wetted facies. In addition, if the slopes (B values in Table 5) are compared, along with their associated confidence intervals, no significant differences, necessary for separation of facies, exist at the 95% confidence level. The data and analyses for Station 1 are inconclusive due to too few observations and therefore are not included in Figure 7. An underlying assumption necessary for the validity of the interpretations of the data in Table 5 is that the depth-load variation is rectilinear. Although it is not exactly rectilinear, this assumption seems justified by the strikingly high correlation coefficients (Table 5).

In contrast to temperature, ram hardness, and stratigraphic evidence, density data suggest only one facies, interpreted as wetted facies by comparison with Benson's data from Greenland and elsewhere. The difficulties arise in part as a consequence of the nature of the parameters themselves. The saturation line is located, by definition, where the 0°C isotherm intersects the upper snow surface of the previous budget year. As the 0°C isotherm is a

TABLE 3. Facies Densities and Load Values According to Benson (1962)

Facies	Av. Density in upper 5 m (g/cm^3)	Load (g/cm^2)
wetted	>0.500	240 – 300 and above
percolation	0.430 to 0.390	200 – 225
dry-snow	<0.375	175 – 200

TABLE 4. Pit Densities and Load Values, Kaskawulsh Glacier

Pit Station	Depth Interval (cm)	Av. Density (g/cm^3)	Load (g/cm^2)
1	0 – 169	0.513	262
2	0 – 420	0.515	258
3	0 – 320	0.517	248
4	0 – 400	0.496	257
4 (1962)*	0 – 500	0.501	250
5	0 – 380	0.475	236

*Measured by the writer in 1962, approximately 10 m from the 1963 snow pit.

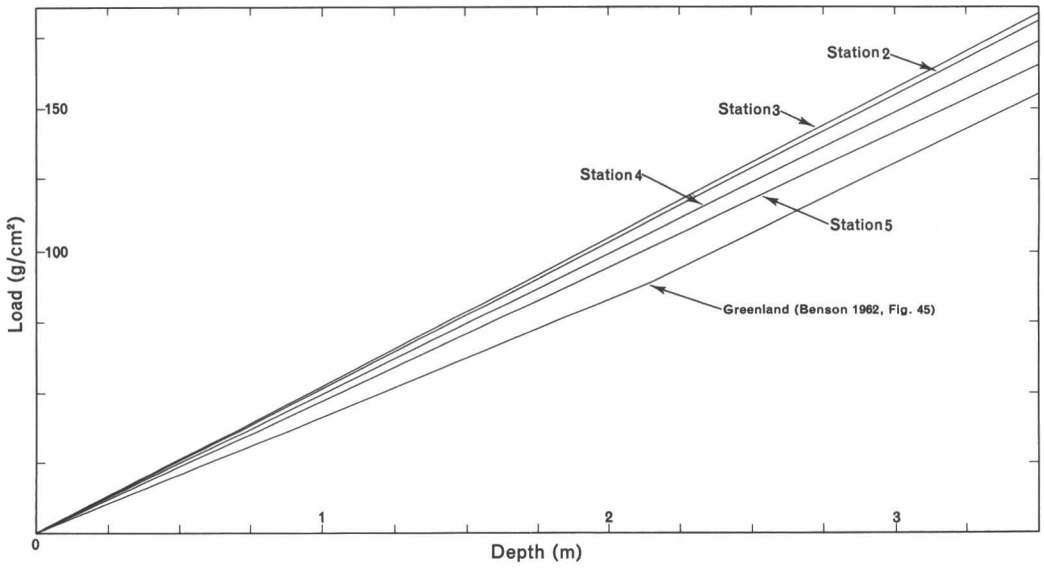

Fig. 7. Regression lines for depth-load variation at pit stations. Curves have been determined from the data in Table 5.

TABLE 5

Pit Station	N	R	<R>	A	B	<B>
1	15	0.636	0.184 to 0.866	12.66	0.306	0.305 to 0.916
2	40	0.995	0.991 to 0.997	0.965	0.519	0.462 to 0.576
3	32	0.997	0.993 to 0.998	1.41	0.516	0.439 to 0.592
4	40	0.995	0.990 to 0.997	−0.590	0.495	0.447 to 0.542
5	37	0.992	0.984 to 0.996	0.420	0.469	0.427 to 0.511

N = number of observations
R = correlation coefficient
<R> = 95% confidence interval on R
A = y intercept of regression line
B = slope of regression line
<B> = 95% confidence interval on B

more or less planar surface, the transition between percolation and soaked facies, that is, the intersection of two fairly planar surfaces, is a line. Ram hardness values, which are in part a function of temperature as discussed by Benson (1962, pp. 63–67), also reflect the position of the saturation line as a fairly sharp break. On the other hand, the saturation line as located by density variations may be a relatively broad transition zone rather than a definite line. Although the difference in amounts of melt above and below the saturation line may produce a grouping of densities as stated by Benson (1962, p. 67) or, in other words, a grouping of rates of load increase with depth, and of density and load values at 5-m depth, a definite break or gap between the groups is not necessary. As a consequence, the saturation line determined by densities may be a zone of gradational density changes. Thus density measurements on valley glaciers such as the Kaskawulsh, where pit stations are necessarily spaced fairly closely and do not span a wide range in elevation, may not exhibit a grouping of densities, but instead show insignificant variations. Furthermore, if the location of the saturation line by temperature, hardness, and stratigraphy is accepted, then the values of density and load at 5 m, and the rates of load increase with depth on the Kaskawulsh Glacier are not comparable with the values from Greenland and elsewhere.

It should be noted that part of the difficulty with the density data may be due to the shallow depths sampled. It is possible that deeper density measurements might demonstrate a facies boundary. Unfortunately, because of the thickness of the annual layer and the short field time available, deeper measurements were not possible.

Conclusions. The central arm of the Kaskawulsh Glacier may be divided into three facies, ablation, wetted, and percolation. The ablation facies extends from the glacier terminus at 810 m to the 1963 budget year firn line at 1990 m. Measurements of snow temperature, hardness, and stratigraphy located the saturation line separating wetted and percolation facies between 2330 and 2420 m. Density measurements do not agree with these interpretations for reasons discussed.

According to Benson's (1962, p. 73) refinement of Ahlmann's (1948) glacier classification, the Kaskawulsh Glacier is a subpolar type. From previous experience in the area, Richard Ragle (1964, personal communication) feels that melt seasons in 1962 and 1963 were similar. In 1961 and 1964, however, the melt seasons were shorter and/or less intense. In view of the location of the 1963 saturation line near the highest elevation of the glacier, it is likely that in 1961 and 1964 the saturation line passed above the glacier surface. Thus the saturation and ablation facies included all of the glacier. In some years, therefore, the Kaskawulsh Glacier would be classified as temperate, and in other years subpolar. Perhaps the glacier is neither typically temperate nor subpolar in any year, but intermediate.

Acknowledgments

The author is grateful to the American Alpine Club for financial assistance, and to Richard Ragle for his advice in the field. Land Washburn lent full-time assistance, and many others helped part time. Dr. Louis I. Briggs assisted the writer in programming the density data; execution of the program was handled by the University of Michigan Computer Center. Dr. Carl S. Benson, Dr. Donald F. Eschman, James M. Havens, and Richard H. Ragle read the manuscript.

References

Ahlmann, H. W. (1948) Glaciological research on the North Atlantic coasts, *Roy. Geogr. Soc. Res. Ser.*, No. 1, 83 pp.

Bader, H., Haefeli, R., Bucher, E., Neher, J., Eckel, O., and Thams, Chr. (1939) Snow and its metamorphism, transl. of Der Schnee und seine metamorphose, *Beitr. Geol. Schweiz, Geo-techn. Ser., Hydrol., Lief. 3,* Bern, *Transl. 14,* 1954, U.S. Army Snow, Ice and Permafrost Res. Estab., Corps of Engineers.

Benson, C. S. (1962) Stratigraphic studies in the snow and firn of the Greenland Ice Sheet, *Res. Rept. 70,* U.S. Army Snow, Ice and Permafrost Res. Estab., 93 pp.

Schaefer, V. J., Klein, G. J., and de Quervain, M. (1951) *Draft of an International Snow Classification,* Commission of Snow and Ice, Intern. Assoc. Sci. Hydrol., Brussels, 10 pp.

O^{18}/O^{16} Ratios in Snow and Ice of the Hubbard and Kaskawulsh Glaciers*

D. S. Macpherson† and H. R. Krouse‡

ABSTRACT. One hundred samples collected from the Hubbard and Kaskawulsh Glaciers in the St. Elias Mountains during the summer of 1963 were analyzed for O^{18}/O^{16} content. The δ_{18} values ranged from −18 to −29, with an average of about −23. Pits that were studied before extensive melting showed definite trends in δ_{18}, with the more negative values corresponding to winter precipitation. Pits studied later in the season had the seasonal trend masked by the action of downward percolating meltwaters. The average of all pits and boreholes studied above the firn line gave no indication of an altitude variation of δ_{18} larger than the sampling error. A longitudinal profile below the firn line showed much scatter in the δ value, but the average trend was a decrease in δ_{18} in going down-glacier from the firn line to the terminus. A transverse profile below the firn line which sampled three main ice streams gave remarkably consistent values of δ near the margins, whereas the stream centers had decidedly more positive or negative δ values. These results are considered in terms of accepted modes of glacier flow. Precipitation studies exhibited much scatter and did not show the expected altitude variation of δ. Comparison of the over-all data with that of other workers shows a number of consistencies. This comparison also suggests that much of the precipitation in the area is derived from the Pacific Ocean rather than from inland sources.

Introduction

Although fractionation of isotopic species of water can occur in a number of physical, chemical, and biological processes, the most extensive alteration arises during repeated condensation and evaporation of surface waters. In this case, the fractionation is due to the different vapor pressures of the isotopic water molecules. For vapor and liquid in equilibrium, the vapor phase is enriched in the lighter isotopic species.

The most important isotopic components of water are H_2O^{16}, HDO^{16}, and H_2O^{18}. The first two are examined experimentally by measuring H/D ratios, whereas the first and last are examined by measuring O^{18}/O^{16} ratios. For the most part, the deuterium and O^{18} concentrations vary parallelly, the fractional separation for deuterium under conditions of fresh precipitation being about 8 times that for O^{18} (Friedmann, 1953; Craig, 1961a; Dansgaard, 1964). Under conditions of significant evaportation, however, the separation factor for deuterium may decrease to about 5 times that of O^{18} (Craig *et al.*, 1956; Craig *et al.*, 1963; Dansgaard, 1964).

In this study, only O^{18}/O^{16} variations were measured. Following the format of other workers, the relative O^{18} content is expressed in terms of a δ value, where

$$\delta_{18} = \left[\frac{(O^{18}/O^{16})_{\text{sample}}}{(O^{18}/O^{16})_{\text{standard}}} - 1 \right] \times 1000$$

The commonly used standard is designated SMOW (standard mean ocean water). A standard sample of SMOW does not exist physically, but its O^{18}/O^{16} ratio is the mean of a large number of ocean samples. SMOW has been related to a physically obtainable water standard, NBS–1 (Craig, 1961b).

Epstein and Mayeda (1953) found that the oceans had a fairly uniform O^{18}/O^{16} ratio with the exception of locations near mouths of fresh continental streams. These locations had more negative δ values. Epstein and Mayeda likened the general meteorological isotope fractionation to a several stage distillation column. Fresh water depleted in O^{18} is being continually evaporated from oceanic waters and being lost to the ice regions of the world. In the absence of remixing, this results in δ_{18} becoming more negative with increasing latitude. Such a trend is retained in continental waters and glaciers (Sharp, 1960), the δ value of precipitation at the south pole being as low as −50 (Epstein and Sharp, 1959b). Circulation tends to maintain the oceanic waters at a constant O^{18}/O^{16} ratio with the exception of locations receiving continental fresh water contributions.

These general conditions are further perturbed by local variations. Dansgaard (1954) has demonstrated that the O^{18} abundance of atmospheric vapor depends on the origin of the vapor, the precipitation temperature, and the cooling of the vapor during circulation. For any single precipitation, the O^{18} content depends on the condensation temperature, cooling since the beginning of the condensation, and evaporation during the fall of the precipitation.

It is expected that, since the temperature gradient between the source and the precipitation area varies with season, the δ value of the precipitation should also vary. This variation has been demonstrated by monitoring precipitation (Dansgaard, 1954; Epstein, 1956; Dans-

*This report has previously appeared in *Isotope Techniques in the Hydrologic Cycle,* edited by Glenn E. Stout, *Geophysical Monograph No. 11,* American Geophysical Union, 1967, pp. 180 – 194, and is reproduced here with permission.

†Department of Geology, University of Alberta, Edmonton, Canada at time of writing. Now at Mobil Oil Canada Ltd., Calgary, Alberta.

‡Department of Physics, University of Alberta, Edmonton, Canada.

gaard, 1964) and by examining the record preserved in glaciers (Epstein and Sharp, 1959a; Gonfiantini *et al.*, 1963). A more negative δ value is associated with a larger temperature gradient or winter precipitation. Considering an air mass that has just picked up water vapor, the δ_{18} of the water vapor would typically be -8 with respect to the source water at 25°C. Any immediate precipitation would have the same O^{18}/O^{16} composition as the source. As the air mass moves, it preferentially deposits water enriched in O^{18} compared with the vapor or leaves the vapor reservoir depleted in O^{18}. Because of this reservoir effect, the precipitation at some later time is quite deficient in O^{18} compared with the source. This depletion will be greatest for the largest temperature gradient between the source and precipitation point. Further depletion of O^{18} results from the dependence of δ on temperature. Reisenfeld and Chang (1963) found that the value for the fractionation factor $\alpha = (H_2O^{18}/H_2O^{16})_{\text{liquid}}/(H_2O^{18}/H_2O^{16})_{\text{vapor}}$ decreased from the value 1.010 at 0°C to the value 1.005 at 100°C. Since the largest temperature gradient between the source and the precipitation point implies a minimum in temperature at the precipitation point, the depletion in O^{18} is enhanced by the temperature dependence of α. Seasonal effects based on these principles are generally more pronounced at higher latitudes because of greater temperature fluctuations.

Consistent with the above description, it is found that the δ value decreases with increasing altitude (Dansgaard, 1954; Sharp *et al.*, 1960).

Expected variations of the O^{18}/O^{16} ratio on an idealized valley glacier will now be considered. The accumulation area at upper altitudes is characterized by snow precipitation greatly exceeding summer melting. Farther down the glacier, the summer melting exceeds snowfall and, as a result, is called the ablation area. As melting progresses in summer, the line that separates these two areas (the firn line) recedes gradually upglacier. The highest position reached by the firn line is termed the 'firn limit.'

If homogenization processes were not present in the accumulation area, two effects should be evident. The δ value should decrease with altitude and evidence of seasonal variation should be preserved. In some pit studies, such as those conducted in Greenland and Antarctica (Epstein and Sharp, 1959b; Gonfiantini *et al.*, 1963), the seasonal variation in δ was found to persist for many years, whereas in more temperate glaciers the seasonal variation has been partly masked by homogenization processes such as downward percolation of meltwaters (Epstein and Sharp, 1959a; Sharp *et al.*, 1960).

The mechanics of glacier flow were discussed very early in the history of glaciology by Reid (1896). Because of its simplicity, Reid's theory has been used to interpret results of contemporary O^{16}/O^{18} studies of glaciers. The essential aspects of his description are shown in Figure 1. According to his theory, snow from the upper parts of the accumulation area should eventually

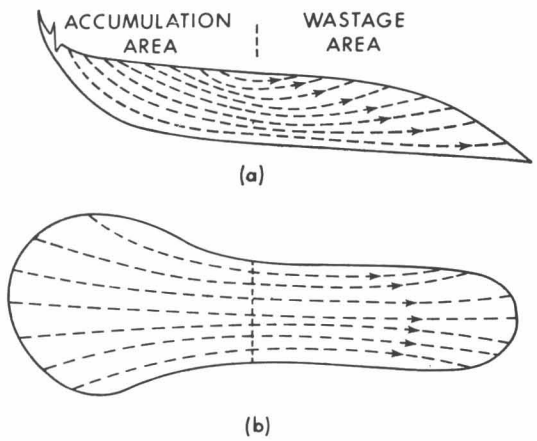

Fig. 1. Idealized valley glacier flow (after Reid, 1896): (a) vertical profile; (b) horizontal profile.

appear at the surface near the terminus, whereas snow deposited just above the firn limit will appear at the surface immediately below the firn limit. On this basis, an 'inverse' altitude effect in the δ value should be found below the firn limit. Such an increase in the δ value with altitude below the firn limit has been found in the Saskatchewan and Blue Glaciers (Epstein and Sharp, 1959a; Sharp *et al.*, 1960).

The variation of the δ value in a transverse profile of an ice stream below the firn line is subject to many factors. A predominant factor is the shape of the surface of the accumulation area. If the surface is bowl-shaped, it would be expected on the basis of the flow lines in Figure 1b that the stream center would arise from a lower altitude than the stream edges. In this case, the center should have a more positive δ value in comparison with the stream edges. Other topographical shapes of the accumulation area may possibly give the opposite trend in the δ value.

There is also the variation of flow velocity with transverse position. Other workers suggest that the slower velocities of the margins of the stream give rise to greater ablation, exposing deeper ice which had its origin at higher altitudes. On this basis, it is expected that the stream margins will have a more negative δ value than the stream center. This argument has been suggested by Epstein and Sharp (1959a) and Sharp *et al.*, (1960) to account for the results obtained with transverse profiles on the Saskatchewan and Blue Glaciers.

General Description of the Glacier System

The Hubbard and Kaskawulsh Glaciers form part of the Icefield Ranges of the St. Elias Mountains (Plate 1[1]). The Kaskawulsh lies near the Alaska-Yukon border and flows toward the interior plateau from a snow catchment basin located to the north of Mount Queen Mary (Figure 2). It forms the source of the Slims River which flows

[1] Plate 1 is a map inside the back cover of this volume.

northward across the Alaska Highway into Kluane Lake. The adjoining Hubbard Glacier flows southward into Yakutat Bay and the Gulf of Alaska. Plate 1 also shows the Malaspina and Seward Glaciers in the same general area, which have been previously studied isotopically (Epstein and Sharp, 1959a).

The accumulation area, examined in this study, was common to two main tributaries of the Hubbard and Kaskawulsh Glaciers. This snow catchment basin is located at longitude 139°40'W, latitude 60°45'N and it ranges in altitude from 2100 to 2700 m.

Glaciological investigations carried out during the summers of 1962 and 1963 have been reviewed by Wagner (1963) and Wood (1963). The Kaskawulsh is described as a temperate valley glacier existing at the pressure melting point and is therefore isothermal throughout the budget year. The glacier is approximately 80 km (~50 miles) long from its geographical divide with the Hubbard Glacier and varies in width up to 6 km, depending on the number of tributaries entering the main stream. The three major contributaries are described as the north, central, and south arms. The north and central arms extend from the snow catchment basin mentioned above; the south arm extends from a separate accumulation area to the southeast. No major ice falls impede the flow of the glacier. Seismological evidence indicates that the average thickness is more than 800 m, and flow data suggest that the north arm moves at a rate of about 100 m per annum.

The general area is characterized by a combination of a cold marine climate, on the slopes bordering the Gulf of Alaska, and a dry cold climate that dominates the interior plateau. The extent to which the moist Pacific air penetrates the St. Elias Mountains is not known, but the large annual accumulation of snow suggests that the Hubbard and Kaskawulsh Glaciers are products of deposition of H_2O derived from the Pacific Ocean.

Havens and Saarela (1964, and pp. 17–22 of this volume) have published a summary of meteorological data for the summer of 1963 which showed occasional intrusions throughout the accumulation season of the cold dry air from the interior plateau. The predominant wind direction was, however, from the south and west throughout the period of observation.

Sampling and Analysis

The field camp for the summer of 1963 has been described by Ragle (1964). It was situated a few miles to the Kaskawulsh side of the geographical divide separating the Hubbard and Kaskawulsh systems and was supported by a base camp at Kluane Lake.

Elevations quoted for the various sampling locations are taken from the St. Elias map sheet of the Yukon Territory published by the Department of Mines and Technical Surveys of the Dominion Government (1961). Approximate elevations above sea level of sites on the Kaskawulsh Glacier are as follows:

Terminus	920 m
Firn Limit	2000 m
Upper camp (Divide Station A)	2500 m
Meteorological station (Divide Station B)	2600 m

Sampling began as soon as logistics permitted the

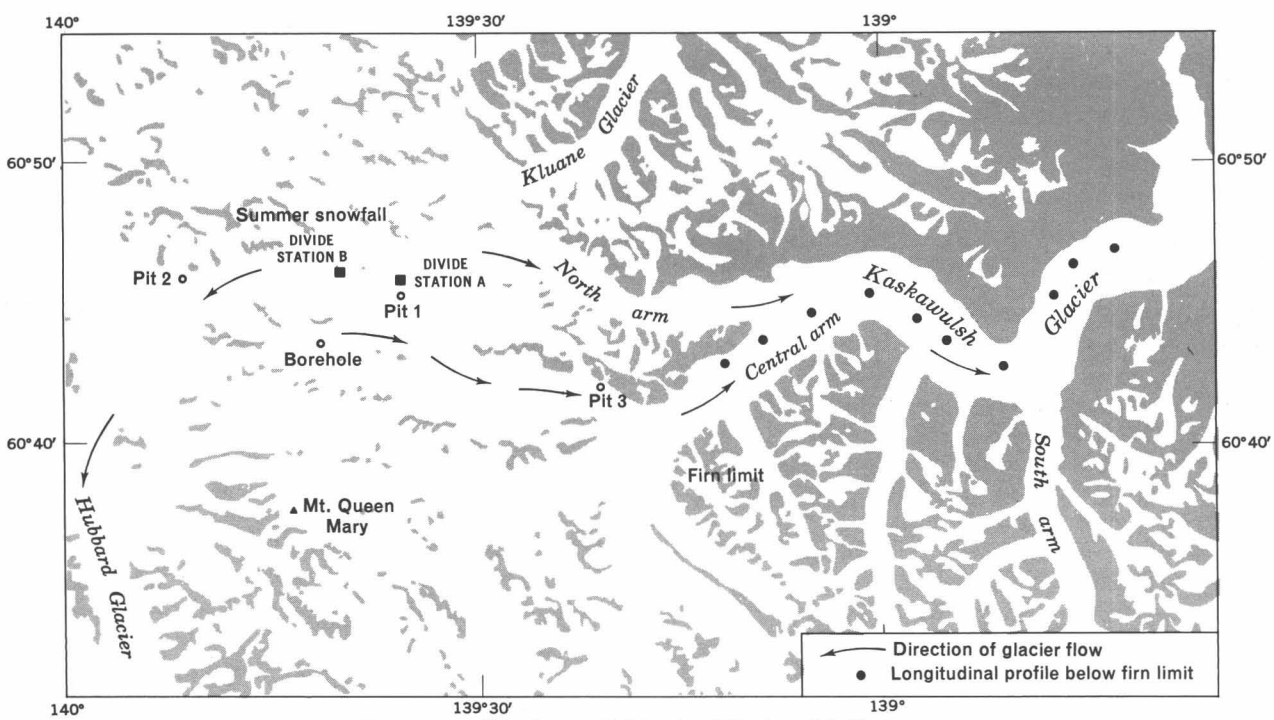

Fig. 2. Sampling sites on Hubbard and Kaskawulsh Glaciers.

establishment of a camp on the glacier. The first samples were taken shortly after the melt season had started as was indicated by the presence of a few ice layers in the first glaciological pit dug on June 20, 1963. Sampling was continued until August 28, 1963, when colder weather suggested that the height of the melt season was over. Pit studies and the down-glacier sample profiles were made with the following purposes in mind:

(1) A study of seasonal variations of the O^{18}/O^{16} ratio
(2) A study of the effects of downward percolation of meltwaters on the O^{18}/O^{16} variations found in (1)
(3) A study of the variation of the O^{18}/O^{16} ratio with altitude in recent precipitation
(4) Studies in the use of the O^{18}/O^{16} ratio as a natural tracer of glacier flow

The sampling sites are shown in Figure 2. Pits were dug at night to avoid melting during the snow sampling. In each case, the depth extended past the previous summer's surface as evidenced by the stratigraphy and density of the various snow layers. Horizontal cores of snow were taken from the side of the pit with an aluminum tube (1-in. ID by 20-in. length). Plastic sample bottles were filled to the top and indented before capping to check on whether the bottles remained airtight.

Sampling of hard ice below the firn line presented problems. Owing to the heavy accumulation during the winter, snow near the 1963 firn limit was completely saturated with water, making sampling impossible. Therefore, collection of samples of hard ice was started 2 miles down-glacier from the firn limit. The Kaskawulsh Glacier is not heavily crevassed, thus simplifying down-glacier travel. Meltwater streams made it necessary, however, to choose slightly elevated areas as sample sites. The technique used was to chop away the dirty surface ice, making a basin 1 foot in diameter and a few inches deep. Clean and relatively dry ice chips were removed from the bottom of the basin. Since Sharp *et al.*, (1960) found systematic variations in the O^{18} content of the different types of ice, only coarse-bubbly ice was sampled to avoid introducing more variables into the interpretation of results.

Summer snowfall samples taken on July 7, 1963 were collected by fashioning an aluminum foil funnel and mounting it on a support, so that water from the wet snow would drip into the bottle upon melting. Evaporation losses were considered negligible.

The O^{18}/O^{16} ratios of the samples were obtained by analyzing CO_2 mass spectrometrically. The method consisted of equilibrating the water sample with purified industrial CO_2 in a fashion similar to methods described by Epstein and Mayeda (1953) and Dansgaard (1961). A drop of dilute HNO_3 was added to 25 ml of the water sample to lower the *p*H and facilitate rapid equilibration (Urey and Mills, 1940). The sample was frozen with a solid CO_2-alcohol bath and evacuated to remove trapped CO_2 and air. The sample was allowed to come to room temperature to further release trapped CO_2, refrozen, and again evacuated for a short time. It was then brought to room temperature again and the CO_2 admitted to a pressure of slightly less tham atmospheric. The bulb with attached breakseal was removed and taken to a water bath thermostatically regulated to 25°C. The bulbs were shaken frequently over the period of equilibration to avoid permanent condensation of water droplets on the walls of the vessel. After three days of equilibration, CO_2 was removed in the breakseal.

In order to relate the measured O^{18}/O^{16} ratios to SMOW, a sample of NBS-1 was obtained and equilibrated in the above fashion. All measured values were then referred through NBS-1 to SMOW, using the δ value of NBS-1 (−7.94) given by Craig (1961b).

A 90°, 12-in.-radius, magnetic analyzer mass spectrometer, which simultaneously collected ion currents corresponding to mass 44 and 46, was used for the analyses. Rapid intercomparison of a sample and standard was facilitated with a magnetic valve system. Digital recording components were used to print the ratio of the signals from the two ion currents to five figures as described by McCullough and Krouse (1965). Measurements of O^{18}/O^{16} ratios in our laboratory have improved since this initial report. Currently precision within an analysis is noticeably better than ± 0.01%, and the reproduceability with duplicate samples is comparable. Table 1a shows the results of a typical comparison of the standard and an unknown during an analysis time of about 25 minutes. R_x and R_s refer to the signals derived from the two ion currents after amplification. It is seen that the standard deviation in the δ value is less than ± 0.08, even when the second value which appears rather high is included. Table 1b, which gives the results of six samples of CO_2 equilibrated with identical samples of distilled water, shows that the reproduceability in sample preparation is ± 0.1 δ units (0.01%) and therefore only one figure after the decimal is quoted in the tables of results.

Experimental Results and Discussion

Pit studies on the Kaskawulsh and Hubbard Glaciers. Pit 1 was dug in the Kaskawulsh Glacier on June 30 at an altitude of about 2520 m with the purpose of sampling before the melt season commenced. Figure 3 shows the variations of δ value, density, and stratigraphy with depth. The slight extent of melting is indicated by the few ice layers near the top of the pit. The δ value shows a marked annual variation with the position of the most negative value (−29.3) corresponding to midwinter precipitation. This is expected, since the most negative δ value should correspond to snow deposited at the lowest temperature.

In Figure 3 the density has been plotted in such a way that its curve resembles that of the δ_{18} variation. The variations due to isotopic composition are too

TABLE 1a. Typical Comparison of Unknown and Standard Sample

Ratio R_s*	Sample ratio R_x*	$R_x - R_s$	$\frac{R_x - R_s}{R_s} \times 1000 = \delta$ value
(1) .83651			
.83662	(1) .83269	− .00393	−393/83362 = − 4.70
(2) .83673	.83269	− .00404	−404/83673 = − 4.84
.83659	(2) .83268	− .00391	−391/83659 = − 4.67
(3) .83645	.83253	− .00392	−392/83645 = − 4.69
.83627	(3) .83237	− .00390	−390/83627 = − 4.66
(4) .83609			

Average δ value = − 4.71 ± 0.08

*Average of 10 printed ratios

TABLE 1b. Measured δ Values of Six Equilibrated Identical Water Samples

− 19.4
− 19.6
− 19.6
− 19.6
− 19.5
− 19.4

Average = − 19.5 ± 0.1

small to account for the wide range of density values, and, further, the observed effect is opposite to the effect expected on this basis. It seems possible that since both the snow density and the δ value are related to the temperature of deposition, there may be a correlation between them. This possibility should be checked with precipitation studies. The limited data from this pit study suggest that a higher density is associated with a more negative δ value. If significant modification has occurred, however, such a correlation would disappear, since the trend would be toward higher densities in the modification processes. Compaction would produce higher densities in the bottom of the pit.

Three ice layers in Pit 1 were found to have O^{18}/O^{16} ratios which were, on the average, five δ units more negative than the surrounding snow (Table 2). The question arises as to whether this represents a fractionation factor between the snow and co-existent ice or whether it is representative of meltwater that has percolated downward and refrozen. With the latter interpretation, however, the meltwater should correspond to spring precipitation and have a higher concentration of O^{18}. Further, the results on Pit 1 are not in agreement with effects generally found on the Blue Glacier (Sharp *et al.*, 1960). It seems unlikely that evaporational loss of O^{16} during percolation would be sufficient to account for these results.

Marked discontinuities exist in both the δ_{18} and the density behavior at the previous summer surface.

Since, with the exception of the top layers, the snow showed little stratigraphic variation beyond slight

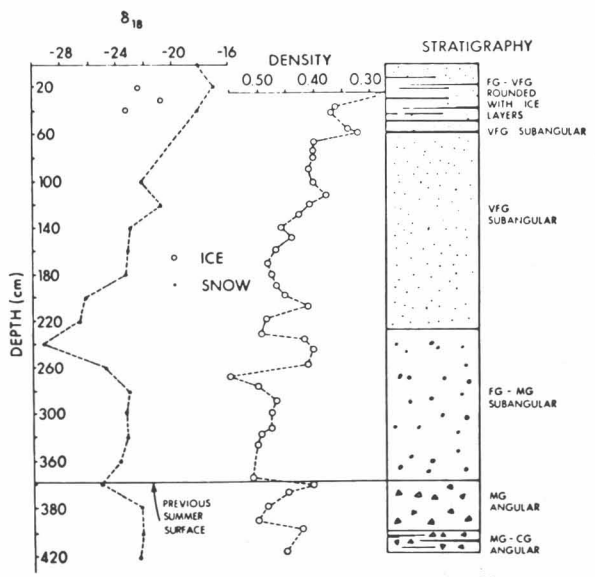

Fig. 3. Pit 1 on Kaskawulsh Glacier; variation of O^{18}, density, and stratigraphy with depth (June 30, 1963, altitude 2560 m). Abbreviations used here and in Figure 5 are: VFG, less than 0.5 mm; FG, less than 1 mm; MG, less than 2 mm; CG, greater than 2 mm.

TABLE 2. Snow Samples and Ice Layers from Pit 1 (Kaskawulsh Glacier)

Sample number	Depth (cm)	δ Value
	Snow Samples	
1	0	− 18.2
2	20	− 17.1
3	40	− 18.3
4	100	− 22.3
5	120	− 20.9
6	140	− 23.1
7	160	− 23.2
8	180	− 23.4
9	200	− 26.3
10	220	− 26.7
11	240	− 29.3
12	260	− 24.9
13	280	− 23.2
14	300	− 23.4
15	320	− 23.3
16	340	− 23.9
17	360	− 25.2
18	380	− 22.3
19	400	− 22.3
20	420	− 22.5
Average δ value for samples above 360 cm = − 23.2		
	Ice Layers	
1	20	− 22.5
2	31	− 20.9
3	39	− 23.4

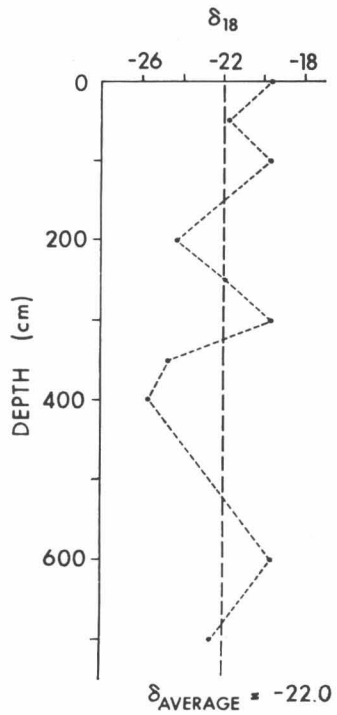

Fig. 4. Auger hole on Kaskawulsh Glacier; variation of O^{18} with depth (August 29, 1963, altitude 2560 m).

changes in grain size, no correlation of O^{18}/O^{16} variations with stratigraphy of the snow is apparent.

The site of Pit 1 was revisited on August 29, 1963, after the peak of the melt season had passed. In the near vicinity, a 7-m auger hole was drilled, and the δ values as a function of depth are shown in Figure 4. Although the sampling was not as detailed, the range in δ values is smaller in this core than in the previous pit (Table 3). This finding is consistent with the idea that downward percolating meltwater has tended to homogenize the O^{18}/O^{16} composition. The difference between the average δ value for the borehole (−22.0) and that of Pit 1 (−23.1) could be attributable to sampling error.

Pit 2 was dug on the Hubbard Glacier (at an altitude of about 2500 m) on July 17. The variations of δ value, density, and stratigraphy with depth are shown in Figure 5. The stratigraphy of this pit showed that melting was well underway as ice layers were evident throughout the total depth. The snow was isothermal to a depth of at least 310 cm. The previous summer layer was located at a depth of 243 cm (compared with 370 cm for Pit 1 on the Kaskawulsh Glacier). It would seem that the accumulation at this site is less than on the Kaskawulsh side of the divide. Again, annual variation of the δ value is evident, but it is noticeably less than in Pit 1 (see Table 4). The decrease in variation presumably resulted from the action of percolating meltwater. It is also noted that the extremely negative δ value occurs much nearer to the top of the Hubbard Pit (~ 80 cm) than in the case of the Kaskawulsh Pit (~ −240 cm). It is interesting, however, that the distances for the extremely negative δ values above the previous summer surfaces are comparable in both pits. This could suggest similar amounts of accumulation up to midwinter, but thereafter the accumulation on the Hubbard was less. During percolation, the distance between the summer surface and the top of the pit would decrease, but it is improbable that the 17 days between the samplings could account for such a large difference of pit depth. Likewise, the possibility that the extremely negative δ value occurred much later in time on the Hubbard Glacier seems unlikely.

It is also seen that the small variation in δ values of this pit is consistent with the small density spread. The

TABLE 3. Samples from 7-m Hole at the Site of Pit 1

Sample number	Depth (cm)	δ Value
1	0	− 19.7
2	50	− 21.8
3	100	− 19.7
4	200	− 24.3
5	250	− 21.9
6	300	− 19.6
7	350	− 24.7
8	400	− 25.7
9	600	− 19.7
10	700	− 22.6
Average value = − 22.3		

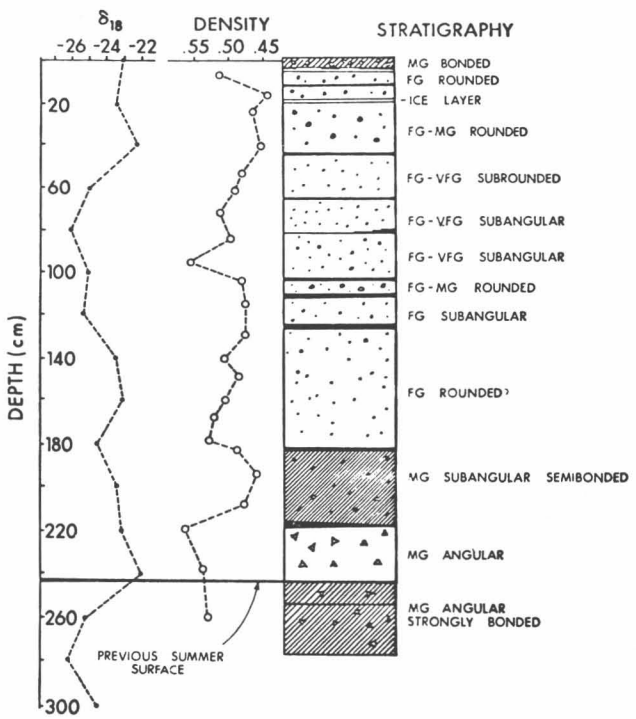

Fig. 5. Pit 2 on Hubbard Glacier; variation of O^{18}, density, and stratigraphy with depth (July 17, 1963, altitude 2370 m).

TABLE 4. Snow Samples from Pit 2 (Hubbard Glacier)

Sample number	Depth (cm)	δ Value
1	0	− 23.2
2	20	− 23.5
3	40	− 22.3
4	60	− 25.1
5	80	− 26.2
6	100	− 25.2
7	120	− 25.5
8	140	− 23.7
9	160	− 23.3
10	180	− 24.8
11	200	− 23.6
12	220	− 23.4
13	240	− 22.3
14	260	− 25.4
15	280	− 26.5
16	300	− 24.8
Average value for samples above 240 cm = − 24.0		

average density is much higher in Pit 2 than in Pit 1 because of the larger extent of homogenization processes. Again, the δ value shows a discontinuity at the previous summer surface, but it is not consistent with that observed in Pit 1.

A third pit was dug on August 22 as close to the firn limit on the Kaskawulsh Glacier as the water content of the snow would allow. The previous summer surface was located at a depth of 122 cm by stratigraphical considerations. The results of this study are shown in Figure 6 and Table 5. The O^{18}/O^{16} ratios obtained are of limited significance because of the water content and were only considered to obtain an average value of the accumulation. The surface sample is heavier isotopically, thereby being consistent with average summer precipitation. Evidence of seasonal variation at depth has either been washed out or requires a more detailed analysis. The density fluctuations are smaller and the average density is higher in comparison with the other pits because of the greater extent of homogenization.

On July 28, seven samples were taken from an auger core through one annual layer at the top of the accumulation area (altitude 2650 m). The δ-value variation with

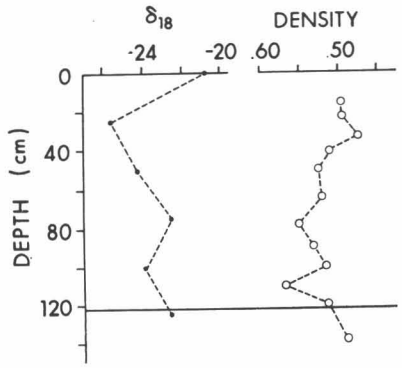

Fig. 6. Pit 3 near firn line on Kaskawulsh Glacier; variation of O^{18} and density with depth (August 22, 1963, altitude 1980 m).

TABLE 5. Snow Samples from Pit 3 (Firn Line)

Sample number	Depth (cm)	δ Value
1	0	− 20.9
2	25	− 25.6
3	50	− 24.2
4	75	− 22.5
5	100	− 23.9
6	125	− 22.6
Average value = − 23.3		

depth is shown in Figure 7 and Table 6. The previous summer surface was located at a depth of 360 cm. As in the firn limit pit, the δ value near the surface is heavier isotopically, being characteristic of summer precipitation. The extremely negative δ value characteristic of mid-winter accumulation is not evident, owing either to the homogenization processes or to insufficiently detailed sampling. The average δ value for this core was slightly

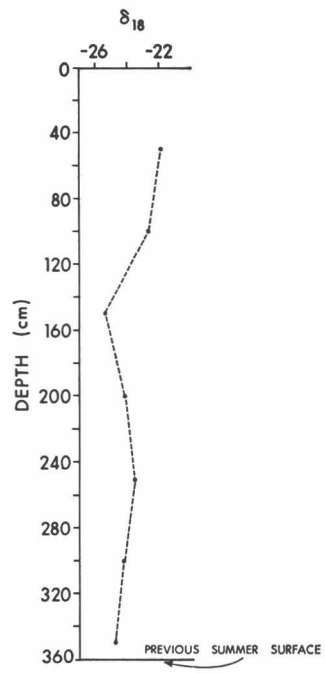

Fig. 7. Auger hole near top of accumulation area; variation of O^{18} with depth (July 28, 1963, altitude 2700 m).

TABLE 6. Samples Taken from an Auger Hole at the Top of the Accumulation Area

Sample number	Depth (cm)	δ Value
1	50	− 21.9
2	100	− 22.3
3	150	− 25.7
4	200	− 24.1
5	250	− 23.5
6	300	− 24.2
7	350	− 24.8
Average value = − 23.8		

more negative (−23.8) than for Pit 1 (−23.1) as predicted by the altitude effect, but this variation is within the sampling error.

Longitudinal profile. In Figure 8, the average δ values have been plotted for pits and cores on the Kaskawulsh Glacier as a function of altitude. Any trend above the firn line is within the sampling error. The results of other studies are shown in this figure.

Shortly after the furthest extent of the melt season, ten hard ice samples were taken on a longitudinal profile from the firn limit to the terminus of the glacier at locations spaced about 3 km apart. Since Sharp *et al.* (1960) found variations in δ for co-existent types of ice, only coarse-bubbly ice was chosen to reduce the number of variables. Coarse-bubbly ice should, however, be fairly indicative of the total ice O^{18}/O^{16} ratio. The results shown in Figure 8 and Table 7 exhibit a large scatter, but the average trend is a decrease in the δ value with decreasing altitude going from the firn line to the terminus. This effect is predicted by glacier flow considerations as discussed in the introduction and has been demonstrated in other studies (Epstein and Sharp, 1959a; Sharp *et al.*, 1960). Since material appearing below the firn line had its initial origin at higher altitudes, the flat geometry of the accumulation basin of the Kaskawulsh Glacier would tend to make the effect more complex. The meteorology of the area will further complicate the simple pattern.

Transverse profile. The site for the transverse profile was chosen to include samples from each of the three ice streams that make up the main body of the glacier. The results are shown in Figure 9. It is seen that the centers of the south and central arms have noticeably more positive δ values than their margins, whereas the opposite occurs in the north arm. As discussed previously, topography of the accumulation area could be a significant factor in determining the δ variation of a transverse profile. More extensive isotopic and physical data are necessary to show such a topographical dependence. The cases of the central and south arms resemble those found on the Saskatchewan and Blue Glaciers (Epstein and Sharp, 1959a; Sharp *et al.*, 1960), and the argument given by these workers could also apply. In comparison with the center of the stream, the slower traveling edges suffer more ablation, and thus deeper layers of ice with origins at higher altitudes are exposed.

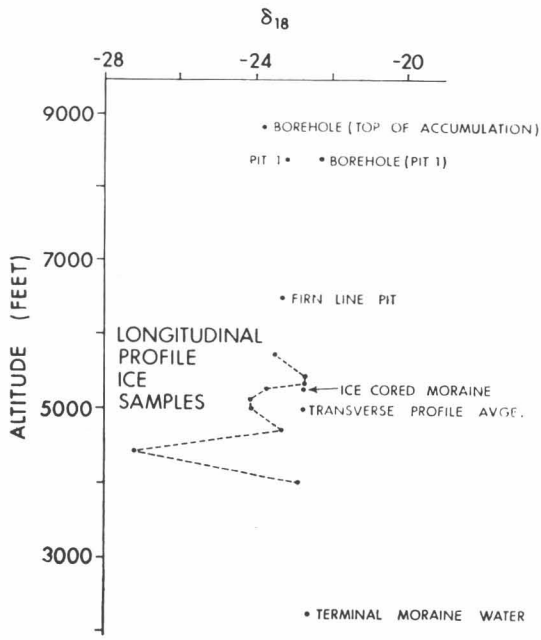

Fig. 8. Longitudinal profile on the Kaskawulsh Glacier.

TABLE 7. Ice Samples from Longitudinal Profile

Sample number	Altitude (m)	δ Value
1	1720	− 23.5
2	1630	− 22.7
3	1600	− 22.7
4	1580	− 23.7
5	1560	− 24.1
6	1500	− 24.1
7	1420	− 23.3
8	1340	− 27.2
9	1300	
10	1200	− 22.9
Average value = −23.8		

It is remarkable that all the margins have consistent δ values, especially since two accumulation areas and varying topography are represented. It seems unlikely that all six measurements are coincidental. These results could suggest either that all the margins originated at similar accumulation altitudes or that a high degree of homogenization occurs near the stream edges.

The range of δ values arising in the transverse profile (Table 8) may explain the scatter in the ice samples of the longitudinal profile study. It is clear that close control in a longitudinal study is required to reproduce the same relative transverse position in the ice stream. More conclusive results could have been obtained if a

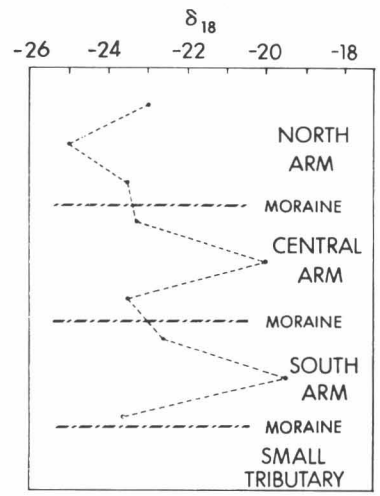

Fig. 9. Transverse profile on the Kaskawulsh Glacier below the firn line (altitude 1520 m).

TABLE 8. Ice Samples from Transverse Profile

Sample number	δ Value
1	− 23.0
2	− 25.0
3	− 23.5
4	− 23.3
5	− 20.0
6	− 23.5
7	− 22.6
8	− 19.5
9	− 23.6
Average value = −22.7	

complete transverse profile had been taken at each longitudinal profile position

It is also noted that the spread in δ values for the ice samples is much less than that of the snow in the first pit study. The ice samples have been subjected to homogenizing processes that have decreased the δ-value spread.

Miscellaneous samples. A sample of ice-cored moraine was obtained from the moraine between the north and central ice streams. This sample was exposed by a crevasse joining the two ice streams and was located near Sample 4 of the longitudinal profile study (see Table 7). The δ value of this sample was − 22.7 (altitude 1580 m). This value is not significantly different from those of the hard ice samples. It is fairly close to the stream-edge values found in the transverse profile study which was conducted nearby (about 70 m lower in altitude); therefore, this sample probably corresponds to one or both of the stream edges.

Measurements on a composite sample from meltwater streams emerging from the terminal moraine gave a δ value of −22.6 (altitude 840 m), which is very close to the average of the hard ice samples and the ice core sample from the medial moraine. The value is also close to the average value for all the samples considered in the pit and auger studies. This water represents the ultimate in homogenization and should have the average δ value if evaporational alterations of the O^{18}/O^{16} ratio are negligible. This result suggests that the total sampling was generally representative of average behavior.

Precipitation studies. On June 29, after a summer snowfall, a series of samples were taken at various altitudes on a nearby peak (location give in Figure 2). The samples represent an altitude gradient of over 600 m. The δ values as a function of altitude are shown in Figure

TABLE 9. Samples of Summer Snowfall on a Nearby Peak

Sample number	Altitude (m)	δ Value
1	2460	− 20.3
2	2560	− 26.6
3	2900	− 25.9
4	3000	− 20.9
5	3150	− 18.8

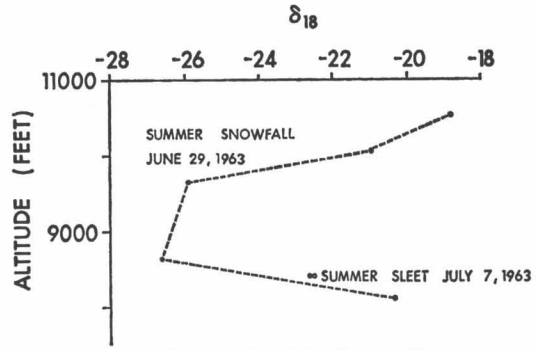

Fig. 10. Precipitation studies.

10 and Table 9. The scatter of results is such that no consistent altitude effect, as predicted theoretically, appears. Furthermore, the results do not show the homogeneity expected in samples from a single snowfall, and the average δ value is more negative than that expected for summer precipitation. The two samples with the large negative δ values may represent previous winter snow if the locations have been significantly windblown.

Three summer sleet samples were collected on July 7 near the base camp. Whereas the wind was westerly during the snowfall discussed above, it was from the east at 2 miles per hour during the sleeting. The average δ value for these samples was − 22.6 (see Table 10). This δ value is significantly more negative than the values found near the tops of pits studied in the same general area. This may be explained by the fact that the prevailing wind direction was from the interior of the Yukon rather than from the Pacific Ocean. In general, an air mass deriving vapor from a continental rather than a marine source at this latitude should have a lower δ value, because continental water bodies do not experience the degree of remixing that ocean waters do. Thus they retain the latitudinal differentiation of the O^{18}/O^{16} ratio.

General Comparisons with Other Data

Sharp (1960) has summarized O^{18}/O^{16} ratios for a number of studies and shown how the O^{18} content decreases with latitude. The δ-value range of the Kaskawulsh Glacier is shown with this summary in Figure 11, which shows that it fits into the general pattern of latitude δ variation. It is also seen that the spread in δ value for the Kaskawulsh is comparable with the spreads found in the Saskatchewan and Blue Glaciers.

The average δ value found for the Malaspina Glacier (Epstein and Sharp, 1959) in the same general area was about two δ units less negative than the average of this study. Since inter-laboratory calibrations do not exist and since the studies were conducted during different

TABLE 10. Summer Sleet Sample

Sample number	δ Value
1	− 22.6
2	− 22.6
3	− 22.5

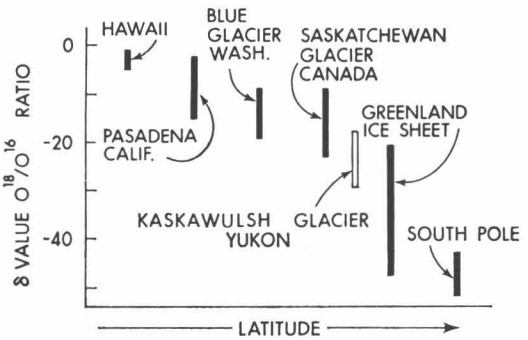

Fig. 11. O^{18}/O^{16} ratios of the Kaskawulsh Glacier compared with locations at other latitudes (after Sharp, 1960).

years, care must be taken in considering this small difference. It is in the right direction, however, to be consistent with the same marine source of water vapor. The δ value for precipitation would become more negative as the vapor is carried farther inland.

Since some evidence shows occasional intrusion of air from the interior of the Yukon, it is of interest to compare the results with precipitation studies being performed at Whitehorse by Dansgaard (1964) as part of the world wide IAEA-WMO precipitation survey. Data over the past five years show that a minimum δ value usually occurs during December or January. Since the amount of precipitation is also recorded at Whitehorse, the seasonal behavior can be compared with that preserved in the Pit 1 study. It is expected, in the absence of complicating factors, that the minimum δ value at locations at one latitude should occur at the same time. For periods other than 1962 – 1963, the seasonal variations resemble the variations of Pit 1 in average δ value, δ variation, and position of minimum δ. The period 1962 – 1963 was, however, unusual at Whitehorse, in that the usual December – January minimum δ value is not apparent in the monthly average as shown in Figure 12 (Dansgaard, personal communication, 1965). Since such a minimum was present in Pit 1, this implies that the majority of the precipitation on the Kaskawulsh Glacier did not have the same source as Whitehorse but was of marine origin.

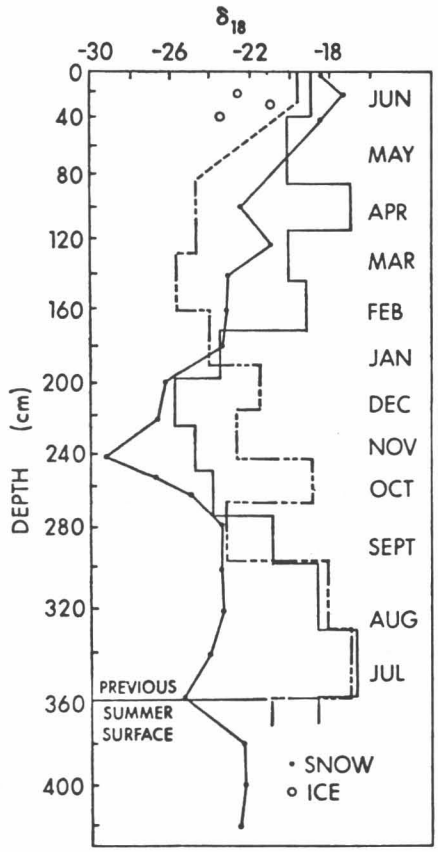

Fig. 12. Comparison of accumulation (density corrected) in Pit 1 with precipitation at Whitehorse (after Dansgaard). Solid line: 5-year average without 1962 – 1963; dashed line: 1962 – 1963.

Acknowledgments

We are indebted to the Arctic Institute of North America for making the sampling of these glaciers possible. We wish to thank P. Wagner (University of Michigan) for making his density determinations available. The National Bureau of Standards, Washington, kindly provided us with a sample of NBS-1.

Colleagues at the University of Alberta who shared an interest in the project include G. L. Cumming and E. R. Kanasewich, of the Department of Physics, and H. Baadsgaard and R. E. Folinsbee, of the Department of Geology.

D.S.M. received financial support from a Geological Survey of Canada–National Advisory Council grant, and the remainder of the financial assistance came from the National Research Council, Ottawa.

References

Craig, H., Boato, G., and White, D. E. (1956) ISOTOPIC GEOCHEMISTRY OF THERMAL WATERS, in NAT, ACAD. SCI. NUCL. SCI. SER., REPT. 19, pp. 29 – 36.

Craig, H. (1961a) Isotopic variations in meteoric waters, SCIENCE, 133, 1702 – 1703.

Craig, H. (1961b) Standard for reporting concentrations of deuterium and oxygen^{18} in natural waters, SCIENCE, 133, 1833 – 1843.

Craig, H., Gordon, L.I., and Horibe, Y. (1963) Isotopic exchange effects in the evaporation of water, J. GEOPHYS. RES., 68, 5079 – 5087.

Dansgaard, W. (1953) The abundance of O^{18} in atmospheric water and water vapour, TELLUS, 5, 461.

Dansgaard, W. (1954) The O^{18} abundance in fresh water, GEOCHIM. COSMOCHIM. ACTA, 6, 241 – 260.

Dansgaard, W. (1961) The isotopic composition of natural waters with special reference to the Greenland ice cap, MEDD. GROENLAND, 165.

Dansgaard, W. (1964) Stable isotopes in precipitation, TELLUS, 16, 436 – 468.

Epstein, S. (1956) Variation of the O^{18}/O^{16} ratio of fresh water and ice, PUBL. 400, U.S. NAT. ACAD. SCI., p. 20,

Epstein, S. (1959) The variations of the O^{18}/O^{16} ratio in nature and some geologic implications, in RESEARCHES IN GEOCHEMISTRY, edited by P.H. Abelson, pp. 217 – 240, John Wiley & Sons.

Epstein, S., and Mayeda, T. (1953) Variations of the O^{18} content of waters from natural sources, GEOCHIM. COSMOCHIM. ACTA, 4, 213 – 224.

Epstein, S., and Sharp, R. P. (1959a) Oxygen isotope variations in the Malaspina and Saskatchewan glaciers, J. GEOL., 67, 88.

Epstein, S., and Sharp, R.P. (1959b) Oxygen isotope studies, IGY BULL., TRANS. AM. GEOPHYS. UNION, 40, 81 – 84.

Friedmann, I. (1953) Deuterium content of natural water and other substances, GEOCHIM. COSMOCHIM. ACTA, 4, 89 – 103.

Gonfiantini, R., Togliatti, V., Tongiorgi, E., DeBreuck, W., and Picciotto, E. (1963) Snow stratigraphy and Oxygen isotope variations in the glaciological pit of King Baudouin station, Queen Maud Land, Antarctica, J. GEOPHYS. RES., 68, 3791 – 3798.

*Havens, J.M., and Saarela, D.E. (1964) Exploration meteorology in the St. Elias Mountains, Yukon, Canada, WEATHER, 19, 342 – 352.

*This article is reprinted in the present volume.

McCullough, H., and Krouse, H.R. (1965) Application of digital recording to simultaneous collection in mass spectrometry, REV. SCI. INSTR., 36, 1132 – 1134.

Ragle, R.H. (1964) The Icefield Ranges Research Project, 1963, ARCTIC, 17, 55 – 57.

Reid, H.G. (1896) The mechanics of glaciers, J. GEOL., 4, 912 – 928.

Reisenfeld, E.H., and Chang, L.T. (1963) Dampfdruck, Siedenpunkt, und Verdampfundswarme von HDO and H_2O^{18}, Z. PHYSIK. CHEM., B. 33, 127 – 132.

Sharp, R.P. (1960) Glaciers, CONDON LECTURES, OREGON STATE SYSTEM OF HIGHER EDUCATION, Eugene, Oregon.

Sharp, R.P., Epstein, S., and Vidziunas, I. (1960) Oxygen isotope ratios in the Blue Glacier, Olympic Mountains, Washington, J. GEOPHYS. RES., 65, 4043 – 4059.

Urey, H.C., and Mills, G. (1940) The kinetics of isotopic exchange between CO_2, bicarbonate ion, carbonate ion, and water, J. AM. CHEM. SOC., 62, 1019.

Wagner, P. (1963) Snow facies on the Kaskawulsh glacier, Yukon Territory, Canada. M.Sc. thesis, Department of Geology and Mineralogy, University of Michigan, Ann Arbor.

Wood, W.A. (1963) The Icefield Ranges Research Project, GEOGR. REV., 53, 163 – 184.

High Snowfields of the St. Elias Mountains*

Edward Grew† and Malcolm Mellor†

ABSTRACT. Observations made during the 1964 summer provide a description of snow and radiation characteristics for the region and give insight into effects of altitude, regarded as a gross variable, when anomalous wind and slope effects are excluded. Divide Camp, Seward Camp, and Lucania Camp were occupied successively within a minimum period of time to compare conditions at different altitudes. Data are presented on snow profiles, snow accumulation measurements, the development of the annual snow layer, snow conditions at depth, the mechanical properties of the snow, snow densification, solar radiation, and the variation of snow properties with surface altitude. It is concluded that as long as local anomalies are avoided, the effects of surface altitude on snow properties and surface processes seem to be simple. However, in mountain regions it is probably a combination of local conditions which produces the most remarkable effects.

Introduction

As part of the continuing program of the Icefield Ranges Research Project, observations were made during the summer of 1964 on three extensive and relatively flat snowfields lying at different altitudes in the St. Elias Mountains, Yukon Territory, Canada. The general area of activity lay between 60°20'N and 61°05'N, and between 139°35'W and 140°00'W, a mountainous terrain ringed by Mt. Logan (6050 m), Mt. Vancouver (4790 m), Mt. Lucania (5230 m) and Mt. Steele (5070 m). The high snowfields are drained by a number of major valley glaciers, including the Kaskawulsh, Kluane, and Donjek on the continental (northeast) side of the range, and the Seward, Hubbard, Logan, and Walsh on the Pacific side. The observations provide a description of snow and radiation characteristics for the region and give some insight into the effects of altitude, regarded as a gross variable, when anomalous wind and slope effects are excluded.

Snow profiles

To compare conditions at different altitudes, three sites were occupied successively over a minimum period of time. The principal site, Divide Camp[1], was at the main glacier station of the expedition, at 2600-m altitude on an extensive snowfield which forms a common accumulation area for the Hubbard and Kaskawulsh Glaciers. The lowest site, Seward Camp[2], was on the Seward Glacier at an elevation of 1900 m, close to sites occupied during "Project Snow Cornice" (Sharp, 1951a, 1951b, 1951c). The highest site, Lucania Camp, lay on a broad snowfield on the southeast flank of Mt. Steele at an altitude of 3600 m.

Snow profiles to a depth of 4 m were obtained at all three sites by standard field methods, yielding the data of Figures 1, 2, 3. At Divide Camp, additional observations were made periodically in pits 1 to 2 m deep in order to follow the changes of snow conditions from late June to mid-August. In cooperation with members of the Hokkaido University Alaskan Glacier Expedition, led by Dr. Akira Higashi, a 15-m hole was drilled with a CRREL coring auger to extend the snow profile (Figure 4).

The stratigraphic sections display evidence of melt water infiltration at all sites, a condition which explains the lateral inhomogeneity evident in density profiles (and also found in Rammsonde profiles). When melt water is actually penetrating cold snow there are appreciable horizontal temperature gradients in the affected layers, but the erratic shape of the plotted temperature profiles is due partly to errors in the well-used bimetal dial thermometers, many of which were incapable of holding a calibration.

Identification of annual snow layers

Without benefit of several months direct observation it is not easy to make a chronological interpretation of snow stratigraphy in this area, since there are usually no clear and unambiguous indicators such as the dirty summer layers found on parts of the Seward Glacier by Sharp (1951b). However, snow accumulation measurements have been made on stakes in the Divide area under the direction of Richard Ragle, project field leader; these show that 3.30 m of snow accumulated from August 1963 to August 1964, and thus give the approximate level of the 1963 summer horizon.

The 1963 summer level (Figure 2) coincides with a pronounced density minimum and with a marked change in grain structure. These may be diagnostic features, since they seemed likely to be reproduced at the 1964 summer surface[3]. From late June to mid-August 1964, density was consistently low at the surface, with sharp increase of density to a

*This report previously appeared as CRREL *Technical Report 177*, March 1966, and is reproduced here with permission.

†Cold Regions Research and Engineering Laboratory (CRREL), U.S. Army Material Command, Hanover, New Hampshire.

[1]Divide Station B of Plate 1 in the back of this volume.

[2]Seward Station A of Plate 1 in the back of this volume.

[3]Since this was written it has been reported (C.M. Keeler, personal communication) that the features discussed were repeated in the 1964 – 65 layer.

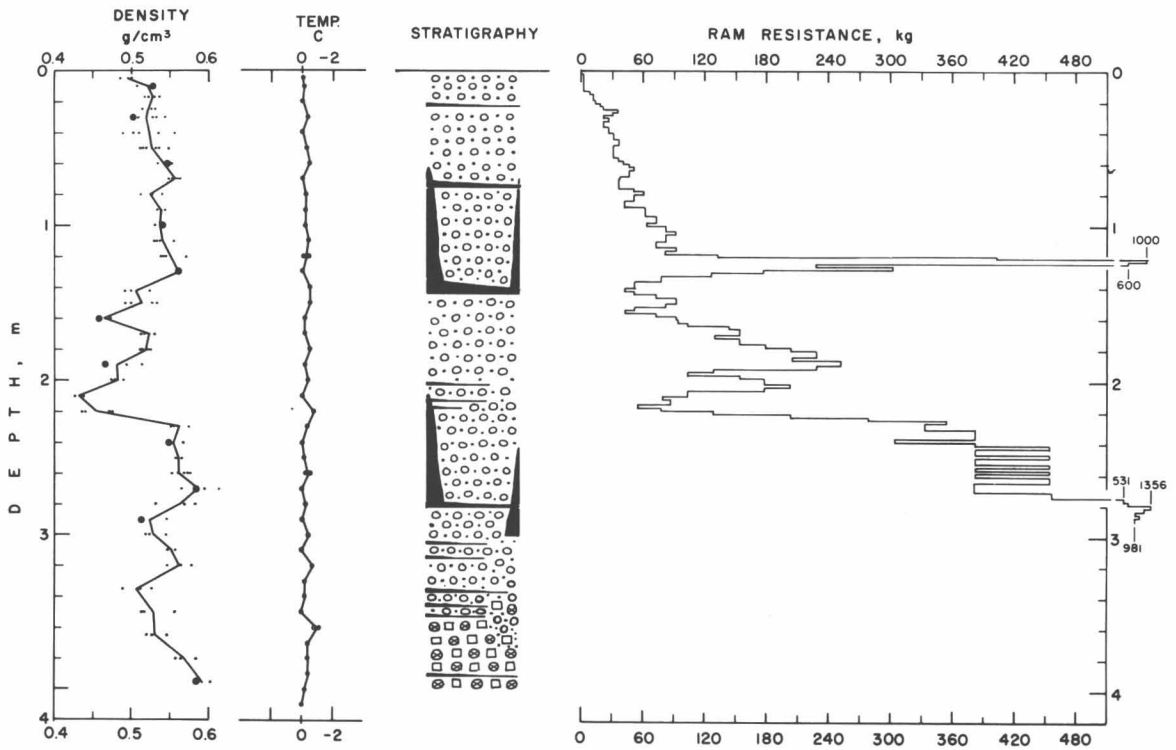

Figure 1. Snow profile at Seward Camp (1900 m) on 3 August 1964.

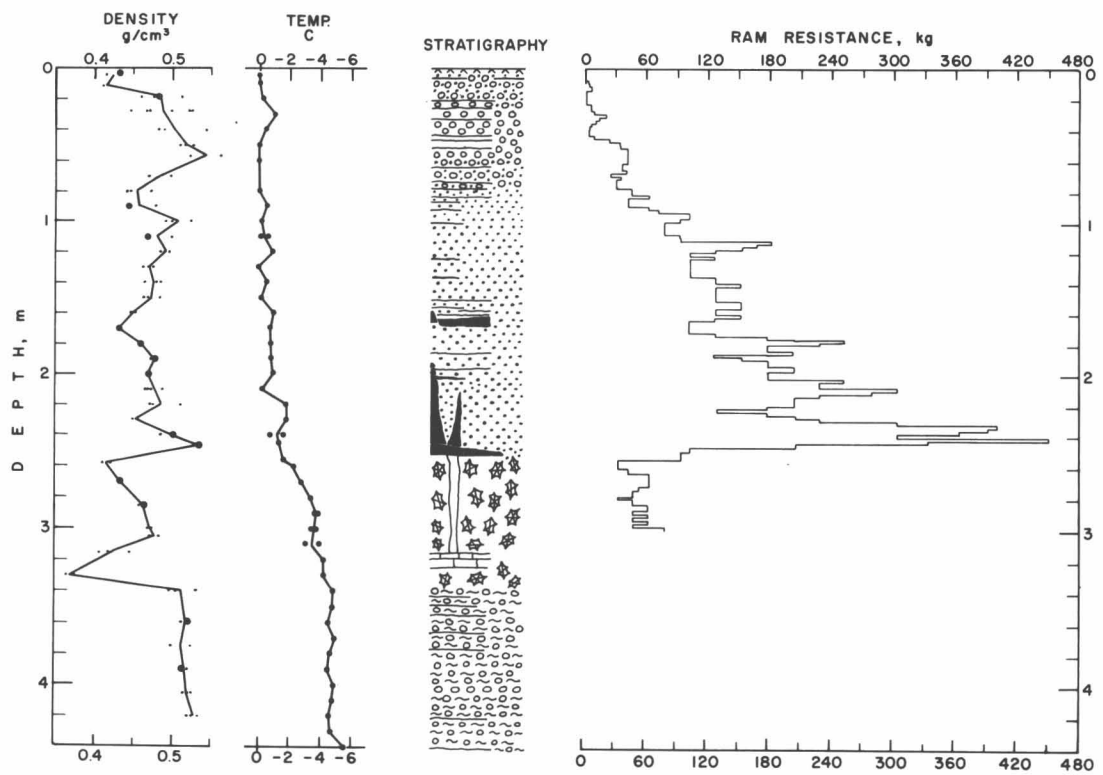

Figure 2. Snow profile at Divide Camp (2600 m) on 22 July 1964.

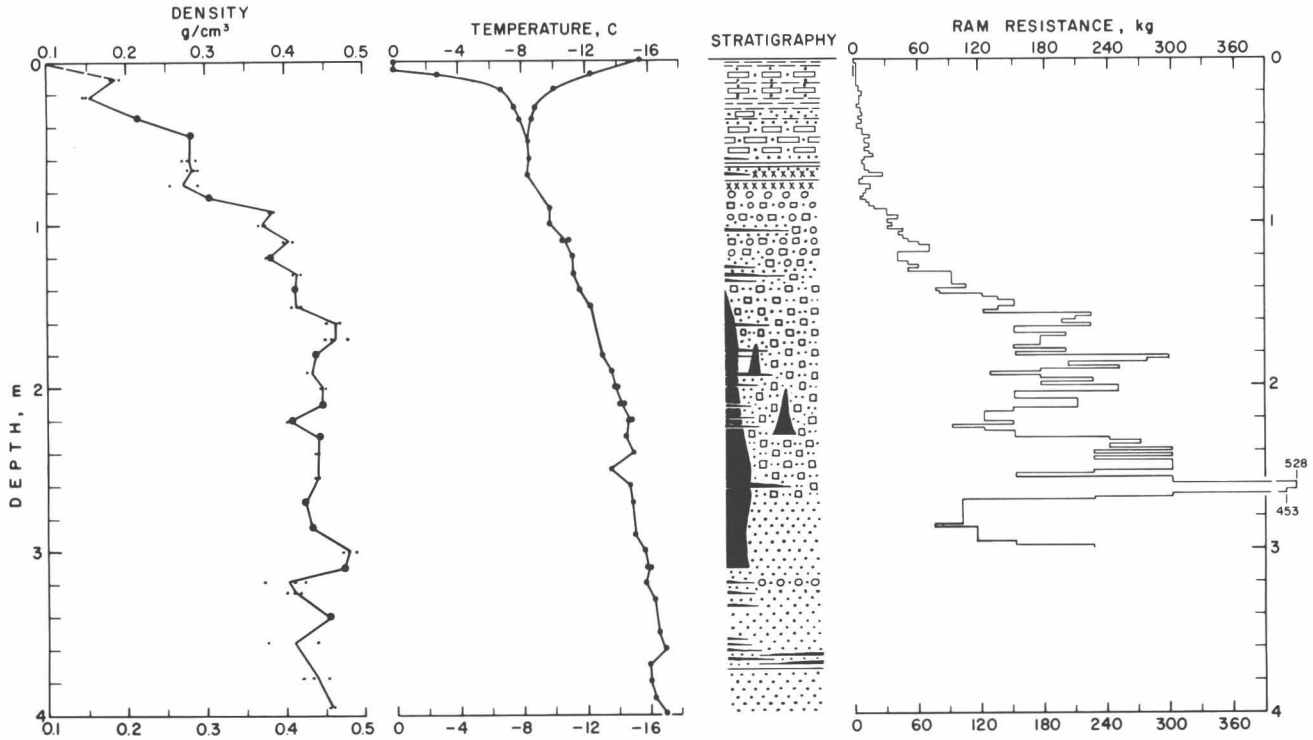

Figure 3. Snow profile at Lucania Camp (3600 m) on 16 July 1964.

TABLE 1. Legend for Figures 1 – 3.

^^^^	Surface hoar, at top of Divide section only.
	Sub-rounded coarse grained snow.
	Sub-rounded fine to very fine grained snow.
	Sub-rounded medium grained snow.
	Thin ice crusts.
	Ice gland. Thin gland at right indicates ice pipe.
	Ice layer and lens; ice lens is discontinuous.
xxxxxxx	Layer of hardened snow.
	Fine to very fine angular equant snow.
	Fine to very fine angular inequant snow.
	Coarse grained. Angular grains resulting from fusion of smaller grains. Snow compact.
	Fine or medium round grains clumped tightly into coarse to medium grain clusters. Inter-cluster bonds weak and snow very friable. Clusters angular.
	Iced firn.
	Melt crusts of considerable stratigraphic extent consisting of rounded, clumped, fused grains.
	Medium grained angular, equant (Lucania section only).

local maximum in the first 50 cm of depth. This density gradient was attributed to melt water migration. By mid-August, daytime temperature of the snow surface was below 0°C and fresh, relatively angular snow grains were able to persist where previously there had been rapid melt alteration of the surface material. It therefore seems that a summer horizon in this snowfield is characterized by a density minimum situated on top of a comparatively dense snow column which shows evidence of melting and melt water infiltration. The horizon may be overlain by unmelted grains fused into clusters, perhaps by vapor diffusion during the autumn period, when a steep positive temperature gradient must exist near the surface.

On the Seward snowfield, Sharp (1951a, 1951b) demonstrated that summer surface layers had low density. In Figure 1 there is a pronounced density minimum at a depth of 2.10 m, which is tentatively identified as the 1963 summer level. An accumulation of 2.1 m is in tolerable agreement with Sharp's 1949 determination that "annual accumulation surplus averages about 60 in. of firn." The stratigraphy shows no significant change of grain structure at the 2.1-m level, or indeed at any other level above 3.5 m; there is merely a slow increase of grain size with depth. This is perhaps not surprising, as the entire annual layer reaches the melting point and is subject to melt water seepage.

At Lucania Camp (Figure 3) the subsurface snow apparently remains at below-freezing tempera-

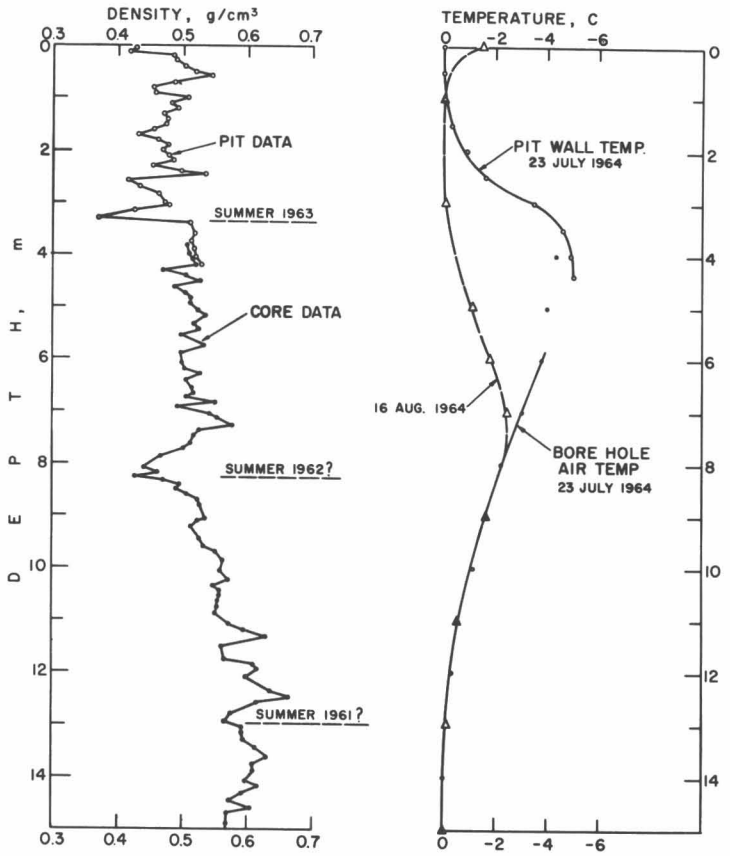

Figure 4. Density and temperature profiles to 15-m depth at Divide Camp on 23 July 1964 (temperature profile repeated on 16 August 1964).

tures throughout the summer. Although ice glands show that percolation has occurred, there are no layers bearing obvious signs of sustained melting. At 3.2-m depth a thin layer of coarse, rounded grains coincides with a low density, and at 3.7 m there are continuous ice crusts just below a layer of low density; while these may indicate a summer level, additional data are needed to establish a dating. On vacating the site a few stakes were planted; although the exposed lengths were only 2.1 to 2.6 m, they should at least give a lower limit for accumulation if the site is revisited in 1965[4].

Development of the annual snow layer

Divide. During summer there is little change of surface level with reference to a shallow subsurface datum (such as a well-defined snow or ice layer). Snowfall is roughly balanced by melting and water infiltration, while evaporation is compensated by nighttime deposition of rime and hoar. (Reports of ablation from this flat-lying area should be treated with caution; there can be very little lateral transfer of water or net loss of mass.) Density remains low at the surface, for low body stresses limit mechanical compaction, and grain growth reduces capillary retention of melt water, thus allowing it to drain to lower layers. The snow below 50-cm depth remains at sub-freezing temperatures until July, so that heavy melting in the early summer leads to water percolation down distinct vertical paths, where refreezing forms ice glands with basal lenses. It seems unlikely that direct solar radiation alone would cause melting at a sufficient rate to form ice glands, for the daytime heating periods are interspersed with nighttime cooling periods. It seems more likely that ice glands are formed from melt water produced by sustained convective heating during "warm spells" of several days duration, or perhaps even from rainwater. By mid-August the surface layers are beginning to cool, and regular melting is coming to an end.

During autumn there will be deposition of snow which remains quite dry, but steep temperature gradients through the surface layers should stimulate considerable vapor diffusion toward the surface. With the onset of winter, lower temperatures and more wind may lead to deposition of snow at higher initial densities. As overburden pressures are developed by accumulation, snow formerly at the surface will begin to densify mechanically at significant rates.

[4]The site was not revisited in 1965 nor subsequently.

Attention might be drawn to the ice lens based at 2.5-m depth in Figure 2. The lens spreads immediately above a layer of low density and apparently high permeability, presumably because of the existence of a crust which was obliterated when the lens formed. The temperature gradient below the lens is relatively steep, but whether this is a consequence of lens formation (latent heat source) or of low thermal conductivity in the coarse, low density snow is not known. Although the coarse layer from 2.5 to 3.4 m is believed to be a result of autumn vapor diffusion, there is a possibility that downward diffusion of vapor after lens formation influenced the structure of this snow.

Seward. On the Seward snowfield it appears that the entire snowpack reaches the melting point in summer (see also Sharp, 1951c), and the stratigraphy suggests that melt water soaks through the complete annual layer and down to greater depths. Deep penetration of melt water offers a possible explanation of Sharp's (1951b) observation that ice layers tend to become thicker and more numerous with depth, for transient sub-freezing temperatures occur to depths of 10 m or more (Sharp, 1951c). It is worthy of note, however, that low density layers persist at depth, perhaps because their constituent snow is highly permeable to water.

The existence of ice glands and lenses at quite shallow depths indicates that the snow is invaded by water while it is still below freezing temperature, that is, prior to mid-June.

Lucania. Summer snow at Lucania Camp is much less dense than that at lower elevations, and there is little evidence of general melting. Although the site was occupied at the height of the melt season, during a period of clear skies and intense solar radiation, there was virtually no melt water production and snow surface temperature varied diurnally from 0°C to − 16°C. Below the level of diurnal temperature variation, temperature decreased steadily from −8.5°C at 50-cm depth to −17°C at 4 m. The stratigraphy shows thin ice crusts distributed through the column; there are definite concentrations at 70 and 370-cm depths, but there are no obvious signs of snow which has melted through any significant depth.

The ice glands shown in Figure 3 are intriguing. These were believed to be of fairly recent origin, since the temperature profile shows some perturbation, but not more recent than spring or early summer in view of the depth of unaffected overlying snow. Temperature records for Yakutat, a coastal station some 165 km to the south, give the year's maximum at the end of May. Applying a lapse rate of 0.65°C/100 m, derived from comparison of temperatures during the comparable period of occupancy for Lucania (which was also one of the warmest times of summer at Yakutat), the air temperature at Lucania at the end of May might have reached +1.6°C on two successive days with much lower overnight temperatures. Even so, after perusal of radiation nomographs (Gerdel, Diamond, and Walsh, 1954) it seems unlikely that this condition could have caused snow to melt at a sufficient rate to form deeply penetrating ice glands, and the possibility of rainfall or sustained heating from a warm air mass (convection plus long-wave radiation) should still be entertained.

Lucania was the only site where the summer surface bore a wind-sculptured microrelief. The patterns were predominantly transverse to the prevailing wind direction, indicating low wind speeds, but their existence gives additional evidence of the dryness of this snowfield even in the height of summer. The density curve down to 1.6-m depth is also characteristic of a "dry" snowfield where densification is by mechanical compaction rather than melt water infiltration.

Snow conditions at depth

The 15-m borehole at Divide provided a density profile and two successive temperature profiles (Figure 4). Density and temperature data to 15-m depth were obtained on the Seward snowfield by Sharp (1951a, 1951b).

The summer horizons of 1962 and 1961 which are tentatively indicated on Figure 4 were placed primarily from density trends, but if the identification is correct, net accumulation between 1961 and 1963 must have been relatively high. In 1961, Wood (1963) estimated accumulation in the 1960-1961 layer at 190 g cm^{-2}, while accumulation in the 1963-1964 layer was about 155 g cm^{-2}; by contrast, the tentative dating in Figure 4 gives 250 and 260 g cm^{-2} for 1962-1963 and 1961-1962 respectively. There is a possibility that a buried layer gains mass from the current annual layer above it by melt water migration, but this hypothesis remains to be tested.

In the 1963-1964 layer, there is an overall tendency for density to decrease with depth, so that melt water infiltration probably outweighs the effects of compactive creep in densifying the snow. This trend changes as depth increases, and in the layer from 8 to 12-m depth there is a positive density gradient which can be attributed to mechanical deformation. One rather remarkable feature of the density profile is the persistence of low density layers at depth; since the compactive viscosity of snow is a function of density, variation of density between adjacent layers of the creeping snow should be attenuated with depth. Although core sampling is somewhat inadequate in laterally inhomogeneous layers, the effect seems to be real, for Sharp (1951b) also shows low density layers persisting at depth. This matter is discussed further in a subsequent section.

The temperature profile in Figure 4 together with similar profiles measured in 1961 and 1962 by Ragle (personal communication) show that the winter cold wave in the snowpack does not completely dissipate before surface cooling resumes. One consequence is that there is a snow layer, between approximately 5-m and 10-m depths, which remains permanently below freezing temperature. This permanently frozen layer effectively blocks the movement of melt water to lower depths, but in doing so it may gain mass from refrozen melt water. The sub-freezing temperatures must also keep mean compactive deformation rates in this layer below those for similar snow in the layer beneath.

From Figure 4 and Ragle's data it is found that the minimum of the cold wave travels down through the snowpack at about 14 cm/day during summer, a rate which is roughly three times the temperature penetration rate commonly observed in the upper layers of dry polar snowfields. The thermal diffusivity of snow at Divide is probably not very different from that for dense polar snow, so that the difference in penetration velocity probably reflects a difference in form of the impressed temperature variation. As far as is known, temperature variation in a snowpack subject to heavy summer melt has not been treated analytically, but for conditions such as those prevailing at Divide it should be feasible to apply conduction theory to the deep layers if a virtual surface is defined at the level where temperature reaches 0°C for a negligibly short period each year (3 to 4-m depth at Divide). The harmonic temperature variation defining the boundary condition at this virtual surface would probably be a skewed wave rather than a symmetric sinusoidal wave, with the "warming" limb of the wave steeper than the "cooling" limb. Benfield's (1953) analysis, which illustrates how the effective penetration depth of a winter cold wave is increased by heavy accumulation, might perhaps be refined by such a treatment.

Mechanical properties of the snow

One objective of the field study was a comparison of mechanical properties between snow in the St. Elias Mountains and snow studied elsewhere, particularly on polar ice caps. Under summer conditions it proved to be unfeasible to perform laboratory-type tests, such as the unconfined compression test, since the coarse-grained snow lacked cohesion at 0°C. Nevertheless, a good deal of information may be gleaned from Rammsonde and density profiles.

Rammsonde data. Ram resistance is a strength index in its own right, having been developed originally for estimating relative shear strength of snow on avalanche slopes. It has been used to define bearing capacity requirements for surface vehicles and aircraft, a topic discussed in several CRREL reports and elsewhere. The St. Elias ram profiles thus can be usefully compared with those for other areas directly. Alternatively, ram resistance from individual layers may be tabulated alongside corresponding density and temperature data to provide plots which define local grain structure parameters more precisely. For broad comparisons between geographically distinct regions, however, there are some advantages to be gained from integrated Rammsonde profiles.

When the Rammsonde is driven through an incremental depth Δz against a resistance Rz, the work done is $R_z \Delta z$, and a summation of all such increments from the surface $z = 0$ to depth z gives the total work done in penetrating to that depth. An integrated ram profile is a plot of

$$\sum_{z=0}^{z} R_z \Delta z, \quad \text{or} \quad \int_0^z R_z \, dz,$$

against z. Figure 5 gives integrated ram profiles taken at different times at Divide, and Figure 6 gives integrated ram profiles for Seward and Lucania. Horizontal steps on the curves indicate ice layers, while vertical steps indicate weak layers of appreciable thickness.

The Divide time sequence shows average strength of the uppermost 1.2 m to decrease during July and then increase again during August. In July this layer underwent no significant density change, but temperatures were still rising to the melting point. In August there was a slight increase of average density, and temperatures near the surface were falling again. Average strength between the surface and 3 m decreased throughout the period of observation, presumably in response to rise of average temperature in the layer.

Comparing profiles of Figure 6 with appropriate interpolations from Figure 5, it is found that the average strength of the uppermost 1.2 m at Seward is almost identical to that at Divide at the end of the melt season. Average density and temperature of this layer at the two stations were closely comparable at the time. Average strength between surface and 3 m was somewhat greater at Seward than at Divide, a difference attributed to higher snow density at depth and prevalence of ice layers between 2 and 3 m at Seward. At Lucania, average strength of the uppermost layers is lower than at Divide, for although temperature is low at Lucania, snow density is very low near the surface. At 3-m depth the snow at Lucania is very cold and density is similar to that at Divide; at this depth, integrated ram profiles for the two stations are converging in response to the relatively high strength of deep snow at Lucania.

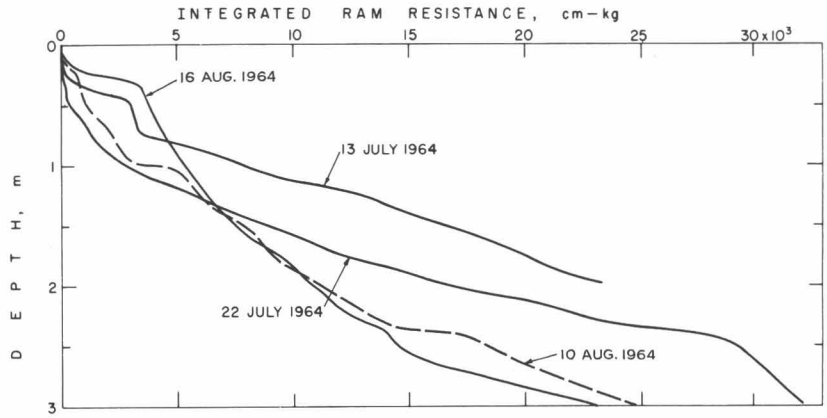

Figure 5. Integrated Rammsonde profiles for Divide Camp.

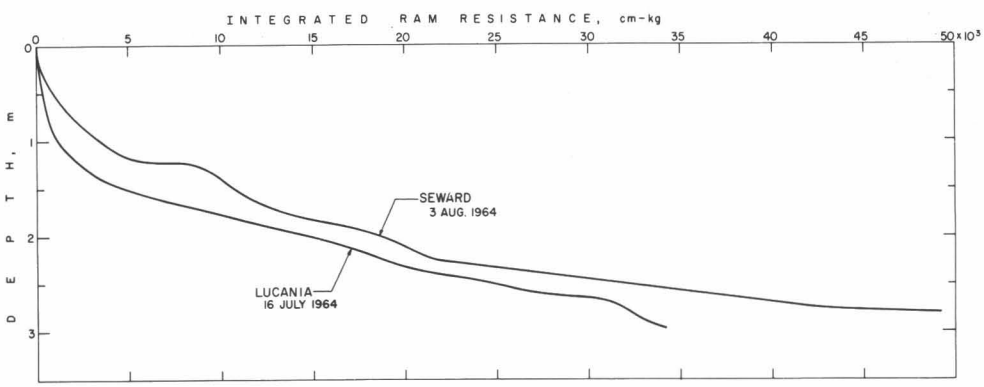

Figure 6. Integrated Rammsonde profiles for Seward Camp and Lucania Camp.

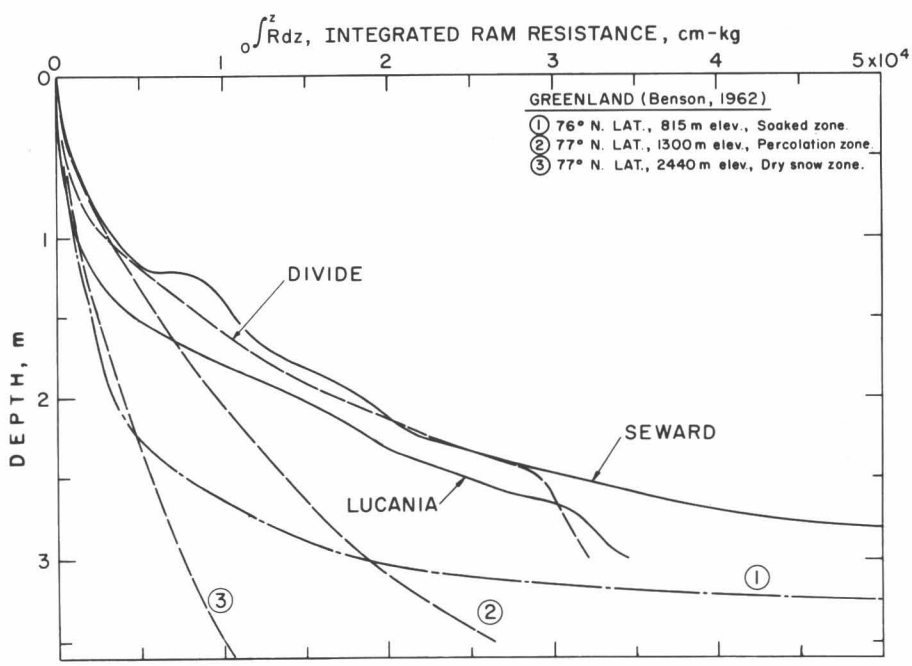

Figure 7. Integrated Rammsonde profiles for Seward, Divide, and Lucania compared with representative profiles from north Greenland (Greenland data from Benson, 1962).

In Figure 7, integrated ram profiles for Seward, Divide, and Lucania are compared with representative profiles from north Greenland, also taken at the height of the melt season. Below the 1.2-m level, the high ice content of St. Elias snows leads to a more rapid strength gain than is found in the percolation zone and dry snow zone of Greenland, although Greenland snow from the soaked zone of the ice cap margin also shows rapid strength gain as ice layers are encountered (see Benson, 1962, for details).

Ram data may also be used to make rough estimates of unconfined compressive strength, although it should be pointed out that unconfined compressive strength itself has little fundamental significance, in spite of its wide currency. Abele (1963) correlated unconfined compressive strength and ram resistance over a limited density range in processed snow to obtain the expression

$$\sigma_c = 4.078 \ln R - 14.72$$

where σ_c is unconfined compressive strength in kg cm^{-2} (at about -13° C) and R is ram resistance in kg. The constants in a corresponding relation for coarse-grained, water-soaked snow might differ from those above, but this need not cause concern here in view of the inconsistencies of existing unconfined data arising from strain rate variation in testing.

Ram data might be expected to give a measure of the energy of disaggregation, an index of both practical and fundamental interest, since the Rammsonde disrupts the structure of the snow it penetrates. On the assumption that structural disruption is closely related to disaggregation, work of disaggregation W is given by

$$W = \frac{R}{K A_c}$$

where A_c is the displacement area of the penetrometer (≈ 12.5 cm^2) and K is the ratio of effective disruption cross section to nominal displacement area (probably of order 2 or 3, and varying with density and grain structure). Since W is work per unit volume it has the dimensions of stress.

If the above two paragraphs are consistent, unconfined compressive strength should also give a measure of work of disaggregation. This seems reasonable, for if test duration is too short to permit significant permanent strain of constituent ice crystals, the energy applied in the test is expended primarily on fragmentation. The net energy expended is the input energy minus the released elastic strain energy, that is $\sigma_c / 2\,[A(\Delta\ell / c - \ell\,\sigma_c/E)]$, where σ_c is the stress at rupture, A is sample cross section area, ℓ is sample length, $\Delta\ell$ is axial deformation at failure, E is Young's modulus, and c is a "plasticity factor" accounting for nonlinearity of the stress-strain curve such that

$$\frac{\sigma_c \Delta\ell}{2c} = \int_0^{\Delta\ell} \sigma d\ell$$

If A' is the total area of failure surfaces and s is the thickness of their associated fragmentation layers,

$$W = \frac{\sigma_c}{2c} \cdot \frac{A}{A'} \cdot \frac{\Delta\ell}{s} \left(1 - c \cdot \frac{\ell}{\Delta\ell} \cdot \frac{\sigma_c}{E}\right).$$

In snow of moderate density the second term can probably be neglected. For competent, fine-grained snow ($A/A' \cdot \Delta\ell / s$) appears to be of order unity, while c is by implication less than unity. Hence W and σ_c are expected to be of the same order.

Published test data (Butkovich, 1956) are in conflict with the above, showing W between 2 and 3 orders of magnitude smaller than σ_c. However, analysis of rotary snow plow performance casts some doubt on these data (Mellor, 1956b).

Snow densification. Below the level of melt water penetration, snow densifies by compaction in a vertical direction. Compaction occurs by a creep process which is apparently Newtonian at low stresses, so that stress σ can be related linearly to strain rate $\dot{\epsilon}$ by a "compactive viscosity" coefficient η:

$$\dot{\epsilon} = \frac{\sigma}{\eta}$$

Compactive viscosity η, which is of both academic and engineering significance, can be calculated for the various snow types using data from the density profile when a stratigraphic chronology has been established. The stress, or overburdening pressure, at any depth is

$$\sigma = \int_0^z \gamma \, dz$$

where γ is bulk density, or unit weight, of the snow. The vertical strain rate is

$$\dot{\epsilon}_z = \frac{1}{\gamma} \left(\frac{d\gamma}{dt}\right)$$

Hence by following density changes in a particular layer, or by comparing densities for corresponding strata in successive annual layers, η can be calculated for the prevailing temperature.

Comparing the low density summer layers of 1962 and 1963 (Figure 4), the mean strain rate over a 1-year period was about 1.7×10^{-9} sec^{-1}, while the mean pressure was about 280 g cm^{-2}. Thus the compactive viscosity of the layer was about 1.6×10^{11} g cm^{-2} sec. Fine-grained polar snow of the same density (0.43 g cm^{-3}) and at similar temperatures would probably have a viscosity an order of magnitude lower, while recently deposited seasonal snow at similar density and temperature might have viscosity two orders of magnitude

lower. Sharp's (1951b) data indicate that Seward snow is similar in the low density summer layer (η is about 2.2×10^{11} for a mean density of 0.47 g cm^{-3}). At both Divide and Seward, average viscosity for a complete annual layer is not significantly different from the viscosities given above when density is taken into account.

The high viscosity of St. Elias snow is attributed to coarse grain size; Bader (1962) has remarked on grain size effects, and has suggested that compactive viscosity is proportional to the third power of grain size.

One implication of these observations is that deformation rates of undersnow tunnels at moderate depth (3-10 m) should be quite similar to those experienced at ice cap sites in Greenland and Antarctica.

Solar radiation

The intensity of global solar radiation (direct component + diffuse sky radiation) received on a horizontal surface was measured at the three sites by an Eppley pyrheliometer. Records were obtained for clear, cloudless days for comparison with theoretically predicted intensities. It was found that standard charts (Fritz, 1949) based on Klein's (1948) analysis gave intensities which agreed quite well with the measured intensities; ignoring dust attenuation and backscattering adjustments for the high albedo of snow, predicted intensities were about 3% lower than measured intensities. It is therefore felt that radiation heat supply on these open mountain snowfields can be calculated with some confidence, at least for clear days. Detailed tables of daily total global radiation at sea level have been prepared by Bolsenga (1964); simple altitude adjustments can be made directly from a table in an earlier work (Gerdel, Diamond, and Walsh, 1954). In confined cirques and valleys both the apparent global intensity and the total daily radiation on a horizontal surface might differ appreciably from the open snowfield values, since surroundings snow walls locally intensify radiation by reflection and also effectively reduce the duration of direct sunlight.

As a basis for estimating radiation absorption, albedo was measured with the Eppley pyrheliometer at the three sites. Spectral reflectance was measured for the visible range (0.4 - 0.7μ), and results have been given elsewhere (Mellor, 1965a). The albedo at Divide varied from 0.69 for coarse-grained wet snow to 0.88 for freshly fallen dry snow; a typical average value for 3 hours either side of noon was 0.82 in July and early August. Only a few measurements were made at Seward, but the average obtained, 0.72, is probably quite representative of the site in melt season. At Lucania the snow was fresh and dry, and brilliantly white to the eye, but the albedo averaged only 0.78 in cloud-free conditions. However, the average albedo jumped abruptly to 0.88 when the sun was obscured by cirro-stratus cloud. Both the comparatively low albedo and its increase during clouding might possibly be due to spectral variation of the snow's reflectance, but only crude, improvised measurements using industrial radiation sensors were made at Lucania. While the Eppley albedo was 0.88, a cadmium sulfide detector peaking at 0.55μ gave visible range reflectance as 0.92, and an uncalibrated lead sulfide detector filtered to exclude visible radiation gave a rough value of 0.81 for the near infrared (0.7 - 3.0μ). This is in broad agreement with spectral measurements made at Divide. If filtering of the sun's rays by cloud produced a shift of the spectral center of gravity toward the shorter wavelengths (selective infrared absorption), some increase in albedo could be expected. There is, however, a further consideration: the snow at Lucania, unlike that at lower elevations, had a wind-sculptured microrelief capable of casting shadows in direct sunlight, and this might have reduced the albedo.

Attempts were made to measure the transmittance of snow *in situ* using inexpensive industrial detectors which could be buried and, if necessary, abandoned. Unfortunately the improvised apparatus gave trouble under field conditions; contacts broke inside the sealed cadmium sulfide ("visible") detectors, and cemented joints on the enclosures of the lead sulfide (infrared) sensors broke open. Nevertheless, it seems that the technique of inserting sensors into undisturbed snow, carefully backfilling the necessary pit, and allowing snow to settle firmly against the sensors has some merit, since disturbance of the radiation field is minimized and cavity ("Holraum") effects are largely eliminated. The visible range sensors, peaking at 0.55μ, gave average extinction coefficients of 0.14 cm^{-1} for the uppermost 20 cm of snow at Divide in early July. Snow temperature at the time was $-1°C$. A few days later, when snow temperatures had risen and the layer was soaked with melt water, the average extinction coefficient dropped to 0.04 cm^{-1}. The mean density of the layer was approximately 0.35 g cm^{-3}. Wet snow of similar texture but of density 0.51 g cm^{-3} was found to have an extinction coefficient of 0.166 cm^{-1} at 0.566 μ during spectral measurements by a slab method (Mellor, 1965a). At Lucania the uppermost 50 cm of snow, of average density about 0.2 g cm^{-3} and $-6°C$, had an average extinction coefficient of 0.065 cm^{-1} for the visible range. The infrared data were discarded, but it might be noted that diurnal changes of flux could

be detected by the simple apparatus to a depth of approximately 25 cm at both Divide and Lucania.

The relatively low extinction coefficients imply a significant penetration of solar radiation into the snow mass, making possible subsurface melting of snow at 0°C. This contrasts with the situation on cold polar snowfields, where typical extinction coefficients for dense, fine-grained snow are probably closer to 1 cm^{-1} (Mellor, 1965a) and radiation effects are likely to be limited to a thin surface layer.

Altitude effects

There has recently been an interest in variation of snow properties with surface altitude when the special effects of slope and exposure are eliminated or randomized.

In the troposphere, some of the more important altitude-dependent factors are as follows:

(1) Mean air temperature decreases with altitude (at a *nominal* rate of 0.65°C/100 m).
(2) Atmospheric pressure and air density decrease with altitude.
(3) As a consequence of (2), optical air mass decreases with altitude and direct solar radiation becomes more intense.

There are also significant changes of wind speed and direction, precipitable moisture content, and cloud distribution with altitude, but these conditions are to some extent dependent on the elevation and topography of the land surface below. In addition, there are other changes which at present have no obvious relevance to deposited snow, for example, variation of potential gradient in the atmospheric electrical field.

Of the above, it seems probable that normal temperature lapse is the most important single factor controlling the condition of snow at various altitudes. Air temperature largely determines the crystalline form of the snow which falls, it governs temperature in the deposited snow, with consequent effect on densification rate and thermal metamorphism, and it establishes a control on melting and evaporation. Atmospheric cooling with altitude is insufficiently compensated by intensification of solar radiation, so that there is always a transition to dry, permanently frozen snow if the surface ascends to great enough altitude. The suggestion that decreased atmospheric pressure may affect evaporation and sintering in the snow mass can be dismissed, since the partial pressure of water vapor is influenced to only a negligible extent by normal terrestrial pressure reductions. For all practical purposes, saturation vapor pressure depends only on temperature for a given surface curvature.

Of prime interest is the gross distribution of snow type with altitude. This includes the height of the temporary snow line, which varies throughout the year, the height of the firn limit, or lowest limit of perennial snow, the height range in which perennial snow is thoroughly soaked by melt water in summer, the height range in which snow melts occasionally to form discrete ice glands and lenses, and finally the dry snow line, above which no melting occurs (see Benson, 1962). As in other regions, the elevations of all these limits except the dry snow line vary to some extent with exposure and accumulation rate, but some broad estimates can be made. Over much of the area the firn limit is at approximately 2000 m, although in the southern sector of the study area (Seward and Hubbard Glaciers) it is lower—approximately 1000 m. The upper limit of snow which is completely soaked by melt water must be close to 2600 m, for 0°C temperatures just penetrate to about the base of the current annual snow layer before the onset of autumn cooling at Divide. The "percolation zone," where snow is infiltrated by melt water but not thoroughly soaked, extends from about 2600 m to the dry snow line somewhere above 3600 m. The dry snow line is not a sharply defined limit, but taking Benson's guidelines it should be at an elevation where the mean annual temperature, at 10-m depth, is approximately 7°C lower than at Lucania camp, that is, between 4300 m and 4700 m, depending on the altitude lapse rate for mean annual temperature.

Since snow density correlates strongly with most physical and mechanical properties, the variation of representative densities with altitude is of interest. In Figure 8 it is shown that mean density decreases with increasing altitude. The data are for mean density between the surface and 4-m depth, and for mean density of a selected layer between 3.5 and 4.0-m depth. The rate of density decrease is approximately 16% per kilometer of altitude. A trend of similar sense and magnitude is found in northern Greenland for snow in transition from the soaked zone to the dry zone. The density variation with altitude reflects temperature change with altitude; at lower altitudes, where temperatures are relatively high, snow densifies more rapidly both by increased melt water penetration and by the temperature dependence of compactive creep. In Antarctica, where there is no melting, mean density of the surface snow (0-15 cm) decreases with decreasing temperature and with increasing surface elevation at a rate of approximately 9% per kilometer. In the Alps and in certain other mountain regions density is found to *increase* with increasing altitude; the Swiss guidelines for avalanche control (1961) give 20% per kilometer of altitude. In this case, however, the consideration is for seasonal snow on steep, exposed slopes and there may be intensification of

wind-packing effects with increasing altitude[5].

In the dry-snow zone and the upper parts of the percolation zone snow temperatures are controlled by conduction, so that the snow temperature at 10-m to 15-m depth, where amplitude of the annual wave becomes negligibly small, gives a reliable measure of the mean annual surface temperature. This is not so in the melt zones; melt water infiltration apparently raises the 10-m temperature above the mean annual air temperature. Nevertheless, it is useful to have altitude lapse rates for deep snow temperature. At Lucania, the measured 4-m temperature (−17°C) was probably quite close to the 10-m temperature and also to the mean annual air temperature. At Divide the winter cold wave does not completely dissipate in summer; the temperature at 10 m still fluctuates to some extent, but the mean about which it fluctuates cannot be higher than −1°C, the summer value. At Seward, sub-freezing temperatures penetrate to 10 m and below in winter (Sharp, 1951c), but for roughly half of the year the 10-m temperature is at 0°C. In Figure 9 the summer 10-m temperatures are plotted against altitude to give some idea of the lapse rate for deep snow temperatures. The resulting gradient, −1.6°C/100 m, is comparable to that found in Greenland at the same latitude, −1.4°C/100 m (Mock and Weeks, 1965). As a matter of interest, free air adiabatic lapse rates of −1.0° and −0.65°C/100 m have been drawn through the Lucania point, which is believed to approximate mean annual air temperature. The gradient of 0.65°C/100 m is reasonably compatible when comparison is made with mean annual air temperatures for Yakutat and Yakataga, the nearest Alaskan coastal stations, and for Haines Junction (60°45'N; 137°35'W), the nearest station in Yukon Territory. Since these stations are snow-free in summer, their mean temperatures would be higher than those over a permanent snowfield at the same elevation. It seems likely that mean snow temperatures in the highest parts of the range can be estimated approximately from base station data and free air lapse rates, and in Figure 10 summer and winter lapse rates for model Arctic atmospheres are given.

The variation of direct radiation intensity with altitude at a given time and latitude depends chiefly on the optical air mass, with minor corrections for dust depletion and change of precipitable moisture. The optical air mass changes with altitude in the same ratio as the barometric pressure, and for convenience the relative pressure and optical air mass have been plotted against altitude in Figure 10 on the basis of model Arctic atmosphere in summer and winter.

[5] More recent studies on Mt. Logan show some increase of density with altitude in windswept locations (C. M. Keeler, personal communication).

Conclusion

The above work was regarded as a reconnaissance of the St. Elias snowfields; there is still a need for detailed studies. The heavy reliance on conjecture in this and similar reports emphasizes a paucity of data on the metamorphism of perennial snow in sub-polar and temperate regions. Although seasonal and polar snowpacks have been studied in detail, most observations on non-polar glacier snowfields have been restricted to the summer period. To improve the situation will require winter observation.

As long as local anomalies are avoided, the effects of surface altitude on snow properties and surface processes seem to be quite simple. However, in mountain regions it is probably a combination of local conditions which produces the most remarkable effects. Future studies might therefore include measurements on steep slopes, in cirques and valleys, and on ridges and peaks. Some care would have to be taken in selecting locations for such measurements, since haphazard choice would make analysis difficult.

References

Abele, G. (1963) A correlation of unconfined compressive strength and ram hardness of processed snow, *Tech. Rept. 85,* U.S. Army Cold Regions Res. Eng. Lab., 14 pp.

Bader, H. (1962) Snow as a material, *Cold Regions Sci. Eng., Pt. 2, Sec. B,* U.S. Army Cold Regions Res. Eng. Lab., 79 pp.

Benfield, A. E. (1953) The effect of accumulation on temperatures within a snowfield, *J. Glaciol., 2,* 250-254.

Benson, C. S. (1962) Stratigraphic studies in the snow and firn of the Greenland ice sheet, *Res. Rept. 70,* U.S. Army Snow, Ice and Permafrost Res. Estab., 93 pp.

Bolsenga, S. J. (1964) Daily sums of global radiation for cloudless skies, *Res. Rept. 160,* U.S. Army Cold Regions Res. Eng. Lab., 124 pp.

Butkovich, T. R. (1956) Strength studies of high density snow, *Res. Rept. 18,* U.S. Army Snow, Ice and Permafrost Res. Estab., 19 pp.

Fritz, S. (1949) Solar radiation during cloudless days, *Heating and Ventilating,* Vol. 46.

Gerdel, R. W., Diamond, M., and Walsh, K. J. (1954) Nomographs for computation of radiation heat supply, *Res. Paper 8,* U.S. Army Snow, Ice and Permafrost Res. Estab., 6 pp.

Klein, W. H. (1948) Calculation of solar radiation and the solar heat load on man, *J. Meteorol.* 5, 119-129.

Mellor, M. (1965a) Optical measurements on snow, *Res. Rept. 169,* U.S. Army Cold Regions Res. Eng. Lab., 19 pp.

Mellor, M. (1965b) Snow removal and ice control, *Cold Regions Sci. Eng., Pt. 3, Sec. A3b,* U.S. Army Cold Regions Res. Eng. Lab., 37 pp.

Mock, S. J., and Weeks, W. F. (1965) Distribution of mean annual temperatures in Greenland and the Antarctic, *Res. Rept. 170,* U.S. Army Cold Regions Res. Eng. Lab., 44 pp.

Sharp, R. P. (1951a) Accumulation and ablation on the Seward–Malaspina glacier system, Canada–Alaska, *Bull. Geol. Soc. Am., 62,* 725-744.

Sharp, R. P. (1951b) Features of the firn on upper Seward Glacier, St. Elias Mountains, Canada, *J. Geol., 59,* 599-621,

Sharp, R. P. (1951c) Thermal regimen of firn on upper Seward Glacier, Yukon Territory, Canada, *J. Glaciol., 1,* 476-487.

U.S. Air Force (1957) *Handbook of Geophysics for Air Force Designers,* Air Force Cambridge Res. Center, Geophys. Res. Directorate.

Wood, W. A. (1963) The Icefield Ranges Research Project, *Geogr. Rev., 53,* 163-184.

Swiss Federal Institute for Snow and Avalanche Research (1961) Lawinenverbau im Anbruchgebiet, *Mitteil. Eidgen. Inst. Schnee. Lawinenforsch.,* No. *15,* Eidg. Inspektion fur Fortwesen, Bern. English translation prepared and issued by Forest Service, U.S. Dept. of Agriculture, Fort Collins, Colorado.

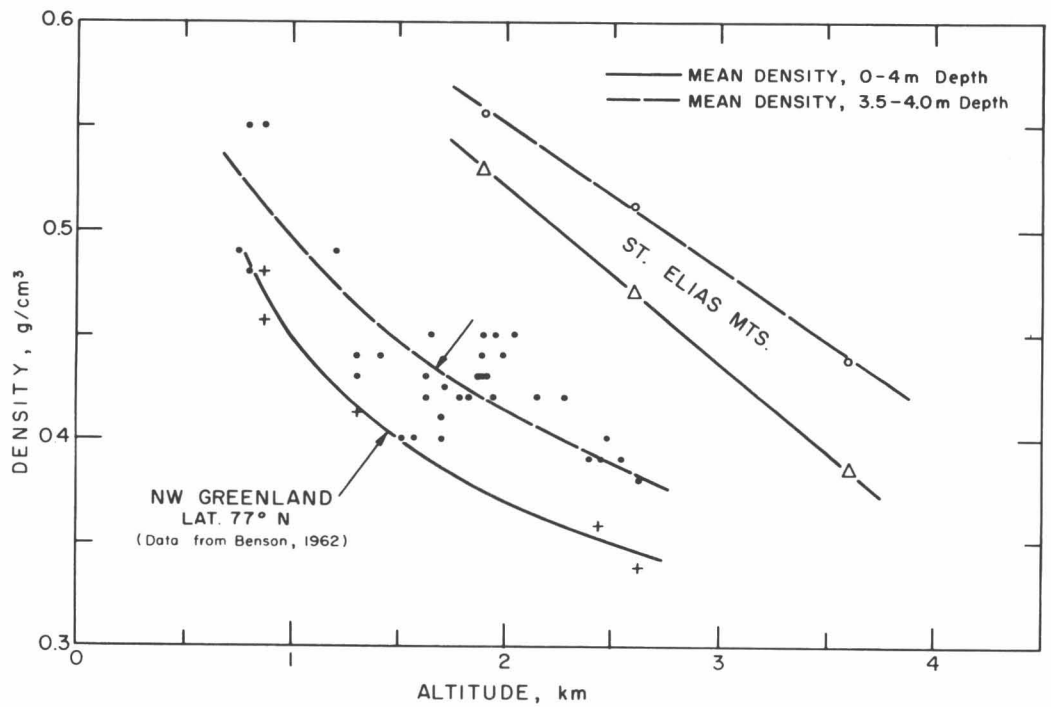

Fig. 8. Variation of snow density with surface elevation.

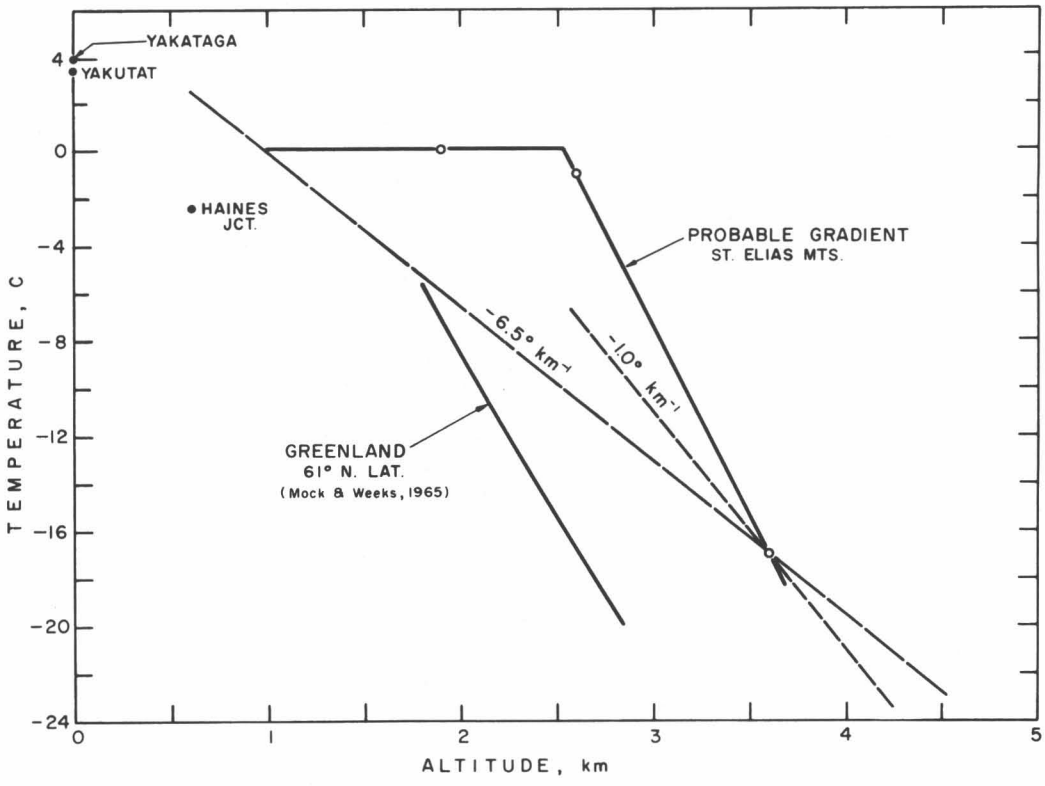

Fig. 9. Variation of snow temperature with surface elevation.

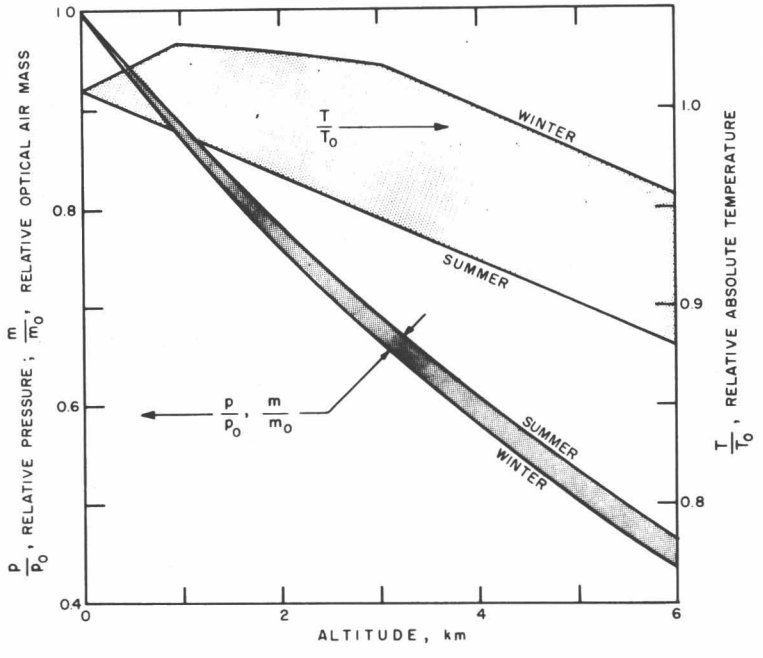

Fig. 10. Variation of atmospheric pressure, optical air mass, and absolute temperature in free air; all values relative to the sea level value. (Based on model Arctic atmospheres for summer and winter, U.S. Air Force, 1957.)

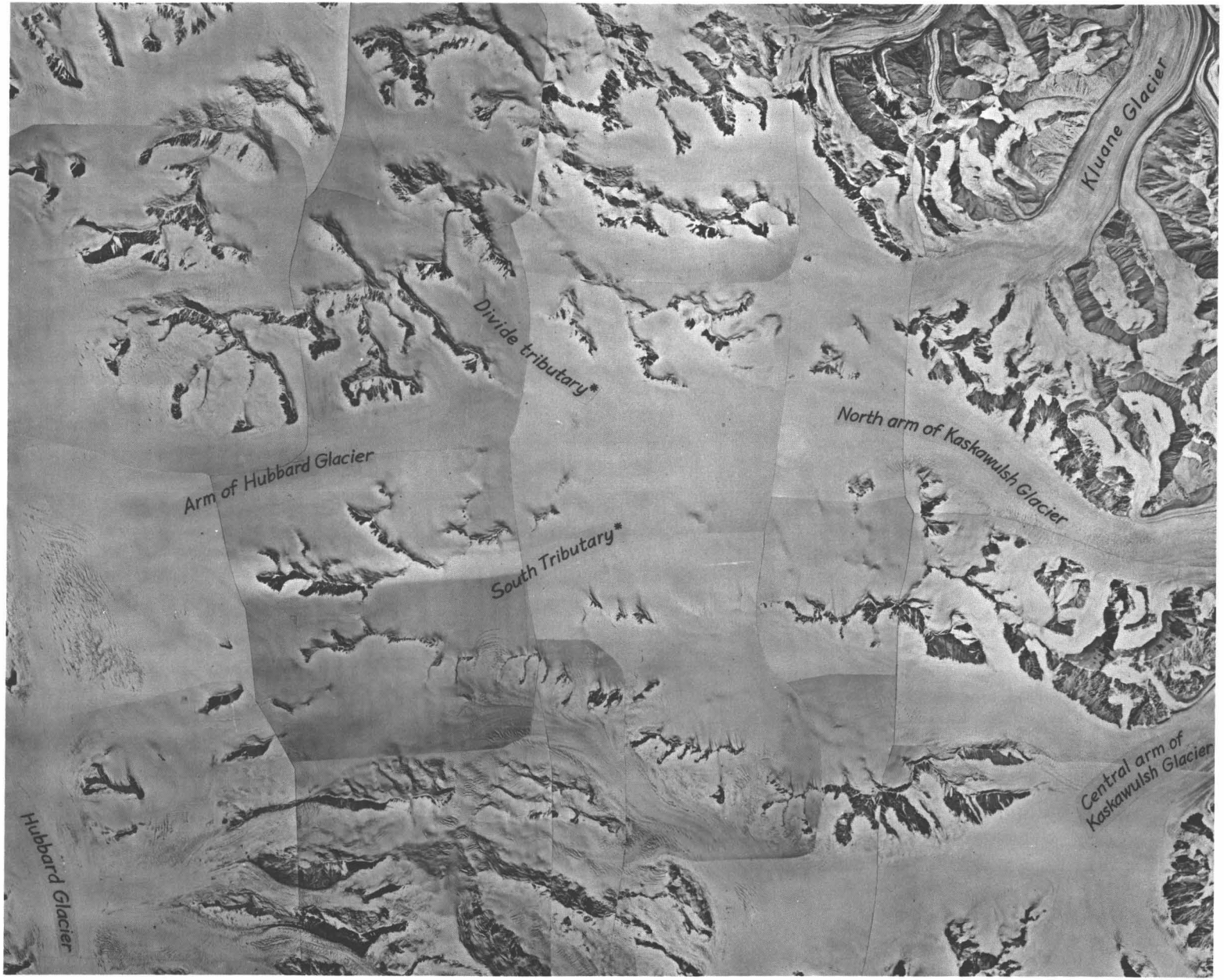

Fig. 1. Photomosaic of a divide between the Kaskawulsh and Hubbard Glaciers.

Geophysical Measurements on the Kaskawulsh and Hubbard Glaciers*

Garry K. C. Clarke†

ABSTRACT. Gravity and seismic measurements made in the summer of 1963 were used to determine ice thickness in the divide region of the Kaskawulsh and Hubbard Glaciers (60° 45'N, 139° 40'W) in the St. Elias Mountains of the Yukon Territory, Canada. Gravity differences were measured for a network of 107 gravity stations and Bouguer anomalies ranged from −199.8 mgal to −162.9 mgal. Crude ice-thickness calculations were made from these results assuming the glacier was an infinite slab. Seismic refraction lines on the Kaskawulsh and Hubbard Glaciers gave a firn thickness of approximately 40 m and an average P-wave velocity of 3710 ± 20 m/sec. One hundred seismic reflection stations were occupied and, discounting poor results, the maximum ice thicknesses found were 778 m at Stake 1 on the Kaskawulsh Glacier and 539 m at Stake 29 on the Hubbard Glacier. The maximum surface flow rates measured were 150m/yr at Stake 1 on the Kaskawulsh Glacier and 132 m/yr at Stake 44 on the Hubbard. A close relationship was found between geophysically-determined ice thicknesses and surface flow measurements. The flow line and the line of the valley center proved to be roughly coincident, although flow was complicated by tributary glaciers. The topographic divide was also the flow divide but no corresponding bedrock divide was found.

Introduction

The development of mathematical theories of glacier flow has emphasized the necessity of knowing the cross-sectional shape of glaciers as a starting point for applying flow theory. At present geophysical methods provide the most practical approach to the problem of finding the dimensions of a glacier. For this reason the Icefield Ranges Research Project has supported seismic and gravity measurements which provide independent and complementary methods of calculating ice thickness and hence of mapping the underlying bedrock surface. This paper describes geophysical work in 1962 and 1963 in the vicinity of the divide between tributaries of the Kaskawulsh and Hubbard Glaciers in the St. Elias Mountains of the Yukon Territory (see Figure 1 and Plate 1)[1].

In 1963 scientific work from the Glacier Camp (see Figure 2)[2] consisted of meteorological observations, glaciological studies, geophysical measurements to determine ice thickness, and theodolite surveys. Meteorological studies were centered at a camp near the divide at elevation 2641 m (Havens and Saarela, 1964, and pp. 17-22 of this volume), with other observations being made from Base Camp, Glacier Camp,[2] and Terminus Station (Ragle, 1964). Glaciological investigations have so far included stratigraphic studies, surface flow measurements, and determination of oxygen isotope abundances. Preliminary studies by Ragle, confirmed by temperature measurements (Wagner, personal communication) would indicate that at 2600 m the glacier is sub-polar by both Ahlmann's geophysical classification (Ahlmann, 1933) and Benson's facies classification (Benson, 1962).

Geophysical studies on the project were initiated by A. Becker in 1962. A high-quality seismic refraction profile was obtained, 14 reflection stations were occupied, and gravity was measured at the metal flow stakes. The following summer geophysical studies were continued by the writer; it is the results of these measurements which form the bulk of this paper. Seismic work during the summer of 1963 consisted of a refraction profile to obtain velocity-depth relations and hence the thickness of the firn layer and the velocity of P waves in the glacier ice, as well as reflection seismic measurements to find the thickness of the glacier and the orientation in space of the reflecting surfaces. A gravity survey was also made, but since the seismic method is considerably more accurate and direct, it was decided to use the gravity results merely to support the seismic results, to check for multiple reflections and, when necessary, to interpolate between high-quality reflection stations.

Reduction and interpretation of gravity measurements

Gravity measurements. Gravimetric surveys of glaciers have a number of attractive features; they are rapid and inexpensive; the gravimeter is light and portable – a significant factor in difficult terrain – and owing to the high density contrast between ice and rock, the

*This report has previously appeared as *Technical Paper No. 20,* Arctic Institute of North America, 1967.

†Department of Physics, University of Toronto.

[1]Plate 1 is a map inside the back cover of this volume.

[2]Glacier Camp is Divide Station A of Plate 1 and Figure 2.

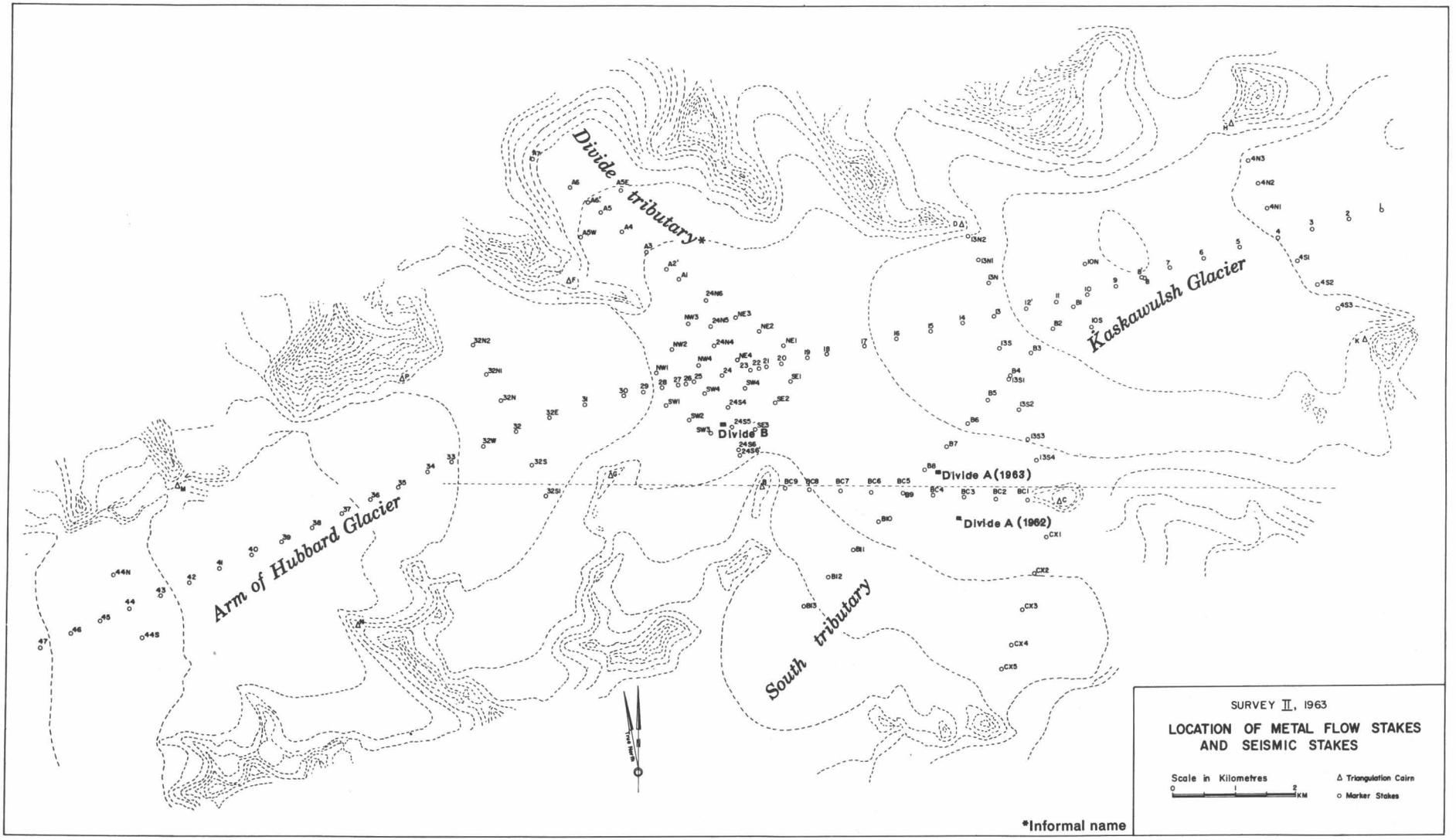

Fig. 2. Location of metal flow stakes and seismic stakes from Survey 2, 1963, by D. Sharni.

anomalies are pronounced. The difficulties to be faced are the severity of climatic conditions, requiring a high degree of temperature stability in the gravimeter, and the roughness of transportation, necessitating a rugged instrument. On mountain glaciers the terrain corrections are often large, and if much of the region is ice covered it may be difficult to estimate these corrections very accurately; moreover in mountainous regions structural trends may give rise to gravity gradients.

A Worden gravimeter was used for the entire 1963 survey. This instrument has a zero-length quartz spring and a thermal compensating spring with the entire system mounted in a vacuum flask to reduce temperature effects (Heiskanen and Meinesz, 1958). The particular Worden gravimeter used, Instrument XPO, had a small-range (185 mgal) dial and a reset screw but not a geodetic dial for long-range measurements. The instrument was calibrated for measuring the gravity difference between the University of Wisconsin Geodetic Station in the Geophysics Laboratory (Rm. 18) of the Physics Building of the University of Alberta, at which g = 981.1695 gals and the Dominion Observatory pendulum station in the basement of the Federal Building in Red Deer at which g = 980.9988 gals (Garland and Tanner, 1957). The Edmonton station was occupied three times and the Red Deer station twice to form an ABABA loop with five readings taken each time. The resulting scale constant was found to be 0.2352(8) mgals/division with a standard deviation of 0.00005 mgals/division compared with the factory-calibrated value of 0.2354(7) mgals/division.

Placing the gravimeter tripod on a sturdy wooden sled proved a satisfactory method of stabilizing the instrument although in a brisk wind the sled tended to vibrate. Unfortunately the particular Worden gravimeter used was highly sensitive to changes in temperature so that many loops had to be repeated to obtain reasonable closure. Loops for which there were readings giving a deviation of more than one scale division from a linear drift line were rejected and the loop was repeated. Stable weather conditions with a light breeze proved ideal for gravity surveying. Repeated measurements between rock stations (at the triangulation cairns) and glacier stations (at the marker stakes) were often poorly duplicated and it is supposed that this was due to their differing temperature conditions. Even when agreement was satisfactory it did not necessarily imply that the actual measurement of the gravity difference was correct owing to the contrasting environments of the two stations. Such an error would appear as poor closure about a loop.

Drift, misclosure, and gravity corrections. Corrections for drift and misclosure were first applied to the raw field measurements to make the data self-consistent. The corrected field values were then converted to gravity units and corrections applied to make each station directly comparable. Such corrections included corrections for latitude, elevation, and terrain and for geology and isostasy if required.

The drift measured by a spring gravimeter is the sum of the tidal or actual drifts and instrument drifts resulting from relaxation of components and thermal effects on components. The tidal drift is of small amplitude and is a smooth sinusoidal-like function. The drift due to relaxation is small and always positive seldom exceeding 0.03 mgal/hr. The thermal drift is minimized by a compensating spring which counteracts length changes in the main spring. Mounting in a vacuum flask further reduces thermal effects. Some systems have a thermostatic heating element which maintains the temperature of the gravimeter at a constant temperature. Ideally thermal drifts can be kept very low, however, the particular instrument used had high and erratic drift suggesting that the gravimeter had lost its vacuum.

The method of looping was used to establish legs of the gravity traverse, a typical sequence of stations being of the form ABABCDEFA. The network of gravity stations consisted of seven large loops allowing the closure of the survey to be checked. Because each measurement of gravity is subject to a small random error, misclosures resulted which were subsequently adjusted by means of a least squares method (Gibson, 1941). The seven loops, the measured gravity differences, and misclosures are represented schematically in Figure 3. Weights were assigned to each branch of the network according to the parameter

$$w = \sqrt{\frac{100n}{t(1+\Delta)}}$$

where n = number of readings at a station
t = average time in minutes required to travel between two end stations
Δ = maximum difference in readings at a station

which proved to give a satisfactory distribution of weights. These weights were normalized and rounded off. The adjusted solution must satisfy two conditions:

(1) the sum of the corrected differences around any loop must be zero

(2) the sum of the weighted corrections at any node must be zero

These are directly analogous to Kirchhoff's circuit laws. It is convenient to define the reciprocal weight as the "adjustability", $a = 1/w$. The desired least squares solution minimizes $\Sigma k_i^2 a_i$ where k_i is the correction to a particular observation, just as $\Sigma i^2 r$ is a minimum for circuitry. The option of a loop or nodal approach is presented. The nodal approach yields the following set of equations. This set of equations was solved by the University of Toronto's 7090 Computer. The resulting adjustments are summarized in Table 1.

$$\begin{Bmatrix} +3.5 & -2.5 & 0 & -2.5 & 0 & 0 & 0 \\ -2.5 & +7.5 & -2.0 & 0 & 0 & 0 & -3.0 \\ 0 & -2.0 & +11.0 & -4.5 & 0 & -1.5 & -3.0 \\ -2.5 & 0 & -4.5 & +14.0 & -5.5 & -1.5 & 0 \\ 0 & 0 & 0 & -5.5 & +11.0 & -1.5 & -4.0 \\ 0 & 0 & -1.5 & -1.5 & -1.5 & +6.0 & -1.5 \\ 0 & -3.0 & -3.0 & 0 & -4.0 & -1.5 & +11.0 \end{Bmatrix} \begin{Bmatrix} g_0 \\ g_1 \\ g_2 \\ g_3 \\ g_4 \\ g_5 \\ g_6 \end{Bmatrix} = \begin{Bmatrix} +2717.0 \\ +2356.0 \\ -5415.5 \\ +6490.3 \\ -2078.8 \\ +1958.0 \\ -927.0 \end{Bmatrix}$$

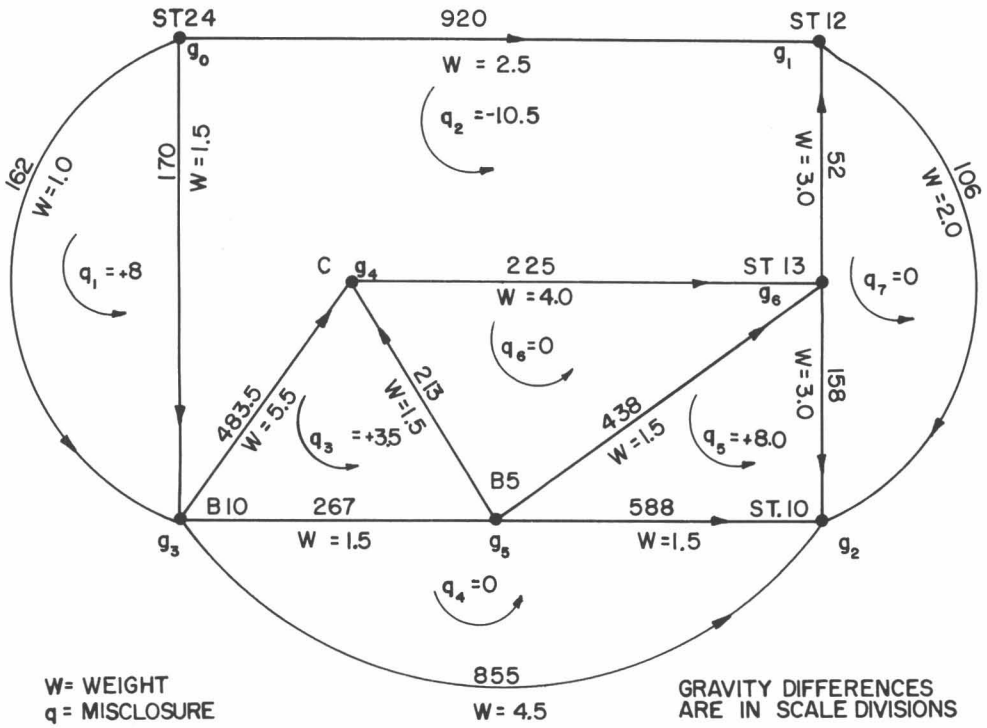

Fig. 3. Schematic diagram of gravity network and misclosures.

TABLE 1. Weights and corrections for gravity differences

Observation	Weight	Difference observed (scale divisions)	Calculated difference	Observed–Calculated
St.24–St.12	2.5	920.0	920.2	−0.2
St.24–G–St.B10	1.0	162.0	166.6	−4.6
St.24–St.B10	1.5	170.0	166.6	+3.4
St.12–St.13	3.0	52.0	50.4	+1.6
St.13–St.10	3.0	158.0	154.4	+3.6
St.12–St.10	2.0	106.0	104.0	+2.0
St.B10–St.10	4.5	855.0	857.6	−2.6
St.B10–C	5.5	483.5	481.1	+2.4
St.B10–St.B5	1.5	267.0	267.5	−0.5
St.B5–St.10	1.5	588.0	590.1	−2.1
St.B5–St.13	1.5	438.0	435.7	+2.3
St.13–C	4.0	225.0	222.1	+2.9
St.B5–C	1.5	213.0	213.6	−0.6

A latitude correction must be applied to measured gravity values to eliminate the combined effects of the earth's rotation and ellipticity of the earth. The 1930 International Gravity Formula defines the theoretical value of gravity for a station located at sea level as $\gamma = (978.0490)\ (1+0.0052884 \sin^2 \phi - 0.0000059 \sin^2 2\phi)$ where ϕ is the latitude of the station. Referring all stations to Divide Station D at latitude $\phi = 60^\circ$ 45'N and assuming the map grid to be spherical the correction for a station a distance y meters north of the reference station is -0.0006938 mgal/meter.

A free air correction must be applied to reduce all gravity measurements to the same datum elevation (usually sea level or the geoid). The expression $\partial g/\partial r = -0.30855 - 0.00022 \cos 2\phi + 0.000144\ h$ mgal/m takes into account the variation in this correction with latitude (Garland, 1956) so that for a latitude $\phi = 60^\circ$ 45' and altitude $h = 2.636$ km the free air correction is -0.30804 mgal/m. To compensate for material between the gravity station and the datum plane the Bouguer correction $g_B = 2\pi k \rho h$ must be added where k is the gravitational constant and ρ is the density of the slab material (Heiskanen and Meinesz, 1958). In the following gravity analysis the glacier ice is taken to be the anomalous material replacing rock. To evaluate the regional density, representative rock samples are usually collected and their densities measured. In the Icefield Ranges outcrops are sparse and often quite inaccessible. Although rock samples were collected at those triangulation cairns at which gravity was measured, it was decided that these samples could in no way be considered representative. The cairns were situated on resistant outcrops, and the very fact that they had not been eroded away by the glacier would suggest that they were not typical of the local geology and possibly of a higher density than the true regional density. Rather than propose a regional density from such a small number of rock samples it was decided to accept $\rho = 2.67$ gm/cm^3 as the regional density so that the Bouguer correction was 0.1119 mgal/m. Hence the complete elevation correction, that is Bouguer correction plus free air correction, was -0.1961 mgal/m.

Since in general the material between the gravity station and the datum plane is not an infinite slab, a further correction must be applied to compensate for variations from the slab, that is, topographic irregularities. This terrain correction is always positive, since any deviation from a slab tends to reduce gravity. If the topographic irregularities are effectively of infinite extent in one dimension then simple two-dimensional corrections may be applied (Hubbert, 1948a, 1948b) using charts or a line-integral method. Unfortunately this situation is not encountered in the area studied. Because of its simplicity the Hammer system of zones (Nettleton, 1940) was used to estimate terrain corrections although this method is not well adapted to the prevailing conditions. First the available maps are not entirely satisfactory for for this purpose; also the Hammer method assumes that terrain effects are due to a single material of constant density whereas in the glacier region there are two materials of widely differing densities, ice and rock. A further difficulty in estimating terrain corrections is that the thickness of the widespread glacier cover is not well known; in some areas there is only a thin cover above the rock and in others deep tributary glaciers join the main glacial channel.

Since the two area maps available are the Ohio University map (1:25,000) of the immediate study area and the Department of Mines and Technical Surveys map (1:250,000) it was decided to divide the terrain correction into two parts: a near-correction including terrain effects within 4470 m of the gravity station determined from the 1:25,000 map, and a far-correction for effects between a 4470- and 21,940-m radius of the station determined from the 1:250,000 map. No correction was made for terrain beyond this outer radius because the effect of this was fairly constant for the entire network of stations. In the near-correction no consideration was given to regions below the station elevation for glacier stations because this was the anomaly being sought. All terrain above the station elevation and not in the main glacier channel was considered to have a density of 2.67 gm/cm^3. No correction was made for areas of the main glacier above the station elevation since this correction was negligible. For the cairn stations the near-correction included a correction for the voids between the station and the elevation of the glacier surface but not for material below this elevation. The far-correction considered terrain effects below the station elevation as well as above.

The value of the far-correction was computed at 14 representative locations and varied from 0.41 to 0.88 mgals. Values at intermediate stations were obtained by contouring the values of the control stations. The near-correction was computed at 47 stations and these results were also contoured to give values at the remainder of the stations. The terrain correction is extremely sensitive to terrain effects very near the station, and without detailed mapping at the station site becomes highly uncertain. This presented no problem for the glacier stations since there were no near-terrain effects. The cairn stations, on the other hand, were often perched on rock pinnacles and hence the near-terrain effects were very large and very uncertain. Little faith can therefore be placed in the values of the Bouguer anomaly for cairn stations and thus a regional trend cannot be established from the cairn stations.

Two additional factors could be considered which are peculiar to gravity measurements on glaciers. First, a glacier is in constant motion so that the surveyed values of the coordinates are not the values of the actual station if there is a time lapse between the survey and the gravity measurement. Secondly, the surface of the glacier changes as a result of ablation and accumulation. Because the maximum interval between the second survey and the gravity measurement was only 27 days, and the maximum annual flow was 150 m no correction for

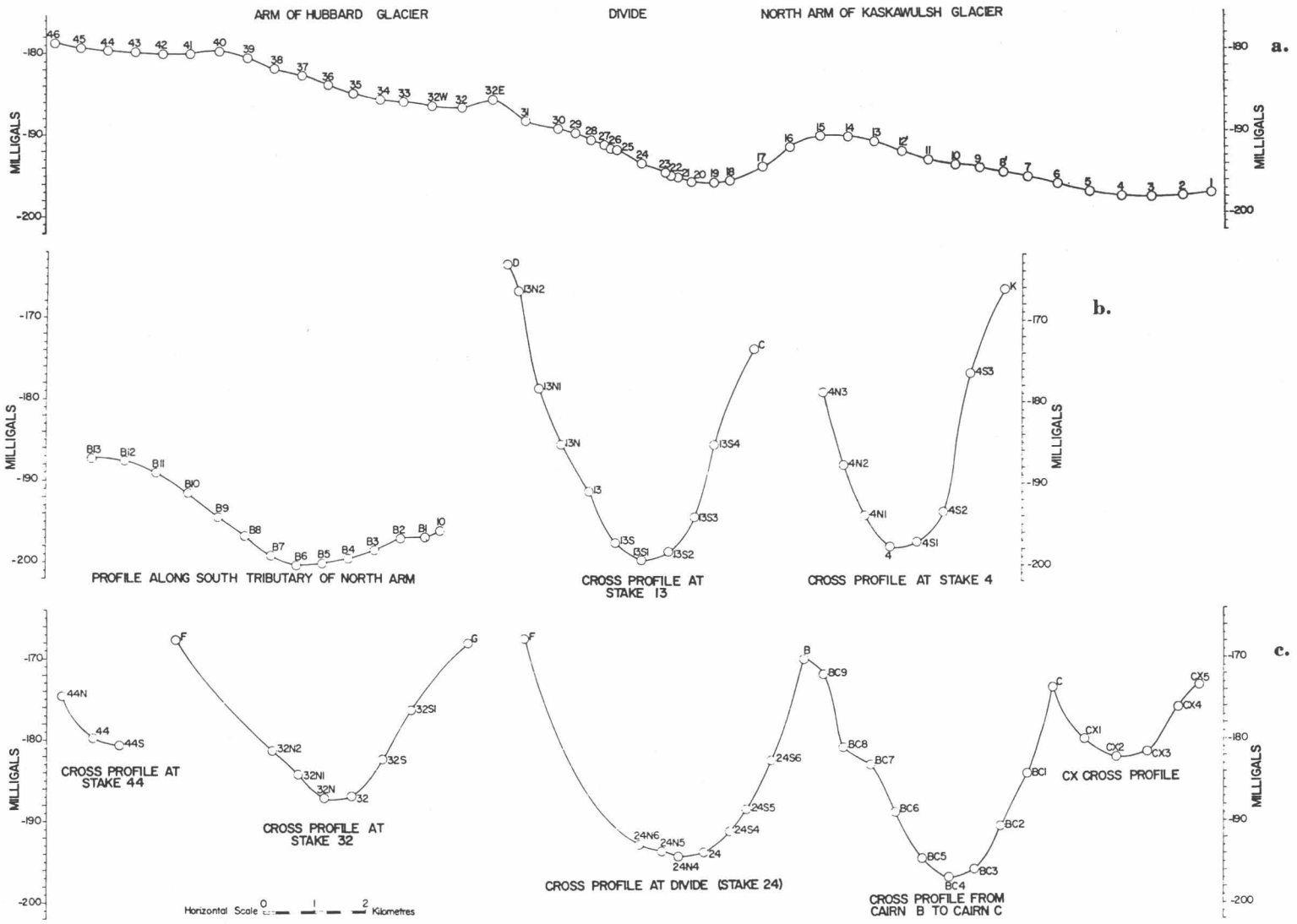

Fig. 4. Bouguer anomaly profiles.

motion was considered necessary. Daily measurements of the changes in the elevation of the snow surface at the divide show the maximum change over the 25-day interval from July 26 to August 19, during which gravity measurements were taken, to be 21.5 cm (Havens, personal communication). Errors resulting from surface lowering are mainly due to differential melting between stations; as such errors are not large and are distributed throughout the entire network it was decided to neglect any correction. Hence the snow surface elevations computed by Sharni for Survey 1 and the Seismic Survey and the coordinates from Survey 2 and the Seismic Survey are used throughout.

Owing to the small range of the gravimeter and the shortage of aircraft time, it was not possible to tie the network of gravity sections to a geodetic station in 1963. However in 1962 Becker (personal communication) measured the gravity difference between Stake 16 and the Dominion Observatory station at Kluane village on the Alaska Highway (Oldham, 1958). No permanent gravity station was established in the region of the glacier at that time to which subsequent gravity measurements could have been tied. However the 1963 survey results show that Stake 24 near the topographic divide has moved only 8 m since 1962 (Sharni, 1963) and the elevation of the snow surface increased by 2.6 m. Using Becker's gravity difference for $g_{24} - g_{16}$ and allowing for 2.6 m of firn of density $\rho = 0.5$ gm/cm^3, the 1963 value of absolute gravity at Stake 24 should be 981,272.4 mgals to within 1.5 mgals. For the other stations the gravity differences are probably correct to ± 0.5 mgals, and these are referred to the value at Stake 24.

Determination of ice thickness from gravity measurements. Before selecting an interpretation approach for the gravity results, a thorough appraisal of the aims and limitations of the particular gravity survey must be made. The simplest but least accurate approach is to imagine the anomaly is due to an infinite horizontal slab of material. The two-dimensional analysis of Hubbert (1948a) or the three-dimensional analysis of Talwani and Ewing (1960) should give better results. In the region of the Glacier Camp the regional density has not been determined and the regional trends have not been isolated. In most of the study area neither the assumption of an infinitely long two-dimensional glacier nor the assumption of an infinite slab give good approximations. However, good seismic results were obtained at almost all gravity stations. The conclusion is that unknown factors are too great to warrant a very sophisticated interpretation approach, and that the Bouguer anomaly profiles should be used only to assist seismic interpretation. The infinite slab assumption, though not very accurate, is easily handled and provides a basis for comparing the seismic and gravity depths directly. The anomaly due to an infinite slab with density contrast ρ and thickness h is

$$g = 2\pi k \rho h.$$

The Bouguer anomalies, assuming a value of absolute gravity of 981,272.4 mgals at Stake 24 and a regional density of 2.67 gm/cm^3, with all pertinent data for each gravity station are to be found in the writer's thesis (Clarke, 1964). To determine the ice thickness from the Bouguer anomaly it is necessary to know what part of the total anomaly is due to regional effects and what part is due to the glacier ice; this establishes a "zero-line" for the anomaly curve. In the absence of satisfactory stations for establishing regional trends these were assumed to be negligible. The zero-line was taken to make the seismic and gravity bedrock profiles as nearly coincident as possible and the density of glacier ice was assumed to be 0.91 gm/cm^3 for this ice-thickness calculation. The Bouguer anomaly profiles are shown in Figure 4;[1] the infinite slab ice-thickness profiles are included in Figure 12. A discussion of the seismic and gravity bedrock profiles is given in the following section on seismic results.

Seismic Measurements

Field work. In 1963 a total of 100 reflection stations was occupied with satisfactory results obtained at the majority of these. A refraction profile was also obtained on the Hubbard Glacier. A twelve-channel high-resolution seismograph manufactured by Houston Technical Laboratories (now Texas Instruments) with a recording oscillograph was used for all seismic work. The speed of the recording paper was 20 inches/sec (50.8 cm/sec) with timing lines every 0.005 sec; 500 cps galvanometers were used as output for all ordinary channels and a 200 cps galvanometer for the Log Level Indicator Trace (which was connected to Channel 10). Up to 40 db of initial suppression were used and automatic gain control was in constant operation. Extensive band-pass filtering was adopted with a double section of M-derived low-cut filters and a single section of M-derived high-cut filters. A pass band of 40 cps to 90 cps was typical although the frequency of reflections varied considerably with the depth of the reflecting layer. Velocity type moving-coil seismometers having a natural frequency of 13 cps were used.

[1] The Bouguer anomaly profiles in Figure 4 were plotted assuming the grid of the map to be oriented so that grid north and true north were coincident. It was later learned that grid north is actually 10° from true north and a slight error in the latitude correction results. Since the character of the Bouguer anomaly profile is unchanged by this error Figure 4 has not been altered.

A variation of the L-spread was resorted to so that the strike and dip as well as the depth of the reflecting "plane" could be calculated. Unfortunately the 50-foot (15.2-m) detector spacing meant that the lengths of the perpendicular arms of the "L" were too short to give the highly accurate step-out times required for the accurate determination of strikes and dips. Nevertheless it was possible to distinguish oblique reflections from near-vertical ones.

A 60 percent high-density high-velocity nitroglycerine-type explosive (CIL Geogel) detonated by No. 8 electrical blasting caps (CIL Seismocaps) supplied the source of seismic energy. The firing current was provided by a capacitor-discharge type blaster which gave a sharp time-break pulse which was recorded on trace 13 of the seismic records. Shots were generally buried in the firn layer at a depth of 3–4 m by means of a SIPRE coring auger. At a depth of 3 m explosions did not penetrate the snow surface but a "second shot" phenomenon presumably caused by slumping at the shot point frequently obscured seismic reflections. At a 4–m shot depth this slumping was not recorded and the coupling of seismic energy was appreciably improved. When repeated shots were required to obtain satisfactory reflections at a particular location, the original shot holes were redrilled and the "sprung" hole was used. This proved a very effective means of coupling seismic energy and high-quality reflections were often obtained. A shot size of 2.5 lb (1.13 kg) of high explosives proved satisfactory at most reflection locations while for the refraction line size shot size ranged from a single blasting cap to 25 lb of high explosives.

Two seismic refraction profiles have been completed in the region of the Glacier Camp: one in 1962 by Becker near Stake 10 on the north arm of the Kaskawulsh Glacier, the other in 1963 by the writer near Stake 32 on the arm of the Hubbard Glacier. These were obtained at the beginning and end of the summer ablation period respectively. Neither of these profiles was reversed since it seemed reasonable that the firn-ice contact would closely parallel the snow surface. For this reason elevation corrections were also considered unnecessary as the snow surface was effectively an inclined plane.

Seismology on glaciers. Above the firn line a glacier is seismically two-layered: a homogeneous layer of glacier ice, density 0.88 – 0.91 gm/cm^3, and an overlying firn layer, with density increasing from as low as 0.4 gm/cm^3 at the surface (Bader *et al.*, 1954) to that of glacier ice at the lower boundary. Seismic refraction enables the determination of the velocity distribution of P waves in the glacier. It has been observed that the hexagonal ice crystals often take on a preferred orientation in which the "c" axis (the slow axis) is near vertical or perpendicular to the maximum shear plane so that the medium is classified as transversely isotropic since it possesses a symmetry axis. Such a medium has five elastic constants not two as does the isotropic solid (Love, 1944). The anisotropy is not usually strong enough to affect seriously the refraction results. By means of perpendicular refraction lines and uphole shots Paterson and Savage (1963) showed that there was no significant anisotropy on the Athabasca Glacier.

The velocity-depth relationship (Figure 6) was computed by numerical integration of the time-distance curve obtained from refracted first arrivals (Figure 5). From the Herglotz-Wiechert solution (Slichter, 1932) the penetration depth, Z_p, for a refracted ray arriving at a detector a distance Δ_p from the shot point is

$$Z_p = \frac{1}{\pi} \int_0^{\Delta_p} \cosh^{-1} \frac{V_p}{V_\Delta} \, d\Delta$$

where V_Δ is the maximum velocity corresponding to a shot-to-detector distance Δ (see Figure 7). Because V_p is the velocity at depth Z_p the time for a wave to travel to a depth h is

$$T = \int_0^h \frac{dZ_p}{V_p} .$$

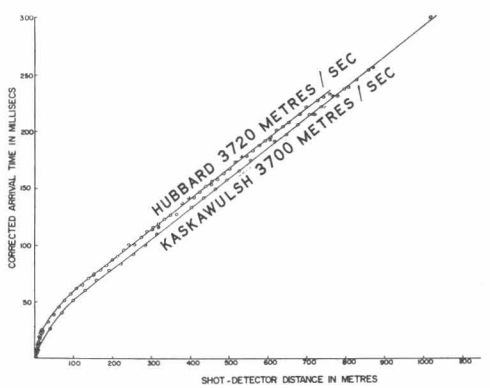

Fig. 5. Refraction arrival times.

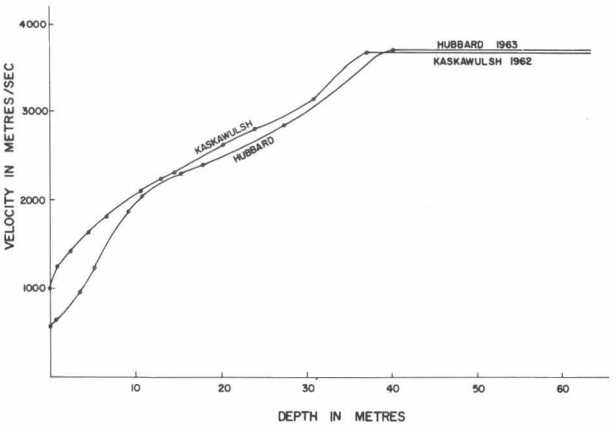

Fig. 6. Velocity of P waves with depth.

When h is the thickness of the firn layer this integration permits the determination of the time required for a vertically-travelling wave to pass through this layer. The results of the two refraction surveys are summarized in Table 2. The determinations of P-wave velocities are probably accurate to 20 ± m/sec. The velocity-depth curves (Figure 6) deserve special comment since both curves differ in character from typical velocity-depth curves for glaciers. In the upper 10-m layer for the Kaskawulsh Glacier curve the velocity increases rapidly but this rapid increase is not seen on the Hubbard Glacier curve. This difference may be caused by the different seismic apparatus used for the two refraction lines or by the deterioration of the upper layer through the summer melting since the refraction profiles for the Kaskawulsh and Hubbard Glaciers were obtained at the beginning and end of the summer ablation period respectively. Although the velocity-depth curves give the impression of a clearly-defined firn thickness this is not the case. The velocity-depth curve is derived from the time-distance curve and the firn thickness corresponds to whatever value of Δ_p is chosen from the time-distance plot. This distance is not apparent as a sharp break on the time-distance curve. The choosing of a value of Δ_p is critical for the determination of Z_p but has a very slight effect on the calculated depths for reflection stations. Table 3 shows P-wave velocities measured on various glaciers of the world.

Application of refraction results to reflection seismic results. Having found the firn thickness, the time required for a vertically-travelling wave to pass through this, and the velocity of P waves in ice, the way the firn layer is to be treated in computing the reflection results must be decided. Solving the two-layer problem for refracted wave paths is hardly warranted since these paths are nearly vertical. More practical approaches are either to strip off the firn layer by subtracting the total travel-time for vertically-travelling P waves in firn, from the times of the reflected arrivals and then calculating the thickness of glacier ice and adding to that the firn

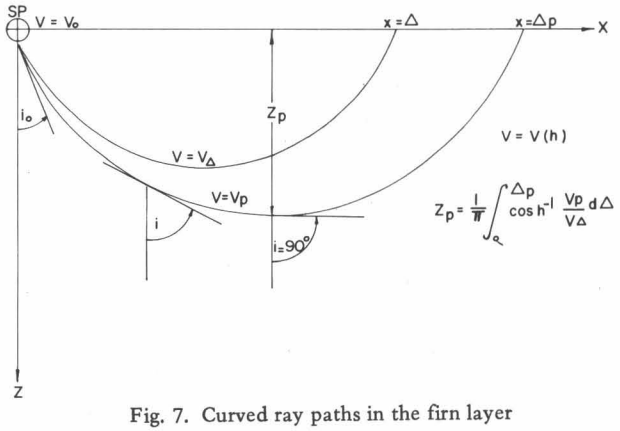

Fig. 7. Curved ray paths in the firn layer

thickness, or to compute an average velocity and solve the problem as a single layer problem. Neither approach considers the effect of curved ray paths in the firn layer but the latter method is less sensitive to the effect of a thick firn layer and was therefore used for all reflection calculations. The average velocity is

$$\bar{V} = V_{ice}\left(1 - 2\frac{T_{firn}}{T_{total}}\right) + 2\frac{Z_{firn}}{T_{total}}$$

where T_{firn} is the one-way vertical travel time in firn and Z_{firn} the firn thickness. In the case of the nth multiple reflection a wave passes through the firn layer 2(n+1) times and the average velocity is

$$\bar{V} = V_{ice}\left(1 - 2(n+1)\frac{T_{firn}}{T_{total}}\right) + 2(n+1)\frac{Z_{firn}}{T_{total}}$$

Since the values of the velocity for P waves in ice (Table 2) from the two refraction surveys agree within the limits of error, it was decided to use the mean value of V_{ice} = 3710 ± 20 m/sec for all calculations. The values of T_{firn} and Z_{firn} for the Hubbard Glacier were used in

TABLE 2. Results of seismic refraction measurements

Glacier	Δ_p	Z_p	one-way time to Z_p	$V_{surface}$	V_{ice}
Kaskawulsh	130 m	37 m	0.016 sec	1010 m/sec	3700 m/sec
Hubbard	99	40	0.020	576	3720

TABLE 3. Velocities of P waves in glacier ice.

Location	Reference	V_p
Taku Glacier, Alaska	Poulter, Allen, Miller[1]	3960 m/sec
Greenland Ice Cap	Bentley *et al.* (1957)	3865
Penny Icecap, Baffin Island	Rothlisberger (1955)	3810
"McGill Ice Cap"[2], Axel Heiberg Island	Redpath (1961)	3790
Hubbard Glacier, Yukon Territory	Clarke	3720
Kaskawulsh Glacier, Yukon Territory	Becker (Pers. comm.)	3700
Athabasca Glacier, Alberta	Paterson and Savage (1963)	3610
		3600

[1] Extracted from a table by Holtzscherer (1954).
[2] Now officially Akaioa Icecap.

computing $\overline{V}$ for Stakes 25 to 46 on the Hubbard Glacier. All other values of $\overline{V}$ were found using the results from the Kaskawulsh refraction profile.

Determination of the depth and spatial orientation of a dipping plane from primary and multiple reflections. It has been established that multiple reflections are routine phenomena in glacier seismic work. It was therefore decided to interpret every supposedly reflected event both as a primary reflection, as a first multiple, and as a second multiple reflection. For simplicity of analysis the glacier was considered to be a one-layer problem in which the firn layer was accounted for by taking an average velocity. This average velocity is exact for waves traveling vertically, and becomes an increasingly poor approximation for waves of high incident angle. Energy and geometry considerations limit the likelihood of high-angle multiple reflections so that the average velocity approach is not unrealistic.

In order to determine the three coordinates which are necessary to locate a point in space (the image shot point) it is necessary to make three independent measurements. For reflection seismology the data from three geophones not in a line are therefore recorded. This requires either shooting along two separate lines or shooting once and recording from a suitable array such as an L-spread. A computer program was prepared to reduce all seismic reflection measurements and to find the depth and space orientation of the reflecting plane (assuming it was a plane). The program consisted of three parts:

(1) reduction of levelling and chaining results
(2) application of time corrections
(3) computation of depth and orientation resulting from interpretation of event as a primary or a first or second multiple reflection.

The elevations of the three principal geophones and the top of the shot hole were found by levelling with a transit and stadia rod; the slope distances were determined by chaining and a knowledge of the inter-geophone spacing. The reduction of these measurements consisted merely of converting chain and level data to angles from the horizontal with respect to the apex geophone (G1 in Figure 8), and of converting all lengths to the metric system.

Corrections to arrival times were necessary to allow for the time lapse between the first break of a reflected arrival and the first trough of the wavelet. The first trough was the arrival picked from the records in all

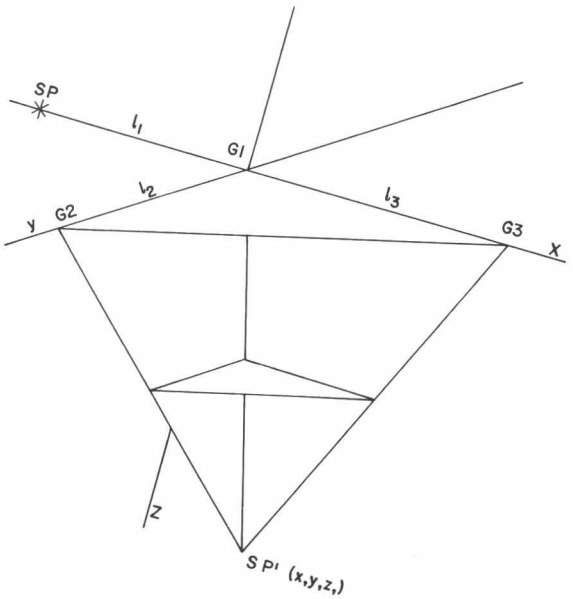

Fig. 8. Coordinates of detectors, shot point, and image shot point.

cases, since it is the most easily distinguished. The time interval between the first break and the first trough was measured from a number of high quality records, averaged and applied as a correction to all records. The extensive filtering required for "clean" records proved a dubious asset since the transmission time curves subsequently supplied by the manufacturer indicated that the transmission times were of the order of 20 m/sec for the filter settings used, and that the delay time was quite sensitive to the frequency of the wave. This injects an unknown into all records and presents a strong case for restricted use of filters. From the five routinely used filter settings, average reflected frequencies were computed from all records for each group. This average frequency was taken as the frequency which characterized the particular filter setting and from this frequency a single lag time was computed for each filter setting and applied as a correction to all records with the same filter settings (Table 4)

Finally a correction for shot depth was applied. This consisted of two parts: a correction to place the shot at the surface and a correction to place the shot from the surface to the plane of the three detectors. From the two refraction profiles an average velocity for P waves at the surface was found to be 793 m/sec and the distance which the shot had to be moved was divided by this

TABLE 4. Filter data

Filter setting	No. of frequency picks	Spread in frequency	Mean frequency	Delay time
MM90 – M140	2	105–142 cps	124 cps	0.020 sec
MM70 – M140	27	88–114	103	0.017
MM40 – M140	1	86	86	0.015
MM40 – M90	68	58–118	76	0.025
MM50 – M90	14	61–91	78	0.023

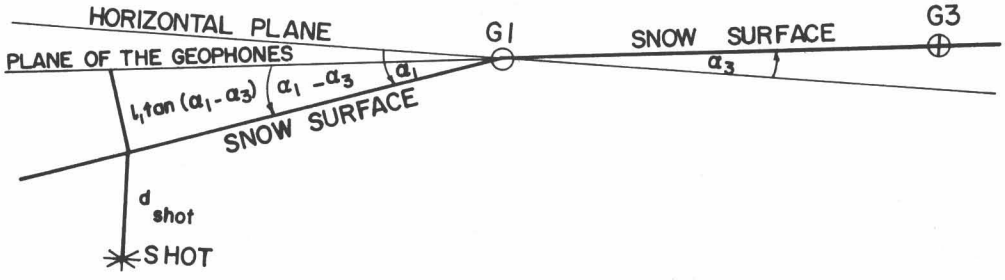

Fig. 9. Correction for shot depth.

velocity to give a time correction. From Figure 9 this correction is seen to be approximately

$$t_{shot} = \frac{d_{shot}}{V_{surface}} + \frac{l_1 \tan(a_1 - a_3)}{V_{surface}}$$

and this was added to the reflection arrival times.

Assume that the shot point and the three detectors are coplanar and have coordinates

$$G1 : (0,0,0)$$
$$G2 : (0,l_2,0)$$
$$G3 : (l_3,0,0)$$
$$SP : (-l_1,0,0)$$

with the apex of the L-spread at the origin (Figure 8), and let the unknown coordinates of the image shot point be x, y, z. Considering the velocity as a constant, and denoting the time required for a wave to travel from the image shot point to detectors *G1*, *G2*, and *G3* as t_1, t_2, t_3 respectively, the resulting expressions are

$$V^2 t_1^2 = x^2 + y^2 + z^2 \quad (1)$$

$$V^2 t_2^2 = x^2 + (y - l_2)^2 + z^2 \quad (2)$$

$$V^2 t_3^2 = (x - l_3)^2 + y^2 + z^2 \quad (3)$$

and

Solving (1) and (2) for y yields

$$y = \frac{V^2(t_1^2 - t_2^2) + l_2^2}{2l_2}$$

and (2) and (3) for x,

$$x = \frac{V^2(t_2^2 - t_3^2) + 2yl_2 + l_3^2 - l_2^2}{2l_3}$$

and finally from (1).

$$z = \sqrt{V^2 t_1^2 - x^2 - y^2}$$

If the three detectors are not in the horizontal plane then the results must be transformed to place the three detectors in their correct orientation (Figure 10). (The previously discussed shot-depth correction renders the shot point coplanar with the three geophones.) Assuming the angles from the horizontal to be small, the transformation can be approximated by successive transformations. First rotate the axes about the y axis by an angle α_3, the angle which the line joining *G1* and *G3* makes with the horizontal plane. Then rotate the resulting axes about the new x axis by the angle α_2, the angle the original y axis made with the horizontal. The resulting transformations are

$$x_1 = x \cos a_3 + z \sin a_3$$

$$y_1 = y$$

$$z_1 = x \sin a_3 + z \cos a_3$$

$$x_2 = x_1 = x \cos a_3 + z \sin a_3$$

$$y_2 = y \cos a_2 + z_1 \sin a_2 = x \sin a_3 \sin a_2 + y \cos a_2 + z \cos a_3 \sin a_2$$

$$z_2 = y_1 \sin a_2 + z_1 \cos a_2 = x \sin a_3 \cos a_2 + y \sin a_2 + \cos a_3 \cos a_2$$

Finally translate the shot point to the origin

$$x_3 = x \cos a_3 + l_1 + z \sin a_3$$

$$y_3 = y_2 \qquad z_3 = z_2$$

Having now obtained the coordinates of the image shot point the depth, dip, and dip direction may be determined. The depth is merely half the value of the z_3 coordinate. The strike of the dip with respect to the axes

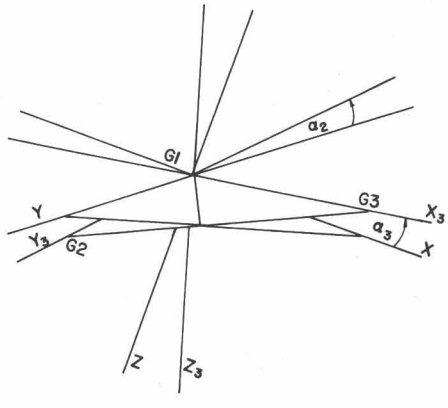

Fig. 10. Spatial orientation of the plane of the three detectors.

(Figure 8) is in the direction of the horizontal projection of the line joining the shot point to the image shot point and is therefore

$$\theta = \tan^{-1}\left(\frac{y_3}{x_3}\right)$$

The dip angle is

$$\delta = \tan^{-1}\left(\frac{\sqrt{(y_3)^2+(x_3)^2}}{z_3}\right)$$

The foregoing calculations may be readily extended to computation for multiple reflections. The problem reduces to that of finding the trigonometric relationship between the image shot points for the primary and multiple reflections.

Consider a plane in space dipping at an angle δ with respect to the horizontal plane (Figure 11). The shot point is located at point O on the surface. Waves are reflected at the two boundary planes so that the waves reflected from the dipping plane will arrive as if propagated from an image source located at point P. The method of images locates the image shot points for the first and second multiple reflections these image sources being $P_1\ (x_1,y_1,z_1)$ and $P_2(x_2,y_2,z_2)$ respectively. The subscripts in this notation are not to be confused with the usage in the previous section to indicate transformation of coordinates. The angles labelled as equal to δ are easily recognized using the fact that for an isosceles triangle the angles opposite equal sides are equal.

For the first reflected arrival

$$\tan^{-1}\frac{\overline{OR}}{\overline{RP}} = \frac{\sqrt{x^2+y^2}}{z} = \delta$$

and for the first multiple reflection

$$\tan^{-1}\frac{\overline{OR_1}}{\overline{R_1P_1}} = \tan^{-1}\frac{\sqrt{x_1{}^2+y_1{}^2}}{z_1} = 2\delta$$

$$\tan^{-1}\frac{\overline{QR_1}}{\overline{R_1P_1}} = \delta$$

so that

$$\overline{R_1Q} = \overline{R_1P_1}\tan\delta = z_1\tan\delta$$

$$\overline{QO} = 2\overline{RP}\tan\delta = 2z\tan\delta$$

$$\overline{OR_1} = \sqrt{x_1{}^2+y_1{}^2} = \overline{R_1Q}+\overline{QO}$$

$$= z_1\tan\delta + 2z\tan\delta$$

Solving for z,

$$z = \frac{\tfrac{1}{2}(\tan2\delta - \tan\delta)\,z_1}{\tan\delta}$$

and

$$z_1 = \frac{2z\tan\delta}{\tan2\delta - \tan\delta}$$

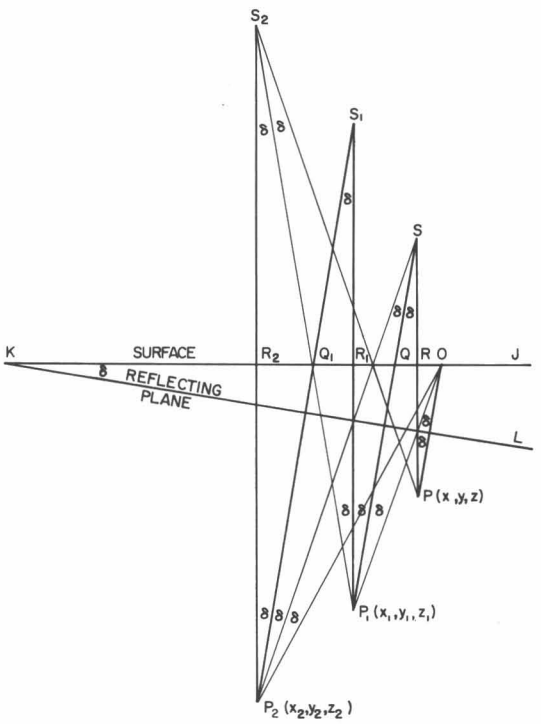

Fig. 11.
Multiple reflections from a dipping plane.

The dip direction with respect to the axes is

$$\theta_1 = \tan^{-1}\frac{y_1}{x_1}$$

and the depth can be found as before using the relationship between z_1 and z.

Similarly for the second multiple reflection with image shot point, $P_2\ (x_2\ y_2\ z_2)$

$$\tan^{-1}\frac{\overline{OR_2}}{\overline{P_2R_2}} = 3\delta = \tan^{-1}\frac{\sqrt{x_2{}^2+y_2{}^2}}{z_2}$$

$$\overline{Q_1R_2} = P_2R_2\tan\delta = z_2\tan\delta$$

$$\overline{QQ_1} = \overline{Q_1R_1}+\overline{R_1Q} = 2\overline{R_1Q} = 2P_1R_1\tan\delta$$

and

$$\overline{QO} = \overline{QR}+\overline{RO} = 2\overline{RO} = 2z\tan\delta$$

$$\overline{OR_2} = \overline{Q_1R_2}+\overline{Q_1Q}+\overline{QO} = \sqrt{x_2{}^2+y_2{}^2}$$

$$= z_2\tan\delta + 2z_1\tan\delta + 2z\tan\delta.$$

Using the previously derived relation for z_1

$$\sqrt{x_2^2 + y_2^2} = z_2 \tan\delta + \frac{4z \tan^2\delta}{\tan 2\delta - \tan\delta} + 2z \tan\delta$$

$$z = \frac{z_2 (\tan 3\delta - \tan\delta)(\tan 2\delta - \tan\delta)}{2 \tan\delta (\tan 2\delta + \tan\delta)}$$

The depth follows immediately from the previously derived relations, and the strike is

$$\theta_3 = \tan^{-1} \frac{y_3}{x_3}$$

with respect to the axes. For the one layer case $\theta_1 = \theta_2 = \theta_3$ but in the above treatment a different average velocity is used for each reflection so that the values of θ change slightly for the primary and multiple reflections.

Results of seismic survey. The results of the computer program to determine the ice thickness are summarized in Clarke (1964); the bedrock profiles for the entire area of coverage are shown in Figure 12; the bedrock contours for a smaller area of detailed coverage are included in Figure 13. Since the reflection times for a record of good quality may be estimated to ±1 m/sec the resulting uncertainty in ice thickness is ±2.0m. Considering the uncertainties in the filter correction and variations in the time between the first break and the first trough of a reflected arrival, the accuracy for relative differences in ice thickness should be with ±10m. Occasionally the arrival time may be in error by one complete cycle, which would cause an error of the order of 25 m in the ice thickness. The estimated accuracy of the absolute values of ice thickness are dependent on the accuracy of the average velocity and the faith one places in the manufacturer's transit-time estimates which seem inordinately high. It would appear that the absolute values of ice thickness are within 5 percent of the actual values.

The resulting ice thicknesses for all reflections identified are shown on the profiles; reflections of low quality which indicate a bedrock profile differing from that indicated by gravity are identified as poor quality reflections. In all cases the reflecting points are projected onto the plane of the profile, for instance the profile may indicate a bedrock high, but the actual case is frequently that the line of the profile does not exactly follow the valley center and reflections from the valley sides are being received. When the reflecting surface was found to be more than 100 m from the line of the profile such reflections were indicated as oblique. On a number of records more than one reflected event was identified. These included supposed multiple reflections from several image sources as well as possible moraine reflections. Not infrequently the various reflections provided valuable additional information from distant reflecting surfaces so that one shot might provide ice thickness information from as many as three distant locations. This was particularly evident from the cross traverses for which the first reflected arrival was an oblique shadow reflection from the valley side followed by deeper less oblique reflections from nearer the valley center. In every case the bedrock surface was determined from the shallowest reflection received except when the first reflection was oblique and a near vertical reflection followed. At several stations gravity profiles differed greatly from the seismic profile and also the seismic depth was not consistent with the trends and adjacent values, the depth being greater than expected. In such cases the depth value assuming a first or second multiple reflection was calculated. If the resulting value fitted the gravity profile and bedrock trends it was accepted and was indicated as a depth obtained from a multiple reflection. The depths for stations at B2 and CX5 are examples of calculations made assuming the reflected event to be a first multiple reflection. The bedrock surface resulting if the reflections at Stations 24S5 and 24S6' are first multiples is dotted in but the evidence for this is dubious.

Records with several reflected events which seem likely to be multiples can be used to test the method of ice thickness calculation. At Stake CX2 events at 242 m/sec and 462 m/sec were detected. Assuming the first event to be a primary reflection the ice thickness is 362 m. Assuming the second event to be a first multiple reflection gives an ice thickness of 376 m. At Stake B2 events at 576 m/sec and 746 m/sec give thicknesses of 481 m and 419 m, assuming these to be first and second multiple reflections, the primary reflection being obscured. The poor coincidence of the last values may be due to several causes. For instance, the primary assumptions may be invalid, or the reflecting surface is not a plane, or reflections may not be simple multiples as assumed.

Investigations of Glacier Flow

Measurement of surface flow on the Kaskawulsh and Hubbard Glaciers. Annual and summer surface flow rates have been determined from three surveys of the metal stakes erected in 1962. The first survey was made by Zissett in 1962; two surveys were made by Sharni in 1963 (Survey 1 and Survey 2). A Wild T2-400^g theodolite was used and coordinates were found by resection and intersection. The coordinates of the 1963 survey are estimated to be correct to within±30 cm and the elevations to be within ±10 cm at the time of the survey. The annual flow rates for the metal stakes are found in Table 5 and a part of Sharni's map of flow vectors is reproduced (Figure 13). Values in Table 5 which are believed erroneous or of low accuracy are indicated by brackets. The summer flow rate proved to be the same as the mean annual flow rate on the Kaskawulsh Glacier but greater than the mean annual flow rate on the Hubbard Glacier. This latter observation may be due entirely or in part to differences in the date of survey, the stakes on the Hubbard Glacier having been erected near the end of the summer of 1962, whereas those on the Kaskawulsh were erected early in the summer. The maximum annual movements were 150 m at Stake 1 on the Kaskawulsh

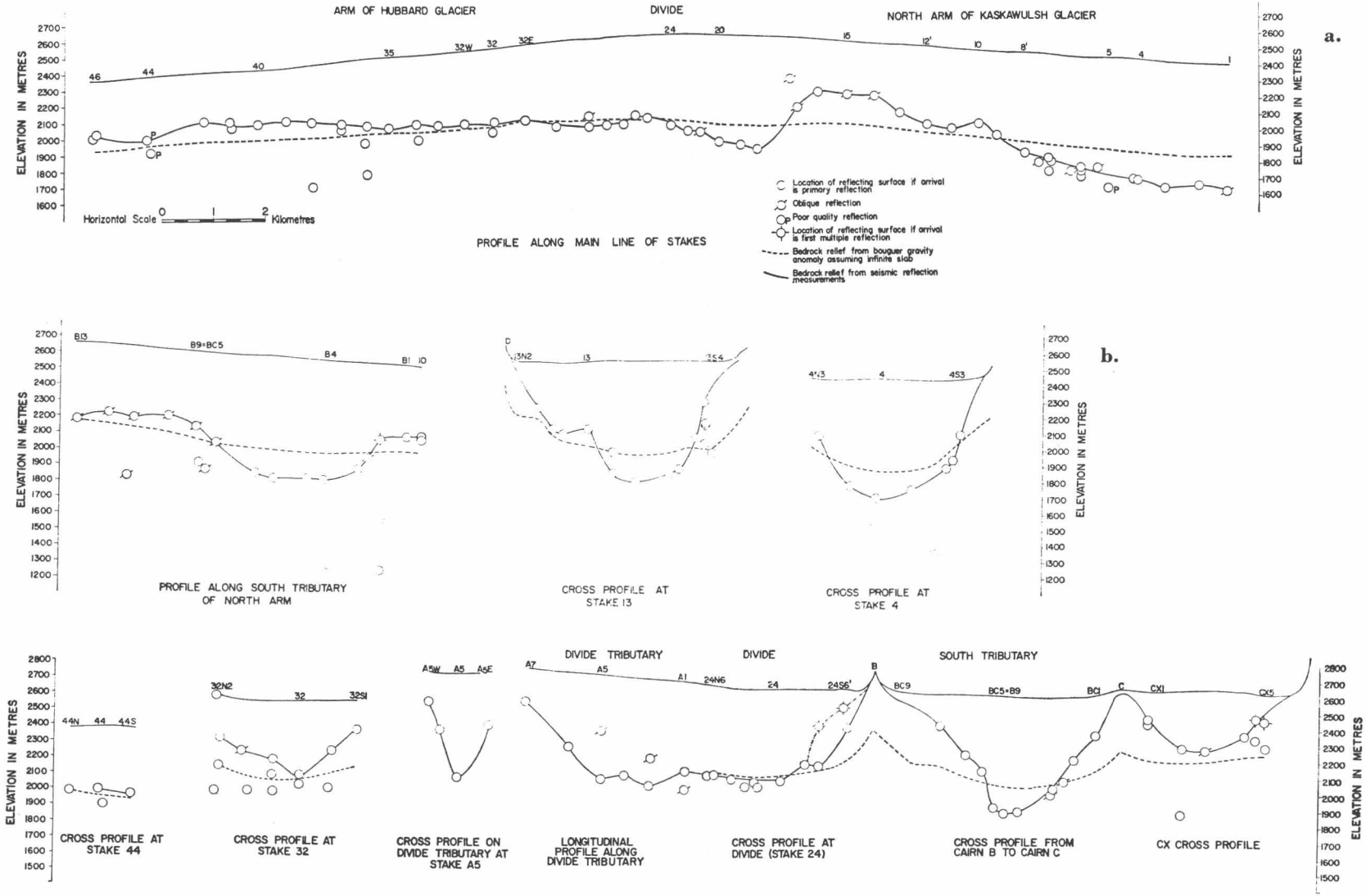

Fig. 12. Bedrock profiles from geophysical measurements.

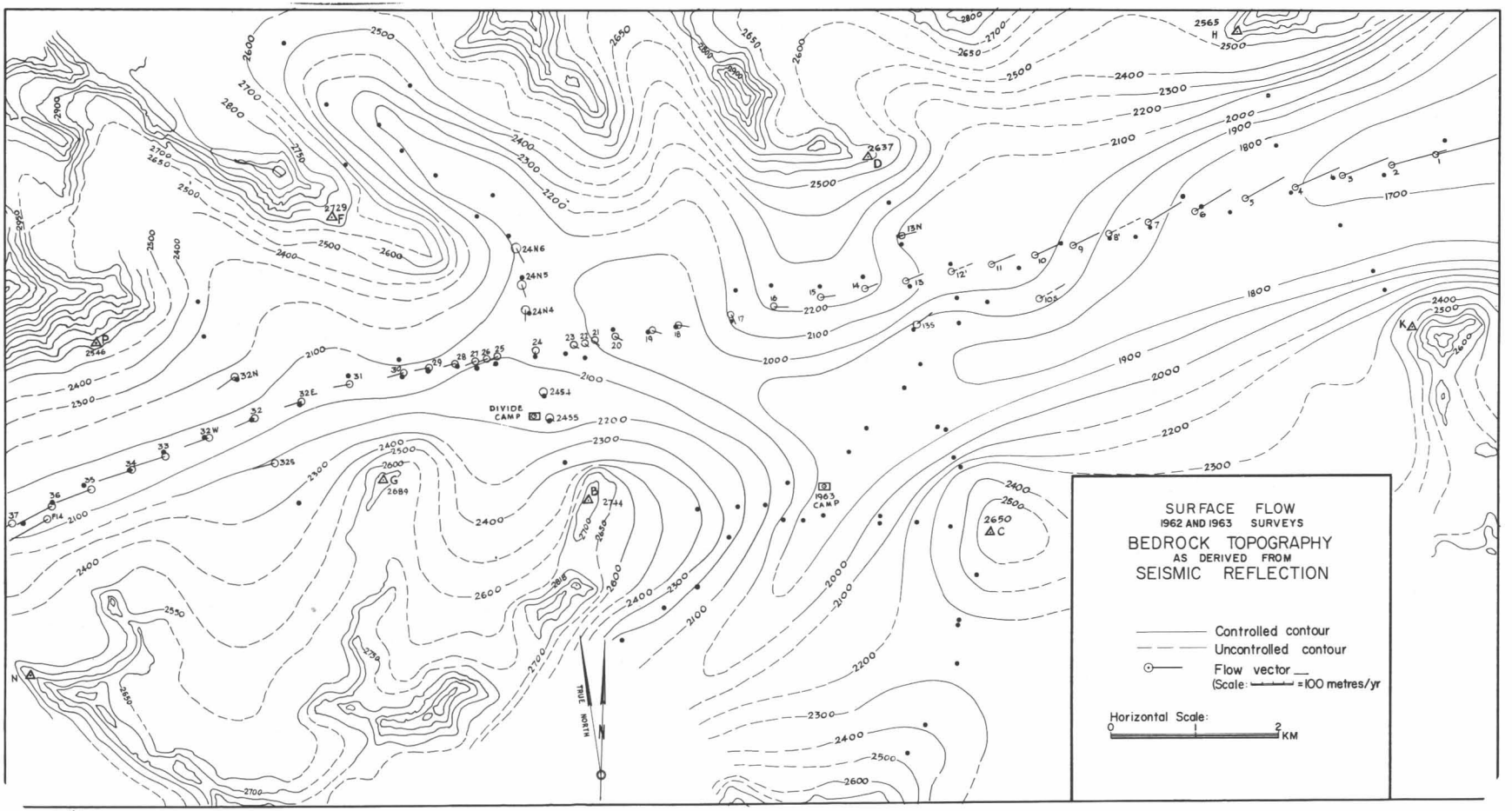

Fig. 13. Bedrock topography and surface flow rates.

TABLE 5. Annual Movements of Flow Stakes.

$$\Delta x = x_{63} - x_{62}$$
$$\Delta y = y_{63} - y_{62}$$
$$\Delta v^2 = \Delta x^2 + \Delta y^2$$

Stake	Δx	Δy	Δv
1	143.1 *m*	45.6 *m*	150
2	127.5	40.0	134
3	111.3	50.7	123
4	103.4	54.0	117
5	95.7	58.7	112
6	87.3	58.2	105
7	76.5	51.0	92
8′	—	—	(85)
9	67.3	35.9	76
10	60.4	32.7	69
11	54.1	28.3	61
12′	—	—	(53)
13	40.6	18.3	45
13S	48.3	32.1	58
13N	34.8	8.7	36
14	35.1	14.3	38
15	33.7	6.5	34
16	29.2	− 0.4	29
17	(66.8)	(35.1)	(22)
18	21.7	− 6.4	23
19	20.2	− 6.6	21
20	16.8	− 7.0	18
21	15.8	−12.2	20
22	12.4	− 8.8	15
23	9.6	− 8.8	13
24	0.7	− 8.1	8
24S5	4.3	− 2.3	5
24S4	2.5	− 1.4	3
24N4	0.9	−22.4	22
24N5	8.5	−31.8	33
24N6	20.7	−34.3	40
25	−14.4	− 8.2	17
26	−16.2	− 7.8	18
27	−18.5	− 7.6	20
28	−22.5	− 7.2	24
29	−26.8	− 6.1	27
30	−30.4	− 7.8	31
31	−34.4	− 7.7	35
32E	−37.8	−14.3	40
32	−44.1	−23.0	50
32W	−59.1	−22.9	63
32S	−33.4	−10.1	35
32N	−41.8	−29.8	51
33	−71.4	−24.9	76
34	−74.7	−28.5	80
35	−79.5	−35.6	87
36	−84.0	−47.7	97
F14	−85.7	−50.7	100
37	−80.4	−54.5	97
38	—	—	(126)
39	−86.9	−69.8	111
40	−98.8	−65.5	118
41	—	—	(155)
42	−114.9	−60.5	130
43	−117.0	−58.8	131
44	−120.6	−54.6	132
45	−118.3	−51.1	129
46	−115.4	−46.7	125

Glacier and 132 m at Stake 44 on the Hubbard Glacier.

The relationship of surface flow to ice thickness measurements. The close relationship that exists between bedrock topography and surface flow is shown in Figure 13 in which the geophysically-determined ice thicknesses form the control points on a contour map of the bedrock surface onto which is superimposed a map of the surface flow vectors. The bedrock surface was contoured from the geophysically-determined ice thicknesses. The flow line and the line of the valley center are roughly coincident. On the Hubbard Glacier the flow line closely follows the line of marker stakes whereas on the Kaskawulsh Glacier the line of stakes is offset from the flow line. Tributary glaciers deflect the flow of the main channel and at the divide the flow is complicated by the swirl effect of the Divide Tributary.

When seismic investigations were first planned in the divide area of the Kaskawulsh and Hubbard Glaciers the question of whether or not a bedrock divide could be related to the flow divide was considered. After two summers of seismic measurements the answer is still not clear. It is often difficult to know whether seismic measurements have been made at the deepest point of the valley cross-section. Perhaps the best plan would be to measure ice thickness along the flow line which should coincide with the deepest channel. In Nye's (1952a, 1952b) discussion of the relative influences of surface slope and bedrock slope in determining surface flow it is made clear that the surface slope is the more significant factor. Hence the observed coincidence of the flow divide with the topographic divide is to be expected but there is no reason to expect a corresponding bedrock divide. Indeed, dismissing the bedrock high between Stake 17 and Stake 8 as being well displaced from the valley center, the glacier trough would appear to be highest at Stake 39 on the Hubbard Glacier. This is hardly a clearly-defined divide, and it seems better to think of a divide in a broader sense and not as a sharply-defined high in the bedrock.

An interesting relationship between surface elevation and bedrock topography is found in the vicinity of Stake 41 near the end of the line of stakes on the Hubbard Glacier. A high in the surface elevation between Stakes 40 and 42 appears to result from a bedrock high at Stake 42 "downstream" from the surface wave. In addition the downslope rate of increase of surface flow suddenly decreases from a fairly uniform rate of the order of 12 m/yr per km downslope to a value near zero. In other words the flow changes from extending to non-extending. Unfortunately discrepancies in both the seismic results and the flow measurements preclude any detailed analysis of these relationships and this would seem to be an area in which further study could prove very rewarding. Detailed seismic work in the vicinity of the flow divide between the arms of the Kaskawulsh and Hubbard Glaciers in conjunction with flow measurements on the Divide Tributary would also be of value.

Summary and conclusions

From gravity and seismic measurements near the divide of the Kaskawulsh and Hubbard Glaciers, calculations of ice thickness were made.

Gravity differences were measured for a network of 107 stations and corrections made for misclosure, latitude, and terrain. In spite of the great uncertainties in making three-dimensional terrain corrections in a largely ice-covered area, the gravity anomalies observed were sufficiently pronounced that errors in terrain correction were not critical except for gravity stations at the cairns. An absolute gravity base was obtained indirectly using a tie made in 1962 to a geodetic station at Kluane village on the Alaska Highway. Observed Bouguer anomalies in the divide region range from −199.8 mgal over ice (at Stake B6) to −162.9 mgal on rock (Cairn D) indicating a large negative Bouguer anomaly for the St. Elias Range.

Seismic reflections were obtained at most of the gravity stations and from two refraction profiles the velocity of P waves in ice was found to be 3710 ± 20 m/sec. The firn thickness was approximately 40 m and the minimum velocity found in the firn layer was 576 m/sec. From an investigation of the maximum possible effects of anisotropy in the ice it was concluded that any effects on the refraction results would be sufficiently small to be ignored. The computation of an average vertical velocity at each seismic station from calculations of the time delay and thickness of the firn layer was made. Using arrival times from three geophones not in a line the depth and spatial orientation of the reflecting surface was found assuming it to be a plane. This calculation was repeated assuming the arrival to be a first or second multiple reflection. A comparison of the depths obtained from a single record on which events were identified as primary and multiple reflections suggested that either some of the events were wrongly identified or that the assumption of a reflecting plane was not satisfactory. The maximum ice thickness was found to be 778 m at Stake 1 on the Kaskawulsh Glacier and 539 m at Stake 29 on the Hubbard Glacier. The ice thickness at Stake 24 on the topographic divide was 539 m. Maximum bedrock elevations on the main line of stakes were found to be 2261 m at Stake 16 and 2102 m at Stake 39 on the Kaskawulsh and Hubbard Glaciers respectively.

Bouguer anomaly profiles were compared with the corresponding seismic profiles and direct comparisons of the ice-thickness determinations were made assuming the glacier to be an infinite slab. This assumption proved to be a poor approximation and effectively smoothed out bedrock relief. Because regional gravity gradients and the regional density were not well established and because of the general high quality of the seismic reflection results, no further refinements were applied to the gravity results. Nevertheless Bouguer anomaly profiles proved an invaluable aid to seismic interpretation.

From the combined gravity and seismic results the bedrock surface was contoured and the boundary of the glacier mapped. Superposition of the flow vectors established from the 1962 and 1963 surveys of the metal stakes showed a clear relationship between the surface flow and the bedrock topography. Maximum annual flow rates were found to be 150 m/yr at Stake 1 on the Kaskawulsh Glacier and 132 m/yr at Stake 44 on the Hubbard Glacier. The minimum measured flow was 3 m/yr at Stake 24S4.

Acknowledgments

The guidance and suggestions of Prof. G. D. Garland and helpful discussions with Prof. J. C. Savage of the University of Toronto are gratefully acknowledged. To all members of the Icefield Ranges Research Project, I am indebted, particularly to project leader R. H. Ragle, my stoic assistants, William Isherwood and Donald Macpherson, and to Dan Sharni, the project surveyor. I was supported by a National Research Council grant throughout this work. Logistic support was received from the Arctic Institute of North America, the American Geographical Society, the Defence Research Board, and the Universities of Alberta and Toronto.

References

Ahlmann, H. W. (1933) Part 8, Glaciology, IN Scientific results of the Swedish-Norwegian Arctic Expedition in the summer of 1931, GEOGR. ANNAL., 15, 161 – 216.

Bader, H., Haefeli, R., *et al.* (1954) Snow and its metamorphism, U. S. Army SIPRE, TRANSLATION 14, 313 pp.

Benson, C. S. (1962) Stratigraphic studies in the snow and firn of the Greenland Ice Sheet, U. S. Army SIPRE, RES. REPT. 70, 93 pp.

Bentley, C. R., Pomeroy, P. W., and Dorman, J. H. (1957) Seismic measurements on the Greenland Ice Cap, ANN. DE GEOPHYS., 13, 253 – 285.

Clarke, G. K. C. (1964) Geophysical measurements on the Kaskawulsh and Hubbard Glaciers, Yukon Territory, Canada, M. A. THESIS, Univ. Toronto, 102 pp.

Garland, G. D. (1956) Gravity and isostasy, HANDBUCH DER PHYSIK, 47, 202 – 245.

Garland, G. D., and Tanner, J. G. (1957) Investigations of gravity and isostasy in the southern Canadian Cordillera, PUBL. DOMIN. OBSERV., Vol. 19, pp. 169 – 222.

Gibson, M. O. (1941) Network adjustment by least squares – alternative formulation and solution by iteration, GEOPHYSICS, 6, 168 – 179.

*Havens, J., and Saarela, D. E. (1964) Exploration meteorology in the St. Elias Mountains, ICEFIELD RANGES RESEARCH PROJECT 1963, PRELIM. REPT. (unpublished)

Heiskanen, W. A., and Vening Meinesz, F. A. (1958) THE EARTH AND ITS GRAVITY FIELD, McGraw-Hill, New York, 470 pp.

Holtzscherer, J. J. (1954) Seismic investigations in Inglefield Land, IN FINAL REPORT, THE SCIENTIFIC PROGRAM, PROGRAM B, OPERATION ICE CAP 1953, U. S. Transportation Corps., pp. 267 – 299.

Hubbert, M. K. (1948a) A line-integral method of computing the gravimetric effects of two-dimensional masses, GEOPHYSICS, 13, 215 – 225.

Hubbert, M. K. (1948b) Gravitational effects of two-dimensional topographic features, GEOPHYSICS, 13, 226 – 254.

Love, A. E. H. (1944) A TREATISE ON THE MATHEMATICAL THEORY OF ELASTICITY, 4 ed., Cambridge Univ. Press, New York, 643 pp.

Nettleton, L. L. (1940) GEOPHYSICAL PROSPECTING FOR OIL, McGraw, New York, 444 pp.

Nye, J. F. (1952a) The mechanics of glacier flow, J. GLACIOL., 2, 82 – 93.

Nye, J. F. (1952b) A comparison between the theoretical and the measured long profile of the Unteraar Glacier, J. GLACIOL., 2, 103 – 107.

Oldham, C. H. G. (1958) Gravity and magnetic investigations along the Alaska Highway, PUBL. DOMIN. OBSERV., Vol. 21, pp. 1 – 22.

Paterson, W. S. B., and Savage, J. C. (1963) Geometry and movement of the Athabasca Glacier, J. GEOPHYS. RES., 68, 4513 – 4520.

Ragle, R. H. (1964) The Icefield Ranges Research Project, 1963, ARCTIC, 17, pp. 55 – 57.

Redpath, B. B. (1961) Seismic operations, IN JACOBSEN-MCGILL ARCTIC RESEARCH EXPEDITION TO AXEL-HEIBERG ISLAND, QUEEN ELIZABETH ISLANDS, PRELIM. REPT. 1959 – 1960, McGill Univ. 219 pp.

Röthlisberger, H. (1955) Studies in glacier physics on the Penny Ice Cap, Baffin Island, 1953, Part 3 Seismic sounding, J. GLACIOL., 2, 539 – 552.

Slichter, L. B. (1932) The theory of the interpretation of seismic travel-time curves in horizontal structures, PHYSICS, 3, 273 – 295.

Sharni, D. (1963) Survey report 1963, ICEFIELD RANGES RESEARCH PROJECT (unpublished)

Talwani, M., and Ewing, M. (1960) Rapid computation of gravitational attraction of three dimensional bodies of arbitrary shape, GEOPHYSICS, 25, 203 – 225.

*This article is reprinted in the present volume.

Radar Sounding of Glaciers in the Icefield Ranges

Donald E. Nelsen *

Introduction

An investigation of the use of a Scott Polar Research Institute (SPRI) Mark II Radio Echo Sounder in the Icefield Ranges of the St. Elias Mountains was performed during the summer of 1967. The radar apparatus was installed on a Model H395B Helio Courier airplane. Measurements were made from the air along the entire length of the Kaskawulsh Glacier, in the divide region between the Kaskawulsh and Hubbard Glaciers, and along the upper Donjek Glacier, to an altitude of 3800 m (12,500 ft.). The object of these experiments was to determine the potential usefulness of the apparatus for mapping and studying glaciers in this region.

Operation of the system is similar to that of radar; a short pulse of electromagnetic energy is emitted, and objects in the path of the signal cause echoes that are received by the apparatus. The time duration between the emission of a pulse and the reception of an echo determines the range from the transmitter to the reflecting object. When the apparatus is operated above a glacier, either on the surface or from an airplane, reflections occur at the surface, at internal inhomogeneities, and at bedrock. If these reflections are strong enough or not too badly distorted when they reach the receiver, the distances to the corresponding reflectors can be determined since the wave speed in ice is known.

Several factors can limit or prevent the usefulness of the sounder. (1) Unwanted echoes (clutter) from valley walls or other objects can mask the nearby bottom echoes. (2) Wet surface snow and streams can highly attenuate the signal and cause reflections. (3) Highly fractured and crevassed areas can cause clutter and multiple internal reflections. One of the main objects of our tests was to determine the extent to which these three factors limited use of the apparatus in the Icefield Ranges region.

The Apparatus

The SPRI system, installed in a Helio Courier aircraft, used separate single-wire dipole antennas for transmitting and receiving. Each antenna was placed under a wing, between wingtip and fuselage. A 50- to 75-ohm ferrite matching transformer was inserted at the center of each dipole. Type RG8 coaxial cable led from each of the matching transformers to the cabin enclosure.

All measurements were made by visually observing an oscilloscope presentation of the return signal as a function of time. Since the echo pattern was frequently very complicated and changing rapidly, interpretation was inefficient and less effective than it would have been had we been able to use either a scope camera or a continuous recorder.

*Department of Electrical Engineering, Massachusetts Institute of Technology, Cambridge.

Measurements Performed

A total of eight flights were made, the first four for the purpose of adjusting the antennas and the apparatus. With the remaining flights the following measurements were performed:

(1) A preliminary search for bottom echoes was made along the entire length of the Kaskawulsh Glacier, up the central arm, across the divide region, and down the north arm.

(2) A careful search for bottom echoes in the region near the confluence of the north and central arms of the Kaskawulsh Glacier was carried out.

(3) A flight was undertaken along the upper reaches of the Donjek Glacier near the southeast flank of Mt. Steele to an altitude of 3800 m. The object here was to see if definite bottom reflections could be observed in the sub-temperate glaciers found at that altitude.

(4) Extensive observations were made in the divide region between the Kaskawulsh and Hubbard Glaciers. Three traverses were flown and several landings made. The object of these measurements was to distinguish between the reflections from nearby nunataks and reflections from the glacier bottom. Our tests were made in an area where detailed depth measurements using seismic and gravity methods had previously been made by Clarke (see pp. 89–106 of this volume). Therefore we could compare our depth estimates with the estimates of Clarke, and knowing the positions of the nunataks, discriminate between the echoes from the nunataks and those from the bottom. Then by moving toward a nunatak, we could observe what happened to the corresponding echoes.

Conclusions

The radar sounding technique was highly successful in the divide region between the Kaskawulsh and Hubbard Glaciers, and would probably be useful in trenches as wide as the upper reaches of the Donjek Glacier. In the divide region, our depth estimates agreed very well with Clarke's. Clutter from nearby nunataks was not a problem when the plane was flying within a few hundred feet of the glacier surface. Because of a highly complicated return signal, no interpretation of the bottom echo could be made in highly fractured regions such as exist in the lower reaches of the Kaskawulsh Glacier. In the upper reaches of the Donjek Glacier, definite echoes were detected. More measurements, however, would have to be made to determine whether these were from valley walls or from the glacier bottom.

An Examination and Analysis of the Formation of Transverse Crevasses, Kaskawulsh Glacier*

Gerald Holdsworth†

ABSTRACT. The main purpose of this investigation was (1) to examine the applicability of Nye's theoretical expression for the longitudinal strain rate on the surface of a valley glacier; namely to test whether:

$$\dot{\epsilon}_x = mV_b \left(mV_b + u_s\right)^{-1} \left(\frac{a}{h} + u_s\, k\cot\alpha - \frac{1}{h}\frac{\partial h}{\partial t} - \dot{\epsilon}_y + \frac{1}{2}h\bar{V}\frac{dk}{dx}\right)$$

and (2) to investigate the mechanics and mode of formation of transverse crevasses.

In an area at the head of a valley glacier, a regional strain rate field was derived from velocity and strain net measurements. The result of a comparison between measured and computed strain rates is inconclusive because the assumptions on which the theoretical equation is dependent are not valid except in one short section, where an approximate agreement is found.-

A value of regional longitudinal extending strain rate of about 3.5×10^{-5} day $^{-1}$ is associated with the occurrance of the first transverse crevasse in previously unfractured firn. The strain rate gradient and hence the rate of stress development associated with this critical strain rate is considered to be important. Localized strain rates and stresses of at least an order of magnitude greater than regional values are deduced to be responsible for fracturing of ice.

Regional values of strain rate do not give a theoretical depth of crevasses close to the observed values. Strain rates of at least an order of magnitude greater are required to produce a rough agreement.

Crevasse spacings average 2.8 x mean crevasse depth, which is about 26 m. Some methods of computing crevasse spacings are given. Nielsen's formula gives a spacing close to the mean of the measured spacings.

A concept of the formation of transverse crevasses is discussed. This follows closely the hypothesis of Meier. The crevasses appear to be forming at the margins of the ice stream and to be propagating quietly towards the center; a plastic rather than an elastic behavior is thus suggested. Suitably placed seismograph stations could be used to locate initial points of failure within the ice.

INTRODUCTION

Statement of Problem

In recent years the theory of glacier mechanics has received much attention, especially from J. F. Nye and J. Weertman. As a result of the steady accumulation of physical theory associated with certain controversial problems, it has become necessary to test the mathematical deductions by conducting precise observations on accessible glaciers. M. F. Meier, J. F. Nye, W. S. B. Paterson and many others have made significant contributions in this field.

The greater part of this report represents an attempt to verify a theoretical relation derived by Nye (1951, 1959a, 1959b, 1959c) which relates the longitudinal rate of strain in a glacier to physical characteristics of the ice mass. An attempt is also made to relate the strain-rate field to the occurrence of transverse crevasses. Certain aspects of the geometry of these crevasses are investigated.

Implications of Research Problem

Previous work that has included an attempt to test the theoretical relation for the longitudinal surface in a glacier (Paterson, 1962) shows inconclusive results. Thus it is considered that a more exhaustive investigation is warranted.

The rheological aspects of the study are at once apparent. Attention is drawn to the behavior of the flow, deformation, and fracture of a sedimentary-diagenetic crystalline aggregate close to or at its pressure melting point.

Structural geologists and glaciologists are faced with many analogous problems. Much of the information obtained from the observations of the dynamics and fracture of glacier ice can be applied to problems involving "hot creep" deformation and fracture of subcrustal rock material which is at present inaccessible to direct observation. Such concepts have been considered in theses on continental drift (for example, Orowan, 1964). Rock joints, which are produced by anisotropic stress conditions of mechanical or thermal origin, are closely analogous to crevasses in glacier ice, but certain significant differences exist so that the stress analyses may not be similar in the two cases.

Some important ideas relating to the flow and fracture of crystalline materials have arisen from metallurgical research. Investigations have been made on the deformation and fracture mechanisms of polycrystalline magnesium at low temperatures (Hauser, Landon and Dorn, 1956). In recent years the analogies between the

*This report is a modified version of the Institute of Polar Studies Report No. 16, (1965), and is printed here with permission.

†Institute of Polar Studies, The Ohio State University, Columbus.

rheology of ice and of certain metals has become evident and much of the work in the two fields is clearly complementary. It is worth noting that because many glaciers are at or near the melting point, the rheological processes are more rapid here than at low temperature (Glen, 1955), whereas most metals generally require considerably elevated temperatures for comparable rates of deformation.

Practical applications of crevasse mechanics also exist. When planning overland traverses, polar and alpine research expeditions are frequently faced with logistical problems which are created when routes traverse regions of crevassed ice. Consequently, a detailed knowledge of the geometry of certain basic crevasse types is essential. Schuster (1954) discusses travel and rescue in crevassed areas.

Related Observations of the Kaskawulsh Glacier Area

Wagner (1963, 1964) recognized that the area near the head of the Kaskawulsh Glacier lies within the saturation zone. This area also lies well above the firn limit which is at 2150 m. The first transverse crevasse field coincides approximately with the formation of the north arm of Kaskawulsh Glacier at 2450 m (Figure 1).

The present project area included 4 km^2 of glacier surface located at approximately 61° 47' N latitude and 139° 28' W longitude and covering part of the upper north arm of Kaskawulsh Glacier. Observations were conducted here for seven weeks between July 4 and August 15, 1964.

THEORETICAL CONSIDERATIONS

The Rheology of Ice

Review of the properties and behavior of ice. Early analyses (for example Lagally, 1929) of the flow and fracture behavior of ice were based on the assumption that ice exhibited the properties of a Newtonian fluid. As new data became available, it was found necessary to revise certain assumptions regarding the properties of ice. Recent works (for example Nye, 1951 to 1963) which develop the theory of glacier flow, have initially assumed, to simplify calculations, that ice behaves as a perfectly plastic solid. That this is a substantial simplification is well known.

Glen (1952, 1953, 1955), Butkovich and Landauer (1959), and others have shown that a flow law exists of the general form, $\dot{\epsilon} = B\sigma^n$ (for $\sigma \geqslant 0.6$ bars) for the material ice when subjected to shear, compressive, or tensile stresses. Rigsby (1958) has shown that for single ice crystals the flow law is independent of hydrostatic

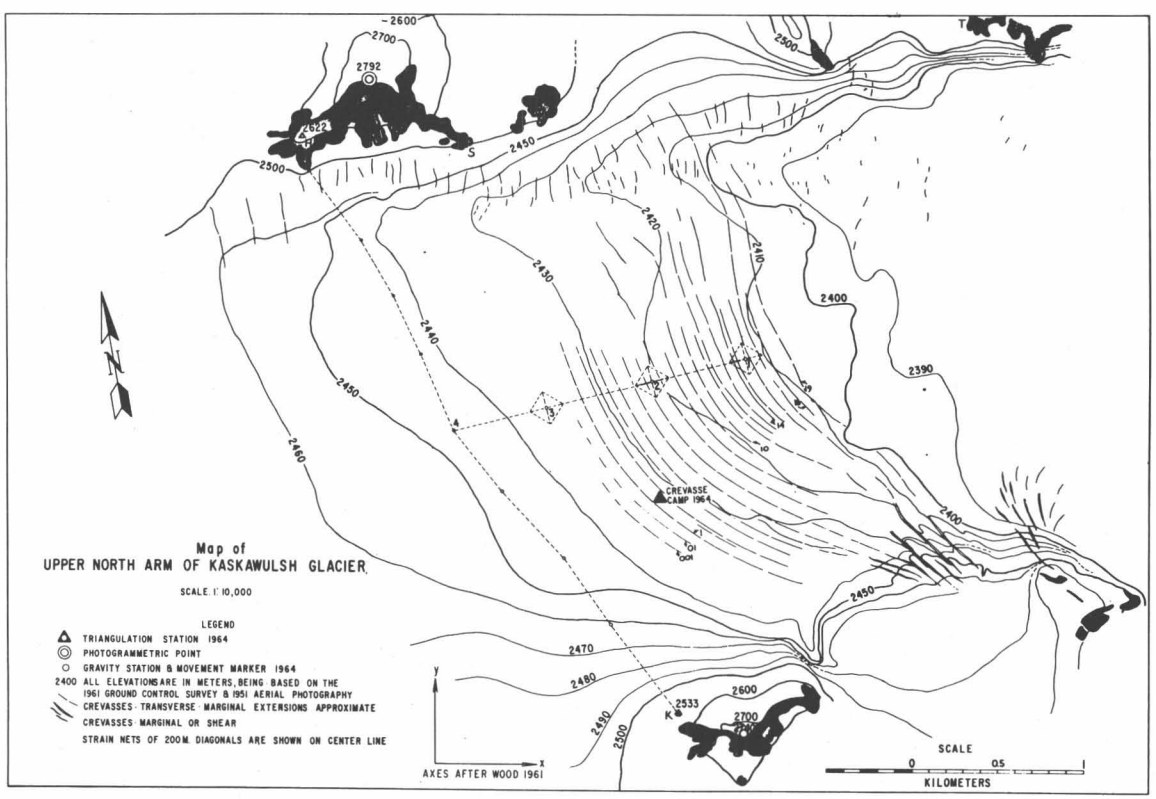

Fig. 1. Geometry of the survey network and the configuration of the transverse crevasse field.

pressure, and this also appears to be valid for polycrystalline ice. This condition holds provided that the difference between the ice temperature and the pressure melting point is kept constant. Crystallographically, ice belongs to the hexagonal system and experiments by Steinemann (1958) and others show that to a good approximation "glide" occurs only along the basal plane (0001). From the flow law and from general observations, it is apparent that ice can exhibit the properties of either a "visco-plastic", a plastic, or a "plasto-elastic" material depending on the magnitude and development of the applied stress. To develop these ideas further it is necessary to refer to the work of Butkovich (1958, p. 2) who examined the behavior of standard cylinders of ice under tensile stresses at different rates of loading. The average tensile strength is related to the rate of stress application within the ice. A "visco-plastic" response occurs below a loading rate of approximately 0.5 kg cm^{-2} sec^{-1}, whereas above this value, a "plasto-elastic" type of response is observed in which the ultimate tensile strength is essentially independent of loading rate. These observations are pertinent in considering the nature of the rupture of glacier ice.

The fracture of ice. In the analyses which follow, ice will be regarded as homogeneous and isotropic. This is a substantial simplification. Furthermore, it will be assumed that the crystallographic orientation of the ice is random. Under these conditions, Glen (1963) has assumed that the maximum principal stress parallels the direction of maximum strain rate in the general case. For other than randomly orientated ice the magnitude of the stress determines the direction of maximum strain. Finally, the effect of temperature on the rheological behavior of ice must be recognized. Glen (1963) states that a reduction in temperature from 0°C to −15°C reduces the flow rate by an order of magnitude. He has shown specifically that the value of B in the flow is an exponential function of temperature. The fact that the value of B is extremely sensitive to changes in temperature is discussed in a later section.

Ice will fracture under tensile or compressive loading (Gold, 1960), but this analysis will consider only tensile failure of glacier ice. For tension failure to occur, the applied stress within the ice must exceed the ultimate strength (u.t.s.). In true glacier ice, the u.t.s. will depend on the direction of stress application, the magnitude of the other principal stresses, the ice temperature, and the bulk physical properties of the ice or firn. Average tensile strengths of ice are given by Bader and others (1951) but the nature of the laboratory tests and the complete physical condition of the ice are not fully specified. Values of u.t.s. ranging from 2.5 kg cm^{-2} to 18.0 kg cm^{-2} have been found. Other sources give values ranging from 6.5 to 17.0 kg cm^{-2}. However, there seems to be little correspondence between laboratory and field measurements of the tensile strength of ice. Calculations by Nye (1959b) indicate that glacier ice will fracture when subjected to tensile stresses of the order of two bars, but others (for example Lliboutry, 1958) have maintained that higher stresses, of the order of 5 to 12 bars, are necessary. It should be understood, however, that the upper parts of most glaciers are not "pure" ice. Furthermore, as will be elaborated later, there is reason to believe that the regional stresses on the surface of a glacier are not necessarily indicative of local stresses which have a greater significance in terms of failure mechanics. Because the surface strain rate only is measured, it is convenient to relate failure of the ice in tension to a critical surface strain rate, but the gradient of strain rate at any point must be specified. In other words, the rate of loading or stress application is important. The stresses are generally considered to be mechanically produced, but there is some evidence to suppose that stresses of thermal origin may be significant (Mellor, 1964). It has been estimated that stresses sufficient to break ice can be produced by a temperature change of about 20°C in the upper five meters of a glacier, but the time of temperature change is not given (Bull, personal communication).

Nielsen (personal communication) and others have witnessed the formation of a transverse crack and describe the phenomenon as being associated with an audible energy release and detectable surface waves. Such a description suggests that ice can exhibit an "elasto-plastic" behavior.

Definition of "crevasse". The origin of the term "crevasse" is not discussed here, but it was evidently in use in the literature of the eighteenth century alpinists. Meier (1960, p. 57) distinguishes between crevasses and cracks by assigning an arbitrary upper limit of 30 cm width to define cracks. Since there is no mechanical or genetic significance implied in this definition, it will not be used here. Instead, the term "crack" will be used to imply an ice or firn fracture which possesses no measurable opening. Thus, cracks are incipient crevasses. All fractures possessing a measurable opening that occur in the surface zones of a glacier are regarded as crevasses. A particular class, namely transverse crevasses, will be considered here. Although marginal crevasses do occur in the area, the mechanics of these are not discussed.

Stress Conditions Existing in Flowing Ice

Stress distribution with depth. Prandtl (1923) has provided the stress solution applicable to a system in which a perfectly plastic material is compressed in plane strain between two parallel plates spaced 2 h apart. The plates are inclined at an angle α to the horizontal and that part of the system below z = h is considered as a model glacier. Reference axes are taken at the bed on which τ_{xz} = K, the yield stress.

Nye (1951, p. 557; 1957c) gives the following solution:

$$\sigma_x = x\left(\frac{K}{h} - \rho g \sin\alpha\right) + z\rho g\cos\alpha \pm 2K\sqrt{1-(1-\tfrac{z}{h})^2} + P \quad (1)$$

$$\sigma_z = x\left(\frac{K}{h} - \rho g \sin\alpha\right) + z\rho g\cos\alpha + P \quad (2)$$

$$\tau_{xz} = K\left(1 - \frac{z}{h}\right) \quad (3)$$

for a material of density ρ.

The depth of crevasses. It is required to find the depth z to which σ_x is still tensile. By placing $\sigma_x = 0$, in equation (1) and using (2),

$$\sigma_z = 2\sqrt{K^2 - \tau_{xz}^2}$$

and substituting for σ_z and τ_{xz},

$$z = \frac{2K}{\rho g\sqrt{1 + 3\sin^2\alpha}}$$

If α is small, $z \cong \frac{2K}{\rho g}$. (4)

Taking K as one bar, z ≅ 23m. This, then, is the depth to which a crevasse might open. Alternatively, it is possible to consider a fracture that has already formed and opened to a depth which is greater than 23 m, but that the extending strain rate is then released. If the normal stress due to air pressure is P, then at a certain depth the lateral stress on the crevasse wall is 2K+P, where 2K is the yield stress in compression. This is equated to an equivalent hydrostatic stress acting in unfractured ice at the same level below the surface, so that,

$$2K + P = \rho g d + P$$

and $d = 2K/\rho g$, as before.

It is conceivable that where the thickness of the ice is not very great compared with $2K/\rho g$, and in places of high flow rate and of excess bending, crevasses could open up to depths exceeding this theoretical depth, which pertains to a slab of ice moving down a uniform slope.

A departure is now made from the perfectly plastic case. Nye (1955) uses a general flow law of the type derived by Glen (1952) to express the yield stress in tension in terms of the strain rate. At the point of failure of the ice at the surface $\sigma_x = \sigma_c$ so that the depth of fracture can be expressed as:

$$d = \frac{2\sigma c}{\rho g} = \frac{2}{\rho g}\left(\frac{\dot{\epsilon}_c}{B}\right)^{\frac{1}{n}} \quad (5)$$

where $\dot{\epsilon}_c = B\sigma_c^n$ provides the relationship between stress and strain rate. $\dot{\epsilon}_c$ can be measured at the surface. Certain complications arise however, in selecting the appropriate value of strain rate. This will be discussed later. Meyerhof (1954) gives some further ideas on crevasse depths but because the theory is based on soil mechanics, the applicability of it to the present problem is very doubtful.

Surface stress distribution. Consideration will be given to the two dimensional stress field existing in the plane of the glacier surface. The model considered is a valley ice stream of constant width, although different "boundary conditions" are included in the analysis. Further assumptions are that the ice depth is small compared with the width and that the surface is horizontal, so that gravity effects can be ignored. This is a good approximation in the case of the north arm of Kaskawulsh Glacier since slopes do not exceed 2° in the area studied.

Rectangular reference axes are adopted so that the x–axis points down-glacier along the central flow line and the y–axis is transverse, in the plane of the surface. Consider σ_x, σ_y, and τ_{xy} to be the only stresses acting in the system. The effect of normal air pressure does not alter the analysis. By considering certain combinations of these stresses, depending on whether the flow is extending or compressive and depending on the type of boundary conditions, the magnitude and direction of the principal stresses at any point may be found by using a Mohr's circle construction.

Nye (1952, p. 91) is able to explain the occurrence of three basic types of crevasses, only one of which is relevant here. Nielsen (1958) considers other combinations of stresses in order to cover all possible cases, but nothing basically new is presented.

To explain transverse crevasse patterns, it is necessary to consider the state of extending flow, namely that $\sigma_x > 0$ over the length of glacier considered. σ_y is controlled by the boundary conditions. According to the theory of plasticity developed by Hill (1950),

$$0 \leqslant |\sigma_y| \leqslant |\tfrac{1}{2}\sigma_x|$$

where the maximum value of σ_y occurs when lateral contraction of the ice is prevented. τ_{xy} varies from a maximum at the boundaries to zero at the centerline of the ice stream.

In real glaciers the idealized pattern of crevasses may be somewhat distorted by irregular boundary conditions, differential surface velocities and anisotrophy of the ice. In the case of the Kaskawulsh Glacier transverse crevasses, a close correspondence with the theoretical pattern is noted. No longitudinal fractures occur, however. Down-glacier, differential surface velocities cause a straightening of the traces, and later, a convexity downstream.

Consideration of Longitudinal Strain Rate

It is necessary now to analyze the conditions which contribute to the states of extending or compressive flow within a body of ice moving downslope under the action of gravity and certain boundary conditions. Nye (1951, 1952, 1959a, 1959c) has developed the theory which follows. In this, the effects of various physical factors are analyzed separately and the principle of superposition is used to combine the component strain rates. Certain simplifying assumptions are made. Ice is considered to be a perfectly plastic material, the shear stress on the bed is considered constant, and the

longitudinal strain rate is considered invariant with depth, or

$$\frac{\partial \dot{\epsilon}_x}{\partial z} = \frac{\partial}{\partial z}\left(\frac{\partial u}{\partial x}\right) = 0 \qquad (6)$$

Consider the effect of accumulation or ablation at the surface of a glacier. Let a=dq/dx be the rate of addition or subtraction of material at the surface of the glacier. A positive sign is used for accumulation, a negative sign for ablation. For simplicity a is assumed to be a constant rate for a yearly period. In order for an equilibrium ice thickness to be maintained, it is necessary for a longitudinal strain rate of (1/h)(dq/dx) to exist. A positive a/h term favors extending flow while a negative term favors compressive flow.

Next consideration will be given to a glacier moving over a bed of variable slope. It is required, however, that dα/dx and dk/dx are small. By considering curvilinear coordinates (x, z) with reference to the bed surface, it can be shown that the longitudinal strain is given by (q/hR) cot α, where q/h can be represented by a mean velocity $\bar{V}_c$ and hence the expression can be rewritten as

$$\bar{V}_c k \cot\alpha \qquad (7)$$

There has been some inconsistency in defining k. Nye (1951, 1957b, 1959a) states that k refers to the surface curvature but in other papers (1952; 1959b, p.400) k is associated with bed curvature. In the derivation of $\bar{V}_c k \cot\alpha$, k and α are associated with the same surface; this fact should be noted.

A slightly different method of derivation will now be used to obtain the above two expressions, a/h and $\bar{V}_c k \cot\alpha$, representing longitudinal strain rate. In addition, further terms will be added by superposition. These ideas were presented by Nye (1959b).

Consideration will be given to a glacier moving partly by internal differential motion and partly by bed slip. The assumptions made at the beginning of this section will be modified. Ice is not, now, assumed to be perfectly plastic and allowance is made for variations of shear stress on the bed of the glacier. The value of n in the flow law is considered to be finite and a relationship of the form,

$$V_b = \left(\frac{\tau}{B'}\right)^m$$

is assumed to hold at the bed of the glacier. $\dot{\epsilon}$ is then expressed as $\partial V_b/\partial x$ and this is assumed to be constant throughout the thickness. Nye (1959c), Paterson (1962) and others state that $\dot{\epsilon}_x$ can vary with depth, but for simplicity of analysis, the assumption is used. Since $\tau = \rho g h \sin\alpha$ the longitudinal strain rate $\dot{\epsilon}_x$ can be written

$$\dot{\epsilon}_x = \frac{\partial V_b}{\partial x} = \frac{\partial V_b}{\partial \tau}\frac{\partial \tau}{\partial \alpha}\frac{d\alpha}{dx} + \frac{\partial V_b}{\partial \tau}\frac{\partial \tau}{\partial h}\frac{dh}{dx}$$

from which,

$$\dot{\epsilon}_x = m V_b k \cot\alpha + \frac{m V_b}{h}\frac{dh}{dx}$$

where $k = \frac{d\alpha}{dx}$.

It is now necessary to consider at any given point the change in height of the ice surface with respect to time. ∂h/∂t can be expressed in terms of three components. The first term is a or dq/dt measured positive if accumulation, negative if ablation. It is also assumed to be a uniform rate of accumulation or ablation.

If the velocity components, respectively parallel and perpendicular on the ice surface be denoted by u_s and v_s then the vertical component of velocity is $v_s - u_s\,(dh/dx)$, being positive in an upward direction. It is noted that for mild slopes the vertical component of v_s is for practical purposes just v_s.

The total effect is obtained by addition of terms so that

$$\frac{\partial h}{\partial t} = a + v_s - u_s\frac{dh}{dx} \qquad (8)$$

Considering now a three-dimensional strain rate system, the longitudinal strain rate can be related to the transverse and vertical strain rate thus: $\dot{\epsilon}_x = -(\dot{\epsilon}_y + V_s/h)$ assuming incompressibility. Hence, $\dot{\epsilon}_x$ can be expressed as

$$m V_b k \cot\alpha + \frac{m V_b}{h}\cdot\frac{1}{u_s}\left(a - h[\dot{\epsilon}_x + \dot{\epsilon}_y] - \frac{\partial h}{\partial t}\right)$$

which reduces to

$$\dot{\epsilon}_x = \frac{m V_b}{m V_b + u_s}\left(\frac{a}{h} - u_s k \cot\alpha - \dot{\epsilon}_y - \frac{1}{h}\frac{\partial h}{\partial t}\right)$$

Nye, (1959c, p. 506) expresses $\dot{\epsilon}_y$ as $(\bar{V}/W)\,(dW/dx)$ but since this is the average value for the whole glacier cross-section it appears more appropriate to use the value of $\dot{\epsilon}_y$ measured near the center line of flow. However, as Nye (personal communication) has pointed out, this ignores any variation of $\dot{\epsilon}_y$ with depth.

Consideration will now be given to an effect of bending of the ice. Simple elastic bending is assumed. Taking curvilinear coordinates (x, z) on the neutral plane of bending so that z is perpendicular to this plane, the strain increment is given by $d\epsilon_x = z\,dk$ at a distance z above the neutral plane. From this,

$$\dot{\epsilon}_x = Z\frac{dk}{dt} = Z\bar{V}\frac{dk}{dx}.$$

If it is assumed that the neutral plane is midway through the thickness then on the upper surface,

$$\dot{\epsilon}_x = \frac{1}{2} h \bar{V}\frac{dk}{dx}.$$

It should be noted that the value of this bending term changes with depth, but since the surface strain rate is being studied, this fact does not affect the argument. The final equation can be written as

$$\dot{\epsilon}_x = \frac{m V_b}{m V_b + u_s}\left(\frac{a}{h} + u_s k \cot\alpha - \frac{1}{h}\frac{\partial h}{\partial t} - \dot{\epsilon}_z + \frac{1}{2} h \bar{V}\frac{dk}{dx}\right) \qquad (9)$$

The coefficient $\frac{m V_b}{m V_b + u_s}$ thus modifies the relation by using results of the experimental flow law for ice.

A numerical value may be assigned to this coefficient by considering typical values of m, V_b and u_s. If plug-flow is assumed (Nye, 1952, p. 83) for a value of m = 2.5 for temperate ice, the coefficient has a value of 0.7. For a condition in which u_s is composed of equal contributions from bedslip and internal movement, the coefficient is 0.6. Judging by vertical velocity profiles in similar glaciers, it is considered probable that the coefficient is of the order of 0.65 for this section of Kaskawulsh Glacier.

Crevasse Spacing

There is a paucity of general information bearing on the problem of crevasse spacing. Approaches to the problem have either been empirical or else analytic but of doubtful validity. Meier and others (1957) find by field measurements in Greenland that the spacing of certain crevasses is roughly four times the mean crevasse depth. However, these were not true transverse crevasses. Nielsen (1958) claims to provide an explanation for the uniformity of crevasse spacing. However, the data from Kaskawulsh Glacier does not suggest a uniformity in spacing (Figure 2).

Nielsen (1958) considers a flowing cantilever ice slab, which, on attaining an unsupported length, s, fractures in elastic bending. If the ice thickness is h and the bending strength is S then it can be shown that

$$s^2 = \frac{Sh}{3\rho g} \qquad (10)$$

Nielsen uses a value of 13.6 kg cm^{-2} for the bending strength and finds that computed values of s are too great by a factor of 4, compared with field measurements of s. Now although some suggestions are made to explain the inappropriate value of S, no recalculation of s is made. Some laboratory tests on the bending of melting ice beams made by Neronov (in Bader and others, 1951, p. 24) yielded an average value of S of 4 kg cm^{-2}. It should be pointed out that the value of S is considerably lower in the upper regions of a glacier where snow and firn are the predominant materials. To counteract this effect in the equation for s, it must be noted that the average value of ρ is lower. Thus, the value of S/ρ is important.

Because the model used by Nielsen does not faithfully reproduce the probable conditions in a real glacier, his approach may be open to some criticism. A similar approach to the problem could be repeated using recent plastic theory for determining the bending moment in beams. However, from general observations of the formation of crevasses (Nielsen, personal communication) it may be thought more appropriate to use elastic theory.

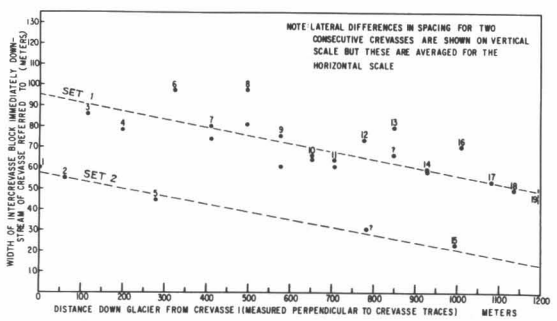

Fig. 2. Plot of crevasse spacing with distance down-glacier.

Another approach to the problem is to consider the conditions occurring near the uppermost crevasse of a set of transverse crevasses. Consideration will be given to the process of fracture taking place on the "dynamic" centerline of flow. Across the crevasse, $\sigma_x = 0$. As the crevasse moves down-glacier the longitudinal stress reaches the critical value σ_c, and another crevasse is formed. Before the point of failure, however, there must exist a gradient of stress, and hence of strain rate. The local stress supposedly varies in some manner from zero to the critical value in a distance s, measured up-glacier from the crevasse which has recently moved away from its point of origin. If a linear variation of stress is assumed as a first approximation, then

$$\frac{\partial \sigma_x}{\partial x} = \frac{\sigma_c}{s},$$

so that

$$s = \sigma_c \Big/ \frac{\partial \sigma_x}{\partial x} .$$

Now

$$\sigma_x = \left(\frac{\dot{\epsilon}_x}{B}\right)^{1/n} \quad \text{from the flow law,}$$

therefore

$$\frac{\partial \sigma_x}{\partial x} = B^{-1/n} \frac{\partial \dot{\epsilon}_x^{1/n}}{\partial x}$$

Previously, an expression (9) was derived for $\dot{\epsilon}_x$ at a point on the surface, but rather than to differentiate this equation, it is obviously simpler to use direct measurements of $\dot{\epsilon}_x$, in order to obtain the value of

$$\frac{\partial \dot{\epsilon}_x^{1/n}}{\partial x} .$$

Where $\dot{\epsilon}_x = \dot{\epsilon}_c$, the spacing is given by

$$s = (\dot{\epsilon}_c)^{1/n} \Big/ \frac{\partial \dot{\epsilon}_x^{1/n}}{\partial x} \qquad (11)$$

It seems probable that crevasse spacing is, at least in part, influenced by crevasse depth. At the edge of an ice sheet in northeast Greenland, Meier and others (1957) found that certain unclassified crevasses having depths, d, of from 22 to 26m possessed spacings of about 4d. Kaskawulsh Glacier transverse crevasses are separated on an average by 2.8d where d ranges from 24 to 26m. It should be noted, however, that these are not similar types of crevasses and the morphologies of the two glaciers are much different. To approach the problem in a more rigorous manner, it will be necessary to examine the stress dis-

tribution with depth and distance up-glacier from a forming crevasse.

FIELD DATA REDUCTION AND RESULTS

Velocity Determination

The velocity vector field was determined over a 25-day period in July and August. Figure 10 in Brecher (p. 142 of this volume) shows a construction of flow-line filaments which are assumed to be a family of smooth curves.

Adopting the rectangular axes (X, Y) established by Wood in 1961, contour diagrams of V, V_X and V_Y have been constructed (Figures 3, 4, and 5). A discussion of the accuracy of velocity measurements is given by Brecher (1966).

An estimate of the mean flow velocity over the depth and width, and of the ice throughflow between H and K has been made. A value of mean surface velocity $\overline{V}_s$ for the transverse profile between Stations H and K, was obtained using standard semigraphical methods. Generally $\overline{V}_s \cong 0.85\ V_c$.

It can be shown that

$$\frac{\overline{V} - V_b}{\overline{V}_s - V_b} = \frac{n+1}{n+2} .$$

Assuming that $V_b \cong 0.25\ V_s$, (although it may reach $0.50\ V_s$ in some temperate glaciers) and putting $n = 3.17$ (Glen, 1953, p. 721; 1955, p. 528) a value of $\overline{V}$ is obtained. Since these velocities pertain to a yearly period, the time unit, one year, will be retained. A value of $71.8\ m\ yr^{-1}$ is obtained for the mean ice velocity $\overline{V}$, between H and K. An estimate of ice throughflow between H and K is obtained from a knowledge of the cross-sectional area of ice measured from a gravity depth profile. A value of $Q \cong 116.3 \times 10^6\ m^3\ yr^{-1}$ is obtained. The throughflow of ice per unit width in the region of the median flow plane at Marker 4 is $q_4 \cong 67 \times 10^3\ m^2\ yr^{-1}$.

Regional Strain Rate Computations

Three main methods have been used for determining the strain rate tensor on the surface of the glacier.

(1) Velocity gradient method. At convenient points on Figures 4 and 5 values of $\frac{\partial V_x}{\partial x}, \frac{\partial V_x}{\partial y}, \frac{\partial V_y}{\partial x}$, and $\frac{\partial V_y}{\partial Y}$ were obtained by semigraphical methods.

Thus, at each point the components of strain rate were determined from

$$\dot{\epsilon}_x = \frac{\partial V_x}{\partial X}$$

$$\dot{\epsilon}_y = \frac{\partial V_y}{\partial Y}$$

and

$$\dot{\Upsilon}_{xy} = \frac{\partial V_x}{\partial Y} + \frac{\partial V_y}{\partial X}$$

The principal strain rate tensors $\dot{\epsilon}_1$ and $\dot{\epsilon}_2$ have been obtained using a Mohr's circle construction. Figures 6, 7, and 8 show contours of the principal strain rate components.

Certain assumptions have been made in the foregoing analysis. These will be mentioned briefly.

a. The surface of the glacier is assumed to approximate a horizontal plane. This is a good approximation since surface slopes do not exceed 2°.
b. Plane strain is assumed. The effect of normal air pressure does not alter the analysis.
c. Strains are assumed to be continuous functions of X and Y, so that regional or average values of strain rate are obtained.
d. Strains are small enough to produce no serious elliptical distortion of Mohr's circle.

(2) Strain diamond method. Methods of data reduction were the same as those given by Nye (1959b). Mea-

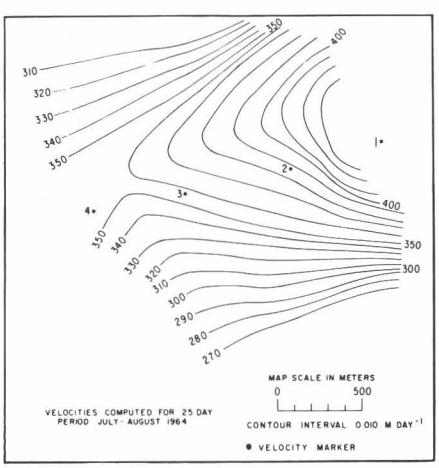

Fig. 3. Contours of total velocity, V, m day $^{-1}$.

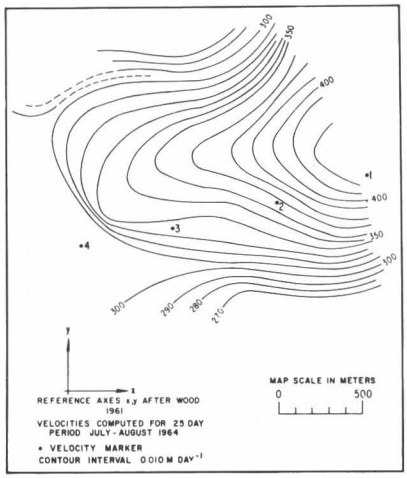

Fig. 4. Contours of velocity component V_x, m day $^{-1}$.

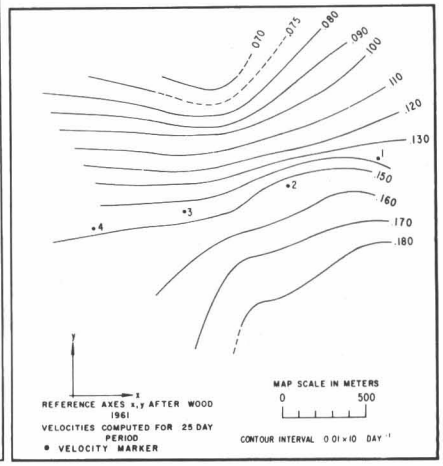

Fig. 5. Contours of velocity component V_y, m day $^{-1}$.

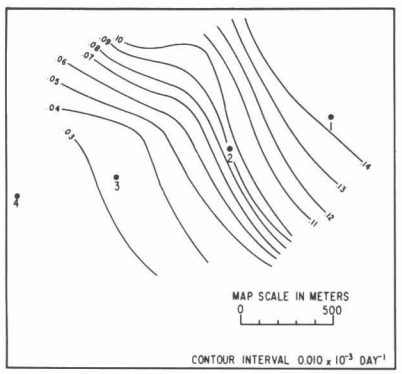

Fig. 6. Contours of principal extending strain rate ($\dot{\epsilon}_1$).

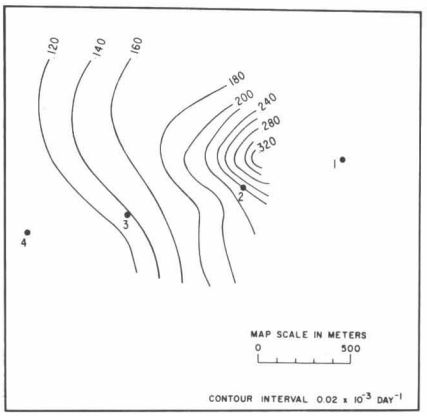

Fig. 7. Contours of principal contracting (least extending) strain rate ($\dot{\epsilon}_2$).

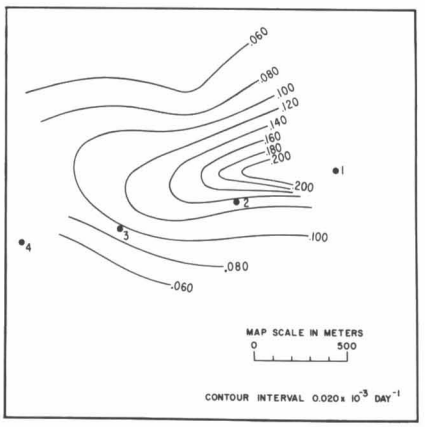

Fig. 8. Contours of maximum shearing strain rate ($|\dot{\epsilon}_1 - \dot{\epsilon}_2|$).

sured lengths for each strain net have been corrected for temperature, slope, and height above sea level. The maximum probable error in the length measurements is estimated as 1 in 20,000. This estimate includes possible movement of corner markers.

The components of strain rate were computed from

$$\dot{\epsilon} = \frac{2.3}{\Delta t} \log_{10} \frac{\ell_2}{\ell_1}$$

$\dot{\epsilon}_1$ and $\dot{\epsilon}_2$ were then computed by the method of Nye (1959b).

(3) Approximate values of longitudinal strain rate have been obtained using the four velocity markers which had been surveyed in 1963 and 1964. The values of strain rate obtained from this strain line are shown in Figure 9-B. Other estimates of strain rate have been made using the relation $\dot{\epsilon}_x = \dot{w}_c/s$. These results are shown in Figure 10 and indicate that the previous assumption that the strain is taken up by opening or closing of a crevasse is a reasonably good one.

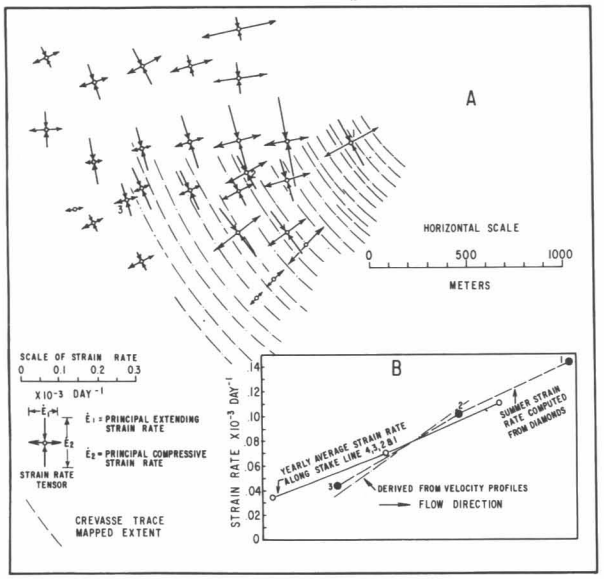

Fig. 9. (A) Configuration of principal strain rate field in region of the transverse crevasses. (B) Longitudinal variation of principal extending strain rate.

Estimate of critical strain rate. Figure 6 shows contours of principal extending strain rate. By overlaying this plot on the map of crevasse traces it is possible to estimate a value of strain rate associated with fracture of the ice. The strain diamond at Marker 3 records a strain rate very close to $\dot{\epsilon}_c$. An approximate regional value of $\dot{\epsilon}_c$ has thus been deduced as 3.5×10^{-5} day^{-1}, $\pm 0.5 \times 10^{-5}$ day^{-1}.

Meier and others (1957) and Meier (1960), from observations in Greenland and on Saskatchewan Glacier, suggest a value of about 1% yr^{-1} (2.8×10^{-5} day^{-1}) while Mellor (1964) considers a value of 10^{-9} sec^{-1} (8.7×10^{-5} day^{-1}) to be of roughly the correct order. Neither of the two sources states the strain rate gradient which is associated with the critical values, but it is considered important here. A regional gradient of about 0.005×10^{-5} day^{-1} m^{-1}

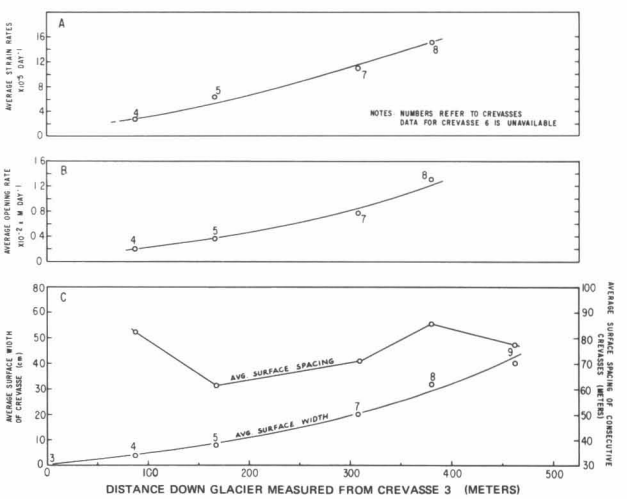

Fig. 10. (A) Approximate extending strain rate gradient perpendicular to crevasse traces ($\dot{\epsilon} = \dot{w}_c/s$). (B) Variation of crevasse opening rate ($\dot{w}_c$) down-glacier. (C) Surface width (w_c) and spacing (s) of crevasses 3 to 9.

is associated with the regional value of 3.5×10^{-5} day^{-1} for the critical strain rate.

It should be noted that great difficulty was experienced in determining the position of the uppermost crevasse. At the beginning of the summer, it was considered that crevasses were forming just upstream of Marker 2, and hence the uppermost strain diamond was established at Marker 3. Later in the season an aerial observation showed that crevasses were forming almost up to Marker 3.

It has been assumed for simplicity that the derived strain rates apply to a particular point although, because of ice movement of the order of 10 m in 35 days, this is not strictly true.

Accumulation and Ablation Data

Accumulation. As a result of observations of snow stratigraphy in pits and of pole measurements since 1961, reasonably reliable estimates of the mean net annual accumulation are available. Observations of snow stratigraphy on the haunch of a crevasse bridge provide values that agree tolerably well with the values for previous years obtained by Ragle (personal communication). Table 1 summarizes the data. Method of determination is by measurement on poles unless otherwise stated. Data other than that from the crevasse have been provided by Ragle (personal communication).

There is clearly an accumulation gradient within the 1800 m in which the observations have been taken. These data are used later in the computation of strain rates. The assumption is made, however, that this accumulation is a uniformly distributed loading rate throughout the year. This will be discussed later in the section.

Ablation. Although the ablation data are not used directly in computing strain rates, the implications are worth noting (see next section on discussion of data and results). Measurements of average surface lowering were taken from velocity poles between July 7 and August 11, 1964. A mean value of 0.98 cm day^{-1} was obtained for this period, but this contains the effect of densification as well as direct ablation. The densification, as estimated from a knowledge of the density profile is, for this short time period, negligible.

Wagner (1963, p. 42) estimates that for July and August, 1963, the average ablation in the region to the west of the crevassed area at altitude 2500 to 2600 m was 0.8 to 0.9 cm day^{-1}. The average surface density is about 0.410 gm cm^{-3}.

Use of data. The effect of accumulation or ablation on the longitudinal strain rate has been considered previously under theoretical considerations.

In the calculations of the a/h term in Equation (9), values of $\underline{a}$ lying between +0.32 cm day^{-1} and +0.46 cm day^{-1} have been used. The values are in terms of centimeters of ice of density 0.9 gm cm^{-3} assumed to be uniformly applied over the year. The effect of a negative a/h term during the summer is considered in the discussion of data and results.

TABLE 1. Mean Annual Net Snow Accumulation on the North Arm of Kaskawulsh Glacier

Pole Number	Accumulation (cm water equivalent)		
	1961 - 62	1962 - 63	1963 - 64
1	--	106, 110†	103, 93†
2	---	130	123
3	---	143	141
4	129*	134	156
5	130*	146	168

* Pit determination

† Crevasse bridge (haunch) stratigraphy

Average snow density has been taken as 0.520 gm cm^{-3}
Note that velocity of Pole 1 is approximately 0.430 m day^{-1}

Field Measurements of Crevasse Depths

General data. Field estimates of crevasse depths are many and variable. There are three main reasons for this:

(1) Direct measurement by "plumbing" from the surface is hindered when the plumbing device becomes jammed before the crevasse terminates. Other pitfalls are evident. Sometimes substantial quantities of water are present in the bottom of the fracture.

(2) Crevasses that are in the process of closing mainly by plastic deformation at depth may be measured as shallower than the original depth.

(3) In fact, in view of the equation for $\dot{\epsilon}_x$, the bending term indicates that it should be possible to have σ_x tensile to a depth greater than that given by the idealized model, and so we expect a considerable range of depth values to be observed.

Nye and others (1954) have discussed, generally, the depth of crevasses. Schuster and Rigsby (1954) state that observed crevasse depths are generally of the order of from 50 to 100 feet (15 to 30 m) but may extend to 150 feet (50 m) or more. According to Seligman (1955) most crevasses in the European alpine glaciers do not exceed 30 m in depth, but Loewe (1955, p. 511) cites a crevasse in the Bernese Oberland as being nearly 40 m deep. This was at an altitude of 3700 m. Goldthwait (1936) using seismic methods on part of Crillon Glacier, Alaska, estimated that crevasse depths averaged 20 m. Miller (in Nye, 1955) reports that crevasses in some Alaskan glaciers average 30 m. Taylor (1962) gives depth values of 10 m for closing crevasses on part of Burroughs Glacier, Alaska. The author's observations on New Zealand glaciers are in general agreement with the above figures. Greenland and Antarctic crevasses have been reported as being up to 150 to 200 feet (45 to 60 m) in depth. Such values may be explained by the change in the ultimate strength properties of ice with temperature and by the measurably slower increase of density with depth. Equation (5) shows the effect of these parameters on the depth d.

Kaskawulsh Glacier transverse crevasse depths. Five consecutive transverse crevasses were plumbed for depth. These values are comparable with the computed depths obtained from Equation (5). Measured values generally lay between 24 and 28 m.The estimated accuracy of individual measurements is probably 5%.

Calculation of crevasse depths. Meyerhof (1954) actually obtains an expression which gives depths of from 23 to 46 m but his methods are suspect since he uses the mechanics of soils. Using Equation (5) the expression developed by Nye (1955), an estimate of theoretical crevasse depth is obtained (Table 2). Data from Glen (1953, p. 721; 1955, p. 519) provides appropriate values of B and n in Equation (5). Strain rate values across crevasses as well as regional values have been used to compute d in Table 2. The critical strain rate of 0.0128 yr^{-1} yields a value of d = 7 m. Results are discussed later.

Field observations of crevasse spacing. Measurements of crevasse spacing are plotted against position on the glacier (Figure 2). Where a lateral variation in spacing between two adjacent crevasses occurred the mean value of $\underline{s}$ perpendicular to the traces was taken. In some cases a 20% variation in spacing was recorded. Figure 2 shows that crevasse spacings in the area vary from about 30 to 100 m., with a mean of about 75 m. A decrease in spacing appears to occur with increasing distance down glacier. It is not known whether this apparent spacing gradient has any significance or not, although individual variations will be discussed shortly.

A re-examination of the major factors influencing fracture spacing may suggest a solution to the above problem. The gradient of surface stress appears to be of utmost importance. Assuming certain conditions, it has been shown earlier under Theoretical Considerations that

$$s \frac{\partial \sigma_x}{\partial x} = \sigma_c$$

Variations in σ_c may be attributed to variations in the bulk properties and physical condition of the ice. Changes in $\partial \sigma_x / \partial x$ are due to variations in the accumulation or ablation gradient and variations in velocity both of which affect the strain rate and also the strain rate gradient. Also to be considered is the rate of change of thickness of the ice downstream (see Equation 8). The occurrence of thermal stresses, which may be of the same order of magnitude as mechanically induced stresses if the temperature changes are rapid enough, should also be considered.

To explain the lateral variation in spacing of any two crevasses it is necessary only to invoke lateral changes in bed profile and velocity gradient profile, and so forth. Moreover, lateral changes in ice properties should be more pronounced than longitudinal ones in this area since the constriction produces heavy fields of shear crevasses close to the boundaries.

To explain the gradient in the spacing down-glacier (Figure 2) it is possible to appeal to a steady change in the sum of all components in Equation (9). In other words substantial changes in velocity, velocity gradients, precipitation or ablation gradients, and so forth, for at least ten years are required. This is roughly the time taken for Crevasse 19 to reach its present position, assuming that it formed in the region of the first crevasse observed recently and assuming a mean velocity of flow of 130 m yr^{-1}. The magnitude of velocity and accumulation changes required to explain the observations does not seem reasonable. In fact, within this area, specific observations concerned with detecting velocity fluctuations show no significant variations for summer flow or yearly flow, although observations have only been conducted over two years (Sharni, 1963; Brecher, 1966, and pp. 127–143 of this volume).

The problem seems best resolved by appealing to changes in structural properties of the ice and firn. Laboratory tests on the ultimate strength of ice (for example Bader and others, 1951) commonly show variations of 200%, and in some cases more. Thus, such a magnitude of variation of σ_c would be more than sufficient to account for the observed variations in $\underline{s}$.

However, this solution does not include a convincing explanation of the apparent increase in spacing with decreasing age. The first solution apparently does this.

TABLE 2. Crevasse Depths

Crevasse No.	Mean Density ($gm\,cm^{-3}$)	T (°C)	B ($bar^{-n}\,yr^{-1}$)	n	$\dot{\epsilon}$ Across Crevasse (yr^{-1})	$\dot{\epsilon}_x$ Regional (yr^{-1})	Depth (d) Calculated Using $\dot{\epsilon}$ Across Crevasse (m)	Depth (d) Calculated Using $\dot{\epsilon}_x$ (m)	Depth (d) Measured (minimum) (m)	Remarks
6	0.70	0	0.17	3.17	1.6	0.020	61.0	16.2	23.5 – 24	------
7	"	"	"	"	1.5	0.022	59.7	16.4	26	------
8	"	"	"	"	1.7	0.025	62.0	17.2	25.5 - 26	------
9	"	"	"	"	2.1	0.032	64.0	18.6	28 – 28.5	Measured value of d suspect.
10	"	"	"	"	1.3	0.037	54.0	19.4	27	
14	"	"	"	"	0.8?	0.046	49.0	20.2	26.5	$\dot{\epsilon}$ across crevasse suspect.
18	"	"	"	"	—	0.053	–	21.6	25.0	

Bearing in mind what has just been said, it seems unnecessary to attempt to explain the apparent existence of the two "sets" of crevasses seen in Figure 2, except for one fact. Whereas the crevasses associated with the narrow spacing (35 m) are conformable in the width sequence (see Figure 10–C), suggesting a consecutive formation, crevasse 18 is only 20 cm wide but flanked by crevasses at least 500 cm wide, both of which must have been formed years before. Thus we are forced to conclude that there has been significant strain on an intercrevasse block which would have had in this case an unbroken width of 112 m, which is considerably larger than any spacings observed. Thus it is concluded that the previous assumption that $\dot{\epsilon}_x = 0$ on an intercrevasse block is only valid for "average" values of spacings. This is well verified by applying the relation:

$$\dot{\epsilon} = \frac{\dot{w}_c}{s}$$

to Crevasses 4 to 8 (Figure 10-A). Strain rates thus derived are comparable to values obtained by other methods.

Hence it is concluded that strain is taken up by opening (or closing) of existing crevasses unless the spacing for some reason is large compared with the average spacing, in which case significant strain can occur.

Calculation of crevasse spacing. Using the formula given by Nielsen (1958, p. 47) and putting

$h = 650$ m

$S = 2$ kg cm^{-2}

$\rho = 0.70$ gm cm^{-3}

$g = 981$ cm sec^{-2}

a value of $s \cong 79$ m is obtained, and this lies within the range of measured values, and is very close to the mean value.

Using the formula involving strain rate characteristics (Equation 11) leads to some difficulties since the detailed local values of surface strain rate up-glacier of the first crevasse are not available. Preliminary estimates indicate that the calculated spacing is an order of magnitude too large.

Thus more detailed strain measurements on the surface of a glacier (as well as within the glacier) need to be undertaken in the region up-glacier from a forming crevasse.

TABLE 3
Comparison Between Computed and Measured Strain Rates

Point	$\dot{\epsilon}_x$ calculated (surface slopes used)	$\dot{\epsilon}_x$ calculated (bed slopes used)	$\dot{\epsilon}_x$ measured (regional)
4	7.7×10^{-5}	0.5×10^{-5}	2.5×10^{-5}
3'A	---	---	2.5 to 2.8×10^{-5}
3'	---	---	4.3 "
2'A	---	---	5.2 "
2'	---	---	10.2 "
1'A	---	---	11.0 "
1'	---	---	14.0 "

Calculation of theoretical longitudinal surface strain rate. Table 3 summarizes all the strain rate data and compares calculated with measured surface $\dot{\epsilon}$ values. Positions 1′ through 4 lie on the dynamic center-line of the glacier which is located in Figure 11. The dynamic or geophysical center-line has been selected on the basis of the symmetry of velocity and strain distribution data. The geographic center-line has been located on the basis of the physical configuration of the ice, and the position of the boundaries.

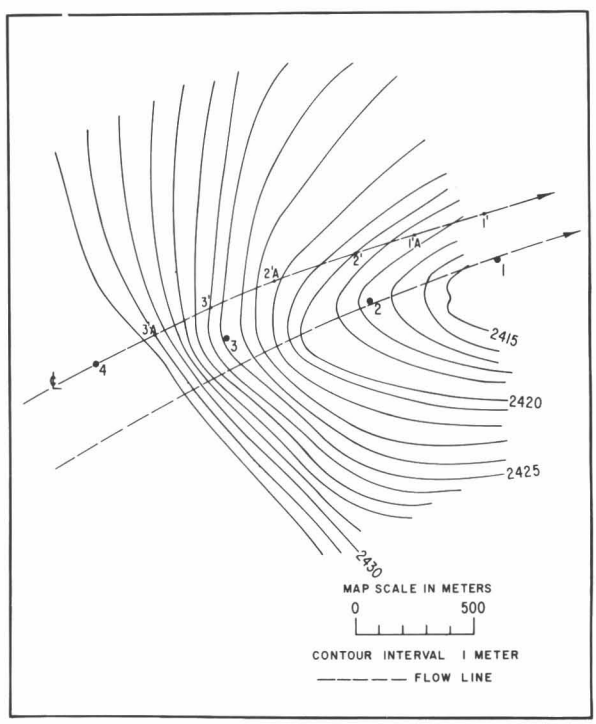

Fig. 11. Average surface configuration, July 1964. Flow-line through Marker 4 is the "dynamic" center-line; flow-line through 1 and 2 is the "geographic" center-line.

DISCUSSION OF DATA AND RESULTS

Discussion of Velocity Data

It is appropriate here to introduce some discussion of the seasonal behavior of the ice stream.

Few comprehensive studies of seasonal ice surface velocity variations are available. Paterson (1964) discusses variations in velocity of Athabaska Glacier. Brecher (1966 and pp. 127–143 of this volume), has attempted to analyze short term velocity measurements made on the north arm of Kaskawulsh Glacier. He finds that in practically every case any possible velocity variation is obscured by the standard error in the velocity values at each point. This applies to weekly, monthly and yearly velocity measurements. Thus no definite statement can be made regarding the velocity characteristics of the glacier, except that if fluctuations in velocity do exist, they are small.

The sliding mechanisms of glaciers on their beds have been dealt with in some detail by Weertman (1957, 1964) and Kamb and LaChapelle (1964). Weertman attributes changes in surface velocity to changes in sliding velocity dependent on the amount of water present at the basal interface and on the existence of traveling waves in the basal water layer.

On the basis of this information it is appropriate to review temperature observations in the upper Kaskawulsh Glacier. Ragle (in Wood, 1963) has classified the divide area as subpolar but measurements by Higashi and Shimizu during the summer of 1964 show that the 0°C isotherm existed to 15 m, thus indicating a temperature classification. Probably the geophysical nature is transitionary (Ragle, personal communication).

Measurements by the author within several crevasses showed that the 0°C isotherm prevailed to 24 m and in mid-August 1964 most crevasses contained about 2 to 4 m of water. The ice region in which this work was accomplished is therefore recognized as "temperate". For this reason an "average" value of V_b for temperate glaciers has been used in calculating $\overline{V}$ in the previous section.

Temperature variations of a seasonal nature could be important in influencing the amount of internal ice motion, but since yearly, seasonal, and weekly velocities have been examined and no pronounced variations are found, it is concluded that the penetration of the winter cold wave is probably shallow. In the cases where seasonal temperature variations are significant for most of the depth, the winter behavior is influenced by accumulation, producing extending flow, while lower temperatures tend to reduce the flow. In the summer, the reverse is the case, since ablation favors compressive flow while higher temperatures induce higher flow velocities. In this way seasonal ice velocity and strain rate fluctuations may be reduced.

It should be noted that approximate strain rates for the year 1963 – 1964 agreed with values obtained during the 1964 summer (see Figure 9-B).

Discussion of Strain Rate Data

Accumulation effect. It has been noted that during the summer the a/h term is negative but that such periods are neglected in order to simplify the calculations. To substantiate this the assumption might be made that the plastic response to the added winter – spring snowload is still occurring during the following summer and that it is only slightly modified by the summer ablation. These ideas are only valid if the response time of the glacier is at least three months, which appears to be a good assumption. Nye (1960,·1963) discusses the response time of valley glaciers.

Curvature effect. In the present analysis this term has proved difficult to interpret. Mention has been made (under Theoretical Considerations) of the fact that confusion exists over the use of the term k.

Theoretical derivations require that k and slope α be referred to the same curved surface; therefore these terms should be referred to either the bed or the ice surface. Preference to the latter is given because of convenience.

In the derivation of the curvature term (Nye, 1951, p. 561) it can be shown that

$$\frac{dh}{dx} = -\frac{h}{R}\cot\alpha$$

and not only must

$$\left|\frac{dh}{dx}\right| \text{ and } \left|\frac{h}{R}\right| \quad << 1$$

but

$$\left|\frac{h}{R}\right| << \frac{dh}{dx}$$

or

$$|hk| << \alpha$$

to a good approximation.

It has been demonstrated in the case of the present study that whether bed slopes or surface slopes are used, this criterion is not fulfilled except in one case. On a plane surface, $\overline{V}_c k \cot\alpha$ vanishes.

Transverse strain rate. It has been suggested that the measured values of $\dot{\epsilon}_y$ on the surface and lying on the central flow line should be used instead of the values derived from $\frac{\overline{V}}{W}\frac{dW}{dx}$ as suggested by Nye (1959b). To use the surface values means that any variation of $\dot{\epsilon}_y$ with depth is neglected, whereas $\frac{\overline{V}}{W}\frac{dW}{dx}$ takes account of this. However, since all the measurements in this case are restricted to the surface of the glacier, the surface value of $\dot{\epsilon}_y$ is more appropriate.

Rate of ice thickness change. This term is positive if the surface at a point is rising with time. Since 1961 the surface of this section of the Kaskawulsh Glacier has lowered and hence the term is negative. The 1964 summer velocity data could not accurately provide an estimate of $\frac{\partial h}{\partial t}$ and hence the results for the years 1962, 1963 and 1964 have been averaged. This is a small term, and is approximate only.

Bending effect. This is the true bending term which takes into account considerable rates of change of curvature. In the present case the value, for either bed or surface, is generally less than 1×10^{-5} day $^{-1}$.

Comparison of Measured and Theoretical Values of Longitudinal Strain Rate

Table 3 shows a final comparison between the values of $\dot{\epsilon}_x$. Unfortunately one of the most important terms is invalidated because the assumptions on which it is based are violated.

At Station 4, however, a calculation of $\dot{\epsilon}_x$ is justified, and using surface slopes, a value of $+7.7 \times 10^{-5}$ day^{-1} is obtained; using bed slopes, a value of 0.5×10^{-5} day^{-1} is obtained. The measured value is seen to lie between these values. Thus, although the computed values of $\dot{\epsilon}_x$ are of

the right order of magnitude, agreement is only approximate. Surface stresses have not been computed from the strain rate data but can be found using methods described in Nye (1959b).

Comparison of Laboratory and Field Measurements of Strain Rates

There is generally little agreement between laboratory measurements of the critical strain rate for tensile failure and measurements made on actual glaciers. The disagreement is generally substantial and may be attributed to the following:

(1) The presence of imperfections in glacier ice, such as inclusions and local deformation, which would locally change the bulk properties of the ice.

(2) The presence of substantial quantities of firn in the upper zones of glaciers which causes a considerable difference in ultimate strength properties from the surface to the base of the tensile layer at which $\sigma_x \leqslant o$.

(3) The development of thermal stresses due to rapid temperature changes at the glacier surface (Mellor, 1964, pp. 85-86).

(4) Differences in the rate of mechanical and thermal stress development within the ice.

Discussion of Crevasse Depths

Table 2 shows that computed values of crevasse depth are of the same order as the measured depths, which average about 26 m. Using values of $\dot{\epsilon}$ across a crevasse the average computed depth is about 55 m, while using regional values of strain rate the average computed depths are about 19 m. Moreover, using the value of critical regional strain rate, a tensile layer of 15 m is obtained. Since measured depths, densities, and the flow law constants are considered to be reliable, the problem becomes one of interpreting the strain rate values. To do this, an examination must be made of the physical significance of the strain rates and the methods of obtaining them.

Two methods were used to obtain $\dot{\epsilon}$ across a crevasse. Several crevasses (3 to 9, Figure 1) were measured for opening rate directly, so that $\dot{\epsilon} = \frac{\dot{w}_c}{w_c}$; others have been estimated from the regional strain rates using known crevasse spacings and fracture widths. Strain on intercrevasse blocks was assumed to be negligible. Thus d is computed from

$$\frac{2}{\rho g}\left(\frac{\dot{\epsilon}_{crev.}}{B}\right)^{\frac{1}{n}}$$

where $\dot{\epsilon}_{crev.}$ is the strain rate across a crevasse. There is one problem, however. It has previously been assumed that $\sigma_x = 0$ across a crevasse and that at the base of an open crevasse $\sigma_x \leqslant 0$; therefore how is the stress associated with the strain rate of an air gap going to be interpreted?

Several methods have been used to compute values of regional strain rates (given in Figure 9-B), and the agreement is within acceptable limits. Values of d approaching the measured depths are obtained if

$$\frac{2}{\rho g}\left(\frac{\dot{\epsilon}_x}{B}\right)^{\frac{1}{n}}$$

is used. $\dot{\epsilon}_x$ is the regional strain rate.

It will be instructive before proceeding with the discussion to review the results of Meier and others (1957). Meier uses regional strain rates such as those corresponding to $\dot{\epsilon}_x$ and in all cases these are very much smaller than the values used in Table 2 of this report. Strangely, the values of strain rate used by Meier are less than the critical strain rate given elsewhere in his report. It would appear the ϵ_x used in the preceeding equation should be such that $\dot{\epsilon}_x \geqslant \dot{\epsilon}_c$. Furthermore the method that Meier uses to obtain the value of B, in the flow law, is obscure. This empirical constant is extremely temperature sensitive and a change from 0° C to -1.5° C decreases B by an order of magnitude; a change from -1.5° C to -12° C changes its value by a further order of magnitude. Meier's calculations show that if the minimum recorded crevasse temperature is used to determine B then a depth of 15 m is obtained (Meier and others, 1957, p. 40). Actual temperatures range from -0.5° C to -6.5° C and the mean is probably -3° C, corresponding to a value of B which would give a computed crevasse depth of about 12 m, which is less than half of the observed depth. Meier assumes a temperature value of -12° C with no apparent justification. However this produces a good correspondence between computed and measured values of d, but it should be noted that Meier has used a depth formula without the factor 2 in the numerator.[1]

To return to the problem of the Kaskawulsh Glacier crevasses, it must be stated that since crevasses are obviously forming during the summer then values of B and n must be those corresponding to the melting temperature. A depth formula given by $d = 13.5\,\sigma_x$ is obtained, where σ_x can be determined directly from the curve given by Glen (1953, p. 721), if the value $\dot{\epsilon}_x$ is known. Nye (1955) implies that $\dot{\epsilon}_x$ should be used to compute d, and as mentioned, Meier and others (1957) use values of $\dot{\epsilon}_x$, but clearly, in the present case this is not accurate. Therefore, to solve this dilemma it could be supposed that prior to failure and during crack propagation, a local concentration of stress develops. This is associated with a strain rate comparable in magnitude with the values of $\frac{\dot{w}_c}{w_c}$ which have been measured for an opening crevasse. The problem may well be analogous to the case concerning the fracture of metals. Minute surface cracks known as "Griffith cracks" are known to exist in metals before rupture, and the local concentrated stress is given by

$$2\sigma_x\left(\frac{\ell}{R}\right)^{1/2},$$

where 2ℓ is the length of the crack, and R is the radius of curvature at the ends of the crack. The average "re-

[1] Author's note: Since this paper was submitted, certain corrections have been made (see Holdsworth, 1969).

gional" tensile stress, σ_x, acts perpendicular to the fracture trace. Clearly, as $R \rightarrow 0$, the local stress may reach very high values. The crack will propagate according to whether this local stress exceeds the ultimate tensile strength of the material.

It is well known that large variations of $\dot{\in}$ occur on the surface of a glacier within short distances (Meier and others, 1957; Nye, 1959b; Paterson, 1962; Wu and Christensen, 1964). Thus the concept of stress concentrations existing on the surface of glacier ice is not unfounded. Finally, it is noted that crevasse depths on temperate glaciers appear to be reasonably consistent.

Discussion of Crevasse Spacing

Crevasse spacing is somewhat of a problem since there is a paucity of analytical work and available data on which to base any hypothesis. As previously stated, it would seem to be necessary to make a stress analysis up-glacier of an already formed crevasse. There has been a suggestion that the spacing of crevasses is related to the depth, but this cannot be a simple function since in the present case $s \cong 2.8$ d whereas Meier and others (1957) finds $s \cong 4$ d for certain crevasses on the edge of the ice sheet in northeast Greenland. However, these were not transverse crevasses, and the physiographic and thermal environments were much different.

If a simple surface stress distribution is assumed, then there is a relation between the spacing, the stress gradient and the critical stress in tension, but in the present case this relation cannot be tested because the local gradient of strain rate near the uppermost crevasse cannot be accurately obtained. Regional values of this gradient are not appropriate since local values of strain rate commonly vary by an order of magnitude in short distances (see Meier and others, 1957; Nye, 1959b; and others).

Using Nielsen's simple bending beam theory, a good approximation for the spacing of fractures is obtained. However, assuming S, ρ, and g to be constant in Equation (10), the spacing s should be a function only of the ice thickness h. This conclusion is suspect. Using the data of Meier and others (1957), for instance, $s \cong 43$ m which is less than half of the measured value of about $4\,d \cong 100$ m. Equation (10), though giving the right order of magnitude of s in the present case, is much too simplified.

There appears to be no reason to associate the spacing of the Kaskawulsh Glacier transverse crevasses with annual movement since the latter is of the order of 110 to 150 m yr^{-1}. Moreover, the velocity distribution in the area observed has probably a weekly, monthly, or yearly variation of less than 10%. There is no evidence to suggest that the formation of crevasses is restricted to any part of the year. Crevasses were presumably forming during the summer on Kaskawulsh Glacier. The spacing values, the velocity data, and the flow law at low temperatures suggest that crevasses are forming in the winter also. It may be added, however, that if the velocity of sliding of the glacier is as high at 50% of the total flow velocity, then internal ice velocities range from 55 to 75 m yr^{-1}, and it is seen that many of the crevasse spacing values lie between 55 and 75 m (Figure 2).

GENERAL CONCEPT OF TRANSVERSE CREVASSE FORMATION

The Kaskawulsh Glacier transverse crevasses appear to be forming under relatively quiet conditions, suggesting a more "visco-plastic" behavior of the ice. Crevasse Camp, shown in Figure 1 was observed at the end of the field season to be situated between two fracture traces, the up-glacier one being a firn crack and the lower one being just measurable in width (that is, by definition, a crevasse). A low altitude flight over the area late in the season revealed the existence of two firn cracks higher up-glacier. These cracks are referred to as 01 and 001 (see Figure 1). Later field measurements of spacing and orientation of these fractures were made, but in no case could more than an ill-defined crack be detected. In the remaining two days of the field season, these had not opened. To detect their existence by ground visual observation was extremely difficult. Most likely, the fracture at depth was more definite but at the surface, firn creep had provided a deep solid bridge which by continuous readjustment removed most of the outward signs of a discontinuity.

To consider the mechanics of formation of these crevasses in previously unfractured firn, it is thought necessary to associate their occurrence with a critical stress and a certain rate of stress development at or near the surface of the glacier. This stress, which is associated with a critical value of extending principal strain rate, is generated by the flow characteristics, dimensions, and shape of the ice mass. To a good approximation the crevasse traces form perpendicular to the principal extending strain rate vector, at a point on the glacier. Presumably the fracture begins at or near the surface and propagates to a certain depth given by Equation (5). Further, it is suggested that the initial fracture occurs at or near the ice margins where "shear" crevasses provide a source of weakness in the ice. Later, the crevasse propagates toward the center of the ice stream. The Kaskawulsh Glacier transverse crevasses appear to be forming near the south boundary of the glacier and to be developing quietly toward the central regions. This type of development may not be general however. As the crevasse just formed moves downstream, a build-up of surface and subsurface stress behind it takes place until the critical strain rate is again reached, when another fracture is formed. The distance between these two crevasses is probably related to the surface stress gradient or the strain rate gradient. Suggestions have been made that the spacing is closely related to the crevasse depth, but as Meier finds that $s \cong 4$ d, and that for the Kaskawulsh Glacier crevasses $s \cong 2.8$ d for comparable depths, the relation cannot be a simple one. In fact a stress analysis around an already opened crevasse needs to be made (Nye, personal communication). If the strain rate is effectively zero on an inter-

crevasse block then the regional strain will be satisfied by the opening, or closing, of the crevasses. However, there is reason to believe that in the present case at least one intercrevasse block had been subjected to sufficient strain so that an intermediate crevasse had formed. This appears to be rather exceptional, however.

Neither detectable vibrations nor the sudden appearance of fractures were ever observed by the occupants of Crevasse Camp, although the camp was not occupied continuously towards the end of the field season. It is suggested that suitably placed seismograph stations on the glacier could be used to locate, in time and position, fracture planes in the ice. Suggestions have been made that model studies could be used to elucidate the processes of fracture taking place in glacier ice. Clay models could be, and have been used for qualitative study while more quantitative experiments could be made using photoplastic techniques.

On real glaciers there is a need for detailed measurements of local strain on the surface and at depth in the region of crevasse origin. Sophisticated methods need to be developed for measuring small strain networks. Further, there is a necessity for obtaining firn and ice samples at depth within the glacier, in order to estimate strength properties of the material.

ACKNOWLEDGEMENTS

This research was conducted as part of The Ohio State University 1964 glaciological program, supervised and led by Dr. C. Bull, on whom the author has been dependent for guidance and valuable consultation.

Financial assistance was gratefully received from the Bownocker Fund (Department of Geology, Ohio State University), the Friends of Orton Hall Fund (Geology Alumni of The Ohio State University) and the Ohio Academy of Science. Travel expenses and some field equipment were provided by the Institute of Polar Studies of The Ohio State University and the Icefield Ranges Research Program.

REFERENCES

Bader, H., and others (1951) Review of the properties of snow and ice, REPT. 4, U.S. Army Snow, Ice and Permafrost Res. Estab., prepared by Univ. of Minnesota, Inst. Technol. Eng. Station, 156 pp.

Brecher, H. H. (1966) Measurements of short term glacier motion, M.S. THESIS, The Ohio State Univ., Columbus (unpublished).

Butkovich, T.R. (1958) Recommended standards for small scale ice strength tests, TECH. REPT. 57, U.S. Army Snow, Ice and Permafrost Res. Estab., 6 pp.

Butkovich, T.R., and Landauer, J.K. (1959) The flow law for ice, RES. REPT. 56, U.S. Army Snow, Ice and Permafrost Res. Estab., 7 pp.

Glen, J.W. (1952) Experiments on the deformation of ice, J. GLACIOL. 2, 111.

Glen, J.W. (1953) Rate of flow of polycrystalline ice, NATURE, 172, 721 – 722.

Glen, J.W. (1955) The creep of polycrystalline ice, PROC. ROY. SOC., Ser. A, Vol. 228, pp. 519–538.

Glen, J.W. (1963) The rheology of ice, in ICE AND SNOW, edited by W.D. Kingery, pp. 3–7, M.I.T., Cambridge.

Gold, L.W. (1960) The cracking activity in ice during creep, CAN. J. PHYS., 38, 1131 – 1148.

Goldthwait, R.P. (1936) Seismic sounding on South Crillon and Klooch Glaciers, GEOGR. J. 87, 503.

Hauser, F.E., Landon, P.R., and Dorn, J.E. (1956) Deformation and fracture mechanisms of polycrystalline magnesium at low temperatures, TRANS. AM. SOC. METALS, 48, 986 – 1002.

Hill, R. (1950) THE MATHEMATICAL THEORY OF PLASTICITY, 356 pp., Clarendon, Oxford.

Holdsworth, G. (1969) Primary transverse crevasses, J. GLACIOL., 8, 109 – 127.

Kamb, B., and LaChapelle, E. (1964) Direct observation of the mechanism of glacier sliding over bedrock, J. GLACIOL., 5, 159.

Lagally, M. (1929) An attempt to formulate a theory of crack formation in glaciers, TRANSL. 47, U.S. Army Snow, Ice and Permafrost Res. Estab., 18 pp.

Lliboutry, L. (1958) Glacier mechanics in the perfectly plastic theory, J. GLACIOL., 3, 167.

Loewe, F. (1955) The depth of crevasses, J. GLACIOL., 2, 511 – 512.

Meier, M.F. (1960) Mode of flow of Saskatchewan Glacier, Alberta, Canada, U.S. GEOL. SURV. PROF. PAPER 351, 70 pp.

Meier, M.F., and others (1957) Preliminary study of crevasse formation, REPT. 38, U.S. Army Snow, Ice and Permafrost Res. Estab., 80 pp.

Mellor, M. (1964) Snow and ice on the earth's surface, COLD REGIONS SCI. ENG., PT. 2, SEC. C, U. S. Army Cold Regions Res. Eng. Lab., pp. 65 – 89.

Meyerhof, G.G. (1954) Crevasse depths, in The mechanics of glacier flow (Discussion), J. GLACIOL., 2, 340.

Nielsen, L.E. (1955) Regimen and flow of ice in equilibrium glaciers, BULL. GEOL. SOC. AM., 66, 1 – 8.

Nielsen, L.E. (1958) Crevasse patterns in glaciers, AM. ALPINE J., 11, 44 – 51.

Nye, J.F. (1951) The flow of glaciers and ice sheets as a problem in plasticity, PROC. ROY. SOC., Ser. A, Vol. 207, pp. 554 – 572.

Nye, J.F. (1952) The mechanics of glacier flow, J. GLACIOL., 2, 82 – 93.

Nye, J.F. (1955) Correspondence on crevasses, J. GLACIOL., 2, 512 – 514.

Nye, J.F. (1957a) The distribution of stress and velocity in glaciers and ice sheets, PROC. ROY. SOC., Ser. A, Vol. 239, pp. 113 – 133.

Nye, J.F. (1957b) Glacier mechanics, J. GLACIOL., 3, 91–93.

Nye, J.F. (1957c) THE PHYSICAL PROPERTIES OF CRYSTALS, pp. 158 – 163, Oxford, Cambridge.

Nye, J.F. (1959a) The deformation of a glacier below an icefall, J. GLACIOL., 3, 387.

Nye, J.F. (1959b) A method of determining the strain rate tensor at the surface of a glacier, J. GLACIOL., 3, 409 – 418.

Nye, J.F. (1959c) The motion of ice sheets and glaciers, J. GLACIOL., 3, 493 – 507.

Nye, J.F. (1960) The response of glaciers and ice sheets to seasonal and climatic changes, PROC. ROY. SOC., Ser. A, Vol. 256, pp. 559 – 584.

Nye, J.F. (1963) The response of a glacier to changes in the rate of nourishment and wastage, PROC. ROY. SOC., Ser. A, Vol. 275, pp. 87 – 112.

Nye, J.F., and others (1954) The mechanics of glacier flow (Discussion), J. GLACIOL., 2, 339 – 341.

Orowan, E. (1964) Continental drift and the origin of mountains, SCIENCE, 146, 1003 – 1010.

Paterson, W.S.B. (1962) Observations on Athabaska Glacier and their relation to the theory of glacier flow, PH.D. THESIS, Univ. of British Columbia, Vancouver.

Paterson, W.S.B. (1964) Variations in velocity of Athabaska Glacier with time, J. GLACIOL., 5, 277.

Prandtl, L., (1923) Z. ANGEW. MATH. MECH., 3, 401.
Rigsby, G.P. (1958) Effect of hydrostatic pressure on velocity of shear deformation of single ice crystals, J. GLACIOL., 3, 273.
Schuster, R.L. (1954) Travel and rescue in crevassed areas, INSTRUCTION MANUAL 2, U.S. Army Snow, Ice and Permafrost Res. Estab., 10 pp.
Schuster, R.L., and Rigsby, G.P. (1954) Preliminary report on crevasses, SPEC. REPT. 11, U.S. Army Snow, Ice and Permafrost Res. Estab., 6 pp.
Seligman, G. (1955) Comments on crevasse depths, J. GLACIOL., 21, 514.
Sharni, D. (1963) Survey Report, ICEFIELD RANGES RES. PROJ., unpublished, 28 pp.
Steinemann, S. (1958) Experimentelle Untersuchungen zur Plastizitat von Eis, BEIT. GEOLOGIE SCHWEIZ. HYRDOLOGIE, No. 10, p. 50.
Taylor, L.D. (1962) Ice structures, Burroughs Glacier, Southeast Alaska, PH. D. DISSERTATION, The Ohio State Univ., Columbus.
Wagner, P. (1963) Snow facies studies on the Kaskawulsh Glacier, Yukon Territory, Canada, M.S. THESIS, Univ. of Michigan, Ann Arbor.
Wagner, P. (1964) Diagenesis and snow facies: I.R.R.P. 1962 – 63, ARCTIC, 17, 56.
Weertman, J. (1957) On the sliding of glaciers, J. GLACIOL., 3, 33.
Weertman, J. (1964) The theory of glacier sliding, J. GLACIOL., 5,287.
Wood, W.A. (1963) The Icefield Ranges Research Project, GEOGR. REV., 53, 163 – 184.
Wu, T.N., and Christensen, R.W. (1964) Measurements of surface strain rate on Taku Glacier, Alaska, J. GLACIOL., 5, 305 – 313.

APPENDIXES

I

LIST OF SYMBOLS USED IN TEST

a	accumulation term expressed as ice equivalent (negative if ablation)
B, B′	empirical constants
d	depth of crevasses
g	acceleration of gravity
h	ice thickness at any position
K	yield stress of ice on perfect plasticity theory
ℓ	length
m	empirical constant $\frac{n+1}{2} \cong 2.1$ (temperate ice)
n	empirical constant in flow law (~ 3.17 for temperate ice)
P	constant (air pressure)
q	rate of flow of ice per unit width at the centerline of flow
Q	total rate of ice flow through a given cross-section
R	radius of curvature of a given surface
s	crevasse spacing
S	ultimate bending strength of ice
t	time
u_s	velocity component parallel to the glacier surface
v_s	velocity component perpendicular to the glacier surface
V	total velocity at a given point
V_X, V_Y	velocity components in direction of X, Y axes
$\overline{V}$	mean velocity of ice flowing through a given cross-section
V_b	velocity of ice at the base of the glacier
V_c	surface velocity on central flow-line
$\overline{V}_c$	mean surface velocity, over the depth
V_s	mean surface velocity, over the width
W	glacier width
w_c	crevasse width
x, y, z	rectangular curvilinear coordinate axes, where x is in the direction of ice flow, y is transverse, and z is perpendicular to x and y
X, Y	rectangular axes established by Wood in 1961 (see Figure 1)
α	surface slope measured from the horizontal direction of a flow line
$\dot{\Upsilon}_{xy}$	shearing strain rate in the x, y plane perpendicular to the z axis
$\dot{\epsilon}_{x,y,z}$	strain rates in the direction of the x,y,z axes respectively
$\dot{\epsilon}_1$	maximum (most extending) principal strain rate
$\dot{\epsilon}_2$	minimum (least extending) principal strain rate
$\dot{\epsilon}_c$	critical extending strain rate for fracture of glacier ice
$\dot{e}$	effective strain rate
θ	angle between the x axis and the axis of principal extending strain rate, measured in the x, y plane
ρ	density of glacier ice (0.9 gm cm^{-3})
σ	"effective" stress
$\sigma_{x,y,z}$	normal stresses in direction of x,y,z axes
σ_c	critical tensile stress associated with rupture
$\sigma_{1,2,3}$	principal stresses at a point
$\sigma'_{1,2,3}$	principal stress deviators at a point
τ	effective shear stress
τ_b	basal shear stress
τ_{xy}	sheer stress in the x, y plane perpendicular to the z axis
k	curvature, $\left(= R^{-1} = \frac{d\alpha}{dx}\right)$
·	denotes differentiation with respect to time

II

COMPUTATION OF SURFACE STRESSES

Nye (1959b, p. 414) outlines a method of computing stresses from the measured surface strain rates by using the experimental results of Glen (1955). The flow law relation, which is of the quasi-viscous type, is not the same as that used in the computation of crevasse depths made in the section on field data and results. The reason for this is due to further research into the flow behavior of ice subjected to low stresses. The stress-strain relation used in the present computations is of the form $\dot{e} = 0.148\,\tau^{4.2}$.

Tables 1 and 2 show the principal stresses at Stations 1, 2 and 3.

Since the relation $\dot{\epsilon}_1 + \dot{\epsilon}_2 + \dot{\epsilon}_3 = 0$ holds for a constant volume condition, the presence of crevasses within most of the diamonds may cause appreciable errors in $\dot{e}$ and hence $\frac{\tau}{\dot{e}}$, σ'_1, σ_1 and σ_2. The last two columns of Table 2 indicate that there is a substantial but consistent difference of between 8° and 15° between the principal extending strain rate direction and the direction of the total velocity vector. Nye (1959b, p. 415) shows differences of between 5° and 22° but these are not consistent with regard to algebraic sign. Estimates from the data of Wu and Christensen (1964) suggest differences of the order 8° to 30°. These are consistent in that principal extending strain rate directions are clock-wise of the total velocity vectors. This is exactly the case for the present results. Some significance may be attached to these results.

TABLE I

Diamond No.	$\dot{\epsilon}_1$	$\dot{\epsilon}_2$	$\dot{\epsilon}_3$	$\dot{e}$ (yr^{-1})	τ (bars)
3	$+4.35 \times 10^{-5}$ day^{-1} ($0.01596\ yr^{-1}$)	-9.10×10^{-5} day^{-1} ($0.03324\ yr^{-1}$)	($+0.01728\ yr^{-1}$)	0.0287	0.677
2	$+10.24 \times 10^{-5}$ day^{-1} ($0.0374\ yr^{-5}$)	-10.26×10^{-5} day^{-1} ($0.03743\ yr^{-1}$)	($+0.0006\ yr^{-1}$)	0.0374	0.721
1	$+14.35 \times 10^{-5}$ day^{-1} ($0.0525\ yr^{-1}$)	-14.0×10^{-5} day^{-1} ($0.0511\ yr^{-1}$)	($-0.0014\ yr^{-1}$)	0.0519	0.781

TABLE 2

						Grid Bearing	
	σ'_1	σ'_2	σ'_3	σ_1	σ_2	$\dot{\epsilon}_1$	Velocity Vector
3	+0.376	−0.785	+0.408	+0.033	−1.194	79.4°	71.0°
2	+0.722	−0.723	+ +0.012	+0.721	−0.724	89.1°	74.5°
1	+0.790	−0.769	−	+0.811	−0.748	87.5°	72.5°

Surface Velocity Measurements on the Kaskawulsh Glacier*

Henry H. Brecher†

ABSTRACT. Positions of 24 markers on the upper north arm of the Kaskawulsh Glacier were determined by intersection or resection on five occasions between July 12 and August 14, 1964. Surface velocities over four time periods of several days and two two-week periods were computed from the position determinations and compared to mean seasonal velocities. It was found that differences from mean seasonal values are randomly distributed. Annual velocities of three markers along the glacier centerline appear to be very slightly greater than summer velocities. An analysis of the errors in the results indicates that the errors in velocity differences are generally about as large as the apparent differences. It is concluded that there are no significant differences from mean seasonal velocities over the short time intervals.

INTRODUCTION

The object of this investigation was to study surface motion on a portion of the Kaskawulsh Glacier in order to determine whether velocities over time periods of several days varied significantly from seasonal and annual mean values. Large short-period variations have been reported for other mountain glaciers (for example Meier, 1960; Paterson, 1964). Since the mean annual surface velocity on the centerline of this portion of the glacier is between 120 and 150 m per year, large variations in velocity should have been readily measurable by standard surveying techniques.

Sharni (1963) measured the velocity over four short time periods during summer 1963 at a point approximately 750 m up the glacier from the present study area. He found that the summer flow rate equals the mean annual rate, to the nearest 5 percent or less.

FIELD WORK

Five surveys of 24 movement markers were carried out between July 12 and August 14, 1964. The weather was suitable for surveying on approximately 35 percent of the field days.

The head of the north arm of the Kaskawulsh Glacier was selected for this study (see map inside back cover). Here the highland ice is channeled between nunataks on the north and south in its easterly progress. The surface area included in the survey is smooth with a slope of less than one degree. A very regular pattern of widely spaced and generally well-bridged transverse crevasses extends across much of the survey area, and there is a heavily crevassed zone along the northern margin of the glacier. The area is bounded on the east by open transverse crevasses. The width of the glacier here is approximately 3 km.

Equipment

A Wild T-2 theodolite, Ser. No. 2334, was used for all of the surveying. This was one of the earliest instruments of this model. As with the later models of the T-2, the instrument can be read directly to the nearest second of arc. The only obvious evidence of the age of the instrument, besides its general appearance, was the rather uncertain illumination of the vertical circle.

An uncalibrated 100-m steel surveying tape was used for the baseline measurement. Heights of the tops of the movement markers above snow level were measured with either a 10-m steel tape or an 8-ft. steel pocket tape.

Procedures

Fixed points. Two fixed points in a previously established local rectangular coordinate system, H on the north and K on the south, were already available in the survey area (see Holdsworth, Figure 1, p. 110, this volume). Station H was difficult to reach so another fixed point, S, was established in a more accessible place. This position also slightly improved the strength of the intersections of most of the surface markers. It must be emphasized, however, that fixed station locations were determined almost entirely by the positions and accessibility of the rock outcrops. A second new station, T, was established in a position suitable for locating the movement markers by resection in conjunction with stations K and H or S. The stations were marked by stone cairns.

The fixed points were tied together by observing all the angles in the two triangles HKS and SKT. Stations H and T were not intervisible. Two sets of observations were made at each station using different portions of the horizontal circle. The scales were coincided and the micrometer read as many times as necessary to obtain three readings not more than 2 seconds apart. This was generally quite easy to accomplish; in fact, most readings agreed within 1 second. Directions were read and recorded to 0.1 second. Several additional sets of observations of most of the angles were made during the season in conjunction with the movement surveys. The final means of the various angles are based on five measurements of angles 2 and 6, four measurements of angles 3 and 5, three measurements of angle 4 and two measurements of angle 1 (see sketch, p. 128). Vertical angles were also taken between all points. Elevation differences are therefore based on several reciprocal observations.

*This report is a modified version of the Institute of Polar Studies Report No. 21, 1966, and is printed here with permission.

†Institute of Polar Studies, The Ohio State University, Columbus, Ohio.

The distance between stations H and K, computed from the previously determined coordinates, was used to provide scale for the survey. A 500-m baseline was laid out with a surveyor's tape on the glacier surface and extended to the line KS through two braced quadrilaterals, to serve as a check.

Motion markers. The three easternmost markers of the network of ablation and motion stakes established on the highland ice in 1962 were located in the area of the present survey. They were spaced roughly 500 m apart and were approximately on the centerline of the glacier. These were lengths of aluminum pipe 3.5 cm in diameter set into the firn with 1 to 1.5 m protruding above the surface. A network of 21 bamboo stakes 2.5 cm in diameter and 3.6 m long, of which approximately 2 m protruded above the surface, were set out in three transverse rows of seven stakes each. In each of the three rows, three markers were at distances of approximately 200, 500, and 1000 m, respectively, from the central markers (Figure 1). Thus the survey area was roughly a 1.5 x 2 km rectangle.

Five determinations of the positions of these 24 markers were made during the season. The first survey, done at the time the markers were emplaced, was by resection on all four stations, with observations on July 12, 14, and 16. The other four surveys were by intersection from stations K and S on July 21 and 29 and August 9 and 14. Intersection was used after the first survey primarily because it required less time than resection. Except during the first survey, redundant observations were not made for every marker. However, in each of the other four surveys observations of all three angles in the triangle were performed at some markers in order to allow an estimate of the errors to be made.

One set of observations, consisting of one forward and one reverse pointing, was made for all angles, horizontal and vertical, in the motion surveys. The same reading accuracy standards were used as in the triangulation of the fixed points. Pointings were to the tops of the stakes. In all but one or two cases the stakes were essentially vertical (judging by their appearance in relation to the vertical hair of the telescope) and no attempt was made to allow for the tilt of the stake. Where there was appreciable tilt, pointings were made to the bottom of the stake. So that all survey heights would refer to the glacier surface, stake heights were measured several times.

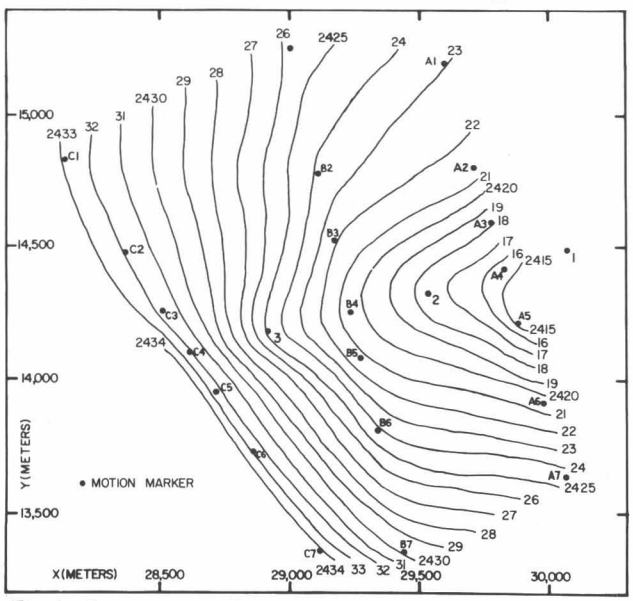

Fig. 1. Contour map of survey area, showing locations of motion markers. Elevations in meters above sea level.

All stakes had 30 x 30 cm bright orange flags fastened near their tops to make them easier to see. No real difficulties were encountered in locating the stakes from either station K or S, but on three occasions pointings were made to a stake which was not part of the present survey network, the pointings being to the same incorrect stake each time.

Aside from the delays that it caused, the weather had no significant effects on the work, except for the third survey. In this instance a fog bank moved into the area while the intersections from station K were being completed, and no reverse pointings could be made on twelve markers from this position. The angles adopted are the forward angles corrected by one half of the mean difference between forward and reverse angles on the thirteen stakes on which full sets of readings were made.

COMPUTATIONS

Angles were rounded off to the nearest second of arc except in the triangulation of the fixed points where tenths of seconds were carried through the computations.

Fixed Points

The two triangles used to establish stations S and T yielded misclosures of 24.8 and 3.9 seconds. They were adjusted separately by adding one-third of the misclosure to each angle. Lengths and coordinates were then computed starting with the length of the line HK (see sketch).

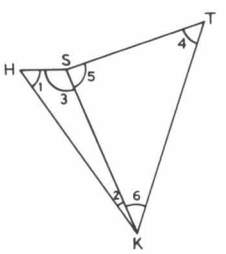

The starting point for height determinations was the elevation of cairn K. Height differences between the fixed points were determined by computing the mean of the 'upward' and 'downward' measurements between each pair of points. The mean height difference

from simultaneous reciprocal observations can generally be taken to be free of refraction errors. In this case the observations were not simultaneous, and therefore errors may be present. Nevertheless it appears that the mean is the best solution obtainable. The results are summarized in Table 1.

TABLE 1. Observed Elevation Differences (Δh) Between Fixed Points

Height difference	Δ h down (m)	Δ h up (m)	Δh mean (m)
1 KS	27.55	25.54	26.54
2 HS	116.00	115.51	115.76
3 HK	90.33	88.14	89.24
4 KT	17.13	14.26	15.70
5 ST	42.85	41.30	42.08

The network was then adjusted by assigning weights to the observations in inverse proportion to the squares of the distances.

The adjusted height differences are

$$h_1 = 26.54 - 0.04 = 26.50 \pm 0.05 \text{ meters}$$
$$h_2 = 115.76 - 0.00 = 115.76 \pm 0.01$$
$$h_3 = 89.24 + 0.02 = 89.26 \pm 0.06$$
$$h_4 = 15.70 - 0.08 = 15.62 \pm 0.07$$
$$h_5 = 42.08 + 0.04 = 42.12 \pm 0.04$$

The height difference between cairns H and K computed from the present observations is 4 cm less than the figure obtained from the existing coordinates for these two points. Since all the elevation figures have been rounded off to the nearest 5 cm in the existing coordinate system and because of the standard errors of the present determinations, no real discrepancy exists. Besides, only the difference in elevation between cairns K and S is of real interest for the present work since all glacier surface height determinations were made only from these two cairns. Table 2 gives the coordinates of the fixed points and the distances between them.

The distance KS, the baseline for the intersections, computed from the taped base after adjustment of the extension by a method given by Clark (1951, pp. 284-87), is 3602.83 m.

Motion Markers

Resection. For the first survey the positions of the markers were determined from resection on cairns S, K and T and H, K and T. The solution was carried out using Burckhardt's method (Jordan and Eggert, 1950). Coordinates were then computed by the same method as in the case of intersection.

Intersection. For the remaining surveys the positions of the markers were determined by intersection from stations K and S. The solution is carried out by first applying the law of sines to compute the two sides, k and s, of the triangle below.

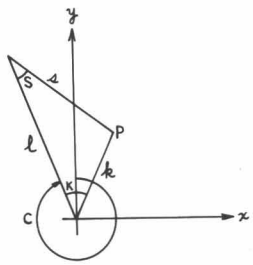

Once the length k and the angle K are known, the x and y coordinates can easily be calculated since the coordinates of K and the grid azimuth C, of the line KS in the local coordinate system, are known. The y axis is parallel to grid north. Then

$$x_p = x_k + k \sin (C+K)$$
$$y_p = y_k + k \cos (C+K)$$

Elevation. Elevation differences were determined by trigonometric leveling to (resection) or from (intersection) cairns K and S. For both resection and intersection the mean elevation of a point Z_p on the glacier, calculated from the known elevation, Z_k, of station K is

$$Z_p = \frac{(Z_k - \Delta Z_k) + (Z_k - \Delta h - \Delta Z_s)}{2}$$
$$= Z_k - \frac{\Delta Z_k + \Delta Z_s + \Delta h}{2}$$

where

ΔZ_k is the elevation difference between cairn K and the point on the glacier

ΔZ_s is the elevation difference between cairn S and the point on the glacier

Δh is the elevation difference between cairns K and S

The refraction and curvature correction used is $r = cD^2$, where r is the correction in meters, c is an empirically determined coefficient, and D is the horizontal distance between the points in kilometers.

TABLE 2. Coordinates of Fixed Points and Distances Between Them

Point	Coordinates (m) x	y	z	Distances (m)			
H	27485.99	15812.26	2622.21	HK	4082.97	KS	3602.90
K	29691.50	12376.22	2532.95	HS	961.35	KT	4484.45
S	28445.74	15756.90	2506.45	HT	4005.62	ST	3078.16
T	31430.41	16509.80	2548.57				

A value of r was adopted which would yield the minimum average difference between elevations determined from stations K and S. This value was found to be 0.065 m/km^2, the same as that used by Sharni (1963).

Corrections for motion during the period between observations from K and from S. Some time necessarily elapsed between the observations from the two fixed points, with the result that the markers on the glacier were slightly farther downglacier at the second observation. The corrections to the angle measurements due to this effect may amount to 15 seconds of arc.

The time at which observations began and ended on each line of markers at each cairn was recorded for each survey. The time of observation of each motion marker was determined by dividing the elapsed time proportionally among the observations in that time period.

The approximate velocity was determined from the positions of the markers at the first and last survey of the season, which were provisionally computed from angles not corrected for motion between observations. Over this relatively long time period the effect of the motion between the observations is negligible. For simplicity, it was assumed that the markers moved at right angles to the baseline in all cases. Although the direction of surface movement relative to the baseline ranged from 75° to 101°, this assumption was justified since even at these extremes the corrections calculated from the true direction of motion and from the assumed direction were identical.

The method of calculating the angular corrections is evident from the following diagram:

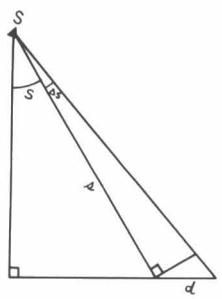

$$\Delta S = \frac{f d \cos S}{s}$$

The angles at S were corrected to the time of the observations from K in each case. Mean values for the angle at S and the distance s were used in computing the corrections for all four surveys. The results of the correction computations are given in Table 3.

Comparison of triangle misclosures in the cases where redundant observations were made shows clearly that these corrections improve the results considerably. The average triangle misclosure was reduced from 28 to 14 seconds. In the two cases where elapsed times between observations were particularly long (0.593 and 0.948 days between observations from K and from the marker, and 0.816 and 0.863 days between observations from S and the marker) the average misclosure was reduced from 82 to 15 seconds.

Motion. Figure 1 is a contour map of the survey area. The maximum slope is only 50 minutes and is in the direction of motion along the glacier centerline. The vertical velocity is only about 3 percent of the horizontal velocity, on the average. The motion in the horizontal direction thus represents the total surface motion for all practical purposes.

The motion in the horizontal direction is

$$d = \sqrt{(x_2 - x_1)^2 + (y_2 - y_1)^2}$$

where x_1, y_1, and x_2, y_2, are the coordinates at the first and second position respectively. The direction of motion with respect to grid north of the local coordinate system is

$$\theta = \tan^{-1} \frac{x_2 - x_1}{y_2 - y_1}$$

The vertical motion of the surface is obtained from the difference in elevation, that is

$$\Delta z = z_2 - z_1$$

Because the measurements refer to the glacier surface this result includes the surface lowering due to ablation.

TABLE 3. Corrections for Motion Between Observations at K and S (seconds)

Marker	Survey 2	Survey 3	Survey 4	Survey 5
1	−5.4	−8.8	3.6	3.3
2	−6.0	−9.8	3.9	3.9
3	7.0	10.2	−3.5	−4.5
A1	9.1	3.9	5.9	6.4
A2	9.7	4.4	6.5	7.0
A3	8.9	4.1	5.9	6.4
A4	8.1	3.8	5.6	5.8
A5	6.6	3.3	4.7	4.9
A6	4.8	2.5	4.0	4.0
A7	3.1	1.7	2.5	2.4
B1	14.8	−15.0	9.6	9.0
B2	12.0	−13.8	8.3	7.7
B3	11.2	−12.4	7.6	6.5
B4	8.4	−9.6	5.6	4.6
B5	7.2	−8.2	4.8	3.9
B6	5.4	−6.4	3.8	2.9
B7	3.3	−3.8	2.1	1.5
C1	−8.5	12.8	−5.1	−4.0
C2	−8.9	11.8	−5.8	−4.2
C3	−7.4	10.2	−5.1	−3.3
C4	−7.7	9.1	−4.4	−2.6
C5	−6.6	8.1	−3.9	−2.1
C6	−5.2	6.8	−3.3	−1.7
C7	−3.5	5.6	−2.1	−1.0

Negative correction means angle S is decreased

The amount and direction of motion between successive position determinations and the velocity for each interval and for the whole summer season were computed for each marker (Table 5, pp. 137 – 139).

Computer Program

Positions, motions, velocities, and errors were computed on an IBM 7094 electronic computer. The facilities of the Ohio State University Numerical Computation Laboratory were employed. A program using the SCATRAN language was developed which accepts both the resection and intersection data and prints out the five positions and the four motions for each point, the standard point errors, the standard errors in the direction of motion (longitudinal) and perpendicular to the direction of motion (transverse) for each position determination, the standard errors in the motion and velocity between two successive positions, the relative errors of velocity, in percent, the elements of the error ellipse for each intersection and the total motion, mean seasonal velocity and their errors for each marker.

ERROR ANALYSIS

Fixed Points

The standard errors of the angles in the two triangles used to establish stations S and T can be computed from the corrections applied to the angles in the triangle adjustments.

Clark (1951, p. 280) gives the following expression for the standard error of an adjusted value obtained from adjustment by conditions

$$m_a = \pm \sqrt{\frac{(t-n)\,[vv]}{tn}}$$

where t is the number of observations
n is the number of conditions
v is the correction.

For each triangle there are three observations and one condition, namely that the sum of the angles in the triangle must be 180°, so that the standard error for triangle HKS is ±11.6, and in a similar manner ± 1.8 seconds is computed as the error for triangle KST.

In spite of this difference in the standard errors, there is every reason to believe that all the observations in both triangles are of the same precision. This is confirmed by the reasonable agreement among the standard errors of the observed angles. Furthermore, the very small misclosure in triangle KST seems entirely unrealistic, particularly in view of the standard errors of the observed angles. It seems more likely that the standard error of an adjusted angle in the cairn triangulation is somewhere between the two values computed; their mean, 6.7 seconds, has therefore been adopted as the best estimate.

The error in the length of the baseline KS from the ends of which the motion markers were intersected, can be determined from the errors in the length HK and the angular errors computed above. Clark (1951, p. 299) gives the following expression for computing the standard error of the exit side, a, of a triangle ABC from the standard error of one side, m_b, and the standard error of the adjusted angles, $m\alpha$.

$$m_a^2 = (m_b \frac{a}{b})^2 + \frac{2}{3} a^2 \frac{m_\alpha^2}{\zeta^2} \quad (\cot^2 A + \cot^2 B + \cot A \cot B)$$

Thus
$$m_{KS} = \pm KS \sqrt{[m_{HK}/HK]^2 + 2/3\ [m/\zeta]^2\ [\cot^2(1) + \cot^2(3) + \cot(1)\cot(3)]}$$

where ζ is 206264.8, the factor for converting radians into seconds.

W. Wood (personal communication) estimates that the scale error in the local coordinate system is 1:30,000, which means an error of ± 0.14 m in the length HK. Assuming this to be the standard error and applying it and the standard error of ± 6.7 seconds in the angles in the expression above, the standard error in the distance KS is ± 0.16 m.

Although reasonable internal agreement for the length of the taped baseline was achieved (standard error = ± 0.006 m), it seems pointless to attempt to estimate the error in the length of KS from the baseline extension because the calibration error of the tape is unknown. It is, however, likely to be considerably larger than the error in the extension from line HK and it therefore appears that the good agreement in the lengths obtained by the two methods is merely fortuitous. The effect of the error in the length of the baseline on the determinations of the motions of the markers is negligible in any case.

Since all the intersections were made from the same two points, errors in their coordinates will have no effect on the relative positions of the intersected points. They will produce errors in the positions relative to the origin of the coordinate system, but these are of no interest here.

The standard errors of the elevation differences can be computed by first obtaining the error of an adjusted difference of unit weight from the expression

$$m_p = \pm \sqrt{\frac{(t-n)\,[pvv]}{tn}}$$

where p is the weight and the other symbols are the same as in the expression for unweighted observations. Then the error of an adjusted value of weight p_i is $m_p/\sqrt{p_i}$. The standard errors for the five elevation differences are

$m_1 = \pm 0.05$ m
$m_2 = \pm 0.01$
$m_3 = \pm 0.06$
$m_4 = \pm 0.07$
$m_5 = \pm 0.04$

The mean of these errors is ± 0.05 m.

Motion Markers

Errors in velocity depend on the errors in the measurements of positions and on the error in the time over which the motion occurred. In this study velocity errors are determined almost entirely by the position errors of the markers since the time between observations is known to 1 part in 500 for the shortest time period and to 1 part in 1000 for the longest time period, based on an estimated error of ± 15 minutes for the time of each position determination.

Errors in Positions

Resection. Since observations were made on four points for each resection, redundant observations are available for determining motion marker position errors. It is to be noted that the adjusted positions are means of the determinations from only two sets of observations, those on cairns H, T and K and those on cairns S, T and K. This procedure was thought to be preferable to an adjustment using all the observations, because in all but two cases these two sets of observations yielded positions which agreed within a few centimeters while the other two combinations of pointings gave positions which were scattered erratically and were not in agreement with each other or with the two other results.

Standard errors in the direction of motion, m_f, and perpendicular to the direction of motion, m_g, were computed from the differences between the results of the two sets of observations used for the position determinations. Although this method is not strictly correct because it does not take into account covariance between the errors in x and y, the values obtained are not appreciably in error. The average directions of motion of the markers, as determined from the first and last positions, have been used in computing these errors. The standard point error, m_p, which by definition is the root mean square of the errors in two perpendicular directions, was also computed.

Intersection. Redundant observations were generally not made in the position determinations by intersection. An estimate of the position errors can be made, however, based on the assumption that all the observations of the motion markers were made with the same precision, which should indeed be the case.

A mean standard error for unadjusted angles has been computed from 11 sets of observations in which all angles in the triangles were observed. The computations give equal weight to angles measured at the cairns and at the motion markers on the glacier surface. This method of computation should result in a conservative value for the angular errors at the cairns since these measurements are likely to be of somewhat higher precision than those at the motion markers, which are adversely affected by settling of the tripod and poorly defined marks for the sightings onto the cairns. The standard error of an intersection angle computed from the observations described is ± 8 seconds. This value has been used in the following analysis.

The error in a position determination by intersection depends on the errors in the angles and on the error in the length of the baseline, and, of course, it varies with the position of the intersected point relative to the baseline. In the present work the effect of the error in the length of the baseline is negligible. For most of the markers it is an order of magnitude smaller than the effect of the angular errors. It averages only 4 mm for all the motion markers and its maximum value is 14 mm. Therefore, the error in the length of the baseline has not been included in the computations which follow.

The position errors in the direction of motion and perpendicular to the direction of motion are desired. These are obtained most easily by partial differentiation of the expressions for the coordinates of a point, P, in the direction of motion, f_p, and perpendicular to this direction, g_p, for each point. The expressions can be derived from the following sketch:

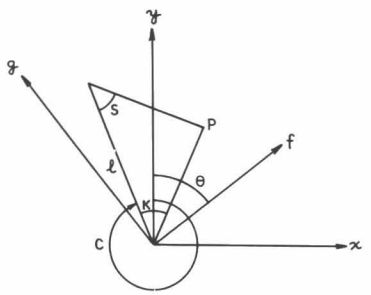

The azimuth, C, is fixed; θ, the direction of motion, is fixed for a given marker; while angles K and S change from observation to observation. Then

$$f_p = \ell \frac{\sin S \cos [K+(C-\theta)]}{\sin (K+S)}$$

and

$$g_p = -\ell \frac{\sin S \sin [K+(C-\theta)]}{\sin (K+S)}$$

The standard error in the direction of motion is

$$m_f = \pm \sqrt{\left(\frac{\partial f}{\partial k}\right)^2 m_k^2 + \left(\frac{\partial f}{\partial s}\right)^2 m_s^2} \quad \text{and} \quad m_k = m_s = m$$

$$\text{so} \qquad m_f = \pm \frac{m\ell}{\zeta \sin^2 (K+S)} \cdot$$

$$\sqrt{\cos^2 [K+(C-\theta)] \sin^2 K + \cos^2 [S-(C-\theta)] \sin^2 S}$$

and similarly the standard error perpendicular to the direction of motion is

$$m_g = \pm \frac{m\ell}{\zeta \sin^2 (K+S)} \cdot$$

$$\sqrt{\sin^2 [K+(C-\theta)] \sin^2 K + \sin^2 [S-(C-\theta)] \sin^2 S}$$

As with the resections, the standard point errors were also computed.

A more general solution can be obtained by calculating the standard error ellipse at each point. This has been done by modifying a method given by Ackerl (1965). When the error ellipse at a point is known, the standard error in any desired direction, m_θ, can be computed from the expression

$$m_\theta = \pm\sqrt{A^2 \cos^2\varphi + B^2 \sin^2\varphi}$$

where A is the semi-major axis of the error ellipse
B is the semi-minor axis and
φ is the angle between the major axis and the desired direction.

A knowledge of the error ellipses generated at various points by the geometry of the survey does not contribute any new information to the evaluation of the errors of the present work, except that by establishing the directions in which the errors are largest and smallest, it gives some indication of whether the locations of the fixed points in the survey are near the optimum.

Figure 2 is a contour diagram of the orientations of the major axes of the error ellipses and the corresponding values of the semi-major and semi-minor axes over the survey area, obtained by computing values at 100-m x and y intervals. Similar diagrams for given baseline lengths and angular errors might be useful in determining optimum locations for fixed points in future surveys.

The standard point errors computed for the intersections are on the average about 6.7 times as large as those obtained for the resections. Since the work was performed with the same precision in both cases, this may be an indication that the accuracy of the intersections has been underestimated. It is more likely, however, that this discrepany is merely due to the geometry of the intersections. The standard position errors in the direction of motion are in reasonably good agreement, the errors for the intersections averaging about 2.6 times the errors for the resections (Table 4). The much higher accuracy of positions in the direction of motion compared with the perpendicular direction is due to the geometry of the intersections. Because of this the standard point errors are of little interest here, but they are given for completeness.

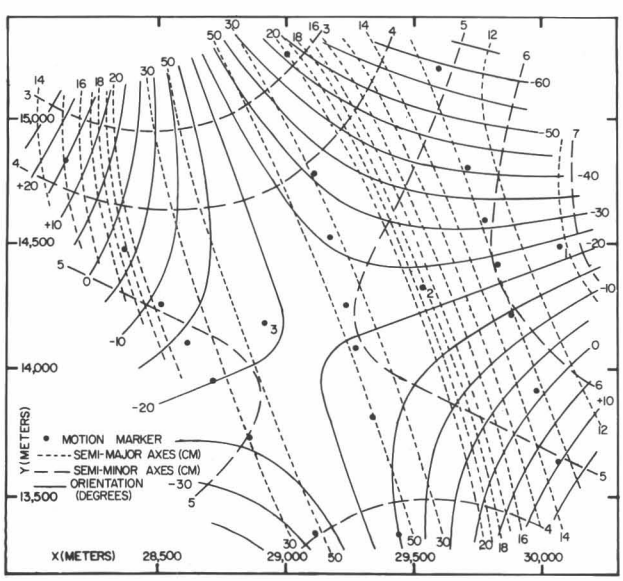

Fig. 2. Elements of error ellipses. Orientations of major axes in degrees from grid north.

TABLE 4. Position Errors for Resections and Intersections

Point	Standard point error (cm)		Standard error in dir. of motion (cm)		Standard error perpendicular to dir. of motion (cm)	
	RESEC	INTERS	RESEC	INTERS	RESEC	INTERS
1	2.9	13.0	1.9	6.8	2.2	11.1
2	2.1	18.8	1.1	5.7	1.8	17.9
3	8.0	99.7	3.8	8.1	7.1	99.3
A1	2.0	13.5	1.3	10.1	1.5	0.9
A2	3.4	13.9	2.1	7.7	2.7	11.5
A3	2.3	14.0	1.4	6.7	1.9	12.3
A4	1.9	14.2	1.2	6.1	1.5	12.8
A5	1.7	14.3	1.1	6.1	1.3	12.9
A6	2.0	14.3	1.5	7.7	1.4	12.1
A7	5.8	14.2	4.7	10.0	3.4	10.1
B1	4.3	20.3	2.7	12.4	3.4	16.1
B2	3.3	28.6	1.7	10.4	2.8	26.6
B3	4.3	33.2	2.0	8.5	3.8	32.1
B4	2.9	38.7	1.3	6.6	2.7	38.1
B5	4.6	42.8	1.9	5.3	4.2	42.5
B6	6.3	50.3	2.4	5.4	5.8	50.1
B7	4.7	69.2	1.3	6.2	4.6	68.9
C1	2.0	15.5	1.8	8.1	0.8	13.2
C2	4.7	19.0	4.4	7.2	1.5	17.6
C3	7.4	21.7	4.1	6.9	6.1	20.6
C4	12.5	23.9	0.1	7.1	12.5	22.9
C5	4.8	26.5	3.2	6.2	3.7	25.7
C6	7.2	30.9	0.7	6.4	7.2	30.2
C7	2.2	42.9	2.0	7.0	1.0	42.3
means	4.3	28.9	2.8	7.4	3.5	27.1

Errors in Motion

The standard error in the motion between two observations is obtained from the position errors in the direction of motion for the two positions, that is

$$m_d = \pm\sqrt{(m_{f_1})^2\,(m_{f_2})^2}$$

Errors in Velocities

The standard error in velocity can then be obtained by partial differentiation of the expression for the velocity. Thus

$$m_v = \pm \sqrt{(m_d/t)^2 + [m_t (d/t^2)]^2}$$

where d is the motion in t and m_d and m_t are their standard errors.

The standard position errors in the direction of motion and standard errors of velocity over the season have been presented as plots of lines of constant error over the study area (Figures 3 and 4). It will be noted that the errors are not symmetrical and the whole pattern may seem rather odd at first glance. However, it must be remembered that the direction of motion changes across the survey area and the error in the direction of the baseline increases very rapidly in its vicinity. Along the line it is as large as the distance between the fixed points. Since the direction of the surface motion is nowhere exactly at a right angle to the baseline, the error in the direction of the baseline contributes a component to the error in the direction of motion. This is the reason for the rapid increase of the errors near the baseline and for the discontinuities in the error contours across it.

Relative Errors

It is evident that the relative errors in motion and velocity decrease as the amount of motion increases, and particularly as the time between position determinations increases. Thus the velocities for the whole season can be given with a good deal of confidence, whereas the velocities over the four short time-intervals are subject to considerable uncertainty. The situation is somewhat better if the season is divided into only two intervals, each about two weeks long. In this case the velocities are determined with a relative accuracy of 1 to 2 percent for most of the markers. The velocity errors are summarized in Table 5.

Errors in Velocity Differences

The standard error of the velocity difference between two velocities is the root mean square of the standard errors of each velocity determination. Since the differences in velocities from the seasonal means are generally very small, their relative standard errors are very large. This is particularly true for the half-season intervals where, although the relative accuracy of the velocities is higher than in the four short intervals, the differences from the mean are so small that the improved accuracy is cancelled out. The medians of the relative errors of the differences range from 72 to 103 percent for all but one interval, where the median is 45 percent. The means are somewhat higher, but this is due to one or two extremely high values resulting from negligibly small velocity differences. The medians therefore give a better picture of the situation. In many cases the errors are several times as large as the velocity differences (Table 5).

Errors in Elevations

The standard error of each elevation can be determined from the difference between the elevations obtained from the two cairns, K and S. The mean of these standard errors is ± 4 cm. It is perhaps statistically more meaningful to compute a single standard error from the differences of all the observations from their means. This yields a standard error of ± 8 cm for one observation. Some additional errors due to inaccuracies in the measurements (or interpolations) of the heights of the motion markers are also present. These cannot be evaluated but are estimated to be no larger than 2 cm.

These figures are not very useful in attempts to judge what systematic errors, primarily those due to refraction, might be present in the results. Since we are primarily interested in differences of elevation, however, it

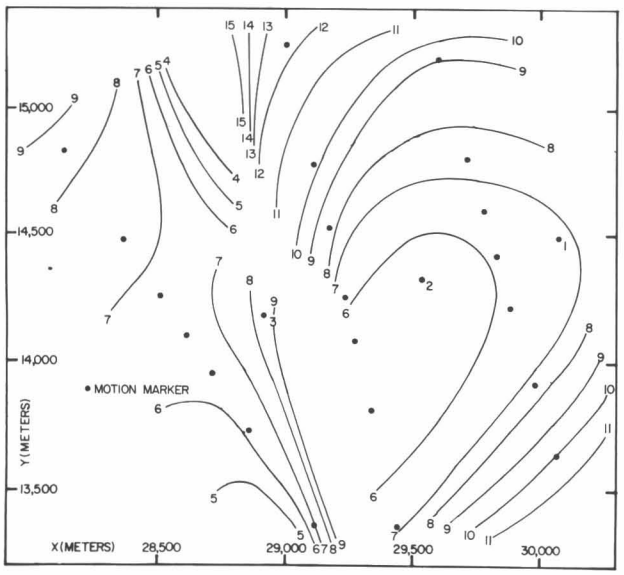

Fig. 3. Standard errors of position in the direction of motion. Errors in centimeters.

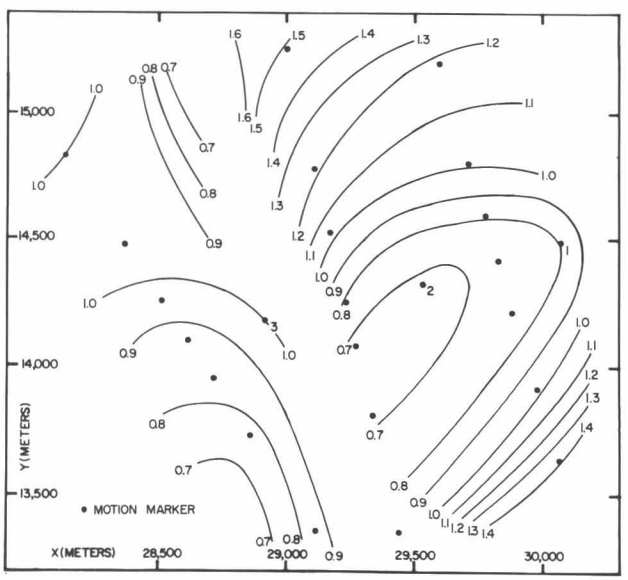

Fig. 4. Standard errors of seasonal velocity. Errors in meters per year.

is not unreasonable to suppose that the results are satisfactory, because any systematic errors which are present are likely to have the same effect each time and therefore do not influence the elevation differences.

Errors Inferred from Results

Plots of the several positions for each marker (Figure 5) seem to indicate that certain systematic errors are present. This is inferred from the fact that the paths of the motions deviate systematically from the straight lines (actually smooth curves, but approximated by straight line segments for the short distances involved here) the motions would be expected to follow. In nearly every case the second and fourth positions are displaced "downward" while the third and fifth positions are displaced "upward" from a hypothetical best straight line for the markers downglacier from the baseline (lines A and B) and in the opposite directions for the upglacier markers (line C). This effect is particularly pronounced for the motion markers in line B, especially in the second position determinations. Inaccurate centering over one (or both) of the fixed points could produce errors in the directions noted but could not account for their magnitude. It has also been suggested that the error in row B may be due to settling of the instrument, since it becomes progressively worse with time. This possibility must be considered, although, since the setup was on a mound of large rocks at cairn S and on solid rock at cairn K, it does not seem very likely.

Consideration was given to correcting the positions by shifting them transversely to make them fall on a straight line. It was decided, however, that there was little to be gained by doing so, since in most cases the effect of such a change on the downglacier distance between positions would be negligible. In the cases where the deviations from a straight line are large, as between markers B4 and B7, it appears that a correction perpendicular to the direction of motion would not represent the true circumstances. Consequently, it was decided to accept the computed positions with the realization that an erroneous result is likely where the deviations from a straight line are large.

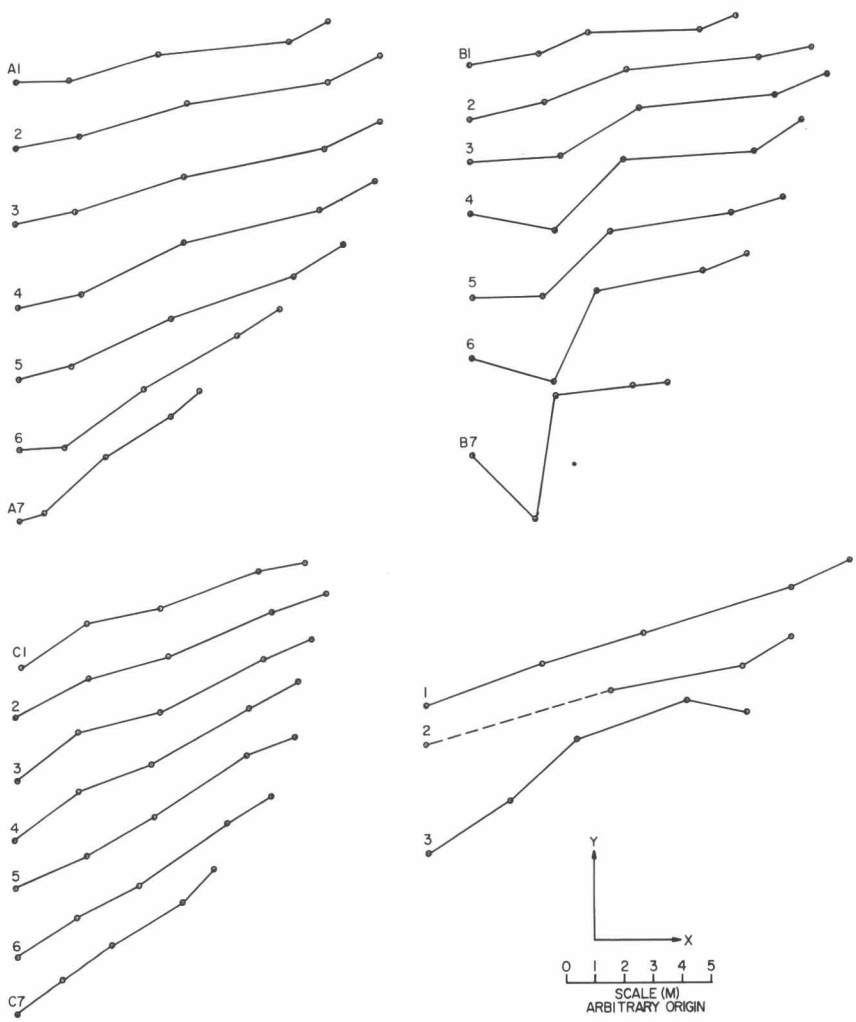

Fig. 5. Positions of markers at each survey and motions between surveys. Approximate time intervals between surveys are 7, 8, 11 and 5 days.

RESULTS

Velocities in the Intervals Between Surveys

Velocities and velocity differences from the season means for the four intervals over which the measurements were made, for the intervals between the first and third survey, the third and fifth survey, and for the season are given in Table 5 with their standard errors and relative errors in percent. These data are also presented as bar graphs in Figure 6.

No systematic pattern of velocity changes emerges from the measurements over the four shortest intervals. The apparent increase in speed in the first half of the season followed by a decrease, indicated by lines A and B, is almost exactly contradicted, period by period (so far as the indications of lines A and B are consistent) in line C.

A more detailed consideration of the results shows that there is an apparent increase in velocity from the first to the second interval for every marker in line A and a corresponding decrease in every case in line C, while line B indicates increasing velocities for three markers and decreasing velocities for two markers. From the second to the third interval there is a decrease in velocity for all but one marker in line A, line B again shows some increases and some decreases, and so does line C, where four markers indicate an increase and three a decrease. All the markers in lines A and B except two (in line A), indicate decreases in velocities from the third to the fourth interval, while all markers in line C indicate an increase. The magnitudes of the velocity differences are generally very similar for all the markers, although a few apparently large differences occur, particularly between the first and second interval in line A.

Another way of looking at these results is to compare the velocities in each time period to the mean seasonal velocity for each marker. This has the advantage that the standard errors of the differences are reduced considerably since the error of the mean velocity is considerably lower than that of a determination over one of the short periods. Comparison to one "standard" is also easier to grasp.

One can summarize the results from this point of view as follows: In line A, velocities appear to be uniformly and considerably higher than the season mean in the second interval and somewhat lower than the mean in the first and fourth intervals. In the third interval, four markers have higher than mean velocities and three have velocities very slightly lower than the season mean.

In line B, the situation is extremely variable and in addition there are no usable data for two markers for the first two intervals. Marker B4 indicates that the velocity was higher than the mean in each interval, an obvious impossibility. For the six remaining markers velocities are higher than the season mean in the third period and lower in the fourth period. Two markers give higher than mean velocities in the first interval and correspondingly lower than mean velocities in the second, while the situation is reversed in the remaining two. Velocities derived from positions determined in the second survey are highly suspect in most of this line, however, unless one postulates some uniquely discontinuous motion for markers B4 to B7. Although these markers straddled a region of incipient transverse crevasses, the opening of which might account for some irregular movement, the fact that all the apparent erratic motions were in the same sense argues against this interpretation because one would expect only the markers on the downglacier side of an opening crevasse to exhibit such motion.

In line C, there is once again a reasonably consistent pattern, with the velocities in the first and fourth intervals usually higher than the mean and those in the second and third intervals usually lower. Markers 1, 2, and 3 do not seem to conform to the patterns of the profiles.

An attempt was made to average out these fluctuations by computing mean velocities for the two halves of the season, that is, for the periods between the first and third and third and fifth surveys. This also eliminated the dubious positions obtained in the second survey and made it possible to take advantage of the higher relative accuracies resulting from the longer time periods.

Again, the results, although generally consistent within each line, are inconsistent among the three lines. The markers in lines A and C (with two exceptions in line C) indicate a decrease in velocity from the first to the second half of the season, while all but one marker in line B indicate an increase. This pattern, incidentally, is also reflected by markers 1, 2, and 3. That is, markers 1 and 3 downglacier from profiles A and C respectively, indicate a decrease in velocity and marker 2 between lines A and B indicates an increase.

Since the lines of markers are only 600 m apart, it is difficult to believe that these differences are real. One would expect that velocity changes, if any, would all be in the same sense, if not necessarily of the same magnitude, over such a limited portion of the glacier.

It is far more likely that these apparent differences result from the errors in the measurements. It has already been indicated that the standard errors of the velocity differences are about as large as the apparent differences, on the average, and in many cases they are several times larger. Furthermore, it must be emphasized that the error given in each case is the standard error; that is, the probability is that 68.3 percent of the results will have errors within this limit, or expressed in another way, one result in every 3.17 will have an error greater than the standard error. Thus, the position in reality is even worse than the numbers would at first lead us to believe. The magnitude of the relative errors then is such as to mask any apparent velocity differences.

An examination of all the velocity differences for each interval also seems to indicate that the distribution of differences is random. There are about the same

TABLE 5. Velocities, Velocity Differences from Season Means and Their Standard Errors.

MARKER	SEASON			INTERVAL 1–2							MARKER	INTERVAL 2–3						
	VEL.	ERROR		VEL.	ERROR		VEL. DIFF.		ERROR OF DIFF.			VEL.	ERROR		VEL. DIFF.		ERROR OF DIFF.	
	(m/yr)	(m/yr)	(%)	(m/yr)	(m/yr)	(%)	(m/yr)	(%)	(m/yr)	(%)		(m/yr)	(m/yr)	(%)	(m/yr)	(%)	(m/yr)	(%)
1	173.2	0.80	0.5	178.9	3.01	1.7	5.7	3.3	3.12	55	1	169.1	4.48	2.7	−4.1	− 2.4	4.56	111
2	146.5	0.65	0.4															
3	134.3	1.00	0.7	141.2	3.76	2.7	6.9	5.1	3.89	56	3	144.9	5.28	3.6	10.6	7.9	5.38	51
A1	137.8	1.34	1.0	129.5	7.57	5.8	−8.3	−6.0	7.70	93	A1	145.8	6.41	4.4	8.0	5.8	6.55	82
A2	162.9	1.01	0.6	158.0	5.69	3.6	−4.9	−3.0	5.79	118	A2	174.3	4.92	2.8	11.4	7.0	5.03	44
A3	164.3	0.87	0.5	150.0	4.88	3.2	−14.3	−8.7	4.96	35	A3	177.5	4.28	2.4	13.2	8.0	4.37	33
A4	163.3	0.78	0.5	152.4	4.39	2.9	−10.9	−6.7	4.47	41	A4	178.5	3.87	2.2	15.2	9.3	3.95	26
A5	152.5	0.79	0.5	136.0	4.50	3.3	−16.5	−10.8	4.57	28	A5	171.1	3.90	2.3	18.6	12.2	3.98	21
A6	128.2	0.99	0.8	111.8	5.66	5.1	−16.4	−12.8	5.74	35	A6	152.3	4.86	3.2	24.1	18.8	4.96	21
A7	96.3	1.39	1.4	66.3	8.04	12.1	−30.0	−31.2	8.16	27	A7	126.8	6.31	5.0	30.0	31.2	6.46	22
B1	110.7	1.49	1.3	125.9	6.51	5.2	15.2	13.7	6.69	44	B1	88.2	8.21	9.3	-22.5	-20.3	8.35	37
B2	142.2	1.24	0.9	136.1	5.42	4.0	− 6.1	−4.3	5.56	91	B2	143.5	6.93	4.8	1.3	0.9	7.06	542
B3	149.7	1.03	0.7	160.0	4.48	2.8	10.3	6.9	4.60	45	B3	149.2	5.65	3.8	− 0.5	− 0.3	5.75	1150
B4	139.8	0.79	0.6	152.8	3.44	2.3	13.0	9.3	3.54	27	B4	156.6	4.39	2.8	− 16.8	12.0	4.47	27
B5	132.7	0.67	0.5	127.0	2.94	2.3	−5.7	−4.3	3.02	53	B5	151.9	3.54	2.3	19.2	14.5	3.60	187
B6	119.9	0.69	0.6								B6							
B7	84.9	0.74	0.9								B7							
C1	124.0	1.00	0.8	143.9	4.45	3.1	19.9	16.0	4.56	23	C1	122.3	5.43	4.4	− 1.7	− 1.4	5.53	326
C2	136.3	1.07	0.8	148.6	4.77	3.2	12.3	9.0	4.90	40	C2	134.9	4.76	3.5	− 1.0	− 1.0	4.88	348
C3	133.6	0.95	0.7	139.3	4.22	3.0	5.7	4.3	4.33	76	C3	138.5	4.58	3.3	4.9	3.7	4.68	96
C4	132.2	0.84	0.6	143.3	3.75	2.6	11.1	0.8	3.84	35	C4	126.2	4.72	3.7	− 6.0	− 4.5	4.80	80
C5	129.2	0.83	0.6	136.9	3.67	2.7	7.7	6.0	3.76	49	C5	125.7	4.13	3.3	− 3.5	− 2.7	4.21	120
C6	122.2	0.77	0.6	129.3	3.38	2.6	7.1	5.8	3.47	49	C6	111.9	4.25	3.8	−10.3	− 8.4	4.33	42
C7	99.2	0.86	0.9	102.8	3.81	3.7	3.6	3.6	3.91	109	C7	96.9	4.68	4.8	− 2.3	− 2.3	4.77	208
								+ 7.0								+10.9		
mean			0.7			3.6		− 9.0		54	mean			3.6		− 4.8		121
maximum										118	maximum							1150
minimum										23	minimum							21
median										45	median							80

Negative differences indicate velocities lower than season means

Negative differences indicate velocities lower than season means

TABLE 5. (Continued) Velocities, Velocity Differences from Season Means and Their Standard Errors

MARKER	INTERVAL 3 – 4							MARKER	INTERVAL 4 – 5						
	VEL. (m/yr)	ERROR (m/yr)	(%)	VEL. DIFF. (m/yr)	(%)	ERROR OF DIFF. (m/yr)	(%)		VEL. (m/yr)	ERROR (m/yr)	(%)	VEL. DIFF. (m/yr)	(%)	ERROR OF DIFF. (m/yr)	(%)
1	177.4	3.20	1.8	4.2	2.4	3.30	79	1	162.1	6.98	4.3	−9.1	−5.2	7.03	79
2	153.5	2.68	1.7	7.0	4.8	2.76	39	2	137.8	5.83	4.2	−8.7	−5.9	5.86	67
3	131.9	3.77	2.9	−2.4	−1.8	3.91	163	3	151.3	8.22	5.4	17.0	12.7	8.29	49
A1	154.5	4.86	3.1	16.7	12.1	5.05	32	A1	106.5	10.29	9.7	−31.3	−22.7	10.38	33
A2	168.1	3.73	2.2	5.2	3.2	3.86	74	A2	143.8	7.90	5.5	−19.1	−11.7	7.97	42
A3	167.9	3.25	1.9	3.6	2.2	3.36	93	A3	153.9	6.89	4.5	−10.4	−6.3	7.00	67
A4	164.6	2.94	1.8	1.3	0.8	3.04	234	A4	154.9	6.24	4.0	−8.4	−5.1	6.30	75
A5	150.2	2.97	2.0	−2.3	−1.5	3.08	134	A5	148.6	6.29	4.2	−3.9	−2.6	6.35	163
A6	124.6	3.70	3.0	−3.6	−2.8	3.84	107	A6	125.6	7.86	6.3	−2.6	−2.0	7.92	305
A7	90.5	4.82	5.3	−5.8	−6.0	5.03	87	A7	94.7	10.23	10.8	−1.6	−1.7	10.33	647
B1	127.3	5.76	4.5	16.6	15.0	5.95	36	B1	96.5	12.69	13.1	−14.2	−12.8	12.79	90
B2	150.8	4.86	3.2	8.6	6.0	5.03	58	B2	134.8	10.69	7.9	−7.4	−5.2	10.76	145
B3	156.5	3.97	2.5	6.8	4.5	4.11	60	B3	139.1	8.73	6.3	−10.6	−7.1	8.80	83
B4	149.1	3.09	2.1	9.1	6.5	3.19	35	B4	142.7	6.81	4.8	2.9	2.1	6.86	236
B5	139.1	2.49	1.8	6.4	4.8	2.58	26	B5	130.7	5.49	4.2	−2.0	−1.5	5.54	278
B6	123.2	2.50	2.0	3.3	2.7	2.60	79	B6	117.4	5.53	4.7	−2.5	−2.1	5.59	223
B7	89.3	2.87	3.2	4.4	5.2	2.96	67	B7	86.9	6.35	7.3	2.0	2.4	6.41	320
C1	118.4	3.77	3.2	−5.6	−4.5	3.90	70	C1	121.4	8.38	6.9	−2.6	−2.1	8.45	326
C2	127.8	3.33	2.6	−8.5	−6.2	3.50	41	C2	143.4	7.40	5.2	7.1	5.2	7.48	106
C3	130.6	3.21	2.5	−3.0	−2.2	3.35	112	C3	133.9	7.13	5.3	0.3	0.2	7.20	2400
C4	128.2	3.31	2.6	−4.0	−3.0	3.42	86	C4	139.6	7.37	5.3	7.4	5.6	7.43	100
C5	126.2	2.90	2.3	−3.0	−2.3	3.02	100	C5	133.3	6.46	4.8	4.1	3.2	6.51	159
C6	122.3	2.99	2.4	0.1	0.1	3.09	3100	C6	129.4	6.66	5.2	7.2	5.9	6.71	93
C7	93.4	3.27	3.5	−5.8	−5.8	3.39	58	C7	113.6	7.31	6.4	14.4	14.5	7.38	51
					+5.1								+5.8		
means			2.7		−3.6		81	means			6.1		−6.3		162
maximum							3100	maximum							2400
minimum							26	minimum							33
median							76	median							103

Negative differences indicate velocities lower than season means

TABLE 5. (Continued) Velocities, Velocity Differences from Season Means, and Their Standard Errors

MARKER	INTERVAL 1 – 3							MARKER	INTERVAL 3 – 5						
	VEL. (m/yr.)	ERROR (m/yr)	(%)	VEL. DIFF. (m/yr)	(%)	ERROR OF DIFF. (m/yr)	(%)		VEL. (m/yr)	ERROR (m/yr)	(%)	VEL. DIFF. (m/yr)	(%)	ERROR OF DIFF. (m/yr)	(%)
1	174.8	1.57	0.9	1.6	0.9	1.76	110	1	172.8	2.14	1.2	−0.5	−0.3	2.29	460
2	146.1	1.28	0.9	−0.4	−0.3	1.44	360	2	148.6	1.83	1.2	2.1	1.4	1.94	92
3	141.9	1.96	1.4	7.6	5.7	2.20	29	3	134.4	2.58	1.9	0.1	0.1	2.76	2800
A1	138.6	2.93	2.1	0.8	0.6	3.22	390	A1	137.9	3.30	2.4	0.1	0.1	3.56	3600
A2	167.7	2.20	1.3	4.8	2.9	2.42	50	A2	159.0	2.52	1.6	−3.9	−2.4	2.72	70
A3	167.0	1.89	1.1	2.8	1.7	2.08	74	A3	163.1	2.20	1.4	−1.3	−0.8	2.37	183
A4	167.5	1.70	1.0	4.2	2.6	1.87	45	A4	160.9	1.99	1.2	−2.4	−1.5	2.14	89
A5	156.1	1.71	1.1	3.6	2.4	1.88	52	A5	149.0	2.02	1.4	−3.5	−2.3	2.17	62
A6	132.6	2.16	1.6	4.4	3.4	2.38	54	A6	125.0	2.52	2.0	−3.2	−2.5	2.71	85
A7	102.6	3.04	3.0	6.3	6.5	3.34	53	A7	92.5	3.26	3.3	−3.8	−3.9	3.54	93
B1	105.0	3.12	3.0	−5.7	−5.1	3.46	61	B1	116.5	3.96	3.4	5.8	5.2	4.74	73
B2	139.4	2.60	1.9	−2.8	−2.0	2.88	103	B2	147.3	3.34	2.3	5.1	3.6	3.57	70
B3	150.4	2.13	1.4	0.7	0.5	2.36	338	B3	149.5	2.72	1.8	−0.2	−0.1	2.91	1500
B4	137.2	1.64	1.2	−2.0	−1.9	1.82	70	B4	143.0	2.13	1.5	3.2	2.3	2.27	71
B5	130.5	1.38	1.1	−2.2	−1.7	1.53	70	B5	137.1	1.70	1.2	4.4	3.3	1.83	42
B6	120.6	1.45	1.2	0.7	0.6	1.61	230	B6	121.0	1.72	1.4	1.1	0.9	1.86	169
B7	86.2	1.56	1.8	1.3	1.5	1.73	133	B7	88.2	1.98	2.2	3.3	3.9	2.12	61
C1	130.0	2.10	1.6	6.0	4.8	2.32	39	C1	119.3	2.60	2.2	−4.7	−3.8	2.78	59
C2	140.2	2.24	1.6	3.9	2.9	2.48	64	C2	133.2	2.29	1.7	−3.1	−2.3	2.53	82
C3	135.1	1.98	1.5	1.5	1.1	2.20	147	C3	131.8	2.22	1.7	−1.8	−1.3	2.40	133
C4	132.2	1.76	1.3	0	0	1.95	∞	C4	131.9	2.29	1.7	−0.3	−0.2	2.44	810
C5	129.3	1.73	1.3	0.1	0.1	1.92	1900	C5	128.0	2.00	1.6	−1.2	−0.9	2.16	180
C6	119.2	1.58	1.3	−3.0	−2.5	1.76	59	C6	125.0	2.07	1.7	2.8	2.3	2.21	79
C7	98.6	1.81	1.8	−0.6	−0.6	2.00	333	C7	102.3	2.25	2.2	3.1	3.1	2.41	78
					+ 2.4		130						+ 2.4		145
means			1.5		−2.0			means			1.8		−1.7		
maximum							∞	maximum							3600
minimum							29	minimum							42
median							72	median							87

Negative differences indicate velocities lower than season means

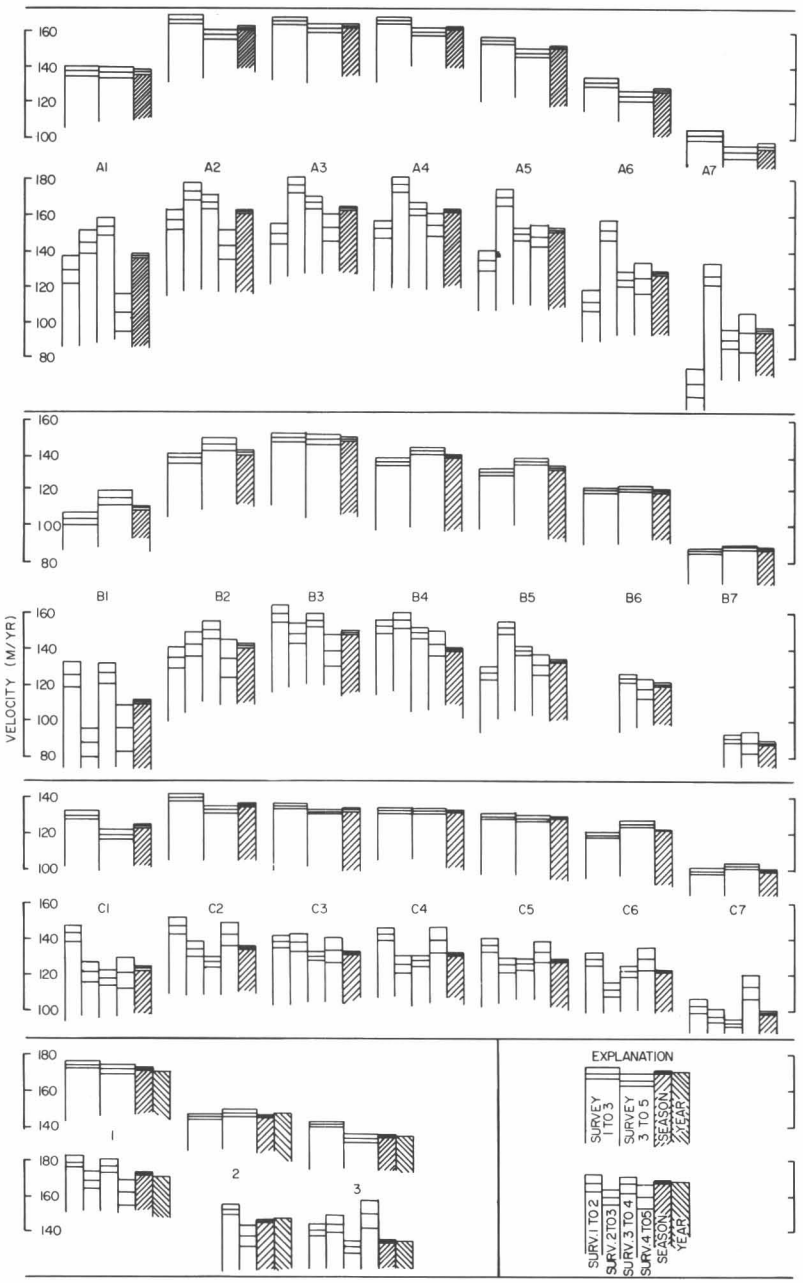

Fig. 6. Velocities and their standard errors. Lower set of bars for each row of markers represents results for four short time periods, upper set for two half-season periods. Highest and lowest line on each bar represent standard error.

number of positive and negative differences from the mean seasonal velocity in each interval, and, as can readily be seen from Figure 7, the frequency distribution of the velocity differences, expressed as percentages of the mean seasonal velocity, is nearly a textbook example of a random distribution. This holds both for the four short intervals and for the two half-season intervals (Table 6).

Even if the error estimates given above are unduly pessimistic, which is unlikely, and we assume that the velocity differences are real, it is clear that velocity differences from the seasonal mean are relatively small. In the four short intervals 80% of the differences are smaller than 10% of the mean seasonal velocity. In the two half-season periods, 90% of the differences are smaller than 4% of the mean seasonal velocity.

Seasonal Velocities

Mean velocities for the season (July 12 to August 14, 1964) have been determined with standard errors which range from 0.4% to 1.4%, the mean error being 0.7% (Table 5). The results are presented as contours of constant velocity over the survey area (Figure 8) and as velocity profiles along lines A, B and C (Figure 9). There

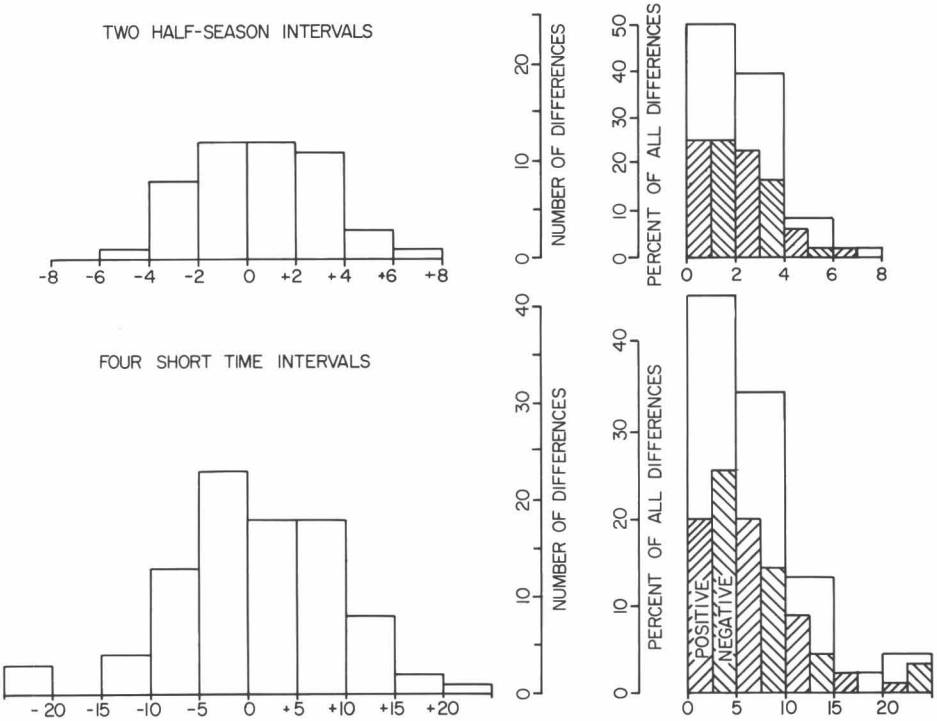

Fig. 7. Frequency distribution of velocity differences. Horizontal scales in percent of difference from seasonal mean velocities. Positive and negative differences are shown separately on left, all differences are shown together on right. Vertical scales apply to both.

TABLE 6. Frequency Distribution of Velocity Differences

Class Interval (% Diff.)	Positive Differences (No.)	Positive Differences (% of Total)	Negative Differences (No.)	Negative Differences (% of Total)	All Differences (No.)	All Differences (% of Total)
Four Short Periods						
0-5	18	20.0	23	25.6	41	45.6
5-10	18	20.0	13	14.5	31	34.5
10-15	8	8.9	4	4.4	12	13.3
15-20	2	2.2	0	0	2	2.2
>20	1	1.1	3	3.3	4	4.4
TOTALS	47	52.2	43	47.8	90	100.0
Two Half-Season Periods						
0-2	12	25.0	12	25.0	24	50.0
2-4	11	22.9	8	16.7	19	39.6
4-6	3	6.2	1	2.1	4	8.3
6-8	1	2.1	0	0.0	1	2.1
TOTALS	27	56.2	21	43.8	48	100.0

is a gratifying lack of anomalies in both presentations. This, together with the reasonably small standard errors, suggests that the seasonal values are quite reliable.

There is a significant velocity increase downglacier and the "dynamic" centerline, that is, the line of greatest velocity, is displaced about 200 m to the true left of the "geographic" centerline (Holdsworth, 1965, and pp. 109 – 125 of this volume).

The velocity profiles have the expected typically parabolic shape. There is a markedly smaller increase in velocity toward the centerline in profile C than in the other two profiles. This may perhaps be due to the slight narrowing of the glacier between lines C and B which may be causing the central portion of the glacier to speed up in this region.

The configuration of the flow-line field in the area has been delineated by Holdsworth (1965) from the seasonal directions of motion (Figure 10). Errors in the individual directions of motion have not been calculated since the values do not need to be known very precisely. Based on an average displacement of about 11 m and the corresponding position errors perpendicular to the direction of motion, the directions have standard errors of 1° to 1.5°.

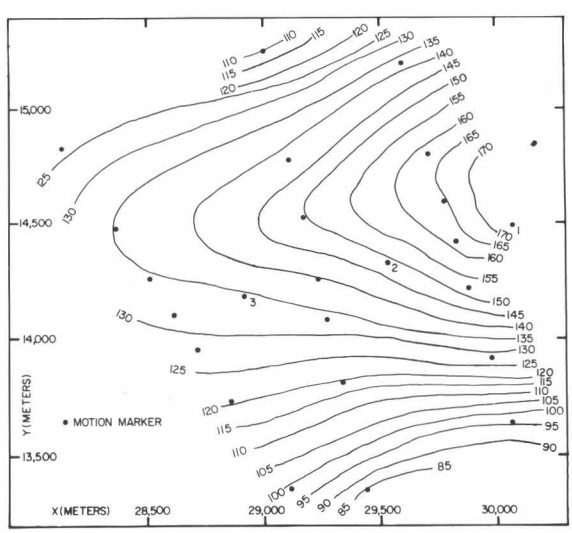

Fig. 8. Contours of seasonal velocity. Velocity in meters per year.

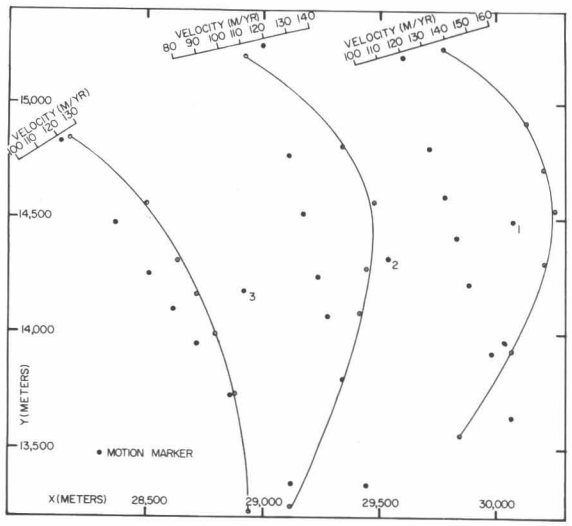

Fig. 9. Seasonal velocity profiles.

Comparison of Summer and Annual Velocities

It is of some interest to compare the summer 1964 velocities with the summer 1963 (June 30 to August 11) values and with the annual velocities for the year 1963-64. Unfortunately the comparison can be made on only three markers, 1, 2, and 3, since the other stakes in the present work were not available before the 1964 season. The positions on June 30 and August 11, 1963 are given by Sharni (1963) with estimated standard errors of ± 30 cm in coordinates.

Since the stakes moved an appreciable amount (about 150 m) in the one-year interval and are thus located in a faster portion of the velocity field in 1964 than they were in 1963, it is meaningless to compare the two velocities directly. What is desired is a comparison of the velocities at a given point in relation to the glacier's surroundings. To accomplish this a velocity was read from the 1964 velocity contour map at the mean location of the marker for the interval for which its velocity was desired. It is estimated that this can be done with a precision of ± 0.5 m per year. The differences from the summer 1964 rates and their standard errors were computed and are summarized in Table 7.

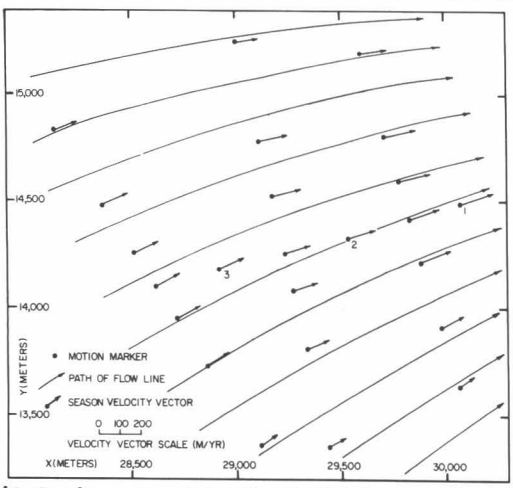

Fig. 10. Configuration of flow-line field (after Holdsworth, 1965, Fig. 7).

Although the errors in the differences are once again rather large, they are at least not so large as to obscure the results entirely. Sharni's error estimates may well be too pessimistic; it is likely that his results are as good as those of the present survey. On the other hand, Sharni determined the marker positions from fixed points which are not specified but could not have included S and T. Some errors due to the errors in the relative positions of the different fixed points are therefore present in the comparison of the 1963 and 1964 positions, but these should be considerably smaller than the other errors in the position determinations.

The results for both comparisons are quite consistent within themselves and appear to be real. It is interesting and somewhat unexpected to find that the velocities in summer 1963 are smaller than in 1964. The mean annual velocities appear to be very slightly larger. Although the differences between the annual and summer 1964 velocities are very small, their consistency makes it very unlikely that they are the results of random errors of measurement. In any case, it appears that if there are any variations in velocity with time on the upper Kaskawulsh Glacier, they are quite small.

Vertical Motion and Ablation

Table 8 is a summary of the results of the vertical motion and ablation measurements. The vertical motion is generally downward, the gradient being about five times as large as the surface slope. That is, there is down-

TABLE 7. Comparison of Summer and Annual Velocities

Marker	Summer 1963 Velocity (m/yr)	Summer 1964 Velocity at same point (m/yr)	Difference (m/yr)	Difference (%)	Relative Error of Difference (%)
SUMMER 1963 AND SUMMER 1964					
1	158.2	165	−6.8	−4.1	55
2	135.6	143	−7.4	−5.2	50
3	125.2	132	−6.8	−5.2	56
YEAR 1963–64 AND SUMMER 1964					
	Year 1963-64 Velocity (m/yr)				
1	171.7	169	+3.2	+1.6	37
2	148.2	145	+3.2	+2.2	40
3	135.1	133	+2.1	+1.6	73

ward motion of the ice particles, as is to be expected above the firn line. The values are large enough in most cases to be significantly greater than the errors in their determination and thus appear to be real. The errors in the differences are such that the difference in the average rate from the first to the second interval is not significant while the difference between the second and third interval appears to be real.

Mean ablation values indicate considerable differences among the intervals. The differences are about twice as large as the errors of the measurements. Because no systematic pattern of vertical velocity fluctuations was detected, no relationship between ablation and velocity can be inferred.

Concluding Remarks

Lliboutry (1965, pp. 624-28) gives a brief summary of the results of various studies on glacier velocity variations. The evidence seems rather conflicting. Numerous workers have found the summer velocity higher than the mean annual velocity in the ablation area and the winter velocity higher than the annual in the accumulation area. The differences amount to 10% to 15%. On the other hand, Lliboutry cites some unpublished results of Elliston which indicate that there is no velocity increase in the winter on the upper portion of the Gorner Glacier while the expected summertime increase is present on its lower portion. He gives the results of several investigations which indicate erratic fluctuations in velocity and others which indicate perfectly regular movement.

Studies which have shown considerable velocity variations over periods of several days, such as those of Finsterwalder (1937), Meier (1960), Friese-Greene and Pert (1965) and Paterson (1961, 1964), have been carried out in the ablation zones of glaciers. In some of the studies strong correlation with ablation and runoff of melt-water is reported, leading to conjectures that the variations are related to varying degrees of "lubrication" of the glacier bed. Since the present study was carried out in an area which is well above the firn line, it is perhaps not surprising that no significant velocity variations were detected.

TABLE 8. Vertical Motion and Ablation (cm/day)

Marker	Interval 1-2		Interval 2-3		Interval 3-4		Means	
	Vertical Motion	Ablation	Vertical Motion	Ablation	Vertical Motion	Ablation	Vertical Motion	Ablation
1	1.3	1.1	2.2	1.3	−.5	.9	1.3	1.1
2		1.3		1.5	.3	1.4	.3	1.4
3	1.2	.8	2.3	1.0	.8	1.6	1.4	1.1
A1	.4	2.4	1.8	.7	−.1	.7	.7	1.3
A2	.2	2.2	2.6	.6	0	.7	.9	1.2
A3	−.6	2.2	2.3	.7	.4	.8	.7	1.2
A4	0	2.3	2.3	.4	.3	.4	.9	1.0
A5	0	1.4	2.3	.6	−.1	.8	.7	0.9
A6	1.6	1.4	3.4	.5	−.9	.7	1.4	0.9
A7	1.0	1.4	1.6	.5	−.7	.6	.6	0.8
B1	1.0	2.3	0	−.1	1.2	.9	.7	1.0
B2	1.7	1.4	1.5	0	1.6	.7	1.6	0.7
B3			.9	0	1.4	1.2	1.2	0.6
B4	1.3	1.0	2.0	−.8	2.2	.7	1.8	0.3
B5	.3	1.0	2.3	.1	1.1	.9	1.2	0.7
B6	4.3	1.4	2.7	−.3	.4	.9	3.8	0.7
B7	.7	1.3	2.2	−.3	1.3	.9	1.4	0.6
C1								
C2	4.2	.4	1.3	−.3			2.8	
C3	4.1	.9	2.0	.3	1.8	.3	2.6	0.5
C4	−4.3	.7	8.6	.3	1.9	.4	2.1	0.5
C5	4.3	1.4	2.8	−.1	1.3	−.2	2.8	0.4
C6	2.6	.9	1.7	.4	1.8	.4	2.0	0.6
C7	1.0	.6	3.6	.4			2.3	0.5
means	1.5	1.4	2.1	0.3	0.7	0.8	1.6	0.8
	=5.5 m/yr		=7.7 m/yr		=2.6 m/yr		=5.8 m/yr	

Negative values indicate upward motion
Blanks indicate no data

ACKNOWLEDGMENTS

It is a pleasure to express my thanks to all who have helped and encouraged me to bring this effort to a satisfactory conclusion.

Thanks are due to Dr. Walter A. Wood and Mr. Richard H. Ragle for valuable discussions and for furnishing some unpublished data. The surveying program could not have been carried out without Mr. Gerald Holdsworth and Mr. Fred W. Erdmann, who willingly took time from their own work to assist me.

I wish to acknowledge the help and guidance of Dr. Simo H. Laurila, my adviser during most of my graduate work. Mr. Solomon Cushman has made valuable suggestions on several points. Dr. Urho A. Uotila, who interited the supervision of my thesis in its final stages, has been most generous with his time and assistance.

REFERENCES

Ackerl, F. (1965) Der Einfluss fehlerhafter Festpunkte auf trigonometrisch abgeleitete Neupunkte, Z. Vermessungs., 90, 279-283.

Clark, D. (1951) Plane and Geodetic Surveying, Vol. 2, 4. ed., Constable, London, 582 pp.

Finsterwalder, R. (1937) Die Gletscher des Nanga Parbat, Z. Gletscherkunde, 25, 57-108.

Friese-Greene, T. W., and Pert, G. J. (1965) Velocity fluctuations of the Bersaekerbrae, East Greenland, J. Glaciol., 5, 739-747.

Holdsworth, G. (1965) An examination and analysis of the formation of transverse crevasses, Kaskawulsh Glacier, Yukon Territory, Canada, Inst. of Polar Studies, Rept. No. 16, The Ohio State Univ., Columbus, 90 pp.

Lliboutry, L. (1965) Traite de Glaciologie, Vol. 2, Masson, Paris, 1040 pp.

Meier, M. F. (1960) Mode of flow of Saskatchewan Glacier, Alberta, Canada, U.S. Geol. Surv. Prof. Paper 351, 70 pp.

Paterson, W. S. B. (1961) Movement of the Sefstrøms Gletscher, northeast Greenland, J. Glaciol., 3, 845-849.

Paterson, W. S. B. (1964) Variations in velocity of Athabasca Glacier with time, J. Glaciol., 5, 277-285.

Sharni, D. (1963) Survey Report, Icefield Ranges Res. Proj., unpublished, 28 pp.

Wood, W. A. (1963) The Icefield Ranges Research Project, Geogr. Rev., 53, 163-184.

Moulins on Kaskawulsh Glacier*

G. Dewart†

In the course of geophysical and glaciological work on Kaskawulsh Glacier (Fig. 1), Yukon Territory, in August 1965, several moulins were examined by the writer and his colleagues on the Icefield Ranges Research Project. The moulins were located near the confluence of the central and north arms of the glacier, about 8 km below the firn line and 40 km from the terminus. The elevation here is approximately 1,750 m, and seismic soundings indicate that the ice is about 500 m thick.

The surface drainage in this area changes significantly from year to year. In the summer of 1964, several square kilometers of glacier surface were drained by two large moulins on either side of the medial moraine a few hundred meters down-stream from the confluence. In 1965 these holes were plugged by snow and the two old basins were combined in a trans-morainal system ending in a 10-m deep gorge which was cut between May and August 1965, and emptied into another moulin. The latter had been small and had drained only a part of the medial moraine the previous year.

Near the main moulin there is a series of smaller ones associated with the closing crevasses of an ice fall about 1 km up-glacier on the central arm. They show a relationship to the crevasses quite like that described by Streiff-Becker (1951). Some of the down-glacier apertures were relatively dry and invited exploration (Fig. 2).

Most of the moulins started as nearly vertical shafts but they changed direction and contained more or less prominent ledges at depth. The largest inactive one found was about 2 m in diameter and dropped vertically for at least 60 m. More typically the moulins were rather tortuous. A manhole-sized shaft that was investigated in some detail dropped at a steep angle for about 6 m to a small ledge. From here a tight corkscrew passage led about the same distance into a large vertical shaft which dropped to a ledge about 20 m below the surface (this was at the limit of perceptible surface light). The floor was about 2 m long, elongated in the direction of the crevasses and contained a plunge pool. The pool was rimmed by blue ice; the surrounding ice was generally bubbly. At the end of this ledge the passage dropped nearly vertically at least another 10 m, where a waterfall entered from the wall and precluded further exploration. Here the shaft was getting larger and receiving many tributary tunnels.

The moulins were found useful as ready-made seismic shot holes. Time did not permit a thorough study of them or their part in the internal hydraulics of the glacier. The party received a strong impression that the "free ground-water system" discussed by Mathews (1964) is very deep in a glacier the size of Kaskawulsh Glacier. A particularly interesting problem here is the relation of this system to the large evanescent lakes that border the glacier.

The writer believes that with the proper equipment, including water-tight suits, extensive subsurface exploration is feasible.

*This note has previously appeared as a letter to the Editor in the *Journal of Glaciology,* 1966, Vol. 6, pp. 320-321, and is reproduced here with permission.

†Institute of Polar Studies, The Ohio State University, Columbus.

References

Mathews, W. H. (1964) Water pressure under a glacier, *J. Glaciol., 5,* 235-240.

Streiff-Becker, R. (1951) Pot-holes and glacier mills, *J. Glaciol., 1,* 488-490.

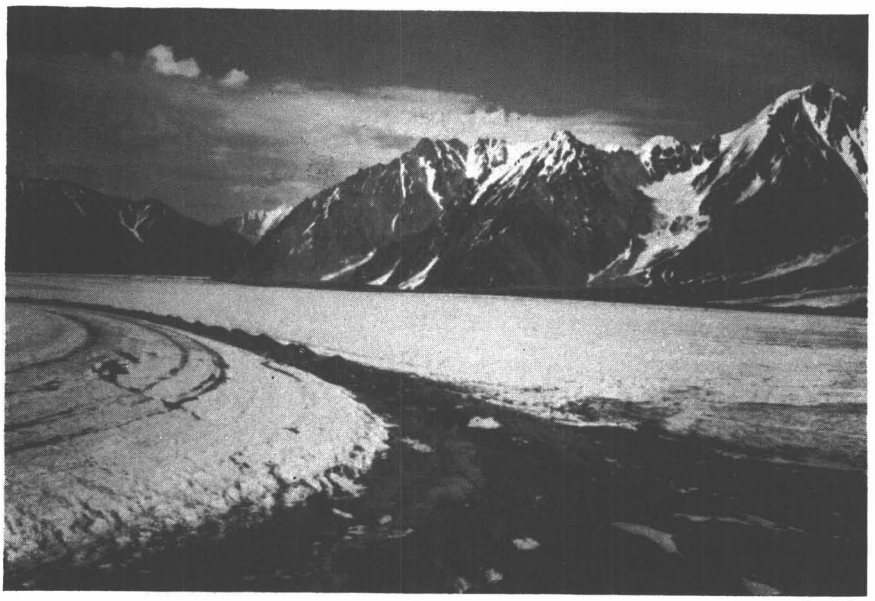

Fig. 1. Confluence area of Kaskawulsh Glacier in July 1965. The central arm is to the right, the north arm to the left.

Fig. 2. An investigator entering a dry moulin on the central arm of Kaskawulsh Glacier.

Water-Spout on Kaskawulsh Glacier*

K. Ewing†, *S. Loomis*†, *and R. Lougeay*†

While conducting field research on Kaskawulsh Glacier, Yukon Territory, Canada, an unusual phenomenon was observed which in this instance related to moulin formation. Thirty meters from the writers' position, at about 11:00 hr. on June 30, 1966, a vertical spout of water suddenly rose from the glacier surface. This was the same area where Dewart (1966) observed several moulins.

The spout of water lasted 7 – 10 sec and reached a maximum height of 4 – 5 m. The only sound noted to accompany the phenomenon was the noise of rushing water; there was no sharp sound of fracturing ice. Immediate investigation of the site revealed that the water had issued from a vertical fissure 7 – 8 cm wide and orientated perpendicular to glacier flow (Figure 1).

The site, which at this time of year was in the vicinity of the snow line, was covered with crusted snow to a depth of 15 – 20 cm. The glacier ice at the fissure itself, however, was blown and washed bare for a distance of more than 1 m along the length of the fissure and 25 cm on either side. This rectangular pattern of snow-free ice, along with the splatter pattern left by the falling water in the snow, suggests that in cross-section the fountain of water was tabular rather than columnar.

Water from surrounding slush areas began to flow into the fissure almost immediately. Within 2 days it was apparent that a distinct circular moulin was developing (Figure 2). By July 9, the original ice fissure had closed, leaving only a circular hole approximately 0.5 m in diameter (Figure 3). This opening was not only being maintained, but also enlarged, by two tributary streams diametrically entering it. Final observations on August 2 revealed that the moulin had a diameter of approximately 1.25 m and the two entering streams had entrenched approximately 1 m into the lip of the moulin (Figure 4). Throughout the observation period there was no evidence suggesting recurrence of spouting action.

An aspect of this moulin, not observed in others of the immediate area, was an irregular pulsation of air from the mouth carrying aloft a fine spray of water. This discharge of air from the moulin was first observed on July 15 and continued to the end of the observation period.

*This note has previously appeared as a letter to the Editor in the Journal of Glaciology, 1967, Vol. 6, pp. 956 – 958, and is reproduced here with permission.

†Department of Geography, University of Michigan, Ann Arbor

Reference

Dewart, G. (1966) Moulins on Kaskawulsh Glacier, Yukon Territory, J. GLACIOL., 6, 320 – 321 (Also p. 145, this volume).

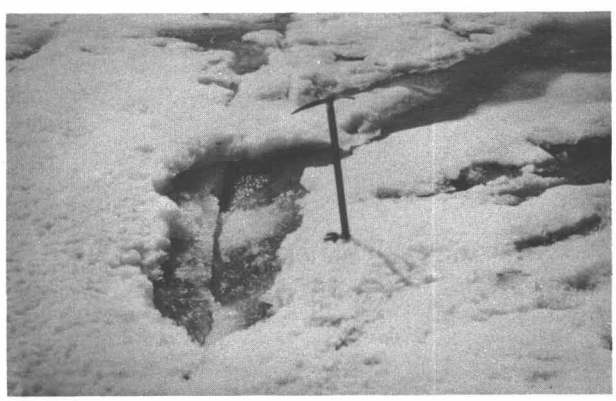

Fig. 1. Site of the water-spout, central arm of Kaskawulsh Glacier, looking south; June 30, 1966.

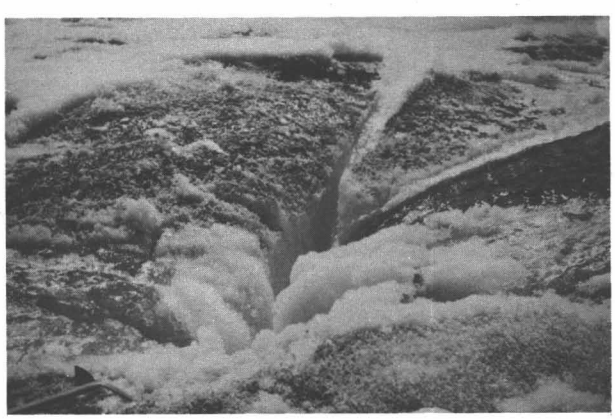

Fig. 2. Developing moulin at the site of the water-spout, looking south-southeast; July 2, 1966.

Fig. 3. Moulin at the site of the water-spout with two tributary melt-water streams, looking west up-glacier (ice-axe at right for scale); July 9, 1966.

Fig. 4. The two streams shown in Figure 3 entrenched into the lip of the enlarged moulin, looking west; August 2, 1966.

Kluane Lake: Its Drainage and Allied Problems*

H. S. Bostock

ABSTRACT. Changes of level of Kluane Lake suggest that the lake has not always drained through the Kluane River as it does today but has, during the Hypsithermal, drained through the Slims River valley into the Kaskawulsh River. This drainage theory was first published by the writer in 1952 and the present paper includes data which have become available since that time. Features of change of level as well as possibilities of drainage reversal are here discussed and it remains the writer's conclusion that the drainage changes suggested in his original paper did indeed occur.

INTRODUCTION

Kluane Lake, which lies in the Shakwak Trench in southwestern Yukon Territory (Figure 1), presents to the researcher a wealth of problems in regard to its origin and history. The Slims River, which flows from the western edge of the Kaskawulsh Glacier terminus, is the main source of its water. On leaving Kluane Lake, the water has to travel about 1400 mi. by the Kluane – Yukon river system to the Bering Sea. In contrast, waters from the eastern part of the Kaskawulsh Glacier terminus drain through the Kaskawulsh River to reach the sea in the Gulf of Alaska by way of the Alsek River, about one-tenth of the distance of the Kluane River passage. The main problem discussed in this paper is whether Kluane Lake has always drained as it does today or whether, after the last major Pleistocene advance – called by Denton and Stuiver (1966 and pp. 173–186 of this volume) the Kluane glaciation – it drained to the Gulf of Alaska through the valleys of the Slims, Kaskawulsh, and Alsek Rivers. Such a course, if formerly open, would have been blocked by the advance of the Kaskawulsh Glacier during the Neoglacial interval, at which time the present drainage via the Kluane River was probably established.

Various features around Kluane Lake suggest that the lake has undergone significant changes in level since the retreat of the Kluane ice and that its outlet by way of the Kluane River is very recent. Some of these features were outlined by the writer in 1952 in a report based on his field work in 1945 (Bostock, 1952, pp. 6 – 8), and the theory that the drainage of the lake has changed from the Kaskawulsh River to the Kluane River was first put forward there.

Since then, new aerial photographs of the area have been produced, and new topographic and other mapping has been done. Considerable research in allied scientific disciplines has also been carried out, and a number of papers that bear on the problems of the Kluane Lake drainage have been published. In view of the suggestion by Raup (Johnson and Raup, 1964, p. 27) that the history of Kluane Lake as outlined in the original paper of 1952 should be modified, the writer has considered these sources of new data. Further, he revisited the area in 1966 and, in addition to certain examinations on the ground, made aerial observations of the lake, the glacier terminus, and the rivers involved in the drainage pattern. Examination of all these sources tends to support his original theory of the changes in the drainage pattern of Kluane Lake.

*This report is already in press as Geological Survey of Canada PAPER NO. 69-28 and is reprinted here with permission.

OUTLINE OF FIELD OBSERVATIONS

Previously Presented Data

The following points summarize the relevant information that has already been presented in the 1952 report:

(1) The modern beaches indicate lake level fluctuations of from 10 to 12 ft. during recent decades (Bostock, 1952, p. 6).
(2) Much greater variations are indicated by the raised beaches, the creek estuaries, notably those of Gladstone and Christmas Creeks, and the presence of stumps of drowned forest in the shallow parts of the lake (Bostock, 1952, pp. 6 – 7). All these indicate levels either higher or lower than the present one.
(3) As the glacier recedes, the steeper gradient of the Kaskawulsh River and the lower level of its head is resulting in its capturing waters from the Slims River. If this process continues, the result could be the complete capture of the Slims River, and possibly Kluane Lake itself, by the Kaskawulsh River.

New and Amended Data

The following summarizes new and amended data:

Lake level. The level of Kluane Lake as measured by the Geodetic Survey of Canada (Canada, Dept. of Mines and Technical Surveys, Datum Publication 24-B, 1960) is 2563 ft. above sea level – 38 ft. higher than the level accepted at the time the writer carried out his original

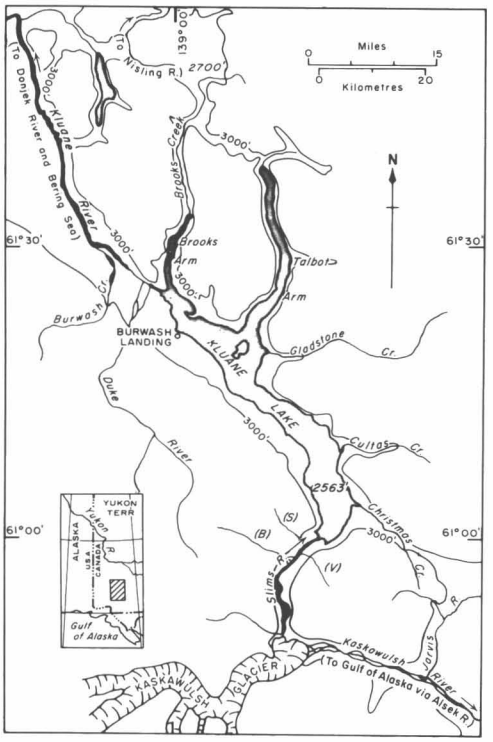

Fig. 1. Drainage routes in the area of Kluane Lake.

field work. This new level was confirmed as being roughly accurate for the summer of 1966 at which time it was measured by the gauge of the Water Resources Branch, Dept. of Energy, Mines and Resources (M. E. Alford, personal communication, 1967). It has been accepted as being roughly accurate for the summer of 1945 also.

Raised beaches. The observed locations of raised beaches around the lake are shown on Figure 2. Those originally recognized by the writer in 1945 – two distinct beaches or wave-cut terraces, one 3 ft. above the other – are located on the steep hillside about one-half mile west of Striation Point. The highest one lies 30 ft. above the present normal lake level. Aerial reconnaissance in 1966 revealed widely scattered beaches at this same elevation, especially on the northeast shores of the lake between Long Point and the abandoned site of the old settlement of Kluane where these raised beaches are particularly well developed.

The beach locality west of Striation Point was the only one closely examined. No excavations were made, but there was no indication that volcanic ash, so widespread in this area (Bostock, 1952, pp. 36 – 38) is associated with these beaches. If this is correct, it would suggest that the ash was removed during the formation of the beaches and that they must therefore be younger than 1425± 50 years B. P. – the indicated time of the ash fall (Stuiver, Borns and Denton, 1964, and pp. 219–220 of this volume).

The slope cut above the beaches in their development is steeper and less clothed with vegetation than the hillsides formed above it since Kluane glaciation. Below them, large spruce trees grow down to the present shoreline. At present, the beaches are protected from wave erosion by their elevation above the lake, but at the time they were formed, the high level of the lake exposed their localities to wave action and, in view of their unconsolidated material, these beaches could have developed quickly.

The existence of the raised beaches has been questioned by Raup (Johnson and Raup, 1964, p. 23) because, along the shores of Kluane Lake where he made his observations, he did not recognize them, and because he believed that the fine textured silts present on much of the low ground on the southwest side of the lake would have been removed in the formation of such beaches and the accompanying flooding. As the writer indicates, the duration of this high water stage was probably very brief.

Creek estuaries. As already stated in the 1952 report, estuaries, or drowned creek valleys, occur at several places around the lake and are evidence of earlier, lower, water levels. The most prominent estuaries are those of Gladstone and Christmas Creeks, the former being the larger (Bostock, 1952, p. 6). Soundings in the inner[1] part of the estuary showed that it was more than 20 ft. deep, but the gradient of the creek and length of the estuary suggest that its outer end is 40 or more feet deep and that the earlier level of the lake was at least as many feet below the present level. Gladstone Creek has cut a deep broad valley through surficial deposits for some miles above the estuary, and material from these deposits must have been built into a large delta beyond the estuary. The same features are common to Christmas Creek, a markedly underfit stream that occupies a major meltwater channel incised to about the 3050-ft. level into the divide separating the Jarvis River drainage from that of Kluane Lake. Glacial Lake Kloo (Kindle, 1953, p. 17) may have used this channel as an outlet, a fact which, if correct, would suggest that the estuary of Christmas Creek began to be cut at the end of the Kluane glaciation, about 12,500 to 9800 B. P.

[1]Due to an unfortunate transposition of phrases, the opposite meaning is conveyed in the 1952 report (p. 7). That sentence should read:

> "The *inner* part of the estuary was observed to be more than 20 feet deep. The creek gradient and length of the estuary suggest that it is 40 feet or more deep *in the outer part,* and that the former level of the lake was at least that much below the present level."

The words in italics represent the correction of the original statement.

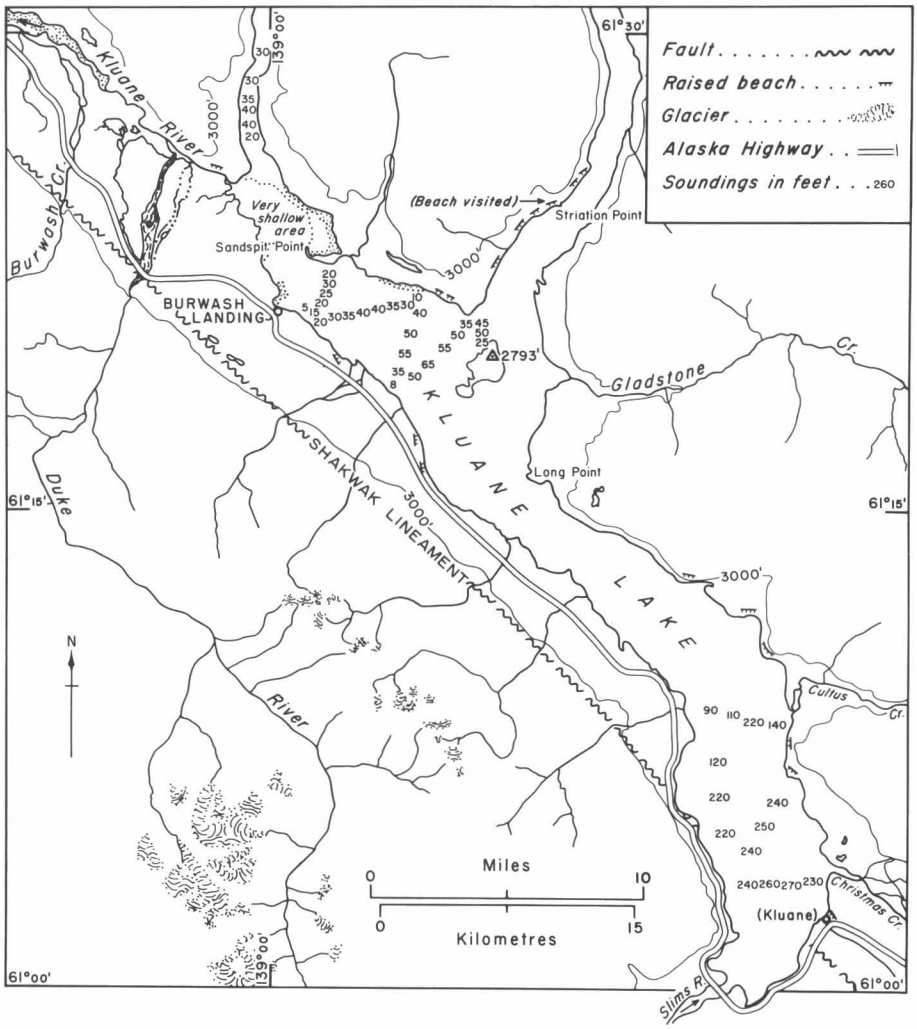

Fig. 2. Kluane Lake, showing water depths and the locations of raised beaches and of the Shakwak Lineament.

Lake depths. Lake soundings taken by the writer's party in 1945 are shown in Figure 2. The few soundings taken in the shallow areas west of Sandspit Point indicate depths of less than 20 ft. and are not shown. Most of the bottom in this shallow area at the northwest end of the lake can be clearly seen in the aerial photographs taken in 1950 at 10,300 ft. They can still be seen vaguely in the 1957 photographs taken at 35,000 ft. which, because they give a panoramic view of the whole outlet area, were selected for Figure 3. There is a channel close to the shore (Figure 6) leading into the Kluane River, but nothing suggests that it is more than 10 to 15 ft. deep. It is certainly not 40 ft. deep and therefore could not have served as an outlet during the lowest stage of Kluane Lake. Near the northeast shore there is also another creek channel leading southeast from Brooks Arm, but it is now blocked by Sandspit Point.

Drowned forest. Under suitable light conditions, stumps of a drowned forest are visible beneath the water in places west of Sandspit Point in the shallow areas at depths to at least 10 ft. Soft, stained, porous wood forms the bulk of the driftwood along the northeastern shore. In many places around the shore, stumps still project above the water (Figure 4).

Stumps of the drowned forest are common in Christmas Bay where, in 1967, wood from a spruce stump was collected for age determinations (GSC-867, collected by J. Look and R. Klaubert for O. L. Hughes). This sample was partly imbedded in beach gravel 6 ft. below the present normal high water level, on the south side of Christmas Bay (36° 03.5' N, 122° 56' W). The stump was excavated to a depth of 18 in. below the gravel surface and was then sawed off. The depth to the base of the stump below the original surface of the gravel is not known but is probably less than 5 ft. The age of this stump, as determined by radiocarbon dating, is 340 ± 130 years B. P. Such features indicate how recent has been the rise of the lake to its present level.

Fig. 3. The northwest end of Kluane Lake. This stereoscopic pair of vertical photographs shows the Kluane River outlet, the coastal channel leading to it, the broad areas of shallow water offshore and, in the right-hand photograph, the tip of Sandspit Point. The Burwash Landing airstrip and the Alaska Highway are seen near the bottom of the photographs. The tip of the Duke Meadows fan appears near the outer edge of the left-hand photograph. Also evident are the northwest-southeast trend characteristic of the surrounding topography and the northeast-trending valleys of the seasonal streams. (Photos: courtesy *Canadian National Air Photographic Library*, Nos. A 15739-53 and 54)

Fig. 4. Kluane Lake, looking east to Striation Point. In the foreground, stumps of drowned forest rise above the water.

OUTLET POSSIBILITIES

In searching for Kluane Lake outlets other than the Kluane River, there are three possibilities within the range of levels dealt with here, that is, roughly between 2500 ft. and 2600 ft. elevation:

(1) the valley system connecting the two northern arms of Kluane Lake to the Nisling and Donjek drainage systems

(2) the Slims River – Kaskawulsh River system which was discussed in the 1952 report.

(3) in the northwest, the wide floor of the Shakwak Trench south of the Kluane River.

The first of these may be eliminated since topographic maps show the divides on these valley floors all lie above the 2700-ft. contour.

Slims – Kaskawulsh Outlet

The junction of the Slims and Kaskawulsh valleys, here referred to as the "valley fork", lies about 15 mi. south of the Kluane Lake (Figure 1) and is dammed by the Kaskawulsh Glacier, whose neoglacial terminal moraines and outwash curve around a drift and bedrock knoll that stands well out in the valley, separated from the mountains to the northeast by an outwash-filled gap about one-third of a mile wide (Figure 5). This knoll projects about 400 ft. above the outwash in the gap whose surface slopes down from the Kaskawulsh lobe of the glacier to the Slims River, from 2682 ft. to 2654 ft. above sea level. The waters of the Slims River issue in several headstreams from the western part of the glacier. The most easterly of these streams pierces the outermost moraine at an elevation 75 ft. above the level of Kluane Lake (R. K. Fahnestock, personal communication). In 1966 the writer measured, by barometer, the difference in level between the outwash surface adjacent to the head of the "eastern" branch of the Slims River, about one-quarter of a mile north of the knoll, and the outwash surface on the Kaskawulsh River side close to the knoll, at the northeast front of the ice. The outwash surface of the Slims River, given by Fahnestock as about 2660 ft. (personal communication) was 90 ft. higher than the outwash surface of the Kaskawulsh River. Farther out in the Kaskawulsh Valley, other headstreams of the river are reported to be more than 100 ft. below the Slims River head (S. G. Collins, personal communication). It is mainly the glacier ice that prevents the Kaskawulsh River from capturing the Slims River. Indeed, in 1967, the Kaskawulsh River was reported to be receiving subglacially a good deal of water which in previous years had flowed into the Slims River (O. L. Hughes and J. P. Johnson, personal communication). These elevations show that the head of the Kaskawulsh River is close to the level of Kluane Lake.

Topography suggests that the knoll in the valley fork was formerly part of the mountain slope to the northeast and that some stream or glacial diversion led to the cutting of the gap. This gap has been used and filled with outwash by meltwater flowing into the Slims River from the Kaskawulsh lobe of the glacier during the recent Neoglacial advance (Borns and Goldthwait,

1966, Figure 4; R. K. Fahnestock, personal communication). Though now filled, the gap would be large enough to contain a buried bedrock canyon sufficiently deep to carry water through at the Kluane Lake level. The existence of such a canyon could be proved by seismographic sounding but the author knows of no such soundings at present.

Some seismographic work has been done in the last few summers by Collins, Fahnestock and Goldthwait (personal communication) on the Kaskawulsh Glacier itself and in the Slims Valley up to a mile north of the glacier. This work indicates that the depth to bedrock in the Slims Valley to this point, as well as under the glacier, is well below the level of Kluane Lake and would permit a stream 40 ft. or more lower than the present lake to flow around the valley fork into the Kaskawulsh Valley.

Denton and Stuiver (1966, p. 581) have shown that the Kaskawulsh Glacier retreated to at least 13.7 mi. above its present terminus during the period following the Kluane glaciation, starting some time between 12,500 B. P. and 9780 B. P. and ending about 2640

Fig. 5. View taken in 1941 looking north from the stagnant terminal ice of the Kaskawulsh Glacier at an elevation of 20,000 ft. The Slims River, seen at the left, drains generally northward to Kluane Lake which is faintly visible in the distance. The Kaskawulsh River, lower right, drains east from the eastern tip of the glacier. Between these two rivers lie the debris-filled gap and the forest-covered knoll surrounded by moraines. (Photo: courtesy U.S.A.A.F., negative 41-F-28-R-79 and GEOLOGICAL SURVEY OF CANADA, negative 104 188).

B. P., and was thus well clear of the valley fork and nearly 30 mi. from Kluane Lake at this time. Although the Neoglacial advance began about 2640 B. P., Denton and Stuiver (1966, p. 594) are of the opinion that the glacier probably did not finally block the valley fork until about 420 B. P. to 300 B. P. The valley fork could therefore have been open to drainage from Kluane Lake from the end of the Kluane glaciation through the Hypsithermal interval as defined by Deevey and Flint (1957, p. 182), and until about 400 years ago. This correlates well with the radiocarbon date given above as the age of the drowned stump from Christmas Bay.

While the level of the bedrock in the valley fork is a crucial factor, other phenomena along the Slims Valley should also be considered. The valley is flanked by a number of alluvial fans, notably those of the Vulcan, Bullion and Sheep Creeks which lie within the first few miles upstream from Kluane Lake. These fans have been mapped and described by Borns and Goldthwait (1966, Figure 2) who draw attention to the fact that they nearly or completely coalesced across the valley during the dissipation of the Kluane glaciation ice from the Kluane Ranges. They consider that the present fans are formed of post-Hypsithermal alluvium but that the "early fans" were constructed "during late Kluane time." They do not say whether or not the "early fans" could have been built in contact with or over bodies of ice lying in Slims Valley. The existence of a drainage channel 40 ft. below Kluane Lake level along the valley when bodies of ice still remained is suggested by the likelihood that Christmas Creek estuary formed part of the spillway for glacial Lake Kloo when, as Kindle (1953, p. 17) notes, ice was still blocking Jarvis River valley. Since the Slims River flows between the present fans without steepening its gradient (Fahnestock, 1966, p. 64), it is possible to envisage a stream from Kluane Lake, at a level 40 ft. below the present lake level, flowing southward through the valley with little hindrance from the fans.

It is interesting to speculate as to what the valley was like before the closing of the valley fork by the Kaskawulsh Glacier. The valley floor is now covered from side to side by Neoglacial outwash, modern fluvial deposits, and aeolian deposits, and it slopes with Slims River down to Kluane Lake. The levels and the grade in the gap do not suggest that the Kaskawulsh River ever flowed into Kluane Lake, so there must originally have been a divide. This would have led to the impounding of Slims River until its water had eroded the obstruction. With all the studies made during the last few years, no sign of a lake from this impounding has been reported, so the divide must have been low and easily eroded. Considering the mass of outwash borne from the glacier by Slims River now (Bostock, 1952, p. 8), the valley must have contained space in the form of lake basins to accommodate this material at or below the level of Kluane Lake.

To the east of the Kluane Lake area, glacial Lake Champagne flooded great stretches of the valleys presently drained by the Alsek River during the end of the Kluane glaciation (Kindle, 1953, pp. 15 – 16). This lake left many miles of beaches at elevations between 2300 and 2800 ft. Most of the beaches shown on the map accompanying Kindle's report are close to or below the 2500-ft. contour. Of the beaches attributed to Lake Champagne, the nearest one to the valley fork, is mentioned by Wheeler (1963, marginal notes) who states, "Terraces at an elevation of 2550 ft. about two miles northwest of the mouth of the Jarvis River were probably formed by this lake."[2]

The topographic maps show that if Lake Champagne lay at 2800 ft., many courses would have been open for its drainage – including one through the Kaskawulsh valley, around the valley fork and through Kluane Lake, provided there was an ice-clear passage. When Lake Champagne dropped to below 2600 ft., it could only drain by the Alsek River or a valley to the east. Had there been a channel around the valley fork, Kluane Lake would have drained into Lake Champagne by way of the Kaskawulsh River. The relative timing of the dissipation of the ice and the cutting of channels through and around the ice in the various valleys remains unresolved.

Northwest Outlet Area

On leaving Kluane Lake, the Kluane River follows a narrow channel close to the northeast side of the Shakwak Trench for 6 mi. The floor of the trench throughout this stretch is about 5 mi. wide and, as far west as the mouth of the Duke River, slopes generally down to the northeast from the mountains on its southwest side. West of the Duke River this slope flattens about a mile from the northeast side. On the southwest side, against the mountains, much of the surface of the trench floor is formed by alluvial fans extending out from gulches. Beyond this, the surface is composed of northwesterly-trending drumlinoid ridges and hollows, more than half of which are eroded or covered by the past and present courses of the larger streams flowing north to the Kluane River. Duke River is outstanding among these streams, with Burwash Creek further west being the next in importance. The surface features of this area are shown in Figure 6. This drawing and the interpretations made in it are based on data extracted from aerial photographs, from information on the 1:50,000 topographic map (Duke River, 115 G/6), from reconnaissance field work during 1945, and from one flight over the area in 1966. For a thorough understanding of the area, much ground work and study are still required.

The information available, however, brings out some interesting points. East of the present course of the Duke River, the floor of the Shakwak Trench is man-

[2] In the context of the notes, a mistake makes "this" read as if another lake were meant, but the statement actually refers to Lake Champagne (J.O. Wheeler, personal communication).

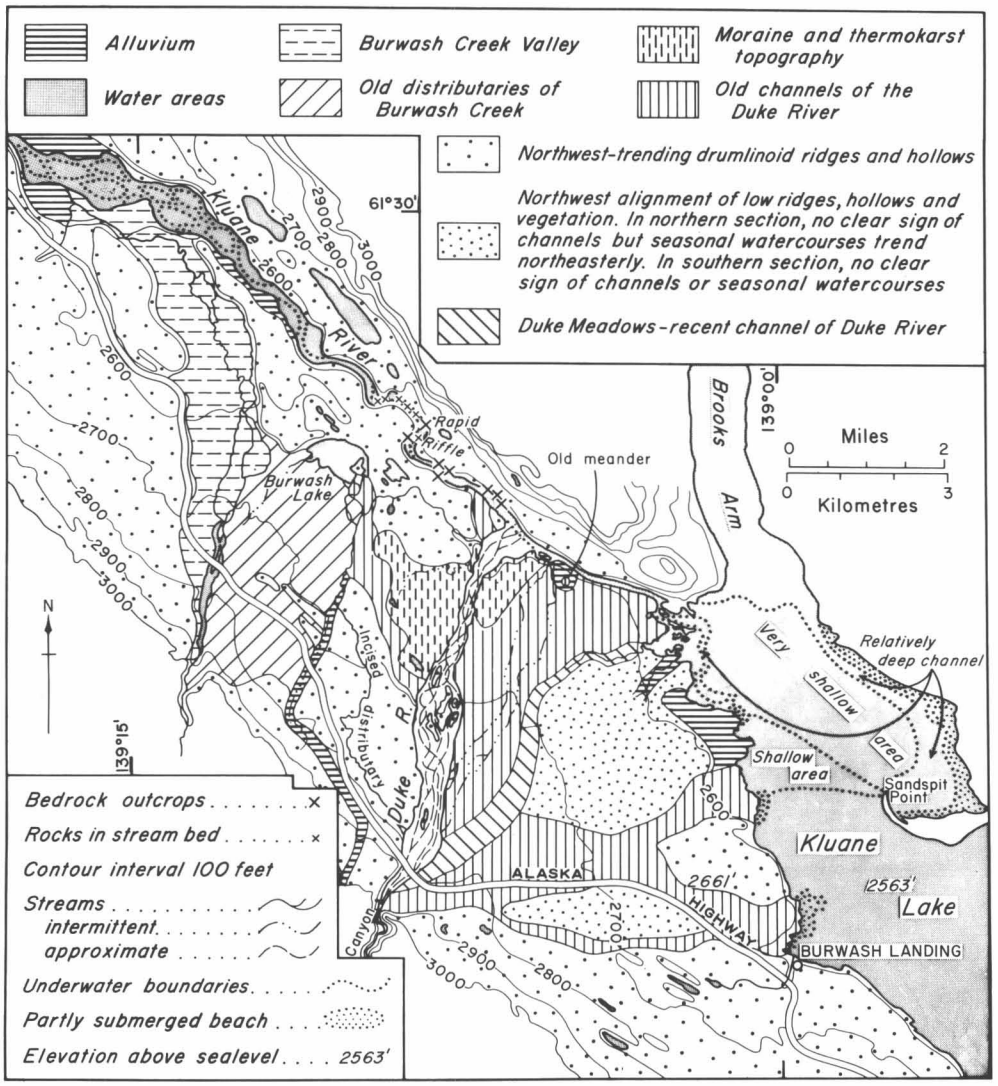

Fig. 6. Geomorphic features in the vicinity of the present outlet to Kluane Lake.

tled by wide, braided, former courses of the Duke River. Raup (Johnson and Raup, 1964, p. 28) refers to these courses, or channels, as outwash fans and says that they are progressively younger from east to west. He further adds, "The earliest one formed what is now nearly all of the shore of Kluane Lake from Burwash Landing to Kluane River. It was just off this shore that Bostock took his 20-foot soundings [see Figure 2 of present paper]. Most of the surface of this fan is forested. It also has volcanic ash on it and some Kluane Silt [also called 'Kluane Loess' by Denton and Stuiver, 1966] indicating that it was deactivated while the deposition of this silt was going on. Further west lie the 'Duke Meadows' [see Figure 7 of present paper], a natural grassland on an adjacent fan that has neither ash or Kluane Silt showing that it was abandoned at some time within the last 1600 – 1700 years. The present active fan is adjacent to this one, still farther to the west .... It is not impossible that the valley of the Kluane River was considerably deeper when the ice melted out of it than it is now, and that it was gradually filled by these huge gravel fans. Most of this work was done prior to Hypsithermal time. If so, the lake would have started its existence at a relatively low level, as Bostock's evidence indicates that it did. But its history would be one of gradual rise to approximately its present level with no requirement for its drainage through the Slims River – Alsek River system. Also, there would be no requirement that it have a level in the recent past, at least for any length of time, that is higher than the present one."

As Figure 6 shows, this oversimplifies the picture and fails to recognize the drumlinoid features northwest of Burwash Landing. In view of this, some of the old channels in this area may be bare of Kluane Silt (Loess) and even volcanic ash and so may have not been abandoned by the Duke River before the end of the Hypsithermal interval or even before the ash fell 1425 ± 50 years B. P.

As suggested by Raup, the old channels shown on

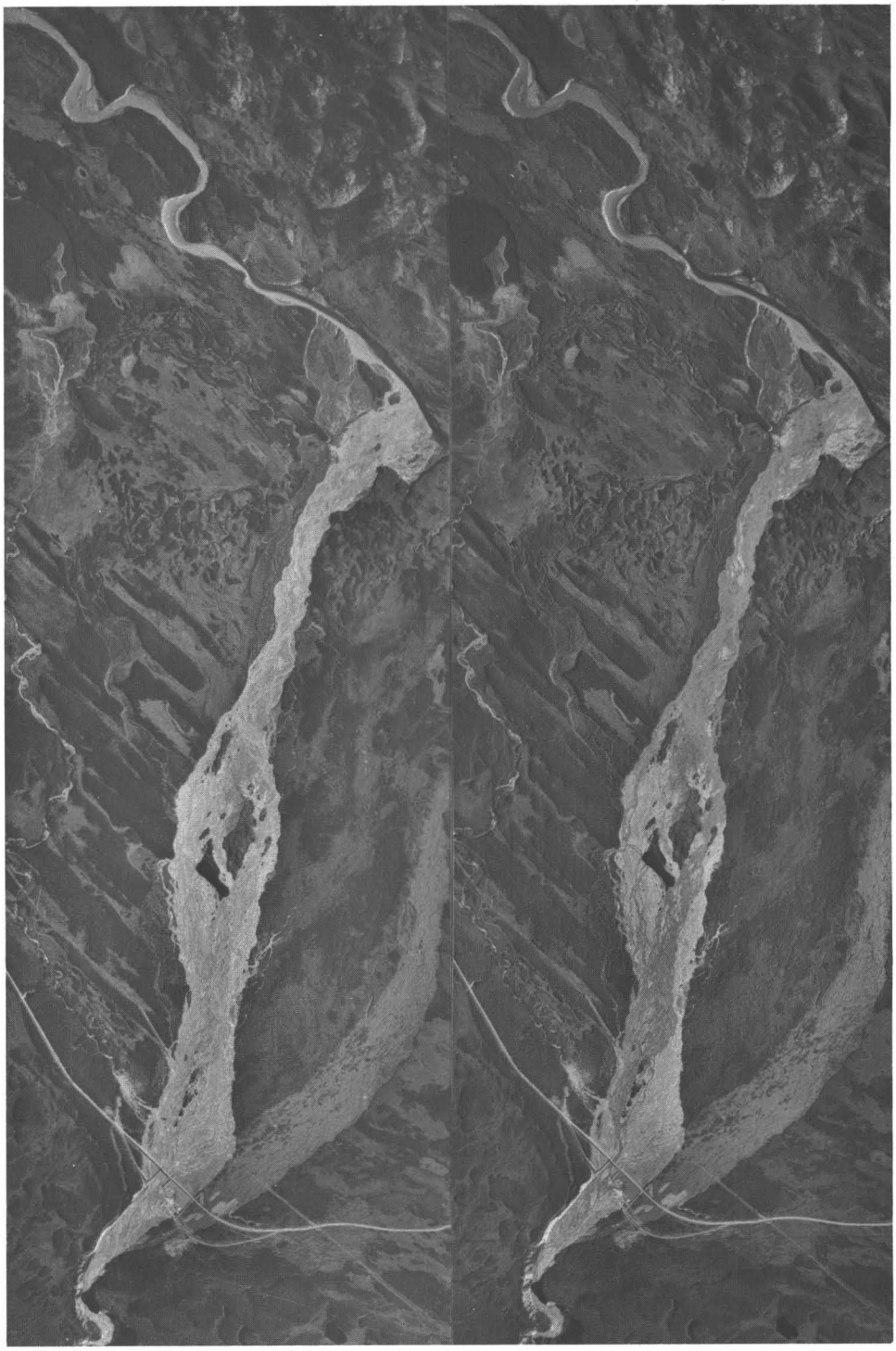

Fig. 7. Stereoscopic pair of vertical photographs showing the junction of the Duke and Kluane Rivers. The Duke Meadows fan lies to the east (right) of the present Duke River channel, and an old channel, now covered with vegetation, lies to the west (left) of the present junction of the two main rivers. Burwash Lake lies in the upper left corner of the right-hand photograph and, extending southeastward from it, two areas of moraine and thermokarst topography lie on either side of the Duke River. The northwest-southeast trending drumlinoid topography is evident on the left bank of the Duke River and traces of old channels may be seen on the right. (Photos: courtesy *Canadian National Air Photographic Library* Nos. A 15739-52 and 53, taken 1957 from 35,000 ft.)

Figure 6 leading eastward from Duke River canyon and reaching the lake shore at points along the coast from Burwash Landing to 2½ mi. to the north, appear to be the first ones used by the river and are certainly the broadest. Their unusual course, turning almost at right angles as they leave the canyon, implies that at the time of their formation the river channel was obstructed by some large feature athwart the natural route straight northward into the Kluane River valley. This feature was probably drift, as there are no bedrock outcrops immediately north of the canyon except along the Kluane River. This also attests to the priority of these channels, as the drift would have had to be removed before a northward course could be established. From the existence and location of these channels, it may be judged that the river was handicapped in filling or occupying any deep former outlet leading westward from the lake. A number of other old channels have also been occupied at various times by the Duke River, including one lying west of its present channel. Some of these channels may have been used by only part of its water or only for a short time. Such appears to have been the case for the Duke Meadows channel and for the old channel which flowed into Burwash Lake but did not fill it. The Duke Meadows channel is comparatively narrow relative to the present Duke River bed (Figure 7) and leads to a narrow inlet rather than to a delta projecting into the shallows of Kluane Lake. The present channel ends in a "delta" that holds the Kluane River against the outcrops on its northeast bank. A short stretch of an older channel on the west side of the "delta" is covered with brush but may have been abandoned quite recently, perhaps twenty years before the aerial photographs were taken. It is uncertain whether the Duke River, when it first reached the north side of the Shakwak Trench, turned eastward to Kluane Lake or westward down the present course of the Kluane River to Burwash Creek.

For more than 6 mi. below Kluane Lake, the Kluane River follows a narrow, relatively fresh channel and the question arises as to whether, at an earlier stage, it followed another course through this area. Burwash Lake, to judge from its shape on the map, might be part of an abandoned river channel. If so, this channel extended from the Kluane River, somewhere between Kluane Lake and the present mouth of the Duke River, and possibly flowed through the two areas of "moraine or thermokarst topography" (Figure 6) to Burwash Lake and thence down Burwash Creek valley. In support of this theory it is noted that Burwash Creek has a broad valley, about 1 mi. wide, which continues as that of the Kluane River below the confluence of these two streams. However, until it reaches the lower Burwash valley, this course lies above the 2600-ft. contour and the theory assumes improbable and prodigious amounts of deposition by the Duke River and Burwash Creek in a comparatively short period of late post-Kluane glacial time. It also assumes the damming of the outlet stream to above the 2600-ft. level, resulting in its re-routing to the present channel of the Kluane River. From aerial photographs, and from the air, Burwash Lake could be a kettle hole rather than an oxbow lake (Figure 8). The peninsula in it has neither the form of a river bar nor a crowfoot of an old channel of the Duke River or Burwash Creek. It is probably an original proglacial topographic feature. Furthermore, no sign of such a river course to the east has been detected on the aerial photographs or among the soundings of Kluane Lake (Figure 2) where it should be deep enough to have permitted the formation of estuaries similar to those at the mouths of Gladstone and Christmas Creeks.

Turning again to the Kluane River, its channel is narrow and has few bars or meanders for 2 mi. above and below its junction with the Duke River. Aerial photographs show an old, dry meander on the southwest bank between the outlet of Kluane Lake and the Duke River. This meander (location indicated on Figure 6) seems to be at a higher level than the present Kluane River, but it is not apparent from the photographs which way the water flowed.

Judging by aerial photographs taken during the summers of 1950 and 1957, the Kluane River is not particularly swift immediately below its junction with the Duke River, a state that might naturally have been expected if the Duke River were overloading it. Rather, the swift water occurs from 1 to 2½ mi. below their confluence at a location where bedrock crops out in its banks, and, apparently, in its bed (Owen, 1962, maps in back pocket). About 4 mi. downstream from its confluence with the Duke River, the Kluane River begins to widen its valley floor, cutting back high banks of drifts and developing broad gravel bars. By the time it reaches Burwash Creek valley, its floor is a mile or more in width and continues so for several miles downstream.

STRUCTURAL MOVEMENT

The Shakwak Lineament, which is assumed to mark a major fault, (Bostock, 1952, pp. 8 – 9; Muller, 1967, pp. 93 – 96) trends northwest – southeast, extending southeast from near the International Boundary (141st Meridian) to beyond Kluane Lake (Figure 2). The trace of this fault is depicted on geological maps as a single fault that follows a line of mounds on the southwest side of the Shakwak Trench. These mounds, clearly visible on trimetrogon photographs taken looking along the fault, continue across a variety of topographic features except where streams have cut them away. On the Donjek River, some 24 mi. northwest of Kluane Lake, they still project as a ridge out onto the floodplain and have not yet been completely eroded away. This suggests that they mark a movement on the fault that took place in recent centuries.

Even if structural faulting were considered as the underlying cause of the changes in lake level inferred from the occurrence of the estuaries, the drowned

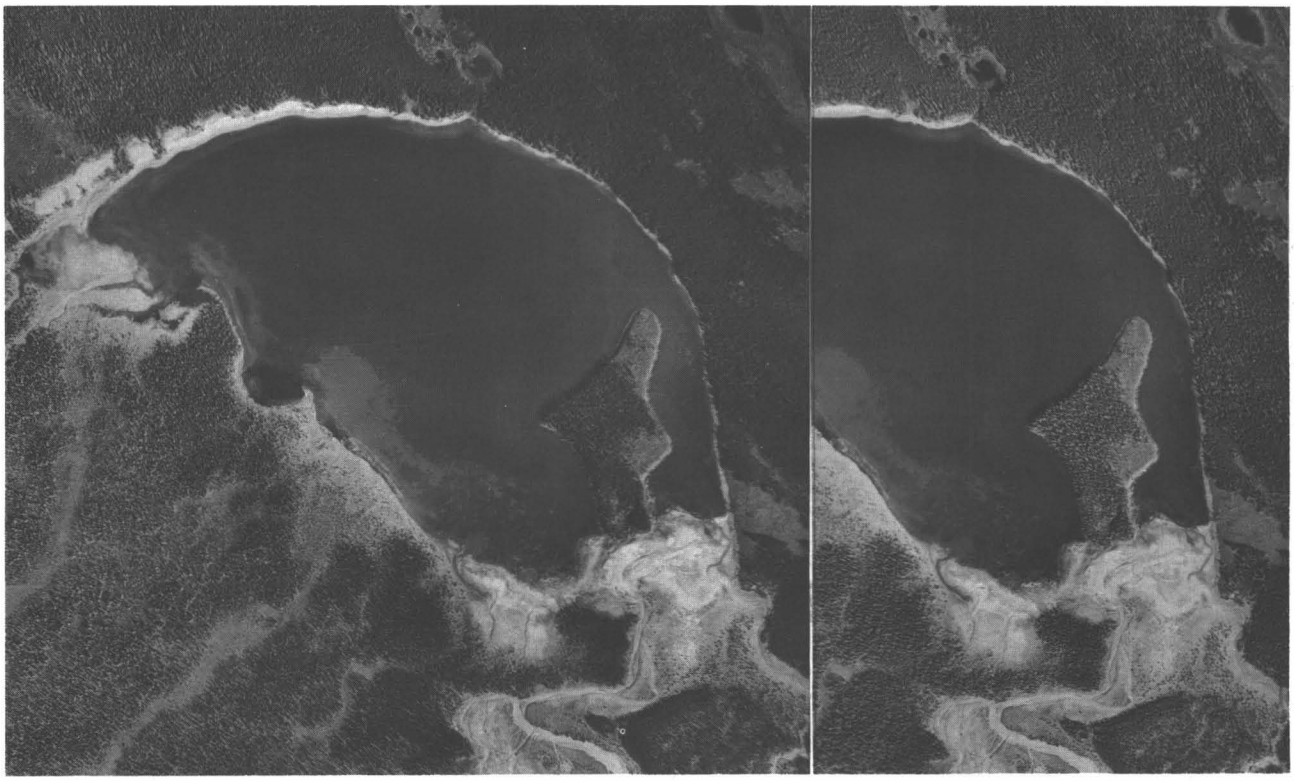

Fig. 8. Burwash Lake. Stereoscopic pair of aerial photographs showing the peninsula which is thought to be a proglacial feature. (Photos: courtesy *Canadian National Air Photographic Library,* Nos. A 12957-235 and 236)

forest, and the raised beaches, the fact still remains that the level of the outlet of Kluane Lake must have changed from 40 ft. below to 30 ft. above its present level before finally establishing its present elevation. Such changes of lake level are difficult to account for by any simple movement along the fault.

CHRONOLOGY

From the phenomena here described, the writer believes the chronology of Kluane Lake to have been as follows:

(1) With the waning of the Kluane glaciation, while ice still filled the Kluane Lake basin, a proglacial stream draining from the ice formed both the broad valley of Burwash Creek and the valley of the Kluane River below their junction.
(2) As the ice in the lake basin was being dissipated, the earliest stage of Kluane Lake developed and drained by way of the valleys of the Slims and Kaskawulsh Rivers via an outlet developed through the valley fork.
(3) By this channel the lake was drained to a level about 40 ft. lower than at present.
(4) At the same time, some of the creeks entering the lake cut the valleys that now form estuaries.
(5) Concurrently, the early fans of the Vulcan, Bullion, Sheep Creeks, and others were built in the Slims Valley, probably partly on bodies of ice, and, on the wasting of this ice, the valley became at first a deep, narrow southern arm of Kluane Lake. Later the creek fans practically coalesced. However, they did not obstruct the outlet stream and probably only increased its gradient and raised the level of the lake by a few feet.
(6) For a very short period, water from glacial Lake Kloo spilled over into the head of Christmas Creek, and cut a valley through deep drift deposits.
(7) The shallow western parts of Kluane Lake became dry land and were later covered by forest.
(8) The Duke River, joined by a stream from Brooks Arm, flowed eastward across this area into Kluane Lake. Their waters added to the volume discharging into the outlet stream in the Slims River valley.

With the final disappearance of the ice, this last drainage pattern persisted through most of the post-Kluane glacial time, including the Hypsithermal interval. With the onset of the Neoglacial, about 2640 B. P., glaciers in the St. Elias Mountains began to advance, and about 400 B. P. the Kaskawulsh Glacier reached its Neoglacial maximum and closed the outlet by way of the valley fork. The direction of the Slims River drainage was reversed and the river began to fill the valley with glacial outwash. With the water of the Slims River now draining the Kaskawulsh Glacier through the Slims Valley, as well as the water contributed by the Duke River, Kluane Lake rose rapidly and flooded its basin to 30 ft. above its present level before finding an over-flow channel to Burwash Creek along the course of the present channel of the Kluane River. Once this channel was opened, the great volume of water from the lake and the Duke and Slims Rivers very quickly cut through the drift deposits and down to the bedrock level that now controls the level of the lake.

As the timing seems to be about right, it is possible that the earthquake that accompanied the movement on the Shakwak Lineament was sufficiently violent to trigger an acceleration in the advance of the Kaskawulsh Glacier and so, indirectly, to close the valley fork.

The Duke River may have found its way north across the "northwest outlet area" before the closing of the valley fork and may have turned either eastward to Kluane Lake or westward to Burwash Creek (see Figure 6, old channels of the Duke River). Normally the gravel load from the Duke River is not sufficient to obstruct the Kluane River and thus raise the level of the lake. However, in some seasons the Duke and the Slims Rivers may have been synchronized so that their input temporarily raised the lake level as much as 10 or 12 ft.

CONCLUSION

In view of the evidence, the author concludes that before the Neoglacial advance of the Kaskawulsh Glacier, Kluane Lake drained south through the Slims Valley into the Kaskawulsh River.

REFERENCES

*Borns, H. W. Jr., and Goldthwait, R. P. (1966) Late-Pleistocene fluctuations of Kaskawulsh Glacier, southwestern Yukon Territory, Canada, AM. J. SCI., 264, 600 – 619.

Bostock, H. S. (1948) Physiography of the Canadian Cordillera, with special reference to the area north of the fifty-fifth parallel, CANADA GEOL. SURV. MEM. 247, 106 pp.

Bostock, H. S. (1952) Geology of northwest Shakwak Valley, Yukon Territory, CANADA GEOL. SURV. MEM. 267, 54 pp.

Deevey, E. S. Jr., and Flint, R. F. (1957) Postglacial Hypsithermal interval, SCIENCE, 125, 182 – 184.

*Denton, G. H., and Stuiver, M. (1966) Neoglacial chronology, northeastern St. Elias Mountains, Canada, AM. J. SCI., 264, 577 – 599.

Fahnestock, R. K. (1966) Morphology of Slims River, Yukon Territory, Canada, GEOL. SOC. AM., PROGR. 1966 ANN. MEETINGS ABSTR., p. 64.

Johnson, F., and Raup, H. M. (1964) Investigations in southwestern Yukon: geo-botanical and archaeological reconnaissance, ROBERT S. PEABODY FOUND. ARCHAEOL. PAPERS, Vol. 6, No. 1, 198 pp.

Kindle, E. D. (1953) Dezadeash map-area, Yukon Territory, CANADA GEOL. SURV. MEM. 268, 68 pp.

Muller, J. E. (1967) Kluane Lake map-area, Yukon Territory, CANADA GEOL. SURV. MEM. 340, 137 pp.

Owen, E. B. (1962) Kluane Canyon damsite, CANADA GEOL. SURV. TOPICAL REPT. 36.

*Stuiver, M., Borns, H. W., and Denton, G. H. (1964) Age of a widespread layer of volcanic ash in the southwestern Yukon Territory, ARCTIC, 17, 259 – 260.

Wheeler, J. O. (1963) Geologic map of Kaskawulsh half of Mt. St. Elias map sheet, Yukon Territory, CANADA GEOL. SURV. MAP 1134A.

*These articles are reprinted in the present volume.

Morphology of the Slims River

*Robert K. Fahnestock**

ABSTRACT. The Alaska Highway crosses the Slims River at mile 1060 where in 1965 the river was building a delta into Kluane Lake. Kaskawulsh Glacier, 14 mi. upstream, was the source of much of the debris being deposited in the valley. Dust clouds from the valley train blanket the surrounding countryside with loess.

On the basis of discharge measurements and observations of gage height and flow phenomena, the discharge of the Slims River ranged from 0 to 20,000 ft.^{3}/sec. The valley train of the Slims River, like those of many other glacial rivers, has 3 zones. In an upstream zone, 1 to 3 channels were cutting down in coarse gravel on a slope lower than that of the intermediate zone. The river was multichanneled in the intermediate zone with considerable bed load transport and some deposition. At all stages it was channel and bar dominated. About mile 1.5 in the intermediate zone, the slope was 15 ft./mi. and at relatively high flows in July 1965, 30 channels covered nearly half of the 6000-ft.-wide valley floor, with an average depth of 1.3 ft., a maximum depth of 4.0 ft., and a velocity of 5 ft./sec at 0.6 of the depth. In the downstream zone at high stages the river had a few bars and graded into a sheet of flowing water. On sand, at mile 6.2 in the downstream zone, on a slope of 4.5 ft./mi. 20 channels covered nearly all of the 5700-ft.-wide valley floor, with an average depth of 0.8 ft., a maximum depth of 3.5 ft., and an average velocity of 2.3 ft./sec.

The stream was regrading the valley train. That is, the slope was gradually being adjusted to the changes in load and discharge, and to the channel form existing in each zone.

Evidence supports the post-glacial drainage reversal suggested by Bostock for the Slims system from the Kaskawulsh – Alsek River to the Yukon River. In 1967, however, the Kaskawulsh Glacier's contribution to the Slims River shifted subglacially to the Kaskawulsh River, imposing a new set of conditions on the valley train and Kluane Lake. Initial changes due to this shift include a major decrease in discharge of Slims River and an increase in amount of blowing sediment.

Introduction

Slims River flows north from the Kaskawulsh Glacier in the Icefield Ranges of the St. Elias Mountains into Kluane Lake near mile 1060 on the Alaska Highway (Figure 1). This broad glacial stream flows in one to more than 30 channels at high flows. The valley is about 6000 ft. wide except where constricted by side stream alluvial fans (Figure 2). As an active glacial stream, it is depositing and modifying its valley train. The Slims River delta in Kluane Lake is approximately 14 mi. from the outermost recent moraine of Kaskawulsh Glacier. Study of the Slims River provides a basis for a better understanding of other valley trains, past and present.

Field work during the summer of 1965 included measurements of valley train slope, stream discharge, size analyses of valley train materials, reconnaissance study of the form and character of the valley, and a survey of valley cross sections.

Earlier measurements of the river consisted of a few stream discharge measurements at the new highway bridge (mile 12.7, Figure 2) and a few stage measurements at the old bridge (mile 10.7, Figure 2) made by Canadian Inland Waters Branch personnel, and some measurements of maximum size of sediment in the main channel, made by S. Chadhuri of The Ohio State University.

*State University College, Fredonia, New York

General description. The Slims and Kaskawulsh Rivers share the runoff from the 800-mi.^{2} drainage basin above the moraine. Approximately 560 mi.^{2} (Richard Ragle, personal communication) of this basin is covered with ice of the Kaskawulsh Glacier system (Figure 3). In 1965 the major share of water from the glacier was going to the Slims River. The Slims River falls about 100 ft. in the 14 mi. to Kluane Lake, and then falls another 2500 ft. in its 1500-mi. route to the Bering Sea via the Kluane, Donjek, White, and Yukon Rivers, a fall of about 1.7 ft./mi. The Kaskawulsh River flows to the Gulf of Alaska via the Alsek River and Dry Bay (Figure 1), and in its 170-mi. length it falls 2500 ft., or about 14.7 ft./mi.

Discharge variations. Large seasonal variations in flow of Slims River are illustrated by the discharge measurements shown in Table 1. If one estimates possible flows under conditions of –75°F and, at the other extreme, the breakout of marginal and perhaps subglacial lakes during the summer, the range could well be 0–20,000 ft.^{3}/sec. or more. The pattern, sediment transport, and channel characteristics vary considerably under these extreme conditions.

A 24-hour period of observations at the old bridge (mile 10.7, Figure 2) on August 5 and 6, 1965 revealed an air temperature high of 68°F at 3:30 p.m. YDT (Yukon Daylight Time) and a low of 44°F at 5 a.m. the following morning. Water temperatures showed a similar pattern reaching a high of 48°F about 4:30 p.m. and a

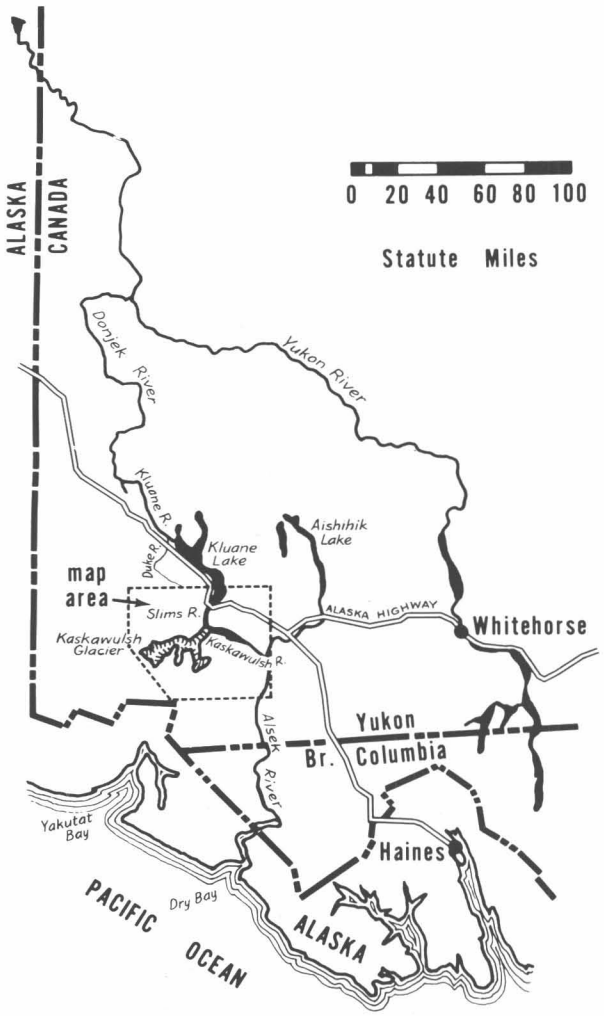

Fig. 1. Location map.

low of about 34°F between 5 and 7 a.m. the following morning. There was a 0.5-ft. variation in water surface elevation during the same period with a low occurring between 12 noon and 2 p.m. and a high sustained from 9 p.m. until 3 a.m. A 0.5-ft. change in stage would represent a flow variation of from 1000 to 2000 ft.^{3}/sec. Continuous recording equipment was not available and the other measurements made were too scattered to establish that these highs and lows were entirely characteristic.

The movement of bars of fine sand and silt caused significant changes in the local water surface elevation and slope in the accessible lower reaches of the river. It was therefore impossible to compile a meaningful relationship of stage to discharge. For example, simultaneous readings of staff gages 1.9 mi. apart showed a difference of 6.16 ft. on July 7 and 4.68 ft. on August 6. Figure 4 shows changes in water surface slope in a shorter reach of river.

Fountains. Slims River emerges from beneath an apparent fill of outwash gravel in several "fountains." Borns and Goldthwait, (1966, and pp. 187 – 196 of this volume) state that in 1963 "around the openings there are accumulations of well-rounded boulders up to 2 or 3 ft. in diameter which have in all probability been ejected." In 1965 the main fountain was 3 to 5 ft. high, considerably lower than previous observations indicated, and perhaps 20 or more feet across (Table 2). Water cascaded in all directions from the base and allowed little view of the nature of the opening or of the materials which composed it. Several small streams also flowed from tunnels in the ice margin. At times of exceptionally high flows, for instance, during the drainage of a marginal lake, there is no doubt that the fountains have reached exceptional heights far exceeding those that have occurred when ground observers were present.

Using the formula $v = \sqrt{2gh}$, for a vertical jet of an ideal fluid, where h is the rise of the jet and g is the acceleration due to gravity, one can calculate a minimum velocity, and therefore a discharge (Table 2).

The 1965 fountain discharge of approximately 4400 to 5000 ft.^{3}/sec. is of the same order of magnitude as the 4000 ft.^{3}/sec. discharge measured at a comparable stage in the main channel through the moraine (Table 1).

Differences in height may be due to changes in head on the orifice, conduit diameter, and the flow resistance of the conduit. Borns and Goldthwait (1966) suggest on the basis of air photos that the two fountains had persisted since at least 1941 and that such persistance is quite remarkable considering rates of ice movement, melting of the ice face, and melting and abrasion of the conduit walls.

Side stream fans. Side stream fans occupy a major part of the Slims River valley floor from the moraine to the lake (Figure 2). They range in size from the large fans of Canada, Bullion, Sheep, and Vulcan Creeks to tiny fans at the mouths of gullies. The fan streams delivered considerable quantities of fine gravel, sand, and finer materials to the valley train. Coarser gravels were deposited higher on the fans, well away from the river. There was evidence of mudflows on some of the smaller and steeper fans. A single small stream flowed on the surface of most fans, although on the larger fans as many as a dozen anastromosing channels changed position rapidly with the higher flows of midsummer.

On the upper portions of the fans, flow was lost by infiltration but reappeared in the lower portions where small channels emerged and flowed into the river (Figure 5). Decrease in grain size and the presence of frozen ground contributed to the decrease in permeability at the fan margins. Cracks and unevenness in once continuous surfaces were the most obvious evidences of ground ice. Wetting by capillary action darkened the surface of the fan margins. Evaporation in these damp areas frequently left films of white powdery material that tasted somewhat like baking soda.

The upper two-thirds of the named tributary fans were wooded, with the notable exception of Canada Creek. The lower one-third of these fans was covered by

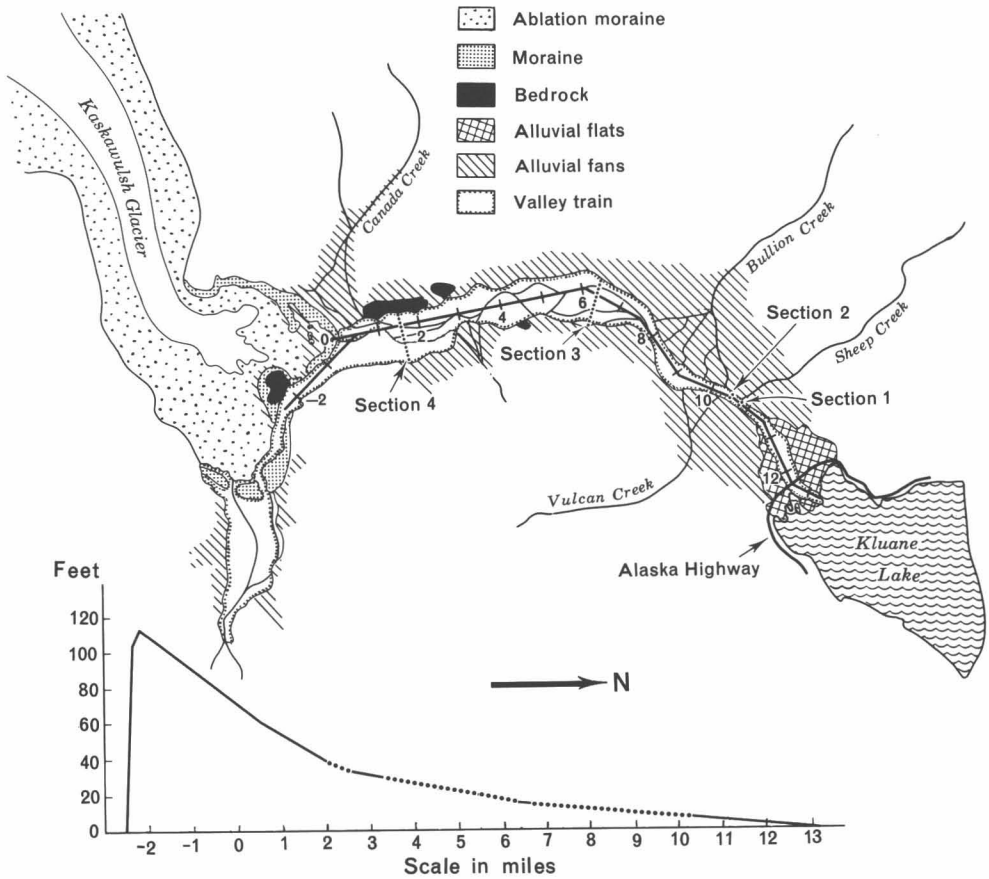

Fig. 2. Slims River valley and profile showing locations of cross sections.

TABLE 1. Slims River Discharge Measurements

	Measurements at Alaska Highway Bridge						Measurements at moraine cable [2, 3]		
	Before 1965[1]			1965			1965		
Month	Day	Year	Discharge (ft.^{3}/sec)	Day	Hour	Discharge (ft.^{3}/sec)	Day	Hour	Discharge (ft.^{3}/sec)
Dec.	27	1962	133						
Feb.	21	1962	8						
May	6	1964	125						
May	25	1955	873						
May	27	1964	1000						
June	27	1962	6400						
June				31	noon	7550			
July	3	1963	6330						
July							27	9 a. m.	3400
July							27	3 p. m.	3900
July							27	6 p. m.	3900
July							28	9 p. m.	4300
Aug.	7	1963	9600						
Aug.				7-8	midnight	9400			
Aug.	9	1962	8870						
Aug.				10-11	midnight	9900			
Aug.	16	1962	11,250						

[1] Miscellaneous measurements by M. E. Alford, Canadian Inland Waters Branch (written communication)
[2] Miscellaneous measurements made for this study
[3] This is the largest of 2 channels draining the Slims lobe of the Kaskawulsh Glacier, containing an estimated 70 – 90 percent of the flow.

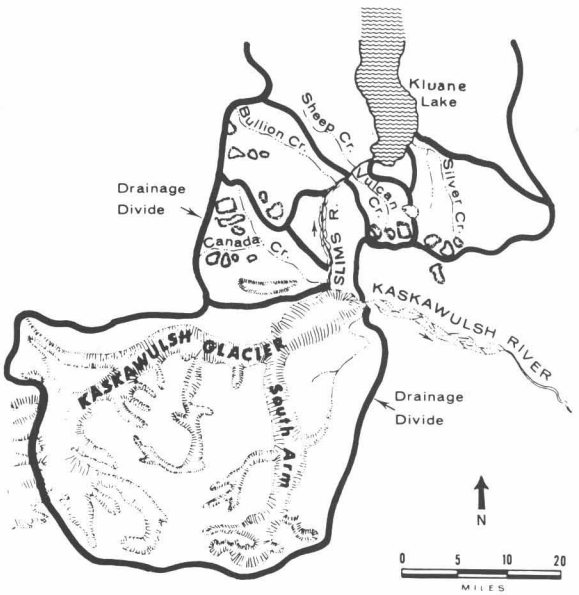

Fig. 3. Drainage basin map.

grasses and muskeg. Portions of the fans bordering the Slims River were covered with silt flats probably deposited by the Slims River itself in previous years. Almost the entire surface of the Canada Creek fan was devoid of vegetation and silt deposits. During the summer of 1965, the braided channels of this creek reworked 15 to 25 percent of the fan surface.

Chien Ning (1961, p. 741), Krigstrom (1962, p. 329), Fahnestock (1963, p. A52) have noted the presence of control points or constriction nodes which decrease the number of channels in the vicinity of the constriction and for some distance downstream.

The large right bank fan at mile 3, Slims River (Figure 2), served to concentrate the flow into one main channel in which occurred one of the greatest depths (about 12.0 ft.) and velocities (about 7 ft./sec.) measured on the entire valley train. This channel collected water from 8 or more channels on the right half of the valley train and distributed it to 6 or more channels on the left, which also received flow from a number of left bank channels (Figure 6).

TABLE 2. Velocity and Discharge of Fountains

Date	Height (ft.)	Velocity[3] (ft./sec.)	Diameter (d) (ft.)	Discharge[4] (ft./sec.)
1962[1]	20	36	10	2700
1963[2]	8	23	10	1800
1965	3 – 4	14 – 16	20	4400 – 5000

[1] Observed from aircraft by Philip Upton (personal communication).

[2] Borns and Goldthwait (1966)

[3] Velocity $= v = \sqrt{2gh}$

[4] Discharge $= \frac{\pi d^2}{4} v$

The alluvial fans of the three named creeks – Bullion, Vulcan, and Sheep Creeks – combined to form similar controls between mile 6.5 mile 11 by constricting the channel and causing similar concentration of flow, relative stability of form, and a decrease in the number of channels and water surface slope.

Similar constrictions caused by smaller fans and bedrock irregularities in the valley margin are evident in Figure 6. Downstream from these points and sometimes extending several times as far into the valley as the actual constriction, islands were larger and channels fewer.

On this valley train, because the flow was separated into many channels, great distances were required for thorough mixing of clear and sediment-laden water. The waters of Canada Creek were darker because of a smaller amount of rock flour, and they retained their identity for two miles along the side of the valley train.

Long profile of the valley train. There are no apparent breaks or discontinuities in the slope of the valley floor (Figure 2). The 10 ft./mi. (0.0019) slope in the single channel upstream reach increases gradually to the 15.0 ft./mi. (0.0028) slope of the multichanneled reach and then merges gradually with the 5 ft./mi. (0.0009) slope of the downstream reach. Where the fans constrict the stream, the slope is as low as 1.6 ft./mi. (0.0003) (Table 3).

The long profile of the valley is based on leveling for the reaches so indicated. The transitional curves have been sketched in from one leveled slope to the next and are averaged from these adjacent slopes to establish the relative elevation of the head of the valley train and other upstream points. Time did not permit running a level line the entire length of the valley. A total of 5.7 mi. of the 13.5 mi. total length of the Slims River valley was leveled, most of it in the steeper portions of the valley train. Distances were determined from maps and air photos. Elevations determined from this profile are not exact but are probably well within ±15 ft. The 75-ft. elevation of the main channel at the moraine (mile 0, Figure 2) checks relatively well with the 90-ft. estimate

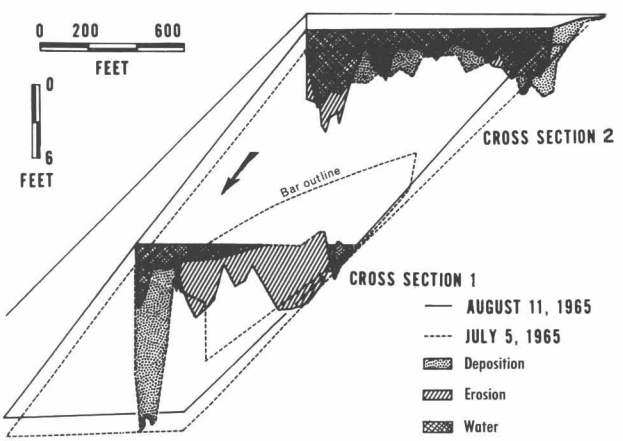

Fig. 4. Cross sections 1 and 2 showing changes between July 5 and August 11, 1965. Note horizontal reference lines.

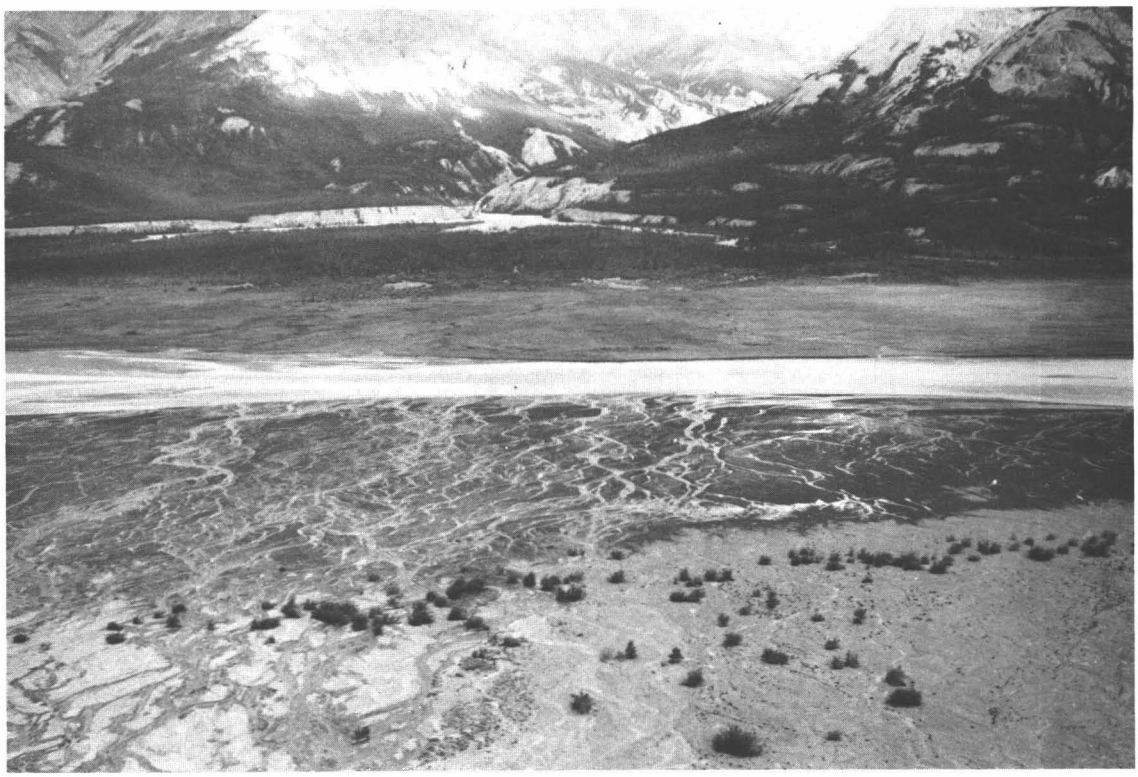

Fig. 5. View west across Vulcan Creek fan toward Bullion Creek. High fan remnants extend from the mouth of Bullion Creek canyon. New channels emerge from the fine materials at the edge of Vulcan Creek fan. Darkening is due to wetting by capillary action. Across the Slims River are five-foot cutbanks in silts at the fan margin.

made by Philip Upton using an aircraft altimeter on several flights between Kluane Lake and the gravel bar air strip near the moraine.

Comparisons of form and phenomena can be made between the Slims River, the White River, which flows from Emmons Glacier on Mt. Rainier, Washington (Fahnestock, 1963), and the Austurfljot of the Hoffellssandur of Iceland (Hjulstrom, 1952).

The slope of the Slims River valley train is much less than that of the White River and the Hoffellssandur (Table 3). The difference in slope between the Slims River and White River is due to the 10 to 20-fold greater discharge of the Slims River and the smaller size of materials available to the Slims.

Where the Slims River is confined by the side stream fans between miles 9.5 and 11 (Figure 2) the water-surface slope was lower (1–2 ft./mi.) than in the wider reaches. A similar relationship between stream width and water-surface slope was noted in studies of the Rio Grande (Fahnestock and Maddock, 1964; Harms and Fahnestock, 1965). All materials transported by the movement of large bars through a wide reach of the Rio Grande were subsequently transported, with no bar formation, though a narrow reach which had approximately 2/3 the slope. The slope of a reach appears to be inversely related to the efficiency of sediment transport through the reach (Gilbert, 1914; Mackin, 1948).

Valley train materials. Both lobes of the Kaskawulsh Glacier and the Hoffellsjokull of Iceland have recently melted back from moraines and have formed debris-collecting lake basins between the receding glaciers and their moraines.

Slims River now deposits in the lake basins much of the load derived from the glacier. The coarser fraction is trapped and all but the silt and clay is lost as the flow passes through the ponds along the glacier margin. The two channels of the Slims River passing through the moraine have entrenched 3 ft. or more below the main channel and as much as 8 ft. in the right bank channel. This trenching is apparent for a half mile along the main stream and for more than one mile in the right bank channel. Similar entrenching occurred in the upper reaches of the Hoffellssandur.

The down-valley decrease in grain size is quite marked in the Slims River valley (Table 3). Pebble counts of the valley train material at the moraine indicated median dia-

Fig. 6. View downstream of the intermediate and downstream zones of Slims River valley showing complex system of channels. Photo by Walter Wood.

meters of 7/8 in. to 2 in. (22 to 52 mm). Lag materials as large as 0.6 ft. (180 mm) were left on the channel bottom when the finer materials were washed out. Most other materials near the moraine were much finer, including those in newly formed bars.

During a discharge measurement made just downstream from the moraine, movement of at least cobble-sized material was noted at average velocities which ranged from 5.5 – 6 ft./sec. (computed by dividing discharge by the cross sectional area of the stream). The highest velocity measured near the bed of the stream was 5.6 ft./sec., at 1.3 ft. above the bed. How far material of this size was transported is not known; its source may have been the nearby moraine.

Within 3 mi. of the moraine, the coarsest particles of the valley train were about 1 in. (25 mm) in diameter, and large amounts of sand were present. Within 5 mi. of the moraine there was no gravel in the main channels, although gravels derived from adjacent fans might have been incorporated in the deposits along the margins. In the reaches having a fine sand bed at about mile 4, the bed was soft (quicksand in some places), the velocities were relatively low, and ripples and dunes were the dominant bed form. Flume studies have suggested that individual pebbles and cobbles are not transported with such bed forms, but, when placed on a sand bed in a flume, roll into scour pockets and are buried (Fahnestock and Haushild, 1962). Such a process might well explain the absence of any gravels introduced from the moraines or side stream fans in the lower Slims River valley.

Median diameters of bed and bank materials collected for the study by M. E. Alford at mile 11.2 were all finer than 230 mesh. Materials sampled during the summer of 1963 showed a decrease in size, from gravel to sand, in the first 3 mi. below the moraine, and a gradual decrease in the sand size materials farther downstream (S. Chadhuri, written communication).

The marked changes in size down the 14 mi. of the Slims River valley train were clearly the result of selective transport and not abrasion or weathering. Much greater distances of transport produce much smaller changes in size in graded streams, that is, in streams more nearly adjusted to transporting all of the sediment supplied. Large size changes in short distances are the rule on an aggrading surface.

TABLE 3. Summary of Valley Train Characteristics

River	Valley train length	Drainage area ($mi.^2$)	Discharge ($ft.^3/sec.$)	Zone 6	Length (mi.)	Slope (ft./ft.)	Debris size	Glacier Position
Slims River, Yukon Terr.	14 mi. (moraine to lake)	ice 560 land 240 800 (above moraine)	8^3 to $15{,}000^4$	U	0.7	0.0019	coarse gravel	1 mi. upstream of moraine (1965)
				I	3	0.0033 – 0.001	med. gravel, sand	
				D	3+	0.0003	sand, silt	
White River Mt. Rainier, Washington	1.1.mi. (glacier to moraine)	ice 5.0 land 2.5 7.5	30^3 to 500^4	U	0.3	0.05 – 0.15	up to 2 ft. (diameter)	1.1 mi. upstream of moraine
				I	0.8	0.015 – 0.05	up to 1 ft. (diameter)	
Hoffellssandur,[1] Iceland	7 + mi. (moraine to sea)	ice 120 land 50 170	100^3 to 5000^4 1000^5 to 9000^5	U	2	<0.007 stream >0.01 valley train	up to 2 ft. (diameter)	0 – 0.2 mi. upstream of moraine (1951)[2]
				I	2 (about)	0.007^2	decreases to fine sand	
				D	3 –	$<0.007^2$		

[1] Based on data from Arnborg (1955).
[2] Based on data from Sundborg, (1952).
[3] Winter.
[4] Summer.
[5] Sum of glacier bursts and normal summer flows.
[6] U (upstream), I (intermediate) and D (downstream) zones (after Krigstrom, 1962) are discussed elsewhere in this paper.

Lateral erosion. A striking aspect of the Slims River valley train was the small amount of lateral erosion. However, at several points near the right-bank margins of the valley train at mile 7.5, boulders were found in or on valley train materials under water. These may have been derived by minor erosion of fan margins or may simply have projected above the buried surface of fan deposits. Such boulders might have been transported across the unconsolidated river silts by mudflows.

The lack of lateral erosion was at least in part a function of the rapid filling of the valley and the lack of a coarse bed load transported by the main stream over most of the valley train. Except for Canada Creek, there were no large fans entering the valley where the valley train was dominantly gravel. Filling appears to be the dominant valley widening process. If the rate of filling had been slower, the mainstream load coarser, or the fan and valley walls less resistant, this would probably not be true.

In contrast, Hjulstrom (1954) briefly described an Icelandic strandflat and ascribed it to lateral erosion on bedrock by a sandur stream. Krigstrom (1962) suggested that a similar lateral erosion was demonstrated in bedrock benches along the Markarfljot in Iceland. At White River, the writer measured lateral erosion of more than 10 ft. in two hours in unconsolidated materials adjacent to the valley train.

No bedrock benches were found in the Slims River valley floor, perhaps due to the filling of the valley. Time may have been an important factor in this lack of lateral erosion. With the rate of upbuilding on the valley train and the rapid shifting of channels, a stream channel would have flowed against the same portion of the valley wall for only a few tens of years at most and more likely for only a few years. The valley wall materials were subglacially plastered till, or bedrock freshly scoured by ice. The fans which showed little or no sign of erosion on their margins had obviously all been growing rapidly and recently, and any cutbanks developed might have been buried by the combined upbuilding of the valley train and extension of the fans.

Sandur Zones

Krigstrom (1962, pp. 329 – 330) described three zones on Icelandic sandurs. The zone nearest the glacier he called the proximal zone and described it as characterized by a few incised, gently sinuous channels commonly with one distinct main channel. A zone farther downstream occupied the larger part of the sandur . According to Krigstrom, " . . . the channel gradually widens and becomes shallower. The banks become less well defined and the channel may merge into a plane on which the streams no longer can be kept together." He notes that in this zone, forkings and junctions become more numerous and the boundaries between the individual streams become increasingly more difficult to determine. Furthermore, he says, "In a zone furthest downstream the intertwined streams merge into a shallow bay with streaming water."

Similar zones were recognized on the Slims River valley train during the flows capable of modifying the form and pattern of the stream. In the upstream zone there were from 1 to 3 channels separated by large islands. At the moraine this upper zone had 2 channels and broad gravel surfaces scarred by many dry channels. These channels became entrenched when the coarse fraction of the load was deposited in the debris basin behind the moraine. During this deposition, water surface slopes must have been equal to or greater than water surface slopes in the present intermediate zone. The water surface slope of the 1965 upstream zone was less than that of the intermediate zone. Cross-sectional relief was greater than in the other zones, and coarse to medium gravels were dominant. Seldom, if ever, would the uppermost reaches of Slims River have been completely flooded because of the high slopes.

In both the upstream and intermediate portions of the Slims River valley train, many streams started at points where abandoned channels intersected the water table. Many of these streams were milky, indicating a relative lack of filtration by the permeable valley train materials. Many minor streams were simply overflows from larger channels which occupied old channels but modified them only slightly, if at all. When enough of these streams joined, a major stream was formed which might fill and rapidly modify its channel.

The number of channels in the intermediate zone continually changed as bars formed in a channel, divided it, or raised the water surface until old channels were reoccupied (Figure 6). As Krigstrom (1962) has indicated, the channel and bar formation typical of the intermediate zone was not dependent upon a few very high flows. Instead, the normal flows of the melt season both formed and altered the bars. The sediments were medium to fine gravel and sand. Most sand and all silt occurred in protected spots where the water was quiet.

At a flow of about 10,000 ft.^{3}/sec. in one of the widest gravel bed reaches at mile 1.5 (Section 4, Figure 7), as many as 30 channels covered half of the 6000-ft.-wide valley floor and most bars were less than 1 ft. out

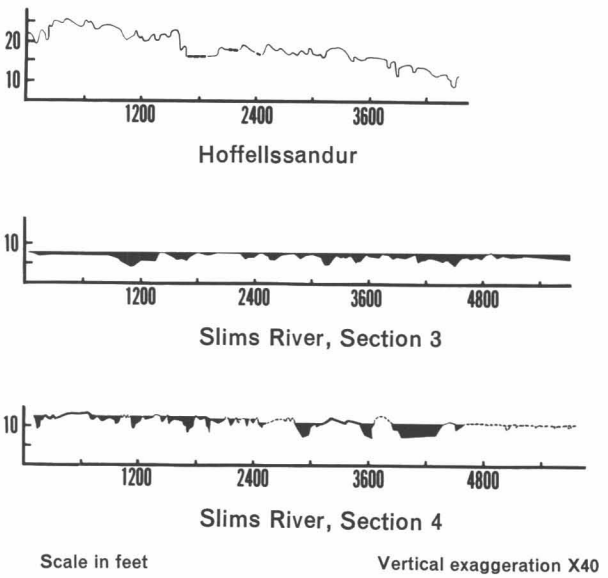

Fig. 7. Comparisons of surface relief on valley-train cross sections.

of water. The valley train here had a slope of about 16 ft./mi. The range in slope over the intermediate zone was 5 – 16 ft./mi. A maximum depth of 4 ft. and a velocity of 5 ft./sec. were found in separate channels of Section 4, while the average depth for all channels was on the order of 1.3 ft. The width – depth ratio was 2300:1.

The intermediate zone of the Slims River had much less relief than streams described by Krigstrom (1962). The relief across the Hoffellssandur recorded by Hjulstrom (1952, 1954) and further described by Krigstrom (1962) was more like that of White River than that of the Slims River (Figure 7). The relatively low Slims River cross-sectional relief is thought to be a function of the lower slope and the nature of the shifting equilibrium.

The Slims River valley train in the downstream zone from mile 5 had very little gravel on its surface. The channels became wider until they were literally a sheet of flowing water with only occasional isolated bars from about mile 5 to mile 7. The load was predominantly sand and silt. In the widest sand bed reaches, 6.2 mi. from the moraine (Section 3, Figure 7) on a slope of 4.5 ft./mi., as many as 20 channels merged into a moving sheet of water 5700 ft. wide at high flows. A maximum depth of 3.5 ft. and a velocity of 2.3 ft./sec. at a depth of 0.6 ft. were found in the main channel of this cross section. The average depth of flow on this cross section was 0.8 ft. and the width – depth ratio was 7100:1.

Downstream between mile 7 and mile 11, the large sidestream fans narrow the valley train to about 1000 ft. In this reach at lower flows, a few bars appeared,

and at much lower flows, bars were the dominant form. An example of the change in the channel with a change in river stage is shown in Figure 4 for Sections 1 and 2.

Stream Equilibrium

The present Slims and White Rivers and the rivers of Iceland are modifying valley trains deposited when the glaciers were up against terminal moraines. The present valley trains exhibit characteristics of regrading, that is, the stream channels are adjusting to a decrease in load at the source by cutting in the upper reaches and depositing in the lower reaches. In addition, the equilibrium of the Slims River is affected by downstream changes in base level.

The three zones described by Krigstrom (1962) are thought to correspond to the zones of a regrading stream. The upstream zone is a degrading reach or one approaching equilibrium after degradation (Mackin, 1948). The intermediate zone, characterized by a high sediment transport rate, is either in equilibrium, slowly degrading, or slowly aggrading. The downstream zone is an aggrading reach dominated by a sand and silt load constantly interchanged between bed and suspended load. As flow conditions vary, the zone boundaries migrate upstream and downstream. All three zones may not exist on all valley trains.

Changes in load or flow reflect variations in precipitation, glacier flow, and melting. The character of the interstream surfaces in the upstream zone suggests that during deposition, when the glacier was up against the moraine, channels were more numerous and there was relatively little relief. An "upstream" zone did not exist at that time; the area instead must have resembled the present intermediate zone.

The gradual melting back of the Kaskawulsh Glacier since the late 1800's suggests a slight negative change in the glacier budget for the Kaskawulsh basin. Although water discharge may have decreased, the effects appear to have been more than offset by the entrapment of load at the retreating glacier margin. Fluctuations in the proportion of discharge going to the Kaskawulsh River provide an additional complication. The net effect has been scour in the upstream zone resulting from a deficit of gravel load for the pre-existing valley train slope. The present water-surface slopes in the upstream zones of the Slims and Hoffellssandur Rivers are more gentle than pre-existing valley-train slopes, and the water-surface slopes in the upstream zones are lower than the water-surface slopes in the present intermediate zones. This reflects more efficient transport of sediment in a single channel.

For the Slims River, the downstream base level controls are the extension of the delta into Kluane Lake and the variation in lake level. Bostock (1952, p.8) reports from local information that the lake level varied as much as 10 ft. between 1900 and 1945 and has had both higher and lower levels during the building of the valley train. Johnson and Raup (1964, p. 27) suggest, on the basis of lichen development, that within the previous 50 years the lake has been no higher than 4½ ft. above the 1944 level.

River silts were present at places adjacent to the stream from mile 8 to the mouth, 3 – 5 ft. above the 1965 water surface. A lower level at least partially occupied by high water and devoid of vegetation may be related to the present lake level and delta position. M. E. Alford (written communication) reports conversations with early residents of the area who had boated over the flats on which the present highway bridge now stands. It is probable that these silt flats are related to such high lake levels. The lake level depends on the inflow from the Kaskawulsh – Slims drainage basin and on the level of the lake outlet, which is controlled by the level of the Duke River alluvial fan over which the lake outlet flows.

The extension of the delta and construction of the 14 mi. of valley train has taken place in less than 2600 years (Denton and Stuiver, 1966; Borns and Goldthwait, 1966) and possibly no more than 500 years (Bostock, 1952, p. 8). The rate of delta advance must have fluctuated widely depending on the level of Kluane Lake, the depth of the water into which the delta was advancing, and the sediment supply to the delta front. Only remnants are left of the older, higher Vulcan Creek and Sheep Creek fans which must have filled the valley when they were fully developed (Borns and Goldthwait, 1966) (Figure 5). Their presence would have increased the rate of the Slims delta advance through this reach as contrasted with the delta's advance in the deeper water of the present Kluane Lake or earlier lakes in the Slims River valley. The present configuration of the downstream valley floor could be explained by a higher lake level in the early 1900's which caused deposition on the lower part of the valley train. A subsequent drop to the 1965 lake level would have brought about a slight trenching of the valley flats (mile 11 to the lake) developed in the previous episode. This is perhaps the simplest explanation for the present (1965) forms.

A depositing stream may be at or near equilibrium if the total quantity of transport is so much larger than the amount deposited that the stream system is nearly in balance (Mackin, 1948). The present rate of building of the Slims River delta of 160 to 240 ft./yr. (Bostock, 1952) clearly demonstrates considerable transport through the Slims River valley train. The volume growth rate of the delta is not known, so the sediment transport rate cannot be estimated. The brimful aspect of the valley train from mile 1.5 to mile 7 shows no evidence of higher levels and suggests that this portion of the valley train is a locus of deposition. Eroded banks of river silt stood 5 ft. or more above the river surface along the lower parts of the tributary fans during the 1965 summer study period (Figure 5). This bank-cutting along the portion of the valley train from the Bullion Creek fan to the mouth was providing some of the materials going into the extension of the delta.

Previous Work on the History of the Slims River – Kluane Lake Valley

As summarized by Borns and Goldthwait (1966) from their own work and that of Denton and Stuiver (1966), Krinsley (1965), Wheeler (1963), and Bostock (1952), loess deposits 15 mi. up valley from the moraine of the Kaskawulsh Glacier indicate that it had retreated considerably up valley from its present position by 12,000 years ago and began to advance approximately 3000 years ago (Table 4). Borns and Goldthwait (1966) mapped 3 moraines of the Slims River lobe. These became stabilized about 1820, 1870, and 1940 respectively, as dated by vegetation recovery.

When there was an active valley train or one recently abandoned in the Slims River Valley, clouds of dust were deposited in a considerable thickness of loess over the surrounding countryside. Bostock (1952), Johnson and Raup (1964), Denton and Stuiver (1966), and Borns and Goldthwait (1966) have worked out a stratigraphy for these deposits, separating them into an upper unweathered loess called the Neoglacial loess and a lower thicker unit, the Kluane Loess, with a weathered zone called the Slims Soil. An ash layer mapped in some detail by Bostock (1952) was found by the other investigators in most deposits near the base of the Neoglacial loess. Capp (1915) and Stuiver, Borns, and Denton (1964 and pp. 219 – 220 of this volume) have dated the ash at about 1425 ± 50 years B.P. The Kluane loess has been dated as accumulated between 9800 and 2600 years ago (Denton and Stuiver, 1966). This period includes both the accumulation of loess and the development of the Slims Soil.

Former lake levels. Bostock (1952) describes the evidence for the former levels of Kluane Lake and cites soundings which indicated that the lake deepens to the southeast or Slims River inlet end. As causes of the fluctuations in lake level, Bostock suggests: (1) variations in the level of the Duke River fan which forms the threshold over which Kluane Lake now spills to the northwest, and the possibility that the Duke River flowed into Kluane Lake rather than joining the Kluane River downstream of the lake, (2) " . . . much of the water from the glacier to its source, which normally flows to Slims River, escaped to Kaskawulsh River as evidenced by the dry channels between the heads of these rivers at the front of the glacier," and (3) variation in precipitation, melting, and runoff.

It must be noted with reference to (2) above that all dry surface channels between the two streams drained *from* the Kaskawulsh *to* the Slims. The oldest and highest valley train surface, mile –2 to about mile + 1.5 (Figure 2) along the right side of the valley train is related to the outlet from the Kaskawulsh Glacier lobe to the Slims River valley. Small bushes have become established on this surface. At least three outlets through the left moraine of the Kaskawulsh lobe lead to this surface. Between the two outlets through the Slims lobe moraine and the junction of the streams is a triangle of slightly lower valley train unoccupied by surface flows for many years. In addition to mosses and grasses, only a few hardy plants have become established, probably because of the excellent drainage of the valley train gravels this close to the glacier and the relatively large depth to the water table. No trees were found although the surface was probably contemporaneous with Drift II or perhaps Drift I, both with trees (Borns and Goldthwait, 1966). This surface sloped across the moraine front from east to west and is thought to be a continuation of the surface related to the now unoccupied outlet from the Kaskawulsh Glacier lobe (mile –2). These two surfaces are separated by the stream from the right outlet which has entrenched as much as 10 ft.

Surface runoff downstream from the moraines resulted in additions to the Slims River rather than losses. However, subsurface conditions may have favored drainage to the Kaskawulsh River, for where it left the glacier it was more than 100 ft. lower than the Slims River.

Bostock (1952, p. 8) suggested that the only way to obtain the lowest Kluane Lake levels, for which there is evidence, was by drainage through the Slims and Kaskawulsh valleys to the southeast prior to the most recent advance of the Kaskawulsh Glacier. The long profile of the Slims River valley (Figure 2) suggests that this was probable. The elevation just beyond the head of the valley train is lower than the surface of Kluane Lake. Seismic work by R. P. Goldthwait (written communication) suggests that there is no bedrock within 100 – 200 ft. of the surface in the vicinity of the outermost moraine (mile 0).

The active ice of the glacier was certainly hundreds of feet thick and this would place the threshold over which Kluane Lake could have spilled well below the present level of the lake. Some idea of a minimum thickness of the Slims lobe of the glacier can be obtained from the thickness of ice exposed in the Kaskawulsh valley. The height of many ice faces is about 100 ft. above the point where the Kaskawulsh River passes through the moraine. In addition, there may be a considerable thickness below this level.

This bedrock threshold was not the only possible barrier to a southward flow of the Slims River, however, the ancient fans of Bullion and Sheep Creeks from the west and Vulcan Creek from the east must have affected the profile of a reversed Slims River much as the Duke River fan now affects the Kluane River. Borns and Goldthwait (1966) suggested, on the basis of a capping of Kluane loess, that these ancient fans reached their maximum elevations not too long after the end of the last major glaciation. Not only would these fans have been as effective as the Duke River fan in damming Kluane Lake, but the flow attacking this barrier would have lacked the drainage from the Kaskawulsh Glacier. In 1965 the Slims River probably contributed more than one half the flow of the present Kluane River. With such a sizable reduction in flow, modifications of barriers in the Slims River valley may have taken place much more slowly than have modifications of the Duke River fan.

It could be that, for a period, the coalesced deltas of Bullion, Sheep, and Vulcan Creeks served as one dam, and the ice of the re-advancing Kaskawulsh Glacier as another, forming two lakes in the Slims – Kluane valley.

Bostock (1952, p. 8) suggested that, as a result of the present continued retreat of the glacier and the steep gradient of the Kaskawulsh River in contrast with the Slims River, the recapture of the Slims by the Kaskawulsh was apt to begin in the near future. The capture of Kluane Lake might follow when a channel had cut back through the unconsolidated drift fill on the floor of Slims valley.

With the Slims River flow erupting from beneath an alluvial fill under a considerable head and with more than a 100-ft. difference in elevation between the valley train at the Kaskawulsh and Slims lobe moraines, a

TABLE 4. Summary of the Post - Kluane (Wisconsin) History of the Slims Area

Years before present (1965)	Glacier	Side stream fans	Loess and soil	Kluane Lake Slims delta
0	Drift IV[1,4]	Extensive development of modern fans, named creeks, and smaller fans		Slims River drained to Kluane Lake and west
40	Ice retreated from moraine of drift III[1,4]			Delta growth into Kluane Lake
77	Ice retreated from moraine of drift II[1,4]		Neoglacial Loess deposited	Valley train of Slims River developed
129	Ice retreated from moraine of drift I[1,4]			
165	Kaskawulsh Glacier advance ceased[2]			
285	Kaskawulsh Glacier reached terminal position about this date[1,4]			Slims River and Kluane Lake valleys flooded to 30 ft. above 1945 elev. when Slims outlet to Kaskawulsh River blocked by glacier[2]
450	Kaskawulsh Glacier advanced. Neoglacial expansion[1,4]			
1425 ± 50			Volcanic ash near base of Neoglacial loess[3,5] which buried Slims Soil	
2600 – 3000	Start of Neoglacial advance[1,4]	Before 2640 Sheep, Bullion, Vulcan Creek fans aggraded then partially degraded; possibly coalesced across Slims valley[1]		Dammed by fans? Drainage alternated west and east?
	Retreated 30 mi. above Kluane Lake valley[4]		Kluane Loess stopped accumulating before 2640 BP; Slims Soil developing	
9700			Kluane Loess buried 9700-yr.-old grass near terminus	
12500	Withdrawal of last Kaskawulsh Glacier expansion into Shakwak Trench			

[1] Borns and Goldthwait, 1966.

[2] Bostock, 1952.

[3] Capps, 1915.

[4] Denton and Stuiver, 1966.

[5] Stuiver, Borns, and Denton, 1964.

break-through under the glacier appeared possible in 1965. During the summer of 1967, such a break-through took place. The flow of the Slims River has been reduced by the amount of the glacier contribution, and blowing dust derived from the Slims River valley train has become much more severe than it was in 1965. During the winter of 1967 – 1968, the Kaskawulsh discharge returned to the Slims River valley only to be lost again during the summer of 1968.

Summary and Conclusion

The Slims River valley train is analogous to the Pleistocene valley trains that existed in many places in North America and elsewhere. Its study provides an insight into the phenomena which are recorded in the alluvial fills. Because of the abundance of fine materials it serves as a source of large amounts of loess. The adjustment of slope to channel pattern and form and the rapid response of the stream to changes in load indicate the near-equilibrium conditions under which the valley train formed and is being modified. The evidence supports the post-glacial drainage reversal for the Slims system suggested by Bostock.

Acknowledgments

R. P. Goldthwait of The Ohio State University suggested the Slims River for study. Logistical support was provided by the Icefield Ranges Research Project. Richard H. Ragle, Philip P. Upton, Walter A. Wood, and Sam G. Collins, in particular, assisted in many ways. William L. Haushild, Jr. served ably as field assistant. M. E. Alford and the Inland Waters Branch of the Department of Energy, Mines and Resources of Canada made essential data and equipment available. The research was supported by National Science Foundation Grant GP–2814.

References

Arnborg, L. (1955) Hydrology of the glacial river, Austurfljot, GEOGR. ANNAL., 37, 185 – 201.

*Borns, H. W. Jr., and Goldthwait, R. P. (1966) Late-Pleistocene fluctuations of Kaskawulsh Glacier, southwestern Yukon Territory, Canada, AM. J. SCI., 264, 600 – 619.

Bostock, H. S. (1952) Geology of northwest Shakwak Valley, Yukon Territory, CANADA GEOL. SURV. MEM. 267, 54 pp.

Capps, S. R. (1915) An ancient volcanic eruption in the upper Yukon basin, U.S. GEOL. SURV. PROF. PAPER 95, pp. 59 – 64.

Chien Ning (1961) The braided stream of the lower Yellow River, SCIENT. SINICA, 10, 734 – 754

*Denton, G. H., and Stuiver, M. (1966) Late Pleistocene glacial chronology, northeastern St. Elias Mountains, Canada, AM. J. SCI., 264, 577 – 599.

Fahnestock, R. K. (1963) Morphology and hydrology of a glacial stream – White River, Mt. Rainier, Washington, U.S. GEOL. SURV. PROF. PAPER 422A, 70 pp.

Fahnestock, R. K., and Haushild, W.L., Sr. (1962) Flume studies of the transport of pebbles and cobbles on a sand bed, GEOL. SOC. AM. BULL., 73, 1431 – 1436.

Fahnestock, R. K., and Maddock, T., Jr. (1964) Sediment transport, bed form and flow resistance of the Rio Grande near El Paso, Texas, U.S. GEOL. SURV. PROF. PAPER 501-B, pp. B140 – B142.

Gilbert, G. K. (1914) The transportation of debris by running water, U.S. GEOL. SURV. PROF. PAPER 86, 263 pp.

Harms, J. C., and Fahnestock, R. K. (1965) Stratification, bed forms and flow phenomena (with an example from the Rio Grande), in PRIMARY SEDIMENTARY STRUCTURES AND THEIR HYDRODYNAMIC INTERPRETATION, SOC. ECON. PALEONTOL. MINERAL. SPEC. PUB. 12, pp. 84 – 115.

Hjulström, F. (1952) The geomorphology of the alluvial outwash plains of Iceland and the mechanics of braided rivers, INTERNAT. GEOGR. CONGR., 17TH, WASHINGTON 1952, EIGHTH GENERAL ASSEMBLY PROC., pp. 337 – 342.

Hjulström, F. (1954) Geomorphology of the area surrounding the Hoffellssandur, Chap. 4 OF The Hoffellssandur – a glacial outwash plain, GEOGR. ANNAL., 36, 169 – 189.

Johnson, F., and Raup, H. M. (1964) Investigations in southwest Yukon: geo-botanical and archaeological reconnaissance, ROBERT S. PEABODY FOUND. ARCHAEOL. PAPERS, Vol. 6, No. 1, 198 pp.

Krigstrom, A. (1962) Geomorphological studies of sandur plains and their braided rivers in Iceland, GEOGR. ANNAL., 44, 328 – 346.

Krinsley, D. B. (1965) Pleistocene geology of the southwest Yukon Territory, Canada, J. GLACIOL., 5, 385–397.

Mackin, J. H. (1948) Concept of a graded river, GEOL. SOC. AM. BULL., 59, 463 – 511.

*Stuiver, M., Borns, H. W., and Denton, G. H. (1964) Age of a widespread layer of volcanic ash in the southwestern Yukon Territory, ARCTIC, 17, 259 – 260.

Sundborg, A. (1954) Map of the Hoffellssandur, Chap. 3 OF The Hoffellssandur – a glacial outwash plain, GEOGR. ANNAL., 36, 162 – 168.

Wheeler, J. O. (1963) Geologic map of Kaskawulsh half of Mt. St. Elias map sheet, Yukon Territory, CANADA GEOL. SURV. MAP 1134A.

*These articles are reprinted in the present volume.

Neoglacial Chronology, Northeastern St. Elias Mountains, Canada*

George H. Denton† and Minze Stuiver‡

ABSTRACT. In the northeastern St. Elias Mountains, Yukon, Canada, drift morphology and stratigraphy, combined with thirteen C^{14} dates, suggest the following Neoglacial and pre-Neoglacial chronology for the Donjek and Kaskawulsh Glaciers: (1) About 12,500 B.P. (Y-1386) ice of the Kluane glaciation (= classical Wisconsin by C^{14} dating) receded from near Kluane Lake and about 9780 B.P. (Y-1483) withdrew behind the position presently occupied by Kaskawulsh Neoglacial moraines. (2) During the Slims nonglacial interval (basically Hypsithermal), glaciers maintained retracted positions; the Kaskawulsh terminus was located at least 13.7 miles up-glacier from its present position. (3) The initial Neoglacial advance, represented by onset of loess deposition, began shortly before 2640 B.P. (Y-1435). (4) Continuous loess deposition suggests that throughout the Neoglaciation glaciers maintained positions more extensive than those occupied during the Slims interval. (5) The youngest major Neoglacial advance, the most extensive of the last 9780 years (Y-1483), occurred through the last few centuries and is bracketed by seven C^{14} dates. Glacier retreat from this maximum began before A.D. 1874 (Donjek Glacier) and A.D. 1865 (Kaskawulsh Glacier).

Comparison of northeastern St. Elias events with those elsewhere supports the concepts that (1) the initial widespread Neoglacial advance shortly antedated 2600 to 2800 B.P. and (2) at least some major Neoglacial events were essentially synchronous throughout the Northern Hemisphere.

Introduction

The purpose of this study was (1) to establish a firmly dated Neoglacial chronology of glaciers in the northeastern St. Elias Mountains and (2) to use this chronology to test and complement existing concepts of widespread Neoglacial fluctuations in the Northern Hemisphere.

The term Neoglaciation is used here in the sense proposed by Sharp (1960, p. 321) as "a short convenient designation for a readvance of ice subsequent to shrinkage during the Hypsithermal interval." In this sense the Neoglaciation (1) is basically equivalent to the "little ice-age" of Matthes (1939, pp. 519-520; 1940, pp. 398-403; 1942, pp. 212-214) and (2) includes all glacier fluctuations during the sub-Atlantic time of northwestern Europe.

The St. Elias Mountains are located in southwestern Yukon Territory, northwestern British Columbia, and southeastern Alaska (Plate 2)[1]; the international boundary between Alaska and Canada passes through the mountains. Much of the central part of the mountains, which includes many of the highest peaks in Cordilleran North America, is presently mantled with an extensive intermontane icefield which is drained on all sides by long outlet valley glaciers. The Neoglacial history and chronology of two of the largest of these, the Donjek (Figure 1) and Kaskawulsh Glaciers, are discussed here. Both glaciers are located within the Yukon Territory on the northeast flank of the mountains (Plate 2). In addition, the Neoglacial history of the Silver and Cairnes Glaciers[2], two small valley glaciers on the northeast border of the mountains, is described.

*This report has previously appeared in *American Journal of Science,* 1966, Vol. 264, pp. 577-599, and is reproduced with permission.

†Department of Geology, Yale University, New Haven, Connecticut.

‡Director, Radiocarbon Laboratory, Yale University.

[1] Plate 2 is a folded map accompanying this volume.

[2] In order to facilitate the following discussion, the names Silver and Cairnes Glaciers are used for two small unnamed valley glaciers on the northeast flank of the St. Elias Mountains (Figure 6).

Pre-Neoglacial Drift and Events

In the northeastern St. Elias Mountains, Yukon Territory, drift morphology and stratigraphic relations of drift sheets and weathering zones indicate that the Neoglaciation was preceded by at least three glaciations and three nonglacial intervals (Denton, ms; Denton and Stuiver, 1967). All three glaciations included ice advances substantially more extensive than those of the Neoglaciation. A summary of these pre-Neoglacial events, with bracketing C^{14} dates, is given in Table 1.

Ice of the Kluane glaciation had receded to the vicinity of the mouth of Slims River valley shortly before 12,500 B.P. as indicated by organic matter from the base of a Kluane kettle (Y-1386) and by 9780 B.P. had withdrawn behind the position presently occupied by Neoglacial moraines fronting the Kaskawulsh Glacier as indicated by grass buried in place at the base of Kluane loess near these moraines (Y-1483). During this recession a widespread layer of loess derived from active Kluane outwash bodies was deposited on all older units of Kluane Drift. This Kluane loess varies in thickness from 14 to 40 inches. Subsequent withdrawal of glaciers into the St. Elias Mountains caused these active outwash bodies on the outskirts of the mountains to become nearly or totally inactive and covered with vegetation. With the source of silt thus removed, deposition of loess ceased or nearly ceased, allowing weathering of the upper 12 to 16 inches of Kluane loess throughout the region. This weathering produced the the Slims Soil (Figure 1).

The Slims Soil occurs on Kluane loess which overlies most pre-Neoglacial deposits below 4500 feet altitude. Near the Donjek and Kaskawulsh Glacier termini the soil is overlain by Neoglacial moraines; near presently active valley trains it is sharply overlain by nonweathered Neoglacial loess. Although the soil is absent on the Neoglacial moraines fringing the present Donjek and Kaskawulsh Glacier termini, it occurs widely on pre-Neoglacial deposits immediately adjacent to these moraines (Figures 2 and 3). Additionally, it is present on the west side of the Kaskawulsh Glacier as a nearly continuous sheet through 8 miles above the terminus and as discontinuous patches

A.

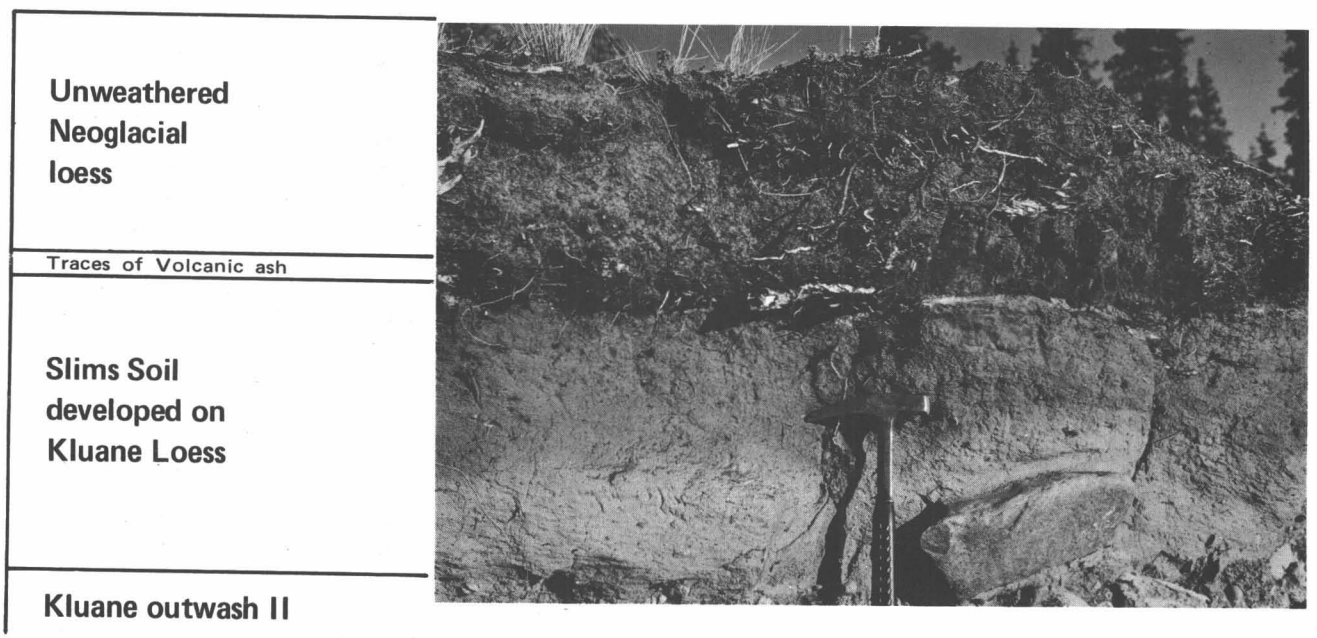

B.

Fig. 1. Neoglacial features, northeastern St. Elias Mountains. A. Aerial photograph of Donjek Glacier terminus and St. Elias Mountains. Photograph taken in summer of 1941 by Walter A. Wood. B. Loess sequence showing, from top to bottom. Neoglacial loess, traces of volcanic ash, Slims Soil developed in Kluane loess, and the upper surface of Kluane outwash II.

through an additional 5.7 miles (Figure 3). The last up-glacier occurrence of Slims Soil is on a bedrock knob 13.7 miles up-glacier from the present terminus and 15 miles from the outermost Neoglacial moraines that fringe the terminus.

The Slims nonglacial interval, which derives its name from the Slims Soil, is the time-transgressive interval that separated the Kluane glaciation from the subsequent Neoglaciation. Radiocarbon dates of the retreat of Kluane ice and the advance of succeeding Neoglacial ice bracket this interval between 2640 (Y-1435) and 9780 (Y-1483) to 12,500 B.P. (Y-1386) and indicate that it includes the Hypsithermal interval as defined by Deevey and Flint (1957, p. 182).

A minimum value of glacier retreat during the Slims nonglacial interval can be obtained from the areal distribution of Slims Soil and Neoglacial loess as follows: (1) all soil localities must have been evacuated by glacier ice, and (2) because Slims Soil formation was related to cessation of loess deposition resulting from deactivation of nearby valley trains, glaciers must have retreated from the immediate vicinity of all soil localities. Substantial retreat is indicated by the occurrences of Slims Soil sharply overlain by Neoglacial loess on the west side of the Kaskawulsh Glacier through 13.7 miles up-glacier from the present terminus. For the vicinities of its occurences, this loess-and-soil sequence (Figure 1) implies (1) loess deposition, (2) cessation of loess deposition, and (3) renewed loess deposition. These events are in turn related to withdrawal of the Kaskawulsh Glacier terminus more than 13.7 miles up-glacier from its present position, followed by renewed advances subsequent to soil formation. This argument for substantial retreat is supported by the continuous, well-defined nature of the soil bordering the lower Kaskawulsh Glacier, which suggests lack of a nearby active valley train during soil formation. A similar argument applies to the Donjek Glacier, where large areas of well-developed soil fringing the terminus suggest retreat during soil formation.

TABLE 1

Late Pleistocene glacial events, with bracketing C^{14} dates; northeastern St. Elias Mountains. Ages in C^{14} years B.P.

Neoglaciation
Start ~ 2640; still current
Slims nonglacial interval
Start ~ 12,500 to 9780; End ~ 2640
Kluane glaciation
Start < 30,100; end ~ 12,500 to 9780
Boutellier nonglacial interval
Start ~ 37,700; end < 30,100
Icefield glaciation
Start > 49,000; end ~ 37,700
Silver nonglacial interval
> 49,000
Shakwak glaciation
> 49,000

Neoglacial Drift

Neoglacial drift, the youngest drift in the northeastern St. Elias Mountains, occurs as loess near presently active valley trains, as well-preserved end-moraine sediments near glacier termini, as small bodies of lacustrine sediment, and as active outwash bodies extending down-stream from glacier termini. In the following discussion the terms Donjek, Kaskawulsh, Silver, and Cairnes drifts are used informally to apply to Neoglacial end-moraine, outwash, and lacustrine sediments surrounding and extending downstream from the termini of these glaciers,

Volcanic ash. A distinct layer of white volcanic ash described in detail by Capps (1916), Bostock (1952, p. 36), and Stuiver, Borns, and Denton (1964) appears at the base of or within Neoglacial loess. In the area of the Donjek and Kaskawulsh Glaciers, the ash ranges in thickness from 0.5 to 1.0 inch. Because it is everywhere synchronous, the ash affords a means of correlating and determining the relative age of Neoglacial drift. Radiocarbon dates (Y-1364 and Y-1363) bracketing the ash indicate that it was deposited about 1425 ± 50 B.P. (Stuiver, Borns, and Denton, 1964).

Loess[3]. Wherever observed, Neoglacial loess (Figure 1) rests on the Slims Soil developed on underlying Kluane loess. The contact is sharp except in a few places where redistribution has resulted in mixing of the two loess units. Because deposition is continuing, Neoglacial loess is not overlain by other sediments, except locally where Donjek and Kaskawulsh end-moraine sediments overlie the basal part of the loess.

Sedimentary and mineralogical characteristics of Neoglacial loess are nearly identical with those of nonweathered Kluane loess. Neoglacial loess consists of well-sorted silt and fine sand; the mineralogy of the particles is complex and reflects the wide variety of bedrock lithologies traversed by the glaciers. Neoglacial loess is not weathered, in sharp contrast to the weathered upper part of the underlying Kluane loess. Along the southeast shore of Kluane Lake, Neoglacial loess is duned and commonly contains buried stumps of white spruce (*Picea glauca*) in growth position. Neoglacial loess is thickest in valley bottoms, thins on gentle valley slopes, and is generally absent from valley walls above about 4500 feet. Although rarely present on the Neoglacial moraines, the loess forms a blanket averaging 30 inches thick on all pre-Neoglacial deposits adjacent to the Donjek and Kaskawulsh Glacier termini and averaging 6 to 15 inches thick on the Slims Soil bordering the west side of the Kaskawulsh Glacier (Figure 3). Additionally, Neoglacial loess covers all pre-Neoglacial deposits fringing the upper Kaskawulsh River and the entire Slims River; average thickness decreases from 30 inches near the Kaskawulsh Glacier to 10 inches near the delta of Slims River. The thickness of Neoglacial loess in Shakwak Trench decreases both northwest and east from the Slims River delta. Northwest, along the southwest shore of Kluane Lake, the average thickness decreases from

[3]Neoglacial loess was informally called Slims Valley silt by Sticht (1963) and Slims River Silt by Johnson and Raup (1964).

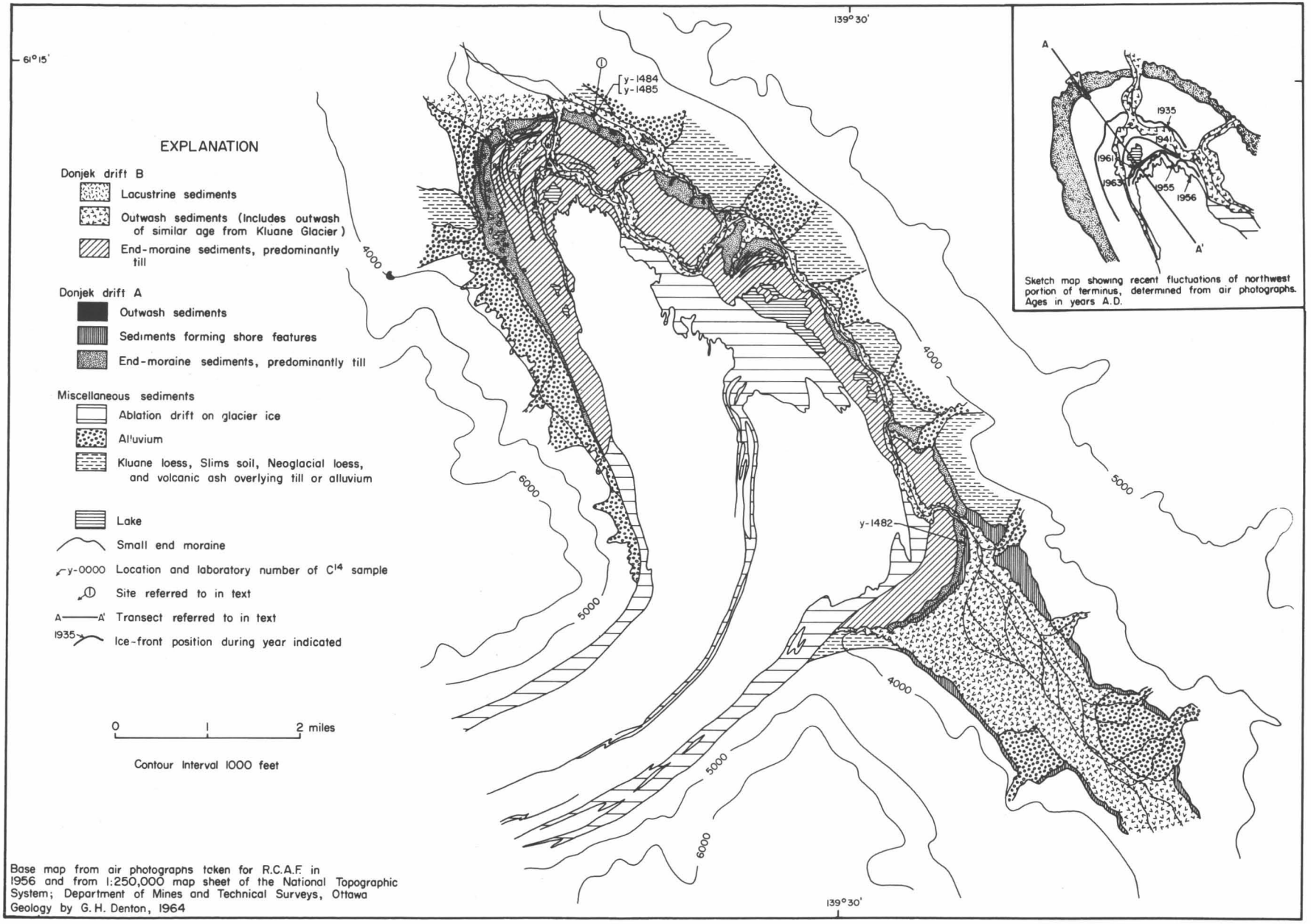

Fig. 2. Glacial features in terminal area of Donjek Glacier.

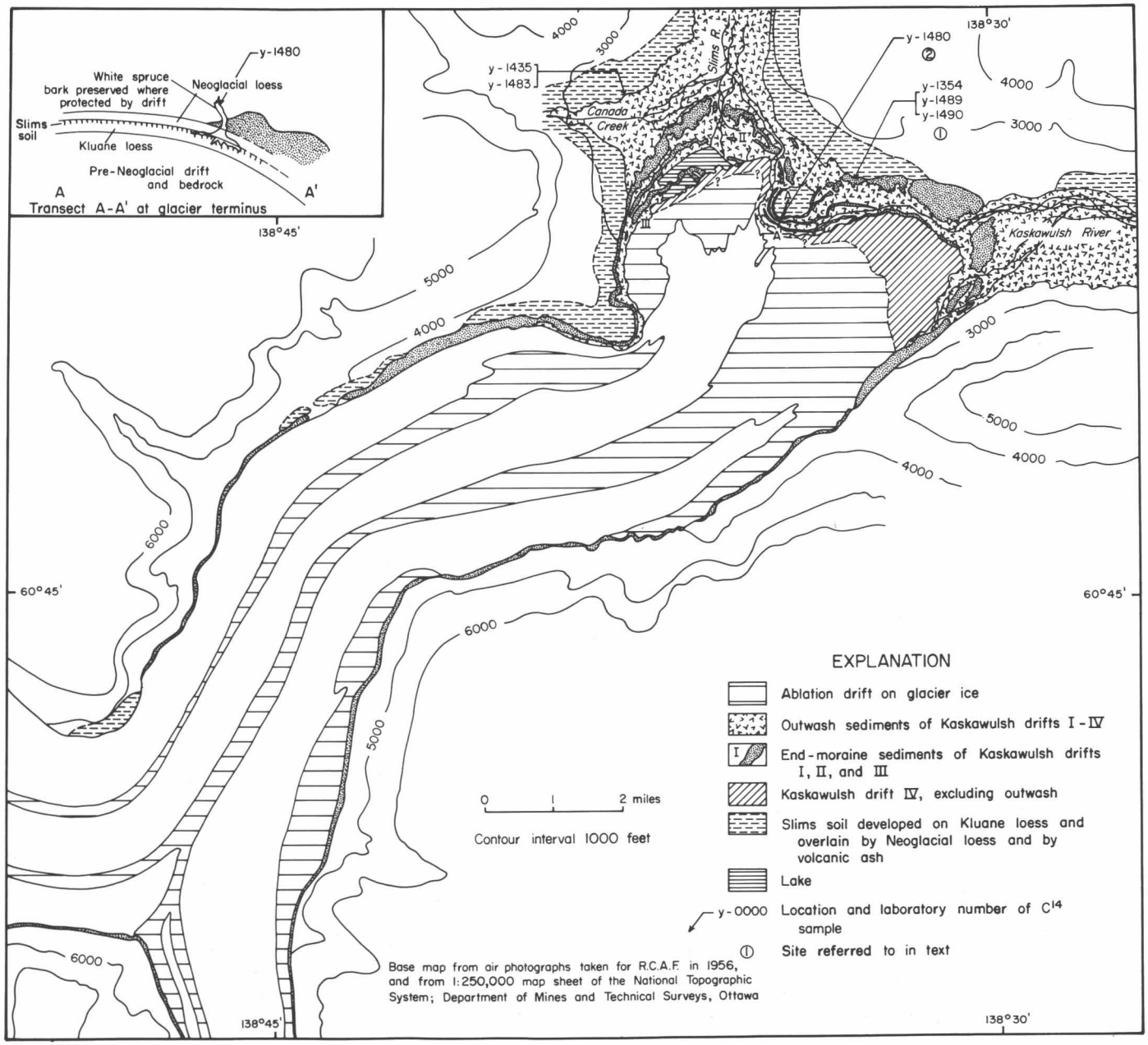

Fig. 3. Glacial features in terminal area of Kaskawulsh Glacier. Positions of end-moraine sediments I, II, and III adapted from Borns and Goldthwait (1966).

5 to 2 to 0 inches over distances from the delta of 4, 10, and 12 miles, respectively. East, it decreases from 14 to 6 to 3 inches over distances from the delta of 5, 8, and 12 miles, respectively. Thus the blanket of loess is thickest near the present termini of the Donjek and Kaskawulsh Glaciers, is slightly thinner in Slims River valley, and in Shakwak Trench thins rapidly with increasing distance from the Slims River delta. Neoglacial loess presently being deposited near the Donjek and Kaskawulsh Glacier termini in Slims River valley and in Shakwak Trench is derived from the Donjek and Slims valley trains. The above relations strongly suggest that the source of the loess was, and still is, active valley trains of large glaciers draining the Icefield Ranges.

Near the termini of the Donjek and Kaskawulsh Glaciers, Neoglacial loess 10 to 30 inches thick occurs beneath the volcanic ash, although 30 inches is exceptional. The thickness of Neoglacial loess underlying the ash decreases with distance from the Kaskawulsh terminus until it reaches zero in Shakwak Trench. This relationship indicates that Neoglacial loess deposition began near the present terminus of the Kaskawulsh Glacier before it began in the lower Slims River valley and Shakwak Trench.

Its relation to active valley trains and its stratigraphic position sharply overlying the Slims Soil imply that Neoglacial loess represents post-Slims reactivation of valley trains resulting from renewed glacier expansion. Thus Neoglacial loess records one or more advances that began at, or slightly before, the start of burial of Slims Soil and continued to recent times. No evidence of significant time breaks in Neoglacial loess deposition has been seen, and accordingly loess stratigraphy does not provide a more detailed record of glacier fluctuations.

Donjek drift. The Donjek Glacier heads in the Icefield Ranges at 9000 feet and flows 35 miles northeast to terminate at 3500 feet in a lobe projecting into and nearly across Donjek River valley. The lobe is 6.7 miles long and 1 to 3 miles wide. Meltwater issuing from the Kluane Glacier, 14 miles farther up the Donjek River valley, and from the Donjek Glacier itself, flows northwest along the valley and covers the valley floor in many localities.

In addition to the loess previously mentioned, Neoglacial drift surrounding the terminus of the Donjek Glacier consists predominantly of fresh end-moraine sediments, which extend 0.5 to 1.7 miles from the ice front, and of active outwash sediments, which surround and extend downstream from the end-moraine sediments (Figure 2). Inclusions of local Slims Soil, early Neoglacial loess, and volcanic ash are embedded in the outermost end moraine (Figure 2, site 1), indicating that the end-moraine sediments postdate these included units and suggesting that the end-moraine sediments may locally overlie both Slims Soil and early Neoglacial loess. Also it is inferred that the end-moraine sediments overlie Neoglacial outwash, which must have been deposited in front of the advancing Donjek Glacier. Only traces of Neoglacial loess overlie the end-moraine sediments.

Slims Soil, developed on Kluane loess and overlain by Neoglacial loess, partially surrounds and locally borders the moraines (Figure 2). This relationship indicates that the outer limit of the moraines marks the maximum Neoglacial extent of the Donjek Glacier, for any more extensive advance would have destroyed or covered with till the surrounding Slims Soil.

On the basis of morphology and vegetation, Donjek drift is divided into an older drift, A, and younger drift, B (Figure 4). The changes in characteristics across the boundary between these two drifts is nearly everywhere sharp. Drift A includes the outer end-moraine sediments which fringe the entire glacier terminus and which are partly covered with vegetation. This drift is comprised of a massive end moraine, consisting mainly of till, on which are superimposed many small end moraines, small outwash fans, and lacustrine sediments in drained kettles. The massive end moraine rises 60 to 100 feet above the Donjek valley train, whereas the small end moraines, many of which are cross cutting, average 30 feet wide, 8 feet high, and 400 feet long. Several fresh cracks associated with nearly vertical till faces suggest that the massive end moraine is at least partly ice cored. Furthermore, comparison of air photographs taken in 1935, 1961, and 1963 shows that a system of lakes on the northwest portion of the moraine is growing, perhaps due to melting and settling of an ice core. The morphology of drift A, although quite fresh, is more subdued than that of drift B; most slopes are stable, and the crests of the small end moraines are rounded. The surface of drift A is unweathered and very bouldery, with all boulders in stable positions.

Shoreline features, including beach ridges and wave-cut cliffs, occur on the outer slope of the southeast part of the outermost moraine of drift A up to 80 feet above the floodplain and also fringe the lower valley walls through 10 miles upstream from the glacier. These shoreline features record a lake, which was dammed when the Donjek Glacier at maximum Neoglacial extent impinged against the northeast wall of Donjek River valley. The lake remained in existence while the outer moraine of drift A was constructed. It was drained after glacier retreat permitted breaching of this moraine. Because comparison of air photographs taken in 1935, 1949, and 1963 shows that modern breaching of moraines by the large quantities of meltwater from the Kluane and Donjek Glaciers is very rapid, drift A was probably breached shortly after withdrawal of the ice from the outermost Neoglacial moraine.

The surface of drift A is sparsely covered with vegetation. The amount of level terrain covered with vegetation decreases gradually and uniformly from about 60 percent on the outer part to about 30 percent on the inner part of drift A. The vegetation cover ceases abruptly at the contact between drifts A and B. Spruce (*Picea glauca*) and poplar (*Populus balsamifera*) trees presently grow only on the drift A end-moraine sediments that fringe the northwest part of the glacier terminus. On the outer part of drift A in this area, cores taken with a Swedish increment borer show that in the summer of 1964 the oldest spruce had from 70 to 86 annual rings

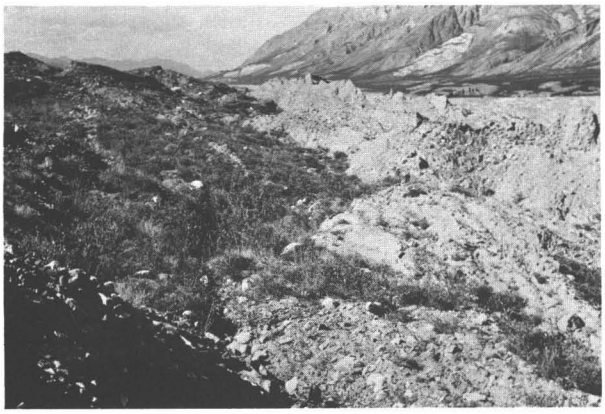

A.

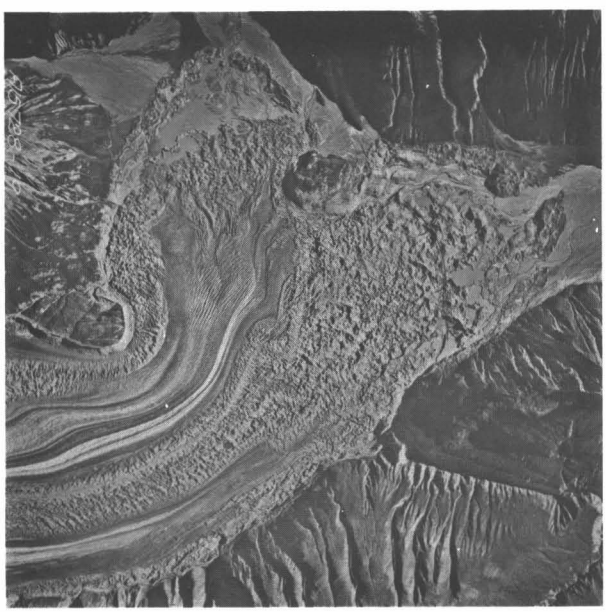

B.

Fig. 4. Neoglacial terminal moraines. A. Contrast between Donjek drifts A and B. B. Aerial photograph of Kaskawulsh Glacier terminus and Neoglacial moraines. Scale about 1:100,00.

whereas the oldest poplars had from 30 to 90 annual rings. On the inner part of drift B only poplars are present, and the oldest had from 20 to 30 annual rings in the summer of 1964. The ages of these trees afford minimum dates for recession of ice from the moraine sectors on which they are growing. Thus, the Donjek Glacier had receded from the outer area of drift A, fringing the northwest portion of the glacier terminus, by at least A.D. 1874. (This estimate is obtained from the age of the oldest poplar.) A more accurate minimum date for retreat can be obtained if the time span required for establishment of trees on the moraine after ice recession is added to their age. However, information concerning this time span is very scarce, and only a crude estimate is possible. First, in view of the age of the oldest poplars (30 years in 1964) and of the lack of spruce on the inner part of drift A, it appears that there spruce trees require at least 30 years for establishment. Second, comparison of air photographs of the northwest Donjek terminus shows that an area of drift B, evacuated by glacier ice between 1935 and 1941, still lacks vegetation, indicating that there poplars require more than 23 years for establishment. When added to the age of the oldest poplars (30 years in 1964), this suggests that the inner portion of drift A has been ice free for at least 53 years and that spruce there take at least 53 years to become established. Addition of this estimate of minimum time required for spruce establishment to the age of the oldest spruce growing on drift A (86 years in 1964) suggests that the northwest Donjek terminus receded from the outermost moraines of drift A before A.D. 1825.

Drift B includes (1) the end-moraine sediments that fringe the glacier terminus inside drift A and are bare of vegetation and (2) active outwash extending downstream from the terminus. The innermost end-moraine sediments are presently being deposited. The end-moraine sediments of drift B consist predominantly of till but also comprise outwash and small bodies of lacustrine sediments. The end moraines include (1) massive embankments of till and (2) small, well-defined ridges, some superimposed on the embankments. Most of the moraines contain ice cores very near the surface, are very bouldery with many boulders in unstable positions, and have steep, unstable slopes. Many features of drift B are continually changing because of glacier fluctuations and shifting of outwash streams.

The history of the Donjek Glacier since Kluane time can be ascertained from the deposits surrounding the glacier terminus and from a comparison of recent air photographs of the terminus. During late Kluane time the glacier withdrew into the Icefield Ranges sufficiently far to allow deactivation of the valley train, cessation of loess deposition, and formation of Slims Soil in the area of the present terminus. Renewed glacier activity following the Slims interval resulted in reactivation of the valley train and deposition of Neoglacial loess over the Slims Soil. During the subsequent Neoglacial advance or advances, the glacier overran Kluane loess, Slims Soil, Neoglacial outwash and loess, and volcanic ash, as well as organic matter in these deposits. This organic matter included logs of spruce (*Picea glauca*) that still retain their bark where protected by drift. Because modern trees of the same species lose all their bark within 6 to 20 years after death (Mr. Donald Merrill, Forestry Superintendent, Yukon Forestry Division, written communication), the trees embedded in the moraine were alive or had been dead for only a very short time when they were overrun by glacier ice.

The Donjek Glacier had reached its maximum Neoglacial extent marked by the outer moraine of drift A, had dammed a lake in Donjek River valley, and had probably begun to retreat by at least A.D. 1825. The lack of abrupt changes in vegetational characteristics on drift A suggests that over the area of drift A, the retreat, although marked by small fluctuations as shown by the cross-cutting moraines, was uninterrupted by major pauses or readvances. The marked contrast between drifts A and B indicates that steady but fluctuating retreat from the area of drift A was interrupted either by a major readvance that terminated at the outer limit of drift B or by a prolonged pause in reces-

sion. That the subsequent recession which resulted in deposition of at least the surficial part of drift B was punctuated by fluctuations is shown by cross-cutting moraines.

Recent fluctuations of the Donjek Glacier terminus can be ascertained from a series of air photographs taken at intervals from August 1935 to July 1964 (Figure 5). The following distances and recessions were measured along a transect of the northwestern part of the glacier (Figure 2, AA'), where the ice terminus is clearly defined. Behavior of the rest of the terminus was probably similar but is harder to measure because ice tended to stagnate rather than waste back. In August 1935, the ice front was about 2640 feet behind the outer limit of the moraines of drift A. Between August 1935 and the summer of 1941, net retreat was about 1760 feet; between the summer of 1941 and the summer of 1955 it was also about 1760 feet; between the summer of 1955 and the summer of 1956 it was about 200 feet. At some time between the summer of 1956 and August 1961, the ice front advanced to a position some 1380 feet in front of its 1956 position. From this position it had retreated about 120 feet by August 1961, 570 feet by August 1963, and 620 feet by July 1964 when the distances were measured.

Kaskawulsh drift. Neoglacial drift near the terminus of the Kaskawulsh Glacier was studied both by Borns and Goldthwait (1966 and pp. 187–196 of this volume) and by the present writers, in part jointly and in part independently. The present writers are grateful for permission to cite their colleagues' work.

The Kaskawulsh Glacier, 45 miles long, flows northeast from the Icefield Ranges and terminates at 2700 feet altitude near the junction of Slims and Kaskawulsh valleys. A bedrock knob divides the terminal portion of the glacier into two lobes, the Slims River lobe and the Kaskawulsh River lobe. Both lobes are fronted by Neoglacial drift (Figure 4) which, in addition to loess previously mentioned, includes (1) end-moraine sediments extending from 0.2 to 2.0 miles in front of active glacier ice and (2) active and inactive outwash sediments (Figure 3).

The age relation of Kaskawulsh end-moraine sediments to surrounding drift units is identical with the comparable Donjek situation as shown by (1) inclusions of Slims Soil and Neoglacial loess in the outer moraine (Figure 3, site 1), (2) end-moraine sediments overlying *in situ* Slims Soil, Neoglacial loess, and volcanic ash in which a sheared spruce (*Picea glauca*) is still rooted in growth position (Figure 3, site 2), and (3) traces of Neoglacial loess on the end-moraine sediments. Additionally, logs of spruce (*Picea glauca*) embedded in the end-moraine sediments (Figure 3, site 1), contain Slims Soil and Neoglacial loess in their roots.

The areal distribution of Slims Soil bordering the Kaskawulsh end-moraine sediments (see also Borns and Goldthwait, pp. 187–196) parallels the Donjek situation and likewise indicates that the outer end moraine marks the maximum Neoglacial extent of the Kaskawulsh Glacier.

Borns and Goldthwait have divided the end-moraine sediments and the associated inactive outwash and lacustrine sediments into Kaskawulsh drifts I, II, and III, mainly on the basis of three distinct end moraines fronting the Slims River ice lobe. The three drifts have a sparse cover of vegetation in comparison to surrounding terrain. Between drift III and active glacier ice there is a deposit of thick, bare ablation drift covering ice which is probably inactive. In front of the Kaskawulsh River lobe, the moraines of drifts I, II, and possibly drift III merge to form an outer fringe of drift which is partly covered with vegetation and nestles around an extensive inner deposit of fresh drift, which is bare of vegetation. The inner drift is ice cored very near the surface and grades into thin ablation drift covering active glacier ice. The contact between the two drifts is sharp. This inner drift, and possibly the inner ablation drift fronting the Slims River lobe, is here called drift IV, following the terminology of Borns and Goldthwait (pp. 187–196). Also included in drift IV is the active outwash extending downstream from the glacier terminus.

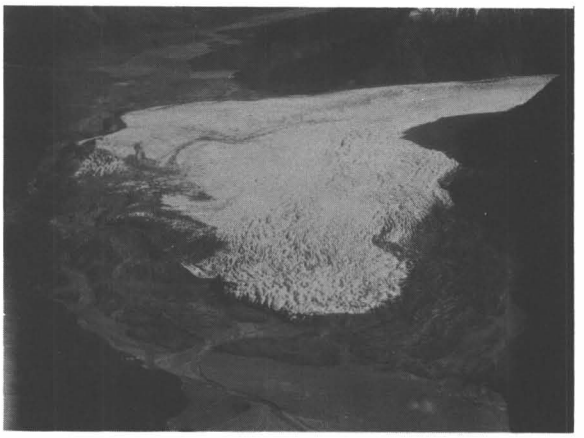

A.

B.

Fig. 5. Aerial photographs of the northwest part of the Donjek Glacier terminus showing recent fluctuations. A. Photograph taken August 1935. B. Photograph taken August 1963. Photographs by Walter A. Wood.

The Neoglacial history of the Kaskawulsh Glacier is revealed by drift and vegetation surrounding the ice. Following the Slims interval, Neoglacial advance(s) caused reactivation of the lower valley train, resulting in deposition of Neoglacial loess, first near the glacier and later in lower Slims River valley and in Shakwak Trench. Spruce logs associated with Slims Soil and Neoglacial loess are embedded in the outermost moraine, indicating that the advancing ice overrode spruce forests growing on these deposits. Where protected by drift, the logs retain their bark, strongly suggesting that the trees were alive when overrun by ice. When it reached its maximum Neoglacial extent, the ice sheared off and partially covered with drift a tree whose stump is still rooted in growth position in Slims Soil, Neoglacial loess, and volcanic ash. Because its bark is still entirely preserved where protected by drift, the tree was probably alive when its top was removed by glacier ice. The total Neoglacial advance of the Kaskawulsh Glacier was at least 15 miles from the retracted position the terminus occupied during the Slims interval.

The most recent fluctuations of the Kaskawulsh Glacier during its general recession from the maximum Neoglacial position are represented by drifts I, II, III, and IV. On the Slims River lobe the moraine of drift I was deposited when the glacier stood at its maximum Neoglacial extent; the moraine of drift II was deposited during a readvance; the moraine of drift III was deposited either during a readvance or a pause in retreat (Borns and Goldthwait, pp. 187–196). On the Kaskawulsh River lobe these advances and/or pauses either are not represented or are recorded by the outer drift. Drift IV represents either a readvance or a stillstand during general recession. Ages of the oldest trees now growing on the outermost moraine suggest that retreat from the Neoglacial maximum began prior to A.D. 1865 (Krinsley, 1965).

Silver and Cairnes drifts. The Silver and Cairnes Glaciers are small valley glaciers located on the northeast flank of the St. Elias Mountains. They head near 8000 feet and terminate at 6000 feet. Well-preserved end-moraine sediments, probably ice cored, surround their termini and active outwash bodies extend downstream from their moraines (Figure 6). No deposits underlying the end-moraine sediments are exposed, and no deposits overlie them. The volcanic ash is absent on both the end-moraine sediments and the surrounding deposits. The latter situation can be interpreted as resulting from the fact that the surrounding deposits consist of active fan and gelifluction sediments that would have disrupted ash beds. On the other hand numerous flat surfaces on the end-moraine sediments afford ideal situations for preservation of the ash, and its absence is interpreted as indicating that the end-moraine sediments are younger than the ash and that they were

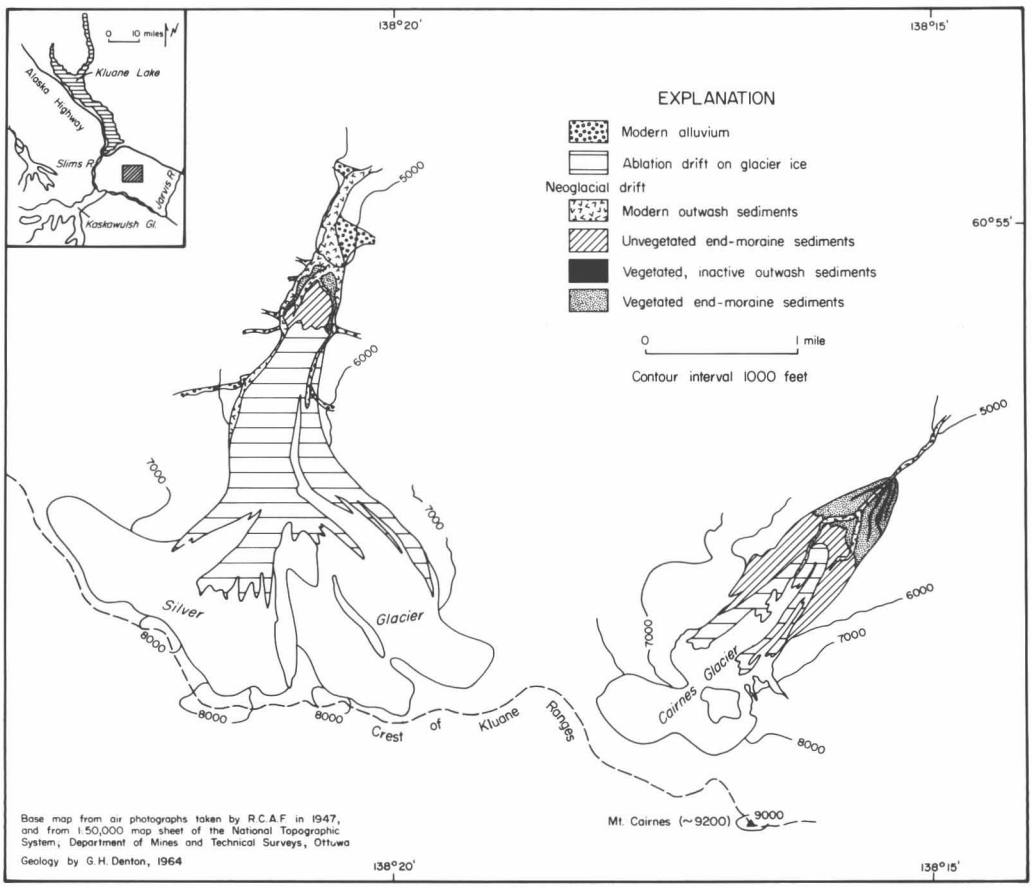

Fig. 6. Glacial features surrounding Silver and Cairnes Glaciers.

therefore constructed subsequent to ash deposition dated at 1425 ± 50 B.P. Because Slims Soil is not present at the altitude of the moraines, its distribution cannot be applied to determination of the maximum Neoglacial extent of these glaciers. In view of the absence of more extensive moraines, it is assumed that the outer moraine probably represents the maximum Neoglacial extent of each of the glaciers. Both the Silver and Cairnes end-moraine sediments have a bipartite arrangement consisting of an outer fringe of drift partly covered with vegetation and an inner barren fringe of drift; in both cases the contact between the inner and outer drifts is sharp.

Only fragments of the Neoglacial history of the Cairnes and Silver Glaciers are revealed by deposits surrounding their termini. Both glaciers probably reached their maximum Neoglacial extent, marked by the outer limit of end-moraine sediments that surround the termini, after deposition of the volcanic ash. At the time of maximum Neoglacial extent, various glaciers now separated from the present Silver Glacier had coalesced to form one large valley glacier. Retreat from the maximum Neoglacial position began recently, as shown by the sparse cover of vegetation on the outer end moraines. The pronounced difference in vegetation cover of the inner and outer drifts indicates that general recession was interrupted by a readvance or a stillstand of the ice.

Østrem (1964, 1965) has shown that ice-cored moraines fronting short glaciers in continental areas may have been constructed during several advances spread over thousands of years. In such cases surface characteristics of moraines represent only the youngest advance. Because they are associated with small glaciers in a continental area, the ice-cored moraines fronting the Silver and Cairnes Glaciers may represent such a situation.

Chronology

The similar Neoglacial histories of the four glaciers studied (Donjek, Kaskawulsh, Silver, and Cairnes) probably represent the general situation for glaciers in the northeastern St. Elias Mountains. The termini of Donjek and Kaskawulsh Glaciers, and probably of the Silver and Cairnes Glaciers, assumed retracted positions during the Slims interval preceding the Neoglaciation. For the Kaskawulsh Glacier, this position was more than 13.7 miles behind its present terminus and 15 miles behind the outermost Neoglacial moraines. The oldest evidence of glacier expansion following the Slims interval is Neoglacial loess, deposited initially near the present termini of the Donjek and Kaskawulsh Glaciers and later farther down-valley.

Lack of evidence of depositional breaks within the Neoglacial loess near the Kaskawulsh and Donjek termini suggests that throughout the Neoglaciation these termini maintained positions farther down-valley than the positions occupied during the preceding Slims interval. Near the present Kaskawulsh Glacier terminus, a C^{14} date of grass buried in place near the base of a 10-foot section of Neoglacial loess provides a close minimum age of 2640 B.P. (Y-1435; Figure 3) for the initial Neoglacial advance(s) of the Kaskawulsh Glacier. Near the Kaskawulsh terminus as much as 30 inches of Neoglacial loess underlie the volcanic ash, whereas in Shakwak Trench near Kluane Lake only 0 to 2 inches underlie the ash. On the shore of Kluane Lake the outer few rings of a spruce stump buried in place in Neoglacial loess 3 inches above the volcanic ash provided a C^{14} date of 870 B.P. (Y-1365); the volcanic ash is dated at about 1425 ± 50 B.P. Thus loess deposition had begun in Shakwak Trench by at least between 870 B.P. and 1425 B.P.

During recent centuries the Kaskawulsh and Donjek Glaciers, and probably also the Silver and Cairnes Glaciers, reached their maximum Neoglacial extent, recorded in each case by the outer end-moraine sediments surrounding the present termini. Sharp (1951) has reported a similar advance of the nearby Steele (Wolf Creek) Glacier. A series of C^{14} samples is associated with this recent advance. In order to present a more realistic chronology and to facilitate correlation with historically dated advances elsewhere, the dates presented are corrected for variations in atmospheric C^{14} (see Stuiver and Suess, 1966). Both the corrected dates and the original C^{14} dates are presented in Table 2.

TABLE 2

Corrected young neoglacial C^{14} dates. All dates in years B.P. Statistical errors not considered.

Sample number	C^{14} ages, in years, B.P., based on 95 percent oxalic acid and a half life for C^{14} of 5568 years	Age range in calendar years B.P. when C^{14} ages are corrected for half life and for fluctuations in atmospheric C^{14} content. Corrections based on data from Stuiver and Suess (1966)
Y-1482	<100	<260
Y-1489	110	130 to 280
Y-1485	230	300 to 400
Y-1480	270	300 to 420
Y-1484	290	300 to 440
Y-1490	390	480
Y-1354	450	500

All corrected dates are on stumps or logs of white spruce, the drift-protected parts of which still retain their bark, indicating that the trees were alive or had been dead only a short time when they were overrun by ice and incorporated into the drift. Radiocarbon dates of the outer few growth rings of logs embedded in Neoglacial end moraines represent (1) a time when the glacier concerned was advancing and (2) a maximum date for construction of the part of the moraine involved. Corrected ages of logs in the outer Kaskawulsh end moraine (Figure 7) suggest that the Kaskawulsh Glacier was advancing about 500 B.P. (Y-1354) and 480 B.P. (Y-1490). The glacier subsequently reached its Neoglacial maximum between 300 and 420 B.P. (Y-1480), the range of corrected ages of the sheared stump at the bedrock knob separating the Slims River lobe from the Kaskawulsh River lobe. A corrected age (130 to 280 B.P. for Y-1489) on a log embedded in the outer moraine is either anomalous or suggests that different parts of the Kaskawulsh terminus reached maximum Neoglacial positions at slightly different times. During this Neoglacial advance the Kaskawulsh Glacier attained its greatest extent of at least the last 9780 years (Y-1483), the age of grass buried in place at the base of Kluane loess immediately outside the Neoglacial moraines.

The corrected ages of wood embedded in the outermost Donjek end moraine (Figure 7; Y-1484 and Y-1485 in Table 3) establish possible dates when the Donjek Glacier was advancing and are maximum for construction of the moraine at the sample localities. These corrected ages range from 440 to 300 B.P. The number of annual growth rings of the oldest trees presently growing on end-moraine sediments imply a minimum date of A.D. 1874 (76 B.P.) for retreat of the northwest part of the Donjek Glacier terminus from its Neoglacial maximum. The date of retreat of the southeast part of the terminus can be estimated from the C^{14} age of a log buried in the highest beach ridge of a lake dammed by the Donjek Glacier at its Neoglacial maximum. The sample, Y-1482, gives a corrected age of <260 B.P. for the highest lake level. Drainage of the lake probably accompanied ice withdrawal from the maximum stand; hence this date suggests that retreat began after 260 B.P.

Retreat from the maximum position began by the Kaskawulsh Glacier before A.D. 1865, a date obtained from the age of the oldest trees now growing on the moraines (Krinsley, 1965). In the case of the Steele Glacier, the Neoglacial advance is estimated to have culminated between A.D. 1840 and 1890 (Sharp, 1951, p. 107). The fluctuating retreat from the maximum Neoglacial extent of the Donjek, Silver, and Cairnes Glaciers, as well as of the Kaskawulsh River lobe of the Kaskawulsh Glacier, was interrupted by at least one major readvance or period of equilibrium, as shown by the bipartite division of drift surrounding the glacier termini. This major interruption in general recession is paralleled in the Steele Glacier, whose moraines also have a bipartite arrangement (Sharp, 1951, p. 107). Recession of the Slims River lobe of the Kaskawulsh Glacier was interrupted by four pauses or readvances, the last probably corresponding to the major pause, or reexpansion, in general recession of the other glaciers discussed above.

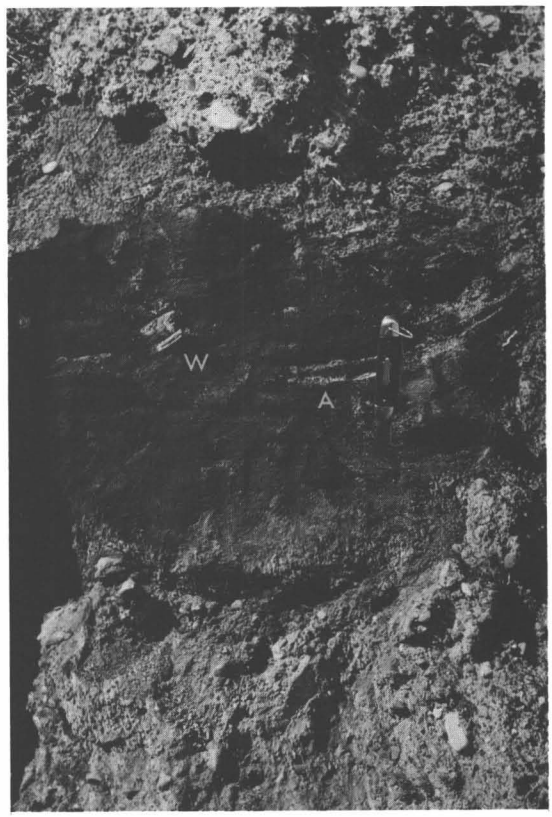

A.

B.

Fig. 7. Neoglacial C^{14} samples. A. Inclusion of Neoglacial loess, volcanic ash (A), and wood (W) embedded in outermost Donjek Neoglacial moraine. B. Spruce stump embedded in outermost Kaskawulsh Neoglacial moraine.

Correlation

Because recently published information concerning the Neoglaciation has not been synthesized, a brief summary of dated events is presented here. Figure 8 shows a representation of dated Neoglacial fluctuations in the Northern Hemisphere, mainly of glaciers in alpine regions. The curve

is based on a detailed synthesis by Porter and Denton (ms) of available Neoglacial data. The curve has several weaknesses. (1) Some of the information is from geographically restricted areas, and thus, if it is to represent the Northern Hemisphere, the curve involves the assumption that major Neoglacial events were synchronous throughout the Hemisphere. (2) Several C^{14} dates of glacier advances in Alaskan coastal mountains contradict the part of the curve representing the Middle Ages. However, neither the extent nor the geographic significance of these Alaskan advances are known, and thus the curve here is based on better-documented data from the North Atlantic region. (3) The horizontal axis of Figure 8 has no absolute dimensions, and the extent shown for each period of glacier expansion is at best relative and represents only an interpretation of available literature.

Data for the timing of the initial Neoglacial advances come mainly from Cordilleran North America. Available

TABLE 3
C^{14} dates

Sample number	Location	Substance and stratigraphic position	C^{14} age in years B.P.
Y-1482	Donjek Glacier (Fig. 2)	Outer rings of spruce log buried in highest beach ridge of lake dammed by Donjek Glacier at Neoglacial maximum	< 100
Y-1485	"	Outer rings of spruce log embedded in outermost Donjek Neoglacial moraine	230 ± 80
Y-1484	"	"	290 ± 80
Y-1489	Kaskawulsh Glacier (Fig. 3)	Outer rings of spruce log embedded in outermost Kaskawulsh Neoglacial moraine	110 ± 80
Y-1490	"	"	390 ± 80
Y-1354	"	" (see Borns and Goldthwait, 1966)	450 ± 100
Y-1480	"	Outer rings of sheared spruce stump in growth position rooted in Slims Soil and Neoglacial loess and partly covered with end-moraine sediments	270 ± 60
Y-1365	South end of Kluane Lake	Outer rings of spruce stump buried in growth position in Neoglacial loess immediately above volcanic ash (see Stuiver, Borns, and Denton, 1964)	870 ± 100
Y-1363	Kaskawulsh Glacier	Peat from immediately above volcanic ash (see Stuiver, Borns, and Denton, 1964)	1460 ± 70
Y-1364	Kaskawulsh Glacier	Peat from immediately below volcanic ash (see Stuiver, Borns, and Denton, 1964)	1390 ± 70
Y-1435	Kaskawulsh Glacier (Fig. 3)	Grass buried in place 4 inches above base of 10 foot section of Neoglacial loess	2640 ± 80
Y-1483	Kaskawulsh Glacier (Fig. 3)	Grass buried in place at base of Kluane loess	9780 ± 80
Y-1386	South end of Kluane Lake	Organic matter from base of kettle in Kluane ice-contact stratified drift	12,500 ± 200

C^{14} dates directly associated with glacier advances during the latter half of the Hypsithermal and during early Neoglacial time are shown in Figure 9. The only C^{14} -dated advance recorded during the Hypsithermal was that of South Cascade Glacier (Meier, 1964). At present it is not known to what extent this advance represents a regional trend, for the only other C^{14} evidence of a glacier advance of comparable age is from the European Alps where wood from a moraine fronting Oberaar Glacier dates from 4600 B.P. (Gfeller and others, 1961, p. 19). Otherwise, the oldest dates of glacier expansion cluster between 2800 and 2600 B.P. and come from areas of such diverse latitudes as the Brooks Range in north-central Alaska (Porter, 1964, p. 457-458), Glacier Bay (Goldthwait, 1963, p. 44), the Juneau district in southeastern Alaska (Heusser and Marcus, 1964, p. 84), and Utah (Richmond, 1962). Such broad areal distribution strongly suggests that widespread advances began shortly before 2800 to 2600 B.P. Evidence supporting this inference is given by the age of initial Neoglacial advance of glaciers on Mt. Rainier, bracketed between 3500 and 2000 B.P. by C^{14}-dated beds of volcanic ash (Crandell, 1965).

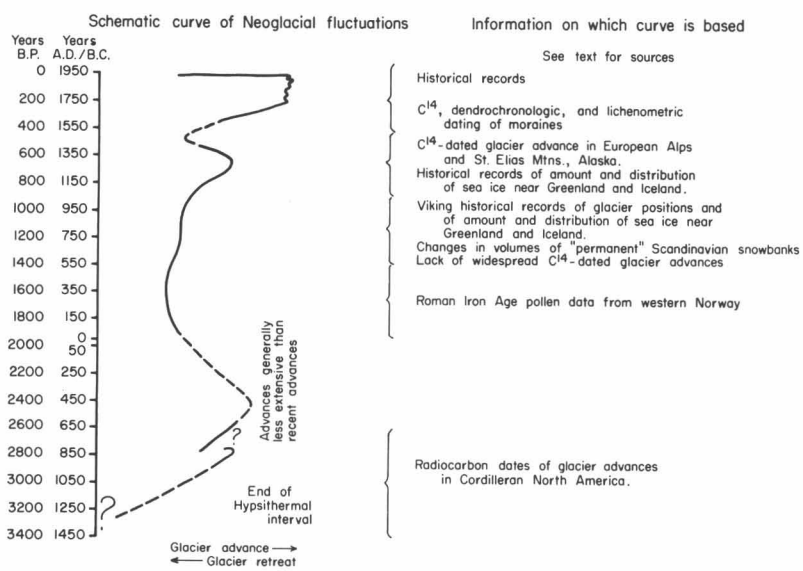

Fig. 8. Neoglacial glacier fluctuations. Most information from alpine areas. Horizontal axis has no absolute scale; known total Neoglacial advance ranged from more than 15 miles for Kaskawulsh Glacier to several miles or less for small Scandinavian glaciers. Although curve probably reflects general situation, for an individual glacier any of the Neoglacial advances represented may have been the most extensive.

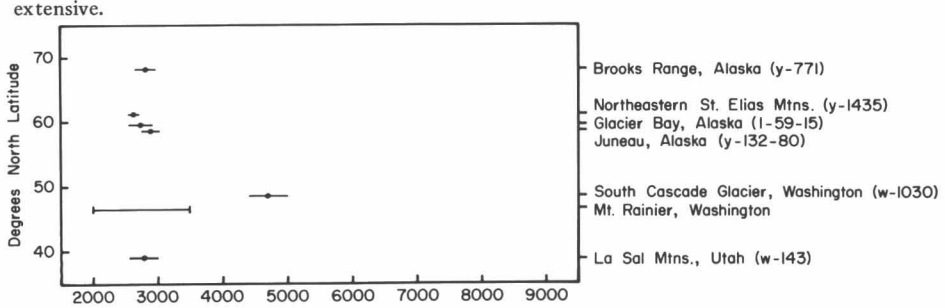

Fig. 9. C^{14} dates of glacier advances in Cordilleran North America during Hypsithermal and early Neoglacial times. —●— represents C^{14} date with statistical error. [——] represents limiting dates of initial Neoglacial advance as imposed by C^{14} -dated beds of volcanic ash. See text for sources.

The best-documented information for the time span between the oldest Neoglacial expansion and the major advances of the last few centuries comes mainly from the North Atlantic region and is based on (1) Roman Iron Age pollen data (see Hafsten, 1960, p. 449-450), (2) historical records relating to relative glacier positions (see Ahlmann, 1953, p. 39) and to amount and distribution of sea ice in waters surrounding Iceland and southern Greenland (see Koch, 1945, p. 243-298), (3) changes in volumes of permanent snow banks in Scandinavian mountains (see Hoel and Werenskiold, 1962, p. 57), and (4) C^{14}-dated advances about A.D. 1200 in the southern St. Elias Mountains (see Plafker and Miller, 1957) and in the European Alps (see Oeschger and Röthlisberger, 1961). Data concerning the widespread later Neoglacial advances of the last few centuries come from many sources and include historical records as well as C^{14}, dendrochronologic, and lichenometric dating of moraines.

Available data from the northeastern St. Elias Mountains agree closely with relevant parts of Figure 8. The close minimum date of 2640 B.P. for the initial Neoglacial advance of the Kaskawulsh Glacier correlates with similar dates from elsewhere in Cordilleran North America and lends strong supporting evidence for the postulate that widespread, essentially synchronous, Neoglacial expansion began shortly before 2600 to 2800 B.P. Furthermore, glaciers of the northeastern St. Elias Mountains were advancing from about 500 B.P. until sometime shortly before A.D. 1874 (Donjek) or A.D. 1865 (Kaskawulsh). This timing agrees with the widespread Neoglacial advances throughout alpine areas of the Northern Hemisphere. Thus, as far as it is known, the St. Elias Neoglacial chronology fits closely with that of other areas and supports the concept that major Neoglacial events were essentially synchronous, at least in alpine regions of the Northern Hemisphere.

In addition, the St. Elias data add the following local dimensions to Figure 8: (1) For the Kaskawulsh Glacier the total distance of advance from its retracted Hypsithermal position to its maximum Neoglacial extent, attained within the last few centuries, exceeded 15 miles. (2) For both the Donjek and Kaskawulsh Glaciers the major Neoglacial advance of the past few centuries was more extensive than any previous Neoglacial advance.

Acknowledgments

The writers thank members of the project, especially Dr. Walter A. Wood, Mr. Richard Ragle, and Mr. and Mrs. Philip Upton, for extensive logistical support. Professor A. L. Washburn and Professor R. F. Flint visited Denton in the field and critically read the manuscript. The writers thank H. W. Borns, Jr., David Fullerton, R. P. Goldthwait, and Barrie McDonald for critical discussions. Funds for the field work by Denton were provided by the Arctic Institute of North America, The Explorers Club, Sigma Xi, and Yale University; support for the C^{14} dating by Stuiver was provided through a National Science Foundation Grant. Able field assistance was provided by Barbara Denton, Paul Nunes, and Julian Orr; Carolyn Morgan and Terry Eisensmith provided assistance for the C^{14} dating. All figures were drafted by Mary Ann Doolittle.

References

Ahlmann, H. W. (1953) Glacier Variations and Climatic Fluctuations, Am. Geogr. Soc., New York, 51 pp.

*Borns, H.W., and Goldthwait, R.P. (1966) Late-Pleistocene fluctuations of Kaskawulsh Glacier, southwestern Yukon Territory, Canada, Am. J. Sci., 264, 600-619.

Bostock, H.S. (1952) Geology of northwest Shakwak Valley, Yukon Territory, Canada Geol. Surv. Mem. 267, 54 pp.

Capps, S.R. (1915) An ancient volcanic eruption in the upper Yukon basin, U.S. Geol. Surv. Prof. Paper 95, pp. 59–64.

Crandell, D.R. (1965) Alpine glaciers at Mount Rainier, Washington, during late Pleistocene and Recent time, Geol. Soc. Am. Spec. Paper 82, pp. 34–35.

Deevy, E.S., and Flint, R.F. (1957) Postglacial hypsithermal interval, Science, 125, 182–184.

Denton, G.H. (ms, 1965) Late Pleistocene Glacial Chronology, Northeastern St. Elias Mountains, Ph.D. Dissertation, 88 pp.

*Denton, G.H., and Stuiver, M. (1967) Late Pleistocene glacial chronology, northeastern St. Elias Mountains, Canada, Bull. Geol. Soc. Am., 78, 485 – 510.

Gfeller, C., Oeschger, H., and Schwarz, U. (1961) Bern radiocarbon dates II, Am. J. Sci. Radiocarbon, 3, 15 – 25.

Goldthwait, R.P. (1963) Dating the Little Ice Age in Glacier Bay, Alaska, Intern. Geol. Congress, Rept. Twenty First Sess., Norden 1960, Pt. 27, pp. 37 – 46.

Hafsten, U. (1960) Pollen-analytic investigations in south Norway, in Geology of Norway, edited by O. Holtedahl (Norges Geol. Undersøkelse No. 208), pp. 434 – 462, H. Ashenhough, Oslo.

Heusser, C.J., and Marcus, M.G. (1964) Historical variations of Lemon Creek Glacier, Alaska, and their relationship to the climatic record, J. Glaciol., 5, 77–86.

Hoel, A., and Werenskiold, W. (1962) Glaciers and snowfields in Norway, Skrifter No. 114, Norsk Polarinstitutt, Oslo, 291 pp.

Johnson, F., and Raup, H.M. (1964) Investigations in southwest Yukon: geobotanical and archaeological reconnaissance, Robert S. Peabody Found. Archaeol. Papers, Vol. 6, No. 1, 198 pp.

Koch, L. (1945) The East Greenland ice, Med. om Grønland, Vol. 130, No. 3, 373 pp.

Krinsley, D.B. (1965) Pleistocene geology of the south-west Yukon Territory, Canada, J. Glaciol., 5, 385–397.

Matthes, F.E. (1939) Report of Committee on Glaciers, Am. Geophys. Union Trans., 20, 518–523.

Matthes, F.E. (1940) Committee on Glaciers, 1939–40, Am. Geophys. Union Trans., 21, 396–406.

Matthes, F.E. (1942) Glaciers, in Physics of the Earth, Pt. 9, Hydrology, edited by O.E. Meinzer, pp. 149–219, McGraw-Hill, New York.

Meier, M.F. (1964) The recent history of advance-retreat and net budget of South Cascade Glacier, Am. Geophys. Union Trans., 21, 396–406.

Oeschger, H., and Röthlisberger, H. (1961) Datierung eines ehemaligen standes des Aletschgletschers durch radioaktivitatsmessung an holzproben und Bemerkungen zu Holzfunden an weiteren gletschern, Z. Gletscherkunde Glazialgeologie, 4, 191–205.

Østrem, G. (1964) Ice-cored moraines in Scandinavia, Geog. Annaler, 46, 282–337.

Østrem, G. (1965) Problems of dating ice-cored moraines, Geog. Annaler, 47A, 1–38.

Plafker, G., and Miller, D.J. (1957) Recent history of glaciation in the Malaspina district and adjoining bays, Alaska, Bull. Geol. Soc. Am., 68, 1909.

Porter, S.C., and Denton, G.H. (unpublished) Chronology of neoglaciation in North American Cordillera.

Richmond, G.L. (1962) Quaternary stratigraphy of the La Sal Mountains, Utah, U.S. Geol. Surv. Prof. Paper 324, 135 pp.

Sharp. R.P. (1951) Glacial history of Wolf Creek, St. Elias Range, Canada, J. Geol., 59, 97–117.

Sharp, R.P. (1960) Pleistocene glaciation in the Trinity Alps of northern California, Am. J. Sci., 258, 305–340.

Sticht, J.H.H. (1951) Geomorphology and Glacial Geology along the Alaskan Highway in Yukon Territory and Alaska, Ph.D. Dissertation, Harvard Univ., 176 pp.

*Stuiver, M., Borns, H.W., and Denton, G.H. (1964) Age of a widespread layer of volcanic ash in the southwestern Yukon Territory, Arctic, 17, 259–260.

Stuiver, M., and Suess, H. (1966) On the relationship between radiocarbon dates and true sample ages, Radiocarbon, 8, 534–540.

*These articles are reprinted in the present volume.

Late-Pleistocene Fluctuations of Kaskawulsh Glacier*

Harold W. Borns, Jr.† and Richard P. Goldthwait‡

ABSTRACT. The 45-mile-long Kaskawulsh is one of many outlet glaciers draining the glacier-filled coastal Icefield Ranges into the dry interior of the Yukon Territory. Its deposits express the major climatic changes of the last 10,000 years. A great retreat, many miles up valley from the present terminus, occurred 12,000 to 9000 years ago leaving drift clinging to valley walls and completed alluvial fans. Winds over the active valley train added up to 8 feet of loess (Kluane loess) on these deposits and buried 9700-year-old vegetation near the present glacier terminus. During the Slims nonglacial interval (essentially the Hypsithermal interval) weathering developed a bright red-yellow paleosol (Slims Soil) in this loess. In the lower parts of a bog, just above the Neoglacial terminal moraine, there are dominant grass pollen and moss spores which suggest a wetter climate than today. But just above the 3300-year-old date in this bog, peat with sedge, spruce, and artemsia pollen show a marked change to a drier climate like that of today. In addition, a new unweathered loess (Neoglacial loess) covers the red-yellow paleosol and 2600-year-old vegetation. The climatic change and reactivated outwash signal the Neoglacial advance 2600 to 3000 years ago. Kaskawulsh Glacier reached its terminal position, where it left a prominent loop moraine, by approximately 300 years ago (C^{14} dates) and was there as late as 145 years ago when it bent over a spruce tree with countable rings. Halting retreat for the last century has left two ice-cored loop moraines: the older one completed and stabilized in 1870 as tree rings show, and the other completely formed in 1939.

Introduction

The Kaskawulsh is one of several easterly draining outlet glaciers of the 7000 to 9000-foot-high icefield astride the Yukon-Alaskan border in the Icefield Ranges of the St. Elias Mountains (Plate 1)[1]. The 45-mile-long Kaskawulsh Glacier terminates at the junction of the Kaskawulsh and Slims River valleys, which respectively carry the glacial meltwater into the Gulf of Alaska via the Alsek River and into the Bering Sea via the Yukon River.

Climate. The southwestern slope of the St. Elias Mountains is characterized by a cold wet climate with an annual precipitation in excess of 125 inches, while on the Yukon Plateau to the northeast of the mountains a cold dry climate prevails. The aridity of the northeastern slope is indicated by the average annual precipitation of 10.6 inches of water equivalent reported for the 1941 to 1950 interval at Whitehorse (Kendrew and Kerr, 1955, p. 194). Richard Ragle (personal communication) reported that the firn line on the Kaskawulsh is at an altitude of approximately 6000 feet.

Previous work. Earlier work in the terminus area of Kaskawulsh Glacier includes that of Bostock (1952, p. 7), Wheeler (1963), Stuiver, Borns, and Denton (1964), Krinsley (1965), and Denton (ms), all of which will be discussed later in context.

Late Wisconsin Events

Introduction. Denton (ms, p. 67) shows that Kaskawulsh Glacier last expanded into Shakwak Trench (Plate 1)[1] sometime after 30,000 years ago (Y-1385) and had withdrawn before 12,500 years ago (Y-1386) indicating that this glacial expansion that he named the Kluane glaciation (Denton, ms, p. 41) is of "classical" Wisconsin age. The great retreat continued until the terminus of Kaskawulsh stood at least 30 miles up valley from Shakwak Trench leaving masses of till clinging to the valley walls and completed alluvial fans in Slims River valley (Plate 1)[1]. Throughout the retreat, winds over the active valley train added 4 to 7 feet of buff, Kluane loess[2] on these deposits and buried 9700-year-old grass (Denton, ms, p. 64; Y-1483) near the terminus.

Alluvial fans. During the dissipation of the ice of the Kluane glaciation from the Kluane Ranges (Plate 1)[1] large outwash alluvial fans aggraded in the valleys. The largest of these fans in the lower Slims River valley were built from alluvium derived from the melting of valley glaciers in Sheep, Bullion, and Vulcan Creeks (Figure 1). These fans nearly or completely coalesced across the Slims River valley at this time. Smaller fans such as at localities 1 and 2 (Figure 1) are veneered over at least 90 percent of their surfaces with Kluane and the younger Neoglacial loess (Figure 2), indicating little activity since Hypsithermal and Neoglacial times. This loess sequence is also present on remnants of the early fans at localities 3, 4, and 5 (Figure 1). Their drainage basins are low and too small to have supported valley glaciers which would have supplied meltwater for their construction.

Rather, they were constructed during late Kluane time when, most probably, the snowline was nearer an altitude of 4000 feet and the greater amounts of melting snow in their drainage basins would have provided sufficient runoff for fan construction. The construction of these fans may not have been related to a lower snowline only but perhaps also to a period of greater rainfall than has subsequently existed.

As the snowline rose and the glaciers continued to shrink during the amelioration of the climate, the fans at localities 1, 2, and 3 (Figure 1) stopped aggrading and

*This report has previously appeared in *American Journal of Science,* 1966, Vol. 269, pp. 600-619, and is reproduced here with permission.

†Department of Geological Sciences, University of Maine, Orono.
‡ Department of Geology, The Ohio State University, Columbus.

[1] Plate 1 is a map inside the back cover of this volume.

[2] The Kluane loess was informally called Kluane silt by Sticht (ms) and Kluane Silt by Johnson and Raup (1964).

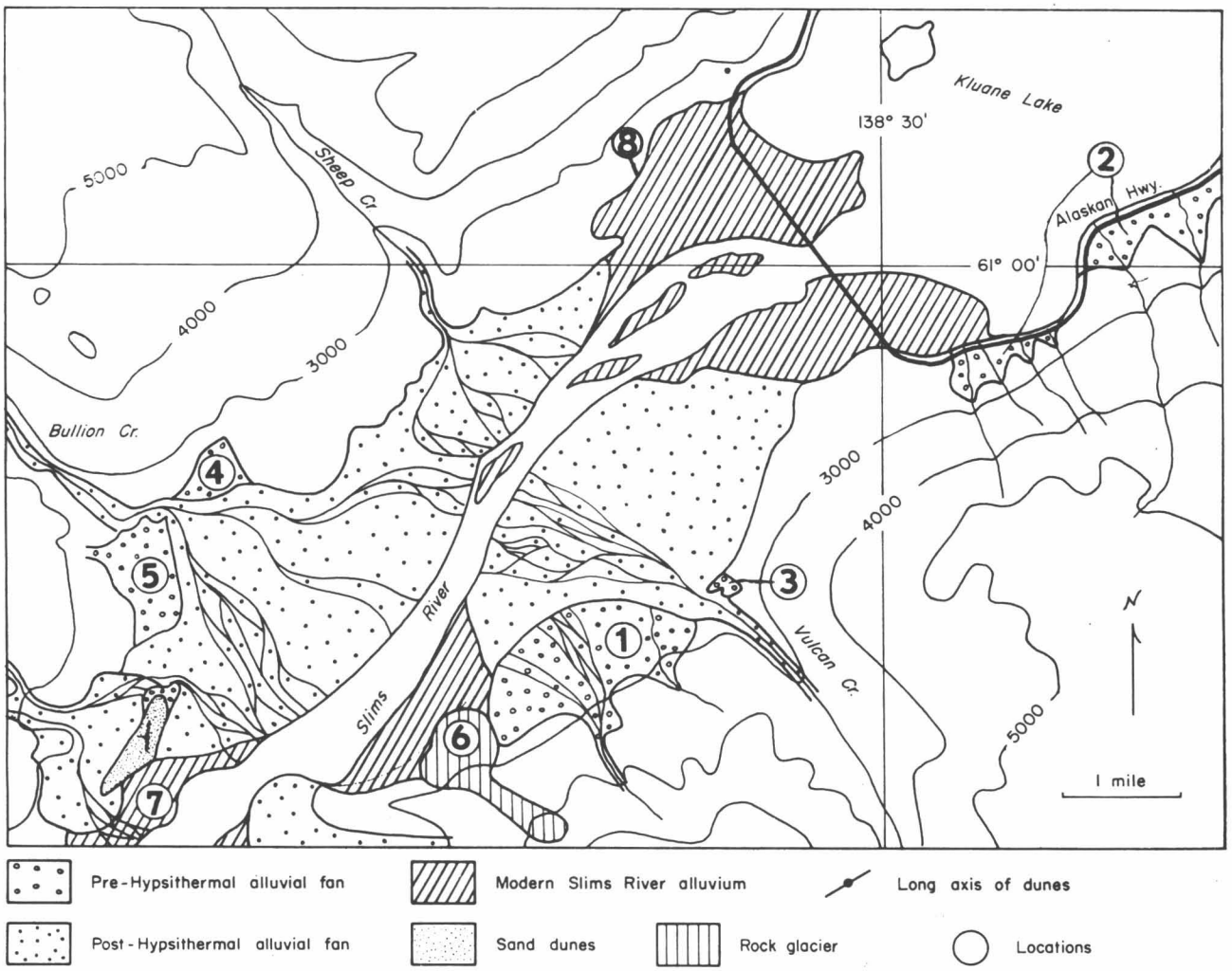

Fig. 1. Pre- and post-Hypsithermal interval alluvial fans and rock glacier in Slims River valley.

were not subsequently degraded prior to accumulation of Kluane loess. However, this is not true for the larger fans at the mouths of Sheep, Bullion, and Vulcan Creeks. These aggraded and were extensively degraded before the Kluane loess had stopped accumulating. This can be clearly seen in the fan remnant at locality 4 (Figure 1). The shift from aggradation to degradation of these earlier, larger fans can be accounted for by the diminution of stream loads, partially a function of waning of the glaciers, and by the size and higher elevation of their drainage basins as contrasted with pre-Kluane loess history of the smaller fans at localities 1, 2, and 3 (Figure 1). It is not known to what depth these larger fans were cut below their present active surfaces. However, the post-Hypsithermal depositional surface of these fans has not been significantly higher than at present. The Slims Soil (Figure 2), developed during the Hypsithermal interval, can be traced down the erosion slope of the pre-Kluane loess fan remnants to the later fan surface (location 4, Figure 1).

Rock glacier. The rock glacier at locality 6 (Figure 1) is presently active as evidenced by its overriding of trees, some of which are less than 10 years old, at its terminus. This rock glacier has been present and probably discontinuously active since ice of the Kluane glaciation retreated up valley as indicated by remnant patches of Kluane loess, Slims Soil, and Neoglacial loess (Figure 2) upon its surface.

Slims Nonglacial Interval

Denton (ms, p. 46) named the time separation between the Kluane and Neoglaciations, the Slims nonglacial interval. As the ice of the Kluane glaciation retreated, Kluane loess deflated from the active valley trains in Slims and other nearby river valleys and accumulated on the older drift. Kluane loess was accumulating in Slims River valley 9780 years ago (Y-1483) and had stopped accumulating by 2640 years ago (Y-1435) (Denton, ms, p. 64). This indicates that the Slims nonglacial interval includes the Hypsithermal interval as defined by Deevey and Flint (1957, p. 182).

Slims Soil. All weathering products of the upper part of the Kluane loess are termed the Slims Soil after the Slims River along whose banks the soil is buried by Neo-

glacial loess and at the terminus of Kaskawulsh Glacier by Neoglacial drift. Denton (ms, p. 44-45) has indicated that these conditions are also present in the valley of the Donjek River and at the terminus of Donjek Glacier (Plate 1)[1]. Areally the buried soil is uniform except for slight variations in thickness. The exposure (location 8, Figure 1) seen in Figure 3 is typical. The upper 9 inches is reddish brown (5YR 4/4) which grades down into a yellowish (5Y 7/6) zone about 8 inches thick. Below this the unoxidized parent Kluane loess is gray (5Y 6/1). These samples were dried before color coding.

The reddish-brown zone is completely leached of calcium carbonate, the yellowish zone is partially leached, and the gray parent material is unleached. Free-iron analyses show 0.06 percent Fe_2O_3 in the reddish brown zone which corresponds with the lack of amphibole. Below this, amphibole is present suggesting that the free-iron oxide was derived from the weathering of the amphibole *in situ*. However, this weathering was not strong enough to produce recognizable changes in the clay mineralogy between the weathered and unweathered portions of the Kluane loess. The pH of the Slims soils is 7.3 and of the parent loess 8.0.

Denton (ms, p. 44-45) has indicated that Slims Soil is not everywhere buried. The soil is exposed at the surface away from the active valley trains, and in these areas the soil is presumably in equilibrium with the existing conditions.

The soil, developed on Kluane loess, has been traced up the west side of Kaskawulsh Glacier by Denton (ms, p. 46) to a point 15 miles up-glacier from the outermost

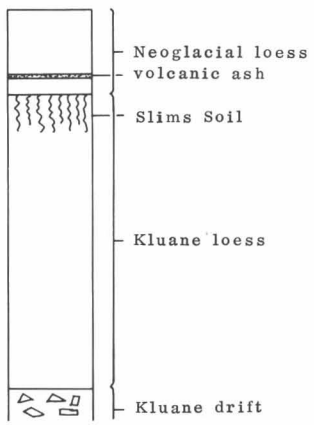

Fig. 2. Typical loess profile in Slims River valley.

Neoglacial moraines that fringe the terminus, suggesting that ice of the Kluane glaciation retreated up-valley at least this far during the Slims nonglacial interval.

Reconnaissance of the distribution of the soil suggests that it is developed upon the Kluane loess, its stratigraphic equivalents, or older deposits over an area of at least 10,000 square miles. This soil was formed during the latter part of the Slims nonglacial interval and, therefore, can be assigned to the Hypsithermal interval.

Climatic shift between the Hypsithermal interval and Neoglacial time. On the top of the interlobate island (location 1, Figure 4) about 400 feet high and half surrounded by the present terminus of Kaskawulsh Glacier is a peat bog (location 2, Figure 4) deposited in a bushy

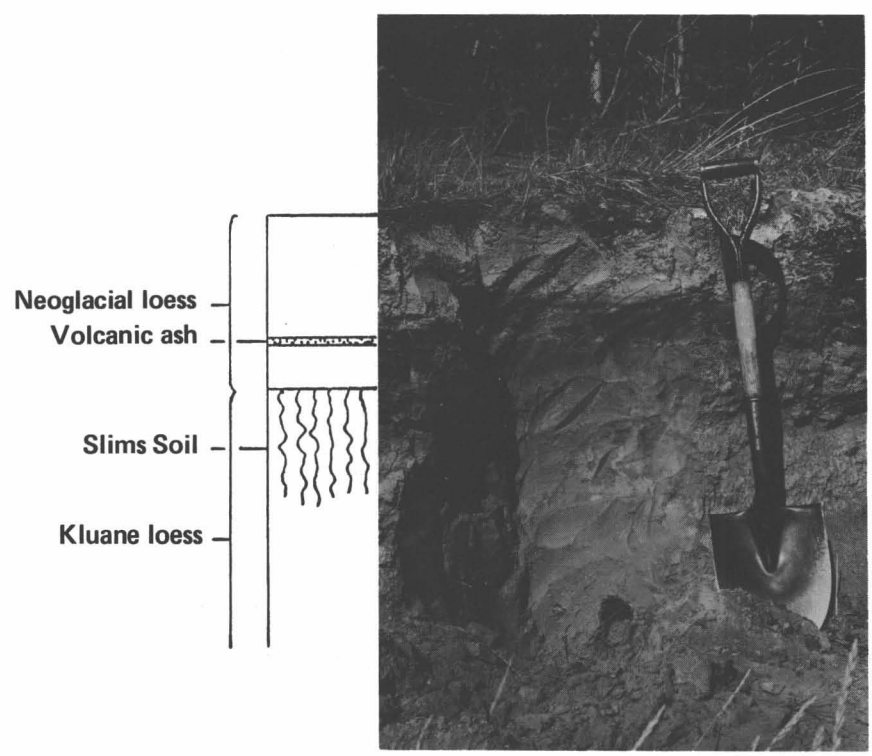

Fig. 3. Complete loess profile (location 8, Fig. 1) typical of Slims River valley (see Fig. 2).

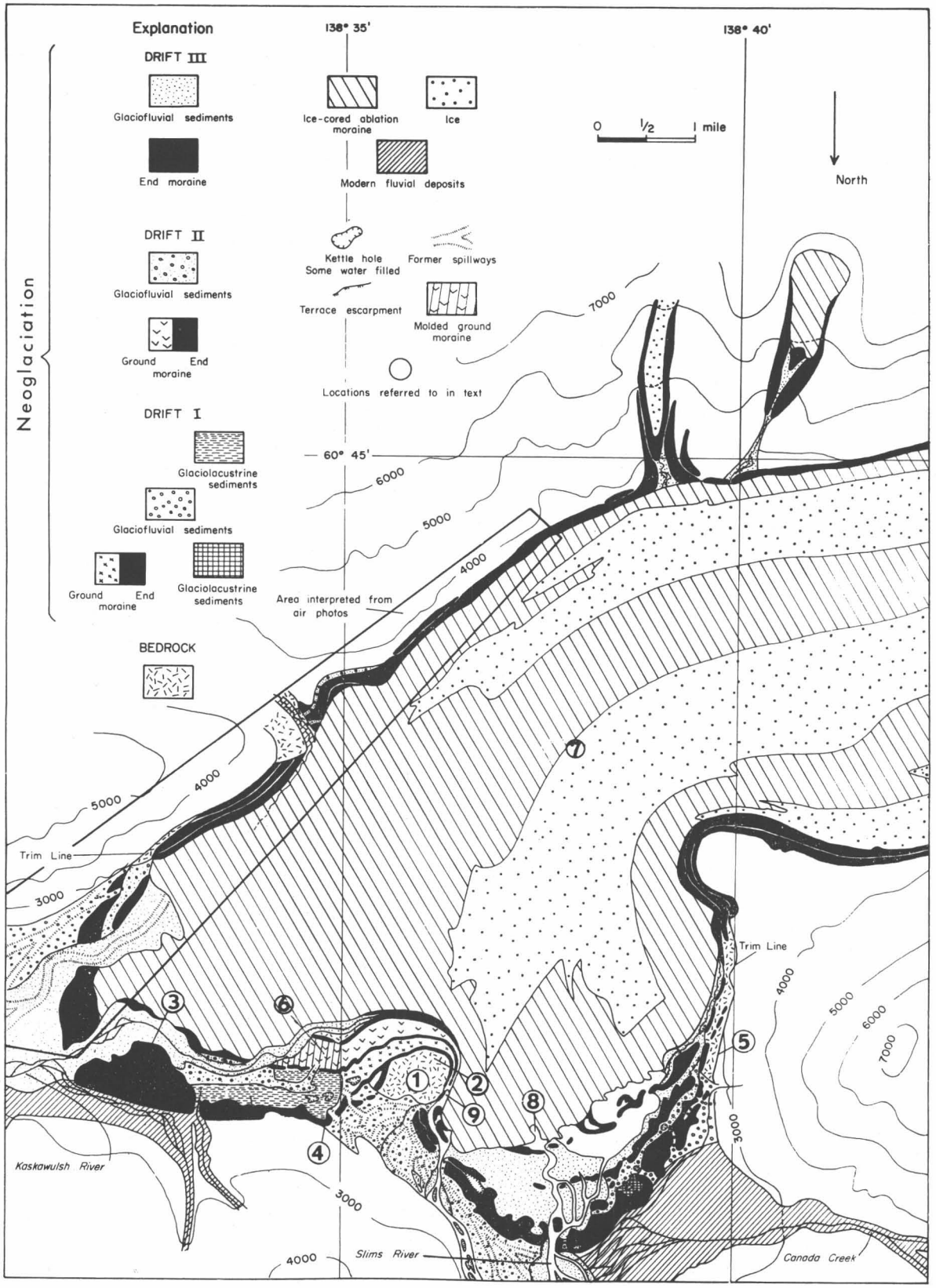

Fig. 4. Glacial geology of Kaskawulsh Glacier, Yukon Territory.

glade in open spruce forest. Because it is only 300 feet outside the outer Neoglacial moraine wrapped up across the knob, it records well the changes of climate.

A 5-foot trench was dug at the deepest location, and samples were taken every inch down to 42 inches and below this every 3 to 8 inches. The upper dark brown peat is 30 inches thick and contains the approximately 1425-year-old white volcanic ash bed 12 inches below the surface. Beneath it is 18 inches of dark gray silt-clay. Deeper to 66 inches total is at least 17 inches of dark greenish silt. Bottom was not reached.

Pollen spores were counted in slides prepared by J. H. Darrell II, under the direction of J. Gordon Ogden III, at Ohio Wesleyan University. Percentages of each pollen type at each depth and total grains counted are presented in Figure 5. Following Dr. Ogden's interpretation the diagram is separable into two main phases, an initial inorganic phase and an upper or later organic phase. The pollen content of the two units is strikingly different. The lower silty unit contains very few pollen grains, primarily grass pollen, with a few sedge and very few spruce pollen grains. The pollen sum in this portion of the profile ranges from 20 to 130 grains, with most of the totals less than 50 grains. For this reason, there is little ground to infer climatic significance for the pollen data recovered from 30 to 65 inches in the sediment profile. The deposit apparently was made in a seasonally moist swale, in which reducing conditions predominated, but whose ability to retain pollen grains was restricted by the exposed nature of the surface. Above 30 inches, there is apparently a real increase in moisture, which resulted in the accumulation of peat. With the onset of peat formation, which would require a significantly greater amount of moisture than the previous "open" conditions, spruce pollen accumulated in abundance, and the dominant herbaceous pollen became sedge instead of grass. It is unlikely that the increase in sedge pollen and decrease in spruce pollen above 30 inches reflect events of climatic significance. It is more probable that this change reflects the increase in local contribution of sedge as conditions in the vicinity of the deposit became increasingly "hydric" while it is possible that the vague maximum of gross pollen from 5 to 18 inches reflects a period of decreased moisture. The change is too small for one to infer climatic control.

The change from predominantly inorganic to predominantly organic sedimentation, however, shown by the change in sediment type and the change from grass to sedge and spruce pollen, is apparently real and reflects a distinct increase in moisture availability at the site. A peat sample collected at the interface between the predominately organic unit above and the predominately inorganic unit below, at a depth of 30 inches, yielded radiocarbon date of 3330 ± 100 years B.P. (Y-1387).

The following mollusk assemblages from the underlying green-gray silt and from peat above and below the ash were identified by Dr. A. LaRocque of Ohio State University.

Green-gray silt 42"-44" depth	Peat below ash 15.5"-19.5" depth	Peat above ash 7.5"-11.5"
Fossaria sp.	*Fossaria* sp.	*Stagnicola* sp.
Pisidium sp.	*Pisidium* sp.	*Gyraulus* sp.
Stagnicola sp.	*Stagnicola* sp.	
Sphaerium sp.		

As Dr. LaRocque points out these suggest a small, permanent lake with an incompletely developed molluskan fauna. *Valvata* and *Physa,* which are the first to enter most Pleistocene lakes, are present elsewhere in Yukon but not here. Reduction in numbers of genera from base to top suggests increasingly acid conditions.

MacNeish (1964, p. 304), in evaluating the megafauna associated with the Kluane loess (Kluane Silt) and the Neoglacial loess[3] (Slims River Silt), concluded that following the last major glaciation (Kluane glaciation) the climate was cooler than at present, and much of the vegetation of the southwest Yukon Territory was tundra or grassland. The muskox, elk, caribou, and bison remains found at archaeological sites associated with the lower portions of Kluane loess attest to this while the later disappearance of muskox and elk, the decrease of bison, and increase of moose and black bear remains indicate a trend toward increasingly warmer and drier conditions. The many bison and caribou remains show that the area was still predominantly grassland, but the steady increase of bear and moose probably indicates that the gallery forest was being extended along the river banks.

With the beginning of the deposition of the Neoglacial loess the associated faunal remains indicate a shift to a dominance of moose over bison suggesting an expansion of the forests. This interpretation of environment is consistent with that of both the geological interpretation of the loess profile and with the interpretation of the pollen sequence.

In conclusion, it can be said that the climatic shift that brought about Neoglaciation in the northeastern St. Elias Mountains was one of a shift from the warmer and drier climate of the Hypsithermal interval in which the Slims Soil was developed and which supported extensive grasslands and grazing animals, to the cooler, wetter climate like the present which supports extensive forests and woodland animals.

Neoglaciation

Sharp (1960, p. 321) defined Neoglaciation as "a short convenient designation for a readvance of ice subsequent to shrinkage during the Hypsithermal interval". The Little Ice Age of Matthes (1939, p. 518) is equivalent to Neoglaciation. All drift deposited in the study area after the Slims nonglacial interval is called Neoglacial drift.

Neoglacial drifts. The Neoglacial drifts deposited by Kaskawulsh Glacier include end-moraine sediments,

[3]The Neoglacial loess was informally called Slims Valley silt by Sticht (ms) and Slims River Silt by Raup (1964).

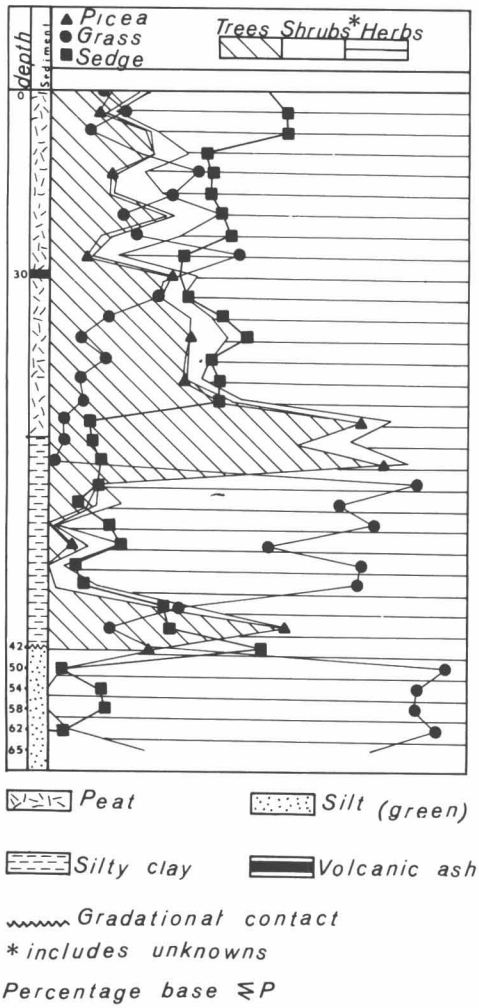

Fig. 5. Pollen diagram for the Slims River valley bog.

inactive and active outwash sediments, and loess. The terminus of the Kaskawulsh is divided into two lobes around a small bedrock "island" (location 1, Figure 4). For purposes of clarity the lobe entering the Slims River valley will be informally called the Slims River lobe and the lobe entering the Kaskawulsh River valley, the Kaskawulsh River lobe (Figure 4).

There are three distinct end moraines of Kaskawulsh Glacier associated with the most recent advance (Figures 4 and 6) all of which are being rapidly dissected and buried by outwash. These end-moraine sediments and associated outwash are divided here into Kaskawulsh I, II, and III, on the basis of the three distinct end moraines fronting the Slims River lobe (Figure 4). The moraine of drift I, the largest and most complete, lies as much as 1 mile in front of the exposed edge of the Slims River lobe while on the Kaskawulsh River lobe this moraine is up to half a mile in front of the exposed glacier edge. Near the eastern side of the Slims River lobe the moraine is clearly composed of two and occasionally three nearly parallel smaller ridges in juxtaposition. Behind this outer moraine, on the Slims lobe, lie the two smaller recessional moraines of drifts II and III. The moraine of drift I is traceable around the bedrock "island" between the lobes along with the two recessionals. However, only the outermost moraine is present completely around the margin of both the Slims and Kaskawulsh River lobes (Figure 4). The relief of the drift I moraine above the adjacent modern outwash varies considerably but averages approximately 15 feet with a few areas as high as 25 feet; however, the depth to the base of the moraine below the outwash is unknown. The relief of the moraines of drifts II and III is considerably less.

Sediments of all three drifts in the terminal area are cored with ice. Nearly all the moraine of drift III has ice within a few feet of the surface, while ice is apparent only a few places within the drift II moraine in the Slims River lobe area. No ice was observed within the drift I moraine of this lobe; however, the temperature of springs issuing from its slopes in several places was 32°F, suggesting, but not proving, the presence of a melting ice core. A seismic traverse between the presently exposed ice edge and the proximal side of the oldest moraine indicated the presence of ice under most of the outwash of drift III along the traverse. The oldest moraine of the Kaskawulsh River lobe is cored with ice at locality 3 (Figure 4), but the presence of ice in other sections of this moraine is questionable.

The moraines on the southern slope of the interlobate bedrock island (location 1, Figure 4) are low, generally less than 8 feet high, but are still distinct and traceable into the more distinct drifts of the lobes. Between the moraines of drifts I, II, and III on the "island" there are many segments of small, cross-cutting moraines, generally less than 5 feet high, which indicate a fluctuating retreat of the ice margin in this area.

The moraine of drift I is composed primarily of till with a clay-silt rich matrix and pebble, cobble, and boulder clasts of metasediment, metaigneous and igneous rocks which reflect the complex bedrock exposed along the main and tributary glacial valleys (Wheeler, 1963). Fluvial sands and gravels and lacustrine silts and clays are intimately associated with the tills in nearly all exposures; however, these are of minor importance volumetrically.

Denton (ms, p. 57) has suggested that the fresh ablation drift covering the ice, which is probably inactive, between drift III and the active glacier, be called Kaskawulsh drift IV. He has further suggested, on the basis of vegetation, that the drift of Kaskawush Glacier is bipartite with an outer drift composed of drifts I, II, III and an inner distinctively younger drift IV.

Vegetation on the drifts. In general, the drifts are young and are just starting to become vegetated. Drifts I and II have sparse and sporadic cover, while drift III is nearly devoid of vegetation. Drift IV of Denton (ms, p. 57) is unvegetated with the exception of a few specimens of *Salix* sp. growing on this unstable ablation material. The highest vegetation density on any drift occurs on drift I where it approaches the valley wall approximately 1 mile north of locality 5 (Figure 4). Here the vegetation easily migrated from the older forested

Fig. 6. Neoglacial end moraines of Kaskawulsh Glacier. Slims River lobe in the foreground.

slopes to the fresh moraine. In well-vegetated areas where comparisons could be made it was estimated that 60 to 70 percent of the surface of drift I was vegetated in contrast with approximately 10 percent on drift II and less than 1 percent on drift III. The plants present on each drift, which were identified by Dr. Rudolph, Ohio State University, are indicated in Table 1.

Trees on each drift were either sampled 1 foot above the base with a Swedish increment corer or cut in order to determine their ages from growth rings. The oldest tree found in drift I was 74 years old, indicating that the glacier had advanced to its terminal position before 1890. However, Krinsley (1965, p. 394) made a brief study of these same drifts and found a tree 97 years old. The oldest trees and their species found on the three drifts are listed in Table 2.

Neoglacial loess. Neoglacial loess rests upon the Slims Soil which developed upon Kluane loess (Figures 2 and 3). In the Slims River valley the Neoglacial loess is generally thickest along the valley bottom and near the terminus of Kaskawulsh Glacier where it averages between 10 and 30 inches. This thickness diminishes rapidly up the valley sides. Downstream on the west side of the valley the loess is forming active dunes. Little or no loess was found on the Neoglacial moraines; however, the loess is being deposited at present downstream from Kaskawulsh Glacier in the Slims and Kaskawulsh River valleys and in Shakwak Trench near the mouth of Slims River valley (Plate 1). The source is the active valley train of Kaskawulsh Glacier. Denton (ms, p. 50) has reported Neoglacial loess is also being developed from the active valley train of nearby Donjek Glacier (Plate 1).

The Neoglacial loess is unweathered and mineralogically is nearly identical to the unweathered Kluane loess. Wherever the Neoglacial loess was observed a layer of white volcanic ash appeared close to its base. This ash was well described by Capps (1915), Bostock (1952, p. 36), and Stuiver, Borns, and Denton (1964). The thickness of the ash within the Slims River valley ranges from 0.5 to 1.5 inches, and it occurs typically 1 to 2 inches above the surface of the Slims Soil. However, occasionally, in places near the Kaskawulsh terminus it is found as much as 2 feet above the Slims Soil indicating a very rapid accumulation of Neoglacial loess prior to the eruption of the ash. This ash forms a marker horizon for the identification of Neoglacial drift in the study area. The age of a wood fragment collected from the base of the Neoglacial loess in the vicinity of the terminus of the Kaskawulsh Glacier (Denton, ms, p. 67-68) places a minimum age for the beginning of the post-Slims nonglacial interval expansion of Kaskawulsh Glacier at approximately 2640 years ago (Y-1435).

The volcanic ash deposited approximately 1425 years ago gives a reliable limiting age for the Neoglacial deposits in this region (Stuiver, Borns, and Denton, 1964, p. 259).

Neoglacial end moraines. No Kluane loess was deposited nor was the Slims Soil developed upon the Neoglacial drifts of Kaskawulsh Glacier. However, masses of Slims Soil are included in, and buried by, the moraine of drift I at several locations, notably on the south slope of the interlobate island and also in the vicinity of locality 4 (Figure 4). In the same area the moraine of drift I was deposited adjacent to the valley wall (Figures 1 and 3). Here the valley slope is veneered by Kluane loess, Slims Soil, and

TABLE 1. Plants Found on the Neoglacial Drifts of Kaskawulsh Glacier

Plants on Drift I
1. *Picea glauca* (Moench) Voss
2. *Populus balsamifera* L.
3. *Salix* sp.
4. *Shepherdia canadensis* (L.) Nutt
5. *Dryas ostopetala* L.

Plants on Drift II
1. *Picea glauca* (Moench) Voss
2. *Populus balsamifera* L.
3. *Salix* sp.
4. *Arctostophlos uva-ursi*
5. *A. alpina* (L.) Spreng
6. *Dryas octopetala* L.
7. (perhaps) *Salix richardsonii* Hooker
8. (perhaps) *Epilobium latifolium* L.
9. *Crepis nana* Richardson

Plants on Drift III
1. *Populus balsamifera* L.
2. *Salix* sp.

Lichens from Drift I
1. *Caloplaca elegans* (Link) Th. Fr.
2. *Omphalodiscus virginis* (Shaer.) Schol.
3. *Umbilicarina arctica* (Ach.) Nyl.

TABLE 2. Ages of the Oldest Trees Found Growing on the Neoglacial Drifts of Kaskawulsh Glacier

	No. of annual rings	Tree species
Drift I	74	*Picea glauca* (Moench) Voss
	51	*Populus balsamifera* L.
Drift II	22	*Picea glauca* (Moench) Voss
	32	*Populus balsamifera* L.
Drift III	16	*Populus balsamifera* L.

Neoglacial loess while the moraine is lightly covered in spots with only Neoglacial loess indicating that the moraine was deposited after the development of the Slims Soil and that the moraine of drift I is the terminal moraine of the post-Slims Soil expansion of Kaskawulsh Glacier. These facts confirm the interpretation of the loess sequence that Kaskawulsh Glacier expanded after the development of the Slims Soil and that the Neoglacial loess, burying the Slims Soil in this area, was, and still is, being developed from the active valley train of this Neoglacial ice expansion.

At locality 4, (Figure 4) several white spruce [*Picea glauca* (Moench) Voss] logs, imbedded in the end moraine of drift I, have been exposed in a former meltwater drainage way (Figure 7). These trees were probably killed by the expanding Kaskawulsh Glacier as indicated by the presence of bark still on the logs. Bark falls off white spruce within a few years after death. A wood sample from the outer 1/2 inch of a 12-inch diameter log at this location yielded a radiocarbon age of 450 ± 100 years (Y-1354). Denton (1965, p. 63) reported the ages of two of the other imbedded logs at this locality as 110 ± 80 (Y-1489) and 390 ± 80 (Y-1490). A sheared spruce stump on the south slope of the interlobate island rooted in Slims Soil and overlain with sediments of drift I yielded an age of 270 ± 60 years (Denton, ms, p. 63) These dates indicate that the Kaskawulsh Glacier was advancing 450 years ago and reached its terminal position by approximately 1680 A.D.

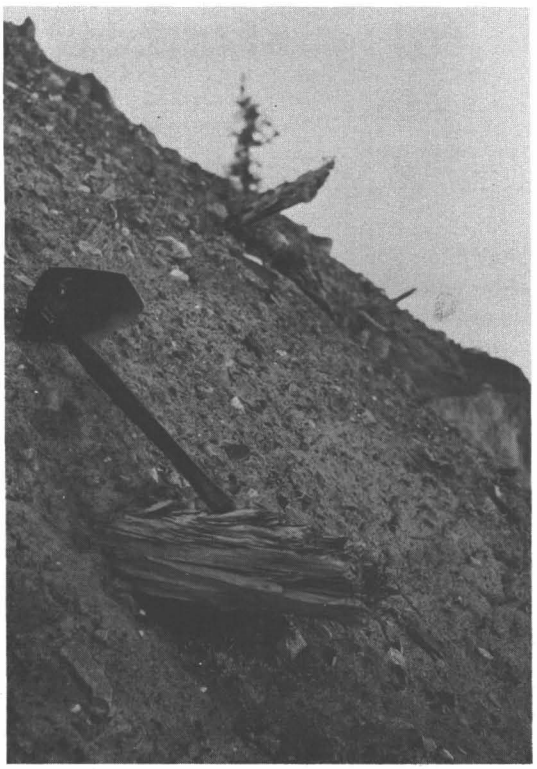

Fig. 7. Log [*Picea glauca* (Moench) Voss] imbedded in the Neoglacial terminal moraine at locality 4 (Fig. 4).

During its Neoglacial expansion Kaskawulsh Glacier advanced below the tree line as evidenced by the logs within drift I at locality 4 (Figure 4) as well as by ice-killed and deformed trees along the trimline. A live tree found at locality 5 (Figure 4) on the prominent trimline in the terminal area was pushed over by the advancing glacier so that its trunk lay parallel to the ground. An increment core of the tree's new vertical growth showed 143 annual growth rings to be present in the summer of 1963. The number of growth rings coupled with the geographic position of the deformed tree indicate that the glacier was present in its Neoglacial terminal position about 1820 A.D. However, the ice first reached its terminal position about 1680 A.D., as indicated by the age of the sheared stump beneath drift I on the interlobate island. Wheeler (1963) suggested that Kaskawulsh Glacier advanced into the same general area between 1730 and 1770 A.D. and again between 1820 and 1860 A.D. He based this on a study of thickness variations between growth rings of trees in the present terminal area. If there was an advance between 1730 and 1770 A.D., as Wheeler has suggested, the terminal position of the glacier was certainly behind the 1820 A.D. terminal position, and no stratigraphic evidence has been found to support its presence. Although the glacier was in its Neoglacial terminal position in 1820 A.D., it is difficult to tell how long it remained there. A minimal date derived from the age of the oldest tree on drift II (Table 2) indicates that the glacier had left the terminal position at least by 1931 A.D. Krinsley (1965, p. 394) in his brief study of Kaskawulsh drifts reported a tree 97 years old on the oldest moraine. However, the oldest tree found on drift I by the authors was a 74-year-old *Picea glauca* (Moench) Voss (Table 2) indicating that this species became established on the moraine by 1889 A.D. This is a minimum figure for the retreat of the ice front from its terminal position. Trees of this species do not establish themselves on unstable, ice-cored drift in this area.

Denton (1965, p. 54) estimated, from his study of Donjek Glacier, that *Picea glauca* (Moench) Voss required at least 53 years to become established on the drift after evacuation of the ice. If this figure is valid for Kaskawulsh Glacier, then it can be assumed that the ice started to retreat from the Neoglacial terminal moraine around 1836 A.D.

The moraine of drift II was clearly built by ice that advanced a minimum of 1000 feet over the dry lake bottom just east of the interlobate island (location 6, Figure 4). This advance left ridges of ground moraine up to 1 foot high between grooves in the lake sediments (Figure 8). These ridges, which meet the low end moraine of drift II at right angles, tail out from single or localized accumulations of boulders and cobbles in crag-and-tail relationships. The fact that no lake sediments were deposited upon the till ridges on the end moraine and that the till rests upon lake sediments implies that the ice advance followed the draining of the lake. The lake was ice-dammed and was drained during the dissipation of the ice from the terminal position.

If 53 years are required for the establishment of white spruce, as Denton (ms, p. 54) has suggested, it can be assumed that the ice retreated from the moraine of drift II about 1888 A.D. (Table 2). The moraine of drift III was built either during a readvance or a pause in the retreat. Denton (ms, p. 54) suggested that *Populus balsamifera* L. require 23 years for establishment on new drift in this area. If this is the case, then the ice retreated from the moraine of drift III about 1925 A.D. (Table 2).

A tripartite division of drift is clear on the Slims River lobe and around the interlobate island; however, only a bipartite division is apparent on the Kaskawulsh River lobe. If the non-vegetated ablation debris presently collecting upon inactive ice (?) at the margin of Kaskawulsh Glacier is considered to be the latest drift (drift IV, Denton, ms, p. 58), then an additional subdivision can be added to the drift sequence of each lobe.

Examination of the two cirque glaciers within the map area (Figure 4) revealed that one of them has three distinct end moraines around its terminus, like the Slims River lobe, while the other has only two distinct end moraines and an ice surface veneered with ablation materials similar to the situation on the Kaskawulsh River lobe.

Denton (ms, p. 61-62) concluded that the Neoglacial history of at least four glaciers, Donjek, Cairnes, Silver, and Kaskawulsh, in the northeastern St. Elias Mountains, was similar and that this history probably was similar for all glaciers in the northeastern St. Elias Mountains. This history, recorded by moraines, is bipartite. The older part of this history is recorded by a larger outer moraine, representing the terminal position of Neoglaciation, and by several small, often cross-cutting, moraines developed during the fluctuating retreat of the Donjek, Cairnes, and Silver Glaciers as well as of the Kaskawulsh River lobe of Kaskawulsh Glacier. This retreat was interrupted by one major readvance or period of equilibrium. Drift accumulated or presently accumulating as a result of this activity is considered representative of the latter phase of the bipartite history.

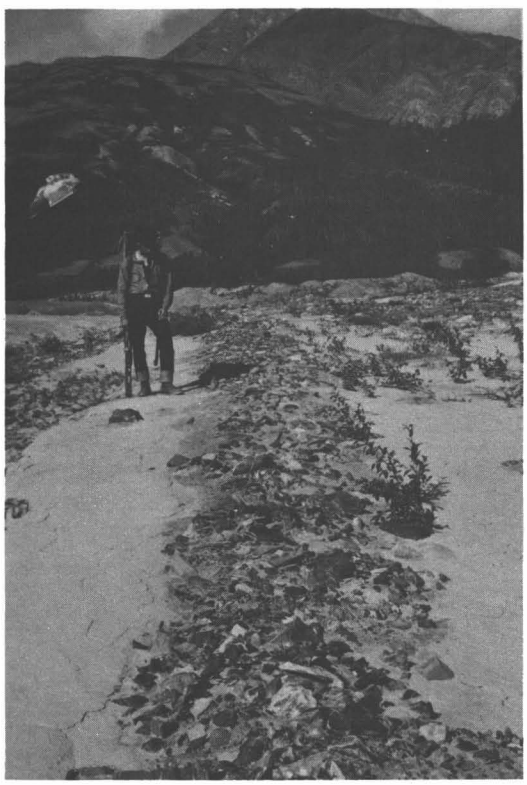

Fig. 8. A till ridge of drift II resting upon glacio-lacustrine silt at locality 6 (Fig. 4). Note the proximal side of drift II end moraine in the immediate background.

The Steele Glacier (formerly Wolf Creek Glacier) also has a bipartite division of drift (Sharp, 1951, p. 107). It appears then from Denton's study of the Donjek, Cairnes, and Silver Glaciers that the bipartite division of Neoglacial drift is common to each. This is also true of the Kaskawulsh River lobe of Kaskawulsh Glacier, and therefore it is suggestive that the distinct tripartite division of drift associated with the Slims River lobe of Kaskawulsh Glacier probably does not represent a regional pattern.

The structure, size, and composition of the moraine of drift I of Kaskawulsh Glacier indicate that it was built over a period of years by an ice front standing essentially in the same position but having an internal forward motion. The size of the Neoglacial terminal moraines of the Donjek and Steele Glaciers implies a similar origin. It is highly improbable that these terminal moraines could have been built by kinematic waves generated by earthquakes in the St. Elias Mountain region. Rather, they were most probably climatically controlled. Therefore, the age of Kaskawulsh drift I is a valid indication of the approximate time of the maximum Neoglacial expansion in the northeastern St. Elias Mountains.[4]

Modern Activity at the Kaskawulsh Glacier Terminus

Measurements of ice motion reported by Wheeler (1963) indicated that the ice stream south of the central ice stream but several miles upstream of locality 7 (Figure 4) moved 700 feet per year between 1953 and 1955 but didn't report any rates from nearer the terminus. Comparison of air photos indicate that the central ice stream at locality 7 (Figure 4) moved approximately 500 feet between September 1956 and July 1957; however, these sporadic measurements are very inadequate in evaluating overall flow in the terminal area.

The topography of the terminal area of the glacier is chaotic with many of the dirty ice faces rising as much as 65 feet. Topography of this type also characterizes the

[4] One may speculate what result the 1963 Alaskan quake will have on the regimen of the glaciers in the Kluane region. Mr. K. Garvis of Silver Creek Lodge at the southeastern end of Kluane Lake indicated by letter the effects of the quake in the area and an interpretation of his data placed the intensity at VI on the Rossi-Forel Earthquake Intensity Scale. These glaciers should be closely observed during the next few years to detect any evidence of kinematic waves.

nearby Kluane and Donjek Glaciers (Plate 1) and was well described by Sharp (1947, p. 35-38) on the Steele Glacier approximately 40 miles to the northwest. In this zone of rapid downwasting the topography is continually being inverted, and when the superglacial mantle comes to rest on the underlying surface the deposit represents an extremely complex mixture of sediments formed in a variety of superglacial environments.

The superglacial mantle differentially covers approximately 9 square miles of the terminal area and generally is less than 2 feet thick on the more gentle ice slopes and thins rapidly as the angle steepens. At the toe of the slopes a 6-foot-thick accumulation is not uncommon. Many of the features, such as glacier tables, debris-covered ice mounds, and dust wells, described by Sharp (1947) on the nearby Steele Glacier are also found on the Kaskawulsh. When the superglacial mantle comes to rest on the surface after complete dissipation of the ice it will probably form an ablation moraine deposit of an inconsequential thickness of 5 to 10 feet at most.

The major meltwater streams draining the ice are either sub- or englacial; however, there are innumerable smaller streams coursing over the ice surface in the ablation zone that do not descend beneath the ice.

The subglacial streams exiting at localities 8 and 9 (Figure 4) are by far the most spectacular. These two streams, which probably contribute the greatest volume of meltwater to the Slims River, exit from sub- or englacial tubes in geyser-like fountains and are under considerable hydrostatic pressure. At locality 8 (Figure 4) the largest stream was observed twice during the season fountaining each time to approximately 8 feet with a a diameter of approximately 10 feet. Philip Upton of the Icefield Ranges Research Project reported that this fountain rose at least 20 feet during August of 1962; however, the summer of 1963 was generally colder than that of 1962, and this difference in height can probably be accounted for by a difference in the volume of meltwater generated. The fountain at locality 9 was about one-half the size of that of locality 8. Examination of air photos indicates that localities 8 and 9 have been the sites of fountaining since at least 1941, which is remarkable in view of the rates of ice motion in the terminal area tending to close the tunnels within the glacier.

Around the openings of these tunnels there are large accumulations of well-rounded boulders up to 2 or 3 feet in diameter which very probably have been ejected from the tube by the hydrostatic pressure and therefore indicate that finer sediment at least cannot be accumulating in the tunnel. One can only speculate as to whether or not eskers can form in such a subsurface environment.

Acknowledgments

This work was done in the summer of 1964 under Grant No. G. P.1125 from National Science Foundation to the Institute of Polar Studies at Ohio State University Research Foundation. The first author spent two months in the area, and the second author two weeks plus a reconnaissance in the previous year. Thanks are especially due to Dr. George Denton of Yale University who coordinated his adjacent work and supplied many observations, to Dr. Minze Stuiver of the Yale University Radiocarbon Laboratory for providing radiocarbon dates, and to field assistants, Richard Bonnett and Land Washburn.

References

Bostock, H.S. (1952) Geology of northwest Shakwak Valley, Yukon Territory, Canada Geol. Surv. Mem. 267, 54 pp.

Capps, S.R. (1915) An ancient volcanic eruption in the upper Yukon basin, U.S. Geol. Surv. Prof. Paper 95, pp. 59--64.

Deevy, E.S., and Flint, R.F. (1957) Postglacial hypsithermal interval, Science, 125, 182--184.

Denton, G.H. (ms, 1965) Late Pleistocene Glacial Chronology, Northeastern St. Elias Mountains, Canada, Ph.D. Dissertation, Yale Univ., 88 pp.

Johnson, F., and Raup, H.M. (1964) Investigations in southwest Yukon: geobotanical and archaeological reconnaissance, Robert S. Peabody Found, Archaeol. Papers, Vol. 6, No. 1, 198 pp.

Kendrew, W.G., and Kerr, D.P. (1955) The Climate of British Columbia and the Yukon Territory, Edmond Cloutier, Ottawa, 222 pp.

Krinsley, D.B. (1965) Pleistocene geology of the southwest Yukon Territory, Canada, J. Glaciol., 5, 385-397.

MacNeish, R.S. (1964) Investigations in southwest Yukon: archaeological excavation, comparisons and speculations, Robert S. Peabody Found, Archaeol. Papers, Vol. 6, No. 2, pp. 201--488.

Matthes, F.E. (1939) Report of Committee on Glaciers, Am. Geophys. Union Trans. 20, 518--523.

Sharp, R.P. (1947) The Wolf Creek glaciers, St. Elias Range, Yukon Territory, Geogr. Rev., 37, 26--52.

Sharp, R.P. (1951) Glacial history of Wolf Creek, St. Elias Range, Canada, J. Geol., 59, 97--115.

Sharp, R.P. (1960) Pleistocene glaciation in the Trinity Alps of northern California, Am. J. Sci., 258, 305--340.

Sticht, J.H.H. (1951) Geomorphology and glacial history along the Alaskan Highway in Yukon Territory and Alaska. Ph.D. Dissertation, Harvard Univ., 176 pp.

*Stuiver, M., Borns, H.W., and Denton, G.H. (1964) Age of a widespread layer of volcanic ash in the southwestern Yukon Territory, Arctic, 17, 259--260.

Wheeler, J.O. (1963) Geologic map of Kaskawulsh half of Mt. St. Elias map sheet, Yukon Territory, Canada Geol. Surv. Map 1134A.

*This article is reprinted in the present volume.

Late Pleistocene Glacial Stratigraphy and Chronology, Northeastern St. Elias Mountains*

George H. Denton† and Minze Stuiver‡

ABSTRACT. Drift morphology and stratigraphic relations of drift sheets and weathering zones indicate four glaciations separated by three nonglacial intervals in the northeastern St. Elias Mountains, Yukon Territory, Canada. Ice of the two oldest glaciations (Shakwak and Icefield) flowed through Slims River valley into Shakwak Valley[1] near Kluane Lake. Ice of the subsequent glaciation (Kluane) entered Shakwak Valley through valleys draining the Icefield Ranges, flowed northwest along Shakwak Valley with a thickness locally exceeding 3530 feet, and terminated in the vicinity of Snag near the Yukon-Alaska boundary. The last glaciation (Neoglaciation) was much more restricted. During the two oldest nonglacial intervals (Silver and Boutellier), Shakwak Valley was ice-free; during the third nonglacial interval (Slims), ice receded more than 13 miles upvalley from the present Kaskawulsh Glacier terminus.

Twenty C^{14} dates combine to give the following late Pleistocene chronology in the areas studied: Shakwak glaciation (>49,000 B.P.), Silver nonglacial interval (>49,000 B.P.), Icefield glaciation (start >49,000 B.P., end approximately 37,700 B.P.), Boutellier nonglacial interval (start approximately 37,700 B.P., end < 30,100 B.P.), Kluane glaciation (start < 30,100 B.P., end approximately 12,500-9780 B.P.), Slims nonglacial interval (start approximately 12,500-9780 B.P., end approximately 2640 B.P.), Neoglaciation (start approximately 2640 B.P., still current).

Comparison of C^{14}-dated glacial events in Yukon-Alaska (as recorded in the St. Elias Mountains and in the Brooks Range) with glacial events in Washington and British Columbia, pluvial events at Searles Lake, California, and fluctuations of the Laurentide Ice Sheet in the Great Lakes region suggests, with reservations, that some major late Wisconsin climatic fluctuations in Yukon-Alaska and these other regions were broadly synchronous. However, sufficient detail is not yet available to make firm conclusions about correlation of minor climatic fluctuations during these times.

INTRODUCTION

The objectives of this study were (1) to examine the chronology of former fluctuations of the St. Elias glacier system as revealed by C^{14}-dated glacial-drift bodies on the northeast flank of the St. Elias Mountains and (2) to investigate temporal relations of glacial and climatic events in various parts of North America by comparing the St. Elias glacial chronology with glacial and pluvial chronologies elsewhere.

The St. Elias Mountains, the largest group of high peaks in Cordilleran North America, are located in southwestern Yukon Territory, northwestern British Columbia, and southeastern Alaska (Plate 1)[2]; the international boundary passes over many of the highest peaks of the mountains. The portions of the mountains considered here are (1) the Icefield Ranges, which form the main group of high peaks and include Mt. Logan (19,850), Mt. St.Elias (18,008), and at least 12 other peaks rising above 15,000 feet in altitude and (2) the Kluane Ranges, which form a narrow front range on the northeast flank of themountains and consist of peaks 6000–10,000 feet in altitude.

Mantling the Icefield Ranges is an extensive intermontane icefield whose average surface altitude decreases from about 8600 feet on the Hubbard-Kaskawulsh glacier divide to about 6000 feet on the accumulation area of the Seward Glacier. This icefield, the most extensive in continental North America, is drained on all sides by long outlet valley glaciers; among the largest are the Lowell, Kaskawulsh, Kluane, Donjek, Walsh, Logan, Seward, and Hubbard. An east-west seismic profile across the Hubbard-Kaskawulsh glacier divide at 8000-8600 feet, in the heart of the Icefield Ranges, indicates that ice thickness here varies from about 800 to 2200 feet (Wood, 1963, Pl. II). Measurements of the thermal regimen of Icefield glaciers indicate two significant facts: (1) The upper part of the Seward Glacier is geophysically temperate, except for a surface layer 40–50 feet thick which attains sub-zero temperatures in winter and warms to 0°C in summer (Sharp, 1951a, p. 480). (2) Ice at 8600 feet on the Hubbard-Kaskawulsh divide lies on the border between geophysically temperate and subpolar ice (Wood, 1963, p. 180). Regimen studies of the Seward-Malaspina glacier system on the south flank of the Icefield Ranges showed a negative budget in 6 of 9 budget years prior to 1954/1955 (Sharp, 1958, p. 622).

In addition to the nearly continuous glacier cover on the Icefield Ranges, valley glaciers and cirque glaciers commonly occur on the flanks of high peaks of the Kluane Ranges.

Three areas were chosen for the study of glacial sediments (Fig. 1) in order to determine the chronology of former fluctuations of the St. Elias glaciers. Twenty C^{14} dates of organic samples from drift bodies in all three areas establish a chronology of glacial events. A part of Shakwak Valley, bounded by the Kluane Hills, the Jarvis River, the Kluane Ranges, and Kluane Lake, was

*This report has previously appeared in *Geological Society of America Bulletin*, 1967, Vol. 78, pp. 485-510, and is reproduced here with permission.

†Department of Geology, Yale University, New Haven, Connecticut.

‡Director, Radiocarbon Laboratory, Yale University, New Haven, Connecticut.

[1] Ed. Note: "Shakwak Valley" is now officially named Shakwak Trench and appears as such in Table 1, though the name "Shakwak Valley" is retained elsewhere throughout the article.

[2] Plate 1 is a map inside the back cover of this volume.

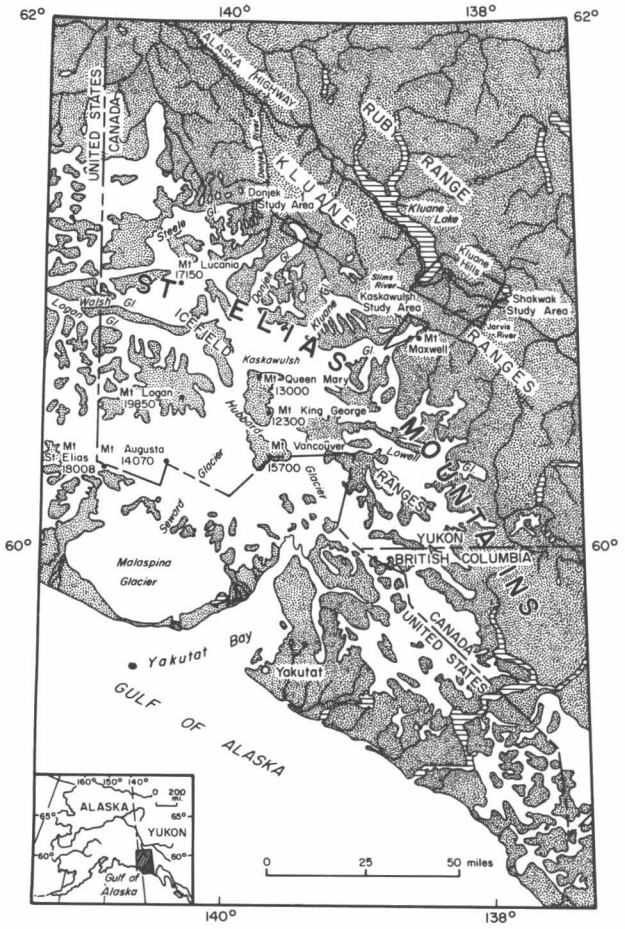

Fig. 1. Locations of three study areas. The three study areas are outlined.

selected because it lies on the major route of Pleistocene glaciers that flowed northwest out of the St. Elias Mountains and because it contains well-preserved drift. The floor of Shakwak Valley in this area is rather flat and is 8–10 miles wide; along the valley axis the floor slopes gently from 3200 feet near Hungry Lake, where it is a drainage divide, northwest to 2560 feet at Kluane Lake, and also southeast to 2600 feet at Jarvis River. The rugged Kluane Ranges, which rise to 9300 feet, form the steep southwest valley wall; and the low, rounded Kluane Hills form the gentle northeast valley wall. Relief averages about 3300 feet and locally reaches 6000 feet.

The areas surrounding the terminal portions of the Donjek and Kaskawulsh Glaciers were chosen for study because the glaciers are fringed by young moraines. Both glacier termini lie in broad, flat valley floors 5–6 miles wide and flanked by peaks 6000–10,000 feet in altitude; the Donjek terminus lies at 3500 feet and the Kaskawulsh terminus, at 2700 feet. Downstream from the young moraines that fringe each glacier, the valley floors are patterned by braided meltwater streams.

Previous work on glacial geology of the northern border of the St. Elias Mountains was essentially reconnaissance. Until very recently all pre-Hypsithermal drift was attributed to one major glaciation regarded as late Wisconsin (Bostock, 1952, p. 13; Sharp, 1951 b, p. 100), or simply Pleistocene, in age (Kindle, 1953, p. 14). Most ice responsible for this drift originated in the Icefield Ranges and entered Shakwak Valley through valleys transecting the Kluane Ranges. In Shakwak Valley most of the ice flowed northwest to a terminal position near Snag (Bostock, 1952, p. 14 and Map 1012A), whereas some flowed northeast along Dezadeash River valley and some north into valleys of the Ruby and Nisling ranges. The ice surface attained altitudes of 6100–6500 feet on the north slope of the Kluane Ranges (Bostock, 1952, p. 13; Kindle, 1953, p. 15; Wheeler, 1963) and 5200 feet on several mountains in the Ruby Range (Bostock, 1952, p. 13). During deglaciation loess and glacial-lake sediments were deposited north of the retreating glaciers; during the Hypsithermal the surface of these sediments was weathered (J. Sticht, 1951, Ph.D. dissert., Harvard Univ.; Johnson and Raup, 1964, p. 22-34). Post-Hypsithermal glacial advance, possibly multiple, caused renewed loess deposition and formed several large proglacial lakes (Sticht, Ph.D. dissert.; Kindle, 1953, p. 21–22; Johnson and Raup, 1964, p. 22–34). Recently, Krinsley (1965) recognized several moraines, near the Yukon-Alaska boundary, to which he has assigned ages ranging from Kansan to classical Wisconsin. Additionally, he has assigned post-Altithermal (post-Hypsithermal) ages to moraines fringing the termini of the Klutlan and Kaskawulsh Glaciers.

Climates on the southwest and northeast flanks of the St. Elias Mountains contrast sharply, reflecting the effectiveness of the mountains as a climatic barrier. The climate of the Gulf of Alaska to the southwest is maritime; at Yakutat from 1941 to 1950 the mean annual temperature was 39.5°F and the mean annual precipitation, 134.08 inches (U. S. Weather Bureau, 1959, p. 826). Northeast of the mountains the climate is continental; the three available stations in southwest Yukon, northeast of the mountains, gave the following average values: Whitehorse (1941–1950) 31°F, 10.6 inches; Aishikik (1943–1950) 25°F, 10.1 inches; and Snag (1943–1950) 22°F, 14.1 inches (Kendrew and Kerr, 1955).

PRESENT AND FORMER FIRN LIMITS

As used here, the term *firn limit* refers to the upper limit on a glacier surface reached by receding winter snow during the succeeding ablation season. By this usage the firn limit is not the same as the equilibrium line of a glacier if superimposed ice is present below the firn limit.

The firn-limit altitude on glaciers of the St. Elias Mountains has been measured at four localities (Fig. 2). On the Malaspina-Seward system the firn-limit altitude averaged 2750 feet between 1947 and 1955, although it ranged from 1000 to 4000 feet depending on climatic variations from year to year (Sharp, 1958, p. 620). On the Kaskawulsh Glacier the firn-limit altitude averaged 6400 feet from 1962 to 1964 (Richard Ragle, personal communication, 1965). On the south flank of the Kluane Ranges, the firn-limit altitude on small glaciers averaged 7400 feet from

1962 to 1964; on the north flank it averaged 7500 feet from 1962 to 1964. Despite the lower inland mean annual temperatures, a line connecting these points (Fig. 2) rises northeast at 60 feet/mile between the Malaspina-Seward system and the Kaskawulsh Glacier and 40 feet/mile between the Kaskawulsh Glacier and the Kluane Ranges. This inland rise of firn-limit altitudes is consistent with the increasingly continental climate across the St. Elias Mountains and suggests that the chief source of precipitation for the St. Elias glaciers is from the Gulf of Alaska to the southwest.

Altitudes of floors of cirques presently empty of glacier ice were plotted for the southwest flank of the St. Elias Mountains near the Malaspina Glacier and for mountains in the Kluane Hills and the Ruby Range. Because most of the cirques were formerly occupied by rather extensive glaciers, the altitude of each cirque floor represents a maximum figure for the firn-limit altitude on the glacier that occupied it. In each case the closest measure of the altitude of the change in slope between the headwall and the floor of the cirque was plotted as representing the cirque-floor altitude. Near the Malaspina Glacier, cirques were identified from topographic maps with a contour interval of 100 feet; in the Kluane Hills and the Ruby Range, cirques were identified from air photographs, and the floors of north-facing cirques were plotted from topographic maps with contour intervals of 100 and 500 feet.

A line connecting the minimum cirque-floor altitudes on both flanks of the St. Elias Mountains rises inland from 900 feet altitude near the Malaspina Glacier to 4400 feet in the Kluane Hills (Fig. 2). The slope of the line is crude because the lowest cirques near the Malaspina Glacier may not have been recognized on the topographic maps and because the effects of recent orogeny on cirque altitudes cannot be ascertained; however, it reflects the correct order of magnitude. Northeast of the mountains a line connecting the minimum altitudes of cirque floors rises northeast at 35 feet/mile from 4400 feet in the Kluane Hills to 5200 feet in an area of the Ruby Range, about 20 miles northeast of Kluane Lake and the Kluane Hills. Northeast of this area of the Ruby Range, cirque floors maintain a constant minimum altitude of about 5200 feet. Because the various cirques plotted on both sides of the mountains may have been repeatedly occupied by glacier ice, minimum cirque altitudes may represent the effects of multiple glaciation.

The inland rise of minimum cirque-floor altitudes is comparable with the rise of the present-day firn limits and indicates that the source of precipitation for the Pleistocene glaciers occupying the cirques, and probably also for the intermontane icefield covering the Icefield Ranges, was the Gulf of Alaska. The initial rise of minimum cirque-floor altitudes in the Kluane Hills and Ruby Range suggests that the main source of precipitation for the Pleistocene glaciers here was also from the south or southwest.

GLACIAL EROSION IN SHAKWAK VALLEY

In the Shakwak study area all bedrock exposed below 6100 feet has been glacially sculptured into rounded knobs, streamlined forms, and blunted spurs. Most ravines have been obliterated. A glacially smoothed valley shoulder near the junction of Slims River Valley and Shakwak Valley at altitudes of 5500-6100 feet indicates particularly strong abrasion. Above 6100 feet there remains alpine morphology characterized by sharp ridges, pyramidal peaks,

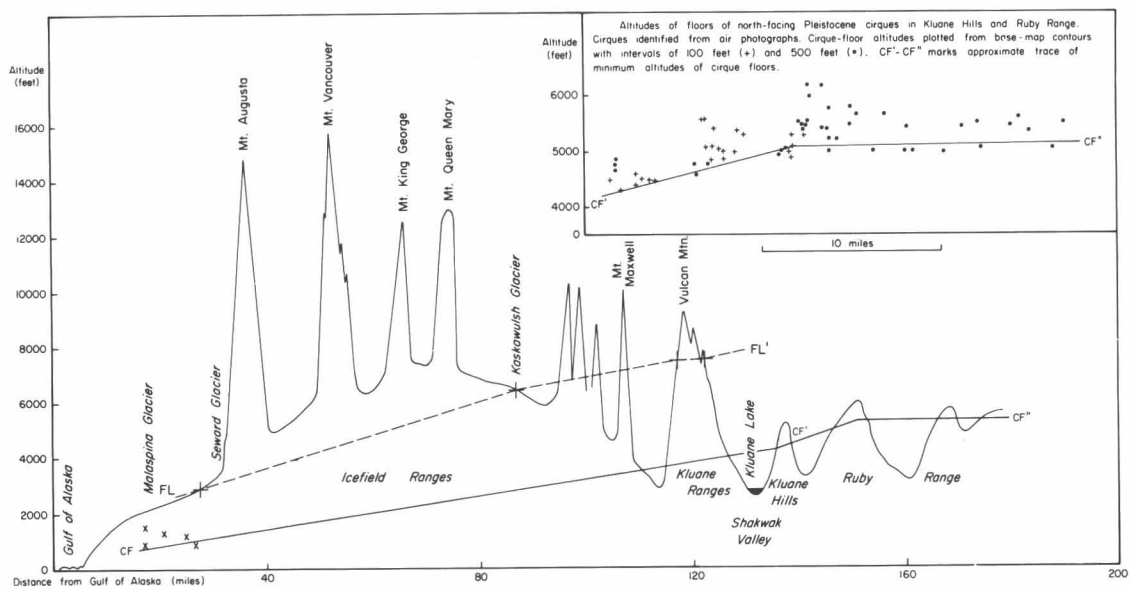

Fig. 2. Southwest-northeast topographic section across the St. Elias Mountains, from Malaspina Glacier to Ruby Range (Fig. 1). Cross marks indicate present altitudes of firn limits, and FL-FL′ is the trace connecting these altitudes. X marks indicate altitudes of Pleistocene cirque floors near the Malaspina Glacier; CF-CF′ connects altitudes of lowest cirque floors to the north and south of the St. Elias Mountains, and CF′-CF″ traces minimum altitudes of floors of north-facing Pleistocene cirques in the Kluane Hills and Ruby Range (see inset for detail).

and many ravines. This morphologic change, present everywhere along the southwest wall of Shakwak Valley, marks an apparent upper limit of glaciation (see Flint and Fidalgo, 1964, p. 341), the minimum upper altitude of former glacier ice.

Both small- and large-scale features of glacial abrasion are present below the apparent upper limit of glaciation. Glacial polish and striations occur on a streamlined hill of chlorite schist in the southeast part of the study area, where all striations trend N 40° W, and also on basalt on a small island in the southeast part of Kluane Lake, where all striations trend N10° W. Elsewhere enough exposed bedrock has been eroded in postglacial time to remove any striations formerly present. Large-scale molding of various types of bedrock by glacier ice has resulted in rounded knobs and flutings. The major positive elements of the flutings are streamlined hills, including drumlins and parallel ridges; the negative elements range from small gouges to large grooves separating the ridges. Most of the parallel bedrock ridges originate to leeward of molded bedrock knobs and grade into similar ridges composed of till of the youngest major glaciation, the Kluane glaciation. The till ridges reach 6 miles in length and are separated by grooves. Relief from groove trough to ridge top ranges from 6 to 50 feet, whereas the distance between ridge crests ranges from 50 to 300 feet. The extent to which these till features are erosional or depositional is not clear.

The surficial features of glacial abrasion below 6100 feet in the Shakwak study area are attributed to the Kluane glaciation because of three considerations: (1) all directional features form a pattern consistent with the flow direction of Kluane ice, as shown by flutings and till fabrics on and in Kluane till III, and are inconsistent with ice-flow directions of older glaciations; (2) flutings in bedrock are continuous with those in Kluane till III; (3) Kluane ice probably would have removed or modified most pre-existing surficial glacial abrasion features. Long axes of flutings, accurately portraying flow directions of Kluane ice, form an arc that parallels Jarvis River valley and Shakwak Valley (Fig. 3). Because flutings consistent with the flow directions of Kluane ice are present up to 6100 feet, and also because Kluane till is present at 6000 feet on the large valley shoulder, the apparent upper limit of glaciation is attributed to the Kluane glaciation.

STRATIGRAPHY

General Statement

In the Shakwak study area, drift mantles the valley floor to thicknesses exceeding 300 feet and thins rapidly with altitude and steepness on valley walls until at 6100 feet, the upper limit of drift, only erratics and patches of drift are preserved. The drift on the valley floor comprises a complex stratigraphic sequence of till, outwash, ice-contact stratified drift, lacustrine sediments, and loess (Fig. 4) that is best exposed in cross section along Outpost, Silver, Boutellier, Christmas, and Inlet Creeks.

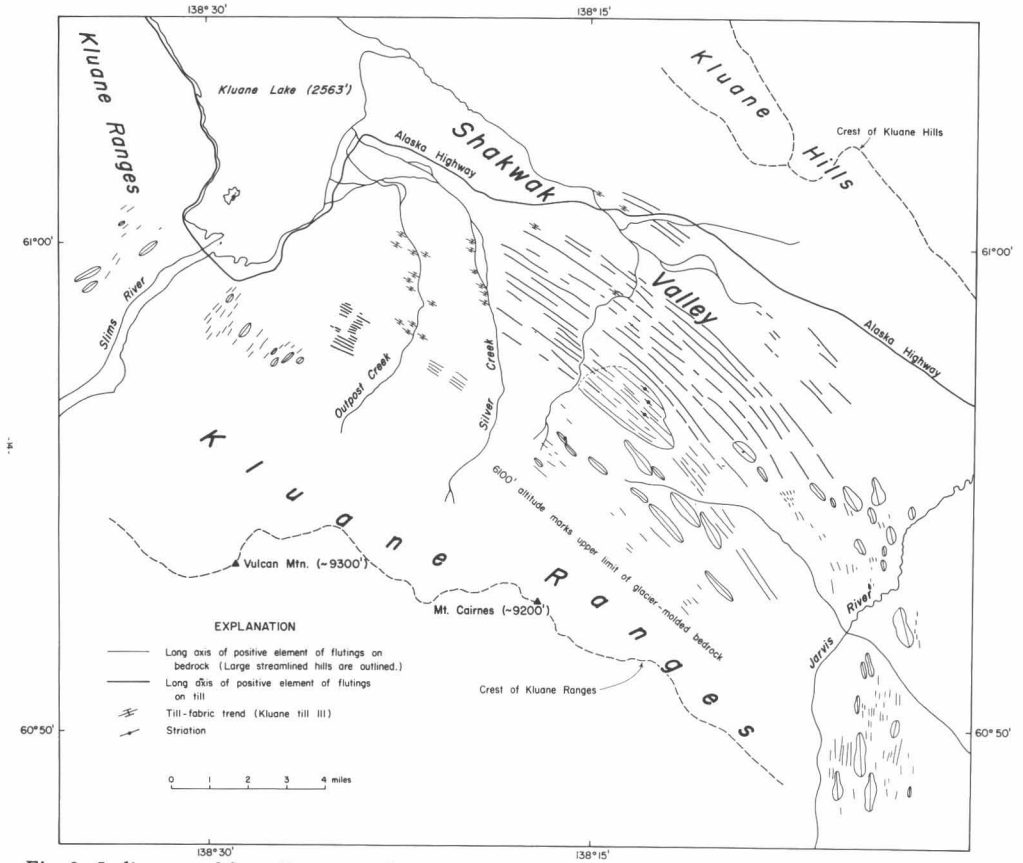

Fig. 3. Indicators of flow directions of glacier ice of the Kluane glaciation within the Shakwak study area and contiguous areas.

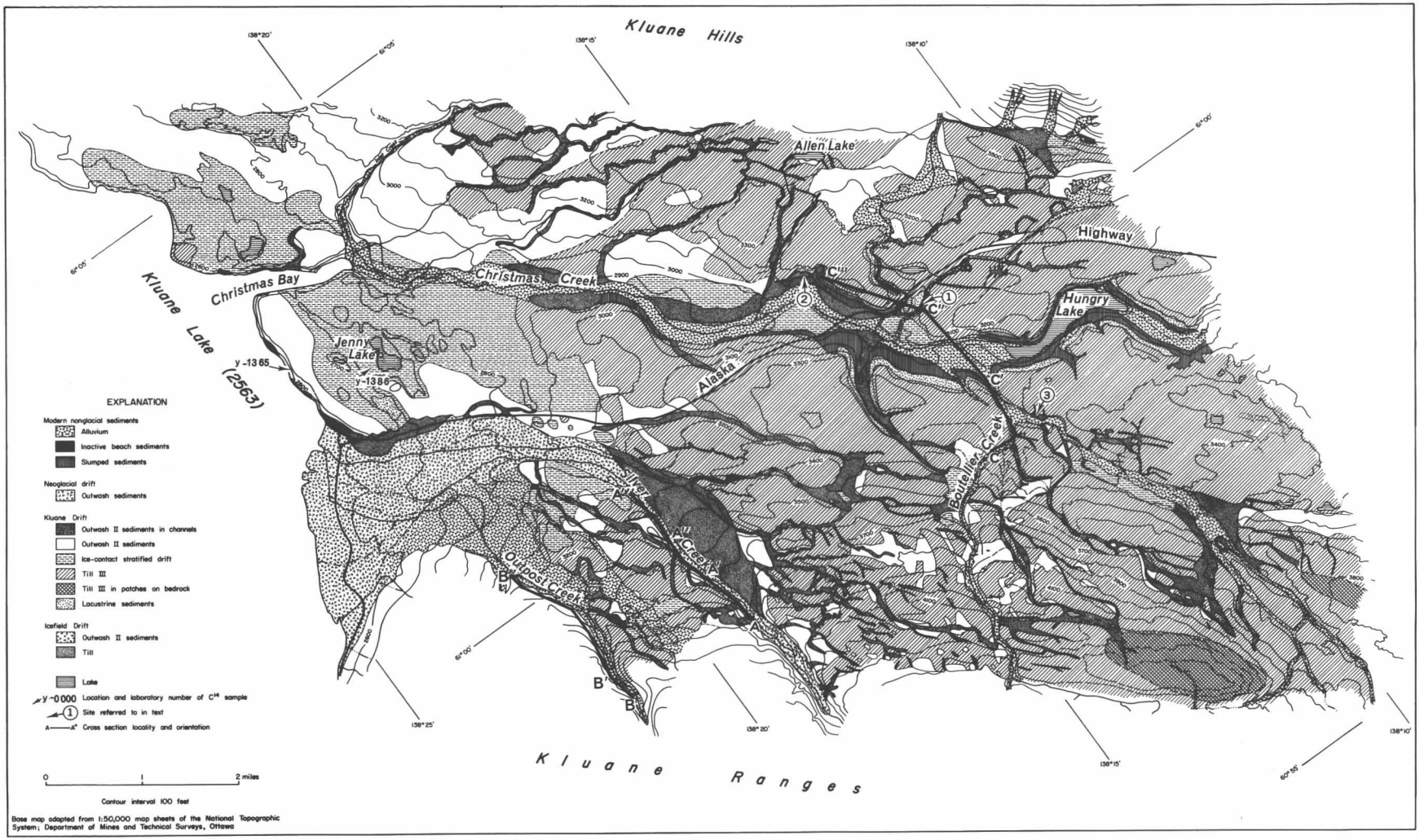

Fig. 4. Glacial drift in part of Shakwak Valley. Surficial loess units and volcanic ash are not shown. Mapping is based on interpretation of air photographs and on 2000 pits dug in glacial drift.

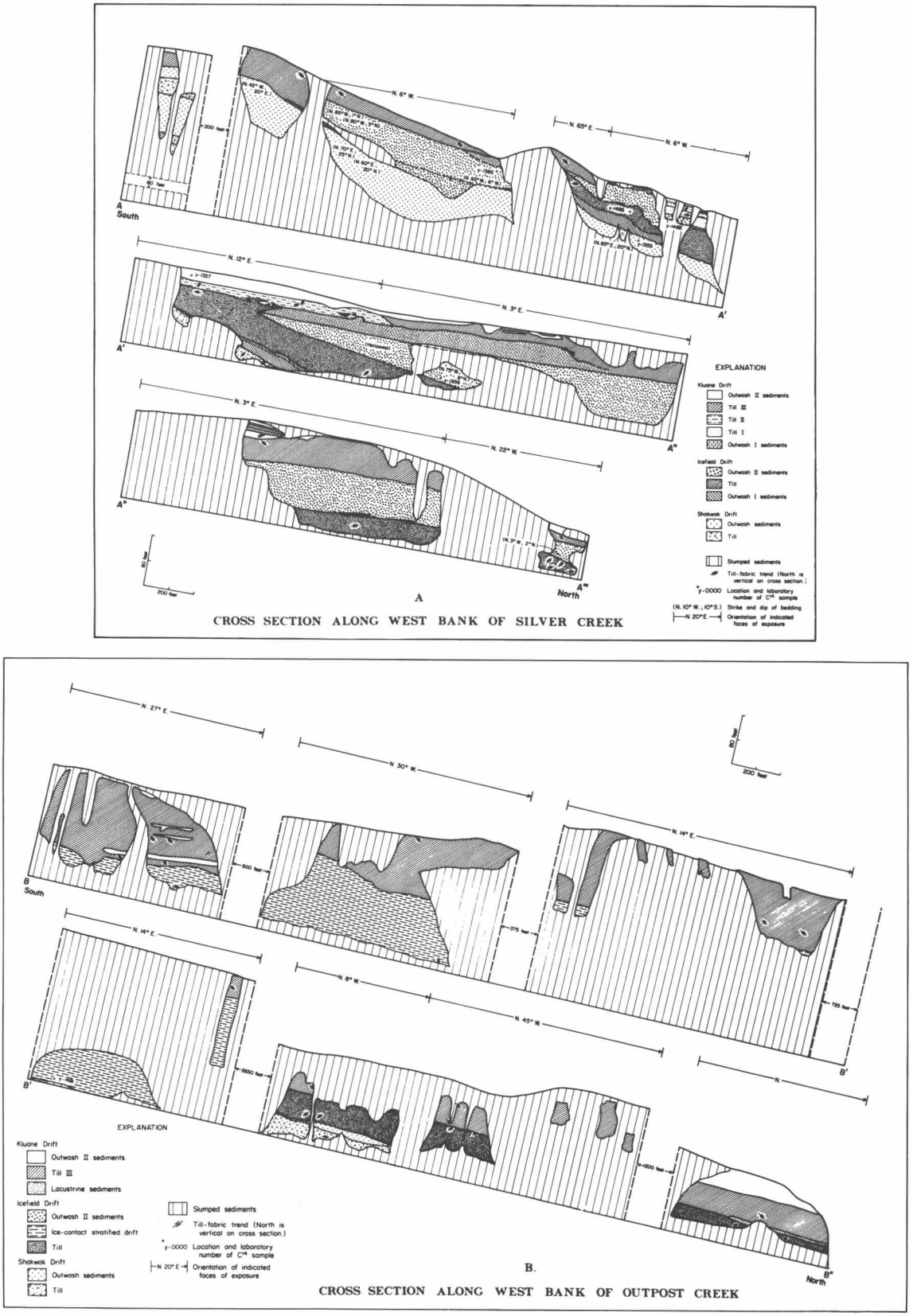

Fig. 5. Cross sections along Silver Creek (A) and Outpost Creek (B), Shakwak Valley. Locations and orientations are designated in Fig. 4. The bottom lines of the cross sections represent the creek beds. Surficial loess units and volcanic ash are not shown.

Additionally, very fresh moraines fringe the termini of glaciers on the north flank of the Kluane Ranges in the study area; these are developed best near the Silver and Cairnes Glaciers[3] (see Denton, 1965; Denton and Stuiver, 1966 and pp. 173–186 of this volume). In the Donjek and Kaskawulsh study areas young end-moraine and outwash sediments surround glacier ice and are flanked in turn by older drift.

The drift bodies are divided into four groups, each representing a glaciation. The grouping is based primarily on marker horizons consisting of two weathering zones and a soil within the stratigraphic sequence, and secondarily on C^{14} dates, characteristics of contacts between units, and drift morphology. The sequence of glaciations and nonglacial intervals thus delineated is as follows, from youngest (top) to oldest:

Neoglaciation
Slims nonglacial interval
Kluane glaciation
Boutellier nonglacial interval
Icefield glaciation
Silver nonglacial interval
Shakwak glaciation.

Drift of the Shakwak and Icefield glaciations as well as weathering products of the Silver and Boutellier intervals were examined solely in the Shakwak study area; drift of the Kluane glaciation and Neoglaciation as well as weathering products of the Slims interval were examined in all three study areas. A cross section of all drift units is shown in Fig. 6.

In the Shakwak study area drift of the Shakwak and Icefield glaciations is everywhere covered with younger glacial sediments and therefore is exposed only in stream cuts. Drift of the Kluane glaciation is generally covered with only a very thin layer of Neoglacial loess; hence both its cross section and its surface morphology are visible. In the study areas, drift of the Neoglaciation, the least extensive of the four glaciations, includes only fresh end-moraine sediments surrounding termini of the Donjek, Kaskawulsh, Cairnes, and Silver Glaciers; outwash bodies extending downstream from these glaciers; and a surface layer of loess, which thins with increasing distance from the Donjek and Kaskawulsh outwash bodies.

Drift units within the Shakwak study area were correlated by (1) physical tracing between closely spaced exposures, (2) comparison of physical characteristics of the deposits, including weathering intensity, (3) stratigraphic position, and (4) C^{14} dates. The younger drift units in and among the three areas were correlated primarily through recognition of a distinctive soil formed during the Slims interval and an equally distinctive white volcanic ash deposited during the Neoglaciation, and secondarily by comparison of physical characteristics of the deposits.

[3]In order to facilitate parts of the following discussion several names were informally used for presently unnamed features. These include Outpost Creek (Figs. 4 and 5) and Cairnes and Silver Glaciers (see Denton, 1965; Denton and Stuiver, 1966 and pp. 173–186 of this volume).

The drift bodies of all glaciations contain a wide variety of sedimentary, metamorphic, and igneous clasts, reflecting the complex bedrock traversed by the glaciers. Many lithology counts showed that rock types in drift bodies of all ages are similar; hence lithology is not a useful guide for the recognition and correlation of individual drift sheets.

Shakwak Drift

General character and stratigraphy. The oldest and stratigraphically the lowest drift sheet recognized in the study areas is here termed Shakwak Drift, after Shakwak Valley where its sole exposures are located. Because it is covered everywhere with younger sediments, the drift crops out only in deep-cut banks of Silver and Outpost creeks; its best exposure is in the west bank of Silver Creek (Fig. 5A).

Along Silver Creek, Shakwak outwash up to 80 feet thick can be traced through 4200 feet between closely spaced exposures (Fig. 5A, sec. A-A′). Upstream, within this outwash body, are two 15-foot layers of Shakwak till separated from the outwash by sharp contacts. Although not demonstrable, interfingering of the till and outwash at this locality is probable. The exposure of outwash farthest downstream is close enough to a Shakwak till body, at least 400 feet long and 10 feet thick, to support the inference that the till conformably overlies the outwash. Along Outpost Creek Shakwak till 3-35 feet thick is exposed through 500 feet laterally and is overlain sharply by 1-10 feet of Shakwak outwash (Fig. 5B, sec. B′-B″).

Shakwak till is compact, nonsorted, and nonstratified. Unaltered till is medium gray (N5 on the Munsell color scale). Although a few clasts are rounded, most are angular or subangular; 10-15 per cent of the fine-grained clasts are striated. Three till-fabric analyses (Fig. 5), each based on 100 stones, show trends ranging from N 40° E to N 50°W, toward Slims River valley, a principal outlet for Pleistocene glaciers that flowed north from the Icefield Ranges

Shakwak outwash exposed on Silver Creek contains parallel stratification throughout the deposit. Individual beds are composed of well-sorted gravel, sand, and silt; average 12-20 inches in thickness; and persist laterally 150-200 feet before pinching out. Most clasts are subround. In upstream exposures bedding is nearly horizontal, whereas in downstream exposures it generally strikes N 60° E and dips as much as 20° N. Shakwak outwash exposed on Outpost Creek is poorly sorted and contains subparellel, nearly horizontal bedding.

Shakwak stratified sediments are inferred to be outwash because (1) they contain till bodies and hence were deposited in close association with glacier ice, and (2) glacier ice is the most probable source for the necessary large quantities of water as well as for the clasts of various lithologies present. Their location stratigraphically above and below Shakwak till suggests that the outwash sediments were deposited during times representing both advances and recessions of Shakwak ice.

The Shakwak till and outwash bodies are ascribed to one episode of glaciation, for two reasons. First, they possess

similar weathering characteristics, discussed later, which differ appreciably from those of all younger drift bodies. Second, nonglacial sediments and other evidence of depositional breaks within and between the drift bodies are lacking. Its similarity to recently dissected outwash fans nearby suggests that Shakwak outwash was deposited as a fan or series of fans by meltwater from the Shakwak Glacier.

Shakwak glaciation. The Shakwak glaciation was the climatic episode, characterized by glacial expansion, during which Shakwak till was deposited. Till-fabric trends indicate that Shakwak ice, derived mainly from the Icefield Ranges, flowed into the Shakwak study area by way of Slims River valley. The inclusion of till bodies within Shakwak outwash implies that the Shakwak glacier terminus fluctuated several times over the area of the drift exposures. The distribution of drift exposures, which determines the minimum extent of Shakwak advance(s), indicates that Shakwak Glacier ice extended at least 22 miles northeast of the present terminus of the Kaskawulsh Glacier and at least 67 miles northeast of the present divide, in the Icefield Ranges, between the Kaskawulsh and Hubbard Glaciers. If such an extensive advance occurred in Slims River valley, similar advances probably occurred in all major valleys draining the Icefield Ranges. Evidence for determining thickness of glacier ice during the Shakwak glaciation is lacking.

Silver Weathering Zone

Character. Throughout its exposed thickness, Shakwak Drift has been modified by subaerial weathering and dissection. The products of this modification are termed the Silver Weathering Zone because they are best exposed in the cut bank of Silver Creek.

The matrix of Shakwak till is oxidized to a minimum depth of 15 feet with oxidation most intense along, and decreasing in intensity with distance from, joints and permeable zones. Small, compact, clayey portions of the till remain unoxidized and are medium gray (N5) compared with dusky yellow (5Y 6/4) for the oxidized till. Analyses for free iron show 0.04 per cent Fe_2O_3 in oxidized till compared with 0.02 per cent in unoxidized till, whereas X-ray diffraction studies indicate that weathering was not sufficiently intense to cause significant alteration of minerals. The till is not leached of calcium carbonate. Only a few clasts are stained with iron oxide; most are fresh. A few globules of iron oxide deposited by ground water are present, but most of the weathering appears to have resulted from oxidation of the till matrix in place.

The outwash is weathered uniformly throughout its exposed thickness of 80 feet. Most clasts, regardless of lithology, are thoroughly coated with iron oxide as much as 0.1 inch thick, and fine particles of iron oxide are disseminated through the matrix. As a result the entire de-

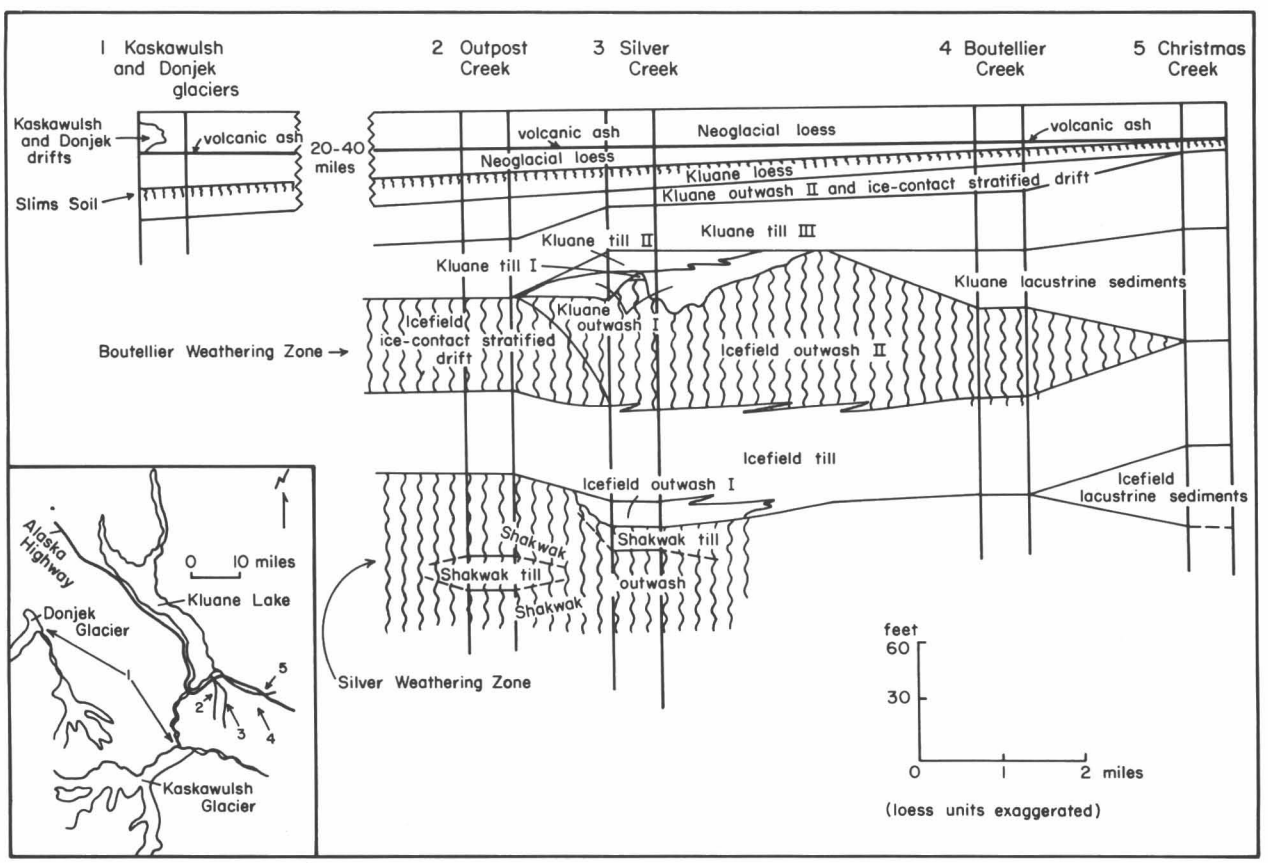

Fig. 6. Composite stratigraphic section of drift units in study areas. Inset shows locations of columnar sections.

posit has an orange color. Iron oxide is especially concentrated immediately above impermeable beds of clayey silt. Partly or wholly disintegrated clasts are scattered randomly throughout the deposit; in the case of granite they amount to 10 per cent of the total granite clasts. Although weathered, the gravel, like the till, is not leached of calcium carbonate. The origin of the iron oxide in the deposit is attributed to ground-water circulation, and because about 10 per cent of the clasts originally contained iron oxide, these were probably a major source of iron for the ground water.

An erosion surface separates Shakwak Drift from overlying sediments. Relief of the surface varies from minor irregularities to channel-shaped troughs 100-200 feet wide and 40 feet deep. Where revealed in the valley of Outpost Creek and in the Silver Creek exposures farthest upstream, the surface is nearly horizontal and stratification above and below the contact is conformable. In exposures of Shakwak Drift farther downstream along Silver Creek, the upper surface of Shakwak outwash generally dips 10° NE and constitutes an interface of angular unconformity between Shakwak outwash, in which stratification dips 17° NE and is truncated at the contact, and overlying Icefield outwash, in which stratification dips 4° NW. The downstream body of Shakwak till, likewise, is truncated by this surface. The volume of Shakwak Drift removed during development of the erosion surface which now forms the angular unconformity is unknown.

Stratigraphic position. Wherever exposed, weathered Shakwak till and outwash are overlain by nonweathered, or in one locality slightly oxidized, basal Icefield till and outwash; the contact is everywhere sharp. Because the weathering of Shakwak Drift could not have taken place beneath a cover of ice, the weathering zone represents an interval in which Shakwak Valley had become free of ice after deposition of Shakwak Drift and before deposition of Icefield Drift. Erosion of Shakwak Drift could have occurred during late Shakwak time, during the nonglacial interval that separated the Shakwak and Icefield glaciations, during early Icefield time, or during all three. Because the upper surface of Shakwak Drift is cut by channels that are not immediately overlain by till, probably at least some of the channel cutting was subaerial rather than subglacial

Silver nonglacial interval. The Silver nonglacial interval, the time-transgressive interval of deglaciation between the Shakwak and Icefield glaciations, is informally named after the Silver Weathering Zone which formed during the interval. Only the minimum extent to which glaciers retreated during the Silver nonglacial interval is known. The withdrawal was long enough along Silver and Outpost Creeks in Shakwak Valley for formation of the Silver Weathering Zone. Neither climatic nor vegetational conditions in the valley during that time are known.

Icefield Drift

General character and stratigraphy. Glacial sediments stratigraphically above Shakwak Drift and below Kluane Drift are here termed Icefield Drift, after the Icefield Ranges, the principal accumulation area of the glaciers responsible for the drift. Icefield Drift is most typically exposed in the west bank of Silver Creek (Fig. 5A; Fig. 7A).

The drift is exposed in cut banks throughout the Shakwak study area, where it is everywhere covered with younger drift 10-150 feet thick. The various units of Icefield Drift are grouped into deposits of one glaciation because (1) they are separated from younger and older drift sheets by weathering zones, and (2) contacts between units are either gradational or interfinger and show no evidence of major depositional breaks.

Icefield Drift overlies sharply the weathered and dissected upper surface of Shakwak Drift. Outwash I, the basal Icefield unit, interfingers with overlying Icefield till, which in turn is partly contemporaneous with a body of lacustrine sediment. The till is overlain by and interfingers with outwash II, as well as being overlain by ice-contact stratified drift. The upper surface of the entire drift sheet is covered with younger Kluane Drift.

Outwash I. Outwash I, stratigraphically the lowest and therefore oldest Icefield Drift unit, is exposed at only two localities, both in the cut bank of Silver Creek (Fig. 5A). At each locality its thickness is 3-15 feet; in the upstream locality (sec. A-A′) its lateral exposure is 400 feet and in the downstream locality (sec. A′ -A″), 350 feet. A sharp contact separates outwash I from underlying Shakwak Drift; a gradational, interfingering contact separates it from overlying Icefield till.

Most clasts are subangular, but in other respects, including grain size, sorting, and stratification, outwash I has great internal variability. Cut-and-fill stratification is common; beds have irregular thickness and extend laterally only 3-4 feet; grain-size changes are abrupt within and among beds; and sorting is poor, with grain size ranging from fine sand to boulders. However, small parts of the deposit have parallel beds, 2-12 inches thick, that consist of well-sorted sand, silt, or clay, and persist laterally 8-20 feet.

Stratigraphic and sedimentary features strongly suggest that outwash I was deposited near the margin of the Icefield glacier by melt-water streams characterized by rapid shifts in the positions of channels and by changes in water volume.

Lacustrine sediments. On a tributary to Christmas Creek (Fig. 4, site 1) and probably, although slumped sediments obscure a clear interpretation, along Christmas Creek (site 2) and along the north shore of Hungry Lake, lacustrine sediments form the lowest exposed Icefield Drift unit (Fig. 8). The base of the lacustrine sediments is not exposed, but a nearly horizontal contact of gradational character separates the unit from overlying Icefield till. The lacustrine sediments are composed of medium-gray (N5), laminated silt and clay with isolated pebbles. Laminae are 0.1-0.2 of an inch thick; some are contorted, but none form varvelike couplets with graded arrangement of particles.

Probably the lake in which the lacustrine sediments were deposited was dammed by ice that flowed from Slims River valley across Shakwak Valley and impinged

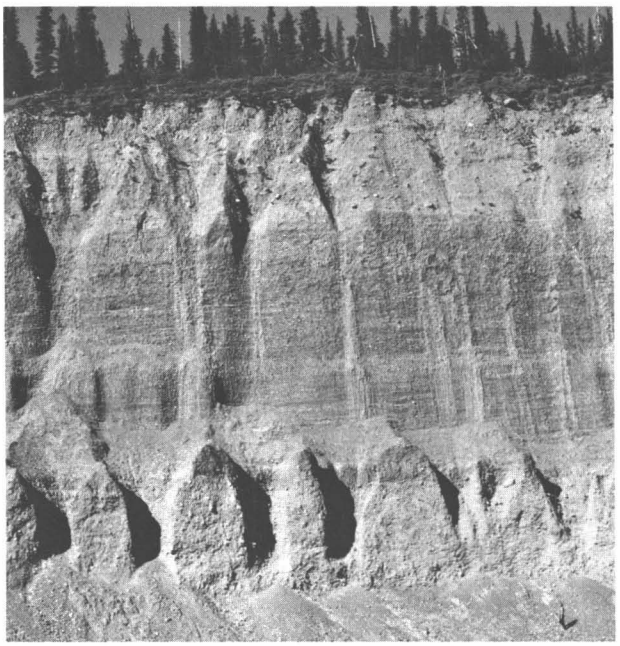

Fig. 7A. Part of a stratigraphic section in west bank of Silver Creek (see Fig. 5A, A″ – A‴). From top to bottom: Kluane till III, Icefield outwash II, Icefield till. Figure in lower right shows scale.

Fig. 7B. Kluane ice-contact stratified drift near Kluane Lake, aerial view. Horizontal extent along bottom of photograph is 0.29 mile.

against the Kluane Hills. That the lake was ice-dammed is suggested by four facts: (1) the presence of the lake at more than 3200 feet altitude, 600 feet above the lowest present outlet for this portion of the valley; (2) lack of pollen in the sediment, probably due at least in part to unfavorable climate for vegetation; (3) isolated, probably ice-rafted, pebbles in the sediment; and (4) lack of evidence for a time break between deposition of the lacustrine sediments and deposition of the overlying till.

Although older than the immediately overlying Icefield till, the lacustrine sediment is contemporaneous with Icefield till deposited by the ice that dammed the lake. The age relation of the lacustrine sediment to outwash I is uncertain; but because it contains no lacustrine characteristics, outwash I probably was deposited prior to creation of the lake.

Till. Icefield till crops out extensively along Inlet Creek, Christmas Creek and several of its tributaries, the north shore of Hungry Lake, Boutellier Creek, Silver Creek, and Outpost Creek. Where its lower contact is exposed, the till overlies Icefield outwash I, Icefield lacustrine sediments, and the weathered and dissected upper surface of Shakwak Drift (Fig. 5; Fig. 8). The till is overlain by outwash II along Silver and Boutellier Creeks (Fig. 5; Fig. 8), where a sharp and interfingering contact separates the two deposits. Thickness of Icefield till along Silver Creek, where both upper and lower contacts are exposed, is 2-50 feet; elsewhere the lower contact is obscured, and only a minimum thickness of 10-40 feet is exposed.

The sedimentary characteristics of Icefield till are uniform throughout the area. The till is medium gray (N5), very compact, nonstratified, and nonsorted, with grain size ranging from clay to boulders. Clasts are generally angular or subangular and commonly are faceted; many have acquired the flatiron shape common among glacially transported clasts (Wentworth, 1936, p. 92). The surfaces of fine-grained clasts are commonly striated. Eighteen till-fabric analyses (Fig. 5; Fig. 8), each based on at least 100 stones, show trends ranging from N 40° E to N 90° E toward Slims River valley and toward the glacially molded shoulder at altitudes of 5500-6100 feet at the junction of Shakwak and Slims River valleys.

Ice-contact stratified drift. Icefield ice-contact stratified drift is revealed in the upstream exposures along Outpost Creek (Fig. 5B). The nature of underlying deposits is unknown because its lower contact is concealed.

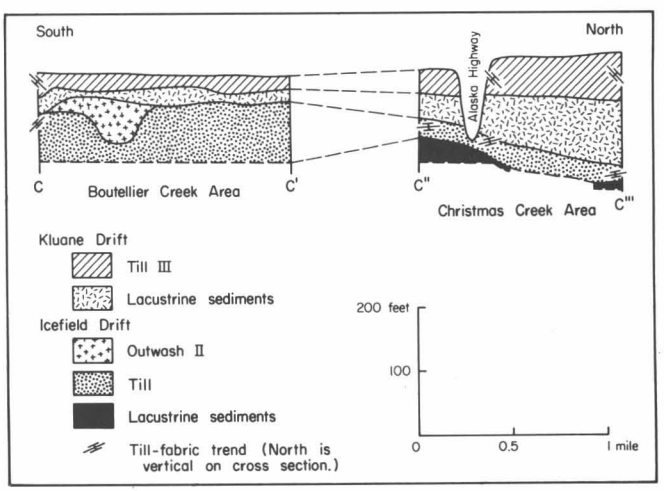

Fig. 8. Cross section of drift in Boutellier Creek and Christmas Creek areas. Location and orientation of section is shown in Fig. 4.

Along its upper surface, the ice-contact stratified drift is overlain sharply by Kluane till III. Its maximum exposed thickness is 120 feet.

The ice-contact stratified drift shows a wide range and abrupt changes of grain size, wide variability of stratification thickness, faulted and slumped stratification, and small till inclusions. No exposures reveal its original topographic characteristics.

Outwash II. Wherever its base is exposed in outcrops along Outpost Creek, Silver Creek, Boutellier Creek, the south shore of Hungry Lake, and several abandoned Kluane meltwater channels, outwash II sharply overlies Icefield till or Shakwak outwash and varies in thickness from several inches to more than 60 feet (Fig. 5; Fig. 8). Along Silver Creek, outwash II and Icefield till interfinger. Outwash II is everywhere separated by a sharp contact from overlying Kluane Drift.

Stratification, grain-size distribution, and shapes of clasts of outwash II are nearly identical to those of Shakwak outwash, except that the stratification everywhere closely parallels the present surface of the ground. Its similarity to recently dissected outwash fans and its interfingering with Icefield till suggest that outwash II originated as a fan or series of fans deposited by meltwater streams from the shrinking Icefield glacier.

Icefield glaciation. The Icefield glaciation was the climatic episode, characterized by glacial expansion, during which Icefield till was deposited. Till-fabric trends indicate that ice, flowing north from the Icefield Ranges, entered the Shakwak study area from Slims River valley. Ice bulging into Shakwak Valley deposited till and outwash I, and after impinging against the Kluane Hills, created the lake in which the lacustrine sediments were deposited. Probably most of the ice flowed northwest along Shakwak Valley, but some advanced into the ice-dammed lake and deposited till over the lacustrine sediments. During general ice shrinkage, outwash II was deposited by proglacial meltwater streams. Some part of the Icefield glaciation was characterized locally by ice stagnation and deposition of the ice-contact stratified drift.

The minimum extent of the Icefield glacier, as ascertained from the distribution of exposures of Icefield Drift, was at least 28 miles northeast of the present Kaskawulsh Glacier terminus and at least 73 miles northeast of the present Hubbard-Kaskawulsh divide in the Icefield Ranges. Minimum thickness of ice in Shakwak Valley, as determined from the maximum difference in altitude of exposures of Icefield Drift, was 1500 feet. It is unlikely that an advance of this magnitude occurred in Slims River valley without occurring also in other valleys that drained the Icefield Ranges.

Boutellier Weathering Zone

Character. The Boutellier Weathering Zone encompasses all products of subaerial weathering and dissection of Icefield Drift, including (1) oxidation of outwash II and, in places, of the upper few feet of Icefield till and (2) local dissection of the upper surface of Icefield Drift by running water.

The Icefield till exposed along Boutellier Creek is slightly oxidized through its uppermost 2-3 feet. The oxidation is confined to the till matrix, which is dusky yellow (5Y 6/4) compared with the medium gray (N5) of the fresh till. Variations in intensity of oxidation are related to cracks and permeable zones in the till; and at the base of the oxidized zone, tongues of oxidized material project down into unoxidized till. Such modification of the till matrix probably resulted both from oxidation of minerals in place and from deposition of iron oxide by ground water. Locally along Silver Creek, the uppermost few feet of Icefield till are oxidized similarly, but elsewhere the exposed upper part of Icefield till is unmodified.

Throughout the exposed thickness of outwash II, iron oxide deposited by ground water occurs as thin, partial stains on 50-80 percent of the clasts and as fine-grained particles in the matrix. Marked variations of iron-oxide concentration within the deposit are not related to depth in a systematic way. In some parts of the deposit, especially above rather impermeable beds of clayey silt and above the lower contact with the relatively impermeable Icefield till, iron oxide thoroughly covers all clasts and is abundant as fine particles in the matrix. As a result the deposit is moderate reddish brown (10R 4/6) to yellow brown (10YR 5/4). These variations of iron-oxide concentration are probably the result of differential circulation of ground water that was carrying iron oxide.

Erosion of the upper surface of Icefield Drift is evident only along Silver Creek, where small channels are carved into outwash II. The channels are filled with basal Kluane outwash and may have been cut by proglacial streams from advancing or retreating ice. Lateral discontinuity of Icefield Drift units (Fig. 5.) may be partly the result of subaerial erosion.

Stratigraphic position. Weathering differences between the upper part of the Icefield Drift and the overlying Kluane Drift indicate that most of the Boutellier weathering took place after deposition of the former drift and before deposition of the latter. Possibly, however, the lower part of Icefield outwash II was undergoing groundwater oxidation while the upper part was being deposited.

The change in weathering intensity across the erosion surface between the Icefield and Kluane drift sheets is abrupt. Through 1300 feet along the Silver Creek exposure a sharp erosion surface with relief of 2-7 feet separates Icefield outwash II from overlying Kluane outwash I (Fig. 5A). The highly oxidized Icefield outwash II contrasts sharply with the unoxidized Kluane outwash I, which is medium gray (N5) in color. In view of the similar permeability of both outwash units, it is unlikely that ground water could have extensively oxidized Icefield outwash II and not overlying Kluane outwash I, if the latter had been present. Therefore, Icefield outwash II was probably deposited and oxidized before deposition of the Kluane outwash I. Similarly, along Boutellier Creek a sharp contact separates Icefield till from

overlying Kluane lacustrine sediments (Fig. 8). Oxidation of the upper part of Icefield till terminates abruptly at the contact, and overlying Kluane lacustrine sediments are unoxidized. This relation is sufficiently consistent and widespread along Boutellier Creek to support the inference that deposition and oxidation of Icefield till preceded deposition of the overlying Kluane lacustrine sediments.

Similar arguments apply to the age distinction between Icefield outwash II and glaciofluvial sediments deposited during recession of Kluane ice. Icefield outwash II, deposited during retreat of the Icefield glacier, is oxidized wherever exposed, whereas overlying Kluane outwash II and the ice-contact stratified drift related to it, both of which were deposited during dissipation of Kluane ice, are unoxidized. Therefore, Icefield outwash II must have been deposited and oxidized before deposition of Kluane outwash II and associated ice-contact stratified drift. Along the wall of one of many valleys cut by meltwater during dissipation of Kluane ice (Fig. 4, site 3), Kluane outwash II was deposited, in the form of a terrace, against Icefield outwash II. Here Icefield outwash II is thoroughly oxidized, whereas the Kluane terrace outwash is unoxidized. From these relations it is again inferred that deposition and oxidation of Icefield outwash II preceded deposition of Kluane outwash II. These glaciofluvial bodies are hence parts of two distinct drift sheets of different ages; and the Boutellier Weathering Zone, formed subaerially, occupies the stratigraphic position between them.

Boutellier nonglacial interval. The Boutellier nonglacial interval separated the Icefield from the Kluane glaciation. The informal name is derived from the Boutellier Weathering Zone which formed during the nonglacial interval. During this time-transgressive interval Shakwak Valley was deglaciated long enough for subaerial oxidation of Icefield outwash II and locally of Icefield till matrix to take place. It is possible that, in places, deposition of the upper part of Icefield outwash II by meltwater from small glaciers in the Kluane Ranges continued throughout the nonglacial interval.

Kluane Drift

General character and stratigraphy. Glacial sediments that overlie Icefield Drift and that underlie Neoglacial drift are here termed Kluane Drift, after Kluane Lake, along whose shores the drift is well exposed. Kluane Drift is well displayed throughout the Shakwak study area (Fig. 7).

Kluane Drift is covered only with a thin, widespread layer of Neoglacial loess, Neoglacial end-moraine sediments fringing the termini of present-day glaciers, and glacier ice; hence, most of its well-preserved surface morphology is discernible. In the Shakwak study area, Kluane Drift, 20-120 feet thick, is revealed in cross section in exposures along most creeks as well as along the shore of Kluane Lake. Wherever its lower contact is revealed, the drift sharply overlies the upper surface of Icefield Drift. The Kluane Drift units are grouped into one drift sheet for three reasons: (1) a soil and a weathering zone separate them from drift sheets, respectively, above and below; (2) the contacts between most of the units are gradational or interfinger; (3) evidence of substantial intervals between the times of deposition of the various units is lacking.

Outwash I, the oldest recognized unit of Kluane Drift, is exposed only along Silver Creek, where it grades upward into and interfingers with overlying Kluane tills II and III. In another part of the Silver Creek exposure, Kluane till II sharply overlies Kluane till I. Both tills are exposed only along Silver Creek, but their stratigraphic position suggests that they are contemporaneous with an extensive body of lacustrine sediments in the east portion of the Shakwak study area. Kluane till III, present throughout the study area, overlies all the drift units previously mentioned, and is overlain in turn by widespread deposits of Kluane outwash II and ice-contact stratified drift. A thin layer of Kluane loess covers all other deposits of Kluane age.

Outwash I. Kluane outwash I is exposed only at two localities along Silver Creek (Fig. 5A); in both places it sharply overlies Icefield Drift. In the upstream locality it is overlain gradationally by Kluane till III; downstream it is overlain with gradational contact by Kluane till III and with interfingering contact by Kluane till II. Its average thickness in both localities is about 20 feet. Individual beds are very irregular in thickness and extend laterally for only a few feet, although well-developed cut-and-fill stratification characterizes parts of the deposit. Outwash I is poorly sorted; grain size ranges from fine sand to boulders, and abrupt changes in grain size are common. Clasts are generally subangular to subround. Both its stratigraphic relationship with overlying till II and its sedimentary characteristics suggest that outwash I was deposited very close to the Kluane Glacier by meltwater streams that fluctuated rapidly in position and capacity.

Till I. The sole exposure of Kluane till I is along Silver Creek (Fig. 5A), where it extends laterally for 150 feet and averages 12 feet in thickness. It overlies Icefield outwash II with a sharp contact that truncates the stratification and is sharply overlain in turn by Kluane till II. The trend of the till fabric (Fig. 5A) is N 70° E toward Slims River valley.

Till II. Kluane till II is exposed along Silver Creek (Fig. 5A, secs. A-A′ and A′ -A″), where its lateral extent is 1300 feet and its average thickness, 20 feet. It overlies Kluane outwash I with a sharp, interfingering contact, Kluane till I with a sharp contact, and Icefield till with a sharp contact except where Icefield till has been incorporated into its base. It is overlain sharply by Kluane outwash II and gradationally by Kluane till III.

Kluane till II is massive, compact, and uniformly moderate yellow (5Y 7/6) in color. Four till-fabric analyses (Fig. 5A) show trends ranging from N 30° E to N 70° E, toward Slims River valley.

Lacustrine sediments. An extensive body of lacustrine sediments is exposed in the eastern part of the Shakwak field area (Figs. 4 and 8), generally at altitudes between

3100 and 3200 feet. Where their base is exposed, the lacustrine sediments abruptly overlie Icefield till and Icefield outwash II; they are overlain gradationally by Kluane till III. Their average thickness is 40 feet where both upper and lower contacts are exposed.

The lacustrine sediments consist of well-sorted, medium-gray (N5), evenly laminated silt and clay, with some pebbles and cobbles surrounded by deformed laminae 0.1-0.2 of an inch thick. Rhythmic couplets with graded arrangement of particles were not recognized.

Glacier damming of the lake in which the sediments were deposited is suggested by four facts: (1) the difference between the altitude of the lacustrine sediments (3200 feet) and the altitude of the present outlet for any lake in this part of the valley (2563 feet); (2) presence of pollen of only alpine, cold-climate plants suggests deposition of the sediments under glacial conditions; (3) some clasts, probably ice-rafted, are present in the sediment; (4) evidence of a time break between deposition of the lacustrine sediments and deposition of overlying Kluane till III is lacking.

Till III. Over large parts of Shakwak Valley Kluane till III forms the youngest Kluane deposit, apart from loess. This till, exposed in stream valleys throughout the Shakwak study area, rests cleanly on Icefield outwash II, and gradationally on Kluane outwash I and lacustrine sediments. It is overlain both gradationally and sharply by Kluane outwash II and ice-contact stratified drift, and sharply by Kluane loess. Its thickness varies from 2 to 45 feet and averages about 25 feet. Kluane till III is massive, nonsorted, and compact and ranges from medium gray (N5) to light olive brown (5Y 5/6) in color. Clasts are generally subangular and are commonly faceted and striated. The lower part of the till is clay-rich because it incorporates lacustrine sediments. Twenty-two till-fabric analyses of clasts in Kluane till III (Figs. 3, 5, and 8) show trends between N 40° W and N 50°W, parallel to the axis of Shakwak Valley and to Jarvis River valley.

As stated in a foregoing section, the surface of Kluane till III is fluted, with parallel ridges and intervening grooves up to 6 miles long (Fig. 3). The flutings are: (1) contiguous with similar flutings in bedrock southeast in the area and in Jarvis River valley, (2) consistent with till-fabric trends of Kluane till III and striations on bedrock immediately below till III, and (3) parallel with streamlined bedrock hills and flutings in bedrock on the southwest wall of Shakwak Valley within the study area. The trends of these consistent directional features parallel the axis of Shakwak Valley everywhere except in the southeast, where they curve south into Jarvis River valley. Thus these directional features indicate that, whereas all older tills were deposited by ice flowing into the study area from Slims River valley, Kluane till III was deposited by ice flowing north into the study area from the Icefield Ranges, by the way of Jarvis River valley.

Ice-contact stratified drift and outwash II. Ice-contact stratified drift and outwash II were deposited contemporaneously, at least in part, during recession of Kluane ice. Because their exposures are rare, the sediments are differentiated mainly by morphology. Extensive deposits of ice-contact stratified drift occur near Kluane Lake (Fig. 7B), whereas less extensive deposits are scattered throughout the Shakwak study area. Outwash II is present as broad outwash plains, as scattered irregular patches, and as linear bodies in meltwater channels.

The ice-contact features, located mainly in a cross-valley belt fringing Kluane Lake (Fig. 4), include eskers, crevasse fillings, and features associated with kettles. Several eskers, up to 1 mile long, 50 feet high, and 200 feet wide, follow a sinuous path nearly parallel with the valley axis. Near Kluane Lake crevasse fillings, consisting of ridges marked by abrupt changes in trend, are oriented perpendicular to the valley axis, except for one group of intersecting ridges which forms a rectilinear pattern. The crevasse-filling sediment is characterized by abrupt grain-size changes, subrounded clasts, and pockets of fine, well-sorted sediments surrounded by poorly sorted pebble-cobble gravel.

The cross-valley belt of ice-contact terrain fringing Kluane Lake near Christmas Bay and Jenny Lake contains a profusion of kettles separated by gravel ridges and surrounded by an outwash plain whose flat upper surface extends to the lip of, and partly encircles, kettles on the outer parts of the complex. The kettles are crudely circular in plan, with longest dimension ranging from 100 to 1000 feet. The surface of the surrounding outwash plain is locally terraced and dips gently toward Kluane Lake; in several exposures the sediments consist of well-sorted, evenly bedded pebble-cobble gravel dipping 2° NW toward Kluane Lake. The formation of this complex required stagnation and detachment of ice blocks during recession of Kluane ice, filling of the intervening area by sediment from the melting ice blocks, and deposition of outwash around and against the stagnant ice by meltwater derived from Kluane ice retreating to the southeast and from glaciers retreating to the Kluane Ranges in the vicinity of upper Silver Creek.

The linear bodies of outwash II were deposited in a complex system of channels, many with depths of as much as 100 feet, carved mainly in Kluane till III by meltwater from shrinking Kluane ice (Fig. 4). Most of the major channels, including that of Christmas Creek, head either in patches of ice-contact stratified drift or in theater-shaped excavations in till. They slope northwest and trend nearly parallel with the valley axis, indicating that the glacier responsible for the meltwater that carved them shrank back southeast along this part of Shakwak Valley. Several channels in the north-central portion of the study area describe crude arcs concave toward the southeast. The trend and position of these channels suggest that they were made by ice-margin rather than proglacial streams. If so, they mark successive terminal positions of a glacier that was withdrawing toward the southeast.

In the south-central part of the area a group of channels forms a rectilinear pattern unrelated to topography (Fig. 4). Several of the channels slope both northwest and south-

east, and short segments of channels without a consistent pattern are scattered throughout the area. This whole complex was probably carved by subglacial streams, the slope reversals being caused by water flowing uphill under hydrostatic pressure. In several other localities channels trend both northwest and southeast from small areas of ice-contact stratified drift and were probably carved by water from a detached block of stagnant ice. Another set of channels, which includes those presently occupied in part by Outpost, Silver, and Boutellier creeks, trends down the southwest wall of Shakwak Valley, transecting many older channels. These transecting channels were cut by meltwater from small valley glaciers in the Kluane Ranges after the main mass of Kluane ice had retreated from Shakwak Valley.

Loess[4]. A blanket of loess forms the youngest unit of Kluane Drift at altitudes below 4500 feet, wherever the drift was examined in the Kluane Lake area, the Slims River valley, and near the Donjek and Kaskawulsh glaciers. Kluane loess consists of well-sorted silt with some fine sand; its particles are composed of a wide range of mineral types, reflecting the complex lithology of source rocks of glacial sediments in the region. Kluane loess thickness varies from 14 to 40 inches, the greatest thickness being in Slims River and Donjek River valleys; elsewhere the thickness varies unsystematically. It is thus inferred that several scattered outwash bodies provided the predominant source for loess during retreat of Kluane ice and that two of the largest of these were the Slims and Donjek valley trains.

Kluane glaciation. The Kluane glaciation was the climatic episode, characterized by glacial expansion, during which the Kluane tills were deposited. Following the close of the Boutellier nonglacial interval, ice advancing north from the Icefield Ranges initially entered the Shakwak study area from Slims River valley, depositing Kluane outwash I and tills I and II, and damming the extensive lake in which lacustrine sediments were deposited. Subsequently, ice from Jarvis River valley flowed northwest through the study area, covering all older Kluane sediments with till III. Jarvis River ice merged with Slims River ice near the junction of Slims River and Shakwak valleys, and the combined ice mass flowed northwest along Shakwak Valley.

Well-defined ridges and grooves on bedrock and till, assumed to be related to the Kluane glaciation, permit the regional flow pattern of Kluane glaciers to be reconstructed from air photographs (Figs. 3, 9, and 10). Glaciers, derived mainly from the Icefield Ranges but also fed by tributary glaciers from the Kluane Ranges, flowed north through all valleys draining the Icefield Ranges and into Shakwak Valley. In southeast Shakwak Valley, ice continued to flow north and northeast. Elsewhere it flowed northwest along the valley, confined by the Ruby Range on the northeast and the Kluane Ranges on the southwest. Some ice escaped north through valleys transecting the Ruby Range; the rest flowed along Shakwak Valley until near the Alaska-Yukon boundary it was no longer confined by the Ruby Range and spread north as a lobe that terminated at or south of the outer limit of glacial drift, about 12 miles north of Snag (Fig. 9).

Kluane ice reached altitudes of 6100 feet on the northeast flank of the Kluane Ranges in the Shakwak study area (see also Wheeler, 1963), as indicated by the altitude of the highest occurrences of Kluane till, of erratics of probable Kluane age, and of bedrock molded by Kluane ice. The molded bedrock is of Kluane age because its directional indicators parallel the flow direction of the Kluane Glacier from Jarvis River valley, rather than the flow directions of older glaciers, and because it is an extension of similar molded forms on Kluane till III. The minimum altitudes of Kluane till III in the valley range from 2570 to 3200 feet; hence, the ice thickness in the Shakwak study area must have ranged from about 2900 to 3530 feet. Altitudes of erratics and drift of probable Kluane age indicate that the upper limit reached by Kluane ice decreased in altitude north and northwest of the mouth of Slims River valley (Bostock, 1952, p. 13).

Several facts suggest that at the maximum of the Kluane glaciation the firn limit on Kluane glaciers lay considerably north of its present position on glaciers of the Icefield Ranges. Because the Kluane glaciation was very extensive, some or all of the presently empty cirques at 4400-5500 feet in the Kluane Hills and the Ruby Range most probably were occupied by glacier ice during the Kluane advance and through its maximum. If so, the firn limit at those times was lower than 5500 feet and must have intersected the upper surface of Kluane ice northwest of the mouth of Slims River valley, because the upper surface of Kluane ice reached at least 6100 feet at that place.

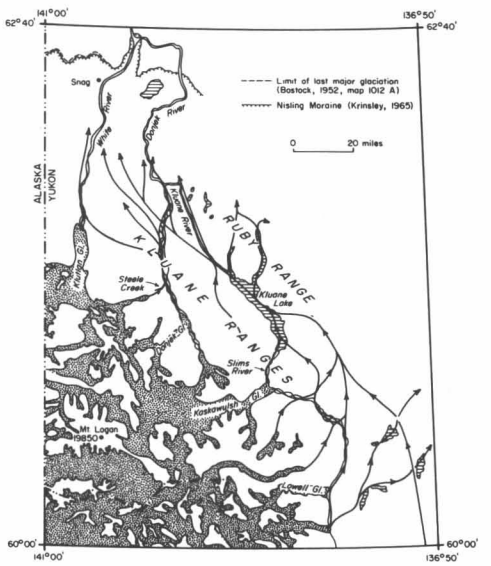

Fig. 9. Probable flow directions of Kluane ice as inferred from striations and flutings. These features are known to be related to Kluane ice within the Shakwak study area and are assumed to be similarly related in immediately adjacent areas. SOURCES: Bostock (1952), Kindle (1953), and air photographs.

[4]The Kluane Loess was informally called Kluane silt by Sticht (1963) and Kluane Silt by Johnson and Raup (1964).

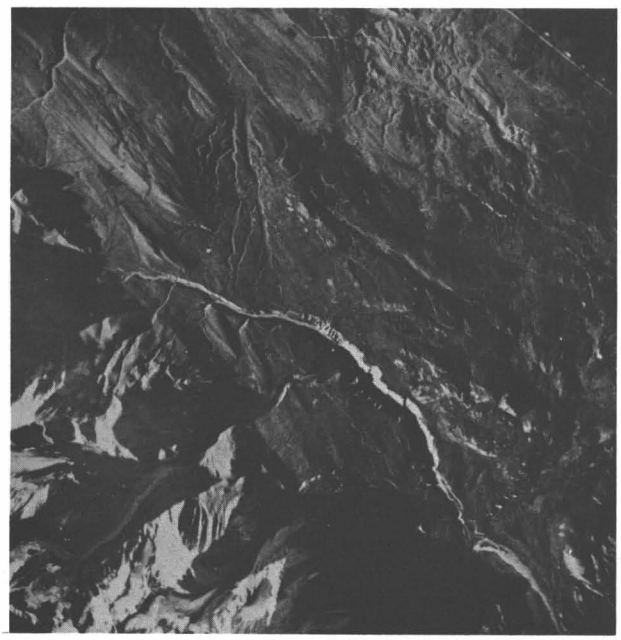

Fig. 10. Air photograph of flutes formed in Shakwak Valley during Kluane glaciation. North is at top of photograph. Scale is about 1: 125,000.

Only limited regional information on Kluane deglaciation is available. In the Shakwak study area the alignment of eskers, the slope of the outwash plain surrounding the kettle complex near Kluane Lake, and the trend and slope of outwash channels all strongly suggest that throughout most of the area ice receded southeast into Jarvis River valley, although to the west and southwest some ice belonged to the glacier retreating into Slims River valley. Ice-contact features indicate that deglaciation was characterized by the stagnation of large masses of ice near the southeast part of Kluane Lake. During deglaciation, loess derived from active outwash plains was deposited as a widespread blanket over all older Kluane deposits below an altitude of about 4500 feet. The only suggestion of fluctuation of ice during general deglaciation of the Shakwak study area, and probably of the rest of the valley through at least 60 miles northwest of the study area, is the cross-valley belt of ice-contact features bordering the southeast part of Kluane Lake. Elsewhere the surface features consist entirely of grooved Kluane till with no clear evidence of fluctuations during Kluane deglaciation.

The belt of ice-contact features forms an arc (not fully shown on Fig. 4 because much of it lies outside the Shakwak study area) concave toward the mouth of Slims River valley and, through much of its length, parallel to and contiguous with the northeast shore of Kluane Lake. A projection of this arc across Kluane Lake about 15 miles northwest of the mouth of Slims River valley intersects a large area of ice-contact features on the southwest shore of the lake. Such a distribution suggests that the features may possibly record the outer position of a stillstand or a readvance of ice from Slims River valley. That this hypothesis is not entirely unreasonable is suggested by the present situation in front of several large glaciers in the region where continued retreat would leave behind mainly ice-contact features to mark the Neoglacial maximum. However, an equally likely alternative is that the ice-contact features formed simply by stagnation of retreating ice owing to topographic conditions, climatic amelioration, or both. In either case ice projecting from Jarvis River valley was certainly present within the study area during formation of these features because (1) the outwash surrounding the kettle complex near Kluane Lake was deposited by streams issuing from Jarvis River ice, and (2) the ice-contact features are dissected by Christmas Creek valley which was carved also by water from Jarvis River ice.

If any further fluctuations occurred during subsequent glacier retreat south through Slims River valley to the position of the Neoglacial moraines, the evidence has been removed by erosion or covered by younger valley-train or fan sediments. Elsewhere, evidence of a temporary pause in recession or of a readvance during late stages of general deglaciation has been found only in Steele (Wolf) Creek valley (Sharp, 1951b, p. 103).

Slims Soil

General character. All weathering products of the upper part of Kluane loess are termed the Slims Soil, after Slims River, along whose banks the soil is particularly well exposed. The Slims Soil has a buried part and a nonburied part. Near the Donjek and Kaskawulsh Glacier termini the soil is overlain by drift of Neoglacial moraines, and near active valley trains such as those of the Slims and Donjek Rivers it is overlain by nonweathered Neoglacial loess. In these places the soil is relict. Away from active valley trains Neoglacial loess is absent, and the soil is exposed at the surface, presumably in equilibrium with existing conditions. Thus the Slims Soil everywhere occupies a stratigraphic position above Kluane loess and locally a position below Neoglacial moraines and loess.

Aside from areal variations of horizon thickness, the soil exposed near the Slims River delta is typical of the buried part. The uppermost horizon, 8 inches thick, is intensely oxidized, is moderate brown (5YR 4/4), and grades down into a less intensely oxidized moderate-yellow (5Y 7/6) horizon, 4 inches thick, which in turn grades down into a light-gray (N7) unoxidized horizon, 10 or more inches thick. The moderate-brown horizon is completely leached of calcium carbonate, the moderate-yellow horizon is partially leached, and the gray horizon is unleached. X-ray diffraction studies show that the mineralogy of oxidized and unoxidized loess is identical except for calcite content. Free-iron analyses show 0.06 per cent Fe_2O_3 in the oxidized loess and 0.10 percent in the unoxidized loess. Globules of iron oxide deposited by ground water are not present in the oxidized zone. Weathering, therefore, was neither of sufficient duration nor of sufficient intensity to cause substantial mineral alteration, consisting mainly of surficial oxidation of iron-

bearing minerals in place and leaching of calcium carbonate.

Nearly everywhere in the Kluane Lake area the Slims Soil occurs at altitudes below 4500 feet. The soil overlies all pre-Neoglacial deposits in the Donjek and Slims River valleys, including pre-Neoglacial deposits that fringe the Neoglacial moraines near the Donjek and Kaskawulsh Glaciers. On the west side of Kaskawulsh Glacier the soil occurs as a nearly continuous sheet through 8 miles above the terminus and as discontinuous patches through an additional 5.7 miles. The last upglacier occurrence of Slims Soil is on a bedrock knob 13.7 miles upglacier from the present terminus and 15 miles upglacier from the outermost Neoglacial moraines that fringe the terminus (see Denton and Stuiver, 1966).

Slims nonglacial interval. The Slims nonglacial interval separated the Kluane glaciation from the Neoglaciation. C^{14} dates, presented later, show that the time-transgressive Slims interval included the Hypsithermal interval (see also Sticht, Ph.D. dissert.; Johnson and Raup, 1964, p. 29) as defined by Deevey and Flint (1957, p. 182).

Both direct and indirect measurements of glacial retreat during the Slims interval can be ascertained from the areal distribution of the Slims Soil. First, because Kluane ice must have evacuated all localities now occupied by the soil, the Donjek and Kaskawulsh Glaciers withdrew at least to their present positions during the interval, and areas adjoining the west side of of the present Kaskawulsh Glacier were evacuated by retreating Kluane ice. Second, conditions prerequisite for the formation of the Slims Soil were deactivation of valley trains subsequent to glacier retreat and the resulting cessation or near cessation of loess deposition (Sticht, 1963; Johnson and Raup, 1964, p. 29). Therefore, presence of the soil at a given locality not only demonstrates the absence of contemporaneous ice at the locality but also suggests withdrawal of glaciers from the immediate vicinity.

Deactivation of much of the lower valley trains resulted from several factors: (1) The volume of meltwater decreased owing to increased infiltration and evaporation over the longer stream courses and to the smaller sizes of the source glaciers. (2) The braided-stream patterns common near the glaciers probably gave way downstream to single larger channels, resulting in smaller areas of the valley trains being covered with meltwater. This situation is common today downstream from glaciers in the region. (3) The abandoned parts of the valley trains were quickly covered with vegetation and with a crust of calcium carbonate, both of which protected silt from further dispersal by wind.

The Slims Soil present along the west side of the Kaskawulsh Glacier through 13.7 miles above the present terminus is sharply overlain by nonweathered Neoglacial loess, implying a sequence of loess deposition, cessation or near-cessation of loess deposition, and renewed loess deposition. This sequence is best explained by a withdrawal of the Kaskawulsh Glacier terminus more than 13.7 miles above its present position, followed by readvance. In the vicinity of the Slims Soil occurrences these events were accompanied by valley-train activity that permitted the deposition of loess, followed by cessation of such activity, allowing soil formation, and finally by renewed valley-train activity with renewed loess deposition. A supporting argument for substantial retreat is provided by the continuous, well-defined nature of the soil bordering the lower Kaskawulsh Glacier. This suggests lack of a nearby active valley train during its formation and therefore implies significant glacier withdrawal. A similar argument applies to the Donjek Glacier, where large areas of well-developed soil fringing the terminus suggest substantial retreat during soil formation.

Neoglacial Drift

General character. The Neoglacial drift and the Neoglaciation were discussed in detail by Denton and Stuiver (1966). A blanket of nonweathered Neoglacial loess sharply overlies the Slims Soil throughout much of the region. The stratigraphic position, distribution, areal-thickness relations, and present source indicate that the loess was derived from large valley trains reactivated by glacial readvance following the Slims nonglacial interval.

Young Neoglacial end-moraine sediments surround termini of all glaciers on the northeastern flank of the mountains and are particularly well displayed in front of the Donjek and Kaskawulsh Glaciers. Prominent sets of end moraines fronting both glaciers extend 0.5-2.0 miles from the ice termini and have common stratigraphic relations: (1) the outermost moraines contain inclusions of Slims Soil, early Neoglacial loess, and a distinct white volcanic ash deposited about 1425 B.P. (Stuiver and others, 1964); (2) the moraines are overlain by little or no Neoglacial loess; and (3) the outermost moraines are closely bordered by undisturbed Kluane loess, Slims Soil, and Neoglacial loess containing the volcanic ash. This last relation indicates that the outermost end moraines represent the maximum Neoglacial extent of the glaciers involved. Both sets of end moraines are sparsely covered with vegetation and are divided into groups on the basis of differences in vegetation cover and morphology. Each group represents a readvance or stillstand during general retreat from the outermost moraines.

Neoglaciation. During the Slims nonglacial interval the Donjek and Kaskawulsh Glaciers receded well into the Icefield Ranges; the terminus of the Kaskawulsh Glacier was more than 13.7 miles behind its present position. Post-Slims glacial readvance(s) reactivated valley trains, causing renewed loess deposition on the northeast flank of the mountains. Lack of evidence of cessation of Neoglacial loess deposition suggests that throughout at least most of Neoglacial time glaciers maintained positions more extensive than those occupied during the Slims nonglacial interval. The youngest and most extensive Neoglacial advance is represented by sets of end moraines fronting the Donjek and Kaskawulsh Glaciers. Ages of trees presently growing on the outermost of these moraines indicate that the fluctuating retreat from the

Neoglacial maximum began before A.D. 1874 by the Donjek Glacier and before A.D. 1865 by the Kaskawulsh Glacier.

C^{14} CHRONOLOGY AND CORRELATION

Twenty samples of organic matter collected from the four drift sheets in the northeastern St. Elias Mountains were processed by the Yale Radiocarbon Laboratory (Fig. 11; Table 1). A half life for C^{14} of 5568 years was used for computation of the sample ages. Descriptions of samples relating mainly to pre-Neoglacial drift units are given in Table 1. For description and discussion of ten additional samples (Y-1354, 1363, 1364, 1365, 1480, 1482, 1484, 1485, 1489, 1490) related to the Neoglaciation and mentioned only briefly in this paper, see Denton and Stuiver (1966) and Stuiver and others (1964).

The date of sample Y-1355, collected from a silt bed in Shakwak outwash (Fig. 5A), indicates that the Shakwak glaciation occurred before 46,400 B.P.

Two other dates, also infinite, relate to the beginning of the Icefield glaciation in Shakwak Valley. Sample Y-1486 consists of sinuous stringers of peat in Icefield till. The peat was probably picked up by advancing ice; and thus the date, >49,000 B.P., is a maximum for the beginning of the Icefield glaciation in Shakwak Valley. Sample Y-1481, from near the base of Icefield ice-contact stratified drift, shows that the Icefield glacier had advanced into Shakwak Valley and had locally stagnated in the vicinity of Outpost Creek before 49,000 B.P. These dates imply, additionally, that both the Shakwak glaciation and the Silver nonglacial interval occurred long prior to 49,000 B.P. The age of organic matter from a silt bed near the base

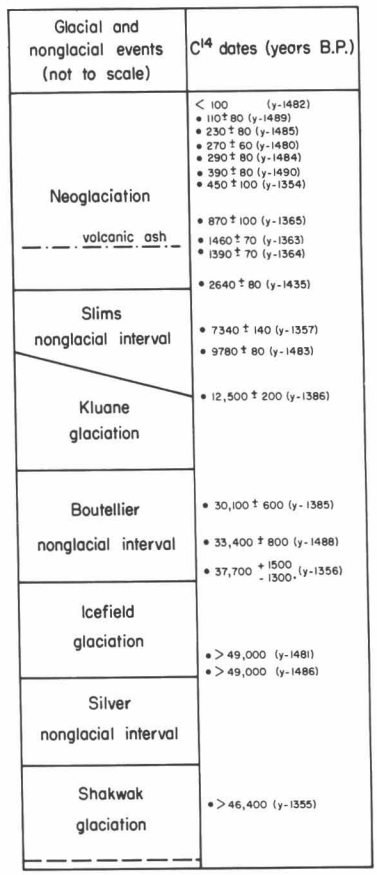

Fig. 11. Late Pleistocene glacial chronology of the northeastern St. Elias Mountains. See Denton and Stuiver (1966) for descriptions of C^{14} dates associated with Neoglaciation.

TABLE 1. C^{14} Dates Related to Glacial Drift (Most Neoglacial Dates Excluded)

Sample number	Location	Substance and stratigraphic position	C^{14} age in years B.P.
Y–1435	Kaskawulsh Glacier	Grass buried in place 4 inches above base of 10-foot section of Neoglacial loess	2640 ± 80
Y–1357	Shakwak Trench (Fig. 5A)	Wood from silt bed in Kluane outwash II. This part of outwash deposited by meltwater from small glaciers in Kluane Ranges	7340 ± 140
Y–1483	Kaskawulsh Glacier	Grass buried in place at base of Kluane loess	9780 ± 80
Y–1386	Shakwak Trench (Fig. 4)	Organic matter from bottom of kettle in Kluane ice-contact stratified drift	12,500 ± 200
Y–1385	Shakwak Trench (Fig. 5A)	Organic matter, including wood, from silt bed in Icefield outwash II, 4 feet below upper surface of outwash II (Fig. 12).	30,100 ± 600
Y–1488	Shakwak Trench (Fig. 5A)	Organic matter, including wood, from a silt bed in Icefield outwash II. Silt bed truncated by Kluane till I	33,400 ± 800
Y–1356	Shakwak Trench (Fig. 5A)	Organic matter, including wood, from silt bed in Icefield outwash II, 12 feet above lower surface	37,700 + 1500 −1300
Y–1481	Shakwak Trench (Fig. 5B)	Organic matter in silt bed at base of Icefield ice-contact stratified drift	> 49,000
Y–1486	Shakwak Trench (Fig. 5A)	Sinuous stringers of peat in Icefield till	> 49,000
Y–1355	Shakwak Trench (Fig. 5A)	Organic matter, including wood, in silt bed 10 feet below upper surface of Shakwak outwash	> 46.400

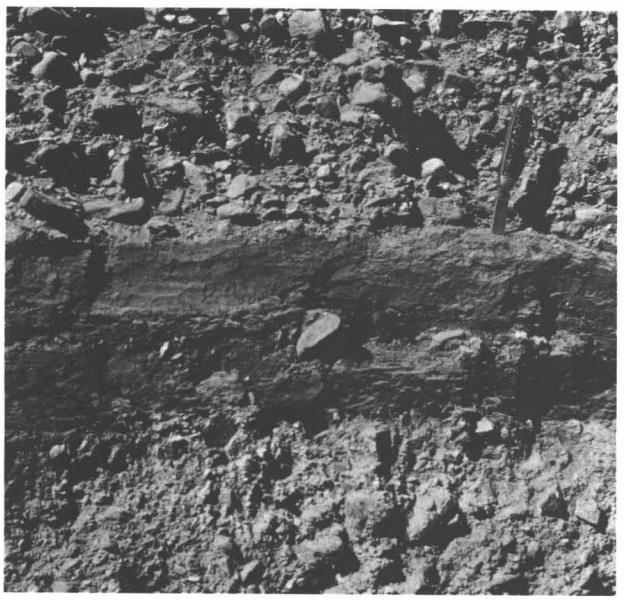

Fig. 12. C^{14} sample Y-1385 in Icefield outwash II.

of Icefield outwash II places the beginning of the fluctuating retreat of the Icefield glacier from Shakwak Valley at shortly before 37,700 B.P. (Y-1356). Thus, within the limits of Shakwak Valley, the Icefield glaciation lasted more than 11,000 years, from before 49,000 B.P. to shortly before 37,700 B.P.

Sample Y-1356 also places the beginning of the Boutellier nonglacial interval in Shakwak Valley shortly before 37,700 B.P. Samples from silt beds in the middle and upper parts of Icefield outwash II, deposited when at least most of Shakwak Valley had become ice-free, have ages of 33,400 (Y-1488) and 30,100 B.P. (Y-1385). The presence of 14 feet of Icefield outwash II and Kluane outwash I between sample Y-1385 and the lower contact of Kluane till III suggests the strong possibility that the end of the Boutellier nonglacial interval may have substantially postdated 30,100 B.P. Thus, dates from Icefield outwash II imply that during the Boutellier nonglacial interval this part of Shakwak Valley was ice-free for at least 7000 years and probably for considerably longer. The main Icefield glacier need not have remained nearby throughout this interval, for the upper part of outwash II may well have been deposited by meltwater from glacierets located in the Kluane Ranges. There is good evidence that this situation existed during the succeeding Slims nonglacial interval.

Sample Y-1385 additionally places the advance, into Shakwak Valley, of ice responsible for Kluane tills II and III after 30,100 B.P., perhaps considerably later. The only control on the maximum age of Kluane till I is sample Y-1488 (33,400 B.P.), located within a silt bed of Icefield outwash II. At the sample locality the silt bed is truncated by Kluane till I, but upstream it is overlain by 12 feet of outwash II. Although till I is probably related to the same advance(s) that deposited tills II and III, there is no evidence to refute the possibility that Kluane till I represents a brief advance postdating 33,400 B.P. and antedating the main Kluane advance that began after 30,100 B.P. Final recession of Kluane ice is locally dated by several samples. Retreat from the cross-valley belt of ice-contact stratified drift near Kluane Lake occurred shortly before 12,500 B.P. (Y-1386), when organic sediments began to accumulate in the base of a kettle. If, as previously suggested, these ice-contact features represent the position of a former major ice front associated with a readvance or stillstand during general deglaciation, this sample gives a close minimum age for construction of the ice-front feature. Grass buried in place at the base of Kluane loess near the Kaskawulsh Glacier terminus gives a close minimum date of 9780 B.P. (Y-1483) for recession of Kluane ice behind the present position of the Neoglacial moraines fringing the present Kaskawulsh terminus.

Samples Y-1386 and Y-1483 show, additionally, that the Slims nonglacial interval had begun in Shakwak Valley and near the Kaskawulsh terminus, respectively, by 12,500 and 9780 B.P. A date of grass buried in place at the base of Neoglacial loess near the terminus of the Kaskawulsh Glacier (see Denton and Stuiver, 1966) provides a close minimum date of 2640 B.P. (Y-1435) for the end of the Slims interval at that locality. During this interval, the upper part of Kluane outwash II in Shakwak Valley was deposited by meltwater from small glaciers in the Kluane Ranges, as indicated by the C^{14} age (7340 B.P., Y-1357) of wood from a silt bed near the top of the deposit. At this time Shakwak Valley was ice-free, as indicated above.

A close minimum age of 2640 B.P. is also given by sample Y-1435 for the initial Neoglacial advance(s) of the Kaskawulsh Glacier. Although deposition of loess near the Kaskawulsh Glacier terminus began shortly before 2640 B.P., it did not commence in much of Shakwak Valley until sometime between about 1425 B.P. (Y-1364 and Y-1363, Stuiver and others, 1964) and about 870 B.P. (Y-1365 Denton and Stuiver, 1966). Otherwise, very little information is available for the time between the initial Neoglacial advance and the youngest advance, although lack of evidence for cessation of loess deposition suggests that glaciers were generally more extensive throughout the Neoglaciation than they were during the Slims interval. Samples Y-1354, Y-1480, Y-1484, Y-1485, Y-1489, and Y-1490 (Denton and Stuiver, 1966) are from spruce logs embedded in or covered with the outermost end-moraine sediments of the Donjek and Kaskawulsh Glaciers and indicate that in recent centuries both glaciers reached their greatest extent of the last 9780 years. The age of sample Y-1482, when corrected for known variations in atmospheric C^{14}, suggests that the Donjek Glacier receded from its Neoglacial maximum less than 260 B.P. (Denton and Stuiver, 1966). The ages of the oldest trees growing on the outermost end moraines suggest that retreat from the Neoglacial maximum occurred before A.D. 1874 by the Donjek Glacier and before A.D. 1865 by the Kaskawulsh Glacier.

The C^{14}-dated glacial stratigraphy in the study areas provides a chronology of major fluctuations of St. Elias glaciers through the last 49,000 years (Fig. 11). However, be-

cause the study areas were restricted in size and because most pre-Neoglacial drift in Slims River valley has been removed or buried, details of late Kluane glacier fluctuations in the St. Elias Mountains are not yet available. A more complete chronology for northwestern North America is obtained by combining data from the St. Elias Mountains with data presented by Porter (1964) for the north-central Brooks Range, Alaska. In the Brooks Range several readvances during general deglaciation from the Itkillik (=Kluane) maximum are C^{14}-dated (Porter, 1964, p. 459). These data complement the St. Elias chronology, and the two groups of dates together constitute a glacial chronology for the northwestern part of the continent during the late Pleistocene (Fig. 13) to supplement those set forth by Péwé and others (1965) and Karlstrom (1964), among many others.

Correlation of Wisconsin Events

The temporal relations of late Pleistocene glacial and pluvial events in areas of North America at widely different latitudes are compared in Figure 13. The sequences were selected because of detailed control by C^{14} dates. Only events within the range of C^{14} dating are shown. All C^{14} dates used to bracket the events are finite except for the oldest date in the St. Elias sequence.

Several of the basic data could cause Figure 13 to be misleading unless the following points are kept in mind: (1) The glacial and nonglacial episodes depicted are time transgressive and vary in age with distance from the center of glacier outflow. In this respect the columnar sections are somewhat unrealistic because the dated sequences from each area are too limited geographically to reflect time-transgressive relations. (2) The precision of correlations may be diminished by different response rates of pluvial lakes and various glacier types to a given climatic change. (3) The closeness with which events are bracketed varies with the stratigraphic position of the C^{14} samples in relation to critical drift bodies. (4) The accuracy of C^{14} dating diminishes rapidly with increasing age. (5) Deevey and others (1954) and Broecker and Walton (1959) have shown that the C^{14}/C^{12} ratio of a lake with high carbonate concentration is lower than that ratio in the atmosphere. This results in initial apparent ages of up to 2000 years for organic debris and carbonates formed within such a lake. If, as probable, Searles Lake had high carbonate concentrations in the past, many or all of the C^{14} dates of the lake sediments may be too old. Because of these five difficulties, positions on Figure 13 of boundaries between events are somewhat arbitrary and are controlled only by the bracketing dates listed.

The major C^{14}-dated responses to late Pleistocene climatic fluctuations are shown on Figure 13 for the northeastern St. Elias Mountains, Washington and British Columbia, and Searles Lake, all within the North American Cordillera. In each area there are three major events, two

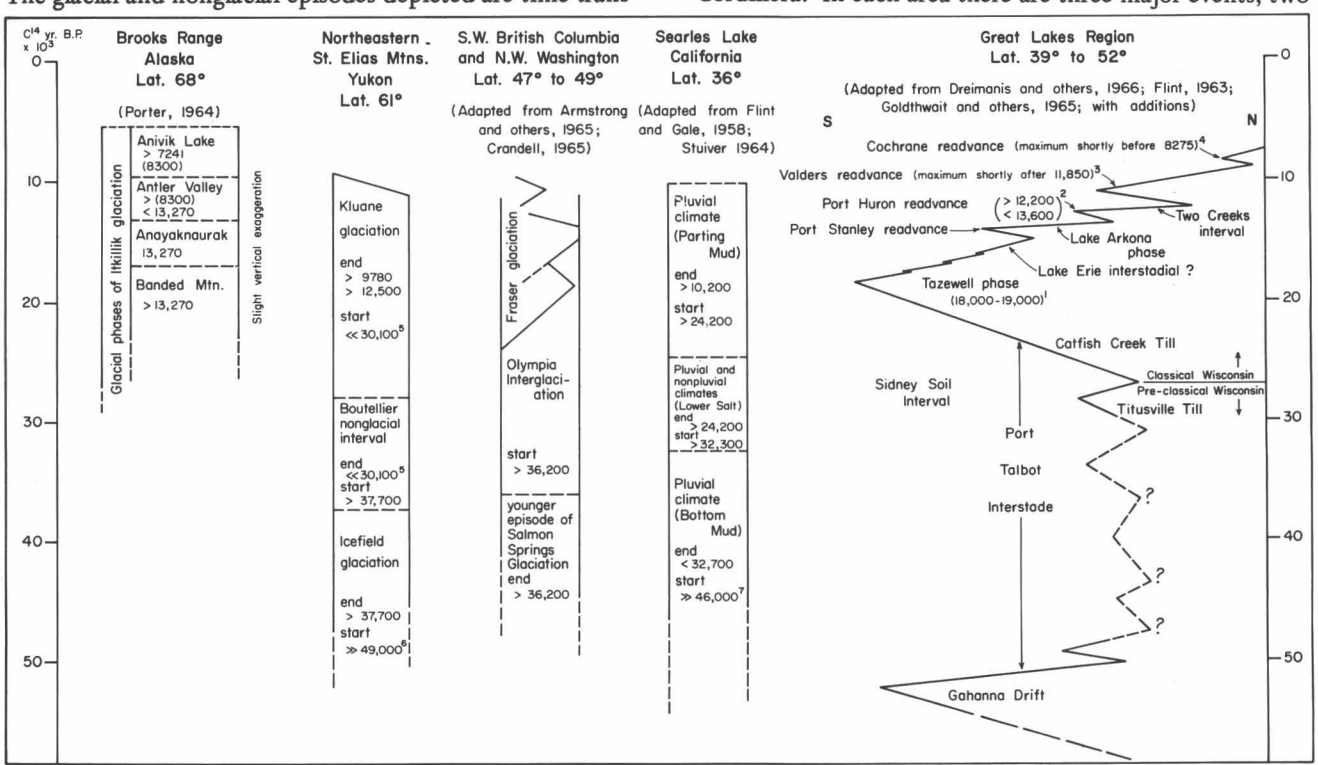

Fig. 13. Correlation chart of late Pleistocene glacial and pluvial events in selected areas of North America. C^{14} dates are given in years B.P.; all C^{14} dates used are finite except for the oldest date in the St. Elias sequence. $<$ or $>$ indicates that C^{14} date closely controls event, whereas $\ll$ or $\gg$ indicates that C^{14} date considerably antedates or postdates event. All boundaries between events are placed at position of bracketing C^{14} date; therefore, correlation of several events is closer than indicated on chart. NOTES: [1]Flint (1956), Flint and Rubin (1955); [2]Flint (1956), Flint and Rubin (1955); [3]Broecker and Farrand (1963); [4]Hughes (1965); [5]C^{14} sample located 14 feet below base of Kluane till III; [6]C^{14} date infinite; [7]C^{14} sample located well above the base of Bottom Mud.

glacial or pluvial intervals separated by a nonglacial or nonpluvial interval. Correlation among the three Cordilleran areas is marred by one apparent discrepancy, the date of 32,500 B.P. (an interpolation of 32,700 B.P. and 32,300 B.P.) at Searles Lake, closely marking a pluvial-nonpluvial boundary. The inconsistency of this date with those of comparable glacial-nonglacial boundaries in the other two areas may reflect a time lag in the response of the lake system, of which Searles is a member, to climatic change. The basic control of sedimentation in Searles Lake is inflow from Owens Lake, in turn related to climatic factors (Flint and Gale, 1958). Although Stuiver (1964, p. 378-381) showed that salt deposition in Searles Lake closely follows cessation of inflow, the time required for cessation of inflow resulting from the climatic change in question is unknown. At the close of the pluvial represented by the Bottom Mud, cessation of inflow may have been delayed by the influx of meltwater into Owens Lake from receding glaciers within the segment of the east slope of the Sierra Nevada that drained into the lake system. Alternatively, a climatic change sufficient to affect glaciers may have occurred before deposition of the Lower Salt, without attaining the necessary magnitude to halt inflow until about 32,500 B.P. A third possibility is that climatic changes were slightly out of phase among the three areas at this time. Data in hand are not sufficient to choose among these possibilities.

Aside from the apparent discrepancy mentioned above, correlation is reasonably close, suggesting that at least some major late Pleistocene glacial and pluvial events and, by inference, the climatic fluctuations that caused them were broadly synchronous at three widely separated latitudes in the North American Cordillera.

Figure 13 also permits comparison of late Pleistocene fluctuations of glaciers in northwestern North America with those of the southern margin of the Laurentide Ice Sheet in the Great Lakes region. For northwestern North America a composite sequence is formed by combining glacial chronologies in the St. Elias Mountains and the north-central Brooks Range, Alaska. For the Great Lakes region the fluctuations of the margin of the ice sheet are broadly traced through much of Wisconsin time (Flint, 1963, p. 403; Goldthwait and others, 1965, p. 94; Dreimanis and others, 1966, p. 323); data for classical Wisconsin events were selected from throughout the Great Lakes region, whereas data for pre-classical Wisconsin events were taken only from the Erie Lobe in Ontario and Ohio because the over-all relations of these events in the Great Lakes region are obscure. Thus pre-classical Wisconsin fluctuations associated with C^{14} dates in Indiana, Illinois, and Wisconsin (Gooding, 1963; Frye and others, 1965) are not shown, nor is correlation with these areas attempted.

Rigid correlation of the oldest dated Wisconsin events on Figure 13 is not possible. As yet the Icefield glaciation has no dated counterpart in the Erie Lobe; however, Dreimanis and others (1966) suggested that throughout this time the fluctuating margin of the ice sheet was located in the St. Lawrence Lowlands. Otherwise, C^{14} dates show that the Boutellier nonglacial interval can be equated with a large part of the Sidney Soil Interval in Ohio (Goldthwait, 1958, p. 210-213; Goldthwait and others, 1965, p. 94) and with the later half of the Port Talbot interstade in southern Ontario (Dreimanis and others, 1966). C^{14} dates show also that the Kluane glaciation occurred during the same time span as the classical Wisconsin glaciation of the Laurentide Ice Sheet in the Great Lakes region.

Several major readvances interrupted general deglaciation of the Great Lakes region by classical Wisconsin ice. In the northeastern St. Elias Mountains, however, areal study was too limited to recognize the effects of comparable fluctuations, with one possible exception: the cross-valley belt of ice-contact features near Kluane Lake may represent the position occupied by a major ice front shortly prior to 12,500 B.P. If so, the associated readvance or stillstand of ice correlates closely with the Port Huron readvance of the Laurentide Ice Sheet. Late Wisconsin glacier fluctuations in northwestern North America are documented in the north-central Brooks Range, where C^{14} dates place readvances during general Itkillik deglaciation within the general time spans occupied by several readvances of late classical Wisconsin ice in the Great Lakes region (Fig. 13; Porter, 1964).

The available evidence suggests that several long-term Wisconsin glacial and nonglacial events in northwestern and central North America were broadly coincident. This strengthens the argument that they represent widespread climatic episodes. Additionally, several readvances during retreat from the classical Wisconsin maximum may have been synchronous. However, climatic inferences based on correlation of these short-term events are tentative in view of (1) the difficulty of relating glacier variations to climatic parameters (Meier, 1965), (2) the possibility of local glacier surges unrelated to climate, and (3) the restriction of most pertinent evidence to morainal morphology, with the result that the relative magnitude of advances is often obscure.

ACKNOWLEDGMENTS

Funds for the field work by Denton were provided by the Arctic Institute of North America, the Explorers Club, Sigma Xi, and Yale University; support for the C^{14} dating by Stuiver was provided through a National Science Foundation grant.

Professor A. Lincoln Washburn and Professor Richard F. Flint visited Denton in the field and critically read the manuscript. Dr. David M. Hopkins reviewed the manuscript and offered valuable criticism. Barbara Denton and Messrs. William Dudley, Paul Nunes, Julian Orr, and Carl Weiman ably assisted in the field work; Mrs. Carolyn Morgan and Mr. Terry C. Eisensmith provided technical assistance for the C^{14} dating. X-ray diffraction studies and analyses of free iron were performed at the Connecticut Agricultural Station.

References

Armstrong, J. E., Crandell, D. R., Easterbrook, D. J., and Noble, J. B. (1965) Late Pleistocene stratigraphy and chronology in southwestern British Columbia and northwestern Washington, *Bull. Geol. Soc. Am., 76,* 321-330.

Bostock, H. S. (1952) Geology of northwest Shakwak Valley, Yukon Territory, *Canada Geol. Surv. Mem., 267,* 54 pp.

Broecker, W. S., and Farrand, W. R. (1963) Radiocarbon age of the Two Creeks forest bed, Wisconsin, *Bull. Geol. Soc. Am., 74,* 795-802.

Broeker, W. S., and Walton, A. (1959) The geochemistry of C^{14} in fresh water systems, *Geochim. Cosmochim. Acta, 16,* 15-38.

Crandell, D. R. (1965) The glacial history of western Washington and Oregon, in *The Quaternary of the United States,* edited by H. E. Wright, Jr. and D. G. Frey, pp. 341-355, Princeton Univ. Press, Princeton, N. J.

Deevey, E. S., and Flint, R. F. (1957) Postglacial hypsithermal interval, *Science, 125,* 182-184.

Deevey, E. S., Gross, M. S., Hutchinson, G. E., and Kraybill, H. L. (1954) The natural C^{14} contents of materials from hard-water lakes, *Proc. Nat. Acad. Sci., 40,* 285-288.

*Denton, G.H., and Stuiver, M. (1966) Neoglacial chronology, northeastern St. Elias Mountains, Canada, *Am. J. Sci., 264,* 577-599.

Dreimanis, A., Terasmae, J., and McKenzie, G. D. (1966) The Port Talbot interstade of the Wisconsin Glaciation, *Canadian J. Earth Sci., 3,* 305-325.

Flint, R. F. (1956) New radiocarbon dates and late-Pleistocene stratigraphy, *Am. J. Sci., 254,* 265-287.

Flint, R. F. (1963) Status of the Pleistocene Wisconsin Stage of central North America, *Science, 139,* 402-404.

Flint, R. F., and Fidalgo, F. (1964) Glacial geology of the east flank of the Argentine Andes between latitude 39°10'S and latitude 41°20'S, *Bull. Geol. Soc. Am., 75,* 335-352.

Flint, R. F., and Gale, W. A. (1958) Stratigraphy and radiocarbon dates at Searles Lake, California, *Am. J. Sci., 256,* 689-714.

Flint, R. F., and Rubin, M. (1955) Radiocarbon dates of pre-Mankato events in eastern and central North America, *Science, 121,* 649-658.

Frye, J. C., Willman, H. B., and Black, R. F. (1965) Outline of glacial geology of Illinois and Wisconsin, in *The Quaternary of the United States,* edited by H. E. Wright Jr. and D. G. Frey, pp. 43-61, Princeton Univ. Press, Princeton, N. J.

Goldthwait, R. P. (1958) Wisconsin Age forests in western Ohio. I. Age and glacial events. *Ohio J. Sci., 58,* 209-230.

Goldthwait, R. P., Dreimanis, A., Forsyth, J. L., Karrow, P. F., and White, G. W. (1965) Pleistocene deposits of the Erie Lobe, in *The Quaternary of the United States,* edited by H. E. Wright Jr. and D. G. Frey, pp. 85-98, Princeton Univ. Press, Princeton, N. J.

Gooding, A. (1963) Illinoian and Wisconsin glaciations in the Whitewater basin, southeastern Indiana, and adjacent areas, *J. Geol., 71,* 665-682.

Hughes, O. L. (1965) Surficial geology of part of the Cochrane district, Ontario, Canada, in *Geol. Soc. Am. Spec. Paper 84,* pp. 535-565.

Johnson, F., and Raup, H. M. (1964) Investigations in southwest Yukon: Geobotanical and archaeological reconnaissance, *Robert S. Peabody Found. Archaeol. Papers,* Vol. 6, 198 pp.

Karlstrom, T. N. V. (1964) Quaternary geology of the Kenai Lowland and glacial history of the Cook Inlet region, Alaska, *U.S. Geol. Surv. Prof. Paper 443,* 69 pp.

Kendrew, W. G., and Kerr, D. (1955) *The Climate of British Columbia and the Yukon Territory,* Edmond Cloutier, Ottawa, 222 pp.

Kindle, E. D. (1953) Dezadeash map-area, Yukon Territory, *Canada Geol. Surv. Mem. 268,* 68 pp.

Krinsley, D. B. (1965) Pleistocene geology of the southwest Yukon Territory, Canada, *J. Glaciol., 5,* 385-397.

Meier, M. F. (1965) Glaciers and climate, in *The Quaternary of the United States,* edited by H. E. Wright Jr. and D. G. Frey, pp. 795-805, Princeton Univ. Press, Princeton, N. J.

Péwé, T. L., Hopkins, D. M., and Giddings, J. L. (1965) The Quaternary geology and archaeology of Alaska, in *The Quaternary of the United States,* edited by H. E. Wright Jr. and D. G. Frey, pp. 355-374, Princeton Univ. Press, Princeton, N. J.

Porter, S. C. (1964) Late Pleistocene glacial chronology of north-central Brooks Range, Alaska, *Am. J. Sci., 262,* 446-460.

Sharp, R. P. (1951a) Thermal regimen of firn on upper Seward Glacier, Yukon Territory, Canada, *J. Glaciol., 1,* 476-487.

Sharp, R. P. (1951b) Glacial history of Wolf Creek, St. Elias Range, Canada, *J. Geol., 59,* 97-115.

Sharp, R. P. (1958) Malaspina Glacier, *Bull. Geol. Soc. Am., 69,* 617-646.

Stuiver, M. (1964) Carbon isotopic distribution and correlated chronology of Searles Lake sediments, *Am. J. Sci., 262,* 377-392.

*Stuiver, M., Borns, H. W., and Denton, G. H. (1964) Age of a widespread layer of volcanic ash in the southwestern Yukon Territory, *Arctic, 17,* 259-260.

U.S. Weather Bureau (1959) *World Weather Records 1941-1950,* U.S. Govt. Printing Office, Washington, D.C., 1361 pp.

Wentworth, C. K. (1936) An analysis of the shapes of glacial cobbles, *J. Sed. Petrol., 6,* 85-96.

Wheeler, J. O. (1963) Geologic map of Kaskawulsh half of Mount St. Elias map sheet, Yukon Territory, *Canada Geol. Surv. Map 1134A.*

Wood, W. A. (1963) The Icefield Ranges Research Project, *Geogr. Rev., 53,* 163-184.

*These articles are reprinted in the present volume.

Age of a Widespread Layer of Volcanic Ash in the Southwestern Yukon Territory*

Minze Stuiver†, Harold W. Borns, Jr.‡, and George H. Denton§

Radiocarbon dates pertaining to a widespread layer of volcanic ash in the southwestern Yukon Territory are here reported. The volcanic ash generally occurs in lacustrine sediments and in peat and loess deposited during the Little Ice Age and thus affords a valuable marker horizon for correlating these deposits. A reliable date for this ash layer will provide future workers with a limiting age for Little Ice Age deposits in this region.

Schwatka (1885) and Dawson (1889) first described a stratum of white volcanic ash from large areas of the southern Yukon Territory and eastern Alaska. This conspicuous deposit occurs at or close to the surface and is easily seen in vertical exposures.

Capps (1915), Bostock (1952), Berger (1960), and Fernald (1962) have since added to the description and interpretation of the ash.

Bostock (1952) constructed an isopach map showing two coalescing fans of ash with a combined area of about 129,000 sq. mi. and a maximum thickness of about 300 ft. near the international boundary about 10 mi. south of the White River. Both Bostock (1952) and Capps (1915) suggested that there was probably the source of the ash.

Moffit and Knopf (1910) reported that a sample of this ash collected in the White River Basin, Alaska was an andesitic pumice. Berger (1960) described ash from the Tepee Lake area, southern Yukon Territory, and concluded that it was of dacitic composition.

Capps (1915) studied the rate of peat accumulation above the ash in a bog exposed in the bank of the White River 25 mi. northwest of the center of eruption and concluded that the ash was deposited about 1400 years ago.

In 1962 Fernald reported radiocarbon dates that placed the age of the ash fall at around 1636 ± 80 years B.P. in the Tanana River valley, Alaska. The value of 1635 ± 80 years was obtained by averaging two dates: 1520 ± 100 years B.P. (sample I-275) and 1750 ± 110 years B.P. (sample I-276) that were derived from peat immediately above and below the ash layer, respectively.

A microscopic analysis of an ash sample collected near the southeast shore of Kluane Lake, southwestern Yukon Territory, in 1963 showed it to be composed of whole and broken euhedral crystals of plagioclase (An 35 to An 50), hornblende, biotite, and a trace of magnetite. The glass sherds have a refractive index of approximately 1.510, suggesting a dacitic composition (George, 1924). The results of this analysis and that of Berger's are consistent, but both differ slightly from the analysis reported by Moffit and Knopf (1910) in the type of plagioclase present. Knopf reported a composition slightly more calcic than Ab 1, An 1, or essentially labradorite, whereas the two analyses from the Yukon Territory show the plagioclase to be andesine.

The ash layer, 1 inch thick, was found in a peat bog in the timbered rocky knob separating the Slims and Kaskawulsh Rivers, southwestern Yukon Territory, approximately 100 yd. north of and about 40 ft. above the Little Ice Age terminal moraine of the Kaskawulsh Glacier. In an excavation the top of the 1-in. thick ash layer in this locality was 13 in. below the surface of the bog. Samples of peat, 0.5 in. thick, were collected from positions immediately above and below the ash for radiocarbon dating. The sample Y-1363 from just above the ash yielded an age of 1460 ± 70 years B. P. and the sample Y-1364 from just below the ash was dated 1390 ± 70 years B. P., indicating that the time of the ash fall was around 1425 ± 50 years ago. Although the lower sample provides a younger date, the difference is not significant in view of the statistical error of ± 70 years. The peat sections are very thin and one can expect that both samples are of about the same age. In a case like this there is a 50 percent chance that the lower sample turns out to be the "younger" one.

Our date is very close to the nonradiometric date of 1400 years ago approximated by Capps, but it is different

*This note has previously appeared in *Arctic*, 1964, Vol. 17, pp. 259-260, and is reproduced here with permission.

†Radiocarbon Laboratory, Yale University, New Haven, Connecticut.

‡Department of Geology, University of Maine, Postdoctoral Fellow for 1963-1964, Department of Geology, Yale University, New Haven, Connecticut.

§Department of Geology, Yale University, New Haven, Connecticut.

from the average radiocarbon date of 1635 ± 80 years presented by Fernald (1962). The difference suggests the possibility that there were two eruptions from the same source separated by approximately 200 years, with the older fan extending northwards.

Bostock (1952) suggested that these fans were probably the result of two different surges during the same eruption with the northward extending fan being the older of the two. If this were so there would be essentially no time difference between the surges. It is suggested that a study of the area of fan coalescence may show two distinct ash layers of essentially the same composition but separated by a thickness of peat or sediment equivalent to about 200 years. From the area of coalescence Moffit and Knopf (1910) reported two separate ash beds in a peat bog exposed in the bank of Holmes Creek, a tributary of the White River, Alaska. They were not sure whether these beds represent two distinct eruptions or whether the top layer had been washed into the bog a considerable time after deposition of the lower. Assuming a constant rate of peat growth for this locality, it would have taken approximately 120 years to form 2 in. of peat between the separate layers.

Near the southeast shore of Kluane Lake, Yukon Territory, the ash occurs near the base of a deposit of loess 4 ft. thick. The center part of a tree buried there in the growth position immediately above the ash was dated at 870 ± years B.P. (sample Y-1365) and gives a minimum age for the ash.

The study of this ash is only a small part of the larger one of the Pleistocene history of Shakwak Trench and Slims River valley which was undertaken with the encouragement and help of Dr. W.A. Wood, director, and Mr. Richard Ragle, field leader of the Icefield Ranges Research Project.

The work of Borns has been supported by the National Science Foundation Grant GP-1125 to the Ohio State University Research Foundation, that of Denton by grants from the Arctic Institute of North America and the Explorers Club, and that of the Yale Radiocarbon Laboratory by the National Science Foundation under Grant GP-1307.

References

Berger, A. R. (1960) On a recent volcanic ash deposit, Yukon Territory, PROC. GEOL. ASSOC. CANADA 12, 117-118.

Bostock, H. S. (1952) Geology of northwest Shakwak valley, Yukon Territory, GEOL. SURV. CANADA MEM. 267, 54pp.

Capps, S. R. (1915) An ancient volcanic eruption in the upper Yukon basin, U. S. GEOL. SURV. PROF. PAPER 95, pp. 59 – 64.

Dawson, G. M. (1889) Report on an expedition in the Yukon district, N. W. T., and adjacent northern portion of British Columbia, GEOL. SURV. CANADA ANN. REPT., Vol 3, Pt. 1, B, 277 pp.

Fernald, A. T. (1962) Radiocarbon dates relating to a widespread volcanic ash deposit, eastern Alaska, U. S. GEOL. SURV. PROF. PAPER 450, pp. B29-B30.

George, W. O. (1924) The relation of the physical properties of natural glasses to their chemical composition, J. GEOL., 32, 353 – 372.

Moffit, F. H., and Knopf, A. (1910) Mineral resources of the Nabesna-White River district, Alaska, with a section on the Quaternary by S. R. Capps, U. S. GEOL. SURV. BULL. 417, pp. 42 – 44.

Schwatka, F. (1885) ALONG ALASKA'S GREAT RIVER, Cassel and Co., New York, 360 pp.

CONVERSION TABLES

LENGTH

Inches to millimeters (1 in. = 25.4 mm)

in.	mm
0	0
2	50.8
4	101.6
6	152.4
8	203.2
10	254.0
12	304.8

Millimeters to inches (1 mm=0.039370 in.)

mm	in.
0	0
10	0.39
20	0.79
30	1.18
40	1.57
50	1.97
60	2.36
70	2.76
80	3.15
90	3.54
100	3.94

Feet to meters (1 ft. = 0.3048 m)

ft.	m
0	0
10	3.05
20	6.10
30	9.14
40	12.19
50	15.24
60	18.29
70	21.34
80	24.38
90	27.43
100	30.48

Meters to feet (1 m = 3.28084 ft.)

m	ft.
0	0
10	32.81
20	65.62
30	98.43
40	131.23
50	164.04
60	196.85
70	229.66
80	262.47
90	295.28
100	328.08

Miles to kilometers (1 mi. = 1.609344 km)

mi.	km
0	0
10	16.1
20	32.2
30	48.3
40	64.4
50	80.5
60	96.6
70	112.7
80	128.7
90	144.8
100	160.9

Kilometers to miles (1 km = 0.621371 mi.)

km	mi.
0	0
10	6.2
20	12.4
30	18.6
40	24.9
50	31.1
60	37.3
70	43.5
80	49.7
90	55.9
100	62.1

VELOCITY

Knots to meters per second and miles per hour

kn (Int)	m/s	mi/h
1	0.51	1.15
2	1.03	2.30
3	1.54	3.45
4	2.06	4.60
5	2.57	5.75
6	3.09	6.90
7	3.60	8.05
8	4.12	9.20
9	4.63	10.36

Miles per hour to meters per second and knots

mi/h	m/s	kn (Int)
1	0.45	0.87
2	0.89	1.74
3	1.34	2.61
4	1.79	3.48
5	2.24	4.34
6	2.68	5.21
7	3.13	6.08
8	3.58	6.95
9	4.02	7.82

Meters per second to miles per hour and knots

m/s	mi/h	kn (Int)
1	2.24	1.94
2	4.47	3.89
3	6.71	5.83
4	8.95	7.77
5	11.18	9.72
6	13.42	11.66
7	15.66	13.61
8	17.90	15.55
9	20.13	17.49

TEMPERATURE

°F to °C

$$\left[°C = \frac{5}{9}(°F - 32)\right]$$

°F	°C
−50	−45.6
−45	−42.8
−40	−40.0
−35	−37.2
−30	−34.4
−25	−31.7
−20	−28.9
−15	−26.1
−10	−23.3
− 5	−20.6
0	−17.8
5	−15.0
10	12.2
15	− 9.4
20	− 6.7
25	− 3.9
30	− 1.1
35	1.7
40	4.4
45	7.2
50	10.0
55	12.8
60	15.6
65	18.3
70	21.1
75	23.9
80	26.7

°C to °F

$$\left[°F = \frac{9}{5}°C + 32\right]$$

°C	°F
−45	−49.0
−40	−40.0
−35	−31.0
−30	−22.0
−25	−13.0
−20	− 4.0
−15	5.0
−10	14.0
− 5	23.0
0	32.0
5	41.0
10	50.0
15	59.0
20	68.0
25	77.0
30	86.0

ICEFIELD RANGES RESEARCH PROJECT STATIONS

Station No.	Name used in this volume	Names used previously by various authors	Used as:		Type of Surface †
			Camp	Scientific station	
1	Base Station	Kluane, Kluane Camp, Base Camp	+	+	Gravel
2	Terminus Station	Moraine Camp, Terminus	+	+	Gravel (outwash)
3	Kaskawulsh Station A	Kask, Kaskawulsh Camp	+	+	Ice-cored moraine
4	Kaskawulsh Station B	Kask Ice		+	Ice (glacier)
5	Kaskawulsh Station C	Kask Knoll		+	Rock (knoll)
6	Crevasse Camp		+	+	Firn (glacier)
7	Divide Station A	Upper Camp, Glacier Central	+	+	Firn (glacier)
8	Divide Station B*	Divide, Meteorological Station	+	+	Firn (glacier)
9	Divide Station C	Divide Cache		+	Rock (nunatak)
10	Divide Station D	Cairn B		+	Snow-covered ridge
11	Seward Station A	Seward	+	+	Rock (nunatak)
12	Seward Station B	Seward Ice		+	Firn (glacier)
13	Lucania Camp		+	+	Firn (glacier)

*Divide Station B used by Havens and Saarela (pp. 17–22) was located ½ mile north of Divide Station B shown on Plates 1 and 2.

†Stations on glaciers move with the glacier at a rate varying from a few centimeters to as much as a meter per day. Therefore, locations of stations on glaciers are only approximate.

PLATE 1

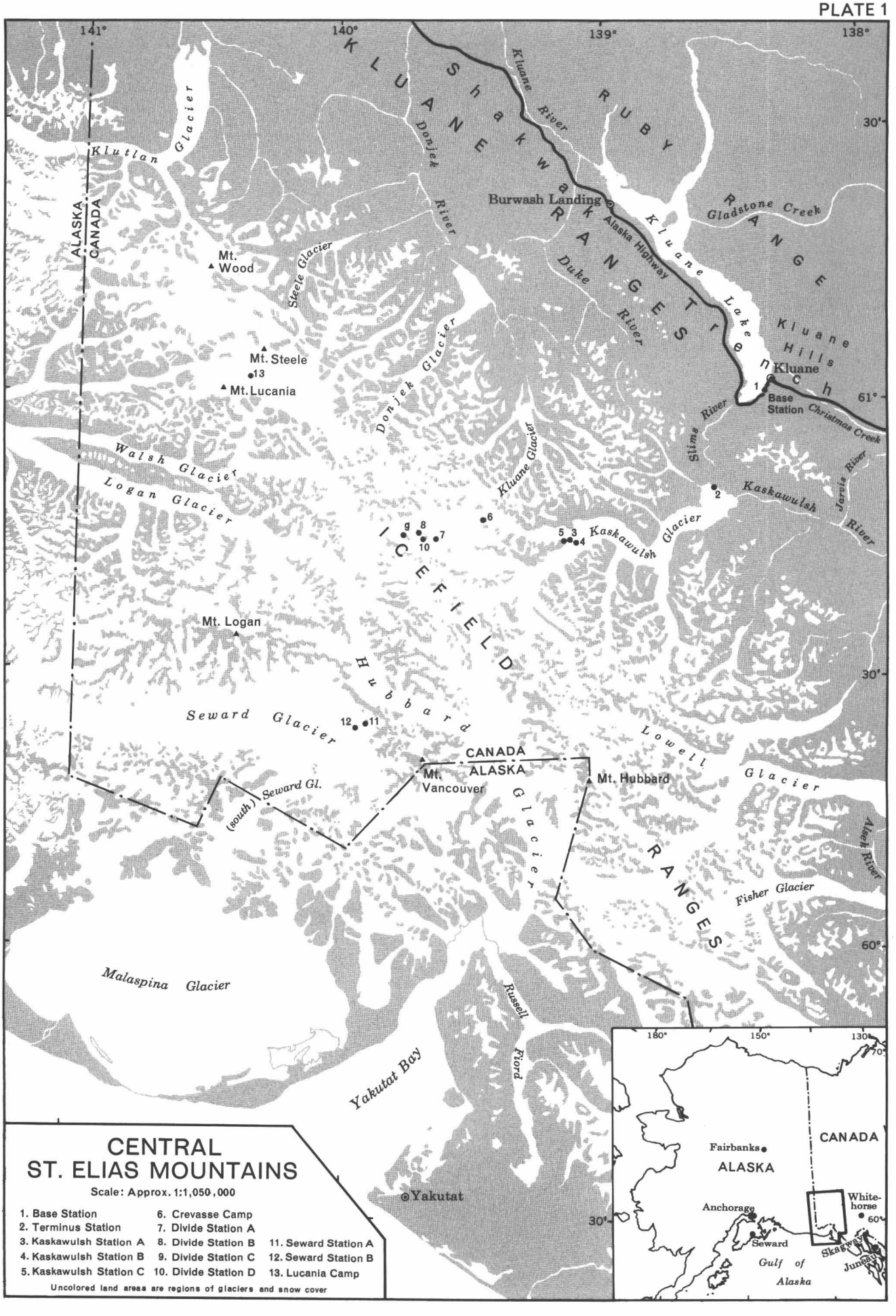

CENTRAL ST. ELIAS MOUNTAINS

Scale: Approx. 1:1,050,000

1. Base Station
2. Terminus Station
3. Kaskawulsh Station A
4. Kaskawulsh Station B
5. Kaskawulsh Station C
6. Crevasse Camp
7. Divide Station A
8. Divide Station B
9. Divide Station C
10. Divide Station D
11. Seward Station A
12. Seward Station B
13. Lucania Camp

Uncolored land areas are regions of glaciers and snow cover